

Development of Advanced Drug Delivery Systems for Respiratory Diseases

by Gabriele De Rubis

Thesis submitted in fulfilment of the requirements for
the degree of

Doctor of Philosophy

under the supervision of:

Dr. Kamal Dua (Principal Supervisor)

Dr. Keshav Raj Paudel (Co-Supervisor)

Prof. Philip Michael Hansbro (Co-Supervisor)

Dist. Prof. Brian Gregory George Oliver (Co-Supervisor)

University of Technology Sydney

Faculty of Health, Graduate School of Health, Discipline of
Pharmacy

Australian Research Centre in Complementary and
Integrative Medicine (ARCCIM)

CERTIFICATE OF ORIGINALITY

I, Gabriele De Rubis, declare that this thesis, is submitted in fulfilment of the requirements for the award of Doctor of Philosophy in the Graduate School of Health at the University of Technology Sydney.

This thesis is wholly my work unless otherwise referenced or acknowledged. In addition, I certify that all information sources and literature used are indicated in the thesis.

This document has not been submitted for qualifications at any other academic institution.

This research is supported by the Australian Government Research Training Program.

Name: Gabriele De Rubis

Signature:

Production Note:
Signature removed prior to publication.

Date: 17 March 2023

ACKNOWLEDGEMENTS

First of all, I would like to thank my principal supervisor, Dr Kamal Dua, for making this possible. Kam, you really are a wonderful mentor and leader, and an example that everyone should follow. Thank you for always believing in me, and for being a fundamental catalyst in my career. Thank you for showing me how research can be fun and hard work at the same time, for showing the power of collaboration, and for re-igniting in me the passion for research. If one day I will be someone in this field, I owe it to you and to all the things you taught me in this relatively short amount of time. I do hope we'll keep wearing the publication hat for a long time!

I would also like to thank my co-supervisors, Dr Keshav Raj Paudel, Prof Phil Hansbro, and Prof Brian Oliver, for all the precious guidance and advice. I am particularly grateful to Keshav for being a great mentor, in and outside the lab. I learned a lot from you and I am extremely grateful to you for sharing your immense knowledge with me.

A big shout and thanks to our amazing, and growing, UTS/Woolcock/Centenary research team: thanks, Bikash, Rashi, Ruby, Alex, Vamshi, Ridhima, for growing with me and making the day-by-day life in the lab and at the office so fun and enjoyable.

I must give a big thanks to all our wonderful collaborators, starting from the UNSW team, with Dr Peter Wich and Vinod. Thanks also to Dr Gang Liu, and to all the Respiratory and Inflammation Research Team. Thanks to Dr Dinesh Kumar Chellappan and Sid. Thanks also to Prof. Sachin Kumar Singh, Prof Vandana Patravale, Dr Gaurav Gupta, and Popat Kumbhar for the advice, support, and collaboration. To a future with always more collaborations and wonderful research outcomes!

Thanks also to our industry partners, whose contribution and input is fundamental for our research. In particular, I want to deeply thank Jessie Shen and Raniya Malik from De'Aurora Pty Ltd, Aniss Chami from Vitex Pharmaceuticals, and Dr Ronan MacLoughlin from Aerogen, Ireland.

A special thanks also goes to Prof Kylie Williams, Prof Toby Newton-John, A/Prof Mojtaba Golzan, and Eddy Dharmadji. Thank you for your immense support throughout these years. And thanks also to the amazing team of Pharmacy academics, for welcoming me so warmly in the team: Dr Rachelle Catanzariti, Dr Helen Benson, Dr Jennifer Wong, Dr Cherie Lucas, Prof Lisa Pont, Dr Monica Kilias.

To my family far from home, my best friends Niko and Michele. Thank you guys, for making me feel at home since day one. Thank you for always sticking with me through good and bad weather, and for always supporting me. Life wouldn't be so colourful without you.

To my real family: Mom, Vito, and Zia Milla. I miss you immensely. Thank you for always believing in me, and for always supporting my dreams and aspirations. I know it's not easy for you to be so far from me, and I wish I will be able to bring you here one day. Thank you for your love and unconditional support.

Last, but definitely not least, a special thanks goes to Eleonora. Thank you for supporting me during the most difficult time of my life. I will never forget your extreme kindness of heart and generosity, and I think that it is people like you who make the world a better place. Please, never stop being the wonderful, genuine person you are.

Finally, I would like to dedicate this work to Dad and Zio Gianni. People never really leave this world if their memory is still alive in the heart of those who loved them.

Grazie!

TABLE OF CONTENTS

Certificate of originality.....	ii
Acknowledgments.....	iii-iv
Table of contents.....	v-viii
Publications from thesis work.....	x-xii
Conference presentations	xiii
List of abbreviations	xiv-xix
Thesis abstract.....	xx-xxiii

CHAPTER 1 – Literature Review: Applications and advancements of nanoparticle-based drug delivery in alleviating lung cancer and chronic obstructive pulmonary disease	1
Abstract	2
1. Introduction	4
2. Impact of cigarette smoking on LC and COPD	5
3. Lung diseases: COPD and LC	6
3.1 COPD	6
3.2 Lung Cancer	7
3.3 The role of tissue remodeling in COPD and lung cancer.....	8
4. Treatment modalities in mitigating LC and COPD	9
4.1 Current therapies in lung cancer and related drawbacks	11
4.2 Current therapies in COPD and related drawbacks	12
5. Emerging pharmacological strategies in the management of LC and COPD	14
5.1 Phytoceuticals.....	14
5.1.1 Berberine.....	15
5.1.2 Agarwood oil	15
5.1.3 Zerumbone	16
5.1.4 Clinical trials investigating the therapeutic efficacy of phytoceuticals	17
5.1.5 Limitations to the clinical application of phytoceuticals	20
5.2 Nucleic acid-based therapy.....	20
5.2.1 Nucleic acid-based therapeutics targeting miRNA in COPD	21

5.2.2 siRNA-based gene knockdown and gene silencing of inflammatory mediators in COPD and inflammatory diseases.....	21
5.2.3 Nucleic acid-based therapy to counteract airway remodelling in COPD	22
5.2.4 Nucleic acid-based therapy in lung cancer	23
5.2.5 Limitations to the clinical translation of nucleic acid-based therapy	23
6. Nanoparticle-based drug delivery approaches to overcome the limitations hampering the use of phytochemicals and nucleic acid-based therapy in lung diseases	24
6.1 Polymeric nanoparticles	28
6.2 Liquid Nanocrystals.....	31
6.3 Nanoemulsions	34
6.4 Liposomes.....	37
6.5 Exosomes.....	39
6.6 Dendrimers	41
6.7 Polymeric micelles	42
6.8 Metal-based nanoparticles	42
7. Clinical trials testing nano-drug delivery systems	50
8. Conclusions and future perspectives	54
References	57
Rationale, hypothesis, and aims of the present work	84
Aims of the thesis.....	85
CHAPTER 2 – Research Paper: Anticancer activity of NFκB decoy oligonucleotide-loaded nanoparticles against human lung adenocarcinoma.....	86
Abstract	89
1. Introduction	91
2. Materials and Methods	94
2.1 Materials	94
2.2 Synthesis of spermine-functionalized acetalated dextran.....	94
2.3 Transcription factor decoy ODN	95
2.4 Nanoparticle preparation	96
2.5 Measurement of particle size and zeta potential.....	96
2.6 Scanning electron microscopy (SEM).....	96
2.7 Determination of ODN loading by RiboGreen assay.....	97

2.8 pH-dependent degradation of SpAcDex particles	97
2.9 pH-dependent release of decoy ODN from SpAcDex particles.....	98
2.10 ODN molecular generation and visualization	98
2.11 Cell culture	98
2.12 Cell viability assessment – MTT assay	99
2.13 Wound healing assay.....	99
2.14 Boyden’s chamber assay	99
2.15 Colony formation assay.....	100
2.16 Real-time qPCR.....	100
2.17 Statistical analysis	102
3. Results	103
3.1 Nanoparticle size and zeta potential	103
3.2 Quantification of decoy ODN loading	104
3.3 pH-dependent particle degradation	105
3.4 pH-dependent decoy ODN release	106
3.5 Anti-proliferative activity of NFκB-ODN-NPs in A549 and BEAS-2B cells	107
3.6 Effect of Dex(NFκB-ODN) NPs on the expression of apoptosis/necroptosis genes in A549 cells.....	109
3.7 Anti-migratory activity of NFκB-ODN-NPs in A549 Cells	110
3.8 Anti-Colony Formation Activity of NFκB-ODN-NPs in A549 Cells	111
4. Discussion	113
5. Conclusions	117
References	119
Supplementary information.....	127

CHAPTER 3 – Research Paper: Agarwood oil nanoemulsion attenuates cigarette smoke-induced inflammation and oxidative stress markers in BCiNS1.1 airway epithelial cells 128

Abstract	130
1. Introduction	132
2. Methods.....	135
2.1 Preparation of agarwood-NE.....	135
2.2 Cell culture and agarwood-NE treatment.....	137
2.3 Cell viability	137
2.4 Real-time qPCR.....	137
2.5 Human cytokine protein array	138

2.6 Statistical analysis	139
3. Results	139
3.1 Identification of an optimal concentration of agarwood-NE for treatment in CSE-induced BCI-NS1.1 cells	139
3.2 Agarwood-NE inhibits the CSE-induced transcription of the pro-inflammatory cytokine IL-8	140
3.3 Agarwood-NE inhibits the CSE-induced protein expression of pro-inflammatory cytokines and mediators	141
3.4 Agarwood-NE stimulates the CSE-inhibited protein expression of anti-inflammatory cytokines and mediators	142
3.5 Agarwood-NE stimulates the CSE-inhibited transcription of antioxidant genes	145
3.6 Agarwood-NE stimulates the CSE-inhibited transcription of the pro-survival gene PI3K	145
4. Discussion	146
5. Conclusion.....	151
References	152

CHAPTER 4 – Research Paper: Berberine-loaded engineered nanoparticles attenuate TGF- β -induced remodelling features in human bronchial epithelial cells 160

Abstract	162
1. Introduction	164
2. Materials and methods	167
2.1 Formulation and physicochemical characterization of BM-LCNs.....	167
2.2 Cell culture	168
2.3 Cell viability assay - MTT.....	168
2.4 Cell viability assay – Trypan Blue staining.....	168
2.5 Wound healing assay.....	169
2.6 Human cytokine protein array	169
2.7 NO levels determination with Griess reagent.....	170
2.7 Statistical analysis	170
3. Results	170
3.1 Identification of a non-toxic concentration of BM-LCNs for treating TGF- β -stimulated BEAS-2B cells.....	170
3.2 Anti-migratory activity of BM-LCNs in TGF- β -induced BEAS-2B cells.....	172
3.3 BM-LCNs counteract the protein expression signature induced by TGF- β	174
3.4 BM-LCNs restore baseline levels of NO.....	175

4. Discussion	176
5. Conclusions	180
References	181
CHAPTER 5 – Discussion, conclusions, and future directions	189
Limitations of the present work and future directions	205
Conclusions	207
References	208
APPENDIX I – Published versions of main thesis chapters	222
APPENDIX II – Additional publications relevant to thesis work	264

PUBLICATIONS FROM THESIS WORK

Introduction – Chapter 1

1) **De Rubis G**, Paudel KR, Oliver BG, Hansbro PM, Dua K. *Applications and advancements of nanoparticle-based drug delivery in alleviating lung cancer and chronic obstructive pulmonary disease*. **Naunyn-Schmiedeberg Archives of Pharmacology (In review)**

Chapter 2

2) Kannaujiya VK[#], **De Rubis G**[#], Paudel KR, Manandhar B, Chellappan DK, Singh SK, MacLoughlin R, Gupta G, Xenaki D, Kumar P, Hansbro PM, Oliver BG, Wich PR, Dua K. *Anticancer activity of NFκB decoy oligonucleotide-loaded nanoparticles against human lung cancer*. **Journal of Drug Delivery Science and Technology**. 2023 Apr 82:104328. doi: <https://doi.org/10.1016/j.jddst.2023.104328>

[#] = authors have contributed equally to this work

Chapter 3

3) **De Rubis G**[#], Paudel KR[#], Manandhar B, Singh SK, Gupta G, Malik R, Shen J, Chami A, MacLoughlin R, Chellappan DK, Oliver BG, Hansbro PM, Dua K. *Agarwood Oil Nanoemulsion Attenuates Cigarette Smoke-Induced Inflammation and Oxidative Stress Markers in BCI-NS1.1 Airway Epithelial Cells*. **Nutrients**. 2023 Feb 17;15(4):1019. doi: [10.3390/nu15041019](https://doi.org/10.3390/nu15041019).

[#] = authors have contributed equally to this work

Chapter 4

4) **De Rubis G**, Paudel KR, Liu G, Agarwal V, MacLoughlin R, Pinto TJA, Adams J, Nammi S, Chellappan DK, Oliver BG, Hansbro PM, Dua K. *Berberine-loaded engineered nanoparticles attenuate TGF-β-induced remodelling in human bronchial epithelial cells*. **Toxicology in vitro**. 2023 92:105660. doi: <https://doi.org/10.1016/j.tiv.2023.105660>

Other Publications Relevant to Thesis Work

5) Alnuqaydan AM, Almutary AG, Azam M, Manandhar B, **De Rubis G**, Madheswaran T, Paudel KR, Hansbro PM, Chellappan DK, Dua K. *Phytantriol-Based Berberine-Loaded Liquid Crystalline Nanoparticles Attenuate Inflammation and Oxidative Stress in*

Lipopolysaccharide-Induced RAW264.7 Macrophages. **Nanomaterials (Basel)**. 2022 Dec 5;12(23):4312. doi: 10.3390/nano12234312.

6) Malya V, Paudel KR, **De Rubis G**, Hansbro NG, Hansbro PM, and Dua K. *Extracellular Vesicles Released from Cancer Cells Promote Tumorigenesis by Inducing Epithelial to Mesenchymal Transition via β -Catenin Signaling*. **International Journal of Molecular Sciences** 2023, 24(4), 3500; <https://doi.org/10.3390/ijms24043500>

7) Ashique S[#], **De Rubis G**[#], Sirohi E, Mishra N, Rihan M, Garg A, Reyes RJ, Manandhar B, Bhatt S, Jha NK, Singh TG, Gupta G, Singh SK, Chellappan DK, Paudel KR, Hansbro PM, Oliver BG, Dua K. *Short Chain Fatty Acids: Fundamental mediators of the gut-lung axis and their involvement in pulmonary diseases*. **Chemico-Biological Interactions**. 2022 Dec 1;368:110231. doi: 10.1016/j.cbi.2022.110231.

= authors have contributed equally to this work

8) Patel VK, Vishwas S, Kumar R, **De Rubis G**, Shukla SD, Paudel KR, Manandhar B, Singh TG, Chellappan DK, Gulati M, Kaur IP, Allam VSRR, Hansbro PM, Oliver BG, MacLoughlin R, Singh SK, Dua K. *Tackling the cytokine storm using advanced drug delivery in allergic airway disease*. **Journal of Drug Release Science and Technology. Journal of Drug Delivery Science and Technology**. 2023 Apr 82: 104366. doi: <https://doi.org/10.1016/j.jddst.2023.104366>

9) **De Rubis G**, Paudel KR, Dua K. *Modernizing traditional medicine: nanoparticle-based drug delivery systems to improve the delivery of phytochemicals in managing chronic respiratory diseases*. **Controlled Release Society, Indian Chapter (CRSIC) – 2023 Newsletter**

10) Paudel KR, **De Rubis G**, Panth N, Singh SK, Chellappan DK, Hansbro PM, Dua K. *Nanomedicine and medicinal plants: Emerging symbiosis in managing lung diseases and associated infections*. **EXCLI Journal**. 2022 Oct 27;21:1299-1303. doi: 10.17179/excli2022-5376

11) Mohamad MSB, Reyes RJ, **De Rubis G**, Paudel KR, Hansbro PM, Dua K, Chellappan DK. *The versatility of 18 β -glycyrrhetic acid in attenuating pulmonary inflammatory disorders*. **EXCLI Journal**, 22, 188–190. <https://doi.org/10.17179/excli2023-5845>

- 12) Malyla V, Paudel KR, **De Rubis G**, Hansbro NG, Hansbro PM, Dua K. *Cigarette smoking induces lung cancer tumorigenesis via upregulation of the WNT/ β -catenin signaling pathway.* **Life Sciences**. 2023 Aug 1;326:121787. doi: 10.1016/j.lfs.2023.121787
- 13) Malyla V, **De Rubis G**, Paudel KR, Chellappan DK, Hansbro NG, Hansbro PM, Dua K. *Berberine nanostructures attenuate β -catenin, a key component of epithelial mesenchymal transition in lung adenocarcinoma.* **Naunyn-Schmiedeberg's Archives of Pharmacology**. 2023 Jun 2. doi: 10.1007/s00210-023-02553-y
- 14) Manandhar B, Paudel KR, Clarence DD, **De Rubis G**, Madheswaran T, Panneerselvam J, Zacconi FC, Williams KA, Pont LG, Warkiani ME, MacLoughlin R, Oliver BG, Gupta G, Singh SK, Chellappan DK, Hansbro PM, Dua K. *Zerumbone-incorporated liquid crystalline nanoparticles inhibit proliferation and migration of non-small-cell lung cancer in vitro.* **Naunyn-Schmiedeberg's Archives of Pharmacology**. 2023 Jul 13. doi: 10.1007/s00210-023-02603-5 (Online ahead of print)

CONFERENCE PRESENTATIONS

- 1) **De Rubis G**, Kannaujiya VK, Paudel KR, Hansbro PM, Oliver BGG, Wich PR, Dua K. *Anticancer activity of NFκB decoy oligonucleotide encapsulated polysaccharide-based nanoparticles against human lung adenocarcinoma. Drug Delivery Australia Conference (DDA2022), Controlled Release Society Australian Local Chapter – Adelaide, Australia, 24-25 November 2022 (Oral Presentation)*
- 2) **De Rubis G**, Paudel KR, Oliver BGG, Hansbro PM, Dua K. *Advanced Drug Delivery Systems for the Delivery of Phytochemicals in the Treatment of Respiratory Diseases. International Conference on Innovations in Biology and Medicine 2023 (ICIBM23) – Nizamabad, India, 21-23 February 2023 (Oral Presentation as Invited Speaker)*
- 3) **De Rubis G**, Paudel KR, Oliver BGG, Hansbro PM, Dua K. *Advanced Drug Delivery Systems for the Delivery of Phytochemicals in the Treatment of Respiratory Diseases. International Conference on Advances in Biology and Medicine 2023 (BioMe23) – Hyderabad, India, 21-23 February 2023 (Oral Presentation as Invited Speaker)*
- 4) **De Rubis G**, Paudel KR, Oliver BGG, Hansbro PM, Dua K. *Berberine-loaded nanoparticles attenuate TGF-β-induced remodelling features in human bronchial epithelial cells. 21st International Symposium on Advances in Technology and Business Potential of New Drug Delivery Systems, Controlled Release Society Indian Local Chapter – Mumbai, India, 24-25 February 2023 (Poster Presentation)*
- 5) **De Rubis G**, Paudel KR, Malik R, Liu G, Kokkinis S, Datsyuk J, Chellappan DK, Oliver B, Hansbro PM, Dua K. *Berberine-loaded nanoparticles attenuate TGF-β-induced remodelling features in human bronchial epithelial cells. Monash INITIATE 2023, Monash University Malaysia – Kuala Lumpur, Malaysia, 25-26 October 2023 (Oral Presentation)*

LIST OF ABBREVIATIONS

AcDex	Acetalated Dextran
AHO	<i>Arachis hypogaea</i>
ANOVA	analysis of variance
AP-1	activator protein-1
α -SMA	alpha-smooth muscle actin
AW-NE	agarwood nanoemulsion
BA	β 2-agonists
BBR	berberine
BCi-NS1.1	basal cell immortalized-nonsmoker 1
BEBM	broncho-epithelial basal media
bFGF	basic fibroblast growth factor
BM-LCNs	berberine-monoolein liquid crystalline nanoparticles
CCL-20	chemokine (C-C motif) ligand 20
COPD	chronic obstructive pulmonary disease
COVID-19	coronavirus disease of 2019
CRD	chronic respiratory disease
CSE	cigarette smoke extract
CTAB	cetyl trimethyl ammonium bromide
CTSB	cathepsin B
CTSD	cathepsin D
CTL	cytotoxic T lymphocyte
CXCL-8	C-X-C motif chemokine ligand 8
CYP450	cytochrome P450

DLS	dynamic light scattering
DMEM	Dulbecco's modified Eagle's medium
DMSO	dimethylsulfoxide
DTT	dithiothreitol
ECM	extracellular matrix
EE	encapsulation Efficiency
EGFR	epidermal growth factor receptor
EMT	epithelial-to-mesenchymal transition
ERK	extracellular signal-regulated kinase
eNOS	endothelial nitric oxide synthase
EPR	enhanced permeability and retention
FAK	focal adhesion kinase
FDA	Food and Drug Administration
FEV1	forced expiratory volume 1
FOXO3a	forkhead box O3a
FVC	forced vital capacity
GAPSH	glyceraldehyde 3-phosphate dehydrogenase
GCLC	glutamate-cysteine ligase catalytic subunit
GDF-15	growth/differentiation factor-15
GH	growth hormone
GLOBOCAN	global cancer observatory
GSTP1	glutathione S-transferase pi 1
GOLD	global initiative for chronic obstructive lung disease
HBE	human bronchial epithelial

HDM	house dust mite
HFF	human foreskin fibroblasts
HIF-1 α	hypoxia-inducible factor-1 α
HO-1	heme oxygenase -1
IFN- γ	interferon- γ
IL	interleukin
IL-18BP	interleukin-18 binding protein
iNOS	inducible nitric oxide synthase
IPF	idiopathic pulmonary fibrosis
JND	jojoba oil dry nanoemulsion
KNTC1	kinetochore-associated 1
LABA	long-acting β 2-agonists
LAMA	long-acting muscarinic antagonist
LAP	latency-associated peptide
LCNs	liquid crystalline nanoparticles
LIMK1/2	LIM kinase 1 and 2
LLC	large latent complex
LNC	liquid nanocrystal
lncRNA	long non coding RNA
LUCAT1	lung cancer associated transcript 1
LPS	lipopolysaccharide
MA	muscarinic antagonist
MDR	multi-drug resistance
MDSC	myeloid-derived suppressor cell

miRNA	microRNA
MLKL	mixed lineage kinase domain like pseudokinase
MMLV	moloney murine leukemia virus
MMP	matrix metalloproteinase
MO	monoolein
MPO	myeloperoxidase
mRNA	messenger RNA
MTT	3-(4,5-Dimethylthiazol-2-yl)-2,5-diphenyltetrazolium bromide
MyD88	myeloid differentiation primary response 88
NADPH	nicotinamide adenine dinucleotide phosphate
NE	nanoemulsion
NEO	neobavaisoflavone
NF-kB	nuclear factor-kappaB
NO	nitric oxide
NOE	<i>Nasturtium officinale</i> extract
Nox	NADPH oxidase
NPs	nanoparticles
Nqo1	NAD(P)H dehydrogenase [quinone] 1
NSCLC	non-small cell lung cancer
ODN	oligodeoxynucleotides
OxAcDex	acetalated oxidized dextran
OxDex	oxidized dextran
P407	poloxamer 407
PAMAM	poly(amidoamine)

PBS	phosphate-buffered saline
PCR	polymerase chain reaction
PDGF-BB	platelet-derived growth factor-BB
PDI	polydispersity index
PEG	polyethylene glycol
PEI	polyethyleneimine
PI3K	phosphatidylinositide-3-kinase
PKGI	cGMP-dependent protein kinase I
PLA	polylactic acid
PLAC2	placenta-specific 2
PLGA	poly(lactic- <i>co</i> -glycolic acid)
PMX	pemetrexed
PNA	peptide nucleic acid
PVP-b-PCL	poly(N-vinylpyrrolidone)-block-poly(ϵ -caprolactone)
RGD	arginylglycylaspartic acid
RIPA	radioimmunoprecipitation assay
RIPK	receptor-interacting serine/threonine-protein kinase
ROS	reactive oxygen species
ROCK1	rho-associated, coiled-coil-containing protein kinase 1
SABA	short-acting β 2-agonists
SABR	stereotactic ablative body radiotherapy
SAMA	short-acting muscarinic antagonists
SARS-CoV-2	severe acute respiratory syndrome coronavirus 2
SCLC	small cell lung cancer

SEM	scanning electron microscope
sGC	soluble guanylate cyclase
shRNA	short hairpin RNA
siRNA	short interfering RNA
SpAcDex	spermine-functionalised acetalated dextran
SREBP	sterol regulatory element-binding proteins
STAT3	signal transducer and activator of transcription 3
TF	transferrin
TFF3	trefoil factor 3
TGF- β	transforming growth factor- β
THBS2	thrombospondin-2
TNF- α	tumor necrosis factor- α
TPA	12-O-tetradecanoylphorbol-13 acetate
TPGS	D- α -tocopherol polyethylene glycol succinate
TQ	thymoquinone
Tregs	regulatory T cells
UV	ultraviolet
VDBP	vitamin D binding protein
VEGF	vascular/endothelial growth factor
VEGFR	vascular/endothelial growth factor receptor
XIAP	X-linked inhibitor of apoptosis protein

THESIS ABSTRACT

Chronic Respiratory Disorders (CRDs) include a group of disease such as Chronic Obstructive Pulmonary Disease (COPD), asthma, and lung cancer (LC). Together, they represent a serious health burden, as CRDs are among the predominant causes of mortality in the world. The current yearly mortality associated to COPD is 3.2 million people. LC is one of the most deadly types of cancer, with around 1.7 million deaths globally in 2020. In Australia, about 30% of the population is reported to be affected by a chronic respiratory condition, and about 5% of all Australians of age more than 45 years old are affected by COPD. Between 2018 and 2020, COPD represented the fifth underlying cause of death in Australia, with about 6000-7000 reported annual deaths. COPD patients have also increased susceptibility to viral infections such as severe acute respiratory syndrome coronavirus 2 (SARS-CoV-2) and Influenza A Virus. With regards to LC, it is estimated that every Australian has a 5% possibility of being diagnosed with LC by the age of 85, and LC was responsible for nearly 8500 deaths in Australia in 2020.

Cigarette smoking is among the main aetiologic factors for these ailments, as well as for many other diseases. CRDs share common pathogenetic mechanisms including inflammation, oxidative stress, and tissue remodelling. Current therapeutic approaches are limited by poor efficacy and serious adverse effects, particularly with regards to LC treatments that include chemotherapy often associated with radiotherapy, surgical ablation, and immunotherapy. Consequentially, LC has a five-year survival of <20%, while COPD and asthma are still incurable. This highlights the necessity for innovative treatment strategies.

Two promising emerging classes of therapy against these diseases include: plant-derived molecules (phytoceuticals) such as berberine, curcumin and others; plant extracts and essential oils such as Agarwood oil; and nucleic acid-based therapies including silencing RNAs and decoy oligodeoxynucleotides. Despite the promising biological activity, the clinical application of these types of therapeutics is limited by many issues. Plant-derived molecules, for example, are often characterised by poor solubility and poor permeability and, in general, an unfavourable pharmacokinetic profile. This translates into the necessity to administer large doses in order to achieve therapeutic efficacy, leading to adverse effects. Nucleic acids, on the other hand, are highly susceptible to enzymatic degradation and have a large size and electrostatic charge density, leading to issues such as poor absorption and unfavourable pharmacokinetic properties. Advanced drug delivery systems are currently being studied and

characterized as flexible systems allowing to overcome the aforementioned limitations. The aim of the present thesis is to provide proof of the suitability of advanced drug delivery systems in improving the delivery of therapeutics including phytochemicals such as berberine and Agarwood oil, and nucleic acid-based therapy (decoy oligodeoxynucleotides). Different types of ADDSs have been tested *in vitro* against various models of disease and disease features such as lung cancer, COPD, and airway remodelling. The core chapters of the present thesis are three main research papers.

In the first research study (Chapter 2), a decoy oligodeoxynucleotide blocking the transcription factor NF- κ B was encapsulated within spermine-functionalised dextran-based nanoparticles (SpAcDex-NPs). These nanoparticles allow a pH-dependent release of the cargo at acidic pH values, which are commonly found in the tumor microenvironment as well as within the endosomal acidic compartments following intracellular uptake of the NPs. The rationale behind the blockade of NF- κ B is provided by the pivotal role played by NF κ B in many cancer hallmarks, as NF- κ B is considered a master regulator of many cancer hallmarks including cell proliferation, migration, metastasis, and epithelial-to-mesenchymal transition. The NPs were characterized for size, morphology, polydispersity index (PDI), size distribution, encapsulation efficiency, zeta potential, pH-dependent degradation and cargo release. The obtained nanoparticles had a spherical morphology with an average size of 190 nm and an average Zeta-potential of about 12 mV. The decoy oligodeoxynucleotides encapsulation efficiency was >99%, and the nanoparticles spontaneously degraded, and released the oligodeoxynucleotide *in vitro*, at a pH of 5.5. The anticancer potential of SpAcDex-NPs was tested on a human LC cell line (A549), where they significantly inhibited cell proliferation, migration, and colony formation. In particular, SpAcDex-NPs at a 10 nM concentration exerted a 37.2% inhibition of cell proliferation. Mechanistically, this was exerted *via* upregulating the expression of mRNAs encoding for four proteins that are considered main mediators of necroptosis: tumor necrosis factor- α (TNF- α), mixed lineage kinase domain-like protein (MLKL), and receptor-interacting serine/threonine-protein kinases 1 and 3 (RIPK1, RIPK3). The effect of SpAcDex-NPs treatment on the cell's migratory capacity was investigated *via* wound-healing assay and modified Boyden's chamber assay, obtaining a consistent inhibition of cell migration across the assays (54.3% and 43.2%, respectively). Finally, treatment with SpAcDex-NPs resulted in a 42% inhibition of the A549 cell's colony formation capacity. This chapter provides evidence of the enormous potential of SpAcDex-NPs as flexible tool to allow the target-selective release of the therapeutic payload directly to cancer cells. This is particularly relevant in the case of

decoy oligodeoxynucleotides targeting NF- κ B, whose application is severely limited by off-target effects.

In the second investigation (Chapter 3), agarwood oil has been formulated in a nanoemulsion through probe sonication and tested against an *in vitro* COPD model achieved by exposing human lung epithelial cells (BCi-NS1.1) to cigarette smoke extract (CSE). Agarwood oil is an essential oil extracted from the wood of *Aquilaria* trees that have been wounded or infested by some species of mould. This product has been used for several centuries in many traditional medicine systems and is renowned for its wide spectrum of antioxidant and anti-inflammatory properties that are exerted through several pathways, including the modulation of the balance between pro- and anti-inflammatory cytokines and the downregulation of inflammatory intracellular signalling pathways. The resulting nanoemulsion exerted significant anti-inflammatory and antioxidant activity. Mechanistically, this activity was exerted through the downregulation of the protein expression of cytokines whose production is stimulated by CSE such as IL-1 α , IL-1 β , I-1Ra, and growth/differentiation factor 15 (GDF-15), as well as through the upregulation of the protein expression of anti-inflammatory cytokines downregulated by CSE, including IL-10, IL-18Bpa, growth hormone (GH), interferon- γ (IFN- γ), platelet-derived growth factor (PDGF-BB), trefoil factor-3 (TFF3), Relaxin-2, and vitamin D binding protein (VDBP). At the mRNA level, treatment with agarwood nanoemulsion (i) restored the expression of transcripts downregulated by CSE such as the antioxidant genes Glutathione S-transferase P (GSTP1) and Glutamate-cysteine ligase (GCLC), as well as the pro-survival gene phosphatidylinositol-3 kinase (PI3K); and (ii) downregulated the expression of IL-8 transcript, a pro-inflammatory cytokine upregulated by CSE. Overall, the study demonstrates the potent antioxidant and anti-inflammatory activity of agarwood oil formulated as a nanoemulsion to increase its otherwise extremely low aqueous solubility.

Finally, in the third experimental set-up of the present thesis (Chapter 4), berberine was encapsulated in a monoolein-based liquid crystalline nanoparticle formulation (BM-LCNs) and tested on an *in vitro* model of pathologic tissue remodelling obtained by stimulating human bronchial epithelial cells (BEAS-2B) with transforming growth factor- β (TGF- β). Berberine is an isoquinoline alkaloid extracted from plants such as barberry and tree turmeric. It is widely known for its antioxidant, anti-inflammatory, and anticancer activities, as well as for its antifibrotic activity in organs such as lungs, heart, liver, pancreas, and kidneys. However, its clinical use is limited by poor cell permeability, which hampers its absorption *in vivo*. In this study, BM-LCNs attenuated TGF- β -induced remodelling features in several ways. First, TGF-

β induced an increased migratory capacity in BEAS-2B cells upon both 24 h and 48 h of treatment (42% and 18% compared to untreated cells, respectively). Treatment with BM-LCNs significantly reversed the effect of TGF- β on cell migration to values comparable with the untreated group. Mechanistically, BM-LCNs counteracted the effect of TGF- β by (i) downregulating the protein expression of cytokines involved in remodelling and upregulated by TGF- β , such as endoglin, thrombospondin-1, vascular endothelial growth factor (VEGF), myeloperoxidase, and basic fibroblast growth factor (bFGF); and (ii) restoring the protein expression of cytokines downregulated by TGF- β such as Cystatin C. Furthermore, treatment with TGF- β resulted in a 36.4% reduction of baseline nitric oxide (NO) levels, a known inhibitor of airway remodelling, which were restored by treatment with BM-LCNs to levels comparable to untreated cells. Due to the fact that TGF- β -induced airway remodelling is a nearly ubiquitous phenomenon present in many CRDs, this chapter underlines the multifaceted therapeutic potential of BM-LCNs and their potential applicability throughout different respiratory ailments.

Collectively, the results discussed in this thesis provide substantial proof of the great capacity of ADDSs in improving the clinical application of promising drugs whose translation into clinic is obstructed by issues such as poor solubility, poor permeability, and adverse pharmacokinetic characteristics. The present work provides a blueprint towards the development of effective treatment strategies to target respiratory diseases, ultimately providing a new direction to pulmonary clinics.

CHAPTER 1

Introduction and Literature Review

Applications and advancements of nanoparticle-based drug delivery in alleviating lung cancer and chronic obstructive pulmonary disease

(Submitted to Naunyn-Schmiedeberg Archives of Pharmacology, in review)

Applications and advancements of nanoparticle-based drug delivery in alleviating lung cancer and chronic obstructive pulmonary disease

Gabriele De Rubis^{1,2}, Keshav Raj Paudel³, Brian Gregory Oliver^{4,5}, Philip Michael Hansbro³, Kamal Dua^{1,2,*}

1. Discipline of Pharmacy, Graduate School of Health, University of Technology Sydney, NSW 2007, Australia

2. Faculty of Health, Australian Research Centre in Complementary and Integrative Medicine, University of Technology Sydney, Ultimo, Australia

3. Centre for Inflammation, Centenary Institute and University of Technology Sydney, Faculty of Science, School of Life Sciences, Sydney, NSW 2007, Australia

4. School of Life Sciences, University of Technology Sydney, Ultimo, NSW 2007, Australia

5. Woolcock Institute of Medical Research, University of Sydney, Sydney, New South Wales, Australia

* Corresponding Author: Dr Kamal Dua, kamal.dua@uts.edu.au

Abstract

Lung cancer (LC) and chronic obstructive pulmonary disease (COPD) are among the leading causes of mortality worldwide. Cigarette smoking is among the main aetiologic factors for both ailments. These diseases share common pathogenetic mechanisms including inflammation, oxidative stress, and tissue remodelling. Current therapeutic approaches are limited by low efficacy and adverse effects. Consequentially, LC has a five-year survival of <20%, while COPD is incurable, underlining the necessity for innovative treatment strategies. Two promising emerging classes of therapy against these diseases include plant-derived molecules (phytochemicals), and nucleic acid-based therapies. The clinical application of both is limited by issues including poor solubility, poor permeability, and, in the case of nucleic acids, susceptibility to enzymatic degradation, large size, and electrostatic charge density. Nanoparticle-based advanced drug delivery systems are currently being explored as flexible systems allowing to overcome these limitations. In this review, an updated summary of the most recent studies using nanoparticle-based advanced drug delivery systems to improve the delivery of nucleic acids and phytochemicals for the treatment of LC and COPD is provided.

This review highlights the enormous relevance of these delivery systems as tools that are set to facilitate the clinical application of novel categories of therapeutics with poor pharmacokinetic properties.

Keywords:

Chronic obstructive pulmonary disease, lung cancer, phytochemicals, drug delivery, nanoparticles, nucleic acid therapeutics, miRNA

1 - Introduction

Chronic respiratory diseases are among the most common causes of death worldwide [1]. Among chronic respiratory diseases, chronic obstructive pulmonary disease (COPD) and asthma represent the main causes of mortality and morbidity [1]. In 2019 alone, COPD accounted for over 3.3 million deaths [2]. The principal risk factor behind the incidence of chronic respiratory diseases, particularly COPD, is cigarette smoking [3-5]. Exposure to the many harmful chemicals contained in cigarette smoke promotes a pro-inflammatory and pro-oxidant state that fuels the development of lung disease [3, 6, 7]. Another disease for which cigarette smoke represents the primary risk factor is lung cancer [8], which is one of the leading causes of death worldwide [9]. COPD and lung cancer are related, as COPD patients are 4-6 times more likely to develop lung cancer compared to healthy individuals [10]. This is likely caused by the fact that COPD is characterized by chronic lung inflammation, dysbiosis, and hypoxia, which are by themselves risk factors for lung cancer [11-13].

Despite several treatment options that are currently available for COPD and lung cancer, patient mortality for these two diseases continues to increase, attributed by limitations of current therapeutic approaches, such as relatively poor efficacy and risk of severe adverse effects. This highlights the need for novel treatment strategies for COPD and lung cancer. Among innovative therapeutic options being currently studied, two strategies are particularly viable and represent promising perspectives: phytochemicals, or plant-derived molecules and extracts, and nucleic acid-based therapeutics. Both therapeutic strategies have limiting factors in their clinical application in the form of unfavourable pharmacokinetic profile. Natural molecules and plant-derived extracts, in fact, are often poorly water-soluble, and this severely limits their bioavailability [14]. With regards to nucleic acid-based therapeutics such as miRNA inhibitors or mimetics, siRNA, and decoy oligodeoxynucleotides, their poor bioavailability is caused by large size and electrostatic charge density, which limit their ability to cross absorption barriers, as well as by their intrinsic sensitivity to nuclease enzymes [15].

To overcome these limitations, numerous types of advanced drug delivery systems, including liquid nanocrystals, nanoemulsions, and liposomes, are currently being developed and are set to revolutionize the delivery of these novel therapeutic moieties [15, 16]. The main feature of most advanced drug delivery systems is the possibility of encapsulating difficult-to-deliver therapeutic moieties, such as plant metabolites or nucleic acids, within nanoparticles or other structures that allow enhanced and more specific delivery of the cargo to the target cell. A

striking example of the enormous relevance of advanced drug delivery systems is represented by the revolutionary mRNA-based COVID-19 vaccines that are currently available, in which the mRNA encoding for the SARS-CoV-2 spike protein is encapsulated within lipidic nanoparticles that allow the nucleic acid to penetrate the host cells [17].

The aim of this review is to provide an updated account of the most recent innovations in terms of advanced drug delivery systems that are being developed to improve the delivery of phytochemicals and nucleic acid-based therapy in the treatment of COPD and lung cancer.

2 - Impact of cigarette smoking on LC and COPD

Cigarette smoke causes COPD and lung cancer through multiple, simultaneous mechanisms. First of all, exposure of lung tissue to the toxic chemicals contained in cigarette smoke causes chronic inflammation, cellular senescence, and oxidative stress [18-21]. These two factors are known to interact, leading to tissue damage and remodelling that are at the root of COPD development [5]. Inflammation and oxidative stress further cause DNA damage [22] and microRNA (miRNA) dysregulation [23], which in turn promote a cancerous phenotype by impacting mechanisms such as apoptosis, cell proliferation, and angiogenesis [24]. Furthermore, the recruitment of inflammatory cells causes the release of many inflammatory mediators and growth factors, including Transforming Growth Factor-beta (TGF- β) [25, 26], which is considered as a master regulator of processes such as tissue remodelling and epithelial-to-mesenchymal transition (EMT), leading to cancer invasion and migration [27]. Another mechanism by which oxidative stress increases the likelihood of cancer development is through the stimulation of the epidermal growth factor receptor (EGFR) pathway [28]. Recently, scientific studies have also highlighted the role of autoimmunity mediated by regulatory T cells, B- cells and their autoantibodies in the pathogenesis of COPD [29]. The main mechanisms by which cigarette smoking causes COPD and lung cancer are summarized in Figure 1.

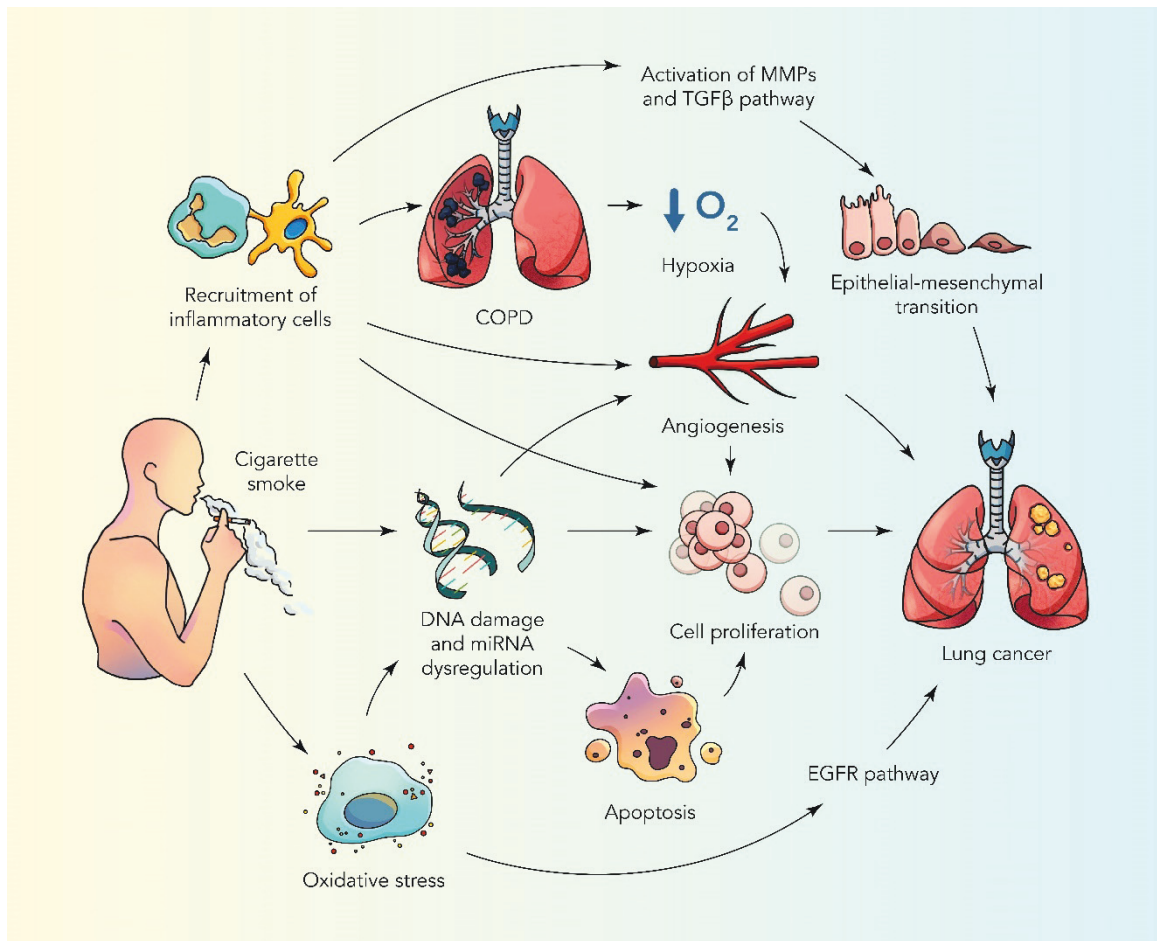


Figure 1 – The interplay of pathways through which cigarette smoking causes lung cancer and COPD

3 - Lung diseases: COPD and LC

This section provides a general introduction of the causes, pathogenesis, diagnosis, and main pathophysiological features of LC and COPD. It also discusses the relevance of airway remodelling as common pathophysiological features underlining both ailments.

3.1 - COPD

COPD is one of the most common respiratory diseases, affecting 251 million people worldwide [30, 31]. In Australia, about 1 in 20 people was affected by COPD in 2017-18 [32]. It is estimated that, by 2030, COPD will be the fourth leading cause of death worldwide unless a fundamental action to reduce underlying risk factors such as primarily tobacco smoking and passive exposure to environmental pollutants, is addressed and adopted [31]. COPD is a chronic inflammatory lung disease that is characterised by progressive airflow limitation and

inflammation leading to structural changes (remodelling) in the lungs [33]. Importantly, COPD symptoms are heterogeneous, ranging from minor or absence of symptoms to complete respiratory failure [34]. The main characteristic feature of COPD is represented by the occurrence of frequent exacerbations of the disease's symptoms, that worsen acutely and often result in the need for patient hospitalization [35]. The most important risk factors for COPD include tobacco use, exposure to indoor and outdoor pollutants, allergens, occupational exposure, unhealthy diet, and obesity [36]. The main pathological signs of COPD include remodelling of small airways, thickening of bronchial walls, destruction of lung parenchyma, and loss of alveolar space [37]. Consequently, diagnosis includes imaging procedures such as X-ray or high-resolution computer tomography. However, the principal diagnostic method remains the monitoring of persistent airflow limitation after administration of bronchodilators, with an FEV1/FVC <70% by pulmonary function test, also known as spirometry. The severity of COPD is classified into 4 groups, A-D, by the Global Initiative for Chronic Obstructive Lung Disease (GOLD) guidelines based on the percentage-predicted FEV1, exacerbation, and dyspnea [30, 38, 39].

3.2 - Lung Cancer

Lung cancer is one the leading causes of mortality worldwide, accounting for almost a fifth of all cancer-related deaths [40]. It is estimated that the number of deaths associated with lung cancer will rise to 10 million per year by 2030 [41, 42]. In Australia, lung cancer alone in 2015 has claimed about 8466 lives, accounting for almost 5.3% of the overall deaths [43]. Although lung cancer is diagnosed relatively less frequently, it leads to more deaths compared to other common cancers such as breast or prostate cancer. The major causes of lung cancer are cigarette smoking, passive exposure to cigarette smoke, and direct exposure to environmental pollutants or toxic substances such as asbestos [44, 45]. Importantly, the symptoms of lung cancer can be minimal, and patients often remain completely asymptomatic during early disease stages. This delayed emergence of symptoms, which results in late diagnosis, contributes to the extremely low 5-year survival rate of lung cancer (~17.8%) [46]. Lung cancer is defined as a heterogenous and genetically complex disease, caused by mutations in oncogenes that leads to the progressive transformation of normal cells to malignant derivatives due to subsequent alterations in the genetics and epigenetics of cancer cells [47]. Lung cancer is classified, based on its cellular origin and phenotype, into two subtypes: non-small cell lung cancer (NSCLC),

and small cell lung cancer (SCLC) [48]. NSCLC ascends from lung epithelial cells, it represents 85% of lung cancer cases, and it is further classified into squamous cell carcinoma, adenocarcinoma, and large cell carcinoma [49]. SCLC accounts for ~15% of lung cancer cases and has distinct histological features of neuroendocrine differentiation, characterised by small cells with limited cytoplasm [50].

3.3 - The role of tissue remodelling in COPD and lung cancer

COPD and lung cancer are both severe multifactorial lung diseases that share the fundamental feature of being characterized by structural changes in the lung tissue, that occurs in diverse morphological compartments including large or small airways and parenchyma. This process is also known as lung remodelling [51]. Tissue remodelling is a complex process that occurs due to an aberrant endogenous response to injury, with the aim of repairing the damaged tissue. This process is characterised by the replacement of lung tissue with abnormal deposition of extracellular matrix (ECM) proteins, and is the root cause of disease symptoms and impaired lung function [51]. One of the key molecular pathways driving the remodelling processes in COPD and lung cancer involves TGF- β [51, 52]. Several studies have reported impaired TGF- β signalling, leading to increased TGF- β levels in smokers and COPD patients [51, 53, 54]. Interestingly, a few studies have shown that this impaired TGF- β signaling can be considered a direct consequence of exposure to cigarette smoke [55, 56]. Besides COPD, higher TGF- β levels have also been reported in NSCLC [57], where they are associated with lymph node metastasis and tumour angiogenesis [58, 59]. TGF- β signalling has pleiotropic functions in lung cancer [57]. In the early stages of lung cancer tumorigenesis, TGF- β is known to suppress epithelial cell proliferation, and loss-of-function mutations in TGF- β signaling are known to increase cancer cell proliferation [60, 61]. In the later stages of cancer progression, TGF- β signalling has a tumor-promoting action [57, 59], and TGF- β is considered the most potent inducer of EMT in NSCLC as well as one of the main drivers of the development of a tumor-promoting microenvironment [57]. One of the mechanisms by which TGF- β induces EMT involves the inhibition of the endogenous nitric oxide (NO) synthase (eNOS). NO administration prevents TGF- β -induced EMT in alveolar epithelial cells [62]. This demonstrates that TGF- β has both deleterious and protective roles in both COPD and lung cancer. Similarly, a pleiotropic action of TGF- β during other inflammatory processes is acknowledged by various studies [57, 63]. In fact, TGF- β exerts a proinflammatory effect early

during inflammation, but functions as an anti-inflammatory cytokine after the establishment of the inflammatory response [57]. Due to its multifaceted role in inflammation, tissue remodelling, and cancer progression, the use of potential therapies targeting the TGF- β signalling should be considered carefully, as the clinical application of these therapies will benefit from further extensive study and validation.

4 - Treatment modalities in mitigating LC and COPD

Numerous treatment options are available for LC and COPD. These include both pharmacological and non-pharmacological approaches, and are summarized in Figure 2. Despite the availability of a wide range of choices in the management of these diseases, a completely effective treatment strategy does not exist for any of these diseases as of today. This section discusses the currently available treatment options for LC and COPD with the related limitations.

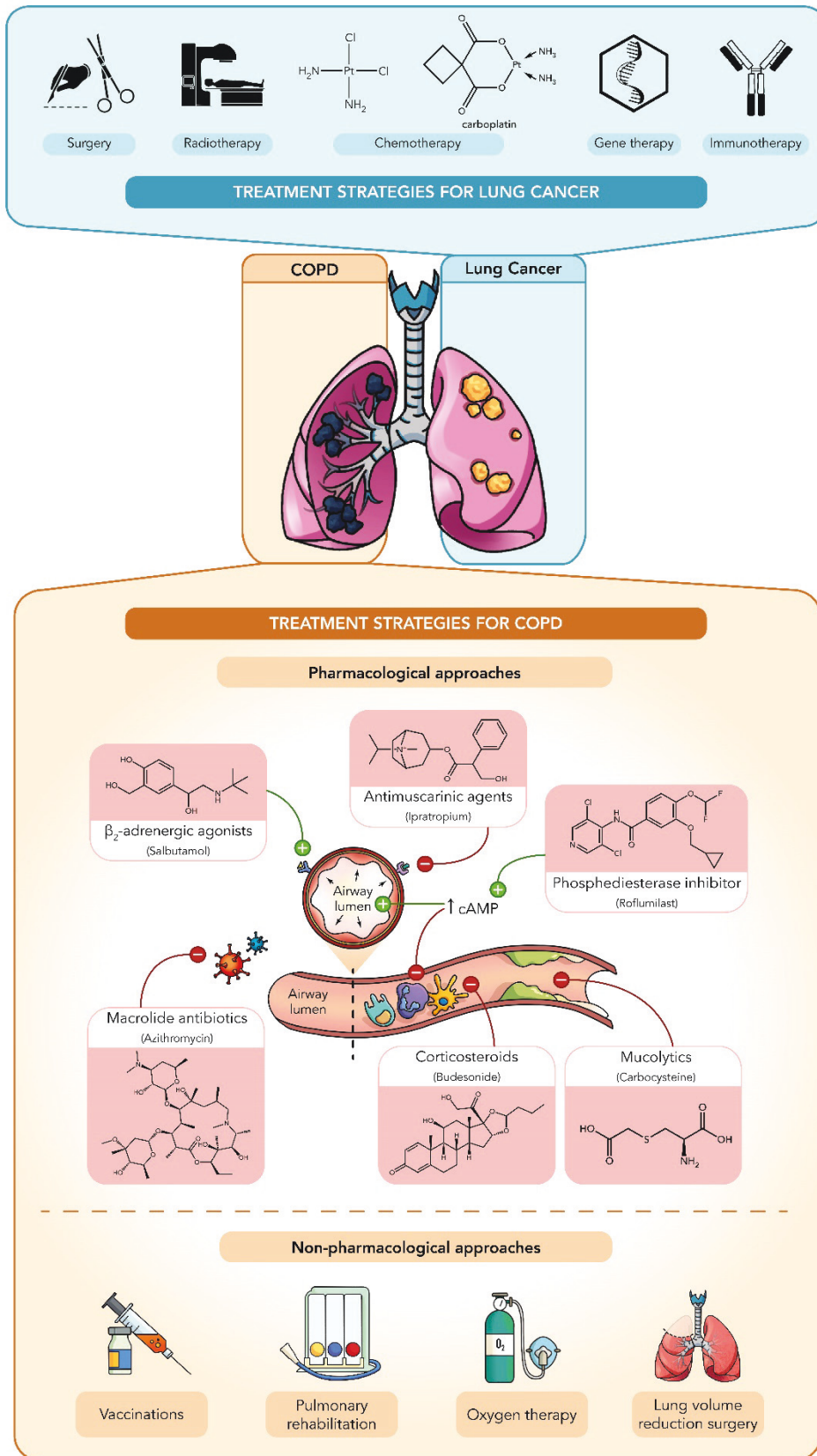


Figure 2 – Summary of the currently available treatment strategies for lung cancer and COPD

4.1 - Current therapies in lung cancer and related drawbacks

The different treatment strategies employed against lung cancer include surgery, radiotherapy, chemotherapy, gene therapy, and immunotherapy. These are summarized in Figure 2. Surgery is the cornerstone treatment preferred for NSCLC of different stages [64]. In stages I, II, and IIIA NSCLC, the tumor is removed *via* surgery if this practice is observed to be favourable [65]. Depending on the type of resection performed, the type of surgery employed in NSCLC are lobectomy (removal of the lung lobe having the tumor), segmentectomy (removal of part of lobes having the tumor), pneumonectomy (removal of a whole lung having the tumor), and sleeve resection (removal of lobe and part of bronchus) [65]. Presently, surgeons perform video-assisted thoracoscopic surgery, which involves making a small incision in the chest and inserting a thoracoscope. Through this tiny incision, a lobe can be removed using the scope, preventing the need for bigger incisions. However, the drawbacks associated with surgery include lack of patient tolerance, adverse reactions to anesthesia, wound infections, pneumonia, excessive bleeding, and blood clotting in the lungs or legs [66].

Radiotherapy is significantly used as a remedial or palliative strategy in the treatment of all-stage lung cancer. Stereotactic ablative body radiotherapy (SABR) is used in patients with peripherally located stage I-IIA NSCLC. Radiotherapy associated with chemotherapy is usually employed in the treatment of patients with stage III NSCLC [67, 68]. The main limitations of radiotherapy include damage to the normal tissues, fatigue, appetite and weight loss, and hair loss. Recently, various technological advancements have been reported in radiation therapy with the aim of avoiding the aforementioned drawbacks by delivering accurate radiation doses at the specific tumor site. Four-dimensional computed tomography is one of the techniques that allow to deliver accurate doses of radiation to the tumor [68]. Moreover, intensity-modulated radiotherapy is used to augment conformity and decrease healthy tissue toxicity *via* directing non-uniform intensity radiations toward the tumor [68].

Chemotherapy is a first-line therapy employed in the treatment of lung cancer based on the stage of cancer. Chemotherapeutic drugs such as docetaxel [69], paclitaxel [70], carboplatin, cisplatin, nitrocamptothecin [71], and doxorubicin [72] have been approved for the treatment of lung cancer. However, the applications of many of these chemotherapeutics have been limited by unfavourable physicochemical characteristics, pharmacokinetic performance, non-selectivity to the tumor, and poor stability [73]. Another important limitation of chemotherapy is the frequent occurrence of multi-drug resistance (MDR), consisting in the simultaneous resistance to different classes of chemotherapeutic drugs, which is among the main causes of treatment failure [74, 75]. Furthermore, another fundamental limitation of chemotherapy is the

toxicity to normal organs such as liver, kidney, and heart. Organ and tissue toxicity also leads to severe side effects such as cough, upper airway toxicity, fibrosis, weight loss, neurotoxicity, nausea, fatigue, dyspnea, bronchitis, bronchial wall thickening, pulmonary edema causing respiratory failure, acute lung injury, dyspnea, severe bronchospasm, wheezing, chest pain hypoxia, and alveolar hemorrhage [76, 77]. The high and often unaffordable cost of chemotherapeutics is a further factor limiting the use of these medicines low and middle-income countries, leading to increased mortality [64].

Immunotherapy assists a patient's immune system in the recognition and destruction of cancer cells, and has shown tremendous promise in the treatment of various types of lung cancer. Among different classes of immunotherapeutics, immune checkpoint inhibitors (pembrolizumab, durvalumab, atezolizumab, and nivolumab) are approved against lung cancer [78]. Nevertheless, key severe drawbacks associated with immunotherapeutics include infusion reactions, difficulty breathing, chills, fever, rash, and skin irritation. Autoimmune reactions, wherein the immune system attacks healthy organs such as liver, kidney, and lungs, are other significant life-threatening adverse effects associated with immunotherapy [79]. Another limitation of immunotherapeutics, which is shared with other classes of biologics, is the susceptibility to degradation with strong pH, organic solvents, elevated temperatures, and freezing stress [80]. To date, treatment strategies associating different classes of therapies such as neoadjuvant therapy (surgery associated with chemotherapy or radiation associated with chemotherapy or immunotherapy) are highly recommended to maximize the chances of success in lung cancer therapy [79, 80].

Although the use of gene therapy for the treatment of lung cancer has received significant attention recently, it is still largely ineffective, and this could be attributed to the lack of specificity, as well as to biosafety, ethical, and budgetary concerns [81]. Low cell permeability due to their large size and high electrical charge density and *in vivo* instability caused by sensitivity to nuclease enzymes are also factors that negatively contribute to the effectiveness of the gene therapy approach in lung cancer [82]. The most recent advances in gene therapy and nucleic acid-based therapy in lung cancer will be discussed in greater detail in the next sections.

4.2 - Current therapies in COPD and related drawbacks

The two main strategies employed in the management of COPD are non-pharmacological and pharmacological strategies. These are summarized in Figure 2. Non-pharmacological strategies include vaccinations, pulmonary rehabilitation, oxygen therapy, and lung volume reduction

surgery. In COPD, vaccination is crucial to prevent exacerbations and further respiratory complications. The influenza vaccine is reported to be effective in the prevention of exacerbations, mortality, and morbidity associated with COPD [83]. The reduced ability to perform exercise in COPD patients, caused by dyspnea (shortness of breath), can be improved with pulmonary rehabilitation. This strategy aims at enhancing ventilation through the application of correct breathing techniques. However, the positive impact of this approach on the COPD-related mortality is still disputable [84]. Oxygen supplementation therapy is another strategy employed as an attempt to reduce COPD-associated mortality, and it has a positive effect on the frequency of exacerbations or hospitalizations [85, 86]. In lung volume reduction surgery, hyperinflation is reduced in patients with severe emphysema through the resection of the apical parts of the lungs. However, patient intolerance and non-compliance is a fundamental drawback of this strategy. Similar to what was discussed about the surgical resection of lung cancer, the use of novel endoscopic procedures has the potential to reduce the invasiveness and adverse effects associated with lung reduction surgery, thereby increasing patient compliance [87].

The most commonly employed pharmacologic strategy in the treatment of COPD is bronchodilator therapy. Bronchodilators include muscarinic antagonists (MAs) such as ipratropium bromide (short-acting MAs-SAMAs) and tiotropium bromide (long-acting MAs-LAMAs), and β_2 -agonists (BAs) such as salbutamol (short-acting BAs- SABAs) and formoterol (long-acting BAs- LABAs) [88-91]. Bronchodilators reduce hyperinflation and airway resistance affecting the airway muscle tone. Both oral and inhalation (metered dose inhaler) formulations of these medications are available. The use of β_2 -adrenergic agonists is limited by serious side effects such as tachyarrhythmias, anxiety, tachycardia, insomnia, and tremor [92-94].

Anti-inflammatory agents (corticosteroids) like prednisone have also shown great promise in the management of COPD by reducing inflammation. These agents are available for both oral and intravenous use. The main drawback of corticosteroids is represented by side effects such as osteoporosis, neuropsychiatric symptoms, hypertension, and hyperglycemia [95]. Another factor seriously limiting the effectiveness of corticosteroids in the management of COPD is the development of steroid resistance, or steroid insensitivity, which usually occurs upon chronic exposure to corticosteroids [96].

Another class of therapeutics employed in the management of COPD is represented by phosphodiesterase inhibitors (PDI). Theophylline (non-selective PDI) and roflumilast (selective PDI) are approved for the treatment of COPD. However, seizures, anorexia,

arrhythmias, and gastrointestinal upset are the main limitations in the use of PDI [97-99]. Moreover, macrolide antibiotics like azithromycin are used in COPD treatment due to their anti-inflammatory and immunomodulatory activities, associated with the antimicrobial action. Although azithromycin significantly decreases COPD exacerbations, prolonged use may cause hearing loss [100].

Finally, to counteract and control mucus hypersecretion, mucolytic agents like N-acetylcysteine are often employed in the management of COPD. These agents are useful to decrease exacerbations to some extent, but present adverse effects such as respiratory discomfort, chest pain, elevated blood pressure, fever, rectal bleeding, skin irritation, headache, vomiting, and diarrhoea that severely restrict their use in COPD [101, 102]. Researchers are interested to investigate if controlling the time of drug administration (chronotherapy) maybe beneficial to treat COPD and lung cancer patients. Although this seems to be a promising approach, there are not enough high-quality clinical trials to support the claimed advantages of chronotherapy [103].

5 - Emerging pharmacological strategies in the management of LC and COPD

Considering the limitations of the current therapies for LC and COPD, there is an unmet need for novel treatment strategies allowing improved treatment outcomes with reduced adverse effects. Among the many novel potential strategies that are currently being investigated, two highly different, but equally promising, sources of active molecules with potential for application against LC and COPD include: plant-derived molecules and extracts, or phytoceuticals, and nucleic acid-based therapeutics. These are the focus of the present review and are discussed in these sections, in which the most recent studies highlighting the potential of these two treatment options against COPD and LC are showcased, together with the current issues that limit their clinical application.

5.1 - Phytoceuticals

Recent research has unravelled the potential benefits of phytoceuticals, or natural product-derived compounds, for the treatment of COPD and lung cancer. Various novel therapeutics have been investigated using *in vitro* experimental models to unravel the molecular mechanisms underlying chronic respiratory diseases [104, 105]. Examples of such phytoceuticals, which will be discussed as the main focus of this section, include berberine, agarwood oil and zerumbone, all of which possess multiple therapeutic benefits [106-112].

These compounds have the advantage of a greater safety profile and lower toxicity over conventional medicines.

5.1.1 - Berberine

Berberine, an isoquinoline alkaloid, is an active constituent that is abundantly found in the root, rhizome and bark of traditional medicinal plants including *Berberis spp.*, *Coptis chinensis*, *Rhizoma coptidi*, and *Hydrastis canadensis*. Studies have shown that berberine induces cytotoxicity in lung cancer cells and protects against the detrimental effects of COPD [110, 113, 114]. Berberine inhibits tumorigenesis by inhibiting proliferation, migration and invasion of lung cancer cells *via* multiple mechanisms [115]. Firstly, berberine induces apoptosis and inhibits the proliferation of on lung cancer cells by activating the tumor suppressors Forkhead box O3a (FOXO3a) and p53 [116, 117]. Secondly, berberine suppresses the protein expression of Nuclear Factor κ B (NF- κ B), c-Fos, and c-Jun thereby downregulating the NF- κ B and Activator Protein-1 (AP-1)-mediated transcription of matrix metalloproteinases (MMP) and urokinase, which are important regulators of lung tumor metastasis [118]. Furthermore, berberine also inhibits Hypoxia-Inducible Factor-1 α (HIF-1 α) and vascular endothelial growth factor (VEGF) expression in A549 lung cancer cells, thus suppressing tumor angiogenesis, growth and metastasis [119]. Besides its anticancer activity, berberine exhibits antioxidant and anti-inflammatory activities in different models of COPD and lung inflammation by inhibiting inducible nitric oxide synthase (iNOS) [120], NF κ B, and myeloperoxidase activity [121], reducing the levels and activity of transforming growth factor- β 1 (TGF- β 1) and Smads signalling [122], downregulating the expression of extracellular signal-regulated kinase (ERK) and p38 [123], and inhibiting I κ B degradation [124]. The inhibitory activity shown by berberine towards TGF- β 1 is particularly relevant in the treatment of both lung cancer and COPD, given the fundamental role played by the TGF- β 1 signalling pathway in driving the tissue remodelling process that occurs in both these diseases [51, 52].

5.1.2 - Agarwood oil

Agarwood oil is derived from the fragrant resinous wood of various species of *Aquilaria* trees and has been used for centuries as a remedy for several ailments under Ayurvedic and Chinese traditional medicine systems [125]. The main therapeutically active principles contained in Agarwood oil include monoterpenes and sesquiterpenes and their derivatives [126, 127]. Recent studies have showed that agarwood oil has antioxidant and anti-inflammatory properties that can be potentially used in COPD treatment [108], along with potent anticancer activity

[125]. Treatment with agarwood oil inhibits the cell growth, attachment, and viability of MCF-7 breast cancer cells with an IC₅₀ value of 44 µg/mL [128]. Similarly, agarwood oil exhibits pro-apoptotic and anti-metastatic activity in MIA PaCa-2 pancreatic cancer cells with an IC₅₀ value of 11 µg/mL [129]. With regards to the anti-inflammatory activity, β-caryophyllene, an active constituent of agarwood oil, was shown to reduce ~88% of the inflammation in a rat model of carrageenan-induced paw edema at a dose of a 200mg/kg [130]. Other active constituents have also shown antioxidant and anti-inflammatory activity by inhibiting nitric oxide (NO) production and NF-κB activation in lipopolysaccharide (LPS)-induced mouse RAW264.7 macrophages [131, 132]. These anti-cancer, anti-oxidative and anti-inflammatory effects of agarwood oil and its constituents make it a viable candidate for the treatment of chronic respiratory diseases such as COPD and lung cancer.

5.1.3 - Zerumbone

Zerumbone is a major bioactive compound found in the rhizome of *Zingiber zerumbet*, which has been traditionally used as a food flavoring agent and a traditional remedy for various ailments [133]. Studies have shown that zerumbone has potent anti-cancer activity and potential therapeutic benefits against lung cancer [111]. Targeting mitochondria-mediated pathogenesis represents a promising strategy to manage chronic respiratory diseases such as asthma, COPD and lung cancer [134-136]. Zerumbone exerts anticancer activity against A549 lung cancer cells through mitochondrial induction of apoptosis, caspase-9 and caspase-3 activation, and upregulation of the expression of p53 and Bax [137]. Zerumbone also shows a complementary effect with cisplatin, as the combination treatment of zerumbone and cisplatin exhibits increased apoptosis and sensitivity to cisplatin treatment in A549 cells [137]. Furthermore, zerumbone inhibits osteopontin-induced migration and invasion of A549 cells by altering the phosphorylation of focal adhesion kinase (FAK), AKT and LIM kinase 1 and 2 (LIMK1/2), decreasing the rho-associated, coiled-coil-containing protein kinase 1 (ROCK1) protein expression, and disrupting the FAK/AKT/ROCK pathway [138]. Together with its anticancer activity, zerumbone is also endowed with anti-inflammatory potential, as evidenced by reports showing that treatment with zerumbone decreased LPS-induced production of pro-inflammatory cytokines in THP-1 macrophages [139], suppressed lung edema in LPS-induced acute lung injury in mice [140], and inhibited innate and adaptive immune responses in mice [141]. Mechanistically, the anti-inflammatory activity of zerumbone is made possible by its ability to inhibit several pro-inflammatory signalling pathways, including Myeloid differentiation primary response 88 (MyD88)-dependent NF-κB/MAPK/PI3K-Akt pathway,

and pro-inflammatory mediators such as iNOS and cyclooxygenase-2 (COX-2) [140, 142]. These studies highlight the potential of zerumbone as a novel therapeutic treatment against COPD and lung cancer.

Besides the phytochemical products described in this section, several other natural products and extracts possess antioxidant, anti-inflammatory, and anticancer activity and therefore represent as potential candidates in the treatment of lung cancer and COPD. These include quercetin [143], curcumin [144, 145], luteolin [146], naringenin [147], piperine [148], boswellic acid [149, 150], and glycyrrhizin [151] to name a few.

5.1.4 - Clinical trials investigating the therapeutic efficacy of phytochemicals

Many clinical trials are currently being conducted to investigate the therapeutic efficacy of phytochemicals. These are summarized in Table 1. Sulforaphane, for example, is being tested in a phase II clinical trial (NCT03232138) to ascertain its activity in preventing the increased risk of lung cancer to which former smokers are subjected. Furthermore, the safety of oral quercetin supplementation was studied in a phase I clinical trial (NCT01708278), where quercetin was found to be safely tolerated at doses up to 2000 mg/day in COPD patients [152]. Furthermore, quercetin is currently being studied in two clinical trials: a phase I/II trial to determine whether a 2000 mg/day quercetin supplementation reduces markers of inflammation and oxidative stress in COPD patients (NCT03989271); and a phase 2/3 study to determine whether isoquercetin is effective in preventing venous thromboembolism in lung cancer, pancreatic cancer, and colorectal cancer (NCT02195232). Berberine is currently under investigation in a phase II clinical trial as a first line therapy for lung cancer in combination with gefitinib (NCT03486496). Similarly, curcumin in combination with tyrosine kinase inhibitors (TKIs) is being investigated as a potential treatment for EGFR-mutant advanced non-resectable adenocarcinoma in a phase 1 trial (NCT02321293). In another study (NCT03598309 – phase II), a preparation called Curcumin C3 complex, in association with fish oil extracts, is being investigated for its activity to reduce the size of smoke-induced lung nodules. A recently completed clinical study investigated the effects of dietary supplementation of curcumin and bioprin on the sputum cytology of COPD patients (NCT01514266) and, in another clinical trial, the effect of curcumin supplementation in addition to the standard of care on COPD is being investigated (NCT04687449).

Table 1 – Clinical trials investigating the therapeutic potential of phytochemicals against lung cancer and pulmonary inflammatory disorders

Study Phase	Clinical trial ID	Title	Aim	Phytochemical	Target disease	Status (as of 05/06/2023)
Phase II	NCT03232138	Clinical Trial of Lung Cancer Chemoprevention With Sulforaphane in Former Smokers	To assess whether sulforaphane supplementation to former smokers reduces the risk of developing lung cancer	Sulforaphane	Lung cancer	Active, not recruiting
Phase I	NCT01708278	Beneficial Effects of Quercetin in Chronic Obstructive Pulmonary Disease (COPD) (Quercetin)	To determine safe quercetin dosage, bioavailability, dose-response relationship, and suitable biomarkers for application of quercetin in large-scale clinical trials	Quercetin	COPD	Completed, has results [152]
Phase I/II	NCT03989271	Biological Effects of Quercetin in COPD	To determine whether quercetin supplementation reduces inflammation and oxidative stress markers in COPD patients	Quercetin	COPD	Recruiting
Phase II/III	NCT02195232	Cancer Associated Thrombosis and Isoquercetin (CATIQ) (CATIQ)	To evaluate whether isoquercetin prevents venous thrombosis in patients with NSCLC, colorectal cancer, and pancreatic cancer	Isoquercetin	NSCLC	Completed
Phase II	NCT03486496	Gefitinib and Berberine in the First-line Treatment of Lung Adenocarcinoma With EGFR Mutation (Geber)	To assess whether administration of berberine associated to gefitinib treatment as first-line strategy for advanced, EGFR-mutated NSCLC increases patients' progression-free survival	Berberine	NSCLC	Not yet recruiting / Unknown
Phase I	NCT02321293	A Open-label Prospective Cohort Trial of Curcumin Plus Tyrosine Kinase Inhibitors (TKI) for EGFR - Mutant Advanced NSCLC (CURCUMIN)	To assess safety and feasibility of administering curcumin associated to EGFR-TKI for the treatment of advanced NSCLC	Curcumin	NSCLC	Recruiting / Unknown

Phase II	NCT03598309	Phase II Trial to Modulate Intermediate Endpoint Biomarkers in Former and Current Smokers	To evaluate the activity of curcumin and fish oil supplementation in reducing the size and number of lung nodules in former heavy smokers	Curcumin	Smoke-associated lung nodules	Recruiting
N/A	NCT01514266	Effect of Curcumin on Lung Inflammation	To evaluate the effect of curcumin and bioprine association on the sputum cytology of COPD patients	Curcumin	COPD	Completed
N/A	NCT04687449	Curcumin in Management of Chronic Obstructive Pulmonary Disease	To evaluate the effect of curcumin supplementation on COPD symptoms, exercise capacity, and decrease risk of acute exacerbations	Curcumin	COPD	Not yet recruiting

COPD: chronic obstructive pulmonary disease; EGFR: epidermal growth factor receptor; NSCLC: non-small cell lung cancer; TKI: tyrosine kinase inhibitor

5.1.5 - Limitations to the clinical application of phytochemicals

Despite the vast array of potential therapeutic benefits of berberine, agarwood oil, zerumbone and other phytochemicals, shortcomings severely limiting their clinical application include their low bioavailability and poor pharmacokinetics. The gastrointestinal (GI) absorption of berberine is poor (less than 5%), and is further reduced by the activity of the multidrug transporter P-glycoprotein [153]. Berberine is also actively metabolized by liver enzymes, resulting in rapid hepatobiliary excretion [154]. As such, high berberine doses are required to achieve therapeutic efficacy, and this can lead to complications in the GI tract [155]. Low water solubility and poor bioavailability are also factors limiting the therapeutic usage of zerumbone in clinical settings. Zerumbone is highly lipophilic and has poor water solubility, which contributes to poor GI absorption and limited bioavailability [156]. Intraperitoneal administration of high doses of zerumbone (2.5–3 g/kg) has been reported to be fatal, with a 0.5 g/kg dose found to be nephrotoxic and hepatotoxic in experimental rats [157]. With regards to agarwood oil, the pharmacological, pharmacokinetics and safety profiles of this extract have been poorly described in literature. Essential oils that contain aromatic terpenes are generally lipophilic and therefore are potentially capable of being readily absorbed in the GI tract and become bioavailable systemically [158]. However, their therapeutic benefits are also accompanied by toxic effects [158]. Furthermore, if essential oils are not stored properly, they can degrade over time resulting in the production of toxic oxidation products. For this reason, improper use of essential oils including agarwood oil may increase the risk of adverse effects such as nephrotoxicity, necrosis, hepatotoxicity, carcinogenicity, phototoxicity and allergic reactions [159]. Besides compounds with therapeutic efficacy, agarwood oil also comprises a range of poorly documented active compounds that may contribute to diverse bioactivity and may even hinder the desired pharmacological effects [107]. Due to the limitations of phytochemicals such as berberine, zerumbone, and agarwood oil discussed in this section, there is an urgent need for the development of novel drug delivery approaches to obtain optimum therapeutic benefits from phytochemicals, optimizing their solubility and pharmacokinetic properties while minimizing toxicity and adverse effects.

5.2 - Nucleic acid-based therapy

Both COPD and lung cancer are linked to the dysregulated expression of many coding and non-coding RNAs, including mRNAs, miRNAs, lncRNAs, and others [89, 160]. For this reason, targeting these nucleic acids and their related molecular pathways represents a suitable potential pharmacological strategy against such diseases. Numerous studies are currently being

performed to investigate the effectiveness of nucleic acid-based therapeutics, including miRNA mimics or inhibitors, short interfering RNAs (siRNA), decoy oligodeoxynucleotides (ODNs), and other classes of therapeutics, in modulating the dysregulated signalling pathways in COPD and lung cancer [161, 162]. These studies are discussed in the present section.

5.2.1 - Nucleic acid-based therapeutics targeting miRNA in COPD

Nucleic acid-based therapeutics are being widely studied to counteract many of the pathological factors typical of COPD, including inflammation, vascular and pulmonary alteration and remodelling, mucus hypersecretion, and exacerbation of disease [89]. With regards to the inflammatory response underlying the development of COPD upon cigarette smoke exposure, a recent study found that the miRNA miR-195 was upregulated in COPD patients, and its expression was induced in mice following exposure to cigarette smoke [163]. Considering the pathogenetic role of miR-195 in COPD, the authors proposed it as a potential therapeutic target [163]. Another miRNA, miR-145-5p, was found to be down-regulated in lung tissues from smokers compared to non-smokers, and overexpression of this miRNA in Human Bronchial Epithelial Cells (HBECs) exposed to cigarette smoke extract counteracted cigarette smoke-induced apoptosis and inflammation [164]. The expression of miR-181c was found to be downregulated in the lung tissue of COPD patients compared to never-smokers, as well as in both HBECs and mice exposed to cigarette smoke [165]. The overexpression of miR-181c reduced the inflammatory response, neutrophil infiltration, and ROS and inflammatory cytokines production caused by cigarette smoke exposure, highlighting the potential of miR-181c as a therapeutic target for COPD [165].

5.2.2 - siRNA-based gene knockdown and gene silencing of inflammatory mediators in COPD and inflammatory diseases

Numerous studies have also highlighted the potential of gene silencing and RNA interference-based approaches in modulating signalling pathways and transcription factors whose activity is dysregulated in the inflammatory processes driving COPD. For example, the siRNA-mediated silencing of the protein Receptor-interacting protein 2 (Rip2), which positively regulates NF- κ B, was shown to improve cigarette smoke extract-induced inflammatory and oxidative markers *in vitro* in mouse macrophages and *in vivo* in a mouse model of cigarette smoke-induced acute lung injury [166]. Similar results were obtained by silencing the Ribosomal Protein S3 (RPS3) protein [167] on both chronic cigarette smoke exposure mouse model and viral exacerbation mouse model, by silencing the mitogen-activated protein kinase

MAP3K19 [168]. The siRNA-mediated knockdown of genes encoding for proinflammatory cytokines such as Tumor Necrosis Factor α (TNF- α) is another viable strategy that is currently being explored for its potential in the treatment of inflammatory lung diseases such as COPD and acute lung injury. Kelly and colleagues, for example, developed poly (lactic-co-glycolic) acid (PLGA) microparticles suitable for inhalation for the delivery of anti-TNF- α siRNA to alveolar macrophages. The microparticles were able to decrease LPS-induced TNF- α expression for up to 72 hours in human THP-1 monocytes [169]. In another study, Ge et al. developed a fluorinated α -helical polypeptide to enhance the delivery of anti-TNF- α siRNA to alveolar macrophages, obtaining significant siRNA uptake, TNF- α gene knockdown, and anti-inflammatory effect against LPS-induced acute lung injury *in vivo* upon intratracheal administration in mice [170]. Similarly, in a more recent study, Jeon and coworkers obtained significant TNF- α silencing in the lung of LPS-challenged mice by intravenously administering cationic polymer/siRNA polyplexes [171].

5.2.3 - Nucleic acid-based therapy to counteract airway remodelling in COPD

Numerous emerging molecular and signalling pathways involved in vascular alteration and airway remodelling are upregulated upon cigarette smoke exposure, and thus their silencing represents a promising strategy to improve these features that contribute to COPD morbidity. Targeting hypoxia-responsive elements such as the calcium binding protein S100A4, for example, has recently been proposed as potential option to prevent vascular remodelling in COPD [172]. Similarly, another hypoxia-responsive factor promoting vascular remodelling with potential as therapeutic target is neuron-derived orphan receptor 1 (NOR1) [173]. With regards to airway tissue repair and remodelling, the siRNA-mediated knockdown of the chondroitin sulfate proteoglycan versican resulted in an increased deposition of insoluble elastin in primary pulmonary fibroblast cells from COPD patients, highlighting the potential of this approach in improving the repair of alveolar elastic fibers [174]. Another potential therapeutic target that is upregulated in both COPD patients' sputum cells and the airways of cigarette smoke-exposed mice is the long non-coding RNA (lncRNA) taurine-up-regulated gene 1 (TUG1) [175]. This lncRNA promotes the pathological alterations associated with cigarette smoke-induced airway remodelling in COPD [175]. Finally, other potentially promising pharmacological targets for COPD are represented by signalling molecules promoting mucus hypersecretion, such as CD147 [176] and the receptor patched homolog 1 (PTCH1) [177], as well as cytokines mediating COPD exacerbations in response to microbes, such as the interleukin IL-17C [178].

5.2.4 - Nucleic acid-based therapy in lung cancer

With regards to lung cancer, a vast number of nucleic acid-based therapies, are currently being investigated in preclinical and early clinical studies. The most prolific class of nucleic acid-based therapies is represented by RNA-based therapies, including antisense RNAs, siRNA, miRNAs, anti-miRNAs, and therapeutic mRNAs [179]. Similar to what was discussed with regards to COPD, the underlying strategy behind RNA-based therapeutics consists of either inhibiting the expression of RNA that is overexpressed or increasing the expression of RNA that is downregulated in lung cancer [179]. In this context, the discovery of RNA-based cancer biomarkers provides an untapped source of novel potential pharmacological targets [180]. Examples of genes with potential as a target for nucleic acid-based therapy that are overexpressed in lung cancer include the X-linked Inhibitor of Apoptosis Protein (XIAP) [181], the miRNA-195 [182], and the lncRNAs lung cancer associated transcript 1 (LUCAT 1) [183] and placenta-specific 2 (PLAC2) [184]. In a recent study, Liu *et al.* showed that the shRNA-mediated inhibition of the Kinetochore-associated 1 (KNTC1) protein inhibits NSCLC tumorigenesis both *in vitro* and *in vivo* [185]. Similarly, targeting the Sterol regulatory element-binding proteins (SREBPs) / miRNA-497-mediated oncometabolite axis *via* shRNA knockdown was shown to reduce cancer stemness and chemoresistance in the lung cancer cell lines A549 and H441 [186]. Finally, many RNA species found in lung cancer patients' circulating extracellular vesicles play oncosuppressor roles, inhibiting cancer hallmarks such as cell proliferation, migration, invasion, metastasis, and chemoresistance, and therefore have potential as therapeutic RNAs. These include: the miRNAs let-7e [187], miR-204 [188], miR-338-3p [189], and the circular RNA circ_PIP5K1A [190].

Another approach for the nucleic acid-based therapy of lung cancer that is gaining particular recognition in recent years is represented by the use of decoy oligodeoxynucleotides (ODNs). These are synthetic double-stranded ODNs that mimic the DNA binding sequence of specific transcription factors, thus binding the active transcription factors and removing them from the pool of molecules available to bring their original target sequence on the genomic DNA. This results in the selective functional inactivation of the intended transcription factors [191]. The rationale of using decoy ODNs as a therapeutic strategy for lung cancer lies in the fact that it would be advantageous to inhibit transcription factors acting as master regulators of cancer progression [15]. Two of such transcription factors for which decoy ODN-based approaches are under investigation are NF- κ B [192] and signal transducer and activator of transcription 3 (STAT3) [193]. Transfection of A549 lung cancer cells with an NF- κ B decoy ODN resulted in a marked reduction of cell proliferation and increased cell cycle arrest in G0/G1 phase [194]

and, in an *in vivo* study, NF- κ B decoy ODNs showed promising activity in inhibiting osteosarcoma lung metastasis [195]. Furthermore, transfection with a STAT3 decoy ODN was shown to inhibit the growth of PG (pulmonary giant) human lung cancer cells *in vitro* [196], and similar results were also obtained *in vitro* on A549 lung cancer cells and *in vivo* in a mouse xenograft model of lung cancer [197]. More recently, a similar degree of anticancer activity was seen on both lung cancer cells and mouse xenografts lung cancer models, by administering a circular STAT3 decoy ODN [198].

5.2.5 - Limitations to the clinical translation of nucleic acid-based therapy

Despite the many pre-clinical studies available or in progress investigating the potential of nucleic acid-based therapy against COPD and lung cancer, very few studies have transitioned to the clinical trial stage, and the clinical application of such innovative treatment strategies is still severely limited. The main factor preventing the widespread clinical application of gene therapy and nucleic acid-based therapeutics is represented by the poor pharmacokinetic behaviour of nucleic acids, which is caused by their large size and charge density and their extreme sensitivity to degradation from nucleases [15, 82]. A poor pharmacokinetic profile represents a fundamental feature that is shared between phytoceuticals and therapeutic nucleic acids. In the next section, the most recent advances in the development of nano-drug delivery systems to overcome these limitations, with the potential of improving the clinical translation of these two classes of therapeutics, are discussed.

6 - Nanoparticle-based drug delivery approaches to overcome the limitations hampering the use of phytoceuticals and nucleic acid-based therapy in lung diseases

An opportunity to overcome the complexities related to the delivery of phytoceuticals and nucleic acid-based therapeutics to the lungs includes the use of advanced drug delivery systems such as vesicular systems, liquid crystals, micelles, and others [199]. Factors such as penetration into the mucus membrane, preferential targeting, and homogeneity of the developed systems account towards the important reasons contributing to the development of pulmonary-based drug delivery systems [200, 201]. Other preferential factors that govern the use of nanosystems targeting phytoceuticals or biologicals to the lungs include: longer residential time in the systemic circulation, extrinsic activation, low immunogenicity, and low toxicity [202]. Typically, the nano-drug delivery systems used to encapsulate phytoceuticals range in the size of 1 to 1000 nm and confer better solubility to poorly soluble moieties by

virtue of their high loading capacity. The loading of the phytoceutical moiety to the nano-drug delivery system is mediated by intermolecular interactions such as ionic forces and dispersion forces [203]. An important advantage of using nanocarriers is that these increase the bioavailability and enhance the stability of phytoceutical/biological therapeutics by shielding them from the physiological processes that can lead to their elimination and deactivation. Furthermore, by virtue of preferential accumulation at the pulmonary site due to hydrostatic pressure, encapsulating these therapeutic moieties might also result in improved therapeutic activity and selectivity [204].

The shape and size of nano-drug delivery systems are two factors that significantly impact the extent of local pulmonary delivery, as the pulmonary deposition of particulates is increased with decreasing particle size range [205]. This suggests that the deposition of nanoparticles in the lungs is based on the mechanism of diffusional deposition [205]. The shape of nano-drug delivery systems for pulmonary delivery also plays a key role in affecting the overall therapeutic activity, especially in cancer. In one study which was carried out to understand the effect of shape of nano-drug delivery carrier on lung cancer, it was found out that, in contrast to identical spheres, needle- and plate-shaped hydroxyapatite structures caused the greatest amount of cell death in human bronchial epithelial cell cultures (BEAS-2B cells) [206]. No clear data is available in literature about any impact of the shape of nano-drug delivery systems on the product's toxicity.

Nano-drug delivery systems possess a multifaceted potential as heterogenous drug delivery systems for the specific targeting of pulmonary cells and their components [207] [208] [209]. The exact mechanism through which the nano-drug delivery systems permeate the lungs is governed by their surface chemistry [210], diversified architecture [211], and intrinsic properties of the nano-drug delivery agents used in the formulation. The chemical properties of the external surface (corona) of nanoparticles can be modified through functionalization with different types of molecules such as membrane fluidization enhancers, tight junction openers, receptor ligands, transcytosis enhancers, protective moieties such as PEG, as well as efflux system inhibitors [212]. These possible modifications are summarized in Figure 3, and they allow increased nanoparticle uptake, protection of the nanoparticle from degradation, and tissue-specific targeting of the nanoparticle.

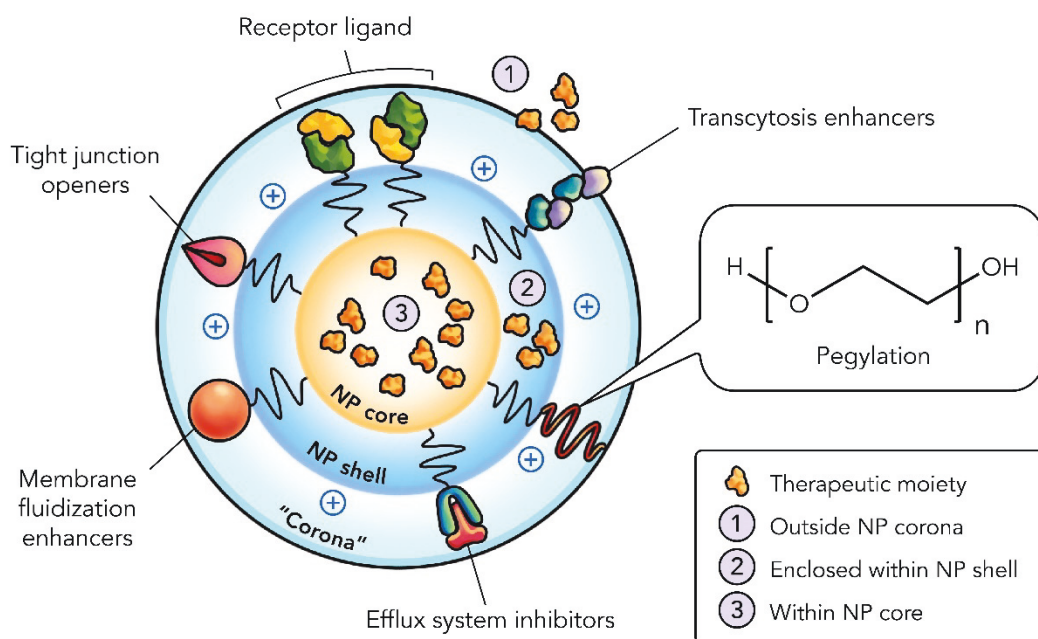


Figure 3 – General structure of a nanoparticle for advanced drug delivery, indicating the possible localizations of the therapeutic moieties and the modifications that can be performed to enhance internalization and penetration of the target cell

There are several pathways through which nanoparticle-based delivery systems allow the delivery of the cargo. First of all, it is well known that nanoparticles widen the tight junctions of epithelial cells, and this allows the cargo embedded in the nanoparticles, along with the carrier, to cross lung epithelial barriers efficiently [213]. Some other studies have reported that the transport of nanoparticles through the epithelial cells of the lung also occurs through transcytosis [214], and other studies also highlight a role for endocytosis [215]. Another factor favouring the accumulation of nanoparticles encapsulating therapeutic moieties at the targeted bronchiolar site is represented by the nanoparticle concentration gradient that is created upon pulmonary administration [216].

To improve the solubility and the physicochemical and pharmacokinetic characteristics of pharmacologically active phytochemicals or biologicals, these two classes of molecules can be efficiently entrapped in nanoparticles. This can be performed either during the nanoparticle synthesis stage or, alternatively, the active principles can be surface-coated on already synthesized nanoparticles [217]. Furthermore, surface modification of nanoparticles can be performed to increase their residence time in the blood by hindering their identification by

phagocytes [218]. Finally, successful active transport of drug-loaded nanocarriers can be achieved, in the treatment of lung cancer and COPD, by functionalizing the nano-drug delivery systems with ligands that bind specifically to receptors present on the intended pulmonary target site. Important receptors in lung cells that have been actively targeted in an attempt to treat lung cancer include: Vascular Endothelial Growth Factor Receptor (VEGFR), $\alpha\beta3$ Integrin, σ Receptor, Transferrin receptor, and CD44 [219]. The ligands that have been used successfully in active targeting include folate, transferrin, antibodies, and peptides [220]. Another way by which selectivity can be conferred to delivery systems targeting cancer cells is through the use of pH-sensitive materials for the encapsulation of the cargo. These materials exploit the fact that the tumor microenvironment and the lysosomes tend to have an acidic pH (4.5-6.8), at which functional groups such as acetals spontaneously hydrolyse, allowing selective cargo release [221, 222].

Various nano-drug delivery systems encapsulating phytochemicals and biologicals have been researched upon in the last few decades for their potential as treatments for pulmonary diseases, with particular focus on the treatment of lung cancer and COPD. Some of these include liposomes, polymeric nanoparticles, dendrimers, and others. Each nanocarriers system has its own strengths and weaknesses. Several types of nanocarriers have been developed for targeted drug delivery in COPD and lung cancer. Some of these include liposomes, polymeric nanoparticles, dendrimers, and others. Liposomes are spherical vesicles composed of phospholipid bilayers and can be modified to carry drugs and target specific cells. While liposomes have good biocompatibility, they are unstable and have low drug loading capacity. Polymeric nanoparticles are made up from biodegradable polymers and can be modified to improve drug stability and targeted delivery. However, they can cause toxicity and an immune response. On the other hand, dendrimers are highly branched, synthetic polymers that can carry large amounts of drug, however they can also cause toxicity and immune responses similarly to polymeric nanoparticles. Therefore, despite their potential advantages, clinical transformation of nanocarriers for COPD and lung cancer is still challenging. The complex nature of these diseases and the lack of efficient drug delivery to the target cells are major obstacles. Additionally, safety concerns related to toxicity and immune responses must be thoroughly evaluated before clinical translation. Overall, more research is needed to address these challenges and improve the clinical outcome [223-227]. These classes of nano-drug delivery systems and the main recent studies showcasing the advantages in using these systems are discussed in detail in the subsequent sections. Table 2 summarizes, in chronological order,

other important studies where these novel drug delivery systems were used to encapsulate phytochemicals or biologicals for use against lung cancer.

6.1 - Polymeric nanoparticles

In the last few decades, extensive studies using biocompatible polymer-based nanosystems for the deposition of therapeutic moieties in the lungs have been performed. Fundamental characteristics of these polymeric nanoparticles that allow effective lung delivery of drugs include surface adaptability and surface charge [228]. The biodegradability and biodistribution of the polymers employed in the synthesis of polymeric nanoparticles also represent an important feature. The polymers that have been extensively studied for pulmonary disposition include both synthetic and natural moieties. Synthetic polymers usually display improved properties such as prolonged half-life compared to polymers of natural origin [229]. Synthetic polymers such as poly(alkylcyanoacrylates), PLGA, poly(methylidene malonate), poly(lactic acid) (PLA), and amino acids (poly(aspartic acid), poly(lysine)) have been extensively utilized to prepare nanoformulations for pulmonary delivery. On the other hand, natural polymers such as polysaccharides (chitosan, alginate, dextran), or proteins (gelatin, albumin) have also been extensively characterized for effective pulmonary delivery [230, 231]. Across the different classes of polymers, PLA has been particularly extensively studied. This is attributed to the fact that it is biocompatible and it undergoes hydrolysis to give lactic and glycolic acids, which get easily cleared through the citric acid cycle [232]. Surface modification with mucoadhesive polymers such as chitosan has also been reported. In a study by Dhanapal *et al.*, surface-modified PLA and chitosan nanoparticles loaded with piceatannol (CS/PLA-PIC) were developed and tested *in vitro* for the treatment of lung cancer. These nanoparticles, synthesized by dropping method, were evaluated for drug loading and for their cytotoxic potential against A549 lung cancer cells [232]. In this study, the cytotoxic potential of CS/PLA-PIC nanoparticles was greater than either CS-PIC nanoparticles or PIC alone [232].

PLGA represents another suitable polymer for use in nanoparticle drug delivery systems. This polymer has been used by Oh *et al.* to develop sustained release nanoparticles for the delivery of budesonide to asthmatic mice, obtaining reduced numbers of inflammatory cells in bronchoalveolar lavage (BAL) fluid and in lung tissue sections. A substantial decrease in bronchial hyperresponsiveness in mice was also obtained upon treatment with budesonide-loaded porous PLGA microparticles [233]. In this context, the major limitation of PLGA is its

hydrophobicity. To overcome this challenge, chemical modifications such as conjugation with poly(ethylene glycol) (PEG) can be performed. In a recent study by Updhyay *et al.* [234], thymoquinone-loaded PEG-PLGA nanoparticles were prepared by modified nanoprecipitation method and decorated with transferrin (TF-TQ-NPs) to selectively target lung cancer cells *in vitro*. The nanoparticle size was of about 25 nm. These TF-TQ-NPs were tested on the A549 lung adenocarcinoma cell line, where they showed potent anticancer activity through several mechanisms, including increased reactive oxygen species (ROS) generation, upregulation of Bax, and downregulation of bcl2 expression. Furthermore, the TF-TQ-NPs induced p53-mediated cell death by modulating the activity of the microRNAs miR-34a and miR-16 [234]. In another study, PEGylated PLGA nanoparticles were used to encapsulate *Nasturtium officinale* extract, and the anticancer activity of these nanoparticles (NOE-PLGA/PEG) was tested on A549 cells. The size of these nanoparticles was in the range of 110-140 nm. Real time PCR revealed that the NOE-PLGA/PEG nanoparticles exerted dose-dependent anticancer activity by upregulating *p53*, *Bax*, and *Caspase 3* transcript expression as well as downregulating *bcl2* and *cyclinD1* expression. The IC₅₀ value of NOE-PLGA/PEG was 40 µg/mL, which was lower as compared to the crude *Nasturtium officinale* extract [235].

With regards to the treatment of COPD, PEGylated immuno-conjugated PLGA-nanoparticles were also employed to deliver ibuprofen to target neutrophil-mediated inflammatory responses in murine models of the disease [236].

In the case of nucleic acid delivery for respiratory diseases, the carrier used to encapsulate the therapeutic nucleic acid should demonstrate a high level of transfection, have a good safety profile, and be biocompatible. PLGA is also a promising carrier for the delivery of therapeutic nucleic acids, and it has been shown to facilitate siRNA delivery to the lungs through the process of pinocytosis and clathrin-dependent endocytosis. However, since PLGA is negatively charged, modification with a cationic ligand is required to allow high affinity binding between the carrier and the polyanionic nucleic acid moieties [229].

Another particularly promising polymer for nucleic acid delivery is polyethyleneimine (PEI). PEI is a cationic polymer which is particularly suitable for delivery of gene/nucleic acid-based therapeutics to mammalian cells due to the presence of positive charges on the amine groups. PEIs are particularly advantageous for lung delivery because they bind to the negatively charged mucin, stimulating the process of endocytosis. Recently, the role of PEIs in the transport of siRNA has also been elucidated [237]. A disadvantage of PEI, which is shared with

many common non-viral gene delivery vectors, is toxicity and low transduction efficiency. To overcome these limitations, Thomas *et al.* [238] screened a combinatorial library of nanoparticles prepared by emulsion/solvent diffusion technique, with the aim of identifying the optimal PEI configuration and branching to maximize the *in vitro* delivery of nucleic acid cargo in the absence of toxicity. The developed nanoparticles, of size of about 150 nm, were capable of releasing the cargo for up to 6 h, and showed high stability in artificial mucus [238]. Branched PEIs tend to interact more strongly with nucleic acids compared to linear polymers, and generally particles containing branched PEIs tend to have better zeta potential, smaller size, and improved compactibility [229].

Another polymer that has gained considerable interest is chitosan [239]. Despite having comparatively lower transfection rates, a dry powder composed of chitosan and siRNA was tested *in vivo* on transgenic mice with metastatic lung cancer, where it showed successful gene silencing with great penetration into the deeper tissues of the lung upon intratracheal administration [240].

Lately, dextran-based nanoparticles are receiving significant interest as delivery systems for lung diseases. Dextran is an FDA-approved polysaccharide with high encapsulation efficiency and good bio-compatibility and biodegradability, that allows many types of chemical modifications to finely tune the drug release behaviour of the formulation [241]. In the context of lung delivery, acetalated dextran (AcDex) represents a highly versatile material for the synthesis of nanocarriers. AcDex nanoparticles are particularly suitable for pulmonary delivery due to their compatibility with aerosolized dry powder inhalation, as well as due to the presence of acetal functional groups, which allow pH-dependent particle degradation and selective therapeutic cargo release in acidic microenvironments [242, 243]. This makes AcDex nanoparticles frontrunner candidates for the treatment of many chronic respiratory diseases, as well as lung cancer [242]. The further functionalization of AcDex with cationic moieties such as polyamines represents a suitable strategy for the high-efficiency encapsulation and delivery of nucleic acid-based therapeutics. For example, AcDex nanoparticles were functionalized with spermine (Spermine-AcDex, or SpAcDex, nanoparticles) and were successfully used to deliver siRNA at high efficiency to HeLa cancer cells [244]. SpAcDex nanoparticles were used, more recently, to deliver a decoy oligodeoxynucleotide inhibiting NF- κ B to A549 lung cancer cells, obtaining potent *in vitro* anti-proliferative, anti-migratory, and anti-colony formation activity [245].

6.2 - Liquid Nanocrystals

Another suitable class of nano-drug delivery system that is gaining particular momentum is represented by liquid nanocrystals (LNCs), also called liquid crystalline nanoparticles (LCNs). These have been extensively studied as versatile drug delivery systems for pulmonary release in inflammatory lung diseases and lung cancer [246]. Thanks to their intrinsic properties, liquid nanocrystals are advantageous as they allow efficient, controlled, homogeneous and target-selective drug delivery [247], with reduced mucociliary degradation and lower macrophage uptake [248]. Furthermore, due to stable phase transition, LCNs have improved bioavailability due to better dissolution, higher diffusion, and improved cargo deposition. Nanocrystals are also known to accumulate passively within solid tumor sites and enter inside the tumor through the enhanced permeability and retention (EPR) effect [249]. The EPR effect consists in the counter-intuitive concept that particles such as liposomes, nanoparticles, and large macromolecular drugs tend to accumulate in solid tumors to a greater extent compared to normal tissues. This is caused by the fact that tumor neovasculature has abnormal architecture, with wide fenestrations that, together with the usually ineffective lymphatic system surrounding solid tumors, allow a superior permeability and accumulation of large macromolecular structures within tumor cells [250]. In addition to their advantage over conventional drug delivery methods due to their large drug loading capacity and their significant role in improving the solubility of poorly soluble drug moieties, nanocrystals also overcome a considerable barrier to drug administration and bioavailability [251]. As a result, poorly water-soluble anticancer drugs that are susceptible to clearance and non-targeted distribution upon systemic administration, ultimately leading to toxicity and frequently therapeutic failure, can be successfully administered *via* the pulmonary route as nanocrystals [249].

Despite these advantages, the identification and degradation of LCNs by the mononuclear phagocytic system severely limits their applicability for pulmonary diseases. To overcome this, surface-modification strategies have been developed, allowing receptor-based targeting of nanocrystals *via* surface functionalization with molecules such as transferrin, folic acid, hereceptin, hyaluronic acid, luciferin, and albumin [252]. In this regard, luciferin-targeted nanocrystals containing camptothecin were prepared using the antisolvent precipitation method. Encapsulation of camptothecin in these nanoparticles resulted in longer half-life and

greater therapeutic efficacy against lung metastasis compared to treatment with camptothecin salt solution upon intravenous administration in mice [253]. In another study, lactoferrin was used as a receptor-based targeting moiety for lung cancer [248]. Here, nanocrystals containing ellagic acid and doxorubicin (DOX) were prepared by antisolvent precipitation and their anticancer activity was studied on A549 cells. The nanocrystals, of size about 190 nm, showed rapid release of ellagic acid and were able to bind to the CD44 receptor (which was overexpressed in cancerous cells), stimulating the process of endocytosis. This resulted in improved internalization of the nanoparticles in the cancer cells, with increased cytotoxicity [248].

Apart from receptor-based targeting, nanocrystal delivery systems allowing stimuli-activated targeting and release of therapeutic moieties have also been studied to treat lung cancer. In this context, pH-sensitive nanocrystal systems that allow degradation and release at acidic pH values have been investigated. Recently, cetyl trimethyl ammonium bromide (CTAB) was used for the development of nanocrystals of 170 nm size using the hydrotrope method. The developed nanocrystals were used for the co-delivery of pemetrexed and resveratrol (PMX-RSV-LNCs). The PMX-RSV-LNCs showed sustained release of the drugs and potent *in vitro* (A549 cell line) and *in vivo* (intravenous injection into urethane-induced lung cancer mice) anticancer activity in the absence of nephrotoxicity and hepatotoxicity [254].

LCNs have been extensively studied for their superior ability to improve the delivery of phytochemicals. One of such phytochemicals is represented by rutin, a flavonol molecule abundantly found in apples, passion flower, buckwheat, and tea and embedded with potent anticancer, antioxidant, and anti-inflammatory activities [255]. In a recent study, Paudel *et al.* [256, 257] prepared a monoolein-based LCN formulation encapsulating rutin using ultrasonication, obtaining nanoparticles of size around 160 nm. This formulation exerted potent anti-inflammatory and antioxidant activities on LPS-stimulated human bronchial epithelial cells (BEAS-2B) *via* the reduction of Reactive Oxygen Species (ROS) and nitric oxide (NO) levels, together with an antiapoptotic effect [256]. The protective activity of these nanoparticles against airway inflammation highlighted the potential of these formulations in the management of airway inflammatory diseases such as COPD. A successive study demonstrated that the rutin-LCNs exert their antioxidant effect by inhibiting the transcription of pro-oxidant genes such as NADPH oxidase (Nox) *Nox4* and *Nox2B* and stimulating the transcription of the antioxidant genes Glutamate-cysteine ligase (*Gclc*) and NAD(P)H dehydrogenase [quinone] 1 (*Nqo1*) [258]. The same nanoparticles were also shown to have potent anticancer activity on

A549 lung cancer cells, where they significantly inhibited proliferation, migration, and colony formation capacity [259].

A similar protocol was also used to encapsulate the phytochemical molecule naringenin within a poloxamer 407/monoolein LCN delivery system [260]. These nanoparticles showed potent anti-inflammatory activity against LPS-stimulated minimally immortalised human airway basal cells (BCi-NS1.1 cells), which was exerted through decreased expression of the cytokines interleukin (IL)-6, IL-8, IL-1 β , and TNF- α [260]. Further to this, the same nanoparticles also showed potent antiproliferative, anti-migratory, and anti-colony formation activity in A549 lung cancer cells [260].

Zerumbone was also encapsulated in monoolein-based LCNs, and the resulting nanoparticles showed potent anticancer activity on A549 NSCLC cells by modulating the expression of several oncogenes and oncosuppressors at both the transcriptional and post-transcriptional levels [261].

Another promising phytochemical known for its anticancer, antioxidant and anti-inflammatory activities is berberine (BBR), discussed in a previous section. To improve its delivery, berberine has been encapsulated in monoolein-based or phytantriol-based LCN systems and tested in many *in vitro* studies. The monoolein-based BBR-LCNs were shown to have potent anticancer activity, successfully inhibiting proliferation, migration, and the ability to form colonies in A549 lung cancer cells, simultaneously inhibiting the EMT process [262]. This activity was exerted at least in part through the inhibition of C-X-C Motif Chemokine Ligand 8 (CXCL-8), heme oxygenase -1 (HO-1), and Chemokine (C-C motif) ligand 20 (CCL-20), all proteins that play a pivotal role in cancer progression [263]. In another study, the same formulation was shown to attenuate the expression of β -catenin, a master regulator of cancer cell proliferation, metastasis, and cell polarity, at both gene and protein levels, in A549 lung cancer cells [264]. A similar, phytantriol-based, BBR-LCN formulation was also evaluated against A549 cells, where it exerted potent cytotoxic and anti-migratory activity by upregulating the transcription of oncosuppressor genes such as *P53* and *PTEN*, downregulating the transcription of the proto-oncogene *KRT18*, and by reducing the levels of many proteins promoting cancer cell migration and proliferation including DKK1, CTSB, CTSD, BCLX, CSF1, and CAPG [265]. In a follow-up study, this formulation was shown to exert its anticancer effect on A549 cells by decreasing the protein expression of survivin and HIF-1 α , as well as by stimulating the expression of p27 [266]. BBR-LCN formulations were also tested

in vitro against different models of inflammation. In a recent study, a monoolein-based BBR-LCN formulation was shown to counteract oxidative stress, senescence, and inflammation in an *in vitro* COPD model obtained by exposure of human bronchial epithelial cells (16HBE) and mouse macrophages (RAW264.7) to cigarette smoke extract [267]. Similarly, a phytantriol-based BBR-LCN formulation was also shown to attenuate inflammation and oxidative stress in LPS-induced RAW264.7 cells through reduction of ROS and NO production, as well as inhibition of the transcription of the pro-inflammatory cytokines TNF- α , IL-6, and IL-1 β [268]. Importantly, in all the studies discussed where berberine-loaded nanoparticles were used, the minimal equivalent berberine concentration necessary to achieve therapeutic efficacy was always lower compared to the pure, non-encapsulated berberine, confirming the advantage of encapsulating therapeutic moieties within LCN systems.

6.3 - Nanoemulsions

Nanoemulsions are isotropically clear, thermodynamically and kinetically stable systems that are composed of a mixture of two immiscible phases: the aqueous phase, and the oil phase, whereby one of the two phases is dispersed in the form of droplets within the other phase [269]. Nanoemulsions are prepared with different techniques, including microfluidization, high-pressure homogenization, and ultrasound-assisted emulsification, and the submicron colloidal system of particles composing nanoemulsions usually ranges in size between 20 and 200 nm [270]. The use of nanoemulsions is advantageous in lung cancer and COPD therapy because, as drug delivery systems, they enhance bioavailability, specificity of delivery, and increase the stability of the formulation by protecting the therapeutic cargo from oxidative and UV degradation. There is also evidence suggesting that nanoemulsions can protect the cargo from certain bacteria, fungi, and viruses [270]. The ability of nanoemulsions to undergo extensive chemical and physical modification is also an added feature in the treatment of lung diseases. In particular, the possibility of modifying the dispersed droplet size to maximize their penetration through the epithelial and ciliary cells of the respiratory tract is a particularly advantageous characteristic of nanoemulsions [271]. Nanoemulsions are also more economical to prepare as compared to other delivery systems. In this regard, many phytochemicals and nucleic acid-based therapeutics have been formulated as nanoemulsions for pulmonary drug delivery. For instance, a curcuminoid extract nanoemulsion was prepared by sonication method and tested on A549 cells. The developed nanoemulsion showed a size range of 12.6-13.7 nm,

and it showed anticancer activity by arresting the cell cycle at the G2/M phase and increasing the expression of caspase-3, caspase-8, caspase-9, and cytochrome C, simultaneously reducing the expression of DK1 [271]. In another study, a curcumin nanoemulsion was prepared by film dispersion sonication method. The developed nanoemulsion contained droplets of size 121 nm, and it exerted superior, dose-dependent anticancer activity on A549 cells by reducing P-gp-mediated efflux, CYP450 metabolism, and enzymatic oxidation of curcumin [272].

Quercetin is a flavonoid found in onion, many vegetables, and fruits such as apples, mangoes, and citrus fruit, which is embedded with anticancer, antioxidant, anti-inflammatory, and antiviral activities [143]. To overcome its poor water solubility, quercetin was formulated as a nanoemulsion compatible with pulmonary delivery using a high-energy emulsification method. The droplet size of the nanoemulsion was found to be 131.4 nm, and the formulation demonstrated dose- and time-dependent cytotoxicity against A549 lung cancer cells, with sustained quercetin release for up to 48h and in the absence of toxic effects against normal cells [273].

In another study, the role of a neobavaisoflavone (NEO) nanoemulsion (nano-NEO) on lung cancer was studied [274]. The size of the nanoemulsion droplets was found to be 110 nm. The nano-NEO was administered intravenously, and it was able to demonstrate improved solubility, bioavailability, antiproliferative action, and reduction in extracellular matrix (ECM) deposition in an *in vivo* model of lung cancer. Furthermore, treatment with nano-NEO improved the activated tumor immune microenvironment by reducing the number of regulatory T cells (Tregs) and myeloid-derived suppressor cells (MDSCs) infiltration and increasing the number of natural killer cells and M2 macrophages [274]. Further, the nano-NEO improved the pharmacokinetic parameters of NEO as compared to naïve NEO [274].

In a further study, a naringenin-loaded nanoemulsion (nano-NAR) was prepared by dispersion technique and optimized by Box-Behnken design. The optimized nano-NAR showed a size of 85.6 nm and a cargo entrapment efficiency of 95.6%, and it exerted dose-dependent cytotoxicity against A549 lung cancer cells through cell cycle arrest in the G2/M phase, reduction of bcl1 expression, and upregulation of Bax and caspase-3 activity. In doing so, the nano-NAR formulation was more potent compared to naringenin alone [275].

In addition to their ability to incorporate single lipophilic moieties, nanoemulsions are particularly prone to be used in improving the solubility and physicochemical characteristics of complex lipophilic mixtures such as the essential oils extracted from different plants,

including, for example, Agarwood oil, which is renowned for its potent antioxidant and anti-inflammatory activities which makes it suitable as a therapeutic strategy for chronic inflammatory diseases [108, 276]. In a recent study, a nanoemulsion containing citrus lemon oil of 30.2 nm average size was developed by modified sonication method. The nanoemulsion demonstrated cytotoxic effect for A549 cells and upregulated the activity of Cas-3, simultaneously exerting antioxidant and anti-angiogenic activities in chick embryo chorioallantoic membrane. [277]. Another natural oil, *Arachis hypogaea* (AHO), was formulated in a nanoemulsion (AHO-NE) for the *in vitro* treatment of lung cancer. The oil was formulated using tween 20 and tween 80 by ultrasonication technique, obtaining droplets of average size 51.3 nm. Treatment of A549 cells with AHO-NE resulted in significant reduction of viability and induction of apoptosis, which was not observed when treating normal cells (human foreskin fibroblasts, HFF) with the same amount of nanoemulsion [278]. In another study, an inhalable jojoba oil dry nanoemulsion (JND) was evaluated for its anti-acute lung injury activity, using a rat model of acute lung injury established upon intratracheal administration of LPS or hydrogen peroxide [279]. Treatment with JND resulted in an anti-inflammatory effect through the reduction of TNF- α , IL-1, IL-6, and NF- κ B p65 subunit, concomitantly with reduced bleeding and inflammatory cell infiltration [279]. Finally, a *Citrus aurantium* essential oil nanoemulsion was prepared by ultrasonication method and it was evaluated for cytotoxicity on A549 cancer cells. The developed nanoemulsion showed a size of 75 nm and exerted a dose-dependent cytotoxic effect on A549 cancer cells, which was attributed to the upregulation of *Cas-3* gene and enhanced-Sub G1 peaks. Upon *in vivo* oral administration in mice, the nanoemulsion also showed antioxidant activity through an upregulation of antioxidant enzymes such as SOD, CAT and GPx [280].

Nanoemulsions are currently being investigated as drug delivery systems for the treatment of inflammatory diseases such as COPD. Our recent work has recently demonstrated that agarwood oil nanoemulsion can significantly attenuate cigarette smoke-induced inflammation and oxidative stress markers in human bronchial epithelial cells [281], as well as the LPS-induced pro-inflammatory cytokines, IL-6 and IL-8, in human bronchial epithelial cells [282]. In another study, Amani et al (2010) developed a nanoemulsion formulation for the respiratory delivery of Budesonide by nebulizers, obtaining improved *in vitro* performance for the nanoemulsion-based preparations due to better aerosol output [283]. With regards to the pulmonary delivery of nucleic acid cargo encapsulated within nanoemulsions, two studies have been published. In one study, a perfluorocarbon (PFC)-based nanoemulsion was used for the

combined pulmonary delivery of a chemokine receptor CXCR4 antagonist and a small interfering RNA (siRNA) targeting the transcription factor STAT3 [284]. This dual nanoemulsion demonstrated effective anticancer activity *in vitro* through inhibition of the invasion capacity, as well as a potent antimetastatic activity *in vivo*, upon pulmonary administration, in an established model of lung metastasis of breast carcinoma [284]. In another study, a chitosan-based cationic nanoemulsion was used for the co-delivery of a siRNA inhibiting the X-linked Inhibitor of Apoptosis Protein and a phytochemical with known anticancer activity, gambogic acid, for the treatment of lung cancer [181]. The nanoemulsion was prepared by high energy emulsification technique, using glycerin and tween 80, obtaining droplets of average size 183 nm. *In vitro* cytotoxicity studies performed on A549 cells revealed that the nanoemulsion had a strong pro-apoptotic activity and inhibited cell proliferation by arresting cells in the G0/G1 phase of the cell cycle. The nanoemulsion was also evaluated in an *in vivo* model of lung cancer obtained by injecting B16F10 cells in BALB/c mice, where it showed potent anticancer activity [181]. Interestingly, in this study, the pulmonary administration of this dual-loaded nanoemulsion exerted a stronger anticancer activity compared to the intravenous administration [181], confirming the great potential of nanoemulsions for the pulmonary delivery of drugs.

6.4 - Liposomes

Liposomes are the most widely known and thoroughly investigated nanocarriers to be used for advanced drug delivery. These heterogeneous drug delivery systems are composed of an aqueous core surrounded by a lipid bilayer [285]. The encapsulated drug is dispersed, according to its solubility, either in the lipid membrane or in the aqueous core, and encapsulation of drugs within liposomes improves the overall pharmacokinetics of the therapeutic moiety under study [286]. Drugs can be loaded within liposomes in two ways, namely active loading and passive loading. In passive loading, the lipids and the drug are mixed and the drug is loaded within the liposome simultaneously with the liposome assembly. Active loading is more advantageous, and it involves loading the drug cargo within pre-formed liposomes by exploiting differences of electric potential or pH gradients between the two sides of the liposome's lipidic membrane [287]. In this regard, liposomes have been successfully used by Konduri et al. to deliver the corticosteroid budesonide in a mouse model of asthma. In this study, weekly treatment with encapsulated budesonide was as effective as daily budesonide therapy in decreasing lung

inflammation by lowering eosinophil peroxidase activity, peripheral blood eosinophils, and total serum IgE levels, highlighting the potential of encapsulation of therapeutics in liposomes in improving patient compliance [288].

Liposomes for delivery of siRNA to treat lung epithelium diseases were developed by McCaskill and coworkers [289] by hydration of a freeze-dried matrix method, for intravenous delivery to target the lung epithelium. The developed liposomes, of size 190.25 nm and zeta potential 52.4 ± 0.25 mV, were successful in protein knockdown in most part of the lungs upon intravenous administration [289].

Liposomes formulated by incorporating phytoceuticals to treat pulmonary related diseases have also been developed and evaluated. In one study, Zhang and coworkers [290] formulated curcumin-loaded liposomes for inhalation delivery using the thin film method. The curcumin encapsulated in these liposomes was uptaken faster and to a greater extent by A549 lung cancer cells as compared to when curcumin alone was administered. Furthermore, a high selection index resulted from curcumin liposomes' low cytotoxicity on normal human bronchial BEAS-2B epithelial cells and simultaneous high cytotoxicity on A549 cancer cells, in part due to enhanced cell death caused by upregulation of caspase-3 expression [290]. In another study, quercetin-loaded liposomes were developed by thin film hydration method and functionalized with the TF7 peptide, allowing to specifically target the transferrin receptor expressed on A549 cells [291]. These liposomes were tested *in vitro* on A549 cells, where they exhibited 3-fold higher cytotoxicity, greater induction of apoptosis and S-phase cell cycle arrest compared to naïve quercetin. Furthermore, the liposomes were able to penetrate tumor spheroids to a depth of 120 μm . Finally, upon *in vivo* pulmonary administration on orthotopic lung tumour-bearing mice, T7-liposomes largely increased the anticancer activity of quercetin, significantly increasing the survival of mice [291]. In another study, quercetin nanoliposomes were formulated for lung cancer targeted therapy [292]. The nanoliposomes were functionalized with arginylglycylaspartic acid (RGD) peptide, which binds integrins that are particularly expressed in the neovasculature surrounding solid tumors, therefore allowing tumor-specific targeting. These liposomes were prepared by thin film hydration technique, and had a size range of 90-99 nm, compatible with penetration in the fenestrated neovasculature typical of cancer, with a zeta potential of -20 to -21 mV [292]. The nanoliposomes of quercetin had good *in vivo* tumor targetability upon intravenous administration, with high penetration capacity and significant anticancer activity in mice with A549 cell tumors [292]. The mechanisms by which these nanoliposomes showed specific tumor-targeting capacity involved the EPR effect and

also RGD-integrin-mediated cell uptake of the nanoliposomes [292]. Another plant-based flavonoid, fisetin, was formulated into liposomes and assessed for its anti-lung cancer activity [293]. The liposomes, of average size 173.5 nm, were prepared by thin film hydration method and assessed for their efficacy *in vivo*, upon intravenous and intraperitoneal administration, against Lewis lung carcinoma (LLC) cell tumor fragments transplanted subcutaneously in the flanks of mice. In comparison to naïve fisetin, liposomal fisetin provided a 47-fold enhancement in relative bioavailability. When compared to naïve fisetin at the same dose, treatment with liposomal fisetin resulted in greater tumour growth latency, highlighting a stronger anticancer effect of liposomal quercetin [293]. In another study, for the treatment of multidrug resistant (MDR) lung cancer cells, resveratrol-loaded liposomes were surface modified to target mitochondria with dequalinium polyethylene glycol-distearoylphosphatidylethanolamine (DQA-PEG(2000)-DSPE). The size of the developed liposomes was found to be 70 nm. The liposomes were evaluated on A549 cells and their MDR variant A549/cDDP. The developed liposomes were able to induce apoptosis on both cell lines by upregulating caspase 9 and caspase 3 and by dissipating the mitochondrial membrane potential. Furthermore, encapsulation of the drug within liposomes resulted in increased tumor penetration ability compared to treatment with naïve resveratrol [294].

6.5 - Exosomes

Exosomes are small extracellular vesicles with a size range of 30 to 150 nm that are delimited by a lipid bilayer, similarly to liposomes [295]. They are physiologically produced by a variety of cell types, both healthy and diseased, and are generally produced in higher numbers by tumor cells [295, 296]. It has been demonstrated that exosomes selectively transport their cargo, composed mainly of proteins and nucleic acids, to different recipient cell types as one of the fundamental mechanisms of cell-to-cell communication [295]. Exosomes released by cancer cells, together with other classes of extracellular vesicles, are key mediators that promote cancer hallmarks such as cell growth, proliferation, migration, invasiveness, and multidrug resistance by delivering growth factors, chemokines, miRNAs, and other molecules [75, 295, 297]. Due to the fact that exosomes are naturally produced by many cells, an indubitable advantage of the exploiting of exosomes as drug delivery systems would be their elevated biocompatibility and reduced immunogenicity [170, 297]. A number of studies highlight the suitability of exosomes as drug delivery vehicles for different types of therapeutics against lung

diseases [297-299]. For example, modified exosomes have been used to co-deliver an anti-CD47 antibody with cisplatin *in vitro* in A549 lung cancer cells and *in vivo* on a LLC tumor-bearing mouse model through intravenous injection, and the exosomes showed a greater anticancer activity compared to non-encapsulated anti-CD47 antibody + cisplatin [300]. Despite this, only a few studies have investigated the potential of exosomes as delivery systems for phytochemical or phytochemical molecules. For example, the phytochemical withaferin A, which is an effective angiogenesis and cancer growth inhibitor, has been encapsulated in bovine milk-derived exosomes [301]. Exosome-loaded withaferin A showed a far more potent anti-tumor activity when compared to its naïve form both *in vitro*, against A549 lung cancer cells, and *in vivo* in a xenograft mouse lung cancer model [301]. In another study, the plant triterpenoid celastrol was encapsulated in exosomes, and treatment with celastrol exosomes displayed a greater anticancer activity, both *in vitro* and *in vivo*, when compared to naïve celastrol [302].

The therapeutic role of nucleic acids, particularly miRNAs and siRNAs, in lung cancer and other pulmonary diseases has recently gained prominence [303]. Exosomes represent a promising system for encapsulation and advanced delivery of nucleic acid cargo. In a recent study, Jeong *et al.* demonstrated that the exosome-mediated delivery of miRNA-496 effectively suppressed the growth of a 3D microfluidic model of lung cancer [304]. The possibility of delivering nucleic acid-loaded exosomes *via* inhalation has been explored in a study by Zhang *et al.* [305]. In this study, serum-derived exosomes loaded with different siRNAs and miRNA mimics or inhibitors were delivered *in vivo* through inhalation. The exosomes were found to selectively transport the cargo to lung macrophages, and were effective in modulating LPS-induced lung inflammation [305]. In a successive study from Han *et al.* [306], exosomes were loaded with a short interfering RNA (siRNA) against the Myd88 transcript (si-Myd88-loaded exosomes) and delivered to mouse lungs through a vibrating mesh nebulizer. The si-Myd88 exosomes showed exclusive lung distribution, with primary localization in macrophage and airway epithelial cells. These exosomes significantly reduced LPS-induced lung injury, supporting the applicability of this system for lung inflammatory diseases such as COPD [306]. In another study, exosomes loaded with a siRNA functionalized with an epidermal growth factor receptor ligand showed potent *in vitro* and *in vivo* antitumor activity against lung cancer [307]. Exosomes loaded with the miRNA miR-7-5p were also shown to enhance the anticancer effect of everolimus against A549 cells [308]. Finally, exosomes derived from MBA-MB-231 breast cancer cells, which are known to selectively bind to lung cancer cells, were used to

successfully deliver the miRNA-126. These exosomes showed strong *in vitro* antitumor effect through suppression of proliferation and migration of A549 lung cancer cells, as well as *in vivo* effective lung homing and antimetastatic activity in a mouse model of lung cancer upon intravenous administration [309].

6.6 - Dendrimers

Dendrimers are clearly structured, monodispersed, branched polymeric macromolecules of size between 1 and 100 nm, whose structure is composed of repeating tree-like branches [310, 311]. Dendrimers offer extreme adaptability, as they can literally be modified in any of their molecular constituents and functionalized in many ways to allow optimization of their physicochemical properties, biodistribution, and tissue or organ targeting. For this reason, dendrimers are particularly suitable as a starting point for the production of contrast agents to be used in different imaging probes to identify diseased tissues or organs [312, 313]. For the same reason, dendrimers have potential to be used as drug carrier systems to precisely deliver therapeutics to the intended diseased area, with the aim of improving the therapeutic effects of conventional treatments while simultaneously minimizing adverse reactions and off-target effects. This makes dendrimers an interesting option for pulmonary drug delivery [314]. In this regard, a poly(amidoamine) (PAMAM) dendrimer was used to successfully deliver an anti-EGFR antisense oligonucleotide to A549 lung cancer cells, successfully reducing their growth [315]. In another study, similar PAMAM dendrimer nanocarriers were produced and tested on *in vitro* and *in vivo* models of the pulmonary epithelium to assess the impact of PEGylation on cell targeting and internalization [316]. As the extent of PEGylation increased, it was observed that the transport from the apical to the basolateral region of polarized Calu-3 cells increased.

This phenomenon was explained by the fact that PEGylation significantly reduced the charge distribution. The findings indicated that PEGylation may be able to influence the pulmonary epithelial transport and internalization of dendrimer nanocarriers, providing an efficient platform for lung tissue targeting in the treatment of respiratory disorders [316].

With regards to nucleic acid delivery, a study by Khan et al. (2015) examined the role of encapsulated siRNA in PAMAM and poly(propylene imine) dendrimers with a lipid substitution for the treatment of inflammatory lung diseases such as COPD. A synergistic effect was observed enabling dendrimers to target tyrosine-protein kinase receptor, Tie-2-expressing endothelial cells within the lung. High levels of potency were observed specifically in PAMAM-

conjugated dendrimers with C15 cholesterol tails and polyphenylene ethynylene (PPE) dendrimers with C15 and C14 cholesterol chains. Additionally, no apparent increase in proinflammatory cytokines and decrease in mice weights was observed [317].

Despite their advantageous characteristics such as high drug-loading and small size, which allow to significantly improve the physicochemical characteristics of poorly soluble drugs and to specifically deliver these drugs to target tissues, a limitation of dendrimers is their potential toxicity and haemolytic activity, which can also be reduced by PEGylation [314, 318].

6.7 - Polymeric micelles

Polymeric micelles are self-assembled amphiphilic polymers in aqueous environment that form supramolecular core-shell structures, which can either have a solid core or a more fluid structure [319]. The ideal diameter of polymeric micelles is approximately between 20 and 200 nm, which allow them to extravasate from the leaky tumor vasculature. Improved, targeted delivery is made possible by the fact that polymeric micelles can encapsulate molecules such as phytochemicals, proteins, and nucleic acids that may be insoluble in aqueous media or otherwise unstable. Polymeric micelles share morphological and functional characteristics with natural transport systems such as lipoproteins and viruses [320]. Extensive chemical modifications can be carried on polymeric micelles to improve their characteristics, as well as to enhance the specificity of delivery or to achieve cargo release in response to specific stimuli. [321]. In a study, Xu *et al.* [322] constructed a tetrandrine-loaded Poly(N-vinylpyrrolidone)-Block-Poly(ϵ -caprolactone) (PVP-b-PCL) micelle system to improve the poor solubility of tetrandrine, and evaluated the drug's distribution and apoptosis induction on A549 lung cancer cells. The mobility, infiltration, and survival of A549 cells were all significantly reduced by the tetrandrine-loaded PVP-b-PCL micelles [322]. In another study, curcumin-loaded nanoparticles prepared with amphiphilic methoxy poly(ethylene glycol)-polycaprolactone (mPEG-PCL) block copolymers were tested against a mouse xenograft model of lung cancer obtained through transplant of A549 cells. The curcumin-loaded nanoparticles achieved greater anticancer activity when compared to naïve curcumin, when administered intravenously, with little toxicity against normal tissues [323]. Using chitosan-epluronic P123 micelles, Zhu *et al.* [324] entrapped acetylthevetin B (a cardiac glycoside with anticancer activity extracted from the seeds of the yellow oleander), obtaining improved therapeutic efficacy in an A549 cell xenograft mouse model of lung cancer when administered intravenously. This was obtained by

means of increased cellular absorption, apoptosis, and improved localization into the orthotopic lung tumour tissue, with simultaneous reduction of acetylthevetin B accumulation in the heart, liver, and spleen [324]. In another study piperine, an alkaloid isolated from black pepper known to possess anticancer activity, was encapsulated by Ding *et al.* using a mixed micelle composition made of D- α -tocopherol polyethylene glycol succinate (TPGS) and Soluplus® [325]. This new excipient, called Soluplus®, is composed of a polyvinyl caprolactame, polyvinyl acetate, and polyethylene glycol graft copolymer (PCLePVAcPEG), and is known to increase the solubility of lipophilic drugs. The goal of the researchers was to increase the solubility of piperine, which is highly hydrophobic. As a result, the cytotoxicity and pharmacokinetics of piperine in A549 cells were enhanced by this mixed micelle formulation [325].

6.8 - Metal-based nanoparticles

Metal-based nanoparticles have emerged as promising drug delivery tools. Reduced peripheral interactions through functional coating ease the transportation of these nanoparticles between the administration site and the target site, thus providing them with unique properties. Therefore, the potential applications of these metal-based nanoparticles include targeted drug delivery, enhanced imaging, and therapeutic interventions in lung conditions like asthma, chronic obstructive pulmonary disease (COPD), and lung cancer [326].

Gold nanoparticles (AuNPs) have garnered considerable attention for their use in lung disease treatment. In a study by Geiser *et al.*, highlighting the potential of AuNPs in targeted drug delivery for respiratory diseases, these nanoparticles were successfully delivered to the alveolar epithelial cells and alveolar macrophages in a COPD mouse model [327]. However, toxicity of AuNPs still remains a major challenge due to the fact that positively charged gold nanoparticles could interact with negatively charged serum proteins, forming aggregates upon intravenous injection. Surface modification of AuNPs with PEG can prevent them from forming aggregates [328]. Furthermore, Yang *et al.*, (2021) used gold nanoparticles to build gold nanocage vehicles capable of delivering doxorubicin and siRNAs, combined to phototherapy. This system achieved potent targeted gene silencing and tumor inhibition in mouse models of lung cancer [329]. In another *in vivo* study, Zhuang *et al.* (2021) used AuNPs to deliver a siRNA inhibiting the expression specificity protein 1 (SPI), obtaining enhanced radiosensitivity in a mouse A549 lung cancer cells xenograft [330].

Table 2 - Nano-drug delivery systems encapsulating phytochemicals or biologicals for treatment against lung cancer

Carrier	Therapeutic Moiety	Polymer/ligand	Year	Particle Size (nm)	Cell line/ Animal Model	Outcome	Reference
Solid Lipid Nanoparticles	AntimicroRNA Oligonucleotides	Glyceryl monosterate and phosphatidyl choline	2011	187	A549	<ul style="list-style-type: none"> • Significant cell uptake as compared to naïve form 	[331]
Nanoparticles	Resveratrol	Gelatin	2012	294	NCI-H460	<ul style="list-style-type: none"> • ↑ Antisense efficiency • Rapid and efficient cellular uptake • Greater antiproliferative effect 	[332]
Solid Lipid Nanoparticles	Curcumin	Polysorbate 50	2013	80	A549	<ul style="list-style-type: none"> • The IC₅₀ value was found to be 1/20th of naïve drug • Inhibition of apoptosis from flow cytometry 	[333]
Nanoparticles	siRNA	PMEP-b-PDEM	2013	50	H2009	<ul style="list-style-type: none"> • Upregulation of p21 and p53 expression • MDM2 protein expression 	[334]
Nanoemulsion	Lycobetaine	Lipoid E80	2013	147	Lewis lung carcinoma animal model	<ul style="list-style-type: none"> • Inhibition of caspase 3 • ↓ of tumor by inhibiting proliferation of tumor cells in rat model 	[335]
Micelles	Curcumin	Pluronic-F127	2015	188	A549	<ul style="list-style-type: none"> • ↑ Circulation time • 3 folds ↑ in cytotoxicity and 55 folds ↑ in bioavailability 	[336]
Nanoparticles	Naringenin	Chitosan	2015	54	A549	<ul style="list-style-type: none"> • ↑ Free radical scavenging • ↑ Cytotoxic effects 	[337]

Dendrimer	MicroRNA-34a	Aptamer	2015	100-200	A549	<ul style="list-style-type: none"> • Apoptotic effect of A549 cells [338] • ↓ Migration and invasiveness
Micelles	Oleanolic acid	P105/d- α -TPGS	2016	95.7	A549	<ul style="list-style-type: none"> • Apoptosis was ↑ as compared to naïve form [339] • Accumulation in tumor
Micelles	Quercetin	DSPE-PEG-TPGS	2016	70	A549	<ul style="list-style-type: none"> • Chromatin condensation and apoptotic body formation of the nuclei [340]
Nanoparticles	<i>Piper nigrum</i>	SnO ₂	2016	8-30	A549	<ul style="list-style-type: none"> • Enhanced cytotoxic and apoptotic effect [341]
Nanoparticles	Silibinin	PL-PEG-Fe ₂ O ₃	2016	130-155	A549	<ul style="list-style-type: none"> • ↓ hTERT gene expression, [342] • ↑ of nano drug as compared to naïve drug
Nanoemulsion	<i>Brucea javanica</i> oil	Cremaphor	2016	43	A549	<ul style="list-style-type: none"> • Killed tumor cells of G0, G1, S, G2, and M phase [343] • Activated caspase 3
Micelles	Curcumin	mPEG-PLA	2017	34	A549	<ul style="list-style-type: none"> • ↓ Migration and invasion of A549 cells [344]
Micelles	Ginsenoside compound K	TPGS/PEG-PCL	2017	53	A549	<ul style="list-style-type: none"> • Enhanced cellular uptake [345] • Showed apoptosis
Micelles	Dihydroergotamine	PLGA-PSPE	2017	297	A549	<ul style="list-style-type: none"> • ↓ Tumor size and mitophagy [346] • ↑ Apoptosis

Nanoparticles	<i>Pleuropterus multiflorus</i>	Silver	2017	275	A549	<ul style="list-style-type: none"> • Increased migration and apoptotic activity [347] • Significantly cytotoxic
Nanoparticles	<i>Musa paradisiaca</i> peel	Gold	2017	50	A549	<ul style="list-style-type: none"> • Inhibited the viability [348] • Showed nuclear morphological changes
Nanoemulsion	<i>Casearia sylvestris</i> leaves	Tween 20	2017	212	A549	<ul style="list-style-type: none"> • EC₅₀ of 4.0 µg/mL [349] • Dose dependent cytotoxicity
Liposomes	Triptolide	Anti-carbonic anhydrase IX antibody	2017	127-160	A549	<ul style="list-style-type: none"> • Efficient cell killing as compared to naïve form [350] • Better apoptotic activity
Micelles	siRNA and curcumin	Chitosan	2018	162	A549	<ul style="list-style-type: none"> • Taken up efficiently by clathrin mediated endocytosis [351]
Nanoparticles	<i>Mangifera indica</i> leaves	Zinc Oxide	2018	48	A549	<ul style="list-style-type: none"> • ↑ Antioxidant effect [352] • Significant cytotoxic effect against A549 cells
Nanoparticles	Naringenin	Hyaluronic acid	2018	221	A549 and J774	<ul style="list-style-type: none"> • Enhanced anticancer effect [353] • Enhanced drug uptake • Superior cytotoxicity and active targeting
Nanoparticles	<i>Matricaria chamomilla</i>	Silver	2018	45	A549	<ul style="list-style-type: none"> • Dose and time dependent effect on cytotoxic cells [354]

Nanoparticles	miR-125b	Hyaluronic acid	2018	92	J774.A1	<ul style="list-style-type: none"> • Upregulation of Bax, caspase-3 and caspase7 • Reduction in size [355] • Significant Increase in iNOS levels
Nanoparticles	<i>Artemisia scoparia</i>	Silver	2018	33	A549	<ul style="list-style-type: none"> • Dose dependent cell toxicity [356] • Apoptotic effect
Nanoemulsion	Carvacrol	Polysorbate 80	2018	106-170	A549	<ul style="list-style-type: none"> • Mitochondrial mediated apoptosis [357] • Dose dependent cytotoxicity
Nanoparticles	<i>Gossypium hirsutum</i> leaves	Silver	2019	100	A549	<ul style="list-style-type: none"> • Arrest of G2/M phase of cell cycle [358] • Enhanced expression of Bax
Nanoparticles	siRNA	Hyaluronic acid	2019	100-200	A549	<ul style="list-style-type: none"> • ↓ Bcl2 expression [359] • Delivered to tumorous tissue by extracellular vascularization
Nanoparticles	<i>Derris trifoliata</i>	Silver	2019	16.05	A549	<ul style="list-style-type: none"> • ↑ DPPH scavenging activity [360] • ↑ Antioxidant effect
Nanoparticles	Boswellic acid	Chitosan	2019	68-188	A549	<ul style="list-style-type: none"> • Arrested SubG0 phase of the cell cycle [149] • Effective cellular uptake and sustained release
Micelles	Retinoic acid and miR-29b	Pluronic® P123 or Pluronic® P103 linked to polyethyleneimine (PEI)	2020	110	A549	<ul style="list-style-type: none"> • ↓ Cell viability and migration [361] • Induced cell cycle arrest •

Nanoparticles	Myricetin	Folic acid conjugated	2020	110	A549 and NCI-H1299	<ul style="list-style-type: none"> • ↓ Cell viability [362] • ↑ Apoptosis, expression of caspase 3
Nanoparticles	Resveratrol	Chitosan-PLGA	2020	341	H1299	<ul style="list-style-type: none"> • Greater cytotoxic and apoptotic activity as compared to naïve form [363] • ↑ Antioxidant effect
Nanoemulsion	Epigallocatechin-3-gallate	Tween 80	2020	150	H1299	<ul style="list-style-type: none"> • ↓ Lung cancer colony formation [364] • ↓ Migration and invasion in a dose dependent manner
Nanoemulsion	<i>Anethum Graveolens</i>	Tween 20 and Tween 80	2021	32	A549	<ul style="list-style-type: none"> • ↓ Cell viability [365] • Demonstrated apoptosis and antioxidant effects
Nanoparticles	<i>Allium sativum</i>	Silver	2022	20-40	A549	<ul style="list-style-type: none"> • Lead to cellular impairment and death [366] • Penetrated cells easily and caspase-3 activation
Nanoemulsion	<i>Boswellia sacra</i>	propylene glycol (PG)	2022	20	A549	<ul style="list-style-type: none"> • ↑ Cytotoxic effect [367] • ↑ Reactive oxygen species
Nanoemulsion	Apricot kernel oil	Ethylene glycol	2022	40	A549	<ul style="list-style-type: none"> • ↑ Number of Sub G1 phase cells [368] • ↑ Expression of Caspases-3, 7 and 9 genes

A549- hypotriploid alveolar basal epithelial cells; DPPH- (2,2-diphenyl-1-picryl-hydrazyl-hydrate); DSPE-PEG-TPGS- 1,2-distearoyl-sn-glycero-3-phosphatidylethanolamine derivative of PEG (DSPE-PEG) and tocopheryl polyethylene glycol 1000 succinate (TPGS); EC₅₀- half maximal effective concentration; H1299- Human non-small lung cell carcinoma; hTERT- Telomerase reverse transcriptase IC₅₀- Half-maximal inhibitory concentration; J774- Macrophage cell lines; L929- NCTC clone 929 Clone of strain L; MDM2- murine double minute 2; mPEG-PLA- Methoxy polyethylene glycol-poly lactide; NCI-H460- Cellosaurus cell line; P105/d- α-TPGS- Pluronic P105/d-α-tocopheryl polyethylene glycol succinate; p21, p53- cyclin-dependent kinase inhibitor; PLGA-PSPE- poly(lactic-co-glycolic acid)-co-polyspermine; PL-

PEG-Fe₂O₃- Poly-d-lactide, polyethylene glycol, and Ferric oxide; PMEP-b ; PDEM- poly(methacryloyloxy ethyl phosphorylcholine)-block-poly(diisopropanolamine ethyl methacrylate); siRNA- small interfering RNA; TPGS/PEG-PCL- alpha-tocopheryl polyethylene glycol 1,000 succinate/poly(ethylene glycol)-poly(ϵ -caprolactone)

7 - Clinical trials investigating the potential of nano-drug delivery systems

Numerous clinical trials are currently being conducted investigating the efficacy of nanoparticle-based advanced drug delivery systems to improve the delivery of phytochemicals and nucleic acid-based therapeutics in the treatment of LC. These are discussed in this section, and summarized in Table 3. There are no clinical trials that are currently in progress to investigate the efficacy of nanoparticle-based advanced drug delivery systems against COPD. The formulation named EP0057 is a cyclodextrin-based nanoparticle encapsulating the topoisomerase I inhibitor camptothecin which allows improved delivery of the cargo and selective release in the tumor microenvironment [369]. This drug is currently being studied, in a Phase I / II clinical trial (NCT02769962), in combination with olaparib in people with relapsed/refractory small cell lung cancer.

Another drug, SNB-101, is composed of double-core shell micelles encapsulating SN38, the active metabolite of irinotecan. A Phase I clinical trial is currently in progress to study the safety, tolerability, and pharmacokinetics of SNB-101 in patients with many cancers including small cell lung cancer (NCT04640480).

With regards to clinical trials involving nucleic acid-based therapy, an interventional phase I clinical trial study (NCT03819387) is currently being executed to identify the optimal NBF-006 (siRNA-based lipid nanoparticles inhibiting Glutathione S-Transferase P (GSTP)) dose and study the pharmacokinetics and preliminary efficacy against NSCLC, colorectal, and pancreatic cancer.

TargomiRs are patented systems used to deliver microRNA mimetic molecules, with the aim of restoring the levels of miRNAs, usually oncosuppressors, that are downregulated in lung cancer [370]. These systems are currently being tested in a clinical trial (NCT02369198, phase I - dose finding) to deliver a miR-16-based microRNA mimetic. The miR-16 family has been implicated as a tumor suppressor in a range of cancer types [371]. The miRNA mimetic being tested in this study is a double-stranded, 23-base pair, synthetic RNA molecule encapsulated in an EnGeneIC delivery vehicle (EDV, consisting of nonliving bacterial minicells [372]) targeted against EGFR using an anti-EGFR bispecific antibody [372]. The study aims at validating the use of this advanced therapeutic as second or third line of treatment for patients with malignant pleural mesothelioma (MPM) and advanced NSCLC [370].

Finally, Quaratusugene Ozeplasmid (Reqorsa) is an experimental non-viral immunogene therapy consisting in the gene encoding for the protein tumor suppressor candidate 2 (TUSC2) encapsulated in cationic lipid nanoparticles. The safety and efficacy of Reqorsa is currently being investigated in two Phase I / II clinical trials: in combination with osimertinib

(NCT04486833) against advanced, metastatic non-small cell lung cancer; and in combination with Pembrolizumab against previously treated non-small cell lung cancer (NCT05062980).

Table 3 – Clinical trials investigating the potential of nano-drug delivery systems

Study Phase	Clinical trial ID	Title	Aim	Carrier	Therapeutic Moiety	Target disease	Status (as of 05/06/2023)
Phase I / II	NCT02769962	Trial of EP0057, a Nanoparticle With Camptothecin and Olaparib in People With Relapsed/Refractory Small Cell Lung Cancer	Testing safety and efficacy of EP0057 and olaparib on small cell lung cancer	Cyclodextrin-based nanoparticle	Camptothecin	SCLC (Relapsed/Refractory)	Recruiting
Phase I	NCT04640480	Dose-finding Study to Evaluate the Safety, Tolerability, and Pharmacokinetics of SNB-101(SN-38) in Patients With Tumors	Studying safety, tolerability, and pharmacokinetics of SNB-101 in cancer patients	Double core-shell micelles	SN-38 (active form of camptothecin)	NSCLC	Recruiting
Phase I	NCT03819387	A Study of NBF-006 in Non-Small Cell Lung, Pancreatic, or Colorectal Cancer	Testing safety, pharmacokinetics and preliminary efficacy of NBF-006 in cancers including NSCLC	Lipid nanoparticle	siRNA inhibiting GSTP	NSCLC	Recruiting
Phase I	NCT02369198	MesomiR 1: A Phase I Study of TargomiRs as 2nd or 3rd Line Treatment for Patients With Recurrent MPM and NSCLC	Dose finding and preliminary efficacy of TargomiRs as second or third line of treatment for MPM and NSCLC	Nonliving bacterial minicells	miR-16 miRNA mimetic	NSCLC	Completed
Phase I / II	NCT04486833	Quaratusugene Ozeplasmid (Reqorsa) and Osimertinib in Patients With Advanced Lung Cancer Who Progressed on Osimertinib (Acclaim-1)	Determination of safety and efficacy of Reqorsa alone and in combination with osimertinib in advanced, metastatic NSCLC	Cationic nanoparticles	lipid TUSC2 gene	Advanced, Metastatic EGFR-Mutant, Metastatic NSCLC	Recruiting
Phase I / II	NCT05062980	Reqorsa (Quaratusugene Ozeplasmid) in Combination With Pembrolizumab in Previously Treated Non-	Determination of safety and efficacy of Reqorsa alone and in combination with pembrolizumab or docetaxel +/- ramucirumab against NSCLC	Cationic nanoparticles	lipid TUSC2 gene	Previously Treated NSCLC	Recruiting

Small Lung Cancer
(Acclaim-2)

GSTP: Glutathione S-Transferase P; MPM: Malignant Pleural Mesothelioma; NSCLC: non-small cell lung cancer; SCLC: small cell lung cancer; TUSC2: tumor suppressor candidate 2

8 - Conclusions and future perspectives

In this review, an overview of the current state-of-the-art advancements in the field of nanoparticle-based drug delivery systems for the advanced delivery of nucleic acid-based therapeutics and phytochemicals in lung cancer and COPD has been discussed.

Lung cancer and COPD are among the most deadly diseases of modern times, and they share common underlying pathogenetic mechanisms. Furthermore, cigarette smoking represents a paramount underlying cause of both ailments. Despite many novel treatment approaches, the medical and financial burden of chronic respiratory diseases is currently substantial and is bound to increase in the next decade [9]. This picture is worsened by the relatively high incidence of comorbidities, in which the diagnosis of ailments such as COPD overlaps with other respiratory diseases such as asthma, lung cancer, bronchiectasis, and interstitial lung disease [373]. The presence of co-morbidities is known to worsen symptom severity and the quality of life of patients [374]. All these listed factors, together with the many limitations of currently available therapies discussed in the present review, underline the necessity for the development of novel therapeutic strategies. In this context, therapies that are effective against more than one type of respiratory disease would be advantageous.

Phytochemicals and nucleic acid-based therapies represent two potentially revolutionary sources of novel therapeutics. Although they are extremely different, these two classes of drugs have one fundamental limitation in common: they are both difficult to deliver to the intended target site. The development of advanced drug delivery systems is set to dramatically expand the applicability of phytochemicals and nucleic acid-based therapies by overcoming these limitations.

The use of phytochemicals, or plant-derived molecules endowed with pharmacological activity, dates back millennia, and the therapeutic use of plants and plant extracts can be considered the earliest application of medicine. The use of nucleic acid-based therapy through systems such as miRNA mimics or inhibitors, siRNA-based gene silencing, or decoy ODN-based transcription factor inhibition, on the other hand, represents the future and is having a profound impact on our approach to the treatment of many diseases, including lung cancer and COPD. Despite the numerous promising studies showcasing the extreme potential of these two different classes of therapeutics to improve the treatment outcomes of lung cancer and COPD, common issues such as poor pharmacokinetic profile, insufficient stability, and poor solubility and/or permeability currently hamper the progression of these therapeutics to the clinical stage.

The different types of nanoparticle-based advanced drug delivery systems showcased in the present review represent an innovative set of tools that is set to finally overcome these limitations, allowing an enhanced, tissue/organ specific, selective delivery of therapeutic cargo that would be otherwise difficult to deliver, simultaneously minimizing the adverse effects associated with this type of therapy. Many advantages are associated with the use of advanced drug delivery systems. These include protection of labile molecules such as RNAs from degradation, improvement of the solubility of poorly soluble molecules such as many phytochemicals, and the possibility of functionalising the delivery systems to selectively target specific cell types and tissues, achieving improved therapeutic efficacy and simultaneously minimising adverse and off-target effects. This is particularly true for respiratory diseases, which are unique compared to other diseases due to the possibility to deliver drugs directly to the lungs through inhalation [64]. Many nanoparticle-based drug delivery systems are considered to be compatible with inhalational delivery and therefore promising in the treatment of respiratory disorders [242].

The topic of advanced drug delivery systems is extremely timely, and it is rapidly gaining momentum, particularly after the breakthrough brought on by the development of the COVID-19 mRNA-based vaccines [17]. In these innovative vaccines, the successful delivery of the mRNA encoding for the viral Spike protein is made possible by its encapsulation within lipid nanoparticles, which exert the double function of protecting the mRNA cargo from degradation and improving its cellular uptake [17]. The approval of this innovative product in such a short amount of time has started what is called an “mRNA revolution” by many scientists [375-377], and advanced drug delivery systems are the tool that made it possible. In particular, one field in which advanced drug delivery systems such as lipidic nanoparticles are set to exert a substantial impact is the field of mRNA-based cancer vaccines, which is currently establishing itself as an innovative cornerstone of cancer immunotherapy [378].

In the next five years, we predict that the further development of advanced drug delivery systems will allow the widespread clinical application of the still largely untapped source of molecules with promising biological activity, but poor solubility and pharmacokinetic properties. These include not only phytochemicals but all the molecules that, in general, do not obey the strict structural and physicochemical rules necessary to be promptly absorbed and exert a therapeutic action such as the Lipinski’s rule of five, ultimately equipping researchers with a significantly expanded arsenal of new molecules to be used in the therapy of all diseases, including respiratory diseases.

To reach this goal, the key area for improvement in the field of advanced drug delivery systems is represented by the target-specific delivery of the therapeutic payload. This will be made possible by the further development of smart drug delivery systems (SDDS), consisting in stimuli-responsive systems that allow to maximize target specificity, distribution, and plasma retention [379]. In order to achieve these goals, efforts must be put in the clinical validation of the safety and efficacy of these nanoparticle-based drug delivery systems. Although numerous clinical trials are currently in progress to assess the feasibility of using nano-delivery systems in the treatment of lung cancer, no clinical trials are currently undergoing to test these systems on COPD. This is an area that necessitates further efforts for improvement.

In conclusion, advanced drug delivery systems are set to revolutionise the way we target and treat lung diseases, and will enormously benefit the quality of life of countless patients in the next decades and the pulmonary clinics.

Declarations

Ethical Approval

Not applicable.

Competing interests

The authors have no competing interests to declare that are relevant to the content of this article.

Authors contributions

GDR and KD conceived the idea of the literature review. All the listed authors contributed to the writing of the first draft of the manuscript and to the subsequent revisions and finalization of the manuscript. KD supervised the project.

Funding

Not Applicable

Availability of data and materials

Not Applicable

REFERENCES

1. Labaki, W.W. and M.K. Han, *Chronic respiratory diseases: a global view*. *Lancet Respir Med*, 2020. **8**(6): p. 531-533.
2. Safiri, S., et al., *Burden of chronic obstructive pulmonary disease and its attributable risk factors in 204 countries and territories, 1990-2019: results from the Global Burden of Disease Study 2019*. *Bmj*, 2022. **378**: p. e069679.
3. Lugg, S.T., et al., *Cigarette smoke exposure and alveolar macrophages: mechanisms for lung disease*. *Thorax*, 2022. **77**(1): p. 94-101.
4. Mehta, M., et al., *Cellular signalling pathways mediating the pathogenesis of chronic inflammatory respiratory diseases: an update*. *Inflammopharmacology*, 2020. **28**(4): p. 795-817.
5. Kc, B.B., et al., *Prevalence and Factors Associated with Tobacco Use among High School Students*. *J Nepal Health Res Counc*, 2022. **20**(2): p. 310-315.
6. MacNee, W., *Pulmonary and systemic oxidant/antioxidant imbalance in chronic obstructive pulmonary disease*. *Proc Am Thorac Soc*, 2005. **2**(1): p. 50-60.
7. Dua, K., et al., *Increasing complexity and interactions of oxidative stress in chronic respiratory diseases: An emerging need for novel drug delivery systems*. *Chemico-Biological Interactions*, 2019. **299**: p. 168-178.
8. Youlden, D.R., S.M. Cramb, and P.D. Baade, *The International Epidemiology of Lung Cancer: geographical distribution and secular trends*. *J Thorac Oncol*, 2008. **3**(8): p. 819-31.
9. Sung, H., et al., *Global Cancer Statistics 2020: GLOBOCAN Estimates of Incidence and Mortality Worldwide for 36 Cancers in 185 Countries*. *CA Cancer J Clin*, 2021. **71**(3): p. 209-249.
10. Young, R.P., et al., *COPD prevalence is increased in lung cancer, independent of age, sex and smoking history*. *Eur Respir J*, 2009. **34**(2): p. 380-6.
11. Xu, Y.R., A.L. Wang, and Y.Q. Li, *Hypoxia-inducible factor 1-alpha is a driving mechanism linking chronic obstructive pulmonary disease to lung cancer*. *Front Oncol*, 2022. **12**: p. 984525.

12. Paudel, K.R., et al., *Role of Lung Microbiome in Innate Immune Response Associated With Chronic Lung Diseases*. *Front Med (Lausanne)*, 2020. **7**: p. 554.
13. Ashique, S., et al., *Short Chain Fatty Acids: Fundamental mediators of the gut-lung axis and their involvement in pulmonary diseases*. *Chem Biol Interact*, 2022. **368**: p. 110231.
14. Liu, C.S., et al., *Research progress on berberine with a special focus on its oral bioavailability*. *Fitoterapia*, 2016. **109**: p. 274-82.
15. Mehta, M., et al., *Recent trends of NFκB decoy oligodeoxynucleotide-based nanotherapeutics in lung diseases*. *J Control Release*, 2021. **337**: p. 629-644.
16. Paudel, K.R., et al., *Nanomedicine and medicinal plants: Emerging symbiosis in managing lung diseases and associated infections*. *Excli j*, 2022. **21**: p. 1299-1303.
17. Hou, X., et al., *Lipid nanoparticles for mRNA delivery*. *Nature Reviews Materials*, 2021. **6**(12): p. 1078-1094.
18. Albano, G.D., et al., *Overview of the Mechanisms of Oxidative Stress: Impact in Inflammation of the Airway Diseases*. *Antioxidants (Basel)*, 2022. **11**(11).
19. Nucera, F., et al., *Role of oxidative stress in the pathogenesis of COPD*. *Minerva Med*, 2022. **113**(3): p. 370-404.
20. Paudel, K.R., et al., *Advancements in nanotherapeutics targeting senescence in chronic obstructive pulmonary disease*. *Nanomedicine (Lond)*, 2022.
21. Wadhwa, R., et al., *Epigenetic Therapy as a Potential Approach for Targeting Oxidative Stress-Induced Non-small-Cell Lung Cancer*, in *Handbook of Oxidative Stress in Cancer: Mechanistic Aspects*, S. Chakraborti, B.K. Ray, and S. Roychoudhury, Editors. 2022, Springer Nature Singapore: Singapore. p. 1545-1560.
22. Nsonwu-Anyanwu, A.C., et al., *Risk of Pulmonary-Reproductive Dysfunctions, Inflammation and Oxidative DNA Damage in Exposure to Polycyclic Aromatic Hydrocarbon in Cigarette Smokers*. *Med J Islam Repub Iran*, 2022. **36**: p. 108.
23. Huang, X., et al., *The roles of microRNAs in the pathogenesis of chronic obstructive pulmonary disease*. *Int Immunopharmacol*, 2019. **67**: p. 335-347.
24. Dos Santos, C.F., et al., *DNA damage and antioxidant capacity in COPD patients with and without lung cancer*. *PLoS One*, 2022. **17**(11): p. e0275873.
25. Su, X., et al., *The effects of epithelial-mesenchymal transitions in COPD induced by cigarette smoke: an update*. *Respir Res*, 2022. **23**(1): p. 225.
26. Liu, G., et al., *Adverse roles of mast cell chymase-1 in chronic obstructive pulmonary disease*. *Eur Respir J*, 2022.

27. Pain, M., et al., *Tissue remodelling in chronic bronchial diseases: from the epithelial to mesenchymal phenotype*. Eur Respir Rev, 2014. **23**(131): p. 118-30.
28. Weng, M.S., et al., *The interplay of reactive oxygen species and the epidermal growth factor receptor in tumor progression and drug resistance*. J Exp Clin Cancer Res, 2018. **37**(1): p. 61.
29. Nucera, F., et al., *Chapter 14 - Role of autoimmunity in the pathogenesis of chronic obstructive pulmonary disease and pulmonary emphysema*, in *Translational Autoimmunity*, N. Rezaei, Editor. 2022, Academic Press. p. 311-331.
30. Han, M.K., et al., *GOLD 2011 disease severity classification in COPDGene: a prospective cohort study*. Lancet Respir Med, 2013. **1**(1): p. 43-50.
31. Mathers, C.D. and D. Loncar, *Projections of global mortality and burden of disease from 2002 to 2030*. PLoS Med, 2006. **3**(11): p. e442.
32. (AIHW), A.I.o.H.a.W. *Chronic obstructive pulmonary disease (COPD)*. 2020 [cited 2022 08/12/2022]; Available from: <https://www.aihw.gov.au/reports/chronic-respiratory-conditions/copd/contents/about>.
33. Dhanjal, D.S., et al., *Concepts of advanced therapeutic delivery systems for the management of remodeling and inflammation in airway diseases*. Future Med Chem, 2022. **14**(4): p. 271-288.
34. Miravittles, M. and A. Ribera, *Understanding the impact of symptoms on the burden of COPD*. Respir Res, 2017. **18**(1): p. 67.
35. Bollmeier, S.G. and A.P. Hartmann, *Management of chronic obstructive pulmonary disease: A review focusing on exacerbations*. Am J Health Syst Pharm, 2020. **77**(4): p. 259-268.
36. Xie, M., et al., *Trends in prevalence and incidence of chronic respiratory diseases from 1990 to 2017*. Respir Res, 2020. **21**(1): p. 49.
37. Barnes, P.J., et al., *Chronic obstructive pulmonary disease*. Nat Rev Dis Primers, 2015. **1**: p. 15076.
38. Yusef, R.D., *Evolution of the GOLD documents for the diagnosis, management, and prevention of chronic obstructive pulmonary disease. Controversies and questions*. Am J Respir Crit Care Med, 2013. **188**(1): p. 4-5.
39. Agustí, A., et al., *FAQs about the GOLD 2011 assessment proposal of COPD: a comparative analysis of four different cohorts*. Eur Respir J, 2013. **42**(5): p. 1391-401.
40. Herbst, R.S., J.V. Heymach, and S.M. Lippman, *Lung cancer*. N Engl J Med, 2008. **359**(13): p. 1367-80.
41. Thun, M.J., et al., *The global burden of cancer: priorities for prevention*. Carcinogenesis, 2010. **31**(1): p. 100-10.

42. Jemal, A., et al., *Global cancer statistics*. CA Cancer J Clin, 2011. **61**(2): p. 69-90.
43. Statistics, A.B.o. 3303.0 - *Causes of Death, Australia, 2015*. 2017 [cited 2022 09/12/2022]; Available from: <https://www.abs.gov.au/ausstats/abs@.nsf/Lookup/by%20Subject/3303.0~2015~Main%20Features~Lung%20cancer~10004>.
44. Abu Rous, F., et al., *Lung Cancer Treatment Advances in 2022*. Cancer Invest, 2022: p. 1-20.
45. Saab, M.M., et al., *A systematic review of interventions to recognise, refer and diagnose patients with lung cancer symptoms*. NPJ Prim Care Respir Med, 2022. **32**(1): p. 42.
46. Wong, M.C.S., et al., *Incidence and mortality of lung cancer: global trends and association with socioeconomic status*. Sci Rep, 2017. **7**(1): p. 14300.
47. Massion, P.P. and D.P. Carbone, *The molecular basis of lung cancer: molecular abnormalities and therapeutic implications*. Respir Res, 2003. **4**(1): p. 12.
48. Dela Cruz, C.S., L.T. Tanoue, and R.A. Matthay, *Lung cancer: epidemiology, etiology, and prevention*. Clin Chest Med, 2011. **32**(4): p. 605-44.
49. Lu, F. and H.T. Zhang, *DNA methylation and nonsmall cell lung cancer*. Anat Rec (Hoboken), 2011. **294**(11): p. 1787-95.
50. Raso, M.G., N. Bota-Rabassedas, and Wistuba, II, *Pathology and Classification of SCLC*. Cancers (Basel), 2021. **13**(4).
51. Morty, R.E., M. Königshoff, and O. Eickelberg, *Transforming growth factor-beta signaling across ages: from distorted lung development to chronic obstructive pulmonary disease*. Proc Am Thorac Soc, 2009. **6**(7): p. 607-13.
52. Aschner, Y. and G.P. Downey, *Transforming Growth Factor- β : Master Regulator of the Respiratory System in Health and Disease*. Am J Respir Cell Mol Biol, 2016. **54**(5): p. 647-55.
53. Chung, K.F., *Cytokines in chronic obstructive pulmonary disease*. Eur Respir J Suppl, 2001. **34**: p. 50s-59s.
54. Takizawa, H., et al., *Increased expression of transforming growth factor-beta1 in small airway epithelium from tobacco smokers and patients with chronic obstructive pulmonary disease (COPD)*. Am J Respir Crit Care Med, 2001. **163**(6): p. 1476-83.
55. Marwick, J.A., et al., *Cigarette smoke-induced oxidative stress and TGF-beta1 increase p21waf1/cip1 expression in alveolar epithelial cells*. Ann N Y Acad Sci, 2002. **973**: p. 278-83.
56. Rennard, S.I., S. Togo, and O. Holz, *Cigarette smoke inhibits alveolar repair: a mechanism for the development of emphysema*. Proc Am Thorac Soc, 2006. **3**(8): p. 703-8.

57. Saito, A., M. Horie, and T. Nagase, *TGF- β Signaling in Lung Health and Disease*. International Journal of Molecular Sciences, 2018. **19**(8): p. 2460.
58. Hasegawa, Y., et al., *Transforming growth factor-beta1 level correlates with angiogenesis, tumor progression, and prognosis in patients with nonsmall cell lung carcinoma*. Cancer, 2001. **91**(5): p. 964-71.
59. Massagué, J., *TGFbeta in Cancer*. Cell, 2008. **134**(2): p. 215-30.
60. Markowitz, S., et al., *Inactivation of the type II TGF-beta receptor in colon cancer cells with microsatellite instability*. Science, 1995. **268**(5215): p. 1336-8.
61. Hahn, S.A., et al., *DPC4, a candidate tumor suppressor gene at human chromosome 18q21.1*. Science, 1996. **271**(5247): p. 350-3.
62. Vyas-Read, S., et al., *Nitric oxide attenuates epithelial-mesenchymal transition in alveolar epithelial cells*. Am J Physiol Lung Cell Mol Physiol, 2007. **293**(1): p. L212-21.
63. Yang, Y.C., et al., *Transforming growth factor-beta1 in inflammatory airway disease: a key for understanding inflammation and remodeling*. Allergy, 2012. **67**(10): p. 1193-1202.
64. Kumbhar, P., et al., *Inhalation delivery of repurposed drugs for lung cancer: Approaches, benefits and challenges*. J Control Release, 2022. **341**: p. 1-15.
65. Howington, J.A., et al., *Treatment of stage I and II non-small cell lung cancer: Diagnosis and management of lung cancer, 3rd ed: American College of Chest Physicians evidence-based clinical practice guidelines*. Chest, 2013. **143**(5 Suppl): p. e278S-e313S.
66. Pathak, N., S. Chitikela, and P.S. Malik, *Recent advances in lung cancer genomics: Application in targeted therapy*. Adv Genet, 2021. **108**: p. 201-275.
67. Bradley, J.D., et al., *Long-Term Results of NRG Oncology RTOG 0617: Standard- Versus High-Dose Chemoradiotherapy With or Without Cetuximab for Unresectable Stage III Non-Small-Cell Lung Cancer*. J Clin Oncol, 2020. **38**(7): p. 706-714.
68. Vinod, S.K. and E. Hau, *Radiotherapy treatment for lung cancer: Current status and future directions*. Respirology, 2020. **25 Suppl 2**: p. 61-71.
69. Haynes, A., et al., *Formulation and evaluation of aerosolized celecoxib for the treatment of lung cancer*. Pharm Res, 2005. **22**(3): p. 427-39.
70. Kim, S.H., et al., *Paclitaxel as third-line chemotherapy for small cell lung cancer failing both etoposide- and camptothecin-based chemotherapy*. Medicine, 2017. **96**(42): p. e8176.
71. Zarogoulidis, P., et al., *Feasibility and effectiveness of inhaled carboplatin in NSCLC patients*. Invest New Drugs, 2012. **30**(4): p. 1628-40.

72. Otterson, G.A., et al., *Phase I study of inhaled Doxorubicin for patients with metastatic tumors to the lungs*. Clin Cancer Res, 2007. **13**(4): p. 1246-52.
73. Yazbeck, V., et al., *An overview of chemotoxicity and radiation toxicity in cancer therapy*. Adv Cancer Res, 2022. **155**: p. 1-27.
74. Li, C., Y. Qiu, and Y. Zhang, *Research Progress on Therapeutic Targeting of Cancer-Associated Fibroblasts to Tackle Treatment-Resistant NSCLC*. Pharmaceuticals (Basel), 2022. **15**(11).
75. De Rubis, G. and M. Bebawy, *Extracellular Vesicles in Chemoresistance*. Subcell Biochem, 2021. **97**: p. 211-245.
76. Verschraegen, C.F., et al., *Clinical evaluation of the delivery and safety of aerosolized liposomal 9-nitro-20(s)-camptothecin in patients with advanced pulmonary malignancies*. Clin Cancer Res, 2004. **10**(7): p. 2319-26.
77. Roa, W.H., et al., *Inhalable nanoparticles, a non-invasive approach to treat lung cancer in a mouse model*. J Control Release, 2011. **150**(1): p. 49-55.
78. Padinharayil, H., et al., *Advances in the Lung Cancer Immunotherapy Approaches*. Vaccines (Basel), 2022. **10**(11).
79. Sham, N.O., et al., *Immunotherapy for Non-small Cell Lung Cancer: Current Agents and Potential Molecular Targets*. Anticancer Res, 2022. **42**(7): p. 3275-3284.
80. Leduc, C., et al., *Comorbidities in the management of patients with lung cancer*. Eur Respir J, 2017. **49**(3).
81. Das, S.K., et al., *Gene Therapies for Cancer: Strategies, Challenges and Successes*. J Cell Physiol, 2015. **230**(2): p. 259-71.
82. Dinh, T.D., et al., *Evaluation of osteoclastogenesis via NFkappaB decoy/mannosylated cationic liposome-mediated inhibition of pro-inflammatory cytokine production from primary cultured macrophages*. Pharm Res, 2011. **28**(4): p. 742-51.
83. Wongsurakiat, P., et al., *Acute respiratory illness in patients with COPD and the effectiveness of influenza vaccination: a randomized controlled study*. Chest, 2004. **125**(6): p. 2011-20.
84. McCarthy, B., et al., *Pulmonary rehabilitation for chronic obstructive pulmonary disease*. Cochrane Database Syst Rev, 2015(2): p. Cd003793.
85. Stoller, J.K., et al., *Oxygen therapy for patients with COPD: current evidence and the long-term oxygen treatment trial*. Chest, 2010. **138**(1): p. 179-87.
86. Cranston, J.M., et al., *Domiciliary oxygen for chronic obstructive pulmonary disease*. Cochrane Database Syst Rev, 2005. **2005**(4): p. Cd001744.

87. Sciruba, F.C., et al., *A randomized study of endobronchial valves for advanced emphysema*. N Engl J Med, 2010. **363**(13): p. 1233-44.
88. Riley, C.M. and F.C. Sciruba, *Diagnosis and Outpatient Management of Chronic Obstructive Pulmonary Disease: A Review*. Jama, 2019. **321**(8): p. 786-797.
89. Mei, D., et al., *Therapeutic RNA Strategies for Chronic Obstructive Pulmonary Disease*. Trends Pharmacol Sci, 2020. **41**(7): p. 475-486.
90. Tashkin, D.P., et al., *Comparison of the anticholinergic bronchodilator ipratropium bromide with metaproterenol in chronic obstructive pulmonary disease. A 90-day multi-center study*. Am J Med, 1986. **81**(5a): p. 81-90.
91. Braun, S.R., et al., *A comparison of the effect of ipratropium and albuterol in the treatment of chronic obstructive airway disease*. Arch Intern Med, 1989. **149**(3): p. 544-7.
92. Wilchesky, M., et al., *Bronchodilator use and the risk of arrhythmia in COPD: part 2: reassessment in the larger Quebec cohort*. Chest, 2012. **142**(2): p. 305-311.
93. *In chronic obstructive pulmonary disease, a combination of ipratropium and albuterol is more effective than either agent alone. An 85-day multicenter trial. COMBIVENT Inhalation Aerosol Study Group*. Chest, 1994. **105**(5): p. 1411-9.
94. Celli, B.R., et al., *Effect of pharmacotherapy on rate of decline of lung function in chronic obstructive pulmonary disease: results from the TORCH study*. Am J Respir Crit Care Med, 2008. **178**(4): p. 332-8.
95. Leuppi, J.D., et al., *Short-term vs conventional glucocorticoid therapy in acute exacerbations of chronic obstructive pulmonary disease: the REDUCE randomized clinical trial*. Jama, 2013. **309**(21): p. 2223-31.
96. Hodge, G., et al., *Steroid resistance in COPD is associated with impaired molecular chaperone Hsp90 expression by pro-inflammatory lymphocytes*. Respir Res, 2016. **17**(1): p. 135.
97. Aubier, M. and C. Roussos, *Effect of theophylline on respiratory muscle function*. Chest, 1985. **88**(2 Suppl): p. 91s-97s.
98. Horita, N., et al., *Chronic Use of Theophylline and Mortality in Chronic Obstructive Pulmonary Disease: A Meta-analysis*. Arch Bronconeumol, 2016. **52**(5): p. 233-8.
99. Martinez, F.J., et al., *Effect of roflumilast on exacerbations in patients with severe chronic obstructive pulmonary disease uncontrolled by combination therapy (REACT): a multicentre randomised controlled trial*. Lancet, 2015. **385**(9971): p. 857-66.
100. Albert, R.K., et al., *Azithromycin for prevention of exacerbations of COPD*. N Engl J Med, 2011. **365**(8): p. 689-98.

101. Poole, P., P.N. Black, and C.J. Cates, *Mucolytic agents for chronic bronchitis or chronic obstructive pulmonary disease*. Cochrane Database Syst Rev, 2012(8): p. Cd001287.
102. Sadowska, A.M., et al., *Role of N-acetylcysteine in the management of COPD*. Int J Chron Obstruct Pulmon Dis, 2006. **1**(4): p. 425-34.
103. Paudel, K.R., et al., *Recent Advances in Chronotherapy Targeting Respiratory Diseases*. Pharmaceutics, 2021. **13**(12).
104. Tan, C.L., et al., *Unravelling the molecular mechanisms underlying chronic respiratory diseases for the development of novel therapeutics via in vitro experimental models*. Eur J Pharmacol, 2022. **919**: p. 174821.
105. Devkota, H.P., et al., *Phytochemicals and their Nanoformulations Targeted for Pulmonary Diseases*, in *Advanced Drug Delivery Strategies for Targeting Chronic Inflammatory Lung Diseases*, D.K. Chellappan, K. Pabreja, and M. Faiyazuddin, Editors. 2022, Springer Singapore: Singapore. p. 95-106.
106. Clarence, D.D., et al., *Unravelling the Therapeutic Potential of Nano-Delivered Functional Foods in Chronic Respiratory Diseases*. Nutrients, 2022. **14**(18).
107. Wang, S., et al., *Chemical Constituents and Pharmacological Activity of Agarwood and Aquilaria Plants*. Molecules, 2018. **23**(2).
108. Alamil, J.M.R., et al., *Rediscovering the Therapeutic Potential of Agarwood in the Management of Chronic Inflammatory Diseases*. Molecules, 2022. **27**(9).
109. Cicero, A.F. and A. Baggioni, *Berberine and Its Role in Chronic Disease*. Adv Exp Med Biol, 2016. **928**: p. 27-45.
110. Och, A., R. Podgórski, and R. Nowak, *Biological Activity of Berberine-A Summary Update*. Toxins (Basel), 2020. **12**(11).
111. Devkota, H.P., et al., *Bioactive Compounds from Zingiber montanum and Their Pharmacological Activities with Focus on Zerumbone*. Applied Sciences, 2021. **11**(21): p. 10205.
112. Mohamad, M.S.B., et al., *The versatility of 18 β -glycyrrhetic acid in attenuating pulmonary inflammatory disorders*. Excli j, 2023. **22**: p. 188-190.
113. Tew, X.N., et al., *Immunological axis of berberine in managing inflammation underlying chronic respiratory inflammatory diseases*. Chem Biol Interact, 2020. **317**: p. 108947.
114. Achi, I.T., et al., *Multi-Target Potential of Berberine as an Antineoplastic and Antimetastatic Agent: A Special Focus on Lung Cancer Treatment*. Cells, 2022. **11**(21).
115. Liu, D., et al., *A Natural Isoquinoline Alkaloid With Antitumor Activity: Studies of the Biological Activities of Berberine*. Front Pharmacol, 2019. **10**: p. 9.

116. Katiyar, S.K., et al., *p53 Cooperates berberine-induced growth inhibition and apoptosis of non-small cell human lung cancer cells in vitro and tumor xenograft growth in vivo*. Mol Carcinog, 2009. **48**(1): p. 24-37.
117. Zheng, F., et al., *p38 α MAPK-mediated induction and interaction of FOXO3a and p53 contribute to the inhibited-growth and induced-apoptosis of human lung adenocarcinoma cells by berberine*. J Exp Clin Cancer Res, 2014. **33**(1): p. 36.
118. Peng, P.L., et al., *Inhibitory effect of berberine on the invasion of human lung cancer cells via decreased productions of urokinase-plasminogen activator and matrix metalloproteinase-2*. Toxicol Appl Pharmacol, 2006. **214**(1): p. 8-15.
119. Fu, L., et al., *Berberine Targets AP-2/hTERT, NF- κ B/COX-2, HIF-1 α /VEGF and Cytochrome-c/Caspase Signaling to Suppress Human Cancer Cell Growth*. PLoS One, 2013. **8**(7): p. e69240.
120. Li, C.L., et al., *Comparison of anti-inflammatory effects of berberine, and its natural oxidative and reduced derivatives from Rhizoma Coptidis in vitro and in vivo*. Phytomedicine, 2019. **52**: p. 272-283.
121. Lin, K., et al., *Berberine attenuates cigarette smoke-induced acute lung inflammation*. Inflammation, 2013. **36**(5): p. 1079-86.
122. Wang, W., et al., *Berberine Attenuates Cigarette Smoke Extract-induced Airway Inflammation in Mice: Involvement of TGF- β 1/Smads Signaling Pathway*. Curr Med Sci, 2019. **39**(5): p. 748-753.
123. Xu, D., et al., *Berberine attenuates cigarette smoke-induced airway inflammation and mucus hypersecretion in mice*. Int J Clin Exp Med, 2015. **8**(6): p. 8641-7.
124. Lee, C.H., et al., *Berberine suppresses inflammatory agents-induced interleukin-1beta and tumor necrosis factor-alpha productions via the inhibition of IkappaB degradation in human lung cells*. Pharmacol Res, 2007. **56**(3): p. 193-201.
125. Hashim, Y.Z., et al., *Aquilaria spp. (agarwood) as source of health beneficial compounds: A review of traditional use, phytochemistry and pharmacology*. J Ethnopharmacol, 2016. **189**: p. 331-60.
126. Chen, H.Q., et al., *Chemical constituents of agarwood originating from the endemic genus Aquilaria plants*. Chem Biodivers, 2012. **9**(2): p. 236-50.
127. Wong, Y.F., et al., *Evaluation of comprehensive two-dimensional gas chromatography with accurate mass time-of-flight mass spectrometry for the metabolic profiling of plant-fungus interaction in Aquilaria malaccensis*. J Chromatogr A, 2015. **1387**: p. 104-15.
128. Hashim, Y.Z., A. Phirdaous, and A. Azura, *Screening of anticancer activity from agarwood essential oil*. Pharmacognosy Res, 2014. **6**(3): p. 191-4.

129. Dahham, S.S., et al., *In vitro antimetastatic activity of Agarwood (Aquilaria crassna) essential oils against pancreatic cancer cells*. Alexandria Journal of Medicine, 2016. **52**(2): p. 141-150.
130. Dahham, S.S., et al. *In vivo anti-inflammatory activity of β -caryophyllene, evaluated by molecular imaging*. 2015.
131. Wang, S.L., et al., *2-(2-Phenylethyl)-4H-chromen-4-one Derivatives from the Resinous Wood of Aquilaria sinensis with Anti-Inflammatory Effects in LPS-Induced Macrophages*. Molecules, 2018. **23**(2).
132. Huo, H.X., et al., *Anti-inflammatory Dimeric 2-(2-Phenylethyl)chromones from the Resinous Wood of Aquilaria sinensis*. J Nat Prod, 2018. **81**(3): p. 543-553.
133. Girisa, S., et al., *Potential of Zerumbone as an Anti-Cancer Agent*. Molecules, 2019. **24**(4).
134. Chellappan, D.K., et al., *Targeting the mitochondria in chronic respiratory diseases*. Mitochondrion, 2022. **67**: p. 15-37.
135. Allam, V., et al., *Nutraceuticals and mitochondrial oxidative stress: bridging the gap in the management of bronchial asthma*. Environ Sci Pollut Res Int, 2022. **29**(42): p. 62733-62754.
136. Chellappan, D.K., et al., *Mitochondrial dysfunctions associated with chronic respiratory diseases and their targeted therapies: an update*. Future Med Chem, 2021. **13**(15): p. 1249-1251.
137. Hu, Z., et al., *Promotion of p53 expression and reactive oxidative stress production is involved in zerumbone-induced cisplatin sensitization of non-small cell lung cancer cells*. Biochimie, 2014. **107 Pt B**: p. 257-62.
138. Kang, C.G., et al., *Zerumbone Suppresses Osteopontin-Induced Cell Invasion Through Inhibiting the FAK/AKT/ROCK Pathway in Human Non-Small Cell Lung Cancer A549 Cells*. J Nat Prod, 2016. **79**(1): p. 156-60.
139. Kim, M.J. and J.M. Yun, *Molecular Mechanism of the Protective Effect of Zerumbone on Lipopolysaccharide-Induced Inflammation of THP-1 Cell-Derived Macrophages*. J Med Food, 2019. **22**(1): p. 62-73.
140. Ho, Y.C., et al., *Zerumbone reduced the inflammatory response of acute lung injury in endotoxin-treated mice via Akt-NF κ B pathway*. Chem Biol Interact, 2017. **271**: p. 9-14.
141. Jantan, I., et al., *Zerumbone from Zingiber zerumbet inhibits innate and adaptive immune responses in Balb/C mice*. Int Immunopharmacol, 2019. **73**: p. 552-559.
142. Haque, M.A., I. Jantan, and H. Harikrishnan, *Zerumbone suppresses the activation of inflammatory mediators in LPS-stimulated U937 macrophages through MyD88-dependent NF- κ B/MAPK/PI3K-Akt signaling pathways*. Int Immunopharmacol, 2018. **55**: p. 312-322.

143. Wang, G., et al., *Pharmacological Activity of Quercetin: An Updated Review*. Evid Based Complement Alternat Med, 2022. **2022**: p. 3997190.
144. Hasan, A.A., V. Tatarskiy, and E. Kalinina, *Synthetic Pathways and the Therapeutic Potential of Quercetin and Curcumin*. Int J Mol Sci, 2022. **23**(22).
145. Hardwick, J., et al., *Targeting Cancer using Curcumin Encapsulated Vesicular Drug Delivery Systems*. Curr Pharm Des, 2021. **27**(1): p. 2-14.
146. Prasher, P., et al., *Luteolin: a flavonoid with a multifaceted anticancer potential*. Cancer Cell Int, 2022. **22**(1): p. 386.
147. Chin, L.H., et al., *Molecular mechanisms of action of naringenin in chronic airway diseases*. Eur J Pharmacol, 2020. **879**: p. 173139.
148. Tripathi, A.K., A.K. Ray, and S.K. Mishra, *Molecular and pharmacological aspects of piperine as a potential molecule for disease prevention and management: evidence from clinical trials*. Beni Suf Univ J Basic Appl Sci, 2022. **11**(1): p. 16.
149. Solanki, N., et al., *Antiproliferative effects of boswellic acid-loaded chitosan nanoparticles on human lung cancer cell line A549*. Future Med Chem, 2020. **12**(22): p. 2019-2034.
150. Solanki, N., et al., *Boswellic Acids: A Critical Appraisal of Their Therapeutic and Nutritional Benefits in Chronic Inflammatory Diseases*. Endocr Metab Immune Disord Drug Targets, 2023.
151. Bakr, A.F., P. Shao, and M.A. Farag, *Recent advances in glycyrrhizin metabolism, health benefits, clinical effects and drug delivery systems for efficacy improvement; a comprehensive review*. Phytomedicine, 2022. **99**: p. 153999.
152. Han, M.K., et al., *Randomised clinical trial to determine the safety of quercetin supplementation in patients with chronic obstructive pulmonary disease*. BMJ Open Respir Res, 2020. **7**(1).
153. Pan, G.Y., et al., *The involvement of P-glycoprotein in berberine absorption*. Pharmacol Toxicol, 2002. **91**(4): p. 193-7.
154. Tsai, P.L. and T.H. Tsai, *Hepatobiliary excretion of berberine*. Drug Metab Dispos, 2004. **32**(4): p. 405-12.
155. Yin, J., H. Xing, and J. Ye, *Efficacy of berberine in patients with type 2 diabetes mellitus*. Metabolism, 2008. **57**(5): p. 712-7.
156. Kesharwani, S.S. and G.J. Bhat, *Formulation and Nanotechnology-Based Approaches for Solubility and Bioavailability Enhancement of Zerumbone*. Medicina (Kaunas), 2020. **56**(11).
157. Ibrahim, M.Y., et al. *Evaluation of acute toxicity and the effect of single injected doses of zerumbone on the kidney and*. 2010.

158. Oliviu, V., H. Simona Codruta, and F. Lorena, *Safety Profile of Essential Oils*, in *Essential Oils*, O. Mozaniel Santana de, C. Wanessa Almeida da, and S. Sebastião Gomes, Editors. 2020, IntechOpen: Rijeka. p. Ch. 3.
159. AbouAitah, K. and W. Lojkowski, *Nanomedicine as an Emerging Technology to Foster Application of Essential Oils to Fight Cancer*. Pharmaceuticals (Basel), 2022. **15**(7).
160. Murugan, D. and L. Rangasamy, *A perspective to weaponize microRNAs against lung cancer*. Noncoding RNA Res, 2023. **8**(1): p. 18-32.
161. Mehta, M., et al., *Interferon therapy for preventing COPD exacerbations*. Excli j, 2020. **19**: p. 1477-1480.
162. Imran, M., et al., *Dressing multifunctional nanoparticles with natural cell-derived membranes for superior chemotherapy*. Nanomedicine (Lond), 2022. **17**(10): p. 665-670.
163. Gu, W., et al., *Role of miR-195 in cigarette smoke-induced chronic obstructive pulmonary disease*. Int Immunopharmacol, 2018. **55**: p. 49-54.
164. Dang, X., et al., *miR-145-5p is associated with smoke-related chronic obstructive pulmonary disease via targeting KLF5*. Chem Biol Interact, 2019. **300**: p. 82-90.
165. Du, Y., et al., *MicroRNA-181c inhibits cigarette smoke-induced chronic obstructive pulmonary disease by regulating CCN1 expression*. Respir Res, 2017. **18**(1): p. 155.
166. Dong, J., et al., *Gene silencing of receptor-interacting protein 2 protects against cigarette smoke-induced acute lung injury*. Pharmacol Res, 2019. **139**: p. 560-568.
167. Dong, J., et al., *Ribosomal Protein S3 Gene Silencing Protects Against Cigarette Smoke-Induced Acute Lung Injury*. Mol Ther Nucleic Acids, 2018. **12**: p. 370-380.
168. Boehme, S.A., et al., *MAP3K19 Is Overexpressed in COPD and Is a Central Mediator of Cigarette Smoke-Induced Pulmonary Inflammation and Lower Airway Destruction*. PLoS One, 2016. **11**(12): p. e0167169.
169. Kelly, C., et al., *Therapeutic aerosol bioengineering of siRNA for the treatment of inflammatory lung disease by TNF α gene silencing in macrophages*. Mol Pharm, 2014. **11**(11): p. 4270-9.
170. Zoulikha, M., et al., *Pulmonary delivery of siRNA against acute lung injury/acute respiratory distress syndrome*. Acta Pharm Sin B, 2022. **12**(2): p. 600-620.
171. Jeon, T., et al., *Engineered Polymer-siRNA Polyplexes Provide Effective Treatment of Lung Inflammation*. ACS Nano, 2023. **17**(5): p. 4315-4326.
172. Reimann, S., et al., *Increased S100A4 expression in the vasculature of human COPD lungs and murine model of smoke-induced emphysema*. Respir Res, 2015. **16**: p. 127.

173. Wang, C.G., et al., *The association of neuron-derived orphan receptor 1 with pulmonary vascular remodeling in COPD patients*. Int J Chron Obstruct Pulmon Dis, 2018. **13**: p. 1177-1186.
174. Wu, L., et al., *Deposition of insoluble elastin by pulmonary fibroblasts from patients with COPD is increased by treatment with versican siRNA*. Int J Chron Obstruct Pulmon Dis, 2017. **12**: p. 267-273.
175. Gu, W., et al., *Long non-coding RNA TUG1 promotes airway remodelling by suppressing the miR-145-5p/DUSP6 axis in cigarette smoke-induced COPD*. J Cell Mol Med, 2019. **23**(11): p. 7200-7209.
176. Yu, Q., et al., *CD147 increases mucus secretion induced by cigarette smoke in COPD*. BMC Pulm Med, 2019. **19**(1): p. 29.
177. Tam, A., et al., *Hedgehog signaling in the airway epithelium of patients with chronic obstructive pulmonary disease*. Sci Rep, 2019. **9**(1): p. 3353.
178. Jamieson, K.C., et al., *Rhinovirus and Bacteria Synergistically Induce IL-17C Release from Human Airway Epithelial Cells To Promote Neutrophil Recruitment*. J Immunol, 2019. **202**(1): p. 160-170.
179. Khan, P., et al., *RNA-based therapies: A cog in the wheel of lung cancer defense*. Mol Cancer, 2021. **20**(1): p. 54.
180. Zhong, Y., et al., *Discovery and validation of extracellular vesicle-associated miRNAs as noninvasive detection biomarkers for early-stage non-small-cell lung cancer*. Mol Oncol, 2021. **15**(9): p. 2439-2452.
181. Xu, M., et al. *Nanoemulsion Co-Loaded with XIAP siRNA and Gambogic Acid for Inhalation Therapy of Lung Cancer*. International Journal of Molecular Sciences, 2022. **23**, DOI: 10.3390/ijms232214294.
182. Tong, J., et al., *microRNA-195 Promotes Small Cell Lung Cancer Cell Apoptosis via Inhibiting Rap2C Protein-Dependent MAPK Signal Transduction*. Technol Cancer Res Treat, 2020. **19**: p. 1533033820977546.
183. Wu, X., et al., *Long non-coding RNA LUCAT1 regulates the RAS pathway to promote the proliferation and invasion of malignant glioma cells through ABCB1*. Exp Cell Res, 2022. **421**(2): p. 113390.
184. Zhao, X., et al., *lncRNA PLAC2 Upregulates CDK6 by Directly Targeting miR-29C to Promote Cell Proliferation in Lung Squamous Cell Carcinoma*. Crit Rev Eukaryot Gene Expr, 2022. **32**(8): p. 55-67.
185. Liu, R., et al., *shRNA-mediated knockdown of KNTC1 inhibits non-small-cell lung cancer through regulating PSMB8*. Cell Death Dis, 2022. **13**(8): p. 685.

186. Tiong, T.Y., et al., *Targeting the SREBP-1/Hsa-Mir-497/SCAP/FASN Oncometabolic Axis Inhibits the Cancer Stem-like and Chemoresistant Phenotype of Non-Small Cell Lung Carcinoma Cells*. *Int J Mol Sci*, 2022. **23**(13).
187. Xu, S., et al., *microRNA-let-7e in serum-derived exosomes inhibits the metastasis of non-small-cell lung cancer in a SUV39H2/LSD1/CDH1-dependent manner*. *Cancer Gene Ther*, 2021. **28**(3-4): p. 250-264.
188. Liu, X.N., et al., *microRNA-204 shuttled by mesenchymal stem cell-derived exosomes inhibits the migration and invasion of non-small-cell lung cancer cells via the KLF7/AKT/HIF-1 α axis*. *Neoplasma*, 2021. **68**(4): p. 719-731.
189. Tian, W., et al., *Exosomal miR-338-3p suppresses non-small-cell lung cancer cells metastasis by inhibiting CHL1 through the MAPK signaling pathway*. *Cell Death Dis*, 2021. **12**(11): p. 1030.
190. Shao, N., L. Song, and X. Sun, *Exosomal circ_PIP5K1A regulates the progression of non-small cell lung cancer and cisplatin sensitivity by miR-101/ABCC1 axis*. *Mol Cell Biochem*, 2021. **476**(6): p. 2253-2267.
191. Ahmad, M.Z., et al., *Application of decoy oligonucleotides as novel therapeutic strategy: a contemporary overview*. *Curr Drug Discov Technol*, 2013. **10**(1): p. 71-84.
192. Cai, Z., K.M. Tchou-Wong, and W.N. Rom, *NF-kappaB in lung tumorigenesis*. *Cancers (Basel)*, 2011. **3**(4): p. 4258-68.
193. Feng, Q. and K. Xiao, *Nanoparticle-Mediated Delivery of STAT3 Inhibitors in the Treatment of Lung Cancer*. *Pharmaceutics*, 2022. **14**(12).
194. Zhang, H.L., Z.X. Zhang, and Y.J. Xu, *[The effects of nuclear factor kappa B decoy oligodeoxynucleotides on ciglitazone-induced differentiation of lung cancer cells A549]*. *Zhonghua Nei Ke Za Zhi*, 2004. **43**(3): p. 201-4.
195. Nishimura, A., et al., *Transfection of NF- κ B decoy oligodeoxynucleotide suppresses pulmonary metastasis by murine osteosarcoma*. *Cancer Gene Ther*, 2011. **18**(4): p. 250-9.
196. Zhang, X., et al., *STAT3-decoy oligodeoxynucleotide inhibits the growth of human lung cancer via down-regulating its target genes*. *Oncol Rep*, 2007. **17**(6): p. 1377-82.
197. Zhang, X., et al., *Therapeutic effects of STAT3 decoy oligodeoxynucleotide on human lung cancer in xenograft mice*. *BMC Cancer*, 2007. **7**: p. 149.
198. Njatcha, C., et al., *STAT3 Cyclic Decoy Demonstrates Robust Antitumor Effects in Non-Small Cell Lung Cancer*. *Mol Cancer Ther*, 2018. **17**(9): p. 1917-1926.
199. Corrie, L., et al. *Multivariate Data Analysis and Central Composite Design-Oriented Optimization of Solid Carriers for Formulation of Curcumin-Loaded Solid SNEDDS: Dissolution and Bioavailability Assessment*. *Pharmaceutics*, 2022. **14**, DOI: 10.3390/pharmaceutics14112395.

200. Tenchov, R., et al., *Lipid Nanoparticles horizontal line From Liposomes to mRNA Vaccine Delivery, a Landscape of Research Diversity and Advancement*. ACS Nano, 2021. **15**(11): p. 16982-17015.
201. Prasher, P., et al., *Targeting mucus barrier in respiratory diseases by chemically modified advanced delivery systems*. Chem Biol Interact, 2022. **365**: p. 110048.
202. Zolnik, B.S., et al., *Nanoparticles and the immune system*. Endocrinology, 2010. **151**(2): p. 458-65.
203. Rizvi, S.A.A. and A.M. Saleh, *Applications of nanoparticle systems in drug delivery technology*. Saudi Pharm J, 2018. **26**(1): p. 64-70.
204. Mikušová, V. and P. Mikuš, *Advances in Chitosan-Based Nanoparticles for Drug Delivery*. Int J Mol Sci, 2021. **22**(17).
205. Löndahl, J., et al., *Measurement techniques for respiratory tract deposition of airborne nanoparticles: a critical review*. J Aerosol Med Pulm Drug Deliv, 2014. **27**(4): p. 229-54.
206. Sukhanova, A., et al., *Dependence of Nanoparticle Toxicity on Their Physical and Chemical Properties*. Nanoscale Res Lett, 2018. **13**(1): p. 44.
207. Devkota, H.P., et al., *Applications of drug-delivery systems targeting inflammasomes in pulmonary diseases*. Nanomedicine (Lond), 2021. **16**(27): p. 2407-2410.
208. Shastri, M.D., et al., *Interleukin-13: A pivotal target against influenza-induced exacerbation of chronic lung diseases*. Life Sci, 2021. **283**: p. 119871.
209. Patel, V.K., et al., *Toll-like receptors, innate immune system, and lung diseases: a vital trilateral association*. Excli j, 2022. **21**: p. 519-523.
210. Aimonen, K., et al., *Role of Surface Chemistry in the In Vitro Lung Response to Nanofibrillated Cellulose*. Nanomaterials (Basel), 2021. **11**(2).
211. Smola, M., T. Vandamme, and A. Sokolowski, *Nanocarriers as pulmonary drug delivery systems to treat and to diagnose respiratory and non respiratory diseases*. Int J Nanomedicine, 2008. **3**(1): p. 1-19.
212. Khursheed, R., et al., *Biomedical applications of metallic nanoparticles in cancer: Current status and future perspectives*. Biomed Pharmacother, 2022. **150**: p. 112951.
213. Shipunova, V.O., et al., *Targeting Cancer Cell Tight Junctions Enhances PLGA-Based Photothermal Sensitizers' Performance In Vitro and In Vivo*. Pharmaceutics, 2021. **14**(1).
214. Garcia-Castillo, M.D., D.J. Chinnapen, and W.I. Lencer, *Membrane Transport across Polarized Epithelia*. Cold Spring Harb Perspect Biol, 2017. **9**(9).

215. Manzanares, D. and V. Ceña, *Endocytosis: The Nanoparticle and Submicron Nanocompounds Gateway into the Cell*. Pharmaceutics, 2020. **12**(4).
216. Paranjpe, M. and C.C. Müller-Goymann, *Nanoparticle-mediated pulmonary drug delivery: a review*. Int J Mol Sci, 2014. **15**(4): p. 5852-73.
217. Khursheed, R., et al., *Expanding the arsenal against pulmonary diseases using surface-functionalized polymeric micelles: breakthroughs and bottlenecks*. Nanomedicine (Lond), 2022. **17**(12): p. 881-911.
218. Nakamura, Y., et al., *Nanodrug Delivery: Is the Enhanced Permeability and Retention Effect Sufficient for Curing Cancer?* Bioconjug Chem, 2016. **27**(10): p. 2225-2238.
219. Barnes, P.J., *Distribution of receptor targets in the lung*. Proc Am Thorac Soc, 2004. **1**(4): p. 345-51.
220. Yoo, J., et al., *Active Targeting Strategies Using Biological Ligands for Nanoparticle Drug Delivery Systems*. Cancers (Basel), 2019. **11**(5).
221. Cohen, J.A., et al., *Acetal-modified dextran microparticles with controlled degradation kinetics and surface functionality for gene delivery in phagocytic and non-phagocytic cells*. Adv Mater, 2010. **22**(32): p. 3593-7.
222. Bachelder, E.M., et al., *Acetal-derivatized dextran: an acid-responsive biodegradable material for therapeutic applications*. J Am Chem Soc, 2008. **130**(32): p. 10494-5.
223. Torchilin, V.P., *Multifunctional nanocarriers*. Adv Drug Deliv Rev, 2006. **58**(14): p. 1532-55.
224. Allen, T.M. and P.R. Cullis, *Drug delivery systems: entering the mainstream*. Science, 2004. **303**(5665): p. 1818-22.
225. Farokhzad, O.C. and R. Langer, *Impact of nanotechnology on drug delivery*. ACS Nano, 2009. **3**(1): p. 16-20.
226. Lamprecht, A., et al., *Biodegradable nanoparticles for targeted drug delivery in treatment of inflammatory bowel disease*. J Pharmacol Exp Ther, 2001. **299**(2): p. 775-81.
227. Kamaly, N., et al., *Targeted polymeric therapeutic nanoparticles: design, development and clinical translation*. Chem Soc Rev, 2012. **41**(7): p. 2971-3010.
228. Mitchell, M.J., et al., *Engineering precision nanoparticles for drug delivery*. Nature Reviews Drug Discovery, 2021. **20**(2): p. 101-124.
229. Begines, B., et al., *Polymeric Nanoparticles for Drug Delivery: Recent Developments and Future Prospects*. Nanomaterials (Basel), 2020. **10**(7).

230. de França, J.O.C., et al., *Polymers Based on PLA from Synthesis Using D,L-Lactic Acid (or Racemic Lactide) and Some Biomedical Applications: A Short Review*. *Polymers (Basel)*, 2022. **14**(12).
231. Prasher, P., et al., *Advances and applications of dextran-based nanomaterials targeting inflammatory respiratory diseases*. *Journal of Drug Delivery Science and Technology*, 2022. **74**: p. 103598.
232. Dhanapal, J. and M. Balaraman Ravindran, *Chitosan/poly (lactic acid)-coated piceatannol nanoparticles exert an in vitro apoptosis activity on liver, lung and breast cancer cell lines*. *Artif Cells Nanomed Biotechnol*, 2018. **46**(sup1): p. 274-282.
233. Oh, Y.J., et al., *Preparation of budesonide-loaded porous PLGA microparticles and their therapeutic efficacy in a murine asthma model*. *Journal of Controlled Release*, 2011. **150**(1): p. 56-62.
234. Upadhyay, P., et al., *Transferrin-decorated thymoquinone-loaded PEG-PLGA nanoparticles exhibit anticarcinogenic effect in non-small cell lung carcinoma via the modulation of miR-34a and miR-16*. *Biomater Sci*, 2019. **7**(10): p. 4325-4344.
235. Adlrahan, E., et al., *Potential activity of free and PLGA/PEG nanoencapsulated nasturtium officinale extract in inducing cytotoxicity and apoptosis in human lung carcinoma A549 cells*. *Journal of Drug Delivery Science and Technology*, 2021. **61**: p. 102256.
236. Vij, N., et al., *Neutrophil targeted nano-drug delivery system for chronic obstructive lung diseases*. *Nanomedicine: Nanotechnology, Biology and Medicine*, 2016. **12**(8): p. 2415-2427.
237. Di Gioia, S. and M. Conese, *Polyethylenimine-mediated gene delivery to the lung and therapeutic applications*. *Drug Des Devel Ther*, 2009. **2**: p. 163-88.
238. Thomas, M., et al., *Identification of novel superior polycationic vectors for gene delivery by high-throughput synthesis and screening of a combinatorial library*. *Pharmaceutical research*, 2007. **24**(8): p. 1564-1571.
239. Corrie, L., et al., *Harnessing the dual role of polysaccharides in treating gastrointestinal diseases: As therapeutics and polymers for drug delivery*. *Chem Biol Interact*, 2022. **368**: p. 110238.
240. Okuda, T., et al., *Gene silencing in a mouse lung metastasis model by an inhalable dry small interfering RNA powder prepared using the supercritical carbon dioxide technique*. *Biol Pharm Bull*, 2013. **36**(7): p. 1183-91.
241. Prasher, P., et al., *Current-status and applications of polysaccharides in drug delivery systems*. *Colloid and Interface Science Communications*, 2021. **42**: p. 100418.
242. Prasher, P., et al., *Versatility of acetalated dextran in nanocarriers targeting respiratory diseases*. *Materials Letters*, 2022. **323**: p. 132600.

243. Bachelder, E.M., E.N. Pino, and K.M. Ainslie, *Acetalated Dextran: A Tunable and Acid-Labile Biopolymer with Facile Synthesis and a Range of Applications*. Chem Rev, 2017. **117**(3): p. 1915-1926.
244. Cohen, J.L., et al., *Acid-degradable cationic dextran particles for the delivery of siRNA therapeutics*. Bioconjug Chem, 2011. **22**(6): p. 1056-65.
245. Kannaujiya, V.K., et al., *Anticancer activity of NF κ B decoy oligonucleotide-loaded nanoparticles against human lung cancer*. Journal of Drug Delivery Science and Technology, 2023: p. 104328.
246. Chan, Y., et al., *Versatility of liquid crystalline nanoparticles in inflammatory lung diseases*. Nanomedicine (Lond), 2021. **16**(18): p. 1545-1548.
247. Mo, J., G. Milleret, and M. Nagaraj, *Liquid crystal nanoparticles for commercial drug delivery*. Liquid Crystals Reviews, 2017. **5**(2): p. 69-85.
248. Abd Elwakil, M.M., et al., *Inhalable lactoferrin-chondroitin nanocomposites for combined delivery of doxorubicin and ellagic acid to lung carcinoma*. Nanomedicine (Lond), 2018. **13**(16): p. 2015-2035.
249. Din, F.U., et al., *Effective use of nanocarriers as drug delivery systems for the treatment of selected tumors*. Int J Nanomedicine, 2017. **12**: p. 7291-7309.
250. Nichols, J.W. and Y.H. Bae, *EPR: Evidence and fallacy*. Journal of Controlled Release, 2014. **190**: p. 451-464.
251. Corrie, L., et al., *Antifibrotic Drugs for COVID-19: From Orphan Drugs to Blockbusters?* Current Respiratory Medicine Reviews, 2021. **17**(1): p. 8-12.
252. Nie, S., *Understanding and overcoming major barriers in cancer nanomedicine*. Nanomedicine (Lond), 2010. **5**(4): p. 523-8.
253. Zhang, H., et al., *Pharmacokinetics and treatment efficacy of camptothecin nanocrystals on lung metastasis*. Mol Pharm, 2014. **11**(1): p. 226-33.
254. Abdelaziz, H.M., et al., *Liquid crystalline assembly for potential combinatorial chemo-herbal drug delivery to lung cancer cells*. Int J Nanomedicine, 2019. **14**: p. 499-517.
255. Ganeshpurkar, A. and A.K. Saluja, *The Pharmacological Potential of Rutin*. Saudi Pharmaceutical Journal, 2017. **25**(2): p. 149-164.
256. Paudel, K.R., et al., *Rutin loaded liquid crystalline nanoparticles inhibit lipopolysaccharide induced oxidative stress and apoptosis in bronchial epithelial cells in vitro*. Toxicol In Vitro, 2020. **68**: p. 104961.
257. Paudel, K.R., et al., *Advances in research with rutin-loaded nanoformulations in mitigating lung diseases*. Future Med Chem, 2022. **14**(18): p. 1293-1295.

258. Mehta, M., et al., *Rutin-loaded liquid crystalline nanoparticles attenuate oxidative stress in bronchial epithelial cells: a PCR validation*. *Future Med Chem*, 2021. **13**(6): p. 543-549.
259. Paudel, K.R., et al., *Rutin loaded liquid crystalline nanoparticles inhibit non-small cell lung cancer proliferation and migration in vitro*. *Life Sci*, 2021. **276**: p. 119436.
260. Wadhwa, R., et al., *Anti-inflammatory and anticancer activities of Naringenin-loaded liquid crystalline nanoparticles in vitro*. *J Food Biochem*, 2021. **45**(1): p. e13572.
261. Manandhar, B., et al., *Zerumbone-incorporated liquid crystalline nanoparticles inhibit proliferation and migration of non-small-cell lung cancer in vitro*. *Naunyn Schmiedebergs Arch Pharmacol*, 2023.
262. Paudel, K.R., et al., *Berberine-loaded liquid crystalline nanoparticles inhibit non-small cell lung cancer proliferation and migration in vitro*. *Environ Sci Pollut Res Int*, 2022. **29**(31): p. 46830-46847.
263. Mehta, M., et al., *Berberine loaded liquid crystalline nanostructure inhibits cancer progression in adenocarcinomic human alveolar basal epithelial cells in vitro*. *J Food Biochem*, 2021. **45**(11): p. e13954.
264. Malyla, V., et al., *Berberine nanostructures attenuate β -catenin, a key component of epithelial mesenchymal transition in lung adenocarcinoma*. *Naunyn Schmiedebergs Arch Pharmacol*, 2023.
265. Alnuqaydan, A.M., et al., *Evaluation of the Cytotoxic Activity and Anti-Migratory Effect of Berberine-Phytantriol Liquid Crystalline Nanoparticle Formulation on Non-Small-Cell Lung Cancer In Vitro*. *Pharmaceutics*, 2022. **14**(6).
266. Paudel, K.R., et al., *Cytotoxic mechanisms of berberine-phytantriol liquid crystalline nanoparticles against non-small-cell lung cancer*. *Excli j*, 2023. **22**: p. 516-519.
267. Paudel, K.R., et al., *Attenuation of Cigarette-Smoke-Induced Oxidative Stress, Senescence, and Inflammation by Berberine-Loaded Liquid Crystalline Nanoparticles: In Vitro Study in 16HBE and RAW264.7 Cells*. *Antioxidants (Basel)*, 2022. **11**(5).
268. Alnuqaydan, A.M., et al., *Phytantriol-Based Berberine-Loaded Liquid Crystalline Nanoparticles Attenuate Inflammation and Oxidative Stress in Lipopolysaccharide-Induced RAW264.7 Macrophages*. *Nanomaterials (Basel)*, 2022. **12**(23).
269. Corrie, L., et al., *Polysaccharide, fecal microbiota, and curcumin-based novel oral colon-targeted solid self-nanoemulsifying delivery system: formulation, characterization, and in-vitro anticancer evaluation*. *Materials Today Chemistry*, 2022. **26**: p. 101165.
270. Jaiswal, M., R. Dudhe, and P.K. Sharma, *Nanoemulsion: an advanced mode of drug delivery system*. *3 Biotech*, 2015. **5**(2): p. 123-127.

271. Chang, H.B. and B.H. Chen, *Inhibition of lung cancer cells A549 and H460 by curcuminoid extracts and nanoemulsions prepared from Curcuma longa Linnaeus*. Int J Nanomedicine, 2015. **10**: p. 5059-80.
272. Wan, K., et al., *Novel nanoemulsion based lipid nanosystems for favorable in vitro and in vivo characteristics of curcumin*. Int J Pharm, 2016. **504**(1-2): p. 80-8.
273. Arbain, N.H., et al., *In vitro evaluation of the inhalable quercetin loaded nanoemulsion for pulmonary delivery*. Drug Deliv Transl Res, 2019. **9**(2): p. 497-507.
274. Ye, H., X. He, and X. Feng, *Developing neobavaisoflavone nanoemulsion suppresses lung cancer progression by regulating tumor microenvironment*. Biomed Pharmacother, 2020. **129**: p. 110369.
275. Md, S., et al., *Formulation Design, Statistical Optimization, and In Vitro Evaluation of a Naringenin Nanoemulsion to Enhance Apoptotic Activity in A549 Lung Cancer Cells*. Pharmaceuticals (Basel), 2020. **13**(7).
276. Xiao, Z., et al., *Protection of agarwood essential oil aroma by nanocellulose-graft-poly(lactic acid)*. Int J Biol Macromol, 2021. **183**: p. 743-752.
277. Yousefian Rad, E., et al., *Citrus lemon essential oil nanoemulsion (CLEO-NE), a safe cell-dependent apoptosis inducer in human A549 lung cancer cells with anti-angiogenic activity*. J Microencapsul, 2020. **37**(5): p. 394-402.
278. Fazelifar, P., M.H. Tabrizi, and A. Rafiee, *The Arachis hypogaea Essential Oil Nanoemulsion as an Efficient Safe Apoptosis Inducer in Human Lung Cancer Cells (A549)*. Nutr Cancer, 2021. **73**(6): p. 1059-1067.
279. Zhang, G., et al., *Inhalable Jojoba Oil Dry Nanoemulsion Powders for the Treatment of Lipopolysaccharide- or H(2)O(2)-Induced Acute Lung Injury*. Pharmaceutics, 2021. **13**(4).
280. Navaei Shoorvarzi, S., et al., *Citrus aurantium L. bloom essential oil nanoemulsion: Synthesis, characterization, cytotoxicity, and its potential health impacts on mice*. J Food Biochem, 2020. **44**(5): p. e13181.
281. De Rubis, G., et al., *Agarwood Oil Nanoemulsion Attenuates Cigarette Smoke-Induced Inflammation and Oxidative Stress Markers in BCI-NS1.1 Airway Epithelial Cells*. Nutrients, 2023. **15**(4).
282. Alamil, J.M.R., et al., *Agarwood oil nanoemulsion attenuates production of lipopolysaccharide (LPS)-induced proinflammatory cytokines, IL-6 and IL-8 in human bronchial epithelial cells*. EXCLI Journal, 2023. **22**: p. 681-685.
283. Amani, A., et al., *Evaluation of a Nanoemulsion-Based Formulation for Respiratory Delivery of Budesonide by Nebulizers*. AAPS PharmSciTech, 2010. **11**(3): p. 1147-1151.

284. Li, Z., et al., *Increased Survival by Pulmonary Treatment of Established Lung Metastases with Dual STAT3/CXCR4 Inhibition by siRNA Nanoemulsions*. *Mol Ther*, 2019. **27**(12): p. 2100-2110.
285. Sercombe, L., et al., *Advances and Challenges of Liposome Assisted Drug Delivery*. *Front Pharmacol*, 2015. **6**: p. 286.
286. Corrie, L., R. Gundaram, and L. Kukatil, *Formulation and Evaluation of Cassia tora Phytosomal Gel Using Central Composite Design*. *Recent Innovations in Chemical Engineering (Formerly Recent Patents on Chemical Engineering)*, 2021. **14**(4): p. 347-357.
287. Nakhaei, P., et al., *Liposomes: Structure, Biomedical Applications, and Stability Parameters With Emphasis on Cholesterol*. *Front Bioeng Biotechnol*, 2021. **9**: p. 705886.
288. Konduri, K.S., et al., *Efficacy of liposomal budesonide in experimental asthma*. *J Allergy Clin Immunol*, 2003. **111**(2): p. 321-7.
289. McCaskill, J., et al., *Efficient Biodistribution and Gene Silencing in the Lung epithelium via Intravenous Liposomal Delivery of siRNA*. *Mol Ther Nucleic Acids*, 2013. **2**(6): p. e96.
290. Zhang, T., et al., *Inhalation treatment of primary lung cancer using liposomal curcumin dry powder inhalers*. *Acta Pharm Sin B*, 2018. **8**(3): p. 440-448.
291. Riaz, M.K., et al., *Pulmonary delivery of transferrin receptors targeting peptide surface-functionalized liposomes augments the chemotherapeutic effect of quercetin in lung cancer therapy*. *Int J Nanomedicine*, 2019. **14**: p. 2879-2902.
292. Zhou, X., et al., *RGD-modified nanoliposomes containing quercetin for lung cancer targeted treatment*. *Onco Targets Ther*, 2018. **11**: p. 5397-5405.
293. Seguin, J., et al., *Liposomal encapsulation of the natural flavonoid fisetin improves bioavailability and antitumor efficacy*. *Int J Pharm*, 2013. **444**(1-2): p. 146-54.
294. Wang, X.X., et al., *The use of mitochondrial targeting resveratrol liposomes modified with a dequalinium polyethylene glycol-distearoylphosphatidyl ethanolamine conjugate to induce apoptosis in resistant lung cancer cells*. *Biomaterials*, 2011. **32**(24): p. 5673-87.
295. Théry, C., L. Zitvogel, and S. Amigorena, *Exosomes: composition, biogenesis and function*. *Nat Rev Immunol*, 2002. **2**(8): p. 569-79.
296. Sharma, K., et al., *The Emerging Role of Pericyte-Derived Extracellular Vesicles in Vascular and Neurological Health*. *Cells*, 2022. **11**(19).
297. Tai, Y.L., et al., *Exosomes in cancer development and clinical applications*. *Cancer Sci*, 2018. **109**(8): p. 2364-2374.
298. Luan, X., et al., *Engineering exosomes as refined biological nanoplatfoms for drug delivery*. *Acta Pharmacol Sin*, 2017. **38**(6): p. 754-763.

299. Manandhar, B., et al., *Applications of extracellular vesicles as a drug-delivery system for chronic respiratory diseases*. *Nanomedicine (Lond)*, 2022. **17**(12): p. 817-820.
300. Cui, Z., et al., *Lung-specific exosomes for co-delivery of CD47 blockade and cisplatin for the treatment of non-small cell lung cancer*. *Thorac Cancer*, 2022. **13**(19): p. 2723-2731.
301. Munagala, R., et al., *Bovine milk-derived exosomes for drug delivery*. *Cancer Lett*, 2016. **371**(1): p. 48-61.
302. Aqil, F., et al., *Exosomal formulation enhances therapeutic response of celastrol against lung cancer*. *Exp Mol Pathol*, 2016. **101**(1): p. 12-21.
303. Wani, J.A., et al., *MiRNAs in Lung Cancer: Diagnostic, Prognostic, and Therapeutic Potential*. *Diagnostics (Basel)*, 2022. **12**(7).
304. Jeong, K., et al., *Exosome-mediated microRNA-497 delivery for anti-cancer therapy in a microfluidic 3D lung cancer model*. *Lab Chip*, 2020. **20**(3): p. 548-557.
305. Zhang, D., et al., *Exosome-Mediated Small RNA Delivery: A Novel Therapeutic Approach for Inflammatory Lung Responses*. *Mol Ther*, 2018. **26**(9): p. 2119-2130.
306. Han, Y., et al., *Nebulization of extracellular vesicles: A promising small RNA delivery approach for lung diseases*. *J Control Release*, 2022. **352**: p. 556-569.
307. Li, Z., et al., *Non-Small-Cell Lung Cancer Regression by siRNA Delivered Through Exosomes That Display EGFR RNA Aptamer*. *Nucleic Acid Ther*, 2021. **31**(5): p. 364-374.
308. Liu, S., et al., *Exosome-mediated miR-7-5p delivery enhances the anticancer effect of Everolimus via blocking MNK/eIF4E axis in non-small cell lung cancer*. *Cell Death Dis*, 2022. **13**(2): p. 129.
309. Nie, H., et al., *Use of lung-specific exosomes for miRNA-126 delivery in non-small cell lung cancer*. *Nanoscale*, 2020. **12**(2): p. 877-887.
310. Abbasi, E., et al., *Dendrimers: synthesis, applications, and properties*. *Nanoscale Res Lett*, 2014. **9**(1): p. 247.
311. Singh, J., et al., *Dendrimers in anticancer drug delivery: mechanism of interaction of drug and dendrimers*. *Artificial Cells, Nanomedicine, and Biotechnology*, 2016. **44**(7): p. 1626-1634.
312. Longmire, M., P.L. Choyke, and H. Kobayashi, *Dendrimer-based contrast agents for molecular imaging*. *Curr Top Med Chem*, 2008. **8**(14): p. 1180-6.
313. Kobayashi, H. and M.W. Brechbiel, *Dendrimer-based macromolecular MRI contrast agents: characteristics and application*. *Mol Imaging*, 2003. **2**(1): p. 1-10.

314. Crintea, A., et al., *The Nanosystems Involved in Treating Lung Cancer*. Life (Basel), 2021. **11**(7).
315. Nakhband, A., et al., *Bioimpacts of anti epidermal growth factor receptor antisense complexed with polyamidoamine dendrimers in human lung epithelial adenocarcinoma cells*. J Biomed Nanotechnol, 2010. **6**(4): p. 360-9.
316. Bharatwaj, B., et al., *Dendrimer nanocarriers for transport modulation across models of the pulmonary epithelium*. Mol Pharm, 2015. **12**(3): p. 826-38.
317. Khan, O.F., et al., *Dendrimer-Inspired Nanomaterials for the in Vivo Delivery of siRNA to Lung Vasculature*. Nano Lett, 2015. **15**(5): p. 3008-16.
318. Palmerston Mendes, L., J. Pan, and V.P. Torchilin, *Dendrimers as Nanocarriers for Nucleic Acid and Drug Delivery in Cancer Therapy*. Molecules, 2017. **22**(9).
319. Ramanunni, A.K., et al., *Nanocarriers for treatment of dermatological diseases: Principle, perspective and practices*. Eur J Pharmacol, 2021. **890**: p. 173691.
320. Zhang, Y., Y. Huang, and S. Li, *Polymeric micelles: nanocarriers for cancer-targeted drug delivery*. AAPS PharmSciTech, 2014. **15**(4): p. 862-71.
321. Hanafy, N.A.N., M. El-Kemary, and S. Leporatti, *Micelles Structure Development as a Strategy to Improve Smart Cancer Therapy*. Cancers (Basel), 2018. **10**(7).
322. Xu, H., et al., *Characterization of the Uptake Efficiency and Cytotoxicity of Tetrandrine-Loaded Poly(N-vinylpyrrolidone)-Block-Poly(ϵ -caprolactone) (PVP-b-PCL) Nanoparticles in the A549 Lung Adenocarcinoma Cell Line*. J Biomed Nanotechnol, 2016. **12**(8): p. 1699-707.
323. Yin, H.T., et al., *In vivo evaluation of curcumin-loaded nanoparticles in a A549 xenograft mice model*. Asian Pac J Cancer Prev, 2013. **14**(1): p. 409-12.
324. Zhu, J.J., et al., *Delivery of acetylthevetin B, an antitumor cardiac glycoside, using polymeric micelles for enhanced therapeutic efficacy against lung cancer cells*. Acta Pharmacol Sin, 2017. **38**(2): p. 290-300.
325. Ding, Y., et al., *Development and evaluation of a novel drug delivery: Soluplus®/TPGS mixed micelles loaded with piperine in vitro and in vivo*. Drug Dev Ind Pharm, 2018. **44**(9): p. 1409-1416.
326. Mishra, B. and J. Singh, *Novel drug delivery systems and significance in respiratory diseases. Targeting Chronic Inflammatory Lung Diseases Using Advanced Drug Delivery Systems*, 2020: p. 57-95.
327. Geiser, M., et al., *Cellular uptake and localization of inhaled gold nanoparticles in lungs of mice with chronic obstructive pulmonary disease*. Particle and Fibre Toxicology, 2013. **10**(1): p. 19.

328. Alkilany, A.M. and C.J. Murphy, *Toxicity and cellular uptake of gold nanoparticles: what we have learned so far?* Journal of Nanoparticle Research, 2010. **12**(7): p. 2313-2333.
329. Yang, Y., et al., *Au-siRNA@ aptamer nanocages as a high-efficiency drug and gene delivery system for targeted lung cancer therapy.* J Nanobiotechnology, 2021. **19**(1): p. 54.
330. Zhuang, M., et al., *Radiosensitizing effect of gold nanoparticle loaded with small interfering RNA-SP1 on lung cancer: AuNPs-si-SP1 regulates GZMB for radiosensitivity.* Transl Oncol, 2021. **14**(12): p. 101210.
331. Shi, S.J., et al., *Solid lipid nanoparticles loaded with anti-microRNA oligonucleotides (AMOs) for suppression of microRNA-21 functions in human lung cancer cells.* Pharm Res, 2012. **29**(1): p. 97-109.
332. Karthikeyan, S., et al., *Anticancer activity of resveratrol-loaded gelatin nanoparticles on NCI-H460 non-small cell lung cancer cells.* Biomedicine & Preventive Nutrition, 2013. **3**(1): p. 64-73.
333. Wang, P., et al., *The formulation and delivery of curcumin with solid lipid nanoparticles for the treatment of on non-small cell lung cancer both in vitro and in vivo.* Mater Sci Eng C Mater Biol Appl, 2013. **33**(8): p. 4802-8.
334. Yu, H., et al., *Induction of apoptosis in non-small cell lung cancer by downregulation of MDM2 using pH-responsive PMPC-b-PDPA/siRNA complex nanoparticles.* Biomaterials, 2013. **34**(11): p. 2738-47.
335. Zhao, H., et al., *Nanoemulsion loaded with lycobetaine-oleic acid ionic complex: physicochemical characteristics, in vitro, in vivo evaluation, and antitumor activity.* Int J Nanomedicine, 2013. **8**: p. 1959-73.
336. Patil, S., et al., *Enhanced oral bioavailability and anticancer activity of novel curcumin loaded mixed micelles in human lung cancer cells.* Phytomedicine, 2015. **22**(12): p. 1103-1111.
337. Kumar, S.P., et al., *Antioxidant studies of chitosan nanoparticles containing naringenin and their cytotoxicity effects in lung cancer cells.* International Journal of Biological Macromolecules, 2015. **78**: p. 87-95.
338. Ceña, V., et al., *Aptamer-Dendrimer Bioconjugates for Targeted Delivery of miR-34a Expressing Plasmid and Antitumor Effects in Non-Small Cell Lung Cancer Cells.* Plos One, 2015. **10**(9): p. e0139136.
339. Wu, H., et al., *Preparation and antitumor evaluation of self-assembling oleanolic acid-loaded Pluronic P105/d- α -tocopheryl polyethylene glycol succinate mixed micelles for non-small-cell lung cancer treatment.* (1178-2013 (Electronic)).
340. Zhao, M.H., et al., *Quercetin-loaded mixed micelles exhibit enhanced cytotoxic efficacy in non-small cell lung cancer in vitro.* Exp Ther Med, 2017. **14**(6): p. 5503-5508.

341. Tammina, S.K., et al., *Cytotoxicity study of Piper nigrum seed mediated synthesized SnO₂ nanoparticles towards colorectal (HCT116) and lung cancer (A549) cell lines*. J Photochem Photobiol B, 2017. **166**: p. 158-168.
342. Amirsaadat, S., et al., *Silibinin-loaded magnetic nanoparticles inhibit hTERT gene expression and proliferation of lung cancer cells*. Artif Cells Nanomed Biotechnol, 2017. **45**(8): p. 1649-1656.
343. Liu, T.T., et al., *Preparation, characterization, and evaluation of antitumor effect of Brucea javanica oil cationic nanoemulsions*. Int J Nanomedicine, 2016. **11**: p. 2515-29.
344. Zhu, W.T., et al., *Delivery of curcumin by directed self-assembled micelles enhances therapeutic treatment of non-small-cell lung cancer*. Int J Nanomedicine, 2017. **12**: p. 2621-2634.
345. Yang, L., et al., *Targeted delivery of ginsenoside compound K using TPGS/PEG-PCL mixed micelles for effective treatment of lung cancer*. (1178-2013 (Electronic)).
346. Qiao, J.-B., et al., *Aerosol delivery of biocompatible dihydroergotamine-loaded PLGA-PSPE polymeric micelles for efficient lung cancer therapy*. Polymer Chemistry, 2017. **8**(9): p. 1540-1554.
347. Castro-Aceituno, V., et al., *Pleuropteris multiflorus (Hasuo) mediated straightforward eco-friendly synthesis of silver, gold nanoparticles and evaluation of their anti-cancer activity on A549 lung cancer cell line*. Biomed Pharmacother, 2017. **93**: p. 995-1003.
348. Vijayakumar, S., et al., *Therapeutic effects of gold nanoparticles synthesized using Musa paradisiaca peel extract against multiple antibiotic resistant Enterococcus faecalis biofilms and human lung cancer cells (A549)*. Microbial Pathogenesis, 2017. **102**: p. 173-183.
349. Pereira, F.G., et al., *Cytotoxic effects of the essential oil from leaves of Casearia sylvestris Sw.(Salicaceae) and its nanoemulsion on A549 tumor cell line*. Boletín Latinoamericano y del Caribe de Plantas Medicinales y Aromáticas, 2017. **16**(5): p. 506-512.
350. Lin, C., et al., *Pulmonary delivery of triptolide-loaded liposomes decorated with anti-carbonic anhydrase IX antibody for lung cancer therapy*. Sci Rep, 2017. **7**(1): p. 1097.
351. Muddineti, O.S., et al., *Cholesterol-grafted chitosan micelles as a nanocarrier system for drug-siRNA co-delivery to the lung cancer cells*. International Journal of Biological Macromolecules, 2018. **118**: p. 857-863.
352. Rajeshkumar, S., et al., *Biosynthesis of zinc oxide nanoparticles using Mangifera indica leaves and evaluation of their antioxidant and cytotoxic properties in lung cancer (A549) cells*. Enzyme and Microbial Technology, 2018. **117**: p. 91-95.
353. Parashar, P., et al., *Hyaluronic Acid Decorated Naringenin Nanoparticles: Appraisal of Chemopreventive and Curative Potential for Lung Cancer*. Pharmaceutics, 2018. **10**(1).

354. Dadashpour, M., et al., *Biomimetic synthesis of silver nanoparticles using Matricaria chamomilla extract and their potential anticancer activity against human lung cancer cells*. Mater Sci Eng C Mater Biol Appl, 2018. **92**: p. 902-912.
355. Parayath, N.N., A. Parikh, and M.M. Amiji, *Repolarization of Tumor-Associated Macrophages in a Genetically Engineered Non-small Cell Lung Cancer Model by Intraperitoneal Administration of Hyaluronic Acid-Based Nanoparticles Encapsulating MicroRNA-125b*. Nano Letters, 2018. **18**(6): p. 3571-3579.
356. Moulaie, S., A. Mirzaie, and E. Aliasgari, *Antibacterial and anticancer activities of silver nanoparticles fabricated by the Artemisia scoparia extract against lung cancer cell line (A549)*. KAUMS Journal (FEYZ), 2018. **22**(5): p. 487-496.
357. Khan, I., et al., *In vitro and in vivo antitumor potential of carvacrol nanoemulsion against human lung adenocarcinoma A549 cells via mitochondrial mediated apoptosis*. Sci Rep, 2018. **8**(1): p. 144.
358. Kanipandian, N., D. Li, and S. Kannan, *Induction of intrinsic apoptotic signaling pathway in A549 lung cancer cells using silver nanoparticles from Gossypium hirsutum and evaluation of in vivo toxicity*. Biotechnology Reports, 2019. **23**: p. e00339.
359. Zhang, W., et al., *Antitumor effect of hyaluronic-acid-modified chitosan nanoparticles loaded with siRNA for targeted therapy for non-small cell lung cancer*. Int J Nanomedicine, 2019. **14**: p. 5287-5301.
360. Cyril, N., et al., *Assessment of antioxidant, antibacterial and anti-proliferative (lung cancer cell line A549) activities of green synthesized silver nanoparticles from Derris trifoliata*. Toxicol Res (Camb), 2019. **8**(2): p. 297-308.
361. Magalhaes, M., et al., *miR-29b and retinoic acid co-delivery: a promising tool to induce a synergistic antitumoral effect in non-small cell lung cancer cells*. Drug Deliv Transl Res, 2020. **10**(5): p. 1367-1380.
362. Song, Y., et al., *Folic acid (FA)-conjugated mesoporous silica nanoparticles combined with MRP-1 siRNA improves the suppressive effects of myricetin on non-small cell lung cancer (NSCLC)*. Biomedicine & Pharmacotherapy, 2020. **125**: p. 109561.
363. Aldawsari, H.M., et al., *Preparation and Characterization of Chitosan Coated PLGA Nanoparticles of Resveratrol: Improved Stability, Antioxidant and Apoptotic Activities in H1299 Lung Cancer Cells*. Coatings, 2020. **10**(5): p. 439.
364. Chen, B.H., et al., *Anticancer effects of epigallocatechin-3-gallate nanoemulsion on lung cancer cells through the activation of AMP-activated protein kinase signaling pathway*. Sci Rep, 2020. **10**(1): p. 5163.
365. Tavakkol Afshari, H.S., et al., *Anethum Graveolens Essential Oil Nanoemulsions (AGEO-NE) as an Exclusive Apoptotic Inducer in Human Lung Adenocarcinoma (A549) Cells*. Nutr Cancer, 2022. **74**(4): p. 1411-1419.

366. Padmini, R., et al., *Cytotoxic effect of silver nanoparticles synthesized from ethanolic extract of Allium sativum on A549 lung cancer cell line*. Journal of King Saud University - Science, 2022. **34**(4): p. 102001.
367. Abd-Rabou, A.A. and A.E. Edris, *Frankincense essential oil nanoemulsion specifically induces lung cancer apoptosis and inhibits survival pathways*. Cancer Nanotechnology, 2022. **13**(1).
368. Etminan, A., et al., *Ultrasonic Nano emulsification of Apricot Kernel Oil and Its Therapeutics Effects on Suppression of Human Lung Cancer Cells (A549)*. Materials Technology, 2022. **37**(14): p. 3231-3240.
369. Duska, L.R., et al., *A phase Ib/II and pharmacokinetic study of EP0057 (formerly CRLX101) in combination with weekly paclitaxel in patients with recurrent or persistent epithelial ovarian, fallopian tube, or primary peritoneal cancer*. Gynecol Oncol, 2021. **160**(3): p. 688-695.
370. Reid, G., et al., *Clinical development of TargomiRs, a miRNA mimic-based treatment for patients with recurrent thoracic cancer*. Epigenomics, 2016. **8**(8): p. 1079-85.
371. Quéméner, A.M., et al., *Non-canonical miRNA-RNA base-pairing impedes tumor suppressor activity of miR-16*. Life Sci Alliance, 2022. **5**(12).
372. Whittle, J.R., et al., *First in human nanotechnology doxorubicin delivery system to target epidermal growth factor receptors in recurrent glioblastoma*. J Clin Neurosci, 2015. **22**(12): p. 1889-94.
373. Lambert, A.A. and M.T. Dransfield, *COPD Overlap Syndromes: Asthma and Beyond*. Chronic Obstr Pulm Dis, 2016. **3**(1): p. 459-465.
374. Park, H., et al., *Prevalence and impact of airway diseases on clinical outcomes in idiopathic pulmonary fibrosis*. Korean J Intern Med, 2022. **37**(2): p. 387-397.
375. Bates, M., *The mRNA Revolution is Coming*. IEEE Pulse, 2021. **12**(6): p. 2-5.
376. Damase, T.R., et al., *The Limitless Future of RNA Therapeutics*. Front Bioeng Biotechnol, 2021. **9**: p. 628137.
377. Baptista, B., et al., *mRNA, a Revolution in Biomedicine*. Pharmaceutics, 2021. **13**(12).
378. Vishweshwaraiah, Y.L. and N.V. Dokholyan, *mRNA vaccines for cancer immunotherapy*. Front Immunol, 2022. **13**: p. 1029069.
379. Darvin, P., A. Chandrasekharan, and T.R. Santhosh Kumar, *Chapter 1 - Introduction to smart drug delivery systems*, in *Biomimetic Nanoengineered Materials for Advanced Drug Delivery*, A.R. Unnithan, et al., Editors. 2019, Elsevier. p. 1-9.

RATIONALE, HYPOTHESIS, AND AIMS OF THE PRESENT WORK

Chronic respiratory diseases (CRDs), including chronic obstructive pulmonary disease (COPD) and lung cancer (LC), are today considered among the major causes of death throughout the world. These diseases share common aetiological factors, particularly cigarette smoking, as well as the exposure to various insults such as environmental pollutants etc and their incidence is currently increasing.

Despite the availability of numerous treatment options for CRDs, the current therapeutic approaches are limited by poor efficacy and severe adverse effects. In COPD, the main pharmacological approaches include the use of bronchodilators and inhaled corticosteroid, which aim at minimizing the symptoms of the disease rather than addressing the underlying causes. The available treatments for LC, which include chemotherapy as first-line treatment, are poorly effective and have several side effects. As a result, COPD is still incurable, and LC has a five-year survival rate of less than 20%, which makes it one of the deadliest types of cancer. This underlines the need for innovative therapies for CRDs.

In the development of an innovative treatment strategy for CRDs, an advantageous approach would involve tackling one or more of the common pathophysiological mechanisms that are shared across all CRDs. These include chronic inflammation, oxidative stress, and airway remodelling.

Two classes of emerging therapies are particularly promising against CRDs include phytoceuticals, or natural moieties such as berberine, agarwood oil, and many others; and nucleic acid-based therapies such as short interfering RNAs (siRNAs), mircoRNAs (miRNAs), and decoy oligodeoxynucleotides (ODNs). The clinical translation of both classes of therapy is hampered by poor pharmacokinetics, which is usually caused by poor solubility and/or permeability, in the case of phytoceuticals, and by the large size, polyanionic nature, and susceptibility to nuclease degradation for nucleic acid-based therapy.

Encapsulating these classes of molecules in advanced drug delivery systems such as liposomes, nanoparticles, nanoemulsions, and others, represents a potentially advantageous strategy to overcome the limitations associated to phytoceuticals and nucleic acid-based therapies. The literature review presented in Chapter 1 of the present thesis summarizes the most recent studies in which these two drug classes have been encapsulated in various advanced drug delivery systems and successfully used to treat *in vitro* and *in vivo* models of CRDs, highlighting the enormous potential of advanced drug delivery systems.

In this context, the principal hypothesis of the present thesis work is that the encapsulation of phytochemicals (berberine and agarwood oil) and nucleic acid-based therapies (NF- κ B decoy ODN) in different advanced drug delivery systems improves their delivery and physicochemical characteristics, resulting as safe and effective therapeutics.

Aims of the thesis

The specific aims of the present thesis are to:

1. encapsulate NF- κ B ODN in spermine-functionalised acetalated dextran nanoparticles (SpAcDex NPs) and test its anticancer activity;
2. encapsulate agarwood oil in a nanoemulsion and test its anti-inflammatory and antioxidant activity;
3. encapsulate berberine in monoolein-Poloxamer 407-based liquid crystalline nanoparticles (LCNs) and test its effect in inhibiting airway remodelling features.

The following studies were conducted to achieve these aims:

1. The NF- κ B ODN SpAcDex NPs were tested on A549 human lung adenocarcinoma cells, and their anticancer activity was assessed by measuring the effect of the NPs on cancer cell migration, proliferation, colony formation, and expression of necroptosis-related genes (Chapter 2).
2. The agarwood oil nanoemulsion was tested on human BCI-NS1.1 airway epithelial cells exposed to cigarette smoke extract (CSE), representing an *in vitro* model of COPD, and its anti-inflammatory and antioxidant potential was evaluated by measuring the relative variation of levels of CSE-modulated pro- and anti-inflammatory cytokines, antioxidant mRNAs, and cell survival genes (Chapter 3).
3. The berberine-LCNs were tested on transforming growth factor- β (TGF- β)-induced BEAS-2B human bronchial epithelial cells, and the inhibitory effect of these nanoparticles against TGF- β -induced remodelling was assessed by evaluating features such as cell migration, the secretion of cytokines stimulating or inhibiting the remodelling process, and the secretion of nitric oxide (Chapter 4).

CHAPTER 2

Research Paper #1

Anticancer activity of NFκB decoy oligonucleotide-loaded nanoparticles against human lung adenocarcinoma

(Kannaujiya VK[#], De Rubis G[#], Paudel KR, Manandhar B, Chellappan DK, Singh SK, MacLoughlin R, Gupta G, Xenaki D, Kumar P, Hansbro PM, Oliver BGG, Wich PR, Dua K. *Anticancer activity of NFκB decoy oligonucleotide-loaded nanoparticles against human lung cancer*, **Journal of Drug Delivery Science and Technology**. 2023 Apr 82; 104328, doi: <https://doi.org/10.1016/j.jddst.2023.104328>.)

[#] Authors contributed equally to this work

Anticancer activity of NFκB decoy oligonucleotide-loaded nanoparticles against human lung cancer

Vinod Kumar Kannaujiya^{1,2#}, Gabriele De Rubis^{3,4#}, Keshav Raj Paudel⁵, Bikash Manandhar^{3,4}, Dinesh Kumar Chellappan⁶, Sachin Kumar Singh^{4,7}, Ronan MacLoughlin^{8,9,10}, Gaurav Gupta^{11,12}, Dia Xenaki¹³, Pradeep Kumar¹⁴, Philip Michael Hansbro^{5,15}, Brian Gregory George Oliver^{13,15*}, Peter Richard Wich^{1,2*}, Kamal Dua^{3,4,*}

¹ School of Chemical Engineering, University of New South Wales, Sydney, NSW 2052, Australia

² Australian Centre for NanoMedicine, University of New South Wales, Sydney, NSW 2052, Australia

³ Discipline of Pharmacy, Graduate School of Health, University of Technology Sydney, Sydney, NSW 2007, Australia

⁴ Faculty of Health, Australian Research Centre in Complementary and Integrative Medicine, University of Technology Sydney, Ultimo, NSW 2007, Australia

⁵ Centre for Inflammation, Centenary Institute and University of Technology Sydney, Faculty of Science, School of Life Sciences, Sydney, NSW 2007, Australia

⁶ Department of Life Sciences, School of Pharmacy, International Medical University, Bukit Jalil 57000, Kuala Lumpur, Malaysia

⁷ School of Pharmaceutical Sciences, Lovely Professional University, Jalandhar-Delhi GT Road, Phagwara 144411, Punjab, India

⁸ IDA Business Park, H91 HE94 Galway, Connacht, Ireland

⁹ School of Pharmacy & Biomolecular Sciences, Royal College of Surgeons in Ireland, D02 YN77 Dublin, Leinster, Ireland

¹⁰ School of Pharmacy & Pharmaceutical Sciences, Trinity College, D02 PN40 Dublin, Leinster, Ireland

¹¹ School of Pharmacy, Suresh Gyan Vihar University, Jaipur 302017, Rajasthan, India

¹² Uttaranchal Institute of Pharmaceutical Sciences, Uttaranchal University, Dehradun 248007, Uttarakhand, India

¹³ Woolcock Institute of Medical Research, University of Sydney, Sydney, New South Wales, Australia

¹⁴ Wits Advanced Drug Delivery Platform Research Unit, Department of Pharmacy and Pharmacology, School of Therapeutic Sciences, Faculty of Health Sciences, University of the Witwatersrand, Johannesburg, South Africa

¹⁵ School of Life Sciences, University of Technology Sydney, Ultimo, NSW 2007, Australia

These two authors contributed equally to this work

* Corresponding Authors: Kamal Dua (kamal.dua@uts.edu.au); Peter Richard Wich (p.wich@unsw.edu.au); Brian Gregory George Oliver (brian.oliver@uts.edu.au).

Abstract (200-300 words)

Non-small cell lung cancer (NSCLC) is among the leading global causes of cancer-related mortality. Current treatment options have limited efficacy and severe adverse effects, underlining the necessity for innovative therapeutic strategies. Among emerging strategies, NFκB inhibition is particularly promising, as NFκB is considered a master regulator of NSCLC pathogenesis. NFκB activity can be efficiently inhibited by double-stranded decoy oligodeoxynucleotides (ODNs). However, therapeutic use of ODNs is strongly limited by enzymatic degradation and poor transport across cell membranes. In this study, we report the encapsulation of a small hydrophilic NFκB decoy ODN into a biodegradable, biocompatible, and acid-responsive dextran-based nanoparticle (NP) system. This formulation has shown excellent encapsulation efficiency (up to 99.5%) with 185 nm average particle size and pH-dependent ODN release at acidic pH. NFκB decoy ODN NPs showed promising anticancer activity, with significant anti-proliferative, anti-migratory, and anti-colony formation activity. These were measured by MTT assay, Boyden chamber and scratch wound healing assays, and crystal violet staining, respectively. Mechanistically, the anti-proliferative effect was exerted through the activation of the expression of key genes regulating apoptosis and necroptosis such as TNF- α , RIPK1, RIPK3, and MLKL. The findings of this study provide the foundations for further investigation of the molecular mechanisms by which NFκB inhibition results in anticancer activity, simultaneously providing proof-of-concept of the therapeutic potential of dextran-based nanoparticles carrying NFκB decoy ODNs against NSCLC.

Keywords: AcDex nanoparticles, decoy oligodeoxynucleotides, lung cancer, NSCLC, migration, proliferation, NFκB, pulmonary delivery

Graphical abstract

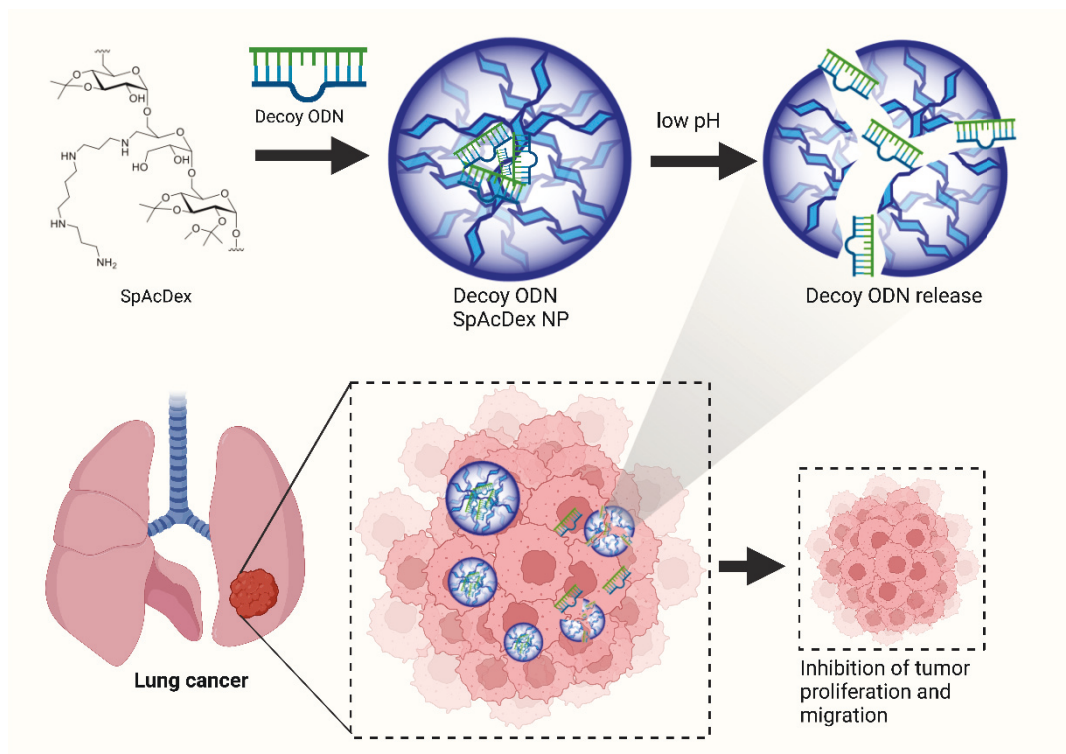


Image created with BioRender.com

1. Introduction

Across all cancer types, lung cancer (LC) is one of the leading causes of death, with more than 1.7 million LC-related deaths recorded in the world in 2020 [1]. Non-small-cell lung cancer (NSCLC) represents the majority (85%) of LC cases [2]. The five-year survival rate of LC is only 17.8%, lower than that of other main cancers [3]. Besides smoking, other factors causing LC include increasing urbanization and environmental pollution [4].

The current mainstay treatment modalities for LC include surgery [5], chemotherapy [6], radiotherapy [7], targeted therapy [8], and immunotherapy [9, 10]. Despite the availability of numerous treatment strategies, a large percentage of patients experience relapse and treatment resistance [9]. This, together with the elevated chemo- and radiation toxicity associated to chemotherapy and radiotherapy [11], demonstrates the urgency for the development of innovative NSCLC treatment strategies with increased efficacy and reduced toxicity [12-14].

Nuclear factor κ B (NF κ B) represents a family of transcription factors that was discovered in 1987 as factors binding to the enhancer of κ immunoglobulins in activated B cells [15]. Since then, NF κ B has been found to have a pivotal role in the transcriptional regulation of a plethora of cellular responses, particularly related to the immune system and inflammation [16]. Besides its role in the immune response, NF κ B is an essential contributor to many cancer hallmarks, as its activation promotes phenomena such as tumour cell proliferation and survival [17], and it is considered the key point of connection between persistent infections, chronic inflammation, and increased cancer risk [18]. In NSCLC, NF κ B is considered a master regulator of cancer pathogenesis and progression, influencing many aspects of this cancer such as proliferation [19], cancer survival, [20], cancer cell migration, infiltration and metastasis [21], and epithelial-to-mesenchymal transition (EMT) [22]. Recently, increased NF κ B expression in NSCLC was associated with reduced overall survival and 5-year survival rate, worsening tumour stage, and lymph node metastasis [23]. This supports the potential of targeting and inhibiting NF κ B as an effective approach for LC therapy [24, 25], and numerous molecules inhibiting the NF κ B pathway are currently being studied [26]. Despite this, no NF κ B targeting treatment has reached clinical approval for application as cancer therapy.

Among the many possible modalities of NF κ B inhibition for therapeutic purposes, the use of decoy oligodeoxynucleotides (ODNs) represents a viable strategy [27, 28]. Decoy ODNs are therapeutic molecules consisting in double-stranded synthetic oligonucleotides with a sequence that mimics the DNA target sequence of the intended transcription factor. As a consequence,

the transcription factor binds specifically to the decoy ODN, and fewer copies of the transcription factor are available to bind the target DNA, resulting in the net inhibition of the transcription factor's activity [29]. For this reason, decoy ODNs represent promising tools to finely regulate the activity of specific transcription factors in many diseases [30, 31]. In a recent study, for example, the transfection with a NFκB decoy ODN resulted in strong suppression of the proliferation of the androgen-independent prostate cancer cell line PC-3M, together with induction of apoptosis [32]. Despite the versatility of decoy ODNs, these therapeutic tools have many limitations, including lack of tissue specificity in the case of systemic administration [33] and, importantly, an unfavourable pharmacokinetic profile [27] characterised by two major issues: (1) low cellular permeability due to the large size and presence of negative charges; and (2) instability of the ODN under *in vivo* conditions due to nuclease activity [34]. This results in reduced therapeutic efficacy [27, 35, 36]. Despite structural ODN modifications such as peptide nucleic acids (PNAs) [37], locked nucleic acids (LNAs) [38] and phosphorothioate-substituted ODNs [33] resulted in increased resistance to degradation, concerns about toxicity, side effects, poor binding efficacy and specificity of these nucleotide derivatives remain [27]. For this reason, there is a need to develop suitable delivery systems for NFκB decoy delivery to the target site of action [39].

One potential strategy to efficiently deliver ODN cargo to target cells is represented by the use of advanced nanocarriers allowing pulmonary delivery through nebulization [40]. *De Rosa et al* have reported a biodegradable polymer, poly(DL-lactic *co*-glycolic acid) (PLGA)-based micro spherical particle, for the delivery of NFκB decoy ODN in RAW 264.7 macrophages, obtaining sustained release of ODN together with inhibition of NFκB at low concentrations [41]. Similarly, NFκB ODN-loaded PLGA microspheres were reported to achieve site-specific delivery of ODN in a rat-carrageenin sponge implant model, inhibiting NFκB activation in chronic inflammation [42].

Polysaccharide-based drug delivery systems have gained a considerable interest due to properties such as biocompatibility, biodegradability, and easy chemical modification [43, 44]. Recently, NFκB/p65 antisense oligonucleotide-loaded chitosan-based nanoparticles (NPs) were reported to achieve an excellent loading efficiency exploiting ionic interactions between cationic chitosan and anionic nucleotides [45]. Similarly, *Cohen et al* have reported an acid-responsive acetalated dextran-based nanocarrier for the delivery of siRNA to HeLa-luc cells [46]. Upon cellular uptake, the acetal groups undergo hydrolysis under slightly acidic environments such as those found in lysosomes/late endosomes and, importantly, in the tumour

microenvironment [47]. This generates water-soluble dextran material, acetone, and methanol as side product [48]. The hydrolysis of the acetal groups initiates the disassembly of NPs and the controlled release of the payload [49]. Additionally, the dextran side chain was modified with spermine to introduce cationic moieties in the polymer, thus facilitating encapsulation of highly polyanionic siRNA molecules through electrostatic interactions. Furthermore, the cationic nature of spermine-modified acetalated dextran (SpAcDex) NPs has shown enhanced cellular uptake due to the electrostatic interactions occurring with the negatively charged cell membrane [50].

In this study, we encapsulated NF κ B double-stranded decoy ODNs into SpAcDex NPs and evaluated the anticancer activity of this formulation in the human A549 NSCLC cell line. The present study is the first in which an NF κ B decoy ODN is encapsulated within a biocompatible, acid-responsive delivery system, which allows selective release of the payload in the acidic tumor microenvironment. This has the potential to minimize adverse effects caused by the off-target, aspecific inhibition of NF κ B in healthy cells. The formulation revealed a strong anticancer activity, with significant inhibition of cancer hallmarks including cancer cell proliferation, migration, and ability to form clonal colonies. Mechanistically, the anti-proliferative effect of this formulation was achieved by enhancing the expression of genes mediating apoptosis and necroptosis such as tumor necrosis factor- α (TNF- α), Receptor-interacting serine/threonine-protein kinases 1 and 3 (RIPK1, RIPK3), and Mixed lineage kinase domain-like (MLKL). This study provides proof-of-concept of the suitability of SpAcDex NP-based ODN formulations for the therapeutic inhibition of NF κ B in NSCLC.

2. Materials and Methods

2.1 Materials

Dextran (Mw 9-11 kDa, from *Leuconostoc mesenteroides*) was purchased from (Sigma Aldrich). Sodium periodate, 2-Methoxy propene, spermine, Sodium borohydride were purchased from Merck. Water used during particle preparation was adjusted to pH 8 with triethylamine (Sigma Aldrich). All buffers and water used for the preparation of SpAcDex-based NPs were in nuclease free and filtrated through syringe filters (Millex, sterile PES membrane, pore size 0.22 μm , Merck). Brandson Digital Sonifier 450 (Power: 400 watts; Line Voltage: 200-245 @ 50/60 Hz, Consonic Tip Micro Tapered 1/8). Dynamic light scattering (DLS) (Malvern Zetasizer Nano ZS). NF κ B decoy ODN and Scramble decoy ODN were purchased from Merck, Bayswater, VIC, Australia MTT (3-[4,5-dimethylthiazol-2-yl]-2,5-diphenyl tetrazolium bromide), crystal violet, DMSO, H/E staining solutions Dulbecco's Modified Eagle's Medium (DMEM), fetal bovine serum (FBS), and penicillin and streptomycin were purchased from Sigma-Aldrich, St. Louis, MO, USA. All remaining agents and solvents used in experiments involving cell culture were purchased from Sigma-Aldrich unless stated otherwise.

2.2 Synthesis of Spermine-Functionalized Acetalated Dextran

The spermine-functionalized acetalated dextran was synthesized over three steps according to literature [46].

Partial Oxidation of Dextran (OxDex): For the synthesis of partially oxidized dextran, dextran (2.0 g, 12.3 mmol) was dissolved in 8.0 mL dd-H₂O. The solution was stirred for 5 h at room temperature after sodium periodate (480 mg, 2.25 mmol) addition. Further, the reaction mixture was dialyzed against dd-H₂O for 3 days using a snakeskin regenerated cellulose membrane with MWCO of 3,500 g/mol. After lyophilization, a colourless powder (1.3 g) was obtained, with an aldehyde content of 8.9 ± 0.02 mol aldehyde per 100 mol anhydrous glucose units (AGU) confirmed by BCA assay.

Acetalation of Partially Oxidized Dextran (OxAcDex): The solubility switch from hydrophilic to hydrophobic dextran was obtained as described by *Bachelder et al.* The oxidized dextran (1 g, 6.17 mmol) was dissolved in DMSO (12.0 mL). Further, 2-methoxypropene (2.6

g, 36 mmol) was added slowly after addition of pyridinium *p*-toluenesulfonate (22 mg, 0.088 mmol). The reaction mixture was stirred for 10 min at room temperature followed by reaction quenching with the help of triethylamine (1 mL) [48]. The resulting reaction mixture was precipitated in dd-H₂O pH 8 (100 mL) and isolated by centrifugation (12,000 g, 20 min, 4 °C). The product was further washed 5 times with dd-H₂O pH 8. After lyophilization, the OxAcDex (1.2 g) was obtained as a colorless powder. The obtained product contains 79.1% acetals, where 30.2% are cyclic and 48.9% are acyclic acetals.

Spermine Modification of OxAcDex (SpAcDex): To further modify oxidized acetalated dextran with spermine, the Ox-AcDex (1.0 g, (AGU) 202 g/mol, 5.05 mmol) was dissolved in DMSO (4.5 mL). After addition of spermine (1 g, 5.05 mmol), the reaction mixture was incubated with continuous stirring for 24 h at 40 °C. Afterwards, sodium borohydride (560 mg, 15.2 mmol) was added, and reaction was stirred for additional 24 h at 50 °C. After purification using similar method as mentioned above, the product was lyophilized to obtain a white powder. The degree of functionalization was determined by elementary analysis (1.36% N, 53.46% C and 7.83% H) and resulted in 4.8 mol spermine per 100 mol AGU.

2.3 Transcription Factor Decoy ODN

Single stranded decoy ODN to double stranded NFκB inhibitor was obtained by annealing. The sequence of sense and antisense oligodeoxynucleotides was annealed in 1×annealing buffer (20 mM Tris-HCl, 20 mM MgCl₂ and 50 mM NaCl, pH 7.5). The mixture was heated at 80 °C for 5 min and allowed to cool slowly at room temperature overnight.

The sequence of the ODN decoy to NFκB used was:

(1) NFκB decoy ODN sequence

5'-CCTTGAAGGGATTTCCCTCC-3'

3'-GGAACTTCCCTAAAGGGAGG-5'

(2) scrambled decoy ODN sequence

5'-TTGCCGTACCTGACTTAGCC-3'

3'-AACGGCATGGACTGAATCGG-5'

2.4 Nanoparticle Preparation

ODN-loaded and empty nanoparticles were prepared by a double emulsion method using a probe sonicator. 10 mg spermine-modified acetalated dextran was dissolved in 800 μL dichloromethane (DCM) and 130 μL phosphate-buffered saline (PBS) with and without 121.5 μg annealed ODN was added for loaded and empty nanoparticle formulations, respectively. The first sonication was performed for 10 second followed by addition of 4 mL polyvinyl alcohol (PVA) solution (3% w/w in PBS, 13–27 kDa, 87–89% partially hydrolyzed) on top of primary emulsion. Further, a second sonication was performed for 30 s to achieve a secondary water-in-oil-in-water emulsion. The resulting emulsion was stirred overnight to allow DCM evaporation followed purification by ultracentrifugation (45,000 x g, 20 min, 20 °C) and was washed three times with 4.0 mL dd-H₂O (pH 8). Before lyophilization, 50 μL PVA solution (0.3% w/w in dd-H₂O pH 8) was added as cryoprotectant. The particle yield was about 60%, based on the initial spermine-modified dextran material.

2.5 Measurement of Particle Size and Zeta Potential

The size of the different dextran-based NP was determined by nanoparticle dynamic light scattering (DLS), using a Malvern Zetasizer Nano ZS. All NP samples were measured in dd-H₂O (pH 8.0) after sonication (Unisonics FXP) for 60 s at 25 °C in triplets. The size calculation was performed with Malvern software. Zeta potential (particle charge) was measured using a clear disposable zeta cell. Three measurements with 20 individual runs each were performed at 25 °C. Particle samples were prepared at concentrations of 0.1 mg/mL in HEPES buffer (25 mm, pH 7.4). The calculation was performed with the Malvern Zetasizer software 6.20. Data shown represent the average zeta potential (standard deviation of distributions of three sequential measurements).

2.6 Scanning Electron Microscopy (SEM)

Particle shape and morphology were analyzed by scanning electron microscopy (SEM). The freeze-dried Dex(ODN-loaded) NPs dispersed in distilled (1 mg⁻¹·mL) were dried and coated with Pt layer under argon atmosphere. Images of the samples were taken on an FEI Nova Nano SEM 230 FE-SEM at an accelerating voltage of 5.0 kV.

2.7 Determination of ODN Loading by RiboGreen Assay

An indirect method of quantification was performed to determine the encapsulated double-stranded decoy ODN in double emulsion particles using the Quant-iT™ RiboGreen® assay [51]. Here, particle solution was centrifuged after particle formation and solvent evaporation. The amount of free decoy ODN present in the supernatant was then quantified and compared with the initial concentration of decoy ODN used in particle formulation [52]. The non-encapsulated decoy ODN present in the supernatant was able to react with the RiboGreen® reagent resulting in a fluorescent compound with an emission maximum at 535 nm ($\lambda_{ex} = 485$ nm). To determine the decoy ODN content, 10 μ L of the supernatant was combined with 90 μ L of PBS in a black, flat-bottom 96-well microplate. Meanwhile, the pure double-stranded decoy ODN was diluted in PBS to a concentration that ensured 100% encapsulation. The RiboGreen® reagent was diluted 1:200 with PBS, and 100 μ L was added to each well, resulting in a total volume of 200 μ L per well. The reaction mixture was then carefully incubated for 5 minutes in the dark before the fluorescence of the reacted dye was recorded using a Tecan microplate reader. To further verify any presence of free decoy ODN in the nanoparticle pellets, the particles were washed twice with nuclease free pH 8.0 water and ODN content were measured in supernatant. The results were compared with the fluorescence of the theoretical amount of encapsulated decoy ODN using Microsoft Excel to determine total ODN loading. Loading content and encapsulation efficiency was calculated according to formula as LC and EE.

$$LC \text{ (wt \%)} = \frac{\text{weight of ODN in particle}}{\text{weight of ODN-loaded particle}} \cdot 100\% \quad \text{eq. 1}$$

$$EE \text{ (wt \%)} = \frac{\text{weight of ODN in particle}}{\text{weight of total ODN used in particle formulation}} \cdot 100\% \quad \text{eq. 2}$$

2.8 pH-Dependent Degradation of SpAcDex Particles

Empty particles were suspended in triplicate at a concentration of 0.25 mg/mL in either a 0.3 M acetate buffer (pH 5.5) or PBS (pH 7.4) buffer and incubated at 37 °C under gentle agitation using a MultiTherm shaker (Eppendorf). At various time points, the size distribution of the

samples was measured using DLS. For visual observation, the particles were incubated at a concentration of 2.5 mg/mL and were photographed at various time points.

2.9 pH-Dependent Release of Decoy ODN from SpAcDex Particles

ODN-loaded particles were incubated at a concentration of 5 mg/mL in either a 0.3 M acetate buffer (pH 5.5) or PBS (pH 7.4) buffer at 37 °C temperature under gentle agitation using a thermo incubator (Eppendorf). At different time interval the aliquots were collected and centrifuged at 10 000g for 10 min to pellet out insoluble materials, and the supernatant was stored at -20 °C. The release ODN in the supernatant sample was quantified by Quant-iT™ RiboGreen® assay. The amount of ODN in each sample was calculated by fitting the emission to a calibration curve using the Quant-iT™ RiboGreen® assay. For this experiment, all solutions included heparin at 25 mg/mL to disrupt electrostatic interactions between polymer amines and decoy ODN to enable quantification.

2.10 ODN Molecular Generation and Visualization

The double stranded molecular structures of NFκB and scrambled ODNs were generated using the default DNA/RNA builder tool in Avogadro 2.0.8.0 Molecule Editor & Visualizer System [53]. The generated ODN structure was then visualized and scanned using UCSF Chimera 1.14 Molecular Modelling System employing conventional Nucleic Acid Database (NDB) colors and formats [54].

2.11 Cell Culture

A549 (human lung epithelial carcinoma) and BEAS-2B (human non-cancerous bronchial epithelial) cell lines (ATCC, USA) were a kind gift from Prof. Alaina Ammit, Woolcock Institute of Medical Research, Sydney, Australia. Cells were cultured in DMEM supplemented with 10% FBS, 1% penicillin and streptomycin, in a humidified 37°C incubator supplied with 5% CO₂.

2.12 Cell Viability Assessment - MTT Assay

The MTT assay was performed to assess A549 and BEAS-2B cell proliferation and viability as previously described [55, 56]. Briefly, 5000 A549 cells/well were seeded in a 96-well plate and, 24 hours post attachment, cells were treated with Dex(NFκB-ODN) NPs or Dex(scrambled-ODN) NPs or empty nanoparticles at different concentrations (corresponding to 0.5, 1, 2.5, 5, 10 nM ODN). Twenty-four hours after treatment, MTT solution (20 μL of a 5 mg/mL stock solution MTT in PBS, for a final concentration of 0.5 mg/mL MTT) was added to the wells and the mixture was incubated at 37 °C for 4 hours. Successively, the supernatant was removed and 100 μL dimethyl sulphoxide (DMSO) were added to each well to dissolve the formazan crystals. The absorbance of the wells was then read using an UV/VIS spectrophotometer at a wavelength of 540 nm. The percent viability of the cells treated with either Dex(NFκB-ODN) NPs or Dex(scrambled-ODN) NPs or empty NPs was reported as percentage compared to the control (untreated) group.

2.13 Wound Healing Assay

The wound healing assay was performed as reported previously [57-59] to assess the anti-migratory activity of the Dex(NFκB-ODN) NPs on A549 cells. Briefly, 3×10^5 A549 cells/well were seeded into 6-well plates and cultured until confluency. The cell monolayer was scratched using the tip of a sterile 200 μL pipette tip, followed by multiple washing steps with PBS. Images at 0 hr time point were taken after PBS washing, then A549 cells were treated with 10 nM Dex(NFκB-ODN) NPs or concentration-matched Dex(scrambled-ODN) NPs for 24 hours. The distance between the edges of the scratch before and 24 h after treatment was measured using the IS capture software after imaging with a light microscope at 10X magnification, and the percentage wound closure was reported compared to the control (untreated) group.

2.14 Boyden's Chamber Assay

To determine A549 cells migration, a modified Boyden's chamber assay was performed as previously described [58, 60], using transwell permeable supports (6.5-mm insert 8-μM pore size polycarbonate membrane). First, the lower surface of the membranes was coated with 2.5% gelatin in 1M acetic acid for 1 hour. Subsequently, cells were seeded in the upper chamber at a density of 10^4 cells/mL in a volume of 200 μL DMEM culture media. The chamber was then placed in a well containing 600 μL DMEM. After attachment, the cells were treated with

10 nM Dex(NFκB-ODN) NPs or concentration-matched Dex(scrambled-ODN) NPs for 24h, and cells were allowed to migrate for 24 hours more after the end of the treatment. Following this, the non-migrated cells remaining in the upper surface of the membrane were removed using cotton swabs, while the cells that successfully migrated reaching the lower surface were fixed in 10% formalin and stained with hematoxylin and eosin. Finally, the cells that had clearly migrated through the pores of the membranes were counted in 5 random fields with a light microscope, with a 20x magnification. Average cells per field of view were then calculated and reported.

2.15 Colony Formation Assay

The colony formation assay was performed as reported previously [58, 61] to test the anti-colony formation activity of Dex(NFκB-ODN) NPs in A549 cells. First, cells were seeded at a density of 500 cells/well into six-well plates. Following adhesion, cells were treated with 10 nM Dex(NFκB-ODN) NPs or concentration-matched Dex(scrambled-ODN) NPs. After colony development (about 2 weeks), the cells were washed with PBS and fixed with 3.7% formaldehyde for 20 minutes. Successively, cells were washed again with PBS and stained with 0.4% crystal violet, then washed four to five times with PBS. The colonies were finally counted using the ImageJ software.

2.16 Real-time qPCR

The effects of Dex(NFκB-ODN) NPs on the mRNA expression levels of proliferation-related genes were assessed through quantitative real-time PCR (qPCR) as described in a previous study [61]. First, 1.5×10^5 A549 cells/well were seeded into 6-well plates and left to attach overnight. The following day, cells were treated with 10 nM Dex(NFκB-ODN) NPs or concentration-matched Dex(scrambled-ODN) NPs for 24 h. After the treatment, the cells were lysed with 500 μL TRI reagent (Sigma-Aldrich, Australia). The samples were vortexed for 45 seconds to ensure complete cell rupture. Successively, 125 μL chloroform (Sigma-Aldrich, Australia) were added and the samples were centrifuged at 12,000 g, 3°C, for 15 minutes. The aqueous layer was transferred into fresh tubes and the RNA was precipitated by adding 250 μL ice-cold isopropyl alcohol (Sigma-Aldrich, Australia). The tubes were then centrifuged at 12,000 g, 3°C, for 10 min. After centrifugation, the supernatant was removed, and the precipitated RNA pellets were washed twice with 1 mL 75% ethanol (Sigma-Aldrich,

Australia), centrifuging the tubes at 8,000 g, 4 °C, for 5 min each time. After the second centrifugation, the ethanol was removed, and dried RNA pellets were dissolved in 20 µL nuclease-free water (Sigma-Aldrich, Australia). Nanodrop (Thermo Fisher Scientific, Waltham, MA, USA) was used to determine the concentration and purity of the RNA samples.

The RNA samples were subjected to DNase I (Sigma-Aldrich, Australia) treatment. Successively, 800 ng total RNA was reverse-transcribed to cDNA using the reaction mixture of M-MLV buffer (Thermo Fisher Scientific), random primers (0.5 µg/µL, Thermo Fisher Scientific), dNTPs (10 mM, Thermo Fisher Scientific) and DTT (100 mM, Thermo Fisher Scientific). For the reverse transcription reaction, a thermal cycler (Eppendorf, Hamburg, Germany) was used with the following steps: denaturation (65 °C, 10 min), annealing (25 °C, 10 min), reverse transcription (37 °C, 50 min), and enzyme inactivation (70 °C, 15 min). An amount of 16 ng of cDNA from each sample was then subjected to real-time qPCR using the iTaq Universal SYBR green (BioRad, Hercules, CA, USA) mix and gene-specific primers (forward and reverse, 0.5 µM each, Sigma-Aldrich, Australia). The thermal cycler used was a CFX96 PCR system (BioRad). The real-time qPCR protocol included the following cycles: 95 °C for 30 s (1 cycle), 95 °C for 15 s (50 cycles) and 60 °C for 30 s (1 cycle). The human gene for Glyceraldehyde 3-phosphate dehydrogenase (GAPDH) has been used as a control for normalization.

The sequences of human primers used were as follows:

Gene name	FW sequence	RV sequence
TNF- α	AGGCAGTCAGATCATCTTC	TTATCTCTCAGCTCCACG
RIPK1	TGATAATACCACTAGTCTGACG	ACAGTTTTTCCAGTGCTTTC
RIPK3	AACTTTCAGAAACCAGATGC	GTTGTATATGTTAACGAGCGG
MLKL	GTGAAGAATGTGAAGACTGG	AAGATTTTCATCCACAGAGGG
GAPDH	TCGGAGTCAACGGATTTG	CAACAATATCCACTTTACCAGAG

2.17 Statistical Analysis

The data are represented as mean \pm SEM. Statistical analysis was performed by ordinary one-way ANOVA, followed by Tukey multiple comparison test. The software used was GraphPad Prism (v.9.4, GraphPad Software, San Diego, CA, USA). In pairwise comparisons, a two-tailed p-value <0.05 was considered statistically significant. In Figure 4d, a Mann-Whitney U test was performed between the 5nM and 10 nM Dex(NF κ B)

3. Results

3.1 Nanoparticle Size and Zeta Potential

The obtained NPs were visualized and characterized by dynamic light scattering (DLS, **Figure 1a**) and scanning electron microscopy (SEM, **Figure 1b**). The spherical morphology of the NPs was confirmed by SEM data. Both empty and double stranded decoy ODN loaded particles have shown similar particle diameter distribution, in the range of 150 to 200 nm. A slight increase in the particle size distribution was observed in loaded particles compared to empty particles. The surface charge of the particles was determined by zeta-potential measurements (**Table 1**). A positive surface zeta-potential of 12.43 mV was observed for empty nanoparticles due to the presence of protonated amines on the particle surface. The encapsulation of the charged decoy ODN slightly reduced the surface zeta potential (11.83-12.37 mV) which is most likely due to the non-covalent adsorption of a small number of negatively charged decoy ODN on the surface of particles.

Molecular modelling was used to predict the three-dimensional structure of the ODNs, which demonstrated self-assembly into well-defined tubular structures with acidic phosphate groups forming the periphery of the tubular structure and amine groups aligning in the centre (**Figure S1**). This is important for efficient encapsulation and loading of the ODNs into spermine-AcDex nanosystems, wherein the amines of the cationic polymer interact with the negatively charged peripheral phosphate groups of the ODNs [62].

Table 1: Physical Characterization of empty, NFκB ODN and scramble ODN loaded Dex NP

Particle Type	Diameter (nm)	PDI	Zeta-Potential / mV
Dex(empty) NP	178 ± 1.0	0.20 ± 0.01	12.4 ± 0.5
Dex(NFκB-ODN) NP	187 ± 1.5	0.23 ± 0.01	11.8 ± 0.3
Dex(scramble-ODN) NP	182 ± 6.0	0.24 ± 0.03	12.4 ± 0.5

(The data obtained from three replicate DLS measurements are represented as the mean ± standard deviation)

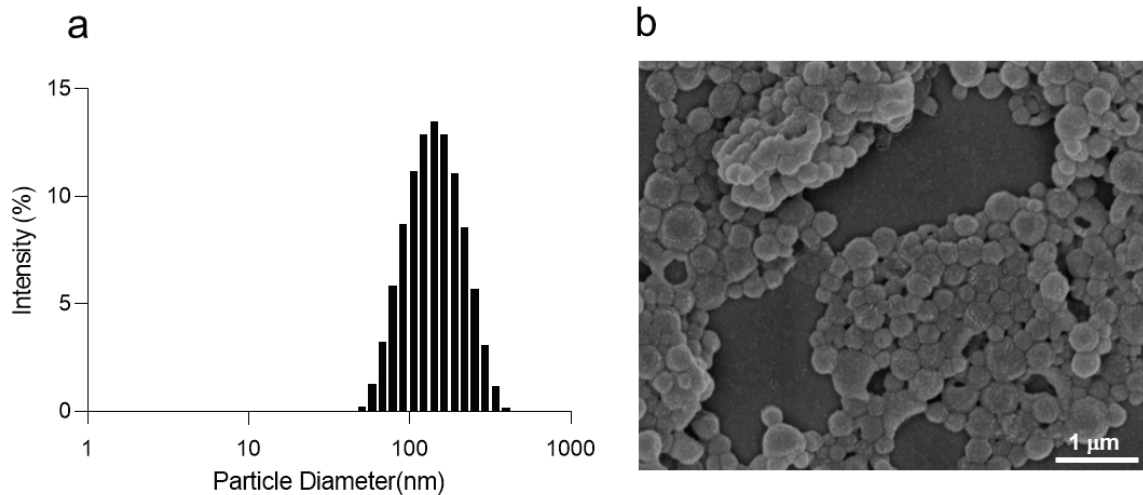


Figure 1. Characterisation of decoy ODN-Encapsulated dextran NPs. (a) Size distribution obtained by DLS; (b) SEM analysis.

3.2 Quantification of Decoy ODN Loading

An indirect method of quantification was performed to validate the successful encapsulation and quantification of decoy ODN loading [52] using the Quant-iT™ RiboGreen assay. The unloaded decoy ODN present in the supernatant was quantified after centrifugation followed by particle formulation and solvent evaporation. The amount of decoy ODN present in the supernatant represent the total amount of free decoy ODN, which has not been encapsulated in the particles. As the decoy ODN is highly soluble in water, any unencapsulated decoy ODN would stay in the supernatant. Furthermore, the particle pellets were washed twice with pH 8.0 nuclease-free water and a negligible amount of free decoy ODN was observed in the supernatant, providing confirmation of the successful encapsulation of the decoy ODN. Both NFκB and scrambled decoy ODN have shown a similar encapsulation efficiency of up to 99.5%. Overall, up to 11.89 µg decoy ODNs were encapsulated per mg NPs, as shown in **Table 2**.

Table 2. *Quantification of Decoy ODN Encapsulation*

Particle type	Decoy ODN in $\mu\text{g}\cdot\text{mg}^{-1}$ NP	Encapsulation efficiency (in %)
Dex(NF κ B-ODN) NP	11.89	99.5
Dex(scrambled-ODN) NP	11.88	99.4

3.3 pH-dependent Particle Degradation

The decoy ODN was encapsulated into an acid-responsive NPs to prevent the premature release of payload under physiological conditions. Under acidic conditions, the acetal groups present on the SpAcDex backbone undergo rapid hydrolysis, forming a water-soluble dextran, acetone and methanol that leads to particle degradation. To determine the degradation behaviour, the NPs were incubated at 37 °C in PBS buffer at pH 7.4 to simulate the physiological conditions of the blood stream and in acetate buffer at pH 5.5 to mimic the acidic tumour microenvironment. The successful pH-dependent particle degradation at acidic pH was confirmed by DLS measurements (**Figure 2a**). The initial increase in particle size (calculated according to number distribution) can be explained by the uncontrolled aggregation of degradation materials and has been observed previously in similar polysaccharide-based nanosystems [63, 64]. The degradation can also be detected by visually observing the particle solutions (**Figure 2b**). While the typical nanoparticulate opaqueness clears under acidic conditions, there was no significant change observed in PBS buffer pH 7.4, indicating the stability of the formulation under physiological conditions.

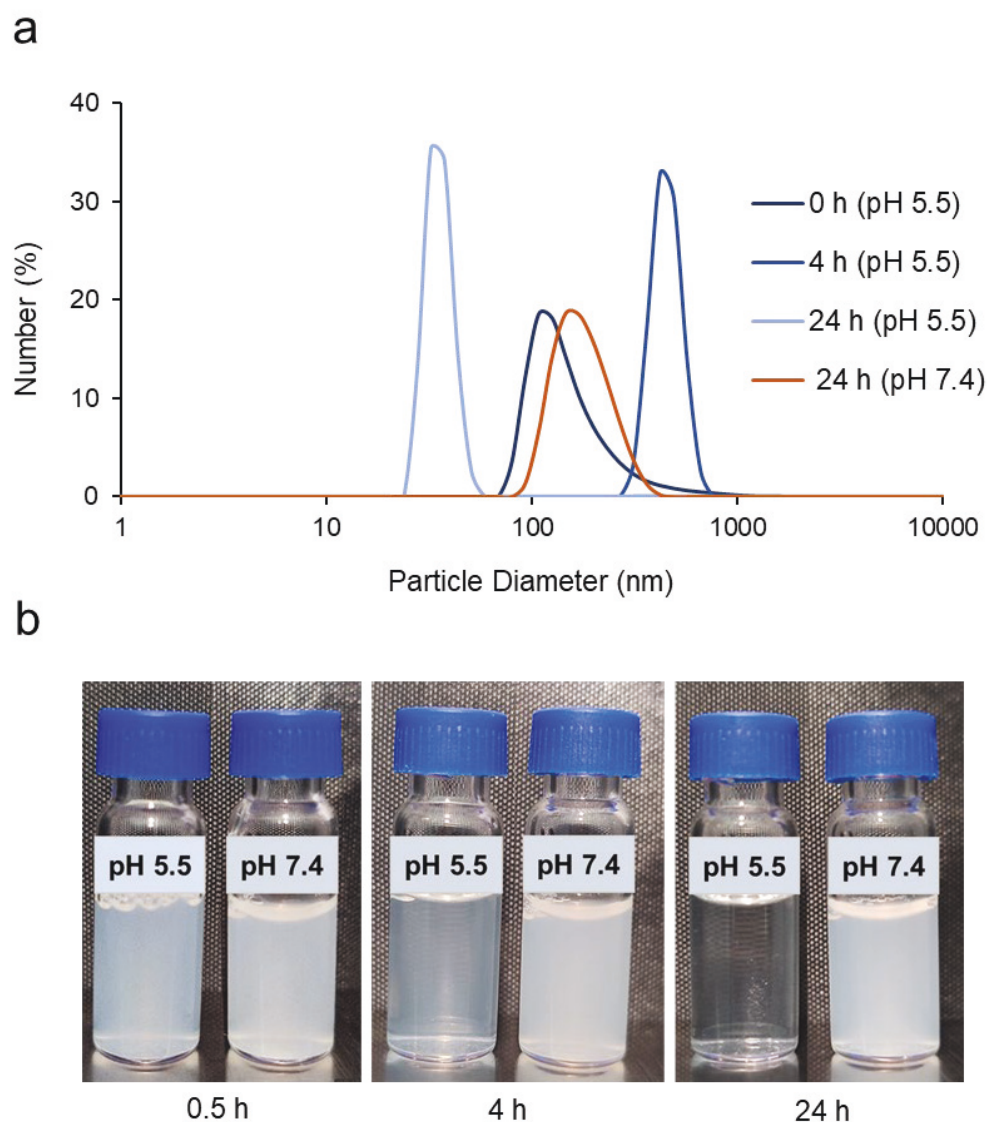


Figure 2. Particle degradation under pH 5.5 and pH 7.4 (a) DLS data; (b) visual observation.

3.4 pH-dependent Decoy ODN Release

The decoy ODN-loaded particles were incubated at different pH values similar to the above experiment. The amount of ODNs released from dextran NPs were quantified by using a Quanti-iT™ RiboGreen® assay. Heparin was used to prevent the electrostatic interactions between water soluble spermine modified dextran and negatively charged ODN. As expected, a fast release of decoy ODN up to 90% was observed within the first 8 h under acidic conditions [46], while physiological pH 7.4 has shown only a slight release of ODN even after 24 h (**Figure 3**). In the first 5 min after incubation, almost 10% ODN release was observed under both

conditions, indicating the adsorption of free ODN on the surface of particles due to electrostatic interaction between particle surface amine and ODN during formulation.

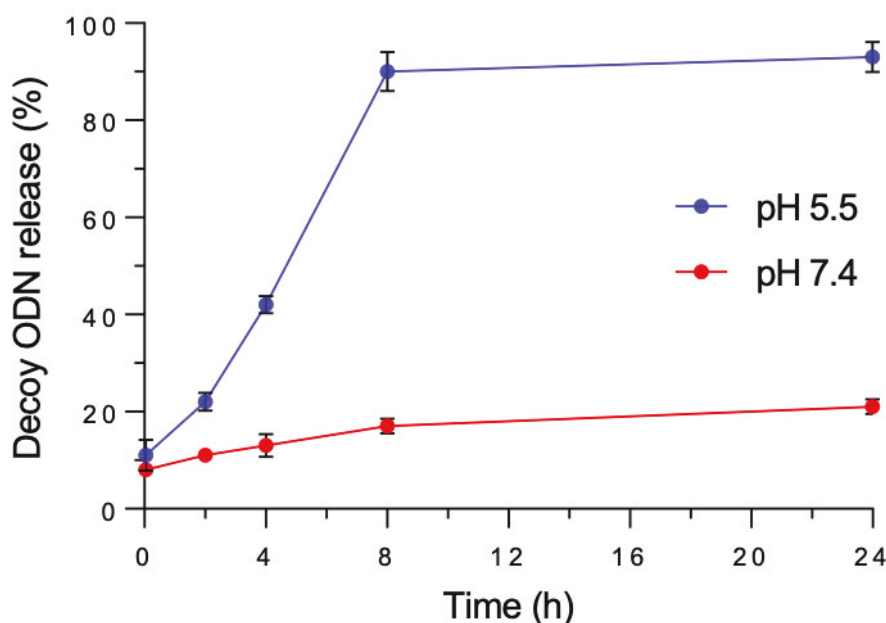


Figure 3. Decoy ODN release under pH 5.5 and pH 7.4 (Data are presented as means \pm SD ($n = 3$))

3.5 Anti-proliferative Activity of NF κ B-ODN-NPs in A549 and BEAS-2B Cells

The effect of Dex(NF κ B-ODN) NPs, Dex(scrambled-ODN) NPs, and empty NPs on the proliferation and viability of A549 and BEAS-2B cells is shown in **Figure 4**. Dex(NF κ B-ODN) NPs at concentrations of 2.5, 5 and 10 nM significantly reduced the proliferation rate of A549 cells by 13.4%, 27.8% and 37.2%, respectively, compared to control (untreated cells) in the MTT assay (**Figure 4a**). Considering that the highest anti-proliferative effect was observed with 10 nM Dex(NF κ B-ODN) NPs, this concentration has been used for the subsequent experiments. In comparison, treatment with the Dex(scrambled-ODN) NPs at 10 nM concentration resulted only in a relatively small reduction of cell viability of 12% (**Figure 4b**). To assess the effect of Dex(NF κ B-ODN) NPs on the viability of non-cancerous cells, the nanoparticles were tested on BEAS-2B human bronchial epithelial cells. Dex(NF κ B-ODN) NPs at concentrations of 1, 2.5, 5 and 10 nM significantly reduced the viability of BEAS-2B cells by 8.5%, 14.3%, 15.1%, and 19.2%, respectively, compared to control (untreated cells) in the MTT assay (**Figure 4d**). The effect of 5nM and 10 nM Dex(NF κ B-ODN) NPs on BEAS-

2B cell viability was significantly lower than the effect obtained by the same concentration of NPs on A549 cells proliferation (**Figure 4d**), indicating the relative safety of these NPs for healthy cells compared to cancer cells. Treatment with Dex(scrambled-ODN) NPs did not result in a significant reduction of BEAS-2B cell viability (**Figure 4e**). Finally, treatment with empty Dex NPs resulted in no significant effect on A549 and BEAS-2B cell viability at concentrations ranging between 0.5 and 10 $\mu\text{g/mL}$ (**Figures 4c and 4f**, respectively).

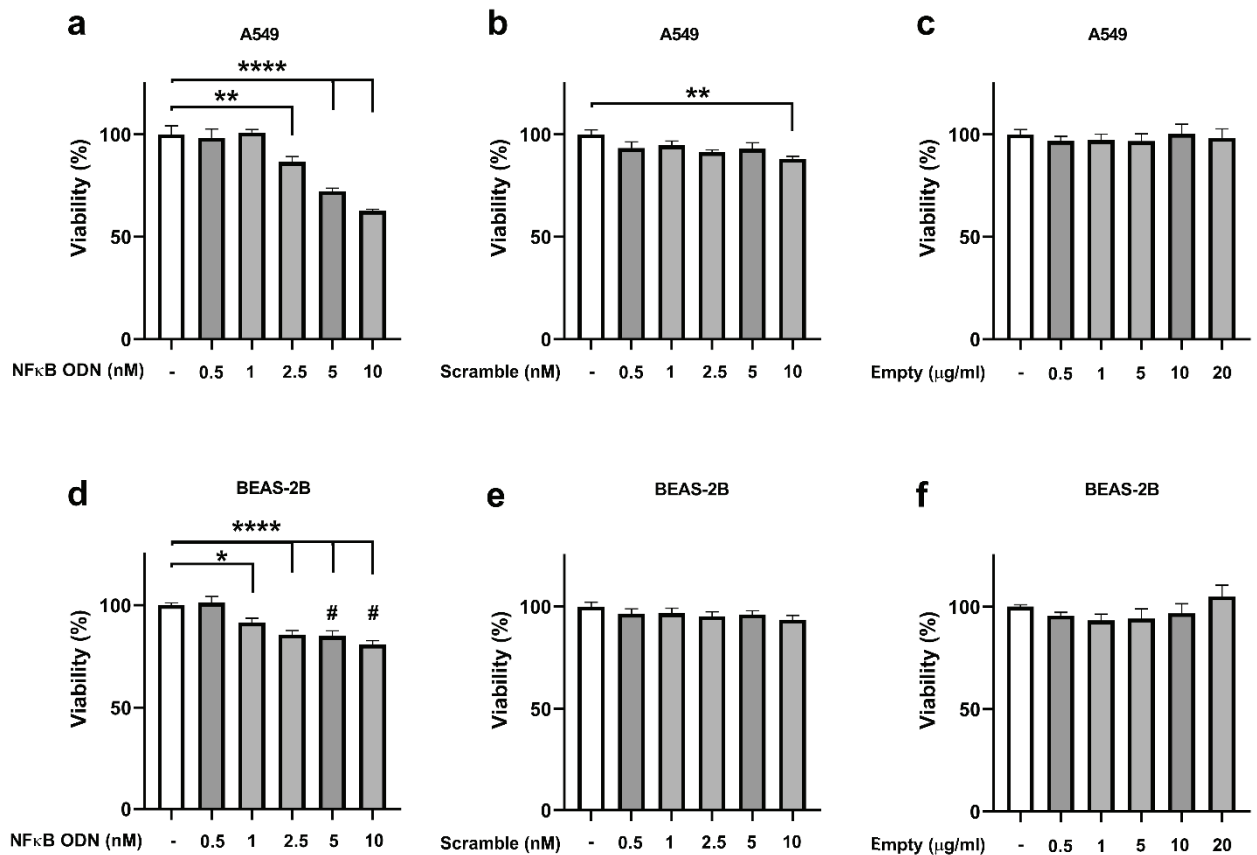


Figure 4. Anti-proliferative activity by MTT assay: The A549 cells (a-c) and BEAS-2B cells (d-f) were treated with various doses of Dex(NFκB-ODN) NPs (a, d) or Dex(scrambled-ODN) NPs (b, e) or empty NPs (c, f) for 24 hours. The values are expressed as average \pm SEM of $n = 3$ independent experiments. Statistical analysis was performed by ordinary one-way ANOVA test. * = $P < 0.05$; ** = $P < 0.01$; **** = $P < 0.0001$ vs control (untreated). In (d), # = $P < 0.05$ vs concentration-matched group on A549 cells as assessed by Mann-Whitney U test.

3.6 Effect of Dex(NFκB-ODN) NPs on the expression of apoptosis/necroptosis genes in A549 Cells

To provide a mechanistic explanation of the anti-proliferative effects of Dex(NFκB-ODN) NPs on A549 cells, the effect of the nanoparticle formulation on the expression of transcripts encoding for TNF-α, RIPK1, RIPK3, and MLKL was assessed via real-time qPCR (**Figure 5**). Dex(NFκB-ODN) NPs at 10 nM concentration induced a significant increase in the expression of RIPK1 (11.3%, **Figure 5a**) and MLKL (10.8%, **Figure 5b**). A similar trend was observed with the expression of TNF-α and RIPK3, which was induced on average by 4.9-fold (TNF-α, **Figure 5c**) and 7.1-fold (RIPK3, **Figure 5d**) upon treatment with 10 nM Dex(NFκB-ODN) NPs, without reaching statistical significance. Treatment with Dex(scramble-ODN) NPs did not result in an increase of the expression of any of the four genes analysed (**Figure 5a-d**).

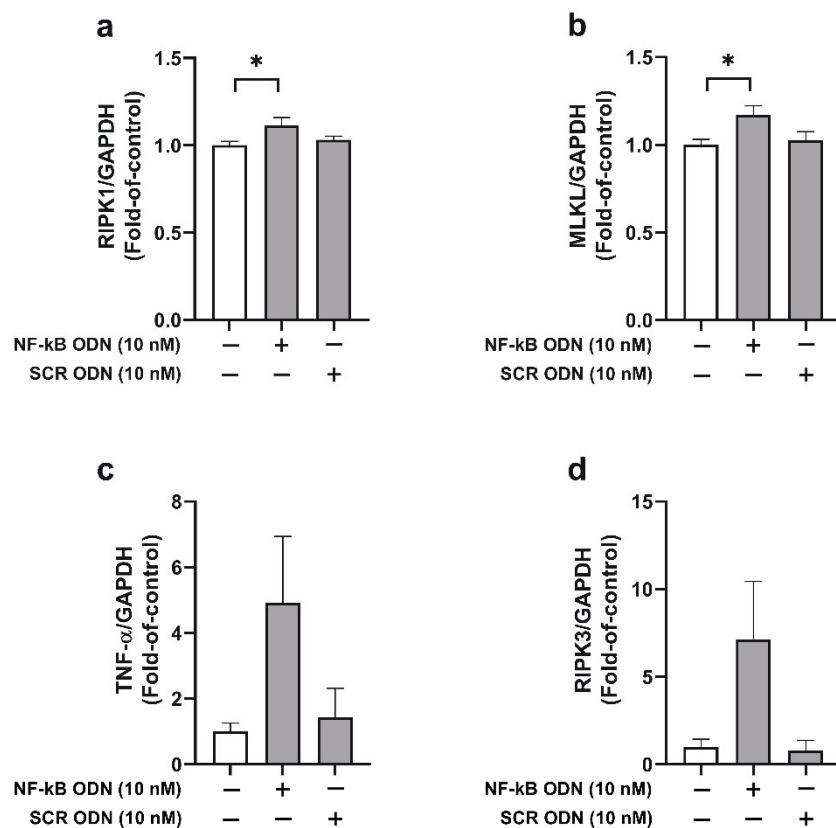


Figure 5. Effect of Dex(NFκB-ODN) NPs on the expression of apoptosis/necroptosis genes in A549 cells. A549 cells were treated with 10 nM Dex(NFκB-ODN) NPs or Dex(Scramble-ODN) NPs and the relative expression of the following genes was measured with real-time qPCR: RIPK1 (a), MLKL (b), TNF-α(c), and RIPK3 (d). Values are expressed as average ±

SEM of $n = 3$ independent experiments. Statistical analysis was performed by ordinary one-way ANOVA test $* = P < 0.05$ vs control (untreated).

3.7 Anti-migratory Activity of NF κ B-ODN-NPs in A549 Cells

The effect of Dex(NF κ B-ODN) NPs on the migration of A549 cells was assessed by a wound healing assay (**Figure 6**) and by a Boyden chamber assay (**Figure 7**). Dex(NF κ B-ODN) NPs successfully suppressed A549 cell migration in the wound healing assay for 24 h. This treatment has shown 54.3% of migration inhibition compared to the untreated control (**Figure 6a**) while the treatment with similar concentration of Dex(scrambled-ODN) NPs has also somewhat suppressed A549 cells migration, although to a lesser extent compared to the Dex(NF κ B-ODN) NPs (27.8% compared to untreated control, **Figure 6b**).

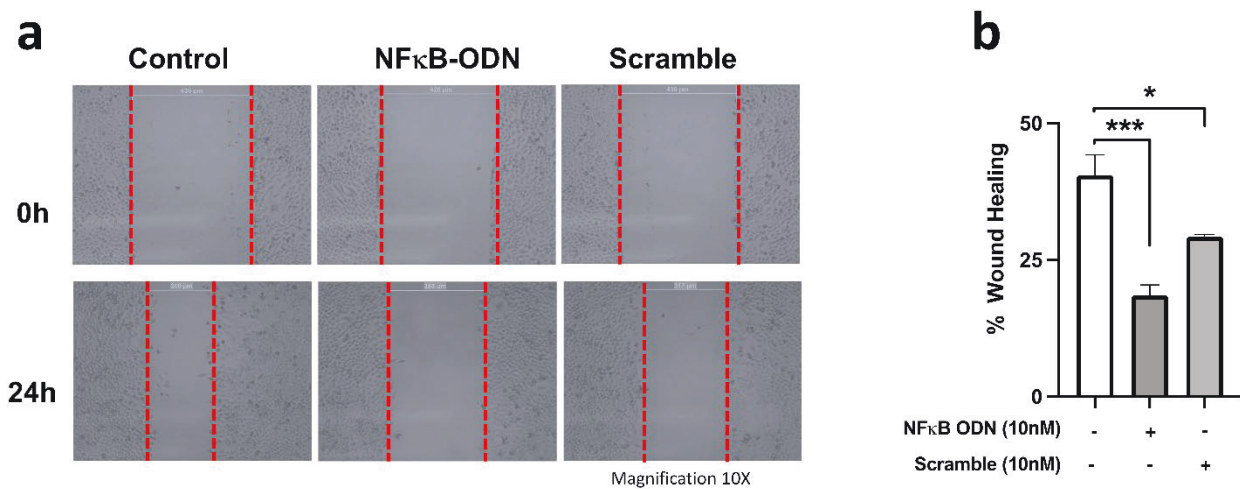


Figure 6. Anti-migratory activity by wound healing migration assay. The wound was created by scratching, with a sterile pipette tip, a confluent layer of A549 cells. Cells were then treated with 10 nM Dex(NF κ B-ODN) NPs or concentration-matched Dex(scrambled-ODN) NPs for 24 h. Photographs were acquired on a light microscope under 10x magnification (a). The distance between the edges of the wounds was measured before treatment (0 h) and after 24 h to calculate the percent wound closure (b). Values are expressed as average \pm SEM of $n = 3$

independent experiments. Statistical analysis was performed by ordinary one-way ANOVA test. * = $P < 0.05$; *** = $P < 0.001$ vs control (untreated).

A similar anti-migratory activity of the Dex(NFκB-ODN) NPs was observed with the transwell chamber assay. In this experiment, the Dex(NFκB-ODN) NPs significantly inhibited A549 cells migration (**Figure 7a**) by 43.2% compared to the untreated control (**Figure 7b**), while upon treatment with Dex(Scrambled-ODN) NPs, no significant inhibition of cells migration was observed as shown in **Figure 7b**.

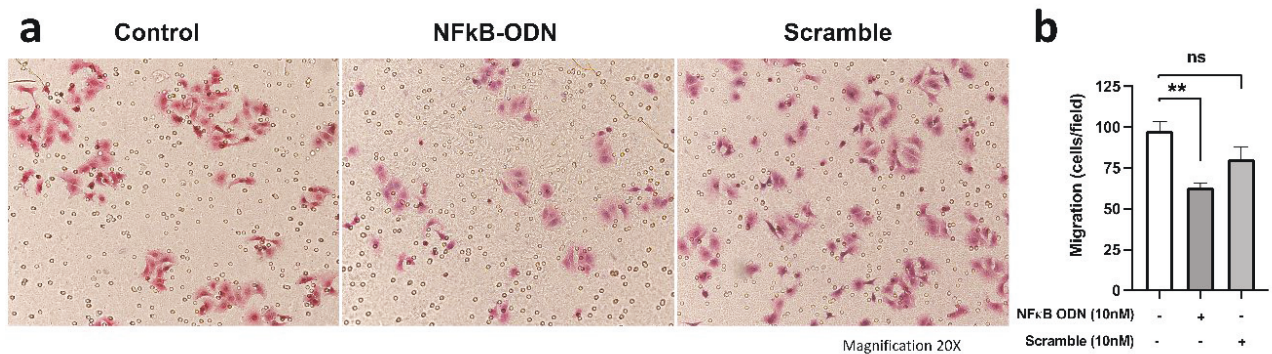


Figure 7. Anti-migratory activity of Dex(NFκB-ODN) NPs in A549 cells: Transwell chamber assay. A549 cells were seeded in a transwell chamber previously coated with gelatin and treated with 10 nM Dex(NFκB-ODN) NPs or concentration-matched Dex(scrambled-ODN)NPs for 24 h. Subsequently, cells were allowed to migrate through the membrane for additional 24 h. The cells that successfully migrated were then stained with hematoxylin-eosin and imaged under a light microscope (a). The migrated cells were counted in 5 random positions per well under a high-power field (b). Values are expressed as average \pm SEM of $n = 3$ independent experiments. Statistical analysis was performed by ordinary one-way ANOVA test. ns = $P \geq 0.05$; ** = $P < 0.01$ vs control (untreated).

3.8 Anti-Colony Formation Activity of NFκB-ODN-NPs in A549 Cells

The anti-colony formation activity of the Dex(NFκB-ODN) NPs in A549 cells was evaluated by colony formation assay after staining with crystal violet. The result of this assay is depicted in **Figure 8**, where the Dex(NFκB-ODN) NPs is shown to inhibit colony formation compared

to the untreated and Dex(scrambled-ODN) NPs treated cells (**Figure 8a**). In particular, treatment with the Dex(NFκB-ODN) NPs resulted in a significantly high inhibition of colony formation up to 42% (**Figure 8b**).

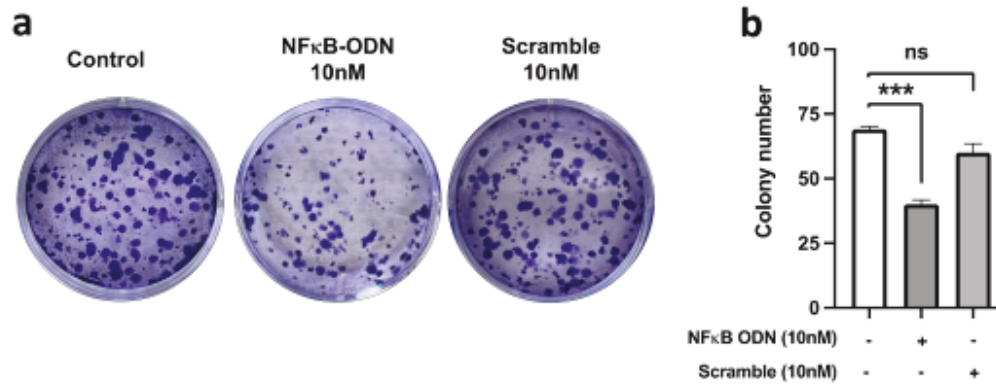


Figure 8. Anti-colony formation activity of Dex(NFκB-ODN) NPs in A549 cells. A549 cells were seeded at low density in 6-well plates and, after adhesion, treated with 10 nM Dex(NFκB-ODN) NPs or concentration-matched Dex(scrambled-ODN) NPs for 24 h. After colony formation (\approx 2 weeks), cells were stained with crystal violet solution and each individual well was imaged using the light microscope (a). The resulting number of colonies in each well has been counted and is plotted in (b). Values are expressed as average \pm SEM of $n = 3$ independent experiments. Statistical analysis was performed by ordinary one-way ANOVA test. ns = $P \geq 0.05$; ** = $P < 0.01$ vs control (untreated).

4. Discussion

In this study, we have shown the potent anticancer activity of a SpAcDex-based NF κ B decoy ODN formulations against an established *in vitro* model of lung cancer, the A549 NSCLC cell line. This anticancer activity was exerted primarily through the inhibition of proliferation, migration, and colony formation.

Both scrambled and NF κ B decoy ODNs were encapsulated into an acid responsive SpAcDex NPs. The spermine-modified acetalated dextran material was synthesized according to *Cohen et al.* [46] The acetal modification of dextran introduces an acid-sensitive functional group to switch the solubility of dextran from hydrophilic to hydrophobic, allowing particle formulation using the emulsion method [49, 65]. These acetalated dextran-based nanocarriers have been effectively used for the delivery of a range of different payloads, including plasmid DNA [66]. To further improve the encapsulation efficiency for small oligonucleotides like siRNA or mRNA, the possibility of additional electrostatic interactions with the phosphate backbone of the RNAs, which is predicted to be exposed on the external surface of dsRNA strands, was provided via functionalization with cationic amines by introducing spermine molecules in the dextran backbone. The spermine modification resulted in an excellent loading of oligonucleotides. The presence of positive charges on the surface of SpAcDex NPs also enhances cellular uptake by improving their interaction with negatively charged cell membranes.

For the particle formulation and ODN encapsulation in spermine-modified acetalated dextran NPs, a double emulsion method was applied [67, 68]. The hydrophilic double-stranded decoy ODN dissolved in PBS buffer was added on top of the DCM layer containing spermine-modified acetalated dextran before the first sonication step to encapsulate this hydrophilic payload into the core of the NPs.

After secondary emulsion and solvent evaporation, narrow size distributed nanoparticles were obtained. The free decoy ODN was quantified by analysing the supernatant after centrifugation using a fluorescence-based indirect method with RiboGreen assay. This confirmed the successful encapsulation of decoy ODN in the nanoparticles. A high encapsulation efficiency was observed, which can be attributed to the electrostatic interaction between the cationic component of spermine AcDex material and the negatively charged decoy ODN [46].

The degradation of particles after incubation in acidic conditions was observed as a result of the hydrolysis of acetal groups. This process led to the conversion of the polysaccharide

component of the particles back to its water-soluble native form which ultimately leads to particle degradation. The pH-dependence of particle degradation was confirmed using dynamic light scattering (DLS) and visual observations over different time periods. Additionally, the release rate of oligonucleotide (ODN) from loaded particles was determined to be dependent on the pH, with a higher rate of release observed in acidic conditions. The observation of limited decoy ODN released under neutral pH 7.4 over a 24 h period acts as a control and highlights the stability of these particles in normal physiological conditions. This stability is critical for ensuring that the particles remain intact to avoid any unwanted leakage and the protection of loaded decoy ODN from nuclease activity in physiological environments such as the bloodstream or typical extracellular spaces, where neutral pH levels are maintained.

Additionally, these particles have been reported to escape endosomes upon cellular uptake via the proton sponge effect, due to the presence of amine content. Upon endocytosis, the degradation of these particles is triggered by low pH in the endosomal compartment. Furthermore, the buffering of the endosome by spermine content leads to accumulation of counterions (such as Cl⁻), which raises the osmotic pressure and causes the endosome to burst [69, 70]. This releases the decoy ODN into the cytoplasm, protecting it from degradation by lysosomal enzymes and ensuring its successful delivery [71].

The overall stability of the particles under physiological conditions reduces the risk of unintended side effects and toxicity, while the acid-triggered release pattern suggests that decoy ODN will only be released in the acidic environment of tumor or endosome/lysosome, which makes this system an attractive candidate for administration of decoy oligonucleotides. The controlled release of decoy ODN from these particles may lead to improved therapeutic outcomes for patients. Next, we tested the anticancer activity of the Dex(NFκB-ODN) NPs formulation against A549 cells. We used A549 cells as an *in vitro* model of NSCLC as this cell line has been extensively characterized and is commonly used in NSCLC studies aimed at investigating mechanisms of action and efficacy of novel experimental anticancer drugs. In particular, the A549 cells are hypotriploid human alveolar basal epithelial cells, with extensive applications as *in vitro* model for lung adenocarcinoma and type II pulmonary epithelial cells [72]. Being cell proliferation and migration/metastasis two hallmarks of cancer progression [73, 74], we have investigated these processes in A549 cells by measuring the impact of treatment with Dex(NFκB-ODN) NPs on the cell ability to proliferate, migrate and form colonies.

As shown by the MTT assay, treatment with Dex(NFκB-ODN) NPs significantly inhibited (37.2%) the proliferation of A549 cells in a dose-dependent manner. Furthermore, we have obtained a low (12%), but significant, anti-proliferative activity when treating A549 cells with the 10 nM concentrated Dex(scrambled-ODN) NPs (here 10 nM concentration represents the concentration of ODNs). Considering that this anti-proliferative activity was sensibly lower compared to the value obtained with the concentration-matched Dex(NFκB-ODN) NPs, we performed the subsequent experiments using 10 nM concentrated ODNs. Furthermore, the fact that the anti-proliferative effect with the 10 nM concentrated Dex(scrambled-ODN) NPs was lower compared to the 10 nM Dex(NFκB-ODN) NPs, confirming that the anti-proliferative activity of the Dex(NFκB-ODN) NPs derives specifically from their NFκB-inhibiting action.

To assess the safety of the Dex(NFκB-ODN) NPs, the formulations were tested on non-cancerous BEAS-2B human bronchial epithelial cells. Although Dex(NFκB-ODN) NPs exerted a significant reduction of BEAS-2B cell viability, the relative safety of our formulation is demonstrated by the fact that, at the highest concentrations tested, the impact on BEAS-2B cell viability was significantly lower compared to the impact on A549 cell viability. This suggests that Dex(NFκB-ODN) NPs specifically inhibit the proliferation of cancerous A549 cells.

To assess whether the materials used in the synthesis of the NPs had any toxic effects on cells, empty nanoparticle were tested on both A549 and BEAS-2B cells. Treatment with empty NPs concentrations of up to 20 μg/mL resulted in no significant reduction of cell viability on both cell lines, in accordance with reports showing that the NPs materials have minimal toxicity against most cells at moderate concentrations [46].

Considering that, in PC-3M androgen-independent prostate cancer cells, the transfection with an NFκB decoy ODN has been reported to induce apoptosis, together with strong suppression of cell proliferation [32], we cannot exclude that, in our experiment, an eventual induction of apoptosis or necroptosis caused by NFκB blockade has at least a partial influence on the reduced metabolic activity reported by the MTT assay. To test this hypothesis, we have assessed the effect of Dex(NFκB-ODN) NPs on the expression of the genes RIPK1, MLKL, TNF-α, and RIPK3, which are collectively considered key mediators of apoptosis and necroptosis [75]. Treatment of A549 cells with Dex(NFκB-ODN) NPs resulted in an overall

increased expression of these genes, which reached statistical significance for RIPK1 and MLKL. The fact that Dex(NFκB-ODN) NPs induced a trend of increase of the expression of TNF-α and RIPK3 genes is caused by a relatively higher variability of the expression of these genes. However, these results collectively confirm that at least part of the anti-proliferative effect of Dex(NFκB-ODN) NPs is caused by the activation of the TNF-α/RIPK1/RIPK3/MLKL pathway which leads to necroptosis.

Furthermore, the inhibition of the NFκB pathway through treatment with the decoy ODN NPs exerted a significant anti-migratory activity, as demonstrated in the wound healing assay as well as in the transwell chamber assay. In the wound healing assay, treatment with Dex(scrambled-ODN) NPs exerted a slight anti-migratory activity, similar to what was observed in the MTT assay. However, a significantly stronger anti-migratory activity was obtained upon treatment with Dex(NFκB-ODN) NPs, which suggests this effect is exerted specifically through the inhibition of NFκB.

The anticancer activity of the Dex(NFκB-ODN) NPs was also supported by the colony formation assay, where a significantly lower number of colonies was formed upon treatment with Dex(NFκB-ODN) NPs compared to Dex(scrambled-ODN) NPs.

Taken together, these results underscore the strong anticancer activity of Dex(NFκB-ODN) NPs, further highlighting the therapeutic potential of NFκB blockage through NP-mediated delivery of decoy ODNs for lung cancer [27, 76].

The robustness and relevance of such a treatment approach would enormously benefit from a mechanistic explanation of the pathways through which the Dex(NFκB-ODN) NPs exert their anti-migratory activity. In the modified Boyden's chamber assay, the surface of the chamber was coated with 2.5% gelatin. Considering that gelatin is degraded by matrix metalloproteinases (MMPs) [77], it can be hypothesized that the reduction of the migratory ability of A549 cells obtained upon NFκB inhibition could be caused by the downregulation of MMPs expression and/or activity. This would also be in agreement with the fact that MMPs, including MMP2 and MMP9, are upregulated upon NFκB activation [78]. Therefore, the assessment of the levels of MMPs via Western blot [58], and/or of their activity through gel zymography [79], could shed further light on the mechanism by which the inhibition of NFκB signalling results in impaired migrating ability. A limitation of our study resides in the fact that only one cell line, A549, has been used to investigate the anticancer activity of Dex(NFκB-ODN) NPs. Although this cell line is a well-established model of LC [72], testing the anticancer

activity of Dex(NFκB-ODN) NPs on further human LC cell lines, as well as on animal models of LC, would surely deepen our comprehension of the exact mechanism(s) by which treatment with Dex(NFκB-ODN) NPs exerts its anticancer activity. This would also be useful in expanding the applicability of this treatment strategy against different subtypes of LC, as well as against other types of cancer, thus strongly enhancing its potential therapeutic range.

A point of strength of the present study lies in the great potential for clinical translation of the Dex(NFκB-ODN) NPs. Acetalated dextran, in fact, is an easy-to-synthesize, bio-compatible material derived by the FDA-approved dextran [80], and it is characterised by extreme versatility and tunability of application as drug delivery system [44, 65]. The application of Dex(NFκB-ODN) NPs in the treatment of lung diseases such as NSCLC is advantageous due to the possibility of deliver the therapeutic agent via inhalational delivery, which represents a privileged administration route for the direct delivery of drug to the lung tissue. Acetalated dextran nanoparticles are suitable for this application, as they can be formulated as dry powder to be administered via inhalation [46, 66, 80]. The *in vivo* study of the delivery and efficacy of Dex(NFκB-ODN) NPs would enormously streamline the clinical translation of this formulation.

5. Conclusions

In conclusion, this study strongly supports the feasibility of inhibiting the NFκB signalling pathway as a therapeutic approach against NSCLC using a cationic dextran-based pH-sensitive delivery system for decoy ODNs. An excellent loading and a controlled release of decoy ODN demonstrated the significance of polysaccharide-based NPs as a novel therapeutic strategy. This resulted in a strong, significant inhibition of three cancer hallmarks: cell proliferation, migration and colony formation. The results of this study provide an innovative direction into the clinical management of lung cancer. Furthermore, these findings represent a blueprint for further medical research and application against lung infectious diseases and other chronic respiratory diseases, providing solid theoretical bases to test similar nanoformulation approaches to enhance the pulmonary delivery of compounds with poor pharmacokinetic properties and bioavailability such as ODNs.

Declaration of interest: none

Acknowledgments

The authors are thankful to the Graduate School of Health, University of Technology Sydney, Australia. KD is supported by a project grant from the Rebecca L Cooper Medical Research Foundation and the Maridulu Budyari Gumal Sydney Partnership for Health, Education, Research and Enterprise (SPHERE) RSEOH CAG Seed grant, fellowship and extension grant; Faculty of Health MCR/ECR Mentorship Support Grant and UTS Global Strategic Partnerships Seed Funding Scheme. GDR is supported by the UTS International Research Scholarship and the UTS President's Scholarship. KRP is supported by a fellowship from Prevent Cancer Foundation (PCF) and the International Association for the Study of Lung Cancer (IASLC). We also thank Maryam Hosseini for her help with SEM imaging.

References

1. Sung H, Ferlay J, Siegel RL *et al.* Global Cancer Statistics 2020: GLOBOCAN Estimates of Incidence and Mortality Worldwide for 36 Cancers in 185 Countries. *CA Cancer J Clin* 71(3), 209-249 (2021).
2. Malyla V, Paudel KR, Shukla SD *et al.* Recent advances in experimental animal models of lung cancer. *Future Med Chem* 12(7), 567-570 (2020).
3. Wong MCS, Lao XQ, Ho KF, Goggins WB, Tse SLA. Incidence and mortality of lung cancer: global trends and association with socioeconomic status. *Sci Rep* 7(1), 14300 (2017).
4. Sharma P, Mehta M, Dhanjal DS *et al.* Emerging trends in the novel drug delivery approaches for the treatment of lung cancer. *Chem Biol Interact* 309 108720 (2019).
5. Onaitis MW, Petersen RP, Balderson SS *et al.* Thoracoscopic lobectomy is a safe and versatile procedure: experience with 500 consecutive patients. *Ann Surg* 244(3), 420-425 (2006).
6. Klastersky J, Awada A. Milestones in the use of chemotherapy for the management of non-small cell lung cancer (NSCLC). *Crit Rev Oncol Hematol* 81(1), 49-57 (2012).
7. Kang TM, Hardcastle N, Singh AK *et al.* Practical considerations of single-fraction stereotactic ablative radiotherapy to the lung. *Lung Cancer* 170 185-193 (2022).
8. Liu SY, Liu SM, Zhong WZ, Wu YL. Targeted Therapy in Early Stage Non-small Cell Lung Cancer. *Curr Treat Options Oncol* doi:10.1007/s11864-022-00994-w (2022).
9. Baci D, Cekani E, Imperatori A, Ribatti D, Mortara L. Host-Related Factors as Targetable Drivers of Immunotherapy Response in Non-Small Cell Lung Cancer Patients. *Front Immunol* 13 914890 (2022).
10. Paudel KR, Panth N, Pangeni R *et al.* Chapter 23 - Targeting lung cancer using advanced drug delivery systems. In: *Targeting Chronic Inflammatory Lung Diseases Using Advanced Drug Delivery Systems*, Dua K, Hansbro PM, Wadhwa R, Haghi M, Pont LG, Williams KA (Ed. ^ (Eds). Academic Press 493-516 (2020).
11. Yazbeck V, Alesi E, Myers J, Hackney MH, Cuttino L, Gewirtz DA. An overview of chemotoxicity and radiation toxicity in cancer therapy. *Adv Cancer Res* 155 1-27 (2022).

12. Paudel KR, Chellappan DK, Macloughlin R, Pinto TJA, Dua K, Hansbro PM. Editorial: Advanced therapeutic delivery for the management of chronic respiratory diseases. *Front Med (Lausanne)* 9 983583 (2022).
13. Paudel KR, Dua K, Panth N, Hansbro PM, Chellappan DK. Advances in research with rutin-loaded nanoformulations in mitigating lung diseases. *Future Med Chem* 14(18), 1293-1295 (2022).
14. Malya V, Paudel KR, Rubis GD, Hansbro NG, Hansbro PM, Dua K. Extracellular Vesicles Released from Cancer Cells Promote Tumorigenesis by Inducing Epithelial to Mesenchymal Transition via β -Catenin Signaling. *International Journal of Molecular Sciences* 24(4), 3500 (2023).
15. Sen R, Baltimore D. In vitro transcription of immunoglobulin genes in a B-cell extract: effects of enhancer and promoter sequences. *Mol Cell Biol* 7(5), 1989-1994 (1987).
16. Zhang Q, Lenardo MJ, Baltimore D. 30 Years of NF- κ B: A Blossoming of Relevance to Human Pathobiology. *Cell* 168(1-2), 37-57 (2017).
17. Xia L, Tan S, Zhou Y *et al.* Role of the NF κ B-signaling pathway in cancer. *Oncotargets Ther* 11 2063-2073 (2018).
18. Taniguchi K, Karin M. NF- κ B, inflammation, immunity and cancer: coming of age. *Nat Rev Immunol* 18(5), 309-324 (2018).
19. Cai Z, Tchou-Wong KM, Rom WN. NF-kappaB in lung tumorigenesis. *Cancers (Basel)* 3(4), 4258-4268 (2011).
20. Jones DR, Broad RM, Madrid LV, Baldwin AS, Jr., Mayo MW. Inhibition of NF-kappaB sensitizes non-small cell lung cancer cells to chemotherapy-induced apoptosis. *Ann Thorac Surg* 70(3), 930-936; discussion 936-937 (2000).
21. Gao M, Yeh PY, Lu YS, Chang WC, Kuo ML, Cheng AL. NF-kappaB p50 promotes tumor cell invasion through negative regulation of invasion suppressor gene CRMP-1 in human lung adenocarcinoma cells. *Biochem Biophys Res Commun* 376(2), 283-287 (2008).
22. Kumar M, Allison DF, Baranova NN *et al.* NF- κ B regulates mesenchymal transition for the induction of non-small cell lung cancer initiating cells. *PLoS One* 8(7), e68597 (2013).
23. Gu L, Wang Z, Zuo J, Li H, Zha L. Prognostic significance of NF- κ B expression in non-small cell lung cancer: A meta-analysis. *PLoS One* 13(5), e0198223 (2018).

24. Wong KK, Jacks T, Dranoff G. NF-kappaB fans the flames of lung carcinogenesis. *Cancer Prev Res (Phila)* 3(4), 403-405 (2010).
25. Yu H, Lin L, Zhang Z, Zhang H, Hu H. Targeting NF-κB pathway for the therapy of diseases: mechanism and clinical study. *Signal Transduct Target Ther* 5(1), 209 (2020).
26. Ramadass V, Vaiyapuri T, Tergaonkar V. Small Molecule NF-κB Pathway Inhibitors in Clinic. *Int J Mol Sci* 21(14), (2020).
27. Mehta M, Paudel KR, Shukla SD *et al.* Recent trends of NFκB decoy oligodeoxynucleotide-based nanotherapeutics in lung diseases. *J Control Release* 337 629-644 (2021).
28. Wardwell PR, Bader RA. Immunomodulation of cystic fibrosis epithelial cells via NF-kappaB decoy oligonucleotide-coated polysaccharide nanoparticles. *J Biomed Mater Res A* 103(5), 1622-1631 (2015).
29. Ahmad MZ, Akhter S, Mallik N, Anwar M, Tabassum W, Ahmad FJ. Application of decoy oligonucleotides as novel therapeutic strategy: a contemporary overview. *Curr Drug Discov Technol* 10(1), 71-84 (2013).
30. Mann MJ. Transcription factor decoys: a new model for disease intervention. *Ann N Y Acad Sci* 1058 128-139 (2005).
31. Imran M, Jha LA, Hasan N *et al.* "Nanodecoys" - Future of drug delivery by encapsulating nanoparticles in natural cell membranes. *Int J Pharm* 621 121790 (2022).
32. Fang Y, Sun H, Zhai J *et al.* Antitumor activity of NF-kB decoy oligodeoxynucleotides in a prostate cancer cell line. *Asian Pac J Cancer Prev* 12(10), 2721-2726 (2011).
33. Morishita R, Higaki J, Tomita N, Ogihara T. Application of transcription factor "decoy" strategy as means of gene therapy and study of gene expression in cardiovascular disease. *Circ Res* 82(10), 1023-1028 (1998).
34. Dinh TD, Higuchi Y, Kawakami S, Yamashita F, Hashida M. Evaluation of osteoclastogenesis via NFκB decoy/mannosylated cationic liposome-mediated inhibition of pro-inflammatory cytokine production from primary cultured macrophages. *Pharm Res* 28(4), 742-751 (2011).
35. De Stefano D. Oligonucleotides decoy to NF-kappaB: becoming a reality? *Discov Med* 12(63), 97-105 (2011).

36. Farahmand L, Darvishi B, Majidzadeh AK. Suppression of chronic inflammation with engineered nanomaterials delivering nuclear factor κ B transcription factor decoy oligodeoxynucleotides. *Drug Deliv* 24(1), 1249-1261 (2017).
37. Mischiati C, Borgatti M, Bianchi N *et al.* Interaction of the human NF-kappaB p52 transcription factor with DNA-PNA hybrids mimicking the NF-kappaB binding sites of the human immunodeficiency virus type 1 promoter. *J Biol Chem* 274(46), 33114-33122 (1999).
38. Crinelli R, Bianchi M, Gentilini L *et al.* Transcription factor decoy oligonucleotides modified with locked nucleic acids: an in vitro study to reconcile biostability with binding affinity. *Nucleic Acids Res* 32(6), 1874-1885 (2004).
39. Farahmand L, Darvishi B, Majidzadeh AK. Suppression of chronic inflammation with engineered nanomaterials delivering nuclear factor kappaB transcription factor decoy oligodeoxynucleotides. *Drug Deliv* 24(1), 1249-1261 (2017).
40. Doroudian M, Macloughlin R, Poynton F, Prina-Mello A, Donnelly SC. Nanotechnology based therapeutics for lung disease. *Thorax* 74(10), 965-976 (2019).
41. De Rosa G, Maiuri MC, Ungaro F *et al.* Enhanced intracellular uptake and inhibition of NF-kappaB activation by decoy oligonucleotide released from PLGA microspheres. *J Gene Med* 7(6), 771-781 (2005).
42. De Stefano D, De Rosa G, Maiuri MC *et al.* Oligonucleotide decoy to NF-kappaB slowly released from PLGA microspheres reduces chronic inflammation in rat. *Pharmacol Res* 60(1), 33-40 (2009).
43. Zhang N, Wardwell PR, Bader RA. Polysaccharide-based micelles for drug delivery. *Pharmaceutics* 5(2), 329-352 (2013).
44. Prasher P, Sharma M, Mehta M *et al.* Current-status and applications of polysaccharides in drug delivery systems. *Colloid and Interface Science Communications* 42 100418 (2021).
45. Ma L, Shen CA, Gao L *et al.* Anti-inflammatory activity of chitosan nanoparticles carrying NF-kappaB/p65 antisense oligonucleotide in RAW264.7 macrophage stimulated by lipopolysaccharide. *Colloids Surf B Biointerfaces* 142 297-306 (2016).
46. Cohen JL, Schubert S, Wich PR *et al.* Acid-degradable cationic dextran particles for the delivery of siRNA therapeutics. *Bioconj Chem* 22(6), 1056-1065 (2011).
47. Boedtkjer E, Pedersen SF. The Acidic Tumor Microenvironment as a Driver of Cancer. *Annu Rev Physiol* 82 103-126 (2020).

48. Bachelder EM, Beaudette TT, Broaders KE, Dashe J, Frechet JM. Acetal-derivatized dextran: an acid-responsive biodegradable material for therapeutic applications. *J Am Chem Soc* 130(32), 10494-10495 (2008).
49. Wang S, Fontana F, Shahbazi MA, Santos HA. Acetalated dextran based nano- and microparticles: synthesis, fabrication, and therapeutic applications. *Chem Commun (Camb)* 57(35), 4212-4229 (2021).
50. Bamberger D, Hobernik D, Konhauser M, Bros M, Wich PR. Surface Modification of Polysaccharide-Based Nanoparticles with PEG and Dextran and the Effects on Immune Cell Binding and Stimulatory Characteristics. *Mol Pharm* 14(12), 4403-4416 (2017).
51. Shi K, Xue J, Fang Y *et al.* Inorganic Kernel-Reconstituted Lipoprotein Biomimetic Nanovehicles Enable Efficient Targeting "Trojan Horse" Delivery of STAT3-Decoy Oligonucleotide for Overcoming TRAIL Resistance. *Theranostics* 7(18), 4480-4497 (2017).
52. Centelles MN, Qian C, Campanero MA, Irache JM. New methodologies to characterize the effectiveness of the gene transfer mediated by DNA-chitosan nanoparticles. *Int J Nanomedicine* 3(4), 451-460 (2008).
53. Hanwell MD, Curtis DE, Lonie DC, Vandermeersch T, Zurek E, Hutchison GR. Avogadro: an advanced semantic chemical editor, visualization, and analysis platform. *Journal of Cheminformatics* 4(1), 17 (2012).
54. Pettersen EF, Goddard TD, Huang CC *et al.* UCSF Chimera—A visualization system for exploratory research and analysis. *Journal of Computational Chemistry* 25(13), 1605-1612 (2004).
55. Lee HH, Paudel KR, Kim DW. Terminalia chebula Fructus Inhibits Migration and Proliferation of Vascular Smooth Muscle Cells and Production of Inflammatory Mediators in RAW 264.7. *Evid Based Complement Alternat Med* 2015 502182 (2015).
56. Paudel KR, Panth N, Manandhar B *et al.* Attenuation of Cigarette-Smoke-Induced Oxidative Stress, Senescence, and Inflammation by Berberine-Loaded Liquid Crystalline Nanoparticles: In Vitro Study in 16HBE and RAW264.7 Cells. *Antioxidants (Basel)* 11(5), (2022).
57. Jun MY, Karki R, Paudel KR, Sharma BR, Adhikari D, Kim DW. Alkaloid rich fraction from Nelumbo nucifera targets VSMC proliferation and migration to suppress restenosis in balloon-injured rat carotid artery. *Atherosclerosis* 248 179-189 (2016).

58. Paudel KR, Wadhwa R, Tew XN *et al.* Rutin loaded liquid crystalline nanoparticles inhibit non-small cell lung cancer proliferation and migration in vitro. *Life Sci* 276 119436 (2021).
59. Paudel KR, Mehta M, Yin GHS *et al.* Berberine-loaded liquid crystalline nanoparticles inhibit non-small cell lung cancer proliferation and migration in vitro. *Environ Sci Pollut Res Int* 29(31), 46830-46847 (2022).
60. Wadhwa R, Paudel KR, Chin LH *et al.* Anti-inflammatory and anticancer activities of Naringenin-loaded liquid crystalline nanoparticles in vitro. *J Food Biochem* 45(1), e13572 (2021).
61. Alnuqaydan AM, Almutary AG, Azam M *et al.* Evaluation of the Cytotoxic Activity and Anti-Migratory Effect of Berberine-Phytantriol Liquid Crystalline Nanoparticle Formulation on Non-Small-Cell Lung Cancer In Vitro. *Pharmaceutics* 14(6), (2022).
62. Wan L, Yao X, Faiola F *et al.* Coating with spermine-pullulan polymer enhances adenoviral transduction of mesenchymal stem cells. *Int J Nanomedicine* 11 6763-6769 (2016).
63. Breitenbach BB, Steiert E, Konhäuser M *et al.* Double stimuli-responsive polysaccharide block copolymers as green macrosurfactants for near-infrared photodynamic therapy. *Soft Matter* 15(6), 1423-1434 (2019).
64. Braga CB, Perli G, Becher TB, Ornelas C. Biodegradable and pH-Responsive Acetalated Dextran (Ac-Dex) Nanoparticles for NIR Imaging and Controlled Delivery of a Platinum-Based Prodrug into Cancer Cells. *Mol Pharm* 16(5), 2083-2094 (2019).
65. Bachelder EM, Pino EN, Ainslie KM. Acetalated Dextran: A Tunable and Acid-Labile Biopolymer with Facile Synthesis and a Range of Applications. *Chem Rev* 117(3), 1915-1926 (2017).
66. Cohen JA, Beaudette TT, Cohen JL, Broaders KE, Bachelder EM, Frechet JM. Acetal-modified dextran microparticles with controlled degradation kinetics and surface functionality for gene delivery in phagocytic and non-phagocytic cells. *Adv Mater* 22(32), 3593-3597 (2010).
67. Foerster F, Bamberger D, Schupp J *et al.* Dextran-based therapeutic nanoparticles for hepatic drug delivery. *Nanomedicine* 11(20), 2663-2677 (2016).
68. Konhauser M, Kannaujiya VK, Steiert E, Schwickert K, Schirmeister T, Wich PR. Co-encapsulation of l-asparaginase and etoposide in dextran nanoparticles for synergistic effect in chronic myeloid leukemia cells. *Int J Pharm* 622 121796 (2022).

69. Nguyen J, Szoka FC. Nucleic acid delivery: the missing pieces of the puzzle? *Acc Chem Res* 45(7), 1153-1162 (2012).
70. Mahajan S, Tang T. Polyethylenimine-DNA Nanoparticles under Endosomal Acidification and Implication to Gene Delivery. *Langmuir* 38(27), 8382-8397 (2022).
71. Akinc A, Thomas M, Klibanov AM, Langer R. Exploring polyethylenimine-mediated DNA transfection and the proton sponge hypothesis. *J Gene Med* 7(5), 657-663 (2005).
72. Lieber M, Smith B, Szakal A, Nelson-Rees W, Todaro G. A continuous tumor-cell line from a human lung carcinoma with properties of type II alveolar epithelial cells. *Int J Cancer* 17(1), 62-70 (1976).
73. Wadhwa R, Paudel KR, Shukla S *et al.* Epigenetic Therapy as a Potential Approach for Targeting Oxidative Stress–Induced Non-small-Cell Lung Cancer. In: *Handbook of Oxidative Stress in Cancer: Mechanistic Aspects*, Chakraborti S, Ray BK, Roychoudhury S (Ed.^(Eds). Springer Nature Singapore Singapore 1545-1560 (2022).
74. Khursheed R, Dua K, Vishwas S *et al.* Biomedical applications of metallic nanoparticles in cancer: Current status and future perspectives. *Biomed Pharmacother* 150 112951 (2022).
75. Seo J, Nam YW, Kim S, Oh D-B, Song J. Necroptosis molecular mechanisms: Recent findings regarding novel necroptosis regulators. *Experimental & Molecular Medicine* 53(6), 1007-1017 (2021).
76. Dimitrakopoulos FD, Kottorou AE, Kalofonou M, Kalofonos HP. The Fire Within: NF- κ B Involvement in Non-Small Cell Lung Cancer. *Cancer Res* 80(19), 4025-4036 (2020).
77. Mook OR, Van Overbeek C, Ackema EG, Van Maldegem F, Frederiks WM. In situ localization of gelatinolytic activity in the extracellular matrix of metastases of colon cancer in rat liver using quenched fluorogenic DQ-gelatin. *J Histochem Cytochem* 51(6), 821-829 (2003).
78. Li J, Lau GK, Chen L *et al.* Interleukin 17A promotes hepatocellular carcinoma metastasis via NF- κ B induced matrix metalloproteinases 2 and 9 expression. *PLoS One* 6(7), e21816 (2011).
79. Frankowski H, Gu YH, Heo JH, Milner R, Del Zoppo GJ. Use of gel zymography to examine matrix metalloproteinase (gelatinase) expression in brain tissue or in primary glial cultures. *Methods Mol Biol* 814 221-233 (2012).

80. Prasher P, Sharma M, Kumar Singh S *et al.* Versatility of acetalated dextran in nanocarriers targeting respiratory diseases. *Materials Letters* 323 132600 (2022).

SUPPLEMENTARY INFORMATION

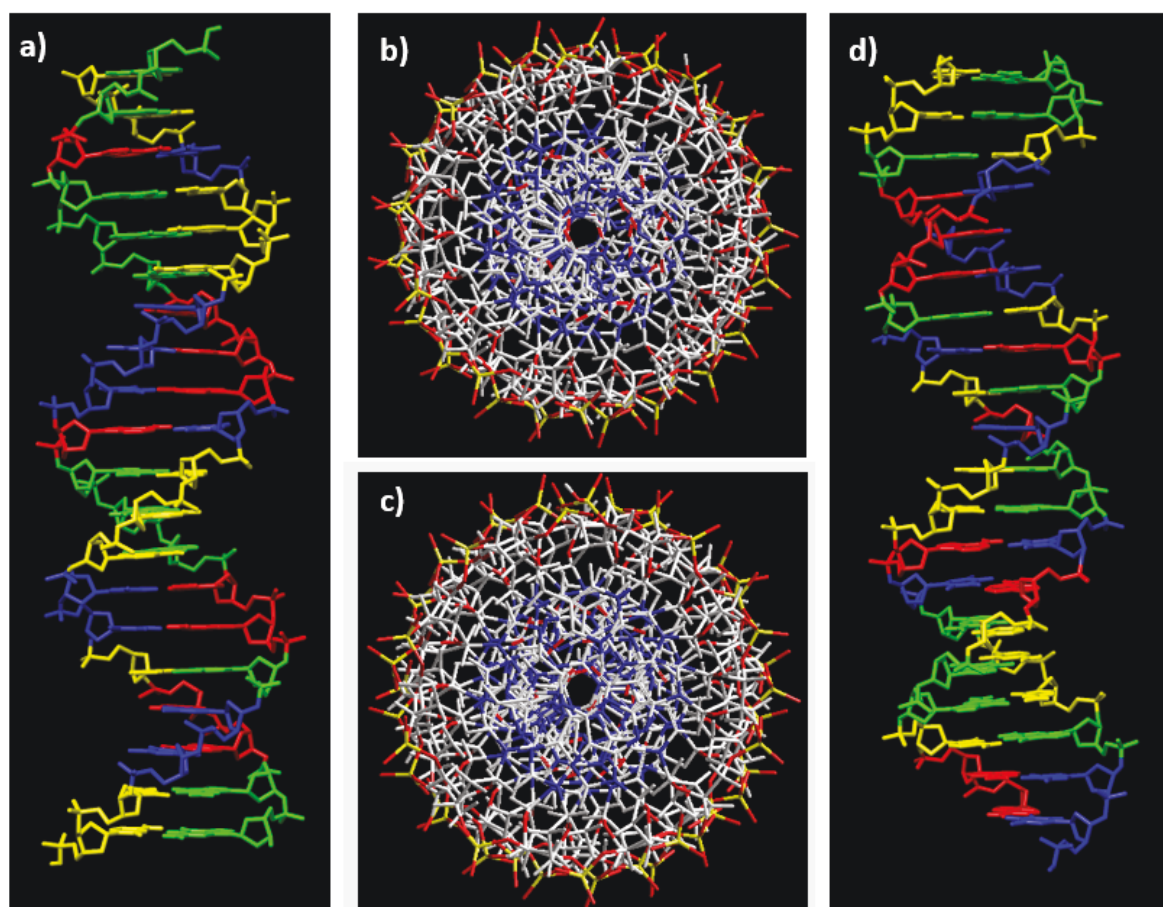


Figure S1. Application of molecular modelling to predict ODN structure

Molecular structures depicting a) NFκB-ODN double-helix, side view; b) NFκB-ODN double helix, top view, showing phosphate functional groups exposed externally; c) scrambled ODN double-helix, side view; and d) scrambled ODN double helix, top view, showing phosphate functional groups exposed externally. NDB Color codes for a) and d): A=red, T=blue, C=yellow, G=green; Elemental color code for b) and c): C=white; O=red; N=blue; P=yellow.

CHAPTER 3

Research Paper #2

Agarwood oil nanoemulsion attenuates cigarette smoke-induced inflammation and oxidative stress markers in B*Ci*NS1.1 airway epithelial cells

(**De Rubis G**[#], Paudel KR[#], Manandhar B, Singh SK, Gupta G, Malik R, Shen J, Chami A, MacLoughlin R, Chellappan DK, Oliver BGG, Hansbro PM, Dua K. *Agarwood Oil Nanoemulsion Attenuates Cigarette Smoke-Induced Inflammation and Oxidative Stress Markers in B*Ci*-NS1.1 Airway Epithelial Cells*. **Nutrients**. 2023 Feb 17;15(4):1019. doi: 10.3390/nu15041019.)

[#] Authors contributed equally to this work

Agarwood Oil Nanoemulsion Attenuates Cigarette Smoke-Induced Inflammation and Oxidative Stress Markers in BCINS1.1 Airway Epithelial Cells

Gabriele De Rubis^{1,2#}, Keshav Raj Paudel^{3#}, Bikash Manhandar^{1,2}, Sachin Kumar Singh^{2,4}, Gaurav Gupta^{5,6,7}, Raniya Malik⁸, Jessie Shen⁸, Aniss Chami⁹, Ronan MacLoughlin^{10,11,12}, Dinesh Kumar Chellappan¹³, Brian Gregory George Oliver^{14,15}, Philip Michael Hansbro^{3*} and Kamal Dua^{1,2*}

¹ Discipline of Pharmacy, Graduate School of Health, University of Technology Sydney, Sydney, NSW 2007, Australia

² Faculty of Health, Australian Research Centre in Complementary and Integrative Medicine, University of Technology Sydney, Ultimo, NSW 2007, Australia

³ Centre for Inflammation, Centenary Institute and University of Technology Sydney, Faculty of Science, School of Life Sciences, Sydney, NSW 2007, Australia

⁴ School of Pharmaceutical Sciences, Lovely Professional University, Jalandhar-Delhi GT Road, Phagwara 144411, Punjab, India

⁵ School of Pharmacy, Suresh Gyan Vihar University, Jaipur 302017, Rajasthan, India

⁶ Uttaranchal Institute of Pharmaceutical Sciences, Uttaranchal University, Dehradun 248007, Uttarakhand, In-dia

⁷ Department of Pharmacology, Saveetha Dental College, Saveetha Institute of Medical and Technical Sciences, Saveetha University, Chennai, India

⁸ DeÁurora Pty Ltd., Dean, VIC 3363, Australia

⁹ Vitex Pharmaceuticals, Eastern Creek NSW 2766, Australia

¹⁰ Aerogen, IDA Business Park, H91 HE94 Galway, Connacht, Ireland

¹¹ School of Pharmacy & Biomolecular Sciences, Royal College of Surgeons in Ireland, D02 YN77 Dublin, Lein-ster, Ireland

¹² School of Pharmacy & Pharmaceutical Sciences, Trinity College, D02 PN40 Dublin, Leinster, Ireland

¹³ Department of Life Sciences, School of Pharmacy, International Medical University, Bukit Jalil 57000, Kuala Lumpur, Malaysia

¹⁴ Woolcock Institute of Medical Research, University of Sydney, Sydney, New South Wales, Australia

¹⁵ School of Life Sciences, University of Technology Sydney, Ultimo, NSW 2007, Australia

These two authors have contributed equally

* Corresponding authors: Kamal Dua (kamal.dua@uts.edu.au); Philip Michael Hansbro (philip.hansbro@uts.edu.au).

Abstract

Chronic obstructive pulmonary disease (COPD) is an irreversible inflammatory respiratory disease characterized by frequent exacerbations and symptoms such as cough and wheezing that lead to irreversible airway damage and hyperresponsiveness. The primary risk factor for COPD is chronic cigarette smoke exposure, which promotes oxidative stress and a general pro-inflammatory condition by stimulating pro-oxidant and pro-inflammatory pathways and, simultaneously, inactivating anti-inflammatory and antioxidant detoxification pathways. These events cause progressive damage resulting in impaired cell function and disease progression. Treatments available for COPD are generally aimed at reducing the symptoms of exacerbation. Failure to regulate oxidative stress and inflammation results in lung damage. In the quest for innovative treatment strategies, phytochemicals, and complex plant extracts such as agarwood essential oil are promising sources of molecules with antioxidant and anti-inflammatory activity. However, their clinical use is limited by issues such as low solubility and poor pharmacokinetic properties. These can be overcome by encapsulating the therapeutic molecules using advanced drug delivery systems such as polymeric nanosystems and nanoemulsions. In this study, agarwood oil nanoemulsion (agarwood-NE) was formulated and tested for its antioxidant and anti-inflammatory potential in cigarette smoke extract (CSE)-treated BCI-NS1.1 airway basal epithelial cells. The findings suggest successful counteractivity of agarwood-NE against CSE-mediated pro-inflammatory effects by reducing the expression of the pro-inflammatory cytokines IL-1 α , IL-1 β , IL-8, and GDF-15. In addition, agarwood-NE induced the expression of the anti-inflammatory mediators IL-10, IL-18BP, TFF3, GH, VDBP, relaxin-2, IFN- γ , and PDGF. Furthermore, agarwood-NE also induced the expression of antioxidant genes such as GCLC and GSTP1, simultaneously activating the PI3K pro-survival

signalling pathway. This study provides proof of the dual anti-inflammatory and antioxidant activity of agarwood-NE, highlighting its enormous potential for COPD treatment.

Keywords: Agarwood; Nanoemulsion; Drug Delivery; Phytochemicals; Nutraceutical; Inflammation; Cigarette Smoke; Chronic Obstructive Pulmonary Disease; Inflammation

1. Introduction

Chronic obstructive pulmonary disease (COPD) is a slow-developing, irreversible disease. It represents the third highest cause of death worldwide, causing approximately 3 million deaths per year [1, 2]. The principal features of COPD are chronic airway inflammation, remodelling, and irreversible damage of the lung parenchyma, that result in mucus retention and severe airflow limitation that lead to symptoms such as difficulty in breathing, coughing, wheezing, increased chest wall diameter, dyspnea, and, progressive and irreversible hyperresponsiveness of the airways [1, 3]. COPD is characterized by frequent exacerbations, consisting of the acute worsening of the disease's symptoms. These often require patient hospitalization, resulting in elevated healthcare costs [4]. The main risk factor for COPD is represented by chronic cigarette smoking, which is associated with airway inflammation, oxidative stress, tissue damage, and fibrosis [5, 6]. The interplay between chronic inflammation, oxidative stress, and tissue damage is particularly relevant for COPD development [7, 8], and cigarette smoke (CS) enhances these processes because it contains several hundreds of compounds with pro-inflammatory and pro-oxidant activities [9].

In the context of inflammation and COPD, CS exposure has been described in several *in vivo* and *in vitro* models to act on broncho-epithelial cells and immune cells such as macrophages, dysregulating many signalling pathways and generally promoting pro-inflammatory, and pro-oxidant states [10]. Effects of CS include the promotion of the release of pro-inflammatory cytokines and mediators such as the interleukins (IL) IL-1 α [11], IL-1 β [12], IL-8 [13], IL-18 [14], and Growth/Differentiation factor-15 (GDF15) [15], as well as inhibition of the release of anti-inflammatory cytokines such as IL-10 [16]. GDF-15 has also been reported to be a biomarker for COPD [15], and circulating GDF-15 levels have been found to be 2.1-fold higher in COPD patients when compared to healthy subjects [17]. Other anti-inflammatory mediators whose release is impacted by CS include IL-18 Binding Protein (IL-18BP), Growth Hormone (GH), and Vitamin D Binding Protein (VDBP). IL-18BP is a protein that acts as a natural IL-18 decoy, blocking the IL-18-mediated inflammatory response [18], and whose expression is reduced in the alveolar macrophages of rats exposed to second-hand smoke [19]. Besides its main activity as a stimulator of tissue growth, cell reproduction and cell regeneration, GH is known to reprogram macrophages towards an anti-inflammatory, reparative phenotype [20], and chronic exposure to CS has been shown to reduce circulating GH levels [21]. VDBP is endowed with cytokine-like activity and is an important mediator of inflammatory tissue injury [22]. VDBP levels are downregulated in the plasma of cigarette smokers compared to non-

smokers [23]. Platelet-derived growth factor (PDGF) is a family of proteins regulating inflammation in the airways. In particular, PDGF-BB has a complex immunomodulatory role in many conditions including asthma, where it was shown to orchestrate lung tissue remodelling [24], and it is known to inhibit inflammatory responses during sepsis through the inhibition of pro-inflammatory cytokines including tumour necrosis factor- α (TNF- α), IL-6, IL-1 β , and IL-8 [25]. Another anti-inflammatory protein with a relevant role in lung health is Relaxin-2, which was recently shown, in a guinea pig model of CS exposure, to counteract CS-induced inflammation, remodelling, and tissue damage when administered exogenously [26].

The neuropeptide Trefoil factor 3 (TFF3) is expressed by many cells of the respiratory tract and modulates the cytokine-induced secretion of inflammatory mediators [27]. By doing so, it affects airway mucus secretion and is involved in maintaining epithelial integrity and healing after mucosal injury [28]. Expression of TFF3 has been reported to be reduced in a rat model of COPD obtained through exposure to CS [29], and this could potentially contribute to tissue damage caused by CS exposure. Further contribution to tissue damage by CS is caused by the direct induction of airway epithelial cell death, which is mediated by many mechanisms including inhibition of the Protein arginine methyltransferase 6 (PRMT6)-phosphatidylinositol 3-kinase (PI3K)-Akt cell survival signalling pathway [30]. Moreover, CS impairs the antiviral response of airway epithelial cells by inhibiting the production of interferon gamma (IFN- γ) [31] and IFN- γ -dependent signalling [32], resulting in further increased susceptibility to infection-associated tissue damage which can, in turn, fuel COPD progression [33].

Another fundamental driving factor of COPD is oxidative stress, which is caused by an imbalance between the production and elimination, through antioxidant detoxification mechanisms, of reactive oxygen species (ROS) [7, 34, 35]. A fundamental mediator of cellular detoxification is glutathione [36]. This molecule is produced by a biosynthetic pathway whose initial and rate-limiting step is catalysed by the enzyme Glutamate-cysteine ligase (GCLC) [37], and it has antioxidant activity as it acts as ROS scavenger [37]. Furthermore, carcinogenic products of tobacco smoke are detoxified upon conjugation with glutathione, and this reaction is catalysed by the enzyme Glutathione S-transferase P (GSTP1) [38]. GSTP1 expression is reduced in lung and sputum specimens of patients with severe COPD [39].

Therapeutic approaches against COPD are aimed at improving the symptoms of exacerbations and involve the use of antibiotics, corticosteroids, and bronchodilators [4, 40]. However, these treatment strategies are symptomatic, and do not essentially address the underlying cause of

the disease. Furthermore, these treatments have several adverse effects including osteoporosis, insomnia, mood swings, and weight gains [4]. For these reasons, there is an unmet need for the development of novel therapeutic strategies allowing the successful, durable pharmacotherapy of COPD with simultaneous minimization of adverse effects.

In the search for novel treatment strategies, a generous source of nutraceuticals or compounds endowed with therapeutic activity is represented by nature, in particular plants [41]. Traditional medicinal plants, for example, are a fundamental source of phytochemical compounds such as berberine [12, 42, 43], curcumin [44], rutin [45], boswellic acid [46], nobiletin [47] with antioxidant, anti-inflammatory, and anticancer activities. Furthermore, numerous plant extracts of complex composition are reported to have anti-inflammatory and anti-oxidant properties [48-50]. One of such extracts is Agarwood oil. Agarwood is a fragrant, dark resinous wood which is derived from the heartwood of trees belonging to the *Aquilaria* species that have been wounded or infested by some species of mould [51], and it has been used in Ayurvedic and Chinese traditional medicine for several centuries [52].

The main active ingredient of Agarwood is its essential oil, which can be extracted from Agarwood using different techniques [53]. Agarwood essential oil has been extensively studied recently, and many of its chemical components, particularly sesquiterpenes and chromones, have been reported to have strong *in vitro* and *in vivo* anti-inflammatory and antioxidant activities [53]. Numerous studies have also demonstrated the anti-inflammatory and antioxidant activities of Agarwood oil as a whole, complex mixture [53]. These activities are exerted through many mechanisms including the inhibition of the production and function of proinflammatory cytokines [54, 55] and prostaglandins [56, 57], increased production of anti-inflammatory cytokines [58], blockade of inflammatory pathways such as NF- κ B [59], and general reduction of oxidative stress and related mediators such as nitric oxide [60]. These studies collectively demonstrate the notable therapeutic potential of Agarwood oil in the management of chronic inflammatory diseases such as COPD [53].

Despite the enormous potential of bioactive plant-derived compounds and extracts, their clinical application is severely limited by issues including low solubility, poor bioavailability, and insufficient intestinal absorption [12, 45, 61-63]. This is particularly true for essential oils such as Agarwood oil which, being an oily extract, has very poor water solubility. With the aim of overcoming these limitations, numerous advanced drug delivery systems have been developed. Many of these successful delivery systems involve the encapsulation of therapeutic

molecules in polymeric nanosystems such as liquid crystalline nanoparticles and solid lipid nanoparticles [64-66]. To improve the properties of highly lipophilic essential oils and extracts, nanoemulsion systems (NEs) are emerging as advanced drug delivery systems of choice, thanks to their relative ease and low cost of preparation, biocompatibility, and physicochemical stability [67, 68]. NEs exist in submicron colloidal particulate systems of size ranging between 20 and 200 nm, that are produced through different techniques including ultrasound emulsification, high-pressure homogenization, and microfluidization [67, 68].

In this study, the antioxidant and anti-inflammatory activities of a Poloxamer 407-based Agarwood oil nanoemulsion (Agarwood-NE) against an *in vitro* model of COPD obtained through exposure of BCI-NS1.1 human basal epithelial cells to 5% cigarette smoke extract (CSE) was investigated [12]. The biological activity of Agarwood-NE was studied using *in vitro* experiments relevant to oxidative stress and inflammation pathways. The results of this study confirm the potent, multifaceted anti-inflammatory and antioxidant activities of Agarwood oil, providing proof of the enormous potential of Agarwood-NE as a therapeutic strategy against chronic inflammatory diseases such as COPD.

2. Methods

2.1. Preparation of Agarwood-NE

Agarwood oil was extracted from *Aquilaria crassna*. The plant material was chopped and ground into powder and left to air dry for 14 days to reduce moist contents. The essential oil was extracted from the dry Agarwood powder through supercritical fluid carbon dioxide extraction at 0.005-0.006% per kg of raw Agarwood powder. The extraction was performed at a pressure of 22MPa and a temperature of 47°C for 2 hours, with a carbon dioxide fluid flow rate of 2 L/h. The separation was performed at 8 MPa and 40°C. The essential oil was characterised by DeÁurora Pty Ltd. The essential oil obtained appeared as a transparent, slightly viscous liquid, with a brown colour and a deep woody aroma. The essential oil was soluble in alcohol and fixed oils and had the following composition:

Component	Actual %
Valerianol	12.31%
gamma-Eudesmol	8.03%
epi-Cyclocolorenone	3.71%
Nootkatone	3.71%
beta-Eudesmol	3.69%
Methyl phenethyl ketone	3.02%
10-epi-gamma-Eudesmol	2.90%
Hinesol	1.74%
dihydro-Columellarin	1.68%
alpha-Curcumene	0.88%
alpha-Humulene	0.85%
alpha-Bulnesene	0.56%
Selina-4,11-diene	0.45%
Debromofiliformin	0.38%
4,5-di-epi-Aristolochene	0.26%
Elemol	0.25%
alpha-Guaiene	0.16%
alpha-Selinene	0.11%

Agarwood nanoemulsion was prepared using a probe sonication method. Briefly, 200 mg of accurately weighed amount of agarwood oil was taken in a 50 ml Falcon conical tube. In another tube, 50 mg of Poloxamer 407 was dissolved with a required amount of purified distilled water (about 10 mL), and vortexed to ensure complete solubilization of the Poloxamer. The prepared solution was gradually added to the agarwood oil at ambient temperature and vortexed for 1 min. The coarse emulsion formed was subjected to probe sonication for 15 min at 80% amplitude in a 1 Hz on/off cycle to minimize heating. This resulted in the formation of a milky nanoemulsion, which was made up to a final volume of 20 mL by adding purified water. The obtained nanoemulsion was characterized for size and polydispersity index (dynamic light scattering), and morphology (transmission electron microscopy). The nanoemulsion was composed of droplets with spherical morphology, of 180 ± 4.7 nm diameter, and 0.36 ± 0.03 polydispersity index.

2.2. Cell culture and Agarwood-NE treatment

Minimally immortalized human airway epithelium derived basal cells (BCi-NS1.1) were purchased from R. G. Crystal (Weill Cornell Medical College, New York, USA). These cells were grown in broncho-epithelial basal media (BEBM) (Lonza) supplemented with various growth factors and other supplements, including bovine pituitary extract, insulin, GA-1000 (Gentamicin sulfate-Amphotericin), retinoic acid, transferrin, triiodothyronine, epinephrine, human Epidermal Growth Factor (BEGM Single Quots, Lonza), at 37 °C under humidified condition in the presence of 5% CO₂. For experiments, the cells were seeded onto a 96-well plate (Corning, NY, USA) or a 6-well plate (Corning) at a density of 1×10⁴/well and 2×10⁵/well, respectively. After 80% confluency, the cells were pre-treated for 1 h with Agarwood-NE at the concentrations indicated, followed by the treatment of with or without 5% cigarette-smoke extract (CSE) for 24 h.

2.3. Cell viability

The cell viability of BCiNS1.1 cells was assessed using 3-(4,5-Dimethylthiazol-2-yl)-2,5-diphenyltetrazolium bromide (MTT, Merck, Rahway, NJ, USA), as described previously [69]. The cells were treated with different concentrations of Agarwood-NE (10–1000 µg/mL) for 24 h in a 96-well plate. Then, MTT solution (250 µg/mL) was added into each well and incubated for 4 h. After incubation, the media was removed and the coloured formazan crystals formed in the reaction were dissolved with 100 µL dimethyl sulfoxide (DMSO, Merck). The absorbance at a wavelength of 540 nm was read using a POLARstar Omega microplate reader (BMG Labtech, Ortenberg, Germany).

2.4. Real time-qPCR

The effects of Agarwood-NE on mRNA expression levels of inflammation-related and oxidative stress-related genes in CSE-induced BCiNS1.1 cells were determined by real time-qPCR, as described previously [70]. The cells were pre-treated with Agarwood-NE at 25 and 50 µg/mL for 1 h, and then treated with or without 5% CSE for 24 h. The cells were then lysed with 500 µL TRI reagent (Merck). 250 µL chloroform was added and the mixture was centrifuged at 12,000 g, 4 °C, for 15 minutes. The aqueous phase was pipetted out into new Eppendorf tubes and 500 µL of isopropyl alcohol was added to precipitate the RNA. The tubes were then centrifuged at 12,000 g, room temperature, for 10 min. After centrifugation, the supernatant was removed, and the RNA pellets were washed 2× with 1 mL 75% ethanol. The tubes were centrifuged again at 8,000 g, 4 °C, for 5 min. After the second round of

centrifugation, the ethanol was removed, and the dry RNA pellets were dissolved in nuclease-free water. Nanodrop (Thermo Fisher Scientific, Waltham, MA, USA) was used to determine the concentration and purity of the RNA.

After subjecting to DNase I (Merck) treatment, 1 µg total RNA was reverse-transcribed to cDNA using the reaction mixture of M-MLV buffer (Thermo Fisher Scientific), random primers (0.5 µg/µL), dNTPs (10 mM) and DTT (100 mM). A thermal cycler (Eppendorf, Hamburg, Germany) was used in the subsequent steps involving denaturation (65 °C, 10 min), annealing (25 °C, 10 min), reverse transcription (37 °C, 50 min) and enzyme inactivation (70 °C, 15 min). Equal amounts (25 ng) of cDNA were then subjected to real-time qPCR with iTaq Universal SYBR green (BioRad, Hercules, CA, USA) and primers (forward and reverse, 0.5 µM each) using a CFX96 PCR system (BioRad). The real-time qPCR involved thermal cycles of 95 °C for 30 s (1 cycle), 95 °C for 15 s (40 cycles) and 60 °C for 30 s (1 cycle).

The sequences of human primers used were as follows:

Gene name	FW sequence	RV sequence
IL-8	GCCTCAAGGAAAAGAATCTG	GGATCTACACTCTCCAGC
GAPDH	TCGGAGTCAACGGATTTG	CAACAATATCCACTTTACCAGAG
GCLC	TTATTAGAGACCCACTGACAC	TTCTCAAATGGTCAGACTC
GSTP1	TTTCCCAGTTCGAGGC	ATAGGCAGGAGGCTTTG
PI3K	GAGTAACAGACTAGCTAGAGAC	AGAAAATCTTTCTCCTGCTC

2.5. Human cytokine protein array

The effects of Agarwood-NE on cytokine expression levels in CSE-induced BCiNS1.1 cells were assessed using a human cytokine protein array kit (R&D Systems, Minneapolis, MN, USA), as described in a previous study [12]. The cells were seeded in 6-well plates as indicated previously and were pre-treated with Agarwood-NE at 25 and 50 µg/mL for 1 h, then treated with 5% CSE for 24 h. The cells were lysed using RIPA buffer (ThermoFisher Scientific, NSW, Australia) that contained protease and phosphatase inhibitors (Roche Diagnostics GmbH, Mannheim, Germany). Equal amounts (300 µg) of protein were loaded onto human cytokine

arrays and incubated overnight at 4 °C. Further incubation with antibodies and reagents were done in accordance with the manufacturer's instructions. The protein spots in the array were photographed using the ChemiDoc MP (Bio-Rad, Hercules, CA, USA) and analysed using Image J. (version 1.53c, Bethesda, MD, USA).

2.6. Statistical analysis

In figures 1, 2, 5, and 6, the data were expressed as Mean \pm SEM and statistically analysed using 1-way ANOVA, followed by Dunnett multiple comparison test. A p-value of <0.05 was considered significant. In Figures 3 and 4, the individual measurements are indicated together with the Mean value of each group.

3. Results

3.1 Identification of an optimal concentration of Agarwood-NE for treatment in CSE-induced BCI-NS1.1 cells

To find a safe Agarwood-NE concentration for cell treatment, a toxicity study was performed, using the MTT assay to measure cell viability upon exposure of 5% CSE-induced BCI-NS1.1 cells to various concentrations of Agarwood-NE. The findings are shown in Figure 1. Treatment with Agarwood-NE amounts corresponding to up to 50 $\mu\text{g}/\text{mL}$ Agarwood oil extract did not result in significant reduction of cell viability (Figure 1). Concentration of 100, 500, and 1000 $\mu\text{g}/\text{mL}$ Agarwood oil significantly decreased cell viability by 9.5%, 78.7%, and 97.7%, respectively (Figure 1, $p < 0.0001$ against untreated control). In the subsequent experiments, cells were exposed to the non-toxic concentrations of 25 and 50 $\mu\text{g}/\text{mL}$ Agarwood-NE.

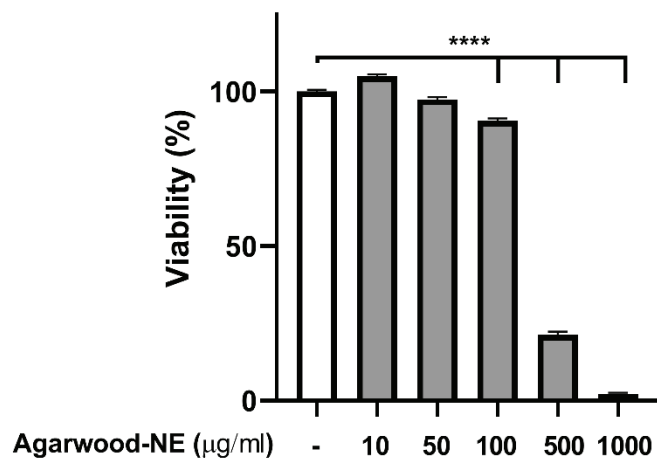


Figure 1. Effect of Agarwood-NE on the cell viability of 5% CSE-induced BCI-NS1.1 cells. BCI-NS1.1 cells were pre-incubated for 1 h in the presence of increasing concentrations of Agarwood-NE (10, 50, 100, 500, or 1000 µg/mL), followed by exposure to 5% CSE for 24h. Upon treatment, MTT assay was used to measure cell viability. Cell viability was normalised as a percentage compared to untreated control. The results are Mean ± SEM of 3 independent experiments (****; $p < 0.0001$).

3.2. Agarwood-NE inhibits the CSE-induced transcription of the pro-inflammatory cytokine IL-8

The anti-inflammatory activity of Agarwood-NE was studied on 5% CSE-induced BCI-NS1.1 cells by measuring the mRNA levels of the pro-inflammatory cytokine IL-8. CSE induced a 6.2-fold increase of the transcription of the IL-8 mRNA compared to control (Figure 2, $p < 0.0001$). Treatment with Agarwood-NE at 25 and 50 µg/mL concentration resulted in the concentration-dependent reduction of IL-8 mRNA levels by 16.1% and 54.9%, respectively, compared to CSE-treated cells (Figure 2, $p < 0.05$ and $p < 0.0001$, respectively).

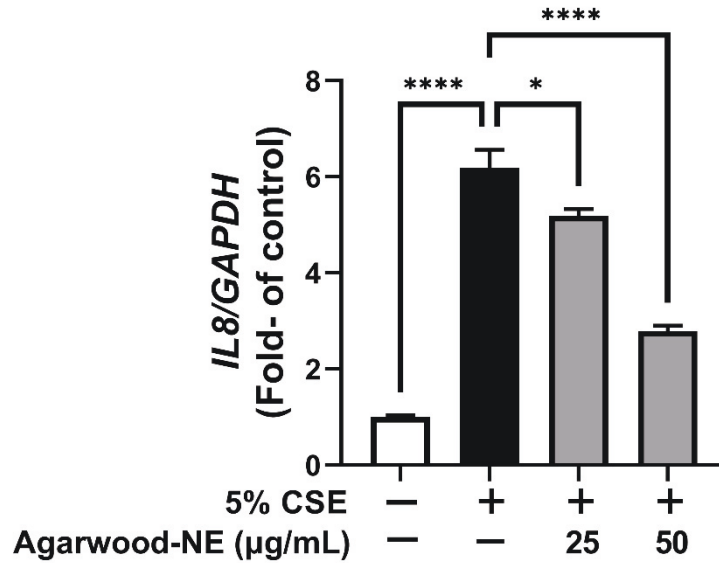


Figure 2. Effect of Agarwood-NE on the CSE-induced transcription of the pro-inflammatory cytokine IL-8. BCI-NS1.1 cells were pre-incubated for 1 h in the presence of 25 and 50 µg/mL Agarwood-NE, followed by exposure to 5% CSE for 24h. The mRNA levels of IL-8 were determined via RT-qPCR. Values are expressed as Mean ± SEM (n=4, *: p<0.05; ****: p<0.0001).

3.3. Agarwood-NE inhibits the CSE-induced protein expression of pro-inflammatory cytokines and mediators

The protein levels of the pro-inflammatory cytokines and mediators IL-1α, IL-1β, IL-1Ra, and GDF-15 are shown in Figure 3. Exposure of BCI-NS1.1 cells to 5% CSE induced a significant increase in the levels of IL-1α (1.6-fold, Figure 3A), IL-1β (1.7-fold, Figure 3B), IL-1Ra (1.1-fold, Figure 3C), and GDF-15 (1.1-fold, Figure 3D) compared to untreated control. The levels of these proteins were significantly reduced to similar extents upon treatment with the two concentrations of Agarwood-NE tested (25 and 50 µg/mL). Upon treatment with 50 µg/mL Agarwood-NE, the levels of IL-1α were reduced by 54.5% (Figure 3A), while the levels of IL-1β were reduced by 35.4% (p<0.0001, Figure 3B). Furthermore, treatment with 50 µg/mL Agarwood-NE resulted in a 15.4% reduction of the levels of IL-1Ra (Figure 3C) and in a 45.3% reduction of the levels of GDF-15 (Figure 3D). Although, treatment with 25 µg/mL Agarwood-NE resulted in a slightly lower extent of reduction of the amount of these four cytokines, no statistically significant difference was detected between the two concentrations of Agarwood-NE tested in all cases.

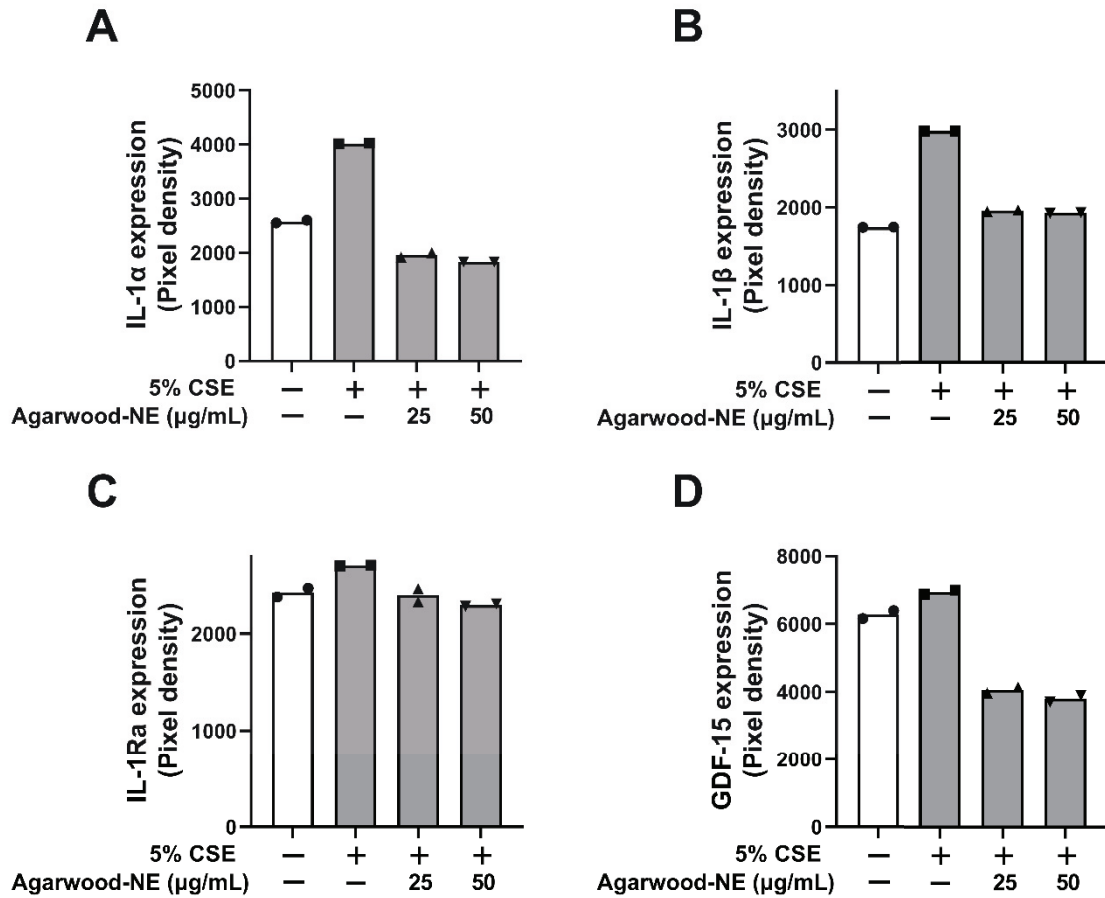


Figure 3. Effect of Agarwood-NE on the CSE-induced production of pro-inflammatory mediators in human cytokine protein array. BCI-NS1.1 cells were pre-incubated for 1 h in the presence of 25 and 50 µg/mL Agarwood-NE, followed by exposure to 5% CSE for 24h. The protein levels of IL-1α (A), IL-1β (B), IL-1Ra (C), and GDF-15 (D) were determined via human cytokine protein array.

3.4. Agarwood-NE stimulates the CSE-inhibited protein expression of anti-inflammatory cytokines and mediators

The protein levels of the investigated anti-inflammatory cytokines and mediators are shown in Figure 4. Treatment of BCI-NS1.1 cells with 5% CSE caused a significant reduction of the protein levels of the following cytokines compared to untreated control: IL-10 (13.3%, Figure 4A), IL-18 Bpa (18.9%, Figure 4B), Growth Hormone (GH, 14.5%, Figure 4C), Vitamin D Binding Protein (VDBP, 7.3%, Figure 4D), Relaxin-2 (14.0%, Figure 4E), Interferon-γ (IFN-γ, 15.9%, Figure 4F), Platelet-derived growth factor (PDGF-BB, 13.3%, Figure 4G), and

Trefoil factor 3 (TFF3, 17.5%, Figure 4H). Exposure to 50 µg/mL Agarwood-NE counteracted the effect of CSE treatment, significantly increasing the levels of all these proteins compared to cells treated with 5% CSE only. In particular, the 50 µg/mL concentration of Agarwood-NE increased the levels of IL-10 by 13.1% (Figure 4A) and the levels of IL-18 Bpa by 11.7% (Figure 4B). The levels of GH were increased by 7.0% (Figure 4C) and the levels of VDBP were increased by 7.0% (Figure 4D). Furthermore, upon treatment with 50 µg/mL Agarwood-NE, Relaxin-2 levels resulted in an increase by 8.0% (Figure 4E), and the levels of IFN-γ increased by 11.8% (Figure 4F). Finally, 50 µg/mL Agarwood-NE treatment increased the levels of PDGF-BB by 10.6% (Figure 4G) and the levels of TFF3 by 12.7% (Figure 4H). Treatment with 25 µg/mL Agarwood-NE significantly increased the levels of IL-18Bpa (6.8%, Figure 4B), Relaxin-2 (8.8%, Figure 4E), and IFN-γ (6.7%, Figure 4F).

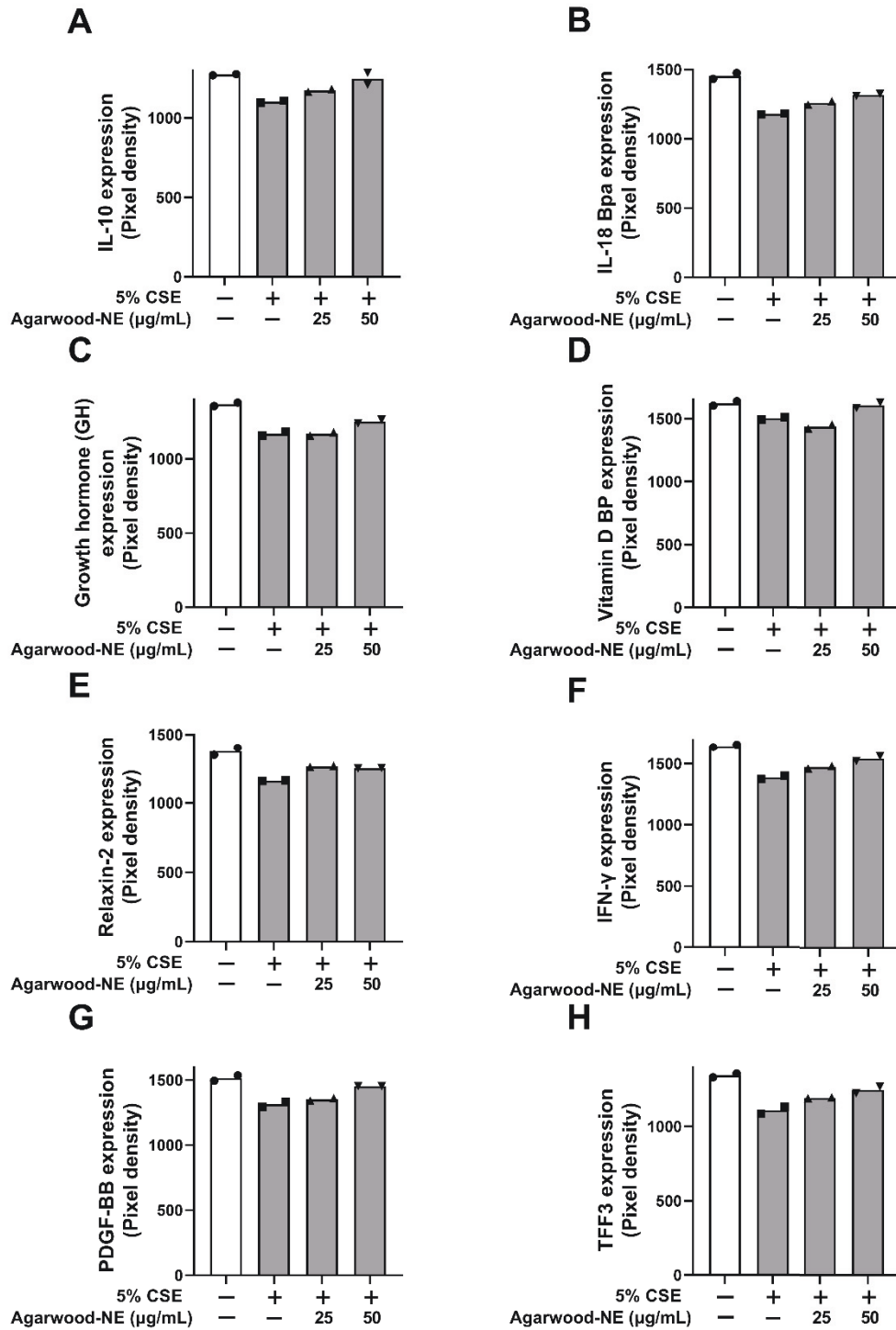


Figure 4. Effect of Agarwood-NE on the CSE-inhibited production of anti-inflammatory mediators in human cytokine protein array. BCI-NS1.1 cells were pre-incubated for 1 h in the presence of 25 and 50 µg/mL Agarwood-NE, followed by exposure to 5% CSE for 24h. The protein levels of IL-10 (A), IL-18Bpa (B), GH (C), VDBP (D), Relaxin-2 (E), IFN-γ (F), PDGF-BB (G), and TFF3 (H) were determined via human cytokine protein array.

3.5. Agarwood-NE stimulates the CSE-inhibited transcription of antioxidant genes

The antioxidant activity of Agarwood-NE was investigated on 5% CSE-induced BCI-NS1.1 cells by measuring the mRNA levels of the genes GCLC and GSTP1 (Figure 5). Compared to the untreated control, CSE induced a 32.7% reduction of the transcription of the GCLC mRNA (Figure 5A, $p < 0.0001$) and a 65.4% reduction of the transcription of the GSTP1 mRNA (Figure 5B, $p < 0.01$). Treatment with Agarwood-NE at 50 $\mu\text{g/mL}$ concentration resulted in a significant 63.6% increase of the mRNA levels of GCLC (Figure 5A, $p < 0.0001$) and in a significant 344.0% increase of the mRNA levels of GSTP1 (Figure 5B, $p < 0.001$), compared to the 5% CSE-treated group. Furthermore, treatment with Agarwood-NE at 25 $\mu\text{g/mL}$ concentration significantly increased the GSTP1 mRNA levels by 138.5% compared to the 5% CSE-treated group (Figure 5B, $p < 0.05$).

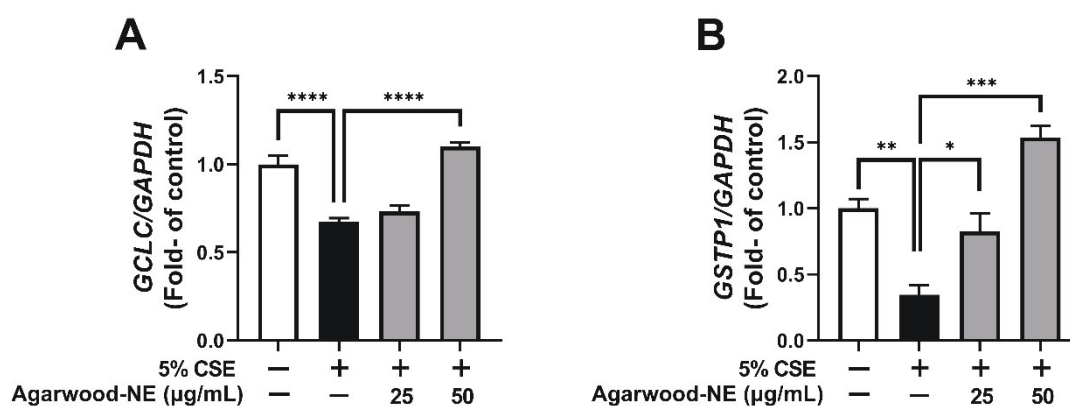


Figure 5. Effect of Agarwood-NE on the CSE-inhibited transcription of antioxidant genes. BCI-NS1.1 cells were pre-incubated for 1 h in the presence of 25 and 50 $\mu\text{g/mL}$ Agarwood-NE, followed by exposure to 5% CSE for 24h. The mRNA levels of GCLC (A) and GSTP1 (B) were determined via RT-qPCR. Values are expressed as Mean \pm SEM ($n=3-4$, *: $p < 0.05$; **: $p < 0.01$; ***: $p < 0.001$; ****: $p < 0.0001$).

3.6. Agarwood-NE stimulates the CSE-inhibited transcription of the pro-survival gene PI3K

Finally, the effect of Agarwood-NE on pro-survival pathways was investigated on 5% CSE-induced BCI-NS1.1 cells by measuring the mRNA levels of the PI3K gene (Figure 6). Exposure of cells to CSE resulted in a significant 31.2% reduction of the PI3K mRNA levels compared to the untreated control group ($p < 0.0001$, Figure 6). Treatment with Agarwood-NE at 25

µg/mL and 50 µg/mL concentration resulted in a significant, concentration-dependent increase of PI3K mRNA levels by 26.5% and 54.8% ($p < 0.001$ and $p < 0.0001$, respectively), compared to the 5% CSE-treated group (Figure 6).

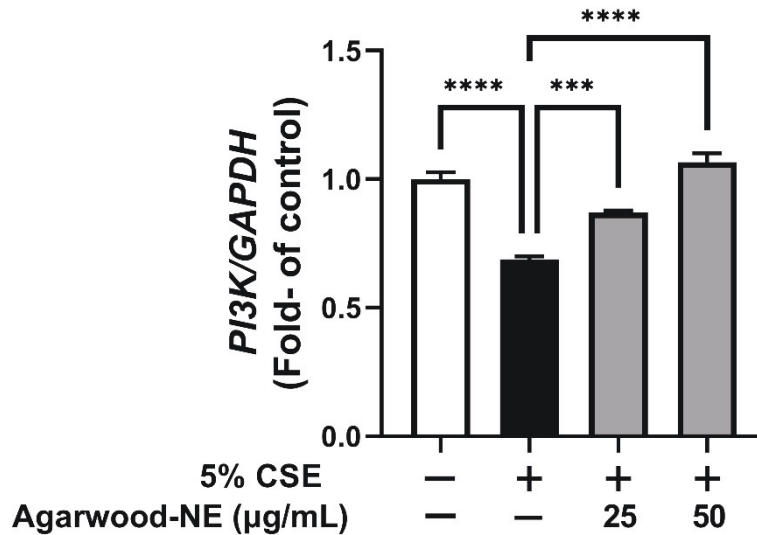


Figure 6. Effect of Agarwood-NE on the CSE-inhibited transcription of the pro-survival gene PI3K. BCI-NS1.1 cells were pre-incubated for 1 h in the presence of 25 and 50 µg/mL Agarwood-NE, followed by exposure to 5% CSE for 24h. The mRNA levels of PI-3K were determined via RT-qPCR. Values are expressed as Mean \pm SEM ($n=4$, ***: $p < 0.001$; ****: $p < 0.0001$).

4. Discussion

COPD is a progressive inflammatory respiratory disease characterized by chronic lung inflammation that causes irreversible obstruction of the airflow and periodic exacerbations [71-73]. This causes significant medical and financial burden worldwide [74]. Cigarette smoking is the main cause of COPD [75], and it is known to cause inflammation and oxidative stress which, together, play fundamental roles in the pathogenesis of chronic inflammatory diseases such as COPD [76, 77]. Current treatment strategies for COPD involve pulmonary rehabilitation, smoke cessation, and pharmacological relief of symptoms through inhalational therapy [78]. Despite this, COPD still represents a leading cause of morbidity and mortality worldwide [79]. This leads to the urgent necessity of novel therapeutic strategies for COPD with increased efficacy and reduced adverse effects. In this context, therapeutic agents embedded with both anti-inflammatory and antioxidant activities would be advantageous,

considering the prominent role played by the interaction between oxidative stress and inflammation in COPD .

In the search for novel therapeutic compounds, the natural world is an endless source of inspiration, and many traditional medicinal plants produce molecules embedded with anti-inflammatory and antioxidant properties. These include, for example, berberine [12] and rutin [80]. Complex mixtures such as the essential oils extracted from many plants [81], including Agarwood oil [53], are also known for their potent anti-oxidant and anti-inflammatory properties. Despite all these, the therapeutic application of plant-based compounds is often hampered by issues such as low water solubility, poor bioavailability and, in general, an unfavourable pharmacokinetic profile [12, 82]. The use of nanoparticles / carriers-based novel drug delivery systems represents a promising strategy to overcome these limitations [62]. This study reports the potent anti-inflammatory and antioxidant properties of Agarwood extract oil formulated in a Poloxamer 407-based nanoemulsion on BCI-NS1.1 human basal epithelial cells exposed to 5% CSE.

Cigarette smoke (CS) is known to contain several hundreds of compounds with oxidative, pro-inflammatory, and carcinogenic properties [9], and each puff of cigarette contains 10^{17} oxidant molecules [83]. These molecules promote inflammation, oxidative stress, and tissue damage, which in turn collectively orchestrate the development of COPD [84, 85]. The chemicals contained in CS are known to interfere with many different signalling pathways in cells of the lung parenchyma, activating DNA damage responses, inflammation, oxidative stress, and autophagy, ultimately leading to increased cellular senescence, cell death, or cancerous transformation [86-88]. CS induces a pro-inflammatory state by (i) activating pathways that lead to the release of pro-inflammatory cytokines and mediators such as IL-8 [89], IL-1 α [11], IL-1 β [90], and GDF-15 [15]; and (ii) inactivating pathways that lead to the production of anti-inflammatory cytokines and mediators such as IL-10 [16], IL-18BP [19], GH [21], and VDBP [23].

This study reports the anti-inflammatory activity of Agarwood-NE which is exerted by counteracting both the aforementioned mechanisms. In particular, the treatment of CSE-induced BCI-NS1.1 with Agarwood-NEs significantly reduced the transcription of the gene encoding for IL-8 as well as the levels of IL-1 α and IL-1 β proteins. With regards to IL-1 α and IL-1 β , our findings are in agreement with previous reports where Agarwood oil, or single components extracted from it, were found to reduce the expression of these cytokines [53].

This study is the first to report that Agarwood oil extract reduces the expression of IL-8. Furthermore, treatment with Agarwood-NE resulted in significant reduction of the levels of GDF-15. The fact that GDF-15 plays a role in the induction of cancer epithelial-to-mesenchymal transition (EMT) [15] also suggests the possibility that Agarwood-NE may possess anti-cancer or anti-metastatic activity. Considering the importance of EMT as a fundamental process contributing to airway remodelling in inflammatory lung diseases [91], the inhibition of GDF-15 represents a potential mechanism by which Agarwood-NE may counteract airway remodelling. IL-1Ra is an anti-inflammatory protein that is released in response to IL-1 β signalling and acts as a negative regulator of IL-1 signalling, with the aim of mitigating hyper-inflammatory states [92]. The fact that the expression of IL-1Ra is stimulated by CSE fits with its role as a negative “buffer” of IL-1 signalling, and the reduction of its expression obtained by concomitant Agarwood-NE treatment may be secondary to the induced downregulation of both IL-1 α and IL-1 β [92].

With regards to the induction of CSE-inactivated anti-inflammatory mediators, treatment with Agarwood-NE, particularly at a 50 μ g/mL concentration, successfully increased the levels of IL-10, IL-18BP, GH, and VDBP to levels comparable to those measured prior to exposure to 5% CSE. The induction of IL-10 is consistent with previous reports where Agarwood oil was shown to increase IL-10 levels in *in vivo* mice models of intestinal injury [58] and gastric ulcer [59]. This current study is the first to report that Agarwood oil induces IL-18BP, GH, and VDBP. Furthermore, this study also reports that treatment of BCI-NS1.1 with 5% CSE significantly decreased the levels of two other anti-inflammatory factors: PDGF-BB and Relaxin-2. To the best of our knowledge, this is the first study to report that CSE causes a reduction of the levels of these two proteins. Considering the anti-inflammatory and immunomodulatory activity of both PDGF-BB and Relaxin-2, the induction of the expression of these two factors represents another pathway by which Agarwood-NE exerts its anti-inflammatory activity, reinforcing its potential against COPD.

Together with the modulation of pro-and anti-inflammatory mediators, another important finding of this study is that treatment with Agarwood-NE successfully counteracted the CSE-induced reduction of the levels of mRNAs encoding for GCLC and GSTP1. Considering the fundamental roles played by these two proteins in the synthesis of glutathione (GCLC, [37]) and in its conjugation with tobacco carcinogens (GSTP1, [38]), this study findings suggest that Agarwood-NE promotes an anti-oxidant state which, together with its anti-inflammatory

activity, makes our formulation suitable as a potential dual antioxidant and anti-inflammatory treatment to counteract these CS-induced processes.

Besides its action on inflammatory and oxidative pathways, the study also shows that another mechanism by which Agarwood-NE counteracts the deleterious effects of CS is through the induction of molecular pathways that are actively involved in protecting cells from damage, infection, and death. These include TFF3, IFN- γ , and PI3K. TFF3 participates in the maintenance of epithelial integrity and in mucosal healing [28], and therefore, may play an important role in protecting the lung parenchyma from CS-induced damage. In this study, treatment of BCI-NS1.1 cells with 5% CSE resulted in a reduction of TFF3 levels, which was counteracted upon treatment with Agarwood-NE. A similar trend was observed for IFN- γ and PI3K. Considering the critical role of IFN- γ in the activation of antiviral responses, as well as in their modulation to minimize collateral tissue damage [93], the fact that treatment with Agarwood-NE increases IFN- γ levels provides a further mechanism by which this formulation exerts its protective activity against CSE-induced damage. Finally, this study report that treatment of BCI-NS1.1 cells with Agarwood-NE increases the levels of PI3K transcript. Due to the fact that PI3K mediates a pro-survival signalling pathway [30, 94], this may represent another mechanism by which Agarwood-NE treatment protects cells from CSE-induced cell death.

Taken together, the findings and observations obtained from this study demonstrate that the Agarwood-NE formulation tested is embedded with potent dual antioxidant and anti-inflammatory activities, which is exerted through a pleiotropic action on many different molecular pathways. The molecular pathways activated or inhibited by the treatment with Agarwood-NE formulation are summarized in Figure 7.

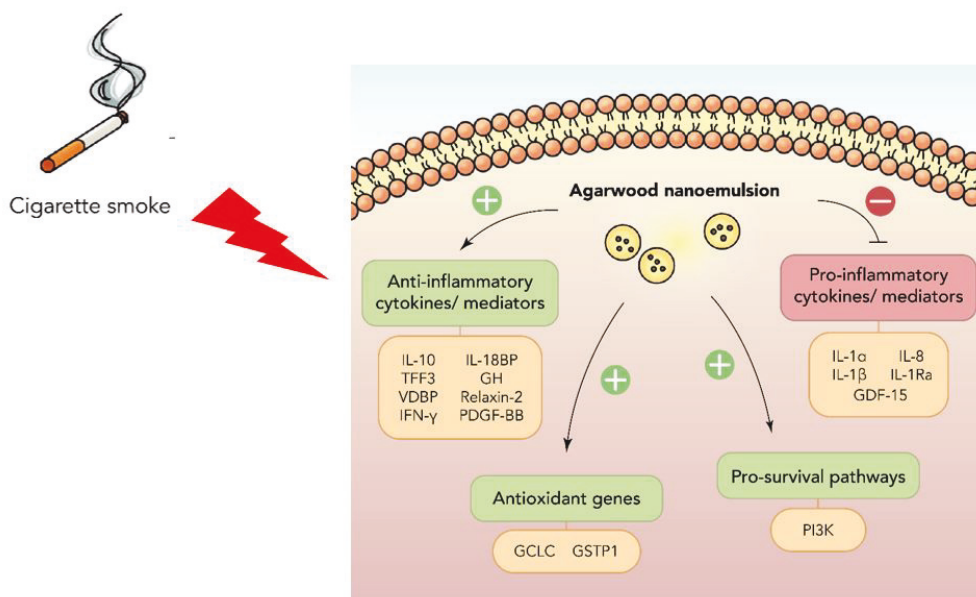


Figure 7. Summary of the anti-inflammatory and antioxidant molecular pathways activated by Agarwood-NE to counteract the effect of cigarette smoke extract in BCi-NS1.1 cells.

This underlines the potential of Agarwood-NE as a treatment strategy for diseases where inflammation and oxidative stress interact significantly, such as COPD.

Although the promising results shown provide a proof of concept of the effect of Agarwood-NE against CSE-induced COPD a limitation of this study is that it only provides information about the effect of Agarwood-NE on basal epithelial cells. To increase the reach and scope of the present findings, the effect of Agarwood-NE should be tested on different cell lines such as macrophages and other cell lines present in the lung, in order to provide a complete and realistic picture of the multifaceted activity of Agarwood-NE against inflammation and oxidative stress. Furthermore, considering the many pathways impacted by the treatment with Agarwood-NE, it would be interesting to investigate the activity of this formulation against other inflammatory diseases such as asthma, and lung cancer. Another exciting future perspective is represented by the investigation of the effect of the Agarwood-NE formulation against other processes occurring in COPD, such as remodelling and cellular senescence. Finally, in order to proceed towards clinical translation, this study must be validated further with suitable *in vivo* animal models of COPD.

5. Conclusions

In this study, we demonstrated that Agarwood-NE exerts potent *in vitro* anti-inflammatory and antioxidant activities by counteracting several pro-inflammatory and pro-oxidant pathways activated by treatment of BCI-NS1.1 human airway epithelium-derived basal cells with 5% CSE. The results of this study provide proof for the enormous potential of Agarwood-NE as dual antioxidant and anti-inflammatory treatment for inflammatory respiratory diseases such as COPD. However, for the results of these studies to be translated into clinic, the findings reported in this study must be validated through further *in vitro* investigation, as well as through *in vivo* pre-clinical studies.

Funding: The authors are thankful to the Graduate School of Health, University of Technology Sydney, Australia. KD is supported by a project grant from the Rebecca L Cooper Medical Research Foundation and the Maridulu Budyari Gumal Sydney Partnership for Health, Education, Research and Enterprise (SPHERE) RSEOH CAG Seed grant, fellowship and extension grant; Faculty of Health MCR/ECR Mentorship Support Grant and UTS Global Strategic Partnerships Seed Funding Scheme. GDR is supported by the UTS International Research Scholarship and the UTS President's Scholarship. KRP is supported by a fellowship from Prevent Cancer Foundation (PCF) and the International Association for the Study of Lung Cancer (IASLC). The authors would also like to thank DeAurora Pty Ltd for providing us with the Agarwood oil along with financial support for the project.

Author Contributions: Conceptualization, G.D.R., K.R.P., K.D., P.M.H., B.G.O.; Methodology, G.D.R., K.R.P., K.D., P.M.H., B.M., D.K.K., S.K.S., R.M., J.S., G.G., R.M.L., A.C.; Formal Analysis, G.D.R., K.R.P., B.M.; Investigation, G.D.R., K.R.P., B.M., R.M.L., R.M., J.S., A.C., G.G., S.K.S.; Resources, R.M., J.S., R.M.L.; Data Curation, G.D.R., K.R.P., B.M.; Writing – Original Draft Preparation, G.D.R.; Writing – Review & Editing, G.D.R., K.R.P., K.D., P.M.H., B.M., D.K.K., S.K.S., R.M., J.S., G.G., R.M.L., A.C., B.G.O.; Supervision, K.D., P.M.H., B.G.O.; Project Administration, K.D., P.M.H.; Funding Acquisition, K.D., P.M.H..

Data Availability Statement: The data presented in this study are available on request from the corresponding authors.

Conflicts of Interest: The authors have no conflict of interest to declare.

References

1. Eapen, M.S., et al., *Airway inflammation in chronic obstructive pulmonary disease (COPD): a true paradox*. *Expert Rev Respir Med*, 2017. **11**(10): p. 827-839.
2. Liu, G., et al., *Adverse roles of mast cell chymase-1 in chronic obstructive pulmonary disease*. *Eur Respir J*, 2022.
3. Vogelmeier, C.F., et al., *Global Strategy for the Diagnosis, Management, and Prevention of Chronic Obstructive Lung Disease 2017 Report: GOLD Executive Summary*. *Arch Bronconeumol*, 2017. **53**(3): p. 128-149.
4. Bollmeier, S.G. and A.P. Hartmann, *Management of chronic obstructive pulmonary disease: A review focusing on exacerbations*. *Am J Health Syst Pharm*, 2020. **77**(4): p. 259-268.
5. Mehta, M., et al., *Cellular signalling pathways mediating the pathogenesis of chronic inflammatory respiratory diseases: an update*. *Inflammopharmacology*, 2020. **28**(4): p. 795-817.
6. Lugg, S.T., et al., *Cigarette smoke exposure and alveolar macrophages: mechanisms for lung disease*. *Thorax*, 2022. **77**(1): p. 94-101.
7. Dua, K., et al., *Increasing complexity and interactions of oxidative stress in chronic respiratory diseases: An emerging need for novel drug delivery systems*. *Chemico-Biological Interactions*, 2019. **299**: p. 168-178.
8. Mehta, M., et al., *Rutin-loaded liquid crystalline nanoparticles attenuate oxidative stress in bronchial epithelial cells: a PCR validation*. *Future Med Chem*, 2021. **13**(6): p. 543-549.
9. Malyla, V., et al., *Recent advances in experimental animal models of lung cancer*. *Future Med Chem*, 2020. **12**(7): p. 567-570.
10. Albano, G.D., et al., *Overview of the Mechanisms of Oxidative Stress: Impact in Inflammation of the Airway Diseases*. *Antioxidants (Basel)*, 2022. **11**(11).
11. Milad, N., et al., *Neutrophils and IL-1 α Regulate Surfactant Homeostasis during Cigarette Smoking*. *J Immunol*, 2021. **206**(8): p. 1923-1931.
12. Paudel, K.R., et al., *Attenuation of Cigarette-Smoke-Induced Oxidative Stress, Senescence, and Inflammation by Berberine-Loaded Liquid Crystalline Nanoparticles: In Vitro Study in 16HBE and RAW264.7 Cells*. *Antioxidants (Basel)*, 2022. **11**(5).

13. Mio, T., et al., *Cigarette smoke induces interleukin-8 release from human bronchial epithelial cells*. Am J Respir Crit Care Med, 1997. **155**(5): p. 1770-6.
14. Kaplanski, G., *Interleukin-18: Biological properties and role in disease pathogenesis*. Immunol Rev, 2018. **281**(1): p. 138-153.
15. Jiang, G., C.T. Liu, and W.D. Zhang, *IL-17A and GDF15 are able to induce epithelial-mesenchymal transition of lung epithelial cells in response to cigarette smoke*. Exp Ther Med, 2018. **16**(1): p. 12-20.
16. Hu, X., B. Hong, and M. Sun, *Peitu Shengjin Recipe Attenuates Airway Inflammation via the TLR4/NF- κ B Signaling Pathway on Chronic Obstructive Pulmonary Disease*. Evid Based Complement Alternat Med, 2022. **2022**: p. 2090478.
17. Mueller, T., et al., *Association of the biomarkers soluble ST2, galectin-3 and growth-differentiation factor-15 with heart failure and other non-cardiac diseases*. Clin Chim Acta, 2015. **445**: p. 155-60.
18. Novick, D., et al., *Interleukin-18 binding protein: a novel modulator of the Th1 cytokine response*. Immunity, 1999. **10**(1): p. 127-136.
19. Kratzer, A., et al., *Role of IL-18 in second-hand smoke-induced emphysema*. Am J Respir Cell Mol Biol, 2013. **48**(6): p. 725-32.
20. Soler Palacios, B., et al., *Growth Hormone Reprograms Macrophages toward an Anti-Inflammatory and Reparative Profile in an MAFB-Dependent Manner*. The Journal of Immunology, 2020: p. ji1901330.
21. Tweed, J.O., et al., *The endocrine effects of nicotine and cigarette smoke*. Trends Endocrinol Metab, 2012. **23**(7): p. 334-42.
22. Kew, R.R., *The Vitamin D Binding Protein and Inflammatory Injury: A Mediator or Sentinel of Tissue Damage?* Front Endocrinol (Lausanne), 2019. **10**: p. 470.
23. Bortner, J.D., Jr., et al., *Proteomic profiling of human plasma by iTRAQ reveals down-regulation of ITI-HC3 and VDBP by cigarette smoking*. J Proteome Res, 2011. **10**(3): p. 1151-9.
24. Kardas, G., et al., *Role of Platelet-Derived Growth Factor (PDGF) in Asthma as an Immunoregulatory Factor Mediating Airway Remodeling and Possible Pharmacological Target*. Front Pharmacol, 2020. **11**: p. 47.
25. Wang, M., et al., *Platelet-derived growth factor B attenuates lethal sepsis through inhibition of inflammatory responses*. Int Immunopharmacol, 2019. **75**: p. 105792.
26. Pini, A., et al., *Protection from cigarette smoke-induced vascular injury by recombinant human relaxin-2 (serelaxin)*. J Cell Mol Med, 2016. **20**(5): p. 891-902.

27. Thim, L. and F.E. May, *Structure of mammalian trefoil factors and functional insights*. Cell Mol Life Sci, 2005. **62**(24): p. 2956-73.
28. Bijelić, N., et al., *Localization of trefoil factor family peptide 3 (TFF3) in epithelial tissues originating from the three germ layers of developing mouse embryo*. Bosn J Basic Med Sci, 2017. **17**(3): p. 241-247.
29. Li, Y.H., et al., *Synergistic anti-inflammatory effect of Radix Platycodon in combination with herbs for cleaning-heat and detoxification and its mechanism*. Chin J Integr Med, 2013. **19**(1): p. 29-35.
30. Li, T., et al., *Cigarette smoke extract induces airway epithelial cell death via repressing PRMT6/AKT signaling*. Aging (Albany NY), 2020. **12**(23): p. 24301-24317.
31. Duffney, P.F., et al., *Cigarette smoke dampens antiviral signaling in small airway epithelial cells by disrupting TLR3 cleavage*. Am J Physiol Lung Cell Mol Physiol, 2018. **314**(3): p. L505-1513.
32. Modestou, M.A., et al., *Inhibition of IFN-gamma-dependent antiviral airway epithelial defense by cigarette smoke*. Respir Res, 2010. **11**(1): p. 64.
33. Leung, J.M., et al., *The role of acute and chronic respiratory colonization and infections in the pathogenesis of COPD*. Respirology, 2017. **22**(4): p. 634-650.
34. Nucera, F., et al., *Role of oxidative stress in the pathogenesis of COPD*. Minerva Med, 2022.
35. Panth, N., K.R. Paudel, and K. Parajuli, *Reactive Oxygen Species: A Key Hallmark of Cardiovascular Disease*. Adv Med, 2016. **2016**: p. 9152732.
36. Ketterer, B., B. Coles, and D.J. Meyer, *The role of glutathione in detoxication*. Environ Health Perspect, 1983. **49**: p. 59-69.
37. Birben, E., et al., *Oxidative stress and antioxidant defense*. World Allergy Organ J, 2012. **5**(1): p. 9-19.
38. Mao, G.E., et al., *Glutathione S-transferase P1 Ile105Val polymorphism, cigarette smoking and prostate cancer*. Cancer Detect Prev, 2004. **28**(5): p. 368-74.
39. Harju, T., et al., *Glutathione-S-transferases in lung and sputum specimens, effects of smoking and COPD severity*. Respiratory Research, 2008. **9**(1): p. 80.
40. Putcha, N. and R.A. Wise, *Medication Regimens for Managing COPD Exacerbations*. Respir Care, 2018. **63**(6): p. 773-782.
41. Allam, V., et al., *Nutraceuticals and mitochondrial oxidative stress: bridging the gap in the management of bronchial asthma*. Environ Sci Pollut Res Int, 2022.

42. Kuo, C.L., C.W. Chi, and T.Y. Liu, *The anti-inflammatory potential of berberine in vitro and in vivo*. *Cancer Lett*, 2004. **203**(2): p. 127-37.
43. Mehta, M., et al., *Berberine loaded liquid crystalline nanostructure inhibits cancer progression in adenocarcinomic human alveolar basal epithelial cells in vitro*. *J Food Biochem*, 2021. **45**(11): p. e13954.
44. Hardwick, J., et al., *Targeting Cancer using Curcumin Encapsulated Vesicular Drug Delivery Systems*. *Curr Pharm Des*, 2021. **27**(1): p. 2-14.
45. Paudel, K.R., et al., *Rutin loaded liquid crystalline nanoparticles inhibit lipopolysaccharide induced oxidative stress and apoptosis in bronchial epithelial cells in vitro*. *Toxicol In Vitro*, 2020. **68**: p. 104961.
46. Solanki, N., et al., *Antiproliferative effects of boswellic acid-loaded chitosan nanoparticles on human lung cancer cell line A549*. *Future Med Chem*, 2020. **12**(22): p. 2019-2034.
47. Kim, E., et al., *ROR activation by Nobiletin enhances antitumor efficacy via suppression of IkappaB/NF-kappaB signaling in triple-negative breast cancer*. *Cell Death Dis*, 2022. **13**(4): p. 374.
48. Rodríguez-Yoldi, M.J., *Anti-Inflammatory and Antioxidant Properties of Plant Extracts*. *Antioxidants (Basel)*, 2021. **10**(6).
49. Kim, T.M., K.R. Paudel, and D.W. Kim, *Eriobotrya japonica leaf extract attenuates airway inflammation in ovalbumin-induced mice model of asthma*. *J Ethnopharmacol*, 2020. **253**: p. 112082.
50. Lee, H.H., K.R. Paudel, and D.W. Kim, *Terminalia chebula Fructus Inhibits Migration and Proliferation of Vascular Smooth Muscle Cells and Production of Inflammatory Mediators in RAW 264.7*. *Evid Based Complement Alternat Med*, 2015. **2015**: p. 502182.
51. Liu, Y., et al., *Whole-tree agarwood-inducing technique: an efficient novel technique for producing high-quality agarwood in cultivated Aquilaria sinensis trees*. *Molecules*, 2013. **18**(3): p. 3086-106.
52. Wang, S., et al., *Chemical Constituents and Pharmacological Activity of Agarwood and Aquilaria Plants*. *Molecules*, 2018. **23**(2).
53. Alamil, J.M.R., et al., *Rediscovering the Therapeutic Potential of Agarwood in the Management of Chronic Inflammatory Diseases*. *Molecules*, 2022. **27**(9).

54. Peng, D.-Q., et al., *Chemical Constituents and Anti-Inflammatory Effect of Incense Smoke from Agarwood Determined by GC-MS*. International Journal of Analytical Chemistry, 2020. **2020**: p. 4575030.
55. Yadav, D.K., et al., *Molecular docking and ADME studies of natural compounds of Agarwood oil for topical anti-inflammatory activity*. Curr Comput Aided Drug Des, 2013. **9**(3): p. 360-70.
56. Chitre, T., et al., *Analgesic and anti-inflammatory activity of heartwood of Aquilaria agallocha in laboratory animals*. Pharmacol Online, 2007. **1**: p. 288-298.
57. Zheng, H., et al., *The protective effects of Aquilariae Lignum Resinatum extract on 5-Fluorouracil-induced intestinal mucositis in mice*. Phytomedicine, 2019. **54**: p. 308-317.
58. Wang, C., et al., *Agarwood Extract Mitigates Intestinal Injury in Fluorouracil-Induced Mice*. Biol Pharm Bull, 2019. **42**(7): p. 1112-1119.
59. Wang, C., et al., *Agarwood Alcohol Extract Protects against Gastric Ulcer by Inhibiting Oxidation and Inflammation*. Evid Based Complement Alternat Med, 2021. **2021**: p. 9944685.
60. Hamouda, A.F., *A biochemical study of agarwood on methanol injection in rat*. Journal of Drug and Alcohol Research, 2019. **8**(1): p. 1-14.
61. Liu, C.S., et al., *Research progress on berberine with a special focus on its oral bioavailability*. Fitoterapia, 2016. **109**: p. 274-82.
62. Ng, P.Q., et al., *Applications of Nanocarriers as Drug Delivery Vehicles for Active Phytoconstituents*. Curr Pharm Des, 2020. **26**(36): p. 4580-4590.
63. Chan, Y., et al., *Versatility of liquid crystalline nanoparticles in inflammatory lung diseases*. Nanomedicine (Lond), 2021. **16**(18): p. 1545-1548.
64. Paudel, K.R., et al., *Editorial: Advanced therapeutic delivery for the management of chronic respiratory diseases*. Front Med (Lausanne), 2022. **9**: p. 983583.
65. Paudel, K.R., et al., *Advances in research with rutin-loaded nanoformulations in mitigating lung diseases*. Future Med Chem, 2022. **14**(18): p. 1293-1295.
66. Clarence, D.D., et al., *Unravelling the Therapeutic Potential of Nano-Delivered Functional Foods in Chronic Respiratory Diseases*. Nutrients, 2022. **14**(18).
67. Jaiswal, M., R. Dudhe, and P.K. Sharma, *Nanoemulsion: an advanced mode of drug delivery system*. 3 Biotech, 2015. **5**(2): p. 123-127.

68. Dupuis, V., et al., *Nanodelivery of essential oils as efficient tools against antimicrobial resistance: a review of the type and physical-chemical properties of the delivery systems and applications*. *Drug Deliv*, 2022. **29**(1): p. 1007-1024.
69. Alnuqaydan, A.M., et al., *Evaluation of the Cytotoxic Activity and Anti-Migratory Effect of Berberine-Phytantriol Liquid Crystalline Nanoparticle Formulation on Non-Small-Cell Lung Cancer In Vitro*. *Pharmaceutics*, 2022. **14**(6).
70. Wadhwa, R., et al., *Anti-inflammatory and anticancer activities of Naringenin-loaded liquid crystalline nanoparticles in vitro*. *J Food Biochem*, 2021. **45**(1): p. e13572.
71. King, P.T., *Inflammation in chronic obstructive pulmonary disease and its role in cardiovascular disease and lung cancer*. *Clin Transl Med*, 2015. **4**(1): p. 68.
72. Chellappan, D.K., et al., *Targeting neutrophils using novel drug delivery systems in chronic respiratory diseases*. *Drug Dev Res*, 2020. **81**(4): p. 419-436.
73. Paudel, K.R., et al., *Role of Lung Microbiome in Innate Immune Response Associated With Chronic Lung Diseases*. *Front Med (Lausanne)*, 2020. **7**: p. 554.
74. May, S.M. and J.T. Li, *Burden of chronic obstructive pulmonary disease: healthcare costs and beyond*. *Allergy Asthma Proc*, 2015. **36**(1): p. 4-10.
75. Eisner, M.D., et al., *An official American Thoracic Society public policy statement: Novel risk factors and the global burden of chronic obstructive pulmonary disease*. *Am J Respir Crit Care Med*, 2010. **182**(5): p. 693-718.
76. Biswas, S.K., *Does the Interdependence between Oxidative Stress and Inflammation Explain the Antioxidant Paradox?* *Oxid Med Cell Longev*, 2016. **2016**: p. 5698931.
77. Chellappan, D.K., et al., *Mitochondrial dysfunctions associated with chronic respiratory diseases and their targeted therapies: an update*. *Future Med Chem*, 2021. **13**(15): p. 1249-1251.
78. Watson, A. and T.M.A. Wilkinson, *Digital healthcare in COPD management: a narrative review on the advantages, pitfalls, and need for further research*. *Ther Adv Respir Dis*, 2022. **16**: p. 17534666221075493.
79. Alqahtani, J.S., *Prevalence, incidence, morbidity and mortality rates of COPD in Saudi Arabia: Trends in burden of COPD from 1990 to 2019*. *PLoS One*, 2022. **17**(5): p. e0268772.
80. Devkota, H.P., et al., *Stinging Nettle (*Urtica dioica* L.): Nutritional Composition, Bioactive Compounds, and Food Functional Properties*. *Molecules*, 2022. **27**(16).
81. Zhao, Q., et al., *Molecular mechanism of the anti-inflammatory effects of plant essential oils: A systematic review*. *J Ethnopharmacol*, 2022: p. 115829.

82. Raman, S., V. Murugaiyah, and T. Parumasivam, *Andrographis paniculata* Dosage Forms and Advances in Nanoparticulate Delivery Systems: An Overview. *Molecules*, 2022. **27**(19).
83. MacNee, W., *Pulmonary and systemic oxidant/antioxidant imbalance in chronic obstructive pulmonary disease*. *Proc Am Thorac Soc*, 2005. **2**(1): p. 50-60.
84. Pahwa, R., A. Goyal, and I. Jialal, *Chronic Inflammation*, in *StatPearls*. 2022, StatPearls Publishing

Copyright © 2022, StatPearls Publishing LLC.: Treasure Island (FL).

85. Hussain, T., et al., *Oxidative Stress and Inflammation: What Polyphenols Can Do for Us?* *Oxid Med Cell Longev*, 2016. **2016**: p. 7432797.
86. Nyunoya, T., et al., *Molecular processes that drive cigarette smoke-induced epithelial cell fate of the lung*. *Am J Respir Cell Mol Biol*, 2014. **50**(3): p. 471-82.
87. Paudel, K.R., et al., *Advancements in nanotherapeutics targeting senescence in chronic obstructive pulmonary disease*. *Nanomedicine (Lond)*, 2022.
88. Nucera, F., et al., *Chapter 14 - Role of autoimmunity in the pathogenesis of chronic obstructive pulmonary disease and pulmonary emphysema*, in *Translational Autoimmunity*, N. Rezaei, Editor. 2022, Academic Press. p. 311-331.
89. Ma, W.J., et al., *Epoxyeicosatrienoic acids attenuate cigarette smoke extract-induced interleukin-8 production in bronchial epithelial cells*. *Prostaglandins Leukot Essent Fatty Acids*, 2015. **94**: p. 13-9.
90. Pauwels, N.S., et al., *Role of IL-1 α and the Nlrp3/caspase-1/IL-1 β axis in cigarette smoke-induced pulmonary inflammation and COPD*. *Eur Respir J*, 2011. **38**(5): p. 1019-28.
91. Feng, K.N., et al., *IL-37 protects against airway remodeling by reversing bronchial epithelial-mesenchymal transition via IL-24 signaling pathway in chronic asthma*. *Respir Res*, 2022. **23**(1): p. 244.
92. Hurme, M. and S. Santtila, *IL-1 receptor antagonist (IL-1Ra) plasma levels are coordinately regulated by both IL-1Ra and IL-1beta genes*. *Eur J Immunol*, 1998. **28**(8): p. 2598-602.
93. Lee, A.J. and A.A. Ashkar, *The Dual Nature of Type I and Type II Interferons*. *Front Immunol*, 2018. **9**: p. 2061.

94. Pungsrinont, T., J. Kallenbach, and A. Baniahmad, *Role of PI3K-AKT-mTOR Pathway as a Pro-Survival Signaling and Resistance-Mediating Mechanism to Therapy of Prostate Cancer*. *Int J Mol Sci*, 2021. **22**(20).

CHAPTER 4

Research Paper #3

Berberine-loaded engineered nanoparticles attenuate TGF- β -induced remodelling features in human bronchial epithelial cells

(**De Rubis G**, Paudel KR, Liu G, Agarwal V, MacLoughlin R, de Jesus Andreoli Pinto T, Singh SK, Adams J, Nammi S, Chellappan DK, Oliver BGG, Hansbro PM, Dua K. Berberine-loaded engineered nanoparticles attenuate TGF- β -induced remodelling in human bronchial epithelial cells. **Toxicology In Vitro**. 2023 92:105660. doi: 10.1016/j.tiv.2023.105660)

Berberine-loaded engineered nanoparticles attenuate TGF- β -induced remodelling in human bronchial epithelial cells

Gabriele De Rubis^{1,2}, Keshav Raj Paudel³, Gang Liu³, Vipul Agarwal⁴, Ronan MacLoughlin^{5,6,7}, Terezinha de Jesus Andreoli Pinto⁸, Sachin Kumar Singh^{2,9}, Jon Adams², Srinivas Nammi¹⁰, Dinesh Kumar Chellappan¹¹, Brian Gregory George Oliver^{12,13}, Philip Michael Hansbro³, Kamal Dua^{1,2,14*}

¹ Discipline of Pharmacy, Graduate School of Health, University of Technology Sydney, Sydney, NSW 2007, Australia

² Faculty of Health, Australian Research Centre in Complementary and Integrative Medicine, University of Technology Sydney, Ultimo, NSW 2007, Australia

³ Centre for Inflammation, Centenary Institute and University of Technology Sydney, Faculty of Science, School of Life Sciences, Sydney, NSW 2007, Australia

⁴ Cluster for Advanced Macromolecular Design (CAMD), School of Chemical Engineering, University of New South Wales, Sydney, Australia

⁵ Aerogen, IDA Business Park, H91 HE94 Galway, Connacht, Ireland

⁶ School of Pharmacy & Biomolecular Sciences, Royal College of Surgeons in Ireland, D02 YN77 Dublin, Leinster, Ireland

⁷ School of Pharmacy & Pharmaceutical Sciences, Trinity College, D02 PN40 Dublin, Leinster, Ireland

⁸ Department of Pharmacy, Faculty of Pharmaceutical Sciences, University of São Paulo, São Paulo, Brazil.

⁹ School of Pharmaceutical Sciences, Lovely Professional University, Phagwara, Punjab, India

¹⁰ School of Science, Western Sydney University, Penrith, NSW 2751, Australia.

¹¹ Department of Life Sciences, School of Pharmacy, International Medical University, Bukit Jalil 57000, Kuala Lumpur, Malaysia

¹² Woolcock Institute of Medical Research, University of Sydney, Sydney, New South Wales, Australia

¹³ School of Life Sciences, University of Technology Sydney, Ultimo, NSW 2007, Australia

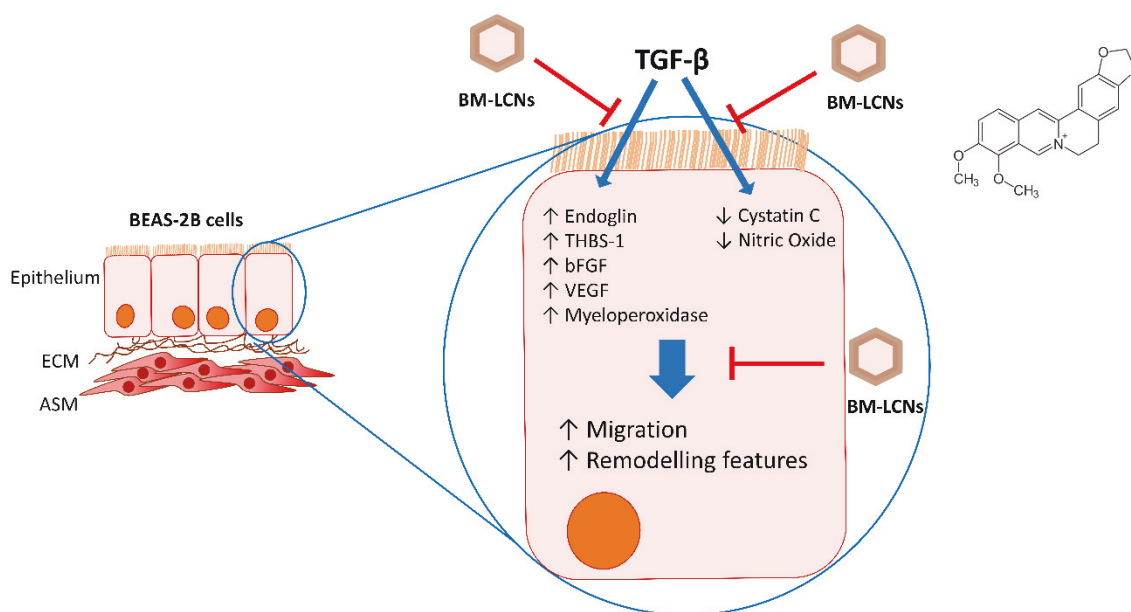
¹⁴ Uttaranchal Institute of Pharmaceutical Sciences, Uttaranchal University, Dehradun, India

* Corresponding Author: Dr Kamal Dua (kamal.dua@uts.edu.au)

Abstract

Airway remodelling occurs in chronic respiratory diseases (CRDs) such as asthma and chronic obstructive pulmonary disease (COPD). It is characterized by aberrant activation of epithelial repair, excessive extracellular matrix (ECM) deposition, epithelial-to-mesenchymal transition (EMT), and airway obstruction. The master regulator is Transforming Growth Factor- β (TGF- β), which activates tissue repair, release of growth factors, EMT, increased cell proliferation, and reduced nitric oxide (NO) secretion. Due to its fundamental role in remodelling, TGF- β is an emerging target in the treatment of CRDs. Berberine is a benzylisoquinoline alkaloid with antioxidant, anti-inflammatory, and anti-fibrotic activities whose clinical application is hampered by poor permeability. To overcome these limitations, in this study, berberine was encapsulated in monoolein-based liquid crystalline nanoparticles (BM-LCNs). The potential of BM-LCNs in inhibiting TGF- β -induced remodelling features in human bronchial epithelial cells (BEAS-2B) was tested. BM-LCNs significantly inhibited TGF- β -induced migration, reducing the levels of proteins upregulated by TGF- β including endoglin, thrombospondin-1, basic fibroblast growth factor, vascular-endothelial growth factor, and myeloperoxidase, and increasing the levels of cystatin C, a protein whose expression was downregulated by TGF- β . Furthermore, BM-LCNs restored baseline NO levels downregulated by TGF- β . The results prove the *in vitro* therapeutic efficacy of BM-LCNs in counteracting TGF- β -induced remodelling features. This study supports the suitability of berberine-loaded drug delivery systems to counteract airway remodelling, with potential application as a treatment strategy against CRDs.

Graphical Abstract



Keywords

Asthma, COPD, lung cancer, airway remodelling, TGF- β , berberine, phytoceuticals, liquid crystalline nanoparticles

1. Introduction

Chronic respiratory diseases (CRDs) are a heterogeneous group of diseases affecting the airways and other lung structures and including asthma, chronic obstructive pulmonary disease (COPD), occupational lung diseases, pulmonary hypertension, idiopathic pulmonary fibrosis, and others [1-3]. Lung cancer (LC), particularly non-small cell lung cancer (NSCLC), is often considered a CRD as well [4]. The main aetiological factor associated with the development of these diseases is cigarette smoking through the exposure to the thousands of toxic chemicals in tobacco smoke, which promote a chronic pro-inflammatory and pro-oxidant state that further prompts disease progression [5-7]. CRDs, particularly asthma, COPD, and LC, are among the leading causes of mortality and morbidity worldwide, and their global burden is significant [8]. According to recent data, in 2017-2019, COPD caused about 3.3 million deaths annually [9], while about 500,000 yearly deaths were associated with asthma [8]. Overall, LC is one of the deadliest types of cancer, with 1.7 million deaths attributed to LC globally in 2020, a trend that is currently increasing [10]. Although less frequent compared to other CRDs, idiopathic pulmonary fibrosis (IPF) is a chronic, progressive disease characterized by the irreversible scarring of the lung's interstitial framework with a median survival of 3-5 years if untreated [11].

Current therapeutic approaches for CRDs include pharmacological and non-pharmacological strategies. These are severely limited and, in the case of asthma, IPF and COPD, aim at improving and managing disease symptoms rather than tackling the underlying disease mechanisms [11-13]. Despite showing some efficacy, the currently available pharmacotherapies for CRDs are limited by severe side effects [11, 14, 15]. With regards to LC, therapeutic approaches include various combinations of surgical removal, radiotherapy, chemotherapy, and immunotherapy, depending on the tumor stage [16]. Chemotherapies are all limited by severe organ toxicity, adverse effects, as well as by the eventual development of cancer multidrug resistance [16-18]. This underlines the need to develop novel therapeutics with improved treatment outcomes and reduced adverse effects. In this context, developing treatment strategies tackling one or more cellular and molecular mechanisms shared by different diseases would be advantageous.

A fundamental feature shared between all these CRDs is the progressive radical deterioration and alteration of the structure of the respiratory tract, also termed airway remodelling [19-21]. Structural transformations in airway remodelling include subepithelial fibrosis, infiltration of

immune cells, disruption of epithelial cell layers, excessive mucus secretion, excessive production of matrix metalloproteinases (MMPs), and thickening of the basement membrane due to excessive collagen deposition [22]. This leads to severe airway obstruction [20, 21, 23]. The thickening of the basement membrane is caused by the presence of an excessive number of highly synthetic myofibroblasts, which express alpha-smooth muscle actin (α -SMA) [23]. Epithelial-to-mesenchymal transition (EMT) of lung epithelial cells, which acquire increased proliferative and migratory capacity, is considered an important source of myofibroblasts contributing to airway remodelling. [23-25].

One of the master regulators of tissue remodelling, particularly in the airways, is transforming growth factor-beta (TGF- β) [25-27]. TGF- β is a multifunctional cytokine present in three different isoforms: TGF- β 1, TGF- β 2, and TGF- β 3, with partially overlapping biological activities [28, 29]. TGF- β is secreted in an inactive form called large latent complex (LLC), in which the functional protein is bound to the latency-associated peptide (LAP) and other proteins [27, 30]. The LLC is primarily localized in the ECM and it functions as a reservoir of inactive TGF- β [27]. The active form of TGF- β is released following different stimuli, including temperature spikes, acidification of the microenvironment, oxidative stress, proteolysis, and integrin binding [27]. Thrombospondin-1 and MMPs are among the main proteins activating TGF- β , and the fact that these proteins are upregulated by TGF- β itself represents an important positive feedback mechanism enhancing TGF- β activation [31, 32]. Upon binding to its receptor, TGF- β regulates the expression of a plethora of target genes mainly through the canonical TGF- β /Smad pathway, in which Smad proteins are phosphorylated and translocated into the nucleus, where they act as transcription factors [33]. Many other proteins are involved in the regulation and action of TGF- β signalling in airway remodelling and EMT. These include growth factors such as the vascular endothelial growth factor (VEGF), which is a known inducer of lung remodelling [34] and whose secretion is enhanced by TGF- β in airway smooth muscle cells [35], as well as the basic fibroblast growth factor (bFGF), which is co-expressed with TGF- β in the lung of ovalbumin (OVA)-induced mice [36] and induces angiogenesis associated to remodelling in asthma and COPD [37]. Other proteins involved in TGF- β -induced remodelling and EMT include myeloperoxidase [38], and endoglin, which is associated with the TGF- β receptors and affects TGF- β responses [39]. TGF- β signalling is also controlled by negative regulators such as cystatin C [40].

An important mechanism through which TGF- β induces EMT in alveolar epithelial cells is through the reduction of baseline nitric oxide (NO) levels [41]. NO, in fact, is a critical factor

that attenuates EMT, and TGF- β reduces its baseline production in the injured lung through the inhibition of the endothelial NO synthase (eNOS) [41] and other enzymes involved in NO production such as soluble guanylate cyclase (sGC) and cGMP-dependent protein kinase I (PKG1) [42].

Physiologically, TGF- β plays a pleiotropic role in lung health and development. Its activity is fundamental in lung organogenesis, and in the regulation of homeostatic alveolar epithelial growth, differentiation, and EMT [43]. Due to its fundamental role in lung homeostasis, dysregulation of TGF- β signalling is common in many diseases where tissue remodelling plays a relevant role, including CRDs [43, 44]. Considering its function as a promoter of EMT in healthy cells, dysregulation of TGF- β signalling is also an important factor contributing to increased cell migration and invasion in many types of cancer, including LC, where it is recognised as the most potent inducer of EMT [43]. Interestingly, increased levels of TGF- β have been detected in the airways of COPD, asthma, and LC patients, as well as tobacco smokers [43, 44].

The multifaceted role played by TGF- β in CRDs makes it a valuable pharmacological target [26]. In the quest for novel pharmacological strategies to treat respiratory disorders, plant-derived molecules, also known as phytochemicals, are an endless source of inspiration [45]. In this context, one promising phytochemical is berberine, an isoquinoline alkaloid found in barberry, tree turmeric, and other plants [46, 47]. Berberine is widely known for its potent antioxidant, anti-inflammatory, and anticancer properties [47-51], and it also exerts antifibrotic activity in the lungs, heart, liver, pancreas and kidneys of rodents [52]. In the lung, in particular, the antifibrotic activity of berberine is exerted through the suppression of nuclear factor- κ B (NF- κ B)-induced TGF- β activation [53]. Furthermore, berberine was shown to counteract TGF- β -induced EMT in vitro on A549 human NSCLC cells [54].

Despite its promising biological activity, the clinical use of berberine, similarly to that of other phytochemicals, is currently limited by its poor solubility and permeability which, together with a high rate of hepatobiliary excretion, translates into poor oral bioavailability and unfavourable pharmacokinetics [55, 56]. To overcome these limitations, encapsulation of phytochemicals within advanced, nanoparticle (NP)-based drug delivery systems is an advantageous strategy [45, 57, 58]. This allows to drastically increase the solubility, permeability, and stability of the encapsulated molecules, improving their bioavailability and pharmacokinetic properties [26, 45, 59, 60]. Among the many available classes of nanoformulations, liquid crystalline

nanoparticles (LCNs) are particularly versatile in the treatment of pulmonary diseases [61]. Our research team has worked extensively with berberine-loaded LCNs, demonstrating their superior *in vitro* anticancer activity against A549 lung cancer cells [49-51], as well as a potent antioxidant, anti-inflammatory, and anti-senescence activity in cigarette smoke-induced BCl-NS1.1 human airway basal cells [47, 62] and antioxidant and anti-inflammatory activity in lipopolysaccharide (LPS)-induced mouse RAW264.7 macrophages [48].

In the present work, we tested a monoolein-based berberine LCN formulation (BM-LCNs) against a model of airway remodelling and EMT obtained by stimulating BEAS-2B human bronchial epithelial cells with TGF- β [23]. We show that BM-LCNs significantly attenuate the functional and molecular features associated with TGF- β -induced remodelling and EMT. This study highlights the enormous potential of nanoparticle-based drug delivery systems in enhancing the use of phytochemicals for the treatment of lung diseases, providing proof of the applicability of BM-LCNs as a potential therapeutic agent tackling the aberrant airway remodelling process that drives the pathogenesis of CRDs.

2. Materials and Methods

2.1. Formulation and Physicochemical Characterisation of BM-LCNs

Berberine hydrochloride (Cat. #B3251), monoolein (Cat. #CRM44893), and poloxamer 407 (Cat. #16758) were purchased from Sigma-Aldrich, Australia, and were used for the preparation of BM-LCNs. BM-LCNs were formulated using the ultrasonication method, and characterised for physicochemical characteristics such as particle size, polydispersity index, zeta potential, entrapment efficiency, morphology, and *in vitro* release, as reported in a previous study [51]. Briefly, 200 mg monoolein were melted at 70 °C in a glass vial. Poloxamer 407 (20 mg) was dissolved in 4.8 mL deionized water and heated to 70 °C in a glass vial. Berberine powder (5 mg) was added to the melted monoolein and vortexed until completely dissolved. Then, the poloxamer 407 solution was added to the berberine-monoolein solution until formation of a coarse dispersion. The coarse dispersion was finally subjected to size reduction using a probe sonicator, using an amplitude of 80 for 5 minutes, with 5-seconds-on and 5-seconds-off cycles.

2.3 Cell Culture

The human bronchial epithelial cells (BEAS-2B, ATCC #CRL-9609) were a kind gift from Professor Alaina Ammit (Woolcock Institute of Medical Research, Sydney, NSW, Australia). These cells were used at passages between 15 and 25 throughout the study, and were cultured at 37 °C in Dulbecco's Modified Eagle Medium (DMEM, Sigma-Aldrich, Australia, Cat. #D6046) supplemented with 5% fetal bovine serum (Sigma-Aldrich, Australia, Cat. #F9423), 100 unit/ml penicillin and 100 µg streptomycin (Pen-Strep solution, Sigma-Aldrich Australia, Cat. #P4333) in a humidified atmosphere containing 5% CO₂.

2.3 Cell viability assay - MTT

The MTT cell viability assay was performed as reported in a previous study [48]. The BEAS-2B cells were seeded at a density of 5,000 cells/well in a transparent, clear-bottom 96-well plate and left to attach overnight. The following day, the cells were incubated in the presence of 5 ng/mL human TGF-β1 (R&D Systems Biotechnology, Minnesota, USA, Cat. # 754BH005), at 37 °C for 24 h. The cells were then incubated for 24 more hours in the presence of BM-LCN concentrations ranging between 0 and 10 µM or with empty LCNs at dilutions representative to the BM-LCNs concentrations tested. Then, 250 µg/mL MTT ((3-(4,5-dimethylthiazol-2-yl)-2,5-diphenyl tetrazolium bromide, Sigma-Aldrich, Australia, Cat. #M2003) was added to each well and incubated at 37°C for further 4 h. Upon incubation, the supernatant was removed, and the formed formazan crystals were dissolved using 100 µL dimethyl sulfoxide (DMSO, Sigma-Aldrich, Australia, Cat. #D8418). The absorbance was read at 570 nm wavelength using a TECAN Infinite M1000 plate reader (Tecan Trading AG, Switzerland).

2.4 Cell viability assay – Trypan Blue staining

The impact of BM-LCNs on cell viability has also been assessed using Trypan Blue staining, similarly to how reported in a previous study [51]. Briefly, 10,000 cells/well were seeded in a 48-well plate and left to attach overnight. The following day, the cells were incubated in the presence of 5 ng/mL human TGF-β1, at 37 °C for 24 h. The cells were then incubated for 24 more hours in the presence of BM-LCN concentrations ranging between 0 and 10 µM. After incubation, the cells were treated with 300 µL 1X Trypsin-EDTA solution (Sigma-Aldrich, Australia, Cat. # T4299), incubating at 37 °C for 2 minutes to allow cell detachment. The trypsin was then inactivated by adding 300 µL FBS-supplemented DMEM, and the cells were centrifuged at 500 x g, for 5 minutes, at room temperature. The cell pellet was then resuspended

in 20 μ L FBS-supplemented DMEM and mixed at a 1:1 ratio with 0.4% Trypan Blue solution (ThermoFisher Scientific, Australia, Cat. #15250061). The number of live cells/mL was counted using a Neubauer Improved haemocytometer, using a light microscope at 10X magnification.

2.5 Wound healing assay

To assess the anti-migratory activity of BM-LCNs on TGF- β -stimulated BEAS-2B cells, the wound healing assay was performed. Briefly, 100,000 BEAS-2B cells/well were seeded into 6-well plates and incubated at 37 °C overnight. The following day, the cell monolayer was scratched using the tip of a sterile 200 μ L pipette tip, and the wells were washed five times with sterile PBS (Sigma-Aldrich, Australia, Cat. #P3813). The cells were then incubated in the presence of 5 ng/mL TGF- β 1 alone or in the presence of 5 ng/mL TGF- β 1 and 0.5 μ M BM-LCNs for up to 48 h. The distance between the edges of the scratch was measured under a light microscope, at 10X magnification, at 0, 24, and 48 h time points. The percentage of wound closure was normalized as a percentage compared to the control (untreated) group.

2.6 Human cytokine protein array

The effect of BM-LCNs on the expression of cytokines and other proteins in TGF- β -induced BEAS-2B cells was studied using the Proteome Profiler Human XL Cytokine Array Kit (R&D Systems, Minneapolis, MN, USA, Cat. #ARY022B), as described previously [47]. The cells were seeded in a 6-well plate at a density of 100,000 cells/well and left to attach overnight. The following day, the cells were incubated in the presence of 5 ng/mL TGF- β 1 and incubated at 37 °C for 24 h. The cells were then incubated for another 24 h in the presence of 0.5 μ M BM-LCNs. Following incubation, the cells were lysed with 500 μ L RIPA buffer (ThermoFisher Scientific, Australia, Cat. #89900) supplemented with protease inhibitor tablets (Roche Diagnostics GmbH, Mannheim, Germany, Cat. #11697498001). An amount of 300 μ g of proteins from each experimental group was loaded onto each array and incubated overnight at 4 °C. The further incubation steps with antibodies and chemiluminescent reagents were performed following the manufacturer's instructions. The arrays were photographed using a ChemiDoc MP (Bio-Rad, Hercules, CA, USA) and the pixel density for each spot was analysed with ImageJ (version 1.53c, Bethesda, MD, USA).

2.7 NO levels determination with Griess reagent

The relative levels of NO released by BEAS-2B cells in the culture supernatants were determined using the modified Griess reagent (Sigma-Aldrich, Australia, Cat. #G4410). The cells were seeded in a 6-well plate at a density of 100,000 cells/well and left to attach overnight. The following day, the cells were incubated in the presence of 5 ng/mL TGF- β 1 and incubated at 37 °C for 24 h. The cells were then incubated for another 24 h in the presence of 0.5 μ M BM-LCNs. Following incubation, the culture supernatants were collected, and 100 μ L of the supernatants were added to a clear-bottom, transparent 96-well plate. The supernatants were mixed in a 1:1 ratio with the Griess reagent and the plates were incubated for 30 min at room temperature in dark. The relative NO levels were determined using a TECAN Infinite M1000 plate reader (Tecan Trading AG, Switzerland) by measuring the absorbance at 540 nm. Unconditioned cell culture media was used as a blank, and its absorbance was subtracted from the absorbance of each sample. Relative NO levels were reported as a percent change compared to the untreated group.

2.8 Statistical analysis

The data are presented as mean \pm SEM. The data were analysed by ordinary one-way ANOVA, followed by Tukey multiple comparison test, using GraphPad Prism (v.9.4, GraphPad Software, San Diego, CA, USA). A two-tailed of p-value <0.05 was considered statistically significant for pairwise comparisons.

3. Results

3.1. Identification of an optimal concentration of BM-LCNs for treating TGF- β -stimulated BEAS-2B cells

To find a non-lethal BM-LCNs concentration to treat BEAS-2B cells, the MTT assay and the Trypan Blue assay were performed to assess the cell viability following treatment of TGF- β -induced BEAS-2B cells with increasing BM-LCNs concentrations. The results are shown in Figure 1a (MTT assay) and Figure 1b (Trypan Blue assay). Furthermore, the toxicity of empty LCNs on BEAS-2B cells was tested through MTT assay (Figure 1c). Treatment with BM-LCNs concentrations of 0.25 and 0.5 μ M resulted in a slight, not statistically significant, reduction in cell viability of 4.5% and 12.8%, respectively (Figure 1a, $p > 0.05$ against the TGF- β -treated group for both groups). At higher concentrations of 1, 2.5, 5, and 10 μ M, treatment

with BM-LCNs caused a significant reduction of cell viability of 28.0%, 29.4%, 26.5%, and 51.9%, respectively (Figure 1, $p < 0.0001$ against the TGF- β -treated group for all groups). In the Trypan Blue assay, treatment with BM-LCNs concentrations of 0.25 and 0.5 μM resulted in a slight, not statistically significant, increase in cell viability of 0.8% and 1.5%, respectively (Figure 1b, $p > 0.05$ against the TGF- β -treated group for both groups). At higher concentrations of 1, 2.5, 5, and 10 μM , treatment with BM-LCNs caused a significant reduction of cell viability of 18.1% ($p < 0.01$ against the TGF- β -treated group), 30.2% ($p < 0.001$ against the TGF- β -treated group), 54.7% ($p < 0.0001$ against the TGF- β -treated group), and 89.4% ($p < 0.0001$ against the TGF- β -treated group), respectively (Figure 1b). The highest non-toxic BM-LCNs concentration resulted to be 0.5 μM across both assays, and this concentration was used to treat cells in the following experiments. Furthermore, treatment of BEAS-2B cells with empty LCNs used at a concentration corresponding to 0.25, 0.5, and 1 μM BM-LCNs resulted in a slight, not significant, reduction in cell viability (of 1.4%, 1.6%, and 4.2% respectively ($p > 0.05$ against the untreated group, Figure 1c). Treatment with higher concentrations of empty LCNs, corresponding to 2.5, 5, and 10 μM BM-LCNs, resulted in a significant reduction of cell viability of 15.8% ($p < 0.001$ against the untreated group), 16.5% ($p < 0.0001$ against the untreated group), and 27.9% 16.5% ($p < 0.0001$ against the untreated group), respectively (Figure 1c). Treatment with either TGF- β alone or with TGF- β and 0.5 μM BM-LCNs did not result in significant changes in the cells' morphology (Figure 1d).

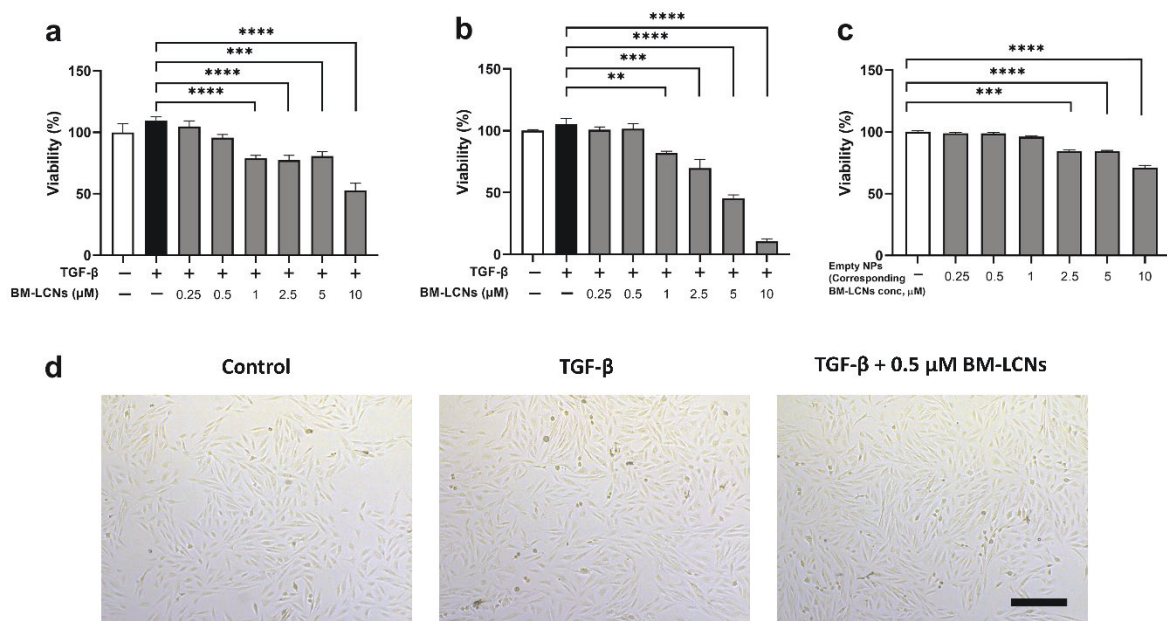


Figure 1. Impact of BM-LCNs treatment on the cell viability and morphology of TGF- β -induced BEAS-2B. BEAS-2B cells were incubated for 24 h in the presence of 5 ng/mL TGF- β and for a further 24 h with increasing concentrations of BM-LCNs (0.25, 0.5, 1, 2.5, 5, 10 μ M, Figure 1a, b). Subsequently, the MTT assay (a) or the Trypan Blue assay (b) was performed to assess cell viability. BEAS-2B cells were incubated for 24 h in the presence of increasing empty LCN concentrations, corresponding to 0.25, 0.5, 1, 2.5, 5, 10 μ M BM-LCNs, and the MTT assay was performed to assess cell viability (c). The BEAS-2B cell morphology upon treatment with TGF- β alone or with TGF- β and 0.5 μ M BM-LCNs is shown in (d). Scale bar = 300 μ m. The results in (a-c) were normalised as a percentage compared to untreated control and indicated as mean \pm SEM (n = 3, **: p<0.01; ***: p<0.001; ****: p<0.0001 with one-way ANOVA test).

3.2. Anti-migratory activity of BM-LCNs in TGF- β -induced BEAS-2B cells

The effect of treatment with 0.5 μ M BM-LCNs on the migratory capacity of TGF- β -induced BEAS-2B cells was assessed through the wound healing assay after 24 and 48 h of treatment (Figure 2a and 2b, respectively). At the 24 h time, the percentage of wound closure of the untreated group was 36.3% (Figure 2a). Treatment with TGF- β resulted in a significant 42% increase in the percentage of wound closure compared to the untreated group (percentage wound closure of 51.5%, p<0.0001, Figure 2a). Simultaneous treatment with BM-LCNs reversed the effect of TGF- β , resulting in a significantly lower percent wound closure similar to the untreated group (34.8%, p<0.0001 vs TGF- β -induced group, Figure 2a). At the 48 h time point, the percentage of wound closure of the untreated group was 65.5% (Figure 2b), and treatment with TGF- β resulted in a significant 18% increase in the percentage of wound closure compared to the untreated group (percentage wound closure of 77.3%, p<0.01, Figure 2b). Simultaneous treatment with BM-LCNs reversed the effect of TGF- β , resulting in a significantly lower percent of wound closure which was similar to the untreated group (63.0%, p<0.01 vs TGF- β -induced group, Figure 2b). Representative figures of the cells at the indicated time points are shown in Figure 2c.

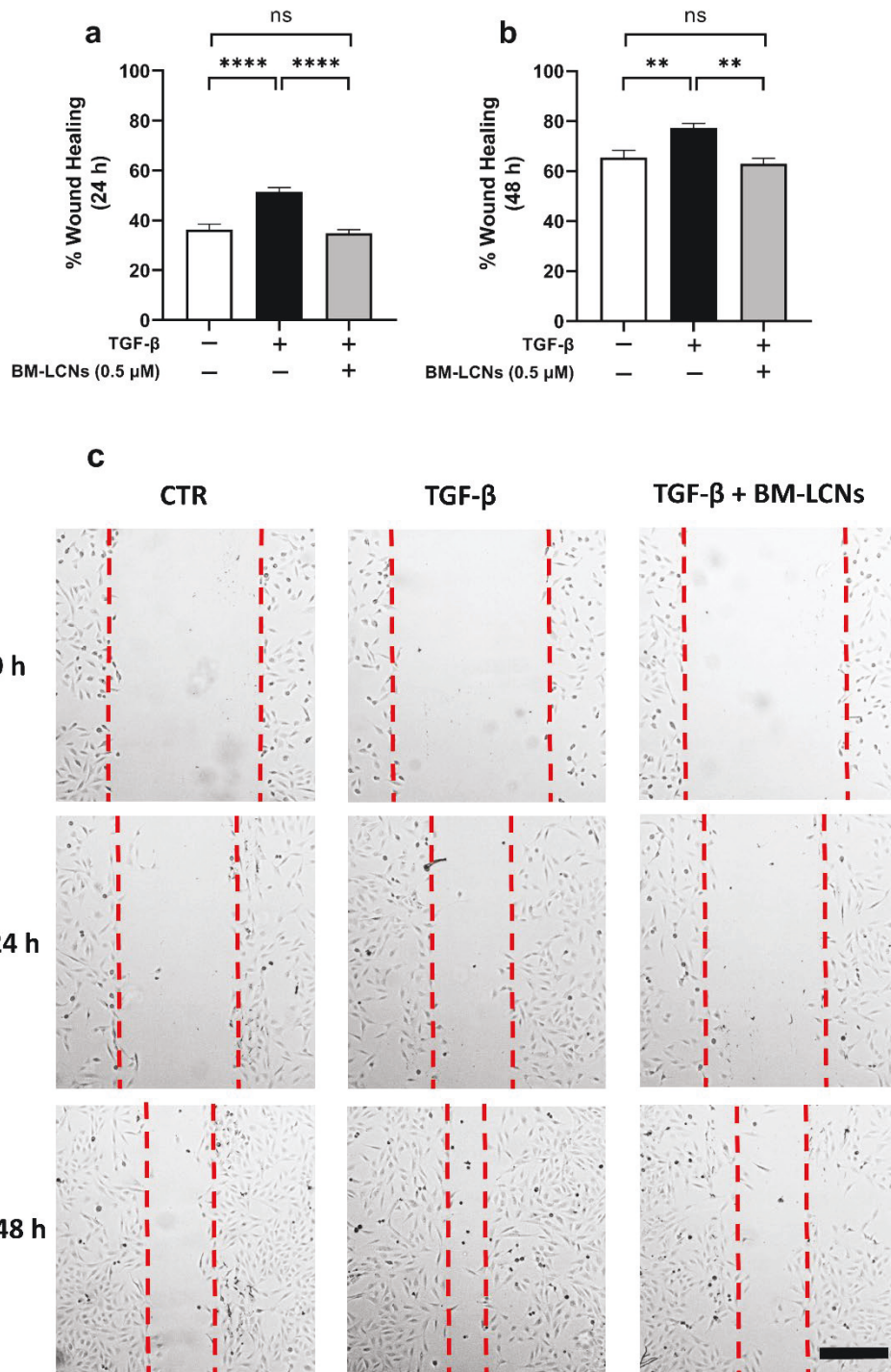


Figure 2. Anti-migratory activity of BM-LCNs in TGF- β -induced BEAS-2B cells. The wound was created by scratching, with a sterile pipette tip, a layer of BEAS-2B cells. Cells were then treated with 5 ng/mL TGF- β 1 with or without the presence of 0.5 μ M BM-LCNs. Photographs were acquired using a light microscope at 10x magnification. The distance between the edges of the wounds was measured before treatment (0 h) and after 24 h (a) and 48 h (b) incubation in order to calculate the percent wound closure. Representative pictures of

the cells at the indicated time points are shown in (c). Magnification: 10X; Scale bar = 300 μm . Values are expressed as mean \pm SEM (n = 3; ns: $p > 0.05$; **: $p < 0.01$; ****: $p < 0.0001$ with one-way ANOVA test).

3.3. BM-LCNs counteract the protein expression signature induced by TGF- β

The relative protein levels of endoglin, basic FGF, myeloperoxidase, thrombospondin-1, VEGF, myeloperoxidase, and cystatin C are shown in Figure 3, as detected using the Human XL Cytokine Protein Array. Treatment with 0.5 μM BM-LCNs counteracted the action of TGF- β by reducing the expression of endoglin, basic FGF, myeloperoxidase, thrombospondin-1, and VEGF (Figure 3a to 3e, respectively), which are induced by TGF- β , as well as by partially restoring the expression of cystatin C, which is suppressed by TGF- β (Figure 3f). A representative array for each experimental group is shown in Figure 3g. In particular, treatment of BEAS-2B cells with TGF- β resulted in a nearly statistically significant increase in the signal intensity correlated to the levels of endoglin (1.14-fold, $p = 0.07$, Figure 3a), as well as a statistically significant increase in the signal of basic FGF (1.37-fold, $p < 0.01$, Figure 3b), and myeloperoxidase (1.35-fold, $p < 0.05$, Figure 3c). Simultaneous treatment with BM-LCNs resulted in a significant reduction of the signal intensity for all these proteins. The signal corresponding to endoglin was reduced by 15.7% ($p < 0.05$, Figure 3a), the signal corresponding to basic FGF was reduced by 21.6% ($p < 0.05$, Figure 3b), and the signal corresponding to myeloperoxidase was reduced by 24.0% ($p < 0.01$, Figure 3c). A similar trend, although not statistically significant, was observed for thrombospondin-1 (THBS1) and VEGF. Upon treatment with TGF- β , THBS1 signal was increased by 1.58-fold and VEGF signal was increased by 2-fold (Figures 3d and 3e, respectively, $p > 0.05$). Treatment with BM-LCNs reduced the signal related to the expression of these proteins by 34.4% ($p > 0.05$, Figure 3d) and 21.2% ($p > 0.05$, Figure 3e), respectively. With regards to cystatin C, its expression was significantly reduced by 65% upon treatment with TGF- β ($p < 0.0001$, Figure 3f). Treatment with BM-LCNs resulted in a 1.68-fold increase in the signal correlated to cystatin C ($p = 0.053$, Figure 3f).

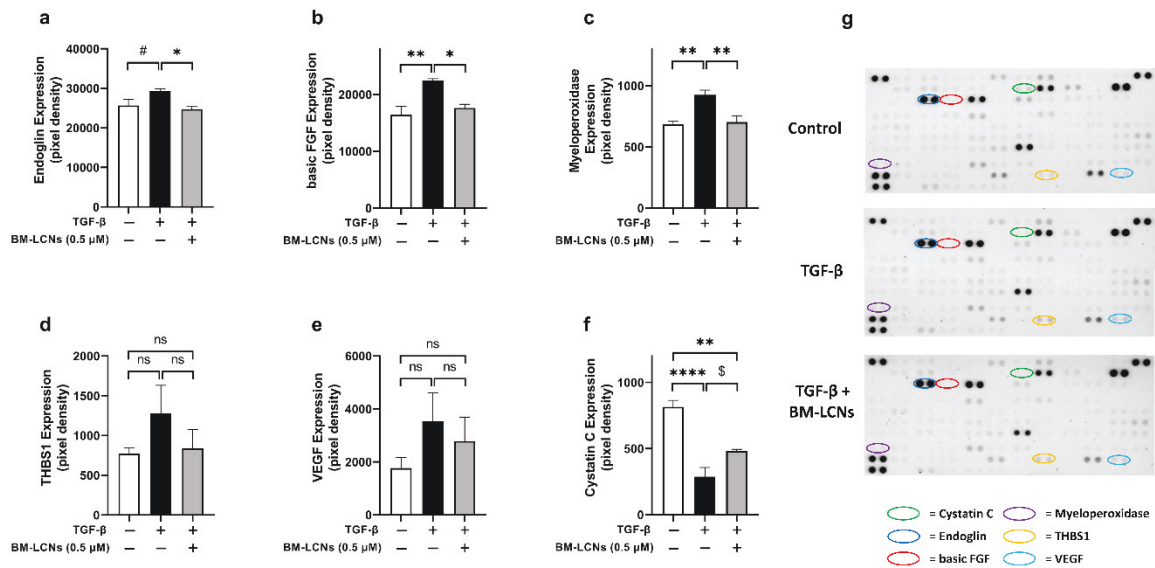


Figure 3. BM-LCNs counteract the expression patterns of proteins induced by TGF-β. BEAS-2B cells were treated with 5 ng/mL TGF-β1 for 24 h with or without a successive 24 h treatment with 0.5 μM BM-LCNs. The relative protein expression levels of endoglin (a), basic FGF (b), myeloperoxidase (c), thrpmbospondin-1 (THBS1) (d), VEGF (e), and cystatin C (f) were determined using the Human XL Cytokine Protein Array. A representative array for each group is shown in (g). Values in (a-f) are expressed as mean ± SEM (n=4, *: p<0.05; **: p<0.01; ****: p<0.0001; #: p=0.07; \$: p=0.053 with one-way ANOVA test).

3.4. BM-LCNs restore baseline levels of NO

The effect of BM-LCNs on NO production in BEAS-2B cells was assessed by measuring NO levels in the cell culture supernatant using the Griess reagent. The results are shown in Figure 4. Treatment of BEAS-2B cells with TGF-β resulted in a significant 36.4% reduction of the NO levels compared to untreated group (p<0.01, Figure 4). The subsequent treatment with BM-LCNs restored the secretion of NO to the same levels as the untreated group (p<0.01 against the TGF-β-treated group, Figure 4). No statistically significant difference was observed between the untreated group and the TGF-β + BM-LCNs treated group (Figure 4).

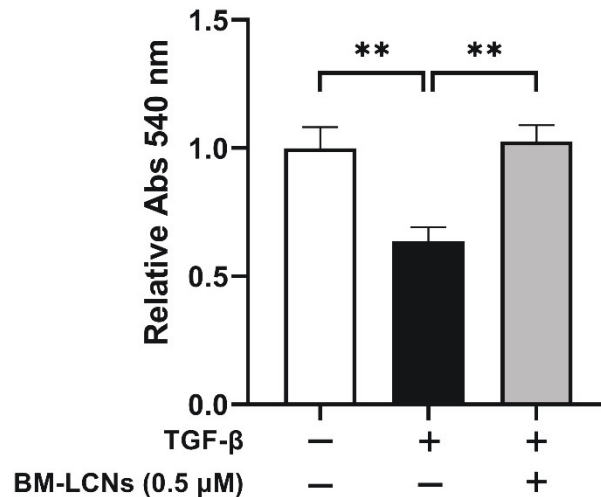


Figure 4. BM-LCNs restore baseline levels of NO. BEAS-2B cells were treated with 5 ng/mL TGF-β1 for 24 h with or without a successive 24 h treatment with 0.5 μM BM-LCNs. The NO levels in the cell culture supernatant were determined using the Griess reagent and measuring the absorbance at 540 nm. The values indicated are mean ± SEM (n=3; **: p<0.01 with one-way ANOVA test).

4. Discussion

CRDs are among the leading causes of morbidity and mortality worldwide, causing substantial medical and economic burdens [8]. Cigarette smoking is considered to be among the main causative factors for this heterogeneous group of diseases due to the fact that it results in the exposure of the respiratory system to thousands of different noxious chemicals, promoting chronic inflammation, oxidative stress, and consequentially severe tissue damage [63-65]. Traditional therapies for CRDs are mainly aimed at improving disease symptoms, and they are often ineffective at restoring the destroyed airways and lung parenchyma [66]. Furthermore, the currently available pharmacological strategies for these ailments are hampered by severe side effects [14]. This is particularly true in the case of LC due to the elevated toxicity of the currently used chemotherapeutic drugs [17].

A common feature shared between the CRDs is the process of airway remodelling, consisting of radical structural changes occurring in both the large and small airways and contributing to severe airway obstruction [21, 26]. The main structural alterations in airway remodelling include EMT of epithelial layers, excessive collagen and mucus secretion, and thickening of

the basement membrane. These processes are orchestrated by TGF- β , whose expression and signalling are aberrant in virtually all CRDs [27, 67]. In this context, a therapeutic agent tackling the TGF- β signalling would be advantageous. It would find widespread clinical application as a therapy for all diseases where tissue remodelling and fibrosis play a fundamental role [68].

The plant world represents an endless source of inspiration for novel compounds, collectively termed phytochemicals or nutraceuticals, with the most disparate pharmacological activities [45]. Many phytochemicals are known to downregulate TGF- β signalling and therefore show great promise in treating CRDs and fibrotic disorders [52]. One of these compounds is berberine, which has been shown to suppress TGF- β expression and signalling and subsequent cell motility, proliferation, and EMT *in vitro* in many types of cancer [69-74] and is embedded with potent multi-organ antifibrotic activity *in vivo* [52]. Despite its potent biological activity, the clinical application of berberine is limited by a poor pharmacokinetic profile, mainly deriving from its scarce permeability. This results in the necessity to administer large doses of berberine to achieve therapeutic efficacy, with an increased risk of adverse effects [55]. To overcome this important obstacle to the clinical application of berberine and other phytochemicals, several types of advanced drug delivery systems are currently being developed [26, 45].

The present study shows that berberine encapsulated in a liquid crystalline nanoparticle formulation attenuates some of the TGF- β -induced remodelling features in BEAS-2B human bronchial epithelial cells. In particular, treatment of TGF- β -induced BEAS-2B cells with BM-LCNs significantly reduced the cells' increased motility up to 48 h of treatment, as assessed through wound healing assay, resulting in an extent of migration that was comparable to that observed in the untreated group. This is in accordance with previous reports showing, in different cell systems, that berberine is capable of inhibiting cell migration [51, 73].

The protein array experiment revealed fundamental mechanistic insights about the pathways impacted by berberine in counteracting TGF- β action. Endoglin is a known interactor of TGF- β receptors I and II. It is an auxiliary component of the TGF- β signalling machinery capable of modulating the downstream signalling [39]. Among its different functions, endoglin is known to regulate actin cytoskeletal organization in endothelial cells, and this could contribute to the increased angiogenesis observed in tissue remodelling [75]. The present study is the first to report that berberine treatment results in the downregulation of endoglin levels, restoring them

to levels compared to untreated cells. Other factors activated upon TGF- β signalling and contributing to various aspects of tissue remodelling, including angiogenesis, are thrombospondin-1, VEGF, and bFGF. In this study, treatment with BM-LCNs reduced the expression of these proteins to levels comparable to the untreated group. Besides being among the main activator factors of latent TGF- β , thrombospondin-1 is involved in physiological tissue repair and pathologic fibrosis in TGF- β -dependent and independent pathways [76]. The present study is the first to report that berberine inhibits the expression of thrombospondin-1.

With regards to VEGF and bFGF, these two cytokines are known to mediate TGF- β -induced remodelling and angiogenesis in various diseases, including asthma and COPD [36-38]. Furthermore, these two cytokines are considered among the most important inductors of angiogenesis in cancers such as NSCLC [77]. The finding that BM-LCNs counteract the TGF- β -induced upregulation of these proteins are in accordance with reports showing that berberine (i) suppresses the expression of bFGF in breast cancer cells, and (ii) downregulates the expression of VEGF in hepatocellular carcinoma cells, concomitantly inhibiting their angiogenic potential [78].

Myeloperoxidase is mainly produced by neutrophils and other body cells [79], and it plays a pivotal role in airway inflammation and tissue remodelling in diseases such as COPD [38]. In the present study, berberine significantly counteracted the TGF- β -induced increase in myeloperoxidase expression in BEAS-2B cells. This is in accordance with a study where berberine was shown to alleviate dextran sulfate sodium (DSS)-induced colitis in mice through the reduction of inflammation and oxidative stress, which was exerted via mechanisms including the downregulation of myeloperoxidase levels [80].

Treatment of BEAS-2B cells with TGF- β further resulted in the downregulation of Cystatin C protein expression. This is a negative regulator of TGF- β signalling [40]. Administration of Cystatin C, in particular, has been shown to have preclinical efficacy against the oncogenic activity of TGF- β in an *in vivo* model of breast cancer [81]. In the present study, BM-LCNs partially restored the TGF- β -induced downregulation of the expression of Cystatin C, further highlighting the potent activity of BM-LCNs in inhibiting TGF- β signalling.

Nitric oxide (NO) plays a fundamental role in preserving the epithelial phenotype of lung epithelial cells by preventing EMT [41]. In this context, one of the mechanisms by which TGF- β induces EMT is the reduction of endogenous NO production via the downregulation and inhibition of eNOS [41], sGC, and PKGI [42]. In the present study, treatment of TGF- β -

induced BEAS-2B cells with BM-LCNs significantly counteracted the effect of TGF- β , restoring the baseline NO production to levels comparable to the untreated group. An increased NO production induced by berberine was shown in a study by Wang et al (2009), in which treatment of high-fat-diet and streptozotocin-induced diabetic rats with berberine resulted in increased eNOS expression and, concomitantly, higher NO levels [82]. Interestingly, in a previous report, treatment of lipopolysaccharide (LPS)-stimulated RAW264.7 mouse macrophages with a similar berberine-LCN formulation resulted in a significant reduction of the elevated NO levels induced by LPS, which was exerted through the downregulation of the expression of the inducible NO synthase (iNOS) [48]. This shows proof of the multifaceted, context-dependent biological activity of berberine, that promotes physiological levels of NO and a generally healthy cell phenotype through its potent anti-inflammatory, antioxidant, and anti-fibrotic properties. The findings reported in this study are summarized in the Graphical Abstract of the present manuscript.

An important advantage of the present study is that BM-LCNs significantly counteracted TGF- β -induced remodelling features at an equivalent berberine concentration of 0.5 μ M. This concentration is substantially lower (10- to 600-fold) compared to the average concentration range of free berberine powder that was shown to be active in counteracting TGF- β -induced features in previous reports (5-300 μ M) [69-74]. Although these mentioned studies were performed on different cell lines and with different experimental setups, this strong discrepancy in active berberine concentration reflects the fact that nanoparticle-based drug delivery systems such as LCNs allow improved delivery of the therapeutic cargo, with resulting lower doses necessary to achieve a significant therapeutic effect. This is in agreement with previous reports from our research team showing that encapsulating phytochemicals in LCNs or other nanoparticle-based delivery systems resulted in potent activity at lower concentrations than the free molecule [47, 48, 83-85].

Despite the promising activity of BM-LCNs in counteracting TGF- β -induced remodelling features, the present study is not exempt from limitations. The main limitation is that these study findings are reported only on TGF- β -induced BEAS-2B bronchial epithelial cells, which represent a rather simplistic *in vitro* model of airway remodelling that does not account for the totality of the cellular and molecular mechanisms involved. Despite the fact that epithelial cell proliferation is one of the key factors driving airway remodelling [22], and that TGF- β signalling plays a central role in this process [86], the lung, like any other organ, is composed of different cell types that, together, orchestrate its function in health and disease. Airway

remodelling itself is an extremely complex process, which involves several other cell types as well as other pro-fibrotic factors that work in synergism with TGF- β [87]. Similar studies performed on other cell types, such as alveolar epithelial cells, endothelial cells, and macrophages, would provide a more complete picture of the true potential of BM-LCNs in counteracting TGF- β -mediated aberrant airway remodelling. In this context, the use of *in vitro* models consisting of the co-culture of different cell lines [87, 88], especially in conjunction with microfluidic [89] and “airway-on-a-chip” devices [90], would provide a more accurate and detailed depiction of the airway remodelling process. Furthermore, to allow the translation of these *in vitro* results to the clinic, BM-LCNs should be tested on suitable animal models of asthma, COPD, and pulmonary fibrosis.

5. Conclusions

This study highlights the potent activity of BM-LCNs in counteracting TGF- β -induced remodelling features in human bronchial epithelial cells. This activity is exerted through the inhibition of TGF- β -induced cell migration, by regulating the expression of several cytokines and mediators dysregulated by treatment with TGF- β , and by restoring physiological baseline NO levels. The findings reported in this manuscript provide further proof of the multifaceted applicability of BM-LCNs as a potential therapy for CRDs where aberrant tissue remodelling plays a pivotal role. However, in order to achieve clinical translation, the results of this finding must be further confirmed and validated by investigating the effect of BM-LCNs on more complex *in vitro* systems, as well as on *in vivo* models of CRDs.

6. Funding

The authors are thankful to the Graduate School of Health, University of Technology Sydney, Australia. KD is supported by a project grant from the Rebecca L Cooper Medical Research Foundation and the Maridulu Budyari Gumal Sydney Partnership for Health, Education, Research and Enterprise (SPHERE) RSEOH CAG Seed grant, fellowship and extension grant; Faculty of Health MCR/ECR Mentorship Support Grant and UTS Global Strategic Partnerships Seed Funding Scheme. The authors would also like to thank Uttaranchal University for their seed grant. GDR is supported by the UTS International Research Scholarship, the UTS President’s Scholarship, and by the Triple I Clinical Academic Group (CAG) Secondment / Exchange Program grant. KRP is supported by a fellowship from Prevent Cancer Foundation (PCF) and the International Association for the Study of Lung Cancer

(IASLC). GL is supported by CREATE Hope Scientific Fellowship from Lung Foundation Australia

7. Data Availability Statement

The data presented in this study are available on request from the corresponding authors.

8. Conflict of Interest

The authors have no conflict of interest to declare.

References

1. Labaki, W.W. and M.K. Han, *Chronic respiratory diseases: a global view*. *Lancet Respir Med*, 2020. **8**(6): p. 531-533.
2. Tan, C.L., et al., *Unravelling the molecular mechanisms underlying chronic respiratory diseases for the development of novel therapeutics via in vitro experimental models*. *Eur J Pharmacol*, 2022. **919**: p. 174821.
3. Prasher, P., et al., *Advances and applications of dextran-based nanomaterials targeting inflammatory respiratory diseases*. *Journal of Drug Delivery Science and Technology*, 2022: p. 103598.
4. Bratova, M., et al., *Non-small Cell Lung Cancer as a Chronic Disease - A Prospective Study from the Czech TULUNG Registry*. *In Vivo*, 2020. **34**(1): p. 369-379.
5. Dua, K., et al., *Increasing complexity and interactions of oxidative stress in chronic respiratory diseases: An emerging need for novel drug delivery systems*. *Chemico-Biological Interactions*, 2019. **299**: p. 168-178.
6. Lugg, S.T., et al., *Cigarette smoke exposure and alveolar macrophages: mechanisms for lung disease*. *Thorax*, 2022. **77**(1): p. 94-101.
7. Kc, B.B., et al., *Prevalence and Factors Associated with Tobacco Use among High School Students*. *J Nepal Health Res Counc*, 2022. **20**(2): p. 310-315.
8. Viegi, G., et al., *Global Burden of Chronic Respiratory Diseases*. *J Aerosol Med Pulm Drug Deliv*, 2020. **33**(4): p. 171-177.
9. Safiri, S., et al., *Burden of chronic obstructive pulmonary disease and its attributable risk factors in 204 countries and territories, 1990-2019: results from the Global Burden of Disease Study 2019*. *Bmj*, 2022. **378**: p. e069679.

10. Sung, H., et al., *Global Cancer Statistics 2020: GLOBOCAN Estimates of Incidence and Mortality Worldwide for 36 Cancers in 185 Countries*. CA Cancer J Clin, 2021. **71**(3): p. 209-249.
11. Martinez, F.J., et al., *Idiopathic pulmonary fibrosis*. Nat Rev Dis Primers, 2017. **3**: p. 17074.
12. Porsbjerg, C., et al., *Asthma*. Lancet, 2023.
13. Riley, C.M. and F.C. Sciurba, *Diagnosis and Outpatient Management of Chronic Obstructive Pulmonary Disease: A Review*. Jama, 2019. **321**(8): p. 786-797.
14. Celli, B.R., et al., *Effect of pharmacotherapy on rate of decline of lung function in chronic obstructive pulmonary disease: results from the TORCH study*. Am J Respir Crit Care Med, 2008. **178**(4): p. 332-8.
15. Leuppi, J.D., et al., *Short-term vs conventional glucocorticoid therapy in acute exacerbations of chronic obstructive pulmonary disease: the REDUCE randomized clinical trial*. Jama, 2013. **309**(21): p. 2223-31.
16. Kumbhar, P., et al., *Inhalation delivery of repurposed drugs for lung cancer: Approaches, benefits and challenges*. J Control Release, 2022. **341**: p. 1-15.
17. Yazbeck, V., et al., *An overview of chemotoxicity and radiation toxicity in cancer therapy*. Adv Cancer Res, 2022. **155**: p. 1-27.
18. Li, C., Y. Qiu, and Y. Zhang, *Research Progress on Therapeutic Targeting of Cancer-Associated Fibroblasts to Tackle Treatment-Resistant NSCLC*. Pharmaceuticals (Basel), 2022. **15**(11).
19. Grzela, K., et al., *Airway Remodeling in Chronic Obstructive Pulmonary Disease and Asthma: the Role of Matrix Metalloproteinase-9*. Arch Immunol Ther Exp (Warsz), 2016. **64**(1): p. 47-55.
20. Dhanjal, D.S., et al., *Concepts of advanced therapeutic delivery systems for the management of remodeling and inflammation in airway diseases*. Future Med Chem, 2022. **14**(4): p. 271-288.
21. Mehta, M., et al., *Incipient need of targeting airway remodeling using advanced drug delivery in chronic respiratory diseases*. Future Med Chem, 2020. **12**(10): p. 873-875.
22. Liu, G., et al., *Therapeutic targets in lung tissue remodelling and fibrosis*. Pharmacol Ther, 2021. **225**: p. 107839.
23. Doerner, A.M. and B.L. Zuraw, *TGF- β 1 induced epithelial to mesenchymal transition (EMT) in human bronchial epithelial cells is enhanced by IL-1 β but not abrogated by corticosteroids*. Respiratory Research, 2009. **10**(1): p. 100.

24. Iwano, M., et al., *Evidence that fibroblasts derive from epithelium during tissue fibrosis*. J Clin Invest, 2002. **110**(3): p. 341-50.
25. Pain, M., et al., *Tissue remodelling in chronic bronchial diseases: from the epithelial to mesenchymal phenotype*. Eur Respir Rev, 2014. **23**(131): p. 118-30.
26. Gupta, G., et al., *Advanced drug delivery approaches in managing TGF- β -mediated remodeling in lung diseases*. Nanomedicine (Lond), 2021. **16**(25): p. 2243-2247.
27. Aschner, Y. and G.P. Downey, *Transforming Growth Factor- β : Master Regulator of the Respiratory System in Health and Disease*. Am J Respir Cell Mol Biol, 2016. **54**(5): p. 647-55.
28. Massagué, J., *TGFbeta in Cancer*. Cell, 2008. **134**(2): p. 215-30.
29. Huang, T., S.L. Schor, and A.P. Hinck, *Biological activity differences between TGF- β 1 and TGF- β 3 correlate with differences in the rigidity and arrangement of their component monomers*. Biochemistry, 2014. **53**(36): p. 5737-49.
30. Liu, G., et al., *Fibulin-1c regulates transforming growth factor- β activation in pulmonary tissue fibrosis*. JCI Insight, 2019. **5**(16).
31. Crawford, S.E., et al., *Thrombospondin-1 is a major activator of TGF-beta1 in vivo*. Cell, 1998. **93**(7): p. 1159-70.
32. Yu, Q. and I. Stamenkovic, *Cell surface-localized matrix metalloproteinase-9 proteolytically activates TGF-beta and promotes tumor invasion and angiogenesis*. Genes Dev, 2000. **14**(2): p. 163-76.
33. Huse, M., et al., *The TGF beta receptor activation process: an inhibitor- to substrate-binding switch*. Mol Cell, 2001. **8**(3): p. 671-82.
34. Lee, C.G., et al., *Vascular endothelial growth factor (VEGF) induces remodeling and enhances TH2-mediated sensitization and inflammation in the lung*. Nat Med, 2004. **10**(10): p. 1095-103.
35. Shin, J.H., et al., *TGF-beta effects on airway smooth muscle cell proliferation, VEGF release and signal transduction pathways*. Respirology, 2009. **14**(3): p. 347-53.
36. Yum, H.Y., et al., *Allergen-induced coexpression of bFGF and TGF- β 1 by macrophages in a mouse model of airway remodeling: bFGF induces macrophage TGF- β 1 expression in vitro*. Int Arch Allergy Immunol, 2011. **155**(1): p. 12-22.
37. Zanini, A., et al., *The role of the bronchial microvasculature in the airway remodelling in asthma and COPD*. Respir Res, 2010. **11**(1): p. 132.
38. Wang, Y., et al., *Role of inflammatory cells in airway remodeling in COPD*. Int J Chron Obstruct Pulmon Dis, 2018. **13**: p. 3341-3348.

39. Guerrero-Esteo, M., et al., *Extracellular and cytoplasmic domains of endoglin interact with the transforming growth factor-beta receptors I and II*. J Biol Chem, 2002. **277**(32): p. 29197-209.
40. Sokol, J.P. and W.P. Schiemann, *Cystatin C antagonizes transforming growth factor beta signaling in normal and cancer cells*. Mol Cancer Res, 2004. **2**(3): p. 183-95.
41. Vyas-Read, S., et al., *Nitric oxide attenuates epithelial-mesenchymal transition in alveolar epithelial cells*. Am J Physiol Lung Cell Mol Physiol, 2007. **293**(1): p. L212-21.
42. Bachiller, P.R., H. Nakanishi, and J.D. Roberts, Jr., *Transforming growth factor-beta modulates the expression of nitric oxide signaling enzymes in the injured developing lung and in vascular smooth muscle cells*. Am J Physiol Lung Cell Mol Physiol, 2010. **298**(3): p. L324-34.
43. Saito, A., M. Horie, and T. Nagase, *TGF- β Signaling in Lung Health and Disease*. International Journal of Molecular Sciences, 2018. **19**(8): p. 2460.
44. Takizawa, H., et al., *Increased expression of transforming growth factor-beta1 in small airway epithelium from tobacco smokers and patients with chronic obstructive pulmonary disease (COPD)*. Am J Respir Crit Care Med, 2001. **163**(6): p. 1476-83.
45. Paudel, K.R., et al., *Nanomedicine and medicinal plants: Emerging symbiosis in managing lung diseases and associated infections*. Excli j, 2022. **21**: p. 1299-1303.
46. Kuo, C.L., C.W. Chi, and T.Y. Liu, *The anti-inflammatory potential of berberine in vitro and in vivo*. Cancer Lett, 2004. **203**(2): p. 127-37.
47. Paudel, K.R., et al., *Attenuation of Cigarette-Smoke-Induced Oxidative Stress, Senescence, and Inflammation by Berberine-Loaded Liquid Crystalline Nanoparticles: In Vitro Study in 16HBE and RAW264.7 Cells*. Antioxidants (Basel), 2022. **11**(5).
48. Alnuqaydan, A.M., et al., *Phytantriol-Based Berberine-Loaded Liquid Crystalline Nanoparticles Attenuate Inflammation and Oxidative Stress in Lipopolysaccharide-Induced RAW264.7 Macrophages*. Nanomaterials (Basel), 2022. **12**(23).
49. Alnuqaydan, A.M., et al., *Evaluation of the Cytotoxic Activity and Anti-Migratory Effect of Berberine-Phytantriol Liquid Crystalline Nanoparticle Formulation on Non-Small-Cell Lung Cancer In Vitro*. Pharmaceutics, 2022. **14**(6).
50. Mehta, M., et al., *Berberine loaded liquid crystalline nanostructure inhibits cancer progression in adenocarcinomic human alveolar basal epithelial cells in vitro*. J Food Biochem, 2021. **45**(11): p. e13954.

51. Paudel, K.R., et al., *Berberine-loaded liquid crystalline nanoparticles inhibit non-small cell lung cancer proliferation and migration in vitro*. *Environ Sci Pollut Res Int*, 2022. **29**(31): p. 46830-46847.
52. DiNicolantonio, J.J., et al., *A nutraceutical strategy for downregulating TGF β signalling: prospects for prevention of fibrotic disorders, including post-COVID-19 pulmonary fibrosis*. *Open Heart*, 2021. **8**(1).
53. Chitra, P., et al., *Berberine attenuates bleomycin induced pulmonary toxicity and fibrosis via suppressing NF- κ B dependant TGF- β activation: a biphasic experimental study*. *Toxicol Lett*, 2013. **219**(2): p. 178-93.
54. Qi, H.W., et al., *Epithelial-to-mesenchymal transition markers to predict response of Berberine in suppressing lung cancer invasion and metastasis*. *J Transl Med*, 2014. **12**: p. 22.
55. Yin, J., H. Xing, and J. Ye, *Efficacy of berberine in patients with type 2 diabetes mellitus*. *Metabolism*, 2008. **57**(5): p. 712-7.
56. Tsai, P.L. and T.H. Tsai, *Hepatobiliary excretion of berberine*. *Drug Metab Dispos*, 2004. **32**(4): p. 405-12.
57. Paudel, K.R., et al., *Advanced therapeutic delivery for the management of chronic respiratory diseases*. 2022, Frontiers Media SA. p. 983583.
58. Khursheed, R., et al., *Expanding the arsenal against pulmonary diseases using surface-functionalized polymeric micelles: breakthroughs and bottlenecks*. *Nanomedicine (Lond)*, 2022.
59. Devkota, H.P., et al., *Phytochemicals and their Nanoformulations Targeted for Pulmonary Diseases*, in *Advanced Drug Delivery Strategies for Targeting Chronic Inflammatory Lung Diseases*. 2022, Springer. p. 95-106.
60. Clarence, D.D., et al., *Unravelling the Therapeutic Potential of Nano-Delivered Functional Foods in Chronic Respiratory Diseases*. *Nutrients*, 2022. **14**(18).
61. Chan, Y., et al., *Versatility of liquid crystalline nanoparticles in inflammatory lung diseases*. *Nanomedicine (Lond)*, 2021. **16**(18): p. 1545-1548.
62. Paudel, K.R., et al., *Advancements in nanotherapeutics targeting senescence in chronic obstructive pulmonary disease*. *Nanomedicine (Lond)*, 2022.
63. Malyla, V., et al., *Recent advances in experimental animal models of lung cancer*. *Future Med Chem*, 2020. **12**(7): p. 567-570.
64. Nucera, F., et al., *Role of oxidative stress in the pathogenesis of COPD*. *Minerva Med*, 2022.

65. Nucera, F., et al., *Chapter 14 - Role of autoimmunity in the pathogenesis of chronic obstructive pulmonary disease and pulmonary emphysema*, in *Translational Autoimmunity*, N. Rezaei, Editor. 2022, Academic Press. p. 311-331.
66. Wang, M.Y., et al., *Current therapeutic strategies for respiratory diseases using mesenchymal stem cells*. *MedComm* (2020), 2021. **2**(3): p. 351-380.
67. Prasher, P., et al., *Targeting mucus barrier in respiratory diseases by chemically modified advanced delivery systems*. *Chemico-Biological Interactions*, 2022: p. 110048.
68. Walton, K.L., K.E. Johnson, and C.A. Harrison, *Targeting TGF- β Mediated SMAD Signaling for the Prevention of Fibrosis*. *Front Pharmacol*, 2017. **8**: p. 461.
69. Huang, C., et al., *Berberine inhibits epithelial-mesenchymal transition and promotes apoptosis of tumour-associated fibroblast-induced colonic epithelial cells through regulation of TGF- β signalling*. *Journal of Cell Communication and Signaling*, 2020. **14**(1): p. 53-66.
70. Du, H., et al., *Berberine Suppresses EMT in Liver and Gastric Carcinoma Cells through Combination with TGF β R Regulating TGF- β /Smad Pathway*. *Oxid Med Cell Longev*, 2021. **2021**: p. 2337818.
71. Kim, S., et al., *Berberine Suppresses Cell Motility Through Downregulation of TGF- β 1 in Triple Negative Breast Cancer Cells*. *Cell Physiol Biochem*, 2018. **45**(2): p. 795-807.
72. Chu, S.C., et al., *Berberine reverses epithelial-to-mesenchymal transition and inhibits metastasis and tumor-induced angiogenesis in human cervical cancer cells*. *Mol Pharmacol*, 2014. **86**(6): p. 609-23.
73. Jin, Y., et al., *Berberine Suppressed the Progression of Human Glioma Cells by Inhibiting the TGF- β 1/SMAD2/3 Signaling Pathway*. *Integr Cancer Ther*, 2022. **21**: p. 15347354221130303.
74. Sun, Y., et al., *Berberine inhibits glioma cell migration and invasion by suppressing TGF- β 1/COL11A1 pathway*. *Biochem Biophys Res Commun*, 2022. **625**: p. 38-45.
75. Sanz-Rodriguez, F., et al., *Endoglin regulates cytoskeletal organization through binding to ZRP-1, a member of the Lim family of proteins*. *J Biol Chem*, 2004. **279**(31): p. 32858-68.
76. Sweetwyne, M.T. and J.E. Murphy-Ullrich, *Thrombospondin1 in tissue repair and fibrosis: TGF- β -dependent and independent mechanisms*. *Matrix Biol*, 2012. **31**(3): p. 178-86.

77. Bremnes, R.M., C. Camps, and R. Sirera, *Angiogenesis in non-small cell lung cancer: The prognostic impact of neoangiogenesis and the cytokines VEGF and bFGF in tumours and blood*. Lung Cancer, 2006. **51**(2): p. 143-158.
78. Jie, S., et al., *Berberine inhibits angiogenic potential of Hep G2 cell line through VEGF down-regulation in vitro*. J Gastroenterol Hepatol, 2011. **26**(1): p. 179-85.
79. Khan, A.A., M.A. Alsahli, and A.H. Rahmani, *Myeloperoxidase as an Active Disease Biomarker: Recent Biochemical and Pathological Perspectives*. Med Sci (Basel), 2018. **6**(2).
80. Zhang, L.C., et al., *Berberine alleviates dextran sodium sulfate-induced colitis by improving intestinal barrier function and reducing inflammation and oxidative stress*. Exp Ther Med, 2017. **13**(6): p. 3374-3382.
81. Tian, M. and W.P. Schiemann, *Preclinical efficacy of cystatin C to target the oncogenic activity of transforming growth factor Beta in breast cancer*. Transl Oncol, 2009. **2**(3): p. 174-83.
82. Wang, C., et al., *Ameliorative effect of berberine on endothelial dysfunction in diabetic rats induced by high-fat diet and streptozotocin*. Eur J Pharmacol, 2009. **620**(1-3): p. 131-7.
83. Paudel, K.R., et al., *Rutin loaded liquid crystalline nanoparticles inhibit lipopolysaccharide induced oxidative stress and apoptosis in bronchial epithelial cells in vitro*. Toxicol In Vitro, 2020. **68**: p. 104961.
84. Chang, H.L., et al., *Naringenin inhibits migration of lung cancer cells via the inhibition of matrix metalloproteinases-2 and -9*. Exp Ther Med, 2017. **13**(2): p. 739-744.
85. Solanki, N., et al., *Antiproliferative effects of boswellic acid-loaded chitosan nanoparticles on human lung cancer cell line A549*. Future Med Chem, 2020. **12**(22): p. 2019-2034.
86. Halwani, R., et al., *Role of transforming growth factor- β in airway remodeling in asthma*. Am J Respir Cell Mol Biol, 2011. **44**(2): p. 127-33.
87. Zhang, S., et al., *Growth factors secreted by bronchial epithelial cells control myofibroblast proliferation: an in vitro co-culture model of airway remodeling in asthma*. Lab Invest, 1999. **79**(4): p. 395-405.
88. Osei, E.T., S. Booth, and T.L. Hackett, *What Have In Vitro Co-Culture Models Taught Us about the Contribution of Epithelial-Mesenchymal Interactions to Airway Inflammation and Remodeling in Asthma?* Cells, 2020. **9**(7).

89. Zeng, Y., et al., *An open microfluidic coculture model of fibroblasts and eosinophils to investigate mechanisms of airway inflammation*. Front Bioeng Biotechnol, 2022. **10**: p. 993872.
90. Bennet, T.J., et al., *Airway-On-A-Chip: Designs and Applications for Lung Repair and Disease*. Cells, 2021. **10**(7).

CHAPTER 5

Discussion, Conclusions, and Future Directions

General Discussion, Conclusions and Future Directions

Chronic Respiratory Diseases (CRDs) include a heterogeneous group of airway diseases such as chronic obstructive pulmonary disease (COPD), asthma, lung cancer (LC), pulmonary fibrosis, and others [1, 2]. Collectively, CRDs constitute one of the main causes of morbidity and mortality worldwide, representing an enormous global healthcare and economic burden [3]. According to recent Global Burden of Diseases Study (GBD) reports, in 2019, 3.3 million deaths were attributed to COPD [4]. In 2020, according to the Global Cancer Observatory (GLOBOCAN) study, LC was responsible for more than 1.7 million deaths globally [5]. In Australia, COPD was the fifth leading cause of death between 2018 and 2020, with about 6300 to 7000 yearly deaths recorded in this period of time [6, 7]. Importantly, the incidence of COPD is higher in Aboriginal Australian populations compared to non-Aboriginal Australian populations [8]. LC is the main cause of cancer-related deaths, and the fifth most commonly diagnosed cancer in Australia, where it caused nearly 8500 deaths in 2020 [9]. CRDs represent a particularly relevant topic in light of the recent COVID-19 pandemic, as the susceptibility to severe acute respiratory syndrome coronavirus 2 (SARS-CoV-2) infection and the resulting disease severity are increased in COPD patients [10, 11] and LC patients [12], and SARS-CoV-2 infection may exacerbate LC [13] and COPD symptoms and outcomes [10, 14].

The prevalent risk factor for the development of CRDs is chronic exposure to tobacco smoke which, due to the thousands of toxic chemicals it contains, severely damages the airways and lung parenchyma causing chronic inflammation, oxidative stress, tissue damage, fibrosis, and airway remodelling [15, 16]. Other important risk factors for CRDs include occupational risks, environmental pollution, and the presence of ambient particulate matter [1, 17].

Despite the high incidence and mortality of CRDs, these ailments are still virtually incurable and, in the case of diseases such as COPD, the main pharmacological treatment strategies available are aimed at improving the symptoms rather than tackling the underlying causes of these diseases [18, 19]. These treatments mainly include the use of short- and long-acting bronchodilators to improve the airflow, and of inhaled corticosteroids (ICS) to counteract the inflammation [19, 20]. A major drawback of these classes of drugs is the occurrence of several adverse effects, including anxiety, insomnia, and tachycardia for bronchodilators [21], and hyperglycemia, hypertension, and osteoporosis for ICS [22]. Furthermore, the long-term use of ICS can lead to steroid insensitivity, further reducing the treatment options available [23].

With regards to LC, chemotherapy often represents the first line of therapy, with many drugs approved including doxorubicin, carboplatin, and docetaxel, which give rise to severe adverse effects [24]. Despite the availability of many treatment options, LC still represents one of the deadliest types of cancer, with a five-year survival rate lower than 20% that is also attributable to the lack of early diagnostic tools [25]. This underlines the urgent necessity for innovative pharmacological treatment strategies against CRDs.

In the context of developing novel pharmacological options to treat CRDs, an advantageous strategy would involve the development of drugs that act on one or more of the main pathophysiological features shared among different CRDs. These include chronic inflammation, oxidative stress, and airway remodelling. Chronic inflammation consists in the aberrant, prolonged activation of the immune response that is caused by the failure of acute healthy inflammation to remove a damaging stimulus, which in the case of lung diseases is represented, for example, by the many toxic carcinogens contained in cigarette smoke, which is one of the main leading cause for COPD and LC [26]. When all the above-mentioned biological events occur, an imbalance between pro-and anti-inflammatory cytokines is reached, and this causes further tissue damage, cell death, oxidative stress, and airway remodelling [26].

Oxidative stress, consisting in the dysregulation of the homeostasis between processes that produce reactive oxygen species (ROS) and processes that eliminate them, represents one of the main hallmarks of CRDs [27]. Oxidative stress and inflammation are deeply interrelated processes that reinforce each other in a positive feedback mechanism [27, 28], causing further tissue damage. In the lung, the continuous exposure to damaging stimuli, inflammation, and oxidative stress causes airway remodelling, consisting in a series of structural transformations that lead to the progressive deterioration of airways and lung parenchyma [29]. These include subepithelial fibrosis, immune infiltration, angiogenesis, epithelial disruption, thickening of the basement membrane, and enhanced extracellular matrix deposition [29, 30]. At the cellular level, epithelial cells undergo epithelial-to-mesenchymal transition (EMT) and acquire increased capacity to proliferate, migrate, and invade surrounding tissues [31, 32], all processes that recapitulate cancerous transformation and may at least partly explain the increased susceptibility to develop LC observed in COPD patients compared to healthy individuals [33]. The main regulator and orchestrator of remodelling processes is transforming growth factor- β (TGF- β), which is overexpressed in virtually all CRDs, including LC [34].

Among several potential novel treatment options targeting one or more of the aforementioned pathophysiological processes occurring in CRDs, two classes of therapeutics are particularly promising: phytoceuticals, or plant-derived molecules, and nucleic acid-based therapeutics such as oligodeoxynucleotides and interfering RNAs. Phytoceuticals include pure active constituents extracted from plant tissues such as berberine, zerumbone, rutin etc [35], as well as complex mixtures, extracts, and essential oils such as agarwood oil [36]. Several phytoceuticals have been used for centuries in different traditional medicine systems, and many are renowned for their potent anti-inflammatory, anti-oxidant, anti-cancer, and anti-fibrotic properties [35-39]. However, the clinical use of these moieties is hampered by common issues such as poor aqueous solubility and/or poor permeability, which result in low bioavailability and poor pharmacokinetic properties [40, 41]. This translates into the necessity to administer excessive doses to achieve therapeutic efficacy, which is often associated with toxicity and adverse effects [42, 43].

Nucleic acid-based therapies include a heterogeneous class of novel therapeutics whose main aim is to target molecular pathways that are dysregulated in diseases, at the transcriptional or post-transcriptional level [44]. These include oligonucleotides acting as miRNA mimics or inhibitors, antisense oligonucleotides (ASOs), short interfering RNAs (siRNAs), decoy oligodeoxynucleotides (ODNs), and others [44]. These classes of drugs are particularly novel, and five oligonucleotide-based products have been approved by the FDA in the last three years [45-47]. Among nucleic acid-based therapies, decoy ODNs are unique as they allow to selectively target transcription factor by mimicking its DNA-binding sequence [48]. In LC, decoy ODNs may be used to block transcription factors acting as master regulators of cancer progression. Two of such master transcription factors are Nuclear Factor- κ B (NF- κ B) and signal transducer and activator of transcription 3 (STAT3) [49, 50]. Despite the promising activity, the clinical translation of nucleic acid-based therapies is an obstacle due to the large poor pharmacokinetic characteristics of these molecules [51, 52], which are particularly manifest when free nucleic acids are administered. These suboptimal pharmacokinetic properties stem from the physicochemical properties of ODNs, which are molecules characterized by large size, high negative charge density, and susceptibility to nuclease degradation at the level of the sugar-phosphate backbone [52]. In the biological environment, the large size and charge density result in poor absorption of the ODNs, whereas the high susceptibility to nuclease digestion results in the rapid, excessive degradation of ODNs upon administration. [51, 53] This further translates into a poor pharmacokinetic profile.

A suitable strategy to overcome the pharmacokinetic issues associated to phytochemicals and nucleic acid-based therapies, with potential to boost the translation of these powerful therapeutics into the clinic, consists in encapsulating these therapeutic moieties within advanced, nanoparticle-based, drug delivery systems [54-57]. These systems allow to improve the solubility and permeability of difficult-to-deliver molecules, simultaneously increasing their stability, and allowing to selectively target the cargo release in the proximity of the cells or tissues of interest, thereby minimising the occurrence and severity of off-target effect [57]. Several nano-formulations are also compatible with inhalational delivery, therefore intrinsically suitable for CRDs [58, 59]. The enormous impact and relevance of the different types of advanced drug delivery systems that are currently being studied to facilitate the clinical application of phytochemicals and nucleic acid-based therapies in CRDs, with a focus on COPD and LC, has been extensively reviewed in the introductory chapter of the present thesis, Chapter 1.

In this context, the aim of the present thesis was to explore and test the efficacy and suitability of different types of drug delivery systems in enhancing the delivery of phytochemicals such as berberine and agarwood oil, and nucleic acid-based therapeutics such as NF- κ B decoy ODN, *in vitro*, using cell-based models of CRDs and CRD features including LC, COPD, and airway remodelling.

In Chapter 2, we encapsulated a decoy ODN inhibiting the transcription factor NF- κ B in acid-responsive, spermine-modified acetalated dextran (SpAcDex) nanoparticles (NPs) and tested the *in vitro* anticancer activity of this formulation on A549 human lung adenocarcinoma cells. NF- κ B is a transcription factor that plays a pivotal role in the regulation of many complex biological processes, most notably innate immunity [60]. In several types of cancer, including LC, the NF- κ B signalling pathway is considered a fundamental regulator of cancer hallmarks such as cell proliferation, dedifferentiation, metastasis, and drug resistance [49, 61, 62].

In LC, in particular, increased NF- κ B expression is considered a prognostic marker associated with worsening tumor stage, disease severity, and low survival rate [63]. This provides the rationale supporting the inhibition of NF- κ B as a potential anti-cancer strategy [62, 64, 65]. This can be achieved in many ways. Several small molecules are known to inhibit the NF- κ B signalling pathway at different levels, and these include phytochemicals such as zerumbone and synthetic molecules such as ibuprofen and hydroquinone [66]. Furthermore, RNA interference-based approaches have been attempted to inhibit NF- κ B [67-69].

Another promising strategy to inhibit the function of transcription factors such as NF- κ B is represented by the use of decoy ODNs [70]. In the context of respiratory diseases, NF- κ B-inhibiting decoy ODNs have been tested in several *in vitro* and *in vivo* models of airway inflammation, acute lung injury, cigarette smoke exposure, cystic fibrosis, and sepsis [51]. Despite promising, the clinical translation of NF- κ B decoy ODNs is limited by the poor pharmacokinetic properties of nucleic acid-based therapies [51, 53]. Another important factor limiting the use of NF- κ B-inhibiting strategies is the fact that NF- κ B plays several fundamental physiological functions, therefore the systemic administration of a drug inhibiting NF- κ B may be particularly prone to deleterious off-target effects [51].

To overcome these limitations, NP-based advanced drug delivery systems can be used to encapsulate NF- κ B decoy ODNs. An advantage of these NP-based systems is that, to minimize the occurrence of off-target effects, the NPs can be functionalised to specifically target the ODN to the intended target cells or tissues. Several types of NP-based formulations have been used to encapsulate NF- κ B decoy ODNs, and their efficacy has been mostly tested against *in vitro* or *in vivo* models of inflammatory processes. NPs were formulated with different materials, including for example poly(DL-lactic *co*-glycolic acid) (PLGA) [71, 72], gelatin [73], exosomes [74] and cationic liposomes [75]. De Rosa *et al.*, developed cationic liposomes to encapsulate NF- κ B decoy ODN, optimizing the formulation and +/- charge ratio to maximize the ODN loading, cellular uptake, and anti-inflammatory effect on LPS-stimulated RAW264.7 macrophages, obtaining limited cytotoxicity and strong inhibition of LPS-induced nitrite production and inducible nitric oxide synthase (iNOS) protein expression [76]. A few more studies reported the formulation of cationic liposomes encapsulating a NF- κ B decoy ODN. Wijagkanalan *et al.*, for example, used mannosylated cationic liposomes to target a NF- κ B decoy ODN to alveolar macrophages in an *in vivo* model of LPS-induced lung inflammation, obtaining significant reduction of the production of LPS-stimulated cytokines such as TNF- α and IL-1 β , and reduced neutrophil infiltration [77]. In this study, the formulation was instilled intratracheally *via* nebulization, highlighting the potential of NP-based formulations as systems to deliver nucleic acid-based therapeutics to the lung [77]. Due to their cationic nature, cationic liposomes are particularly suitable for the delivery of polyanions such as nucleic acids, however, the application of these systems is still limited by the problem of toxicity [78]. Furthermore, considering the ubiquitous role of NF- κ B in many physiological processes occurring throughout the body and in different cell types, there is the necessity for a drug

delivery system allowing a selective release of the NF- κ B decoy ODN only in proximity of cancer cells, in order to avoid adverse effects deriving from off-target delivery.

Two polymers are particularly suitable for the delivery of nucleic acids as therapeutic agents: PLGA, and acetalated dextran (AcDex). PLGA represents one of the most successful polymeric biomaterials to be used as a drug delivery system [79]. In an *in vivo* study by De Stefano *et al.*, PLGA-based NF- κ B ODN NPs have been delivered intratracheally to a rat model of LPS-induced lung inflammation, where they achieved a sustained ODN release, and concomitant inhibition of LPS-mediated inflammation markers, up to 72 h [80]. An advantage of PLGA is the possibility to be functionalised with acid-responsive moieties, allowing targeted cargo delivery to cancer cells [81]. However, a limitation of PLGA is the usually slow degradation rate, which cannot be extensively tuned [82].

A valid alternative to PLGA in this context is AcDex [83], a highly tunable, bio-compatible polymer of easy synthesis and with a wide range of applications [84]. Dextran is a non-toxic, bio-compatible and FDA-approved polysaccharide which can easily be chemically modified [83, 85-88]. Its functionalization with acetal functional groups (AcDex) results in the polymer's spontaneous disassembly, and payload release, at slightly acidic pH values such as those found in the tumor microenvironment [86, 89, 90], thus allowing selective tumor targeting. An advantage of AcDex NPs resides in the fact that their degradation rate can be finely regulated by controlling the reaction time during the polymer's synthesis, which is the main determinant of the ratio of cyclic vs acyclic acetals that ultimately determines the degradation rate [90]. Furthermore, AcDex systems represent a promising option for respiratory diseases due to their inherent compatibility with pulmonary delivery [88]. AcDex NPs were used by Wang and colleagues to encapsulate collagenase (Col-NPs) and deliver it *in vivo* to a mouse model of lung cancer [91]. Pretreatment of mice with Col-NPs, which showed no toxicity, achieved a significant 15% reduction of the tumor's collagen content, improving the intratumoral accumulation of subsequently administered Doxorubicin-loaded liposomes [91]. More recently, Gao and co-workers used AcDex as a starting point to assemble high affinity glycan ligand-decorated glyconanoparticles to be used as a vehicle for the development of next-generation protein-based vaccines against cancer and SARS-CoV-2 [92]. In this study, both vaccines elicited strong, specific, and sustained cytotoxic T lymphocytes (CTL) response and high immunoglobulin G (IgG) titers in mice against the respective antigens utilised, resulting in potent antitumor and anti-SARS-Cov-2 *in vivo* [92]. In a similar study, Gao *et al.*, also used oxidized AcDex NPs (OxAcDex-NPs) as delivery systems to immunize mice with human

mucin-1 (MUC-1), a cancer antigen, and a SARS-CoV-2 antigen, obtaining strong CTL-mediated immune responses [93].

Among the several types of moieties that can be used to functionalise AcDex NPs, modification with spermine – a cationic polyamine – is advantageous because it allows an enhanced uptake of polyanionic molecules such as ODNs through ionic electrostatic interactions and, simultaneously, an improved cellular uptake due to the presence of negative charges on cell membranes [94]. Cohen *et al.*, used the double emulsion method to develop a spermine-functionalized AcDex formulation (SpAcDex), and used it to successfully deliver a siRNA to HeLa cells [86]. In this study, SpAcDex achieved a transfection efficiency comparable to Lipofectamine 2000 [86], a commercially available cationic lipid that is commonly used *in vitro* for its high transfection efficiency, but whose clinical translation is hampered by toxicity [95]. The SpAcDex NPs have been recently used by Zheng *et al.*, to encapsulate and deliver an antisense miRNA-21 oligonucleotide to glioblastoma cells [96]. In this study, the NPs achieved very high oligonucleotide loading efficiency (>90%) and allowed to efficiently deliver the oligonucleotide cargo both *in vitro* and *in vivo* in an orthotopic glioblastoma mouse model, achieving significant inhibition of tumor growth and angiogenesis [96]. This confirms the potential of SpAcDex NPs as a biocompatible system for the enhanced delivery of nucleic acid-based therapeutics.

In the present study, we employed SpAcDex as the polymer of choice to encapsulate NF- κ B decoy ODNs. The obtained NPs resulted to be homogeneously distributed in terms of size, which ranged between 100 and 200 nm, and the ODN encapsulation efficiency was >99%. These SpAcDex NPs underwent spontaneous degradation and released the ODN at an acidic pH of 5.5 (Chapter 2, Figures 2 and 3). The size, encapsulation efficiency, and pH-dependent ODN release behaviour obtained are in agreement with those obtained by Cohen *et al.* [86] and by Zheng *et al.* [96]. The anticancer activity of these NPs was assessed on A549 human lung adenocarcinoma cells, where they showed significant anti-proliferative activity at 10 nM ODN concentration (Chapter 2, Figure 4). A further mechanistic investigation revealed that the upregulation of the transcription of the genes Receptor-interacting serine/threonine-protein kinase 1 (*RIPK1*), mixed lineage kinase domain-like (*MLKL*), Tumor Necrosis Factor- α (*TNF- α*), and *RIPK3*, all encoding for proteins that mediate necroptosis and that are downregulated by NF- κ B [97], was at least partly responsible for the anti-proliferative activity of our decoy ODN formulation (Chapter 2, Figure 5). This finding is in agreement with a report from Kumari *et al.*, showing that the inhibition of NF- κ B signalling in keratinocytes causes RIPK1-dependent

necroptosis [98]. The anti-migratory activity of the formulation was also tested *via* the wound-healing assay (Chapter 2, Figure 6) and with a modified version of the Boyden's chamber assay whereby the transwell chamber was coated with gelatin [99] (Chapter 2, Figure 7), obtaining a consistent anti-migratory effect across the two assays at the concentrations tested. The use of gelatin in the assay allows us to hypothesize that the inhibition of the migratory capacity of A549 cells could be caused by the inhibition of the matrix metalloproteinases (MMPs) MMP2 and MMP9, which are known to degrade gelatin and are upregulated by NF- κ B [100]. Finally, the SpAcDex NF- κ B decoy ODN NPs exerted anti-colony formation activity, as measured *via* crystal violet staining (Chapter 2, Figure 8).

In summary, in Chapter 2 of the present thesis we have demonstrated the strong anti-lung cancer potential of a NF- κ B decoy ODN encapsulated in pH-responsive SpAcDex NPs, which was exerted through the inhibition of three fundamental cancer hallmarks: proliferation, migration/invasion, and colony formation. This study provides proof to support the validity of the inhibition of NF- κ B signalling by using a decoy ODN as a potential therapeutic strategy to treat LC, simultaneously highlighting the enormous advantage of encapsulating nucleic acid-based therapies in cationic, biocompatible, pH-responsive NPs to improve their poor pharmacokinetic properties and to achieve tumor-targeted delivery of decoy ODN.

In Chapter 3, agarwood oil was formulated into a nanoemulsion (AW-NE), and the anti-inflammatory and anti-oxidant activity of this formulation was tested *in vitro* on cigarette smoke extract (CSE)-exposed human airway epithelial cells (BCi-NS1.1). Exposure to cigarette smoke is one of the main causes of COPD [101] due to the hundreds of toxic, pro-inflammatory, and pro-oxidant compounds it contains [102]. For this reason, the *in vitro* exposure of airway epithelial cells such as BCi-NS1.1 or 16HBE to CSE is widely used as a relatively simple system to model the molecular changes associated with inflammation, oxidative stress, carcinogenesis, and senescence caused by cigarette smoke [103]. Agarwood oil is renowned for containing several compounds embedded with strong anti-oxidant and anti-inflammatory activity [36, 37]. The main limitation associated with the use of Agarwood oil is its extremely poor water solubility, which in the present study has been improved by formulating agarwood oil into a nanoemulsion through probe sonication. To the best of our knowledge, we are the first to report the encapsulation of agarwood oil in a nanoemulsion, or in any other type of advanced drug delivery system, to improve its solubility.

The AW-NE obtained exerted significant anti-inflammatory and anti-oxidant activity, successfully counteracting many of the molecular features induced by CSE. The experimental design included a pre-treatment of the cells with AW-NE for 1 h followed by exposure to CSE for 24 h, therefore we investigated the efficacy of AW-NE in preventing CSE-induced inflammation and oxidative stress features. To assess the effect of AW-NE on CSE-induced cytokine protein expression, we used the Proteome Profiler Human XL Cytokine Array Kit (R&D Systems), which allows the simultaneous detection and relative quantitation of up to 105 human cytokines. We observed that exposure to CSE resulted in an increased expression of several pro-inflammatory cytokines, including the interleukins (IL) IL-1 α and IL-1 β , which play a central role in regulating immune and inflammatory responses [104], as well as Growth/Differentiation factor-15 (GDF15). This protein is a member of the TGF- β superfamily of growth factors, and its expression is increased in response to different types of cellular stress [105, 106]. Circulating GDF-15 levels are higher in COPD patients compared to healthy volunteers, making GDF-15 a potential biomarker of COPD [107]. Treatment with AW-NE significantly reversed the CSE-induced increased expression of these pro-inflammatory cytokines (Chapter 3, Figure 3). With regards to IL-1 α and IL-1 β , the finding that treatment with AW-NE reduces the expression of these two cytokines is concordant with previous studies. Yadav *et al.*, for example, reported that the topical application of agarwood oil reduced 12-O-tetradecanoylphorbol-13 acetate (TPA)-induced ear edema, in mice, through the reduction of many pro-inflammatory cytokines including IL-1 β [108], while Wang *et al.*, reported that the intraperitoneal administration of agarwood oil reduced the stress-induced production of cytokines such as IL-1 α in mice [109]. With regards to GDF-15, no previous report showed that the expression of this protein is impacted by agarwood oil.

On the other hand, CSE treatment resulted in the downregulation of the expression of several cytokines playing a generally protective, anti-inflammatory role. These include IL-10 [110], IL-18 binding protein (IL-18 BPa) [111], growth hormone (GH) [112], vitamin D binding protein (VDBP) [113], Relaxin-2 [114], interferon- γ (IFN- γ) [115], platelet-derived growth factor (PDGF-BB) [116], and trefoil factor-3 (TFF3) [117]. Treatment with AW-NE prevented this trend, resulting in a significant restoration of the expression of these cytokines to levels comparable to untreated cells (Chapter 3, Figure 4). The stimulation of IL-10 production is in agreement with two reports from Wang *et al.*, whereby agarwood extracts were found to increase IL-10 production in a mouse model of fluorouracil-induced intestinal injury [118] and in a mouse model of ethanol-induced gastric ulcer [119]. The present study is the first to report

that CSE downregulates the expression of PDGF-BB and Relaxin-2 in airway epithelial cells, and that agarwood oil induces the expression of GH, IL-18BP α , VDBP, Relaxin-2, IFN- γ , PDGF-BB, and TFF3.

At the gene expression level, CSE treatment resulted in an increased mRNA expression of the gene encoding for IL-8, which is one of the main pro-inflammatory cytokines expressed in COPD and a biomarker of COPD exacerbations [120]. The CSE-induced expression of IL-8 was previously reported by Ko *et al.*, in human primary bronchial epithelial cells (hPBECS) [121]. Treatment with AW-NE reduced the levels of IL-8 mRNA in a concentration-dependent way (Chapter 3, Figure 2). We are the first to show that agarwood oil suppresses IL-8 production. Furthermore, CSE exposure resulted in a reduced mRNA expression of two genes: glutamate-cysteine ligase catalytic subunit (*GCLC*), and Glutathione S-transferase Pi (*GSTP1*). *GCLC* and *GSTP1* are two fundamental proteins with anti-oxidant activity. *GCLC*, in particular, is an enzyme involved in the biosynthesis of glutathione, for which it catalyses the rate-limiting reaction step [122], while *GSTP1* is involved in cell detoxification from tobacco carcinogens through their conjugation with glutathione [123]. Treatment with AW-NE successfully restored the expression of these two antioxidant genes (Chapter 3, Figure 5). The agarwood-induced stimulation of *GSTP1* is concordant with a study from Wang *et al.*, where orally administered agarwood oil was shown to exert antioxidant activity in fluorouracil-induced intestinal injury, in mice, via several mechanisms, including increased levels of glutathione and increased expression of glutathione-S-transferase [118]. Finally, in our study, AW-NE restored the expression of the Phosphoinositide 3-kinase (*PI3K*) gene, which was downregulated by CSE exposure (Chapter 3, Figure 6). *PI3K* mediates a pro-survival signal, therefore its downregulation may represent one of the many mechanisms through which cigarette smoke causes cell death [124]. The fact that AW-NE restored *PI3K* expression supports its role in rescuing epithelial cells from CSE-induced cell death.

In summary, the study presented in Chapter 3 of this thesis demonstrates the potent *in vitro* efficacy of AW-NE in counteracting CSE-induced markers of inflammation and oxidative stress, confirming the enormous potential of agarwood oil as a treatment for chronic inflammatory diseases such as COPD and, simultaneously, highlighting the advantages of nanoemulsion-based formulations in improving the delivery of poorly water-soluble phytochemicals such as essential oils.

In Chapter 4, we tested a liquid crystalline nanoparticle (LCN)-based formulation encapsulating berberine (BM-LCNs) on TGF- β -stimulated BEAS-2B human bronchial epithelial cells. Considering the fundamental role played by TGF- β as a master regulator of tissue remodelling in CRDs [31], and the fact that this hormone is overexpressed across all CRDs [34], this system represents a suitable *in vitro* model that recapitulates the main molecular pathways and features of airway remodelling activated by TGF- β [32]. Berberine is an isoquinoline alkaloid extracted from turmeric and other plants which is renowned for its multifaceted anti-inflammatory, anti-oxidant, anti-cancer, and anti-fibrotic properties [57, 125, 126], exerted through various mechanisms including the suppression of some TGF- β -activated pathways [127]. However, berberine is characterised by poor pharmacokinetic properties stemming from issues such as low permeability and hepatobiliary excretion [128].

Among several suitable advanced drug delivery systems that could have been used to encapsulate berberine, we selected a monoolein-poloxamer 407-based LCN formulation [129]. Lyotropic LCNs are advanced drug delivery systems resulting from the spontaneous self-assembly of amphiphilic molecules, such as monoolein, phytantriol, and poloxamer, in aqueous environments, resulting in the concentration-dependent organization of lipids in different three-dimensional structures called mesophases [130]. As drug delivery systems, LCNs are advantageous because they allow superior drug loading, dissolution, and stabilization compared to other delivery systems, together with enhanced and highly tunable controlled release profiles [130, 131]. Furthermore, LCNs are versatile delivery systems with great applicability in inflammatory respiratory diseases [59].

The present study represents an extension of a series of studies performed recently in our laboratory, whereby phytantriol- or monoolein-based berberine-LCN formulations have shown to be effective *in vitro* as a treatment for LC [129, 132, 133], cigarette smoke-induced inflammation, oxidative stress, and cellular senescence [103], and lipopolysaccharide (LPS)-induced inflammation and oxidative stress [134]. In the present study, treatment with BM-LCNs significantly counteracted TGF- β -induced remodelling features in BEAS-2B cells.

The first remodelling feature investigated was cell migration, using the scratch-wound assay. TGF- β induced an increase in BEAS-2B cells migration, which was reversed by simultaneous treatment with BM-LCNs to levels comparable to untreated cells at both 24 and 48 h post-treatment (Chapter 4, Figure 2). The anti-migratory activity of berberine was recently shown by Jin *et al.*, who reported that treatment of U-87 and LN229 glioma cells with free berberine

at concentrations between 5 and 10 μM significantly decreased their migratory ability, as assessed through wound-healing assay, through the inhibition of the TGF- β 1/SMAD2/3 signalling pathway [135]. Furthermore, Alnuqaydan *et al.*, [133] and Paudel *et al.*, [129] reported a similar anti-migratory activity of berberine-loaded LCNs in A549 human adenocarcinoma cells. Mechanistically, the Human XL Cytokine Array experiment revealed that BM-LCNs counteracted TGF- β -induced changes in protein expression by (i) reducing the expression of proteins upregulated by TGF- β (Chapter 4, Figure 3), and (ii) restoring the expression of proteins downregulated by TGF- β (Chapter 4, Figure 3). Proteins belonging to the former group promote various features of TGF- β -induced remodelling and include: endoglin, thrombospondin-1 (THBS1), vascular endothelial growth factor (VEGF), basic fibroblast growth factor (bFGF), and myeloperoxidase. Endoglin is considered a TGF- β co-receptor that contributes to the increased angiogenesis occurring in remodelling [136], while THBS1, VEGF, and bFGF are known to mediate TGF- β -induced remodelling and angiogenesis in asthma, COPD, and LC [137-139]. Myeloperoxidase is also involved in TGF- β -induced remodelling and cell migration [140]. The suppressive effect of berberine towards the expression of bFGF was reported by Li *et al.*, who showed that free berberine at a 90 μM concentration significantly counteracted the IL-8-induced cell migration in MDA-MB-231 breast cancer cells by inhibiting the expression of this and other growth factors [142]. Furthermore, Liu and co-workers previously showed that free berberine at a concentration of 100 to 200 μM significantly inhibited the expression of inflammatory-invasive cytokines, including VEGF, in human ectopic endometrial stromal cells [143]. In another report, Li *et al.*, demonstrated that berberine at a minimal concentration of 60 μM significantly reduced the expression of VEGF in A549 human lung cancer cells [144]. Finally, Zhang *et al.*, reported that berberine administration reduced increased levels of myeloperoxidase expression in the serum and colon of dextran sodium sulfate-induced colitis in mice [145]. The present study is the first to show that berberine downregulates the expression of endoglin and THBS1.

Furthermore, BM-LCNs partially restored the expression of one proteins downregulated by TGF- β : cystatin C (Chapter 4, Figure 2). This protein is a known negative regulator of TGF- β signalling [146, 147]. To the best of our knowledge, this is the first study showing that berberine increases the production of cystatin C. With regards to the berberine-induced increased cystatin C production, the relevance of this result is underlined by a study by Tian *et al.*, which demonstrated that exogenous administration of cystatin C had preclinical efficacy in

counteracting TGF- β -induced cancer progression and angiogenesis in an *in vivo* model of breast cancer lung metastasis [148].

Finally, treatment with BM-LCNs restored baseline nitric oxide (NO) secretion, which was downregulated by TGF- β (Chapter 4, Figure 5). NO is a negative regulator of TGF- β signalling, known to attenuate TGF- β -induced EMT and remodelling [149], and TGF- β reduces NO secretion by inhibiting the enzymes involved in its synthesis, including the endogenous NO synthase (eNOS) [149]. Consistently with our findings, Wang *et al.*, showed that free berberine at a concentration ranging between 5 and 25 μ M significantly increased the phosphorylation and activation of eNOS, and concomitant NO production, *in vitro* in human umbilical vein endothelial cells (HUVECs), protecting these cells from hyperglycemia-induced injury [150]. Interestingly, in a recent study performed in our laboratory, Alnuqaydan *et al.*, showed that a similar berberine-LCN formulation reduced the LPS-induced secretion of NO in RAW264.7 mouse macrophages through the inhibition of the iNOS expression, as part of its anti-inflammatory and anti-oxidant activities [134]. Taken together, these results support the notion that berberine promotes, in a context-dependent manner, the maintenance of physiologically balanced levels of NO secretion.

In summary, BM-LCNs counteracted many TGF- β -induced features of remodelling in BEAS-2B human bronchial epithelial cell. Importantly, BM-LCNs exerted this activity at a low equivalent free berberine concentration of 0.5 μ M, which is 10 to 600-fold lower compared to the concentrations of free berberine powder that were reported to inhibit TGF- β -induced features in other *in vitro* studies, such as those reported previously and many others, using different cell models [135, 142, 143, 145, 150-155]. This confirms the enormous potential of advanced drug delivery systems such as LCNs in improving the delivery of poorly soluble and/or permeable molecules such as berberine and other phytochemicals.

The overall results of the present thesis are summarized in Figure 1.

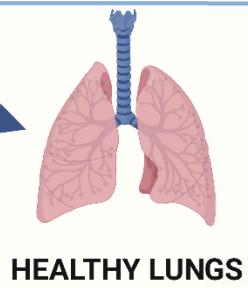
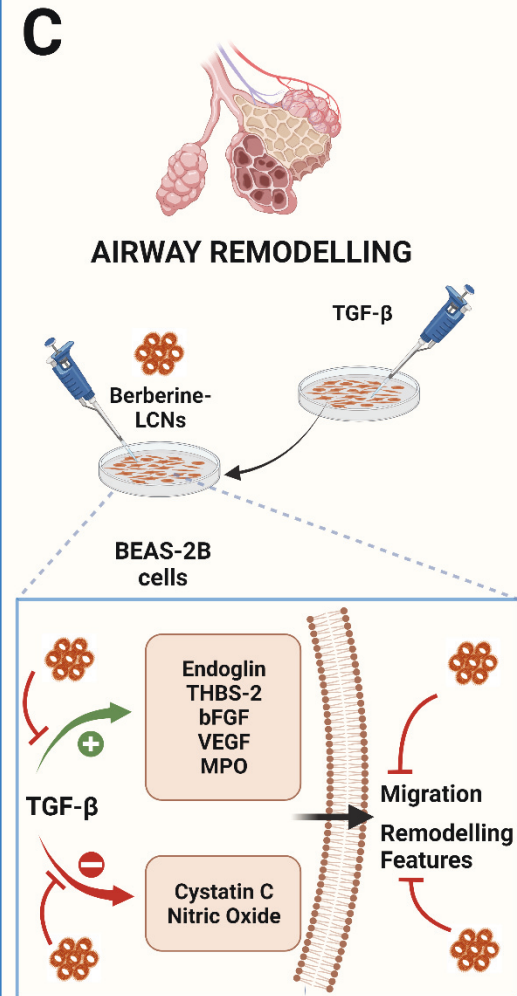
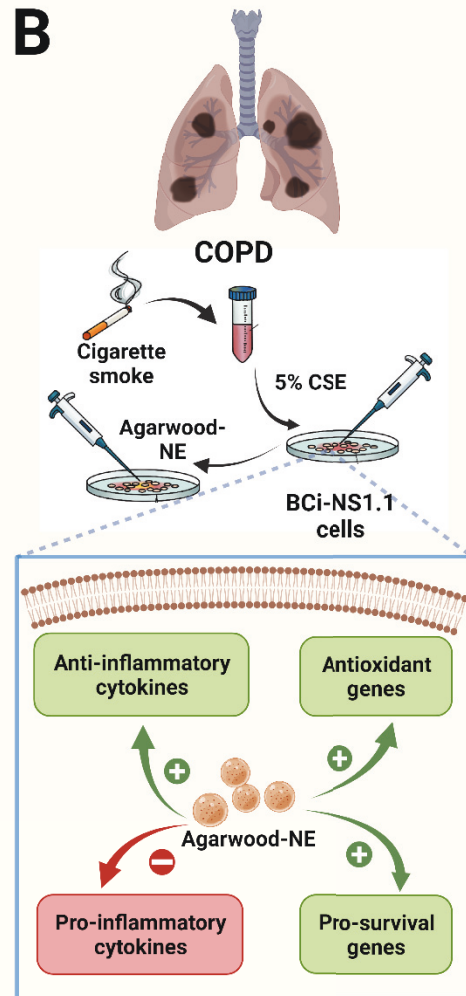
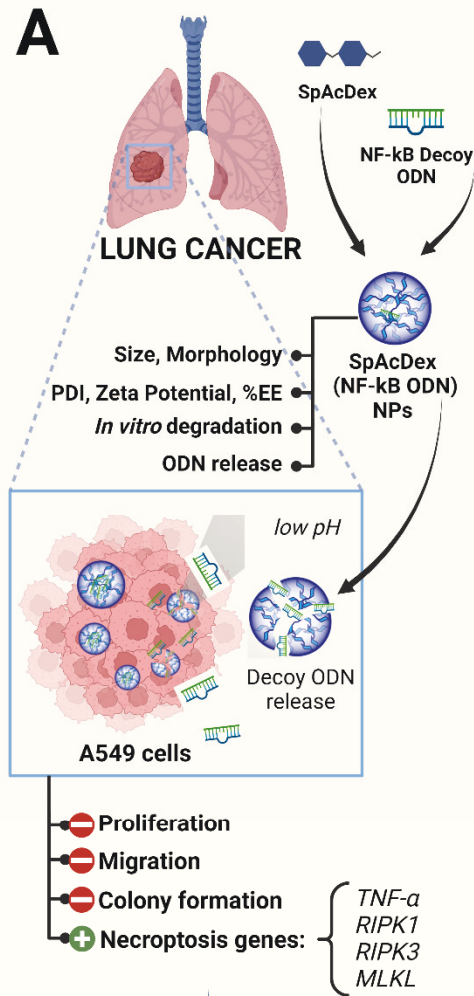


Figure 1 – Overview of Research Findings. (A) **Chapter 2:** NF- κ B decoy ODN has been encapsulated in pH-sensitive SpAcDex-NPs. The NPs have been characterized for size, morphology, zeta potential, polydispersity index, pH-dependent *in vitro* degradation (at pH 5.5), and ODN release. The anticancer activity of the SpAcDex (NF- κ B ODN) NPs was tested *in vitro* on A549 human lung adenocarcinoma cells, obtaining significant inhibition of cell proliferation, migration, and colony formation. Mechanistically, SpAcDex (NF- κ B ODN) NPs upregulated the transcription of four genes involved in necroptosis: TNF- α , RIPK1, RIPK3, and MLKL. (B) **Chapter 3:** agarwood oil was loaded in a nanoemulsion (NE) and tested on an *in vitro* model of COPD obtained by treating human BCI-NS1.1 airway epithelial cells with 5% cigarette smoke extract (CSE). Agarwood-NE significantly counteracted many of the effects of CSE, demonstrating a strong anti-inflammatory and antioxidant activity obtained through (i) stimulation of the production of anti-inflammatory cytokines (IL-10, TFF3, VDBP, IFN- γ , IL-18BP, GH, Relaxin-2, PDGF-BB); (ii) inhibition of the production of proinflammatory cytokines (IL-1 α , IL-1 β , IL-1Ra, IL-8, GDF-15); (iii) stimulation of the expression of antioxidant genes (GCLC, GSTP1) and (iv) stimulation of the expression of pro-survival genes (PI3K). (C) **Chapter 4:** berberine was encapsulated in monoolein-based liquid crystalline nanoparticles (LCNs) and tested on an *in vitro* model of airway remodelling obtained by treating BEAS-2B human bronchial epithelial cells with TGF- β for 48 h. Berberine-LCNs significantly reversed TGF- β -induced remodelling features, including the increase in cell migration, *via* (i) inhibiting the expression of TGF- β -induced cytokines mediating the remodelling process, such as endoglin, THBS2, bFGF, VEGF, and MPO), (ii) stimulating the expression of Cystatin C, a cytokine that negatively regulates the remodelling process, which is repressed by TGF- β , and (iii) stimulating the secretion of nitric oxide (NO), which is repressed by TGF- β .

BCi-NS1.1: basal cell immortalized-nonsmoker 1 (BCi-NS1); bFGF: basic fibroblast growth factor; COPD: chronic obstructive pulmonary disease; CSE: cigarette smoke extract;; EE: Encapsulation Efficiency; GCLC: glutamate-cysteine ligase catalytic subunit; GDF-15: growth/differentiation factor-15; GH: growth hormone; GSTP1: glutathione S-transferase pi 1; IFN- γ : interferon- γ ; IL: interleukin; IL-18BP: interleukin-18 binding protein; LCNs: liquid crystalline nanoparticles; MLKL: mixed lineage kinase domain like pseudokinase; MPO: myeloperoxidase; NE: nanoemulsion; NF- κ B: nuclear factor-kappaB; NPs: nanoparticles; ODN: oligodeoxynucleotide; PDGF-BB: platelet-derived growth factor-BB; PDI: polydispersity index; RIPK: Receptor-interacting serine/threonine-protein kinase; SpAcDex:

spermine-functionalised acetalated dextran; TFF3: trefoil factor 3; TGF- β : transforming growth factor- β ; THBS2: thrombospondin-2; TNF- α : tumor necrosis factor- α ; VDBP: vitamin D binding protein; VEGF: vascular/endothelial growth factor; ζ : zeta-potential.

Limitations of the present work and future directions

The results shown in the present thesis provide proof supporting the enormous potential of different types of advanced drug delivery systems in enhancing the delivery of molecules, such as phytochemicals and nucleic acid-based therapies, whose clinical application is hampered by issues such as poor solubility, poor permeability, and suboptimal pharmacokinetics, providing a blueprint for the development of novel treatment approaches to be used in the treatment of CRDs. However, this research is not exempt from limitations. The limitations discussed below represent the starting point for the future directions of the present work, and many of the proposed experiments discussed in this section are either in progress or at the planning stage in our laboratories, functioning as a starting point for future research.

The first limitation of the present thesis, which is shared across all three main research chapters discussed, is that the different formulations have been tested only one cell line. Although the experimental setups used are all well-established *in vitro* models of non-small cell LC (NSCLC) (A549 cells [156]), cigarette smoke-induced COPD (CSE-treated airway epithelial cells [103]), and TGF- β -induced remodelling (TGF- β -stimulated bronchial epithelial cells [32]), testing these formulations on different cell lines would be advantageous in order to expand the breadth, scope, and applicability of this research. For example, testing the NF- κ B SpAcDex formulation on different LC cell lines, including different types such as squamous cell carcinoma and small cell carcinoma [157], would extend the potential applicability of this therapeutic towards different LC subtypes. Similarly, it would be interesting to test this formulation on other types of cancers, as well as on inflammatory diseases including CRDs, considering the fundamental role played by NF- κ B in the pathogenesis and progression of these diseases [158]. With regards to the AW-NE and BM-LCNs formulations, the results discussed in this work would benefit enormously by further investigating the activity of these formulations on other cell types present in the lung, such as macrophages (for example: RAW264.7 mouse macrophages, or U-397 human macrophages) and pneumocytes (for example: type I hAELVi cells or type II NCI-H441 cells), exposed to the same types of stimuli. The use of co-culture systems, mimicking the complex interactions between different cell types

that physiologically occur in the lungs, would provide further benefit, providing more physiologically relevant models to test these formulations [159, 160]. In this context, the use of microfluidics-based lung-on-a-chip systems would be advantageous, as these systems allow to model the complex cellular and molecular architecture of the airways and lung parenchyma, therefore providing *in vitro* models that are closer, in terms of structure and physiology, to the real organ [161].

Another limitation of this work consists of the fact that the formulations have only been tested *in vitro*. To provide valid proof of these systems as potential therapeutic options for CRDs and to support their clinical translation, *in vivo* studies to assess the efficacy of these formulations on suitable animal models are necessary. These include orthotopic LC models [162], animal COPD models obtained through acute cigarette smoke exposure or intratracheal LPS administration [163, 164], as well as models of diseases showing airway remodelling such as the Dust mite, Ragweed, Aspergillus (DRA) model of chronic asthma [165]. Considering the possibility of developing these formulations to be delivered *via* inhalational administration [59], further obstacles that must be tackled to ensure a smooth transition to the clinic include the possibility that the shear stress to which the nanoparticles are subjected during the spray/nebulization process leads to their rupture [166], as well as the mucus barriers that these nanoparticles need to overcome in order to reach the intended site in the lungs [58]. Only upon thorough testing in the aforementioned *in vivo* models, formulations like the ones explored in the present thesis would be suitable to be tested in in-human clinical trials.

Even though the three formulations used in this study were tested on *in vitro* models of different diseases, the biological activity obtained was directed against pathophysiological features and hallmarks, such as NF- κ B activation, inflammation, oxidative stress, and remodelling, that are common across virtually all CRDs. This increases the possibility that these formulations are effective on other *in vitro* CRD models. For example, the NF- κ B decoy ODN formulation might be tested on the CSE-exposure COPD model or on the TGF- β -induced remodelling model, whereas the AW-NE formulation might be tested on A549 cells for its anticancer activity and on the TGF- β model. Furthermore, it would be interesting to assess the *in vitro* activity of these formulations on asthma models obtained through exposure of airway epithelial cells and other cells to house dust mite (HDM) [167].

Conclusions

Despite the availability of several treatment options, CRDs still represents the leading cause of morbidity and mortality worldwide. This is at least partly caused due to the limited efficacy and severe adverse effects associated with the current pharmacological treatment strategies. For this reason, novel pharmacological treatment options are needed. Among several potential new drug candidates, phytoceuticals and nucleic acid-based therapies are particularly promising, but their clinical use is limited by poor pharmacokinetic properties. To address this issue, we have developed different nanoparticle-based advanced drug delivery systems encapsulating nucleic acids (NF- κ B decoy ODN) and phytoceuticals (agarwood oil, berberine), and tested them *in vitro*, demonstrating their potent therapeutic efficacy on cell-based models of LC, COPD, and aberrant airway remodelling.

In Chapter 2, we used an acid-responsive SpAcDex polymer to formulate NPs encapsulating a decoy ODN inhibiting the transcription factor NF- κ B. We tested this formulation *in vitro* against A549 human adenocarcinoma cells, obtaining potent anticancer activity which was exerted through the inhibition of cell proliferation, migration, and colony formation. Mechanistically, we showed that the anti-proliferative activity was at least partially exerted through the activation of necroptosis-related signalling, mediated by TNF- α , RIPK1, RIPK3, and MLKL. This study highlights the suitability of acid-responsive systems such as SpAcDex NPs in the cancer-specific delivery of nucleic acid-based therapies, supporting the use of decoy ODNs as a therapeutic strategy for LC.

In Chapter 3, we formulated agarwood oil in a nanoemulsion (AW-NE) and demonstrated its potent anti-inflammatory and antioxidant activities on CSE-treated BCI-NS1.1 human airway epithelial cells, representing an *in vitro* model of the molecular pathways activated in the airways upon cigarette smoke exposures, which cause the inflammation and oxidative stress that lead to COPD. The anti-inflammatory activity of AW-NE was obtained through the downregulation of pro-inflammatory cytokines upregulated by CSE (IL-1 α , IL-1 β , IL-1Ra, IL-8 and GDF-15) and through an increased expression of anti-inflammatory cytokines downregulated by CSE (IL-10, IL-18Bpa, GH, IFN- γ , PDGF-BB, TFF3, Relaxin-2, and VDBP). The antioxidant activity was mediated by the restoration of the mRNA levels of GSTP1 and GCLC, two enzymes that are fundamental for the synthesis and conjugation of glutathione and whose expression is downregulated by CSE. Finally, AW-NEs restored the mRNA expression of PI3K, a pro-survival gene whose expression was ablated by CSE. The

results of this study demonstrate that the formulation of poorly water-soluble oil and extracts such as agarwood oil is a convenient strategy to improve their delivery, allowing to fully exploit the potent, multifaceted therapeutic activity of such extracts.

In the study shown in Chapter 4, a monoolein-based LCN formulation (BM-LCNs) was used to encapsulate berberine, a phytochemical with poor permeability that has been extensively characterised for its antioxidant, anti-inflammatory, and anticancer potential, and deliver it to TGF- β -stimulated human bronchial BEAS-2B epithelial cells. This system represents a suitable *in vitro* model of airway remodelling, a pathophysiological feature common across all CRDs. This study showed that BM-LCNs significantly counteracted TGF- β -induced increased cell migration, which is one of the main phenomena occurring during remodelling. From a molecular point of view, BM-LCNs blocked the TGF- β -induced overexpression of cytokines mediating the remodelling process (endoglin, thrombospondin-1, VEGF, myeloperoxidase, and bFGF), simultaneously restoring the expression cystatin C, which was blocked by TGF- β . Furthermore, BM-LCNs restored the secretion of baseline levels of NO, a negative regulator of remodelling whose production is reduced by TGF- β . This study underlines the versatility of LCNs as a delivery system for poorly soluble or poorly permeable phytochemicals such as berberine, with potential as a therapeutic option targeting the phenomenon of airway remodelling, which is ubiquitous across CRDs and therefore represents an advantageous target for a wide range of pulmonary diseases.

Overall, this work demonstrates the enormous potential of advanced drug delivery systems to treat highly prevalent pulmonary diseases such as COPD and LC, providing the foundation for future development of next-generation treatment strategies with great potential to improve the survival and quality of patients affected by CRDs.

REFERENCES

1. *Prevalence and attributable health burden of chronic respiratory diseases, 1990-2017: a systematic analysis for the Global Burden of Disease Study 2017*. Lancet Respir Med, 2020. **8**(6): p. 585-596.
2. Bratova, M., et al., *Non-small Cell Lung Cancer as a Chronic Disease - A Prospective Study from the Czech TULUNG Registry*. In Vivo, 2020. **34**(1): p. 369-379.
3. Viegli, G., et al., *Global Burden of Chronic Respiratory Diseases*. J Aerosol Med Pulm Drug Deliv, 2020. **33**(4): p. 171-177.

4. Safiri, S., et al., *Burden of chronic obstructive pulmonary disease and its attributable risk factors in 204 countries and territories, 1990-2019: results from the Global Burden of Disease Study 2019*. *Bmj*, 2022. **378**: p. e069679.
5. Sung, H., et al., *Global Cancer Statistics 2020: GLOBOCAN Estimates of Incidence and Mortality Worldwide for 36 Cancers in 185 Countries*. *CA Cancer J Clin*, 2021. **71**(3): p. 209-249.
6. (AIHW), A.I.o.H.a.W. *Chronic Respiratory Conditions*. 2023 09/02/2023 [cited 2023 09/03/2023]; Available from: <https://www.aihw.gov.au/reports/chronic-respiratory-conditions/chronic-respiratory-conditions/contents/chronic-obstructive-pulmonary-disease>.
7. Welfare, A.I.o.H.a. *Chronic respiratory conditions*. 2023; Available from: <https://www.aihw.gov.au/reports/chronic-respiratory-conditions/chronic-respiratory-conditions/contents/summary>.
8. Heraganahally, S.S., et al., *Chronic Obstructive Pulmonary Disease In Aboriginal Patients Of The Northern Territory Of Australia: A Landscape Perspective*. *Int J Chron Obstruct Pulmon Dis*, 2019. **14**: p. 2205-2217.
9. Australia, A.G.-C. *Lung cancer in Australia statistics*. 2022 [cited 2023 09/03/2023]; Available from: <https://www.canceraustralia.gov.au/cancer-types/lung-cancer/statistics>.
10. Singh, D., A.G. Mathioudakis, and A. Higham, *Chronic obstructive pulmonary disease and COVID-19: interrelationships*. *Curr Opin Pulm Med*, 2022. **28**(2): p. 76-83.
11. Sunkara, K., et al., *COVID-19 in underlying COPD Patients*. *Excli j*, 2021. **20**: p. 248-251.
12. Passaro, A., et al., *Severity of COVID-19 in patients with lung cancer: evidence and challenges*. *J Immunother Cancer*, 2021. **9**(3).
13. Wu, M., et al., *Is COVID-19 a high risk factor for lung cancer?: A protocol for systematic review and meta-analysis*. *Medicine (Baltimore)*, 2021. **100**(1): p. e23877.
14. Shastri, M.D., et al., *Smoking and COVID-19: What we know so far*. *Respir Med*, 2021. **176**: p. 106237.
15. Lugg, S.T., et al., *Cigarette smoke exposure and alveolar macrophages: mechanisms for lung disease*. *Thorax*, 2022. **77**(1): p. 94-101.
16. Nucera, F., et al., *Role of oxidative stress in the pathogenesis of COPD*. *Minerva Med*, 2022. **113**(3): p. 370-404.

17. Sharma, P., et al., *Emerging trends in the novel drug delivery approaches for the treatment of lung cancer*. Chem Biol Interact, 2019. **309**: p. 108720.
18. Riley, C.M. and F.C. Sciurba, *Diagnosis and Outpatient Management of Chronic Obstructive Pulmonary Disease: A Review*. Jama, 2019. **321**(8): p. 786-797.
19. Holgate, S.T., et al., *Asthma*. Nat Rev Dis Primers, 2015. **1**(1): p. 15025.
20. Barnes, P.J., et al., *Chronic obstructive pulmonary disease*. Nat Rev Dis Primers, 2015. **1**: p. 15076.
21. Wilchesky, M., et al., *Bronchodilator use and the risk of arrhythmia in COPD: part 2: reassessment in the larger Quebec cohort*. Chest, 2012. **142**(2): p. 305-311.
22. Leuppi, J.D., et al., *Short-term vs conventional glucocorticoid therapy in acute exacerbations of chronic obstructive pulmonary disease: the REDUCE randomized clinical trial*. Jama, 2013. **309**(21): p. 2223-31.
23. Thomson, N.C., *Addressing corticosteroid insensitivity in adults with asthma*. Expert Rev Respir Med, 2016. **10**(2): p. 137-56.
24. Howington, J.A., et al., *Treatment of stage I and II non-small cell lung cancer: Diagnosis and management of lung cancer, 3rd ed: American College of Chest Physicians evidence-based clinical practice guidelines*. Chest, 2013. **143**(5 Suppl): p. e278S-e313S.
25. Wong, M.C.S., et al., *Incidence and mortality of lung cancer: global trends and association with socioeconomic status*. Sci Rep, 2017. **7**(1): p. 14300.
26. Anderton, H., I.P. Wicks, and J. Silke, *Cell death in chronic inflammation: breaking the cycle to treat rheumatic disease*. Nature Reviews Rheumatology, 2020. **16**(9): p. 496-513.
27. Dua, K., et al., *Increasing complexity and interactions of oxidative stress in chronic respiratory diseases: An emerging need for novel drug delivery systems*. Chemo-Biological Interactions, 2019. **299**: p. 168-178.
28. Biswas, S.K., *Does the Interdependence between Oxidative Stress and Inflammation Explain the Antioxidant Paradox?* Oxid Med Cell Longev, 2016. **2016**: p. 5698931.
29. Dhanjal, D.S., et al., *Concepts of advanced therapeutic delivery systems for the management of remodeling and inflammation in airway diseases*. Future Med Chem, 2022. **14**(4): p. 271-288.
30. Mehta, M., et al., *Incipient need of targeting airway remodeling using advanced drug delivery in chronic respiratory diseases*. Future Med Chem, 2020. **12**(10): p. 873-875.

31. Pain, M., et al., *Tissue remodelling in chronic bronchial diseases: from the epithelial to mesenchymal phenotype*. Eur Respir Rev, 2014. **23**(131): p. 118-30.
32. Doerner, A.M. and B.L. Zuraw, *TGF- β 1 induced epithelial to mesenchymal transition (EMT) in human bronchial epithelial cells is enhanced by IL-1 β but not abrogated by corticosteroids*. Respiratory Research, 2009. **10**(1): p. 100.
33. Durham, A.L. and I.M. Adcock, *The relationship between COPD and lung cancer*. Lung Cancer, 2015. **90**(2): p. 121-7.
34. Saito, A., M. Horie, and T. Nagase, *TGF- β Signaling in Lung Health and Disease*. International Journal of Molecular Sciences, 2018. **19**(8): p. 2460.
35. Devkota, H.P., et al., *Phytochemicals and their Nanoformulations Targeted for Pulmonary Diseases*, in *Advanced Drug Delivery Strategies for Targeting Chronic Inflammatory Lung Diseases*, D.K. Chellappan, K. Pabreja, and M. Faiyazuddin, Editors. 2022, Springer Singapore: Singapore. p. 95-106.
36. Wang, S., et al., *Chemical Constituents and Pharmacological Activity of Agarwood and Aquilaria Plants*. Molecules, 2018. **23**(2).
37. Alamil, J.M.R., et al., *Rediscovering the Therapeutic Potential of Agarwood in the Management of Chronic Inflammatory Diseases*. Molecules, 2022. **27**(9).
38. Cicero, A.F. and A. Baggioni, *Berberine and Its Role in Chronic Disease*. Adv Exp Med Biol, 2016. **928**: p. 27-45.
39. Devkota, H.P., et al., *Bioactive Compounds from Zingiber montanum and Their Pharmacological Activities with Focus on Zerumbone*. Applied Sciences, 2021. **11**(21): p. 10205.
40. Pan, G.Y., et al., *The involvement of P-glycoprotein in berberine absorption*. Pharmacol Toxicol, 2002. **91**(4): p. 193-7.
41. Kesharwani, S.S. and G.J. Bhat, *Formulation and Nanotechnology-Based Approaches for Solubility and Bioavailability Enhancement of Zerumbone*. Medicina (Kaunas), 2020. **56**(11).
42. Yin, J., H. Xing, and J. Ye, *Efficacy of berberine in patients with type 2 diabetes mellitus*. Metabolism, 2008. **57**(5): p. 712-7.
43. AbouAitah, K. and W. Lojkowski, *Nanomedicine as an Emerging Technology to Foster Application of Essential Oils to Fight Cancer*. Pharmaceuticals (Basel), 2022. **15**(7).
44. Mei, D., et al., *Therapeutic RNA Strategies for Chronic Obstructive Pulmonary Disease*. Trends Pharmacol Sci, 2020. **41**(7): p. 475-486.

45. Mullard, A., *2020 FDA drug approvals*. Nat Rev Drug Discov, 2021. **20**(2): p. 85-90.
46. Mullard, A., *2021 FDA approvals*. Nat Rev Drug Discov, 2022. **21**(2): p. 83-88.
47. Mullard, A., *2022 FDA approvals*. Nat Rev Drug Discov, 2023. **22**(2): p. 83-88.
48. Ahmad, M.Z., et al., *Application of decoy oligonucleotides as novel therapeutic strategy: a contemporary overview*. Curr Drug Discov Technol, 2013. **10**(1): p. 71-84.
49. Cai, Z., K.M. Tchou-Wong, and W.N. Rom, *NF-kappaB in lung tumorigenesis*. Cancers (Basel), 2011. **3**(4): p. 4258-68.
50. Feng, Q. and K. Xiao, *Nanoparticle-Mediated Delivery of STAT3 Inhibitors in the Treatment of Lung Cancer*. Pharmaceutics, 2022. **14**(12).
51. Mehta, M., et al., *Recent trends of NFκB decoy oligodeoxynucleotide-based nanotherapeutics in lung diseases*. J Control Release, 2021. **337**: p. 629-644.
52. Dinh, T.D., et al., *Evaluation of osteoclastogenesis via NFkappaB decoy/mannosylated cationic liposome-mediated inhibition of pro-inflammatory cytokine production from primary cultured macrophages*. Pharm Res, 2011. **28**(4): p. 742-51.
53. De Stefano, D., *Oligonucleotides decoy to NF-kappaB: becoming a reality?* Discov Med, 2011. **12**(63): p. 97-105.
54. Corrie, L., et al., *Multivariate Data Analysis and Central Composite Design-Oriented Optimization of Solid Carriers for Formulation of Curcumin-Loaded Solid SNEDDS: Dissolution and Bioavailability Assessment*. Pharmaceutics, 2022. **14**(11).
55. Paudel, K.R., et al., *Editorial: Advanced therapeutic delivery for the management of chronic respiratory diseases*. Front Med (Lausanne), 2022. **9**: p. 983583.
56. Manandhar, B., et al., *Applications of extracellular vesicles as a drug-delivery system for chronic respiratory diseases*. Nanomedicine (Lond), 2022. **17**(12): p. 817-820.
57. Paudel, K.R., et al., *Nanomedicine and medicinal plants: Emerging symbiosis in managing lung diseases and associated infections*. Excli j, 2022. **21**: p. 1299-1303.
58. Prasher, P., et al., *Targeting mucus barrier in respiratory diseases by chemically modified advanced delivery systems*. Chem Biol Interact, 2022. **365**: p. 110048.
59. Chan, Y., et al., *Versatility of liquid crystalline nanoparticles in inflammatory lung diseases*. Nanomedicine (Lond), 2021. **16**(18): p. 1545-1548.
60. Baltimore, D., *Discovering NF-kappaB*. Cold Spring Harb Perspect Biol, 2009. **1**(1): p. a000026.
61. Xia, L., et al., *Role of the NFκB-signaling pathway in cancer*. Onco Targets Ther, 2018. **11**: p. 2063-2073.

62. Jones, D.R., et al., *Inhibition of NF-kappaB sensitizes non-small cell lung cancer cells to chemotherapy-induced apoptosis*. *Ann Thorac Surg*, 2000. **70**(3): p. 930-6; discussion 936-7.
63. Gu, L., et al., *Prognostic significance of NF-κB expression in non-small cell lung cancer: A meta-analysis*. *PLoS One*, 2018. **13**(5): p. e0198223.
64. Yu, H., et al., *Targeting NF-κB pathway for the therapy of diseases: mechanism and clinical study*. *Signal Transduct Target Ther*, 2020. **5**(1): p. 209.
65. Wong, K.K., T. Jacks, and G. Dranoff, *NF-kappaB fans the flames of lung carcinogenesis*. *Cancer Prev Res (Phila)*, 2010. **3**(4): p. 403-5.
66. Gupta, S.C., et al., *Inhibiting NF-κB activation by small molecules as a therapeutic strategy*. *Biochim Biophys Acta*, 2010. **1799**(10-12): p. 775-87.
67. Chiang, H.I., L.R. Berghman, and H. Zhou, *Inhibition of NF-kB 1 (NF-kBp50) by RNA interference in chicken macrophage HD11 cell line challenged with Salmonella enteritidis*. *Genet Mol Biol*, 2009. **32**(3): p. 507-15.
68. Li, N., et al., *Small interfering RNA targeting NF-κB attenuates lipopolysaccharide-induced acute lung injury in rats*. *BMC Physiol*, 2016. **16**(1): p. 7.
69. Müller, E.K., et al., *Nanoparticles Carrying NF-κB p65-Specific siRNA Alleviate Colitis in Mice by Attenuating NF-κB-Related Protein Expression and Pro-Inflammatory Cellular Mediator Secretion*. *Pharmaceutics*, 2022. **14**(2).
70. Mann, M.J., *Transcription factor decoys: a new model for disease intervention*. *Ann N Y Acad Sci*, 2005. **1058**: p. 128-39.
71. De Rosa, G., et al., *Enhanced intracellular uptake and inhibition of NF-kappaB activation by decoy oligonucleotide released from PLGA microspheres*. *J Gene Med*, 2005. **7**(6): p. 771-81.
72. De Stefano, D., et al., *Oligonucleotide decoy to NF-kappaB slowly released from PLGA microspheres reduces chronic inflammation in rat*. *Pharmacol Res*, 2009. **60**(1): p. 33-40.
73. Hoffmann, F., et al., *A novel technique for selective NF-kappaB inhibition in Kupffer cells: contrary effects in fulminant hepatitis and ischaemia-reperfusion*. *Gut*, 2009. **58**(12): p. 1670-8.
74. Nordmeier, S., et al., *Exosome mediated delivery of functional nucleic acid nanoparticles (NANPs)*. *Nanomedicine*, 2020. **30**: p. 102285.

75. Higuchi, Y., et al., *Suppression of TNF α production in LPS induced liver failure in mice after intravenous injection of cationic liposomes/NF κ B decoy complex*. Pharmazie, 2006. **61**(2): p. 144-7.
76. De Rosa, G., et al., *Novel cationic liposome formulation for the delivery of an oligonucleotide decoy to NF- κ B into activated macrophages*. European Journal of Pharmaceutics and Biopharmaceutics, 2008. **70**(1): p. 7-18.
77. Wijagkanalan, W., et al., *Intratracheally instilled mannosylated cationic liposome/NF κ B decoy complexes for effective prevention of LPS-induced lung inflammation*. J Control Release, 2011. **149**(1): p. 42-50.
78. Cui, S., et al., *Correlation of the cytotoxic effects of cationic lipids with their headgroups*. Toxicol Res (Camb), 2018. **7**(3): p. 473-479.
79. Hines, D.J. and D.L. Kaplan, *Poly(lactic-co-glycolic) acid-controlled-release systems: experimental and modeling insights*. Crit Rev Ther Drug Carrier Syst, 2013. **30**(3): p. 257-76.
80. De Stefano, D., et al., *A decoy oligonucleotide to NF- κ B delivered through inhalable particles prevents LPS-induced rat airway inflammation*. Am J Respir Cell Mol Biol, 2013. **49**(2): p. 288-95.
81. Palanikumar, L., et al., *pH-responsive high stability polymeric nanoparticles for targeted delivery of anticancer therapeutics*. Communications Biology, 2020. **3**(1): p. 95.
82. Broaders, K.E., et al., *Acetalated dextran is a chemically and biologically tunable material for particulate immunotherapy*. Proc Natl Acad Sci U S A, 2009. **106**(14): p. 5497-502.
83. Petrovici, A.R., M. Pinteala, and N. Simionescu, *Dextran Formulations as Effective Delivery Systems of Therapeutic Agents*. Molecules, 2023. **28**(3).
84. Bachelder, E.M., E.N. Pino, and K.M. Ainslie, *Acetalated Dextran: A Tunable and Acid-Labile Biopolymer with Facile Synthesis and a Range of Applications*. Chem Rev, 2017. **117**(3): p. 1915-1926.
85. Cohen, J.A., et al., *Acetal-modified dextran microparticles with controlled degradation kinetics and surface functionality for gene delivery in phagocytic and non-phagocytic cells*. Adv Mater, 2010. **22**(32): p. 3593-7.
86. Cohen, J.L., et al., *Acid-degradable cationic dextran particles for the delivery of siRNA therapeutics*. Bioconj Chem, 2011. **22**(6): p. 1056-65.

87. Prasher, P., et al., *Current-status and applications of polysaccharides in drug delivery systems*. Colloid and Interface Science Communications, 2021. **42**: p. 100418.
88. Prasher, P., et al., *Versatility of acetalated dextran in nanocarriers targeting respiratory diseases*. Materials Letters, 2022. **323**: p. 132600.
89. Boedtkjer, E. and S.F. Pedersen, *The Acidic Tumor Microenvironment as a Driver of Cancer*. Annu Rev Physiol, 2020. **82**: p. 103-126.
90. Wang, S., et al., *Acetalated dextran based nano- and microparticles: synthesis, fabrication, and therapeutic applications*. Chem Commun (Camb), 2021. **57**(35): p. 4212-4229.
91. Wang, J., et al., *Collagenase-loaded pH-sensitive nanocarriers efficiently remodeled tumor stroma matrixes and improved the enrichment of nanomedicines*. Nanoscale, 2021. **13**(20): p. 9402-9414.
92. Gao, Y., et al., *Developing Next-Generation Protein-Based Vaccines Using High-Affinity Glycan Ligand-Decorated Glyconanoparticles*. Adv Sci (Weinh), 2023. **10**(2): p. e2204598.
93. Gao, Y., et al., *Developing Acid-Responsive Glyco-Nanoplatfrom Based Vaccines for Enhanced Cytotoxic T-lymphocyte Responses Against Cancer and SARS-CoV-2*. Adv Funct Mater, 2021. **31**(41): p. 2105059.
94. Bamberger, D., et al., *Surface Modification of Polysaccharide-Based Nanoparticles with PEG and Dextran and the Effects on Immune Cell Binding and Stimulatory Characteristics*. Mol Pharm, 2017. **14**(12): p. 4403-4416.
95. Kongkaneromit, L., et al., *Dependence of reactive oxygen species and FLICE inhibitory protein on lipofectamine-induced apoptosis in human lung epithelial cells*. J Pharmacol Exp Ther, 2008. **325**(3): p. 969-77.
96. Zheng, T., et al., *Anti-MicroRNA-21 Oligonucleotide Loaded Spermine-Modified Acetalated Dextran Nanoparticles for B1 Receptor-Targeted Gene Therapy and Antiangiogenesis Therapy*. Adv Sci (Weinh), 2022. **9**(5): p. e2103812.
97. Seo, J., et al., *Necroptosis molecular mechanisms: Recent findings regarding novel necroptosis regulators*. Experimental & Molecular Medicine, 2021. **53**(6): p. 1007-1017.
98. Kumari, S., et al., *NF- κ B inhibition in keratinocytes causes RIPK1-mediated necroptosis and skin inflammation*. Life Science Alliance, 2021. **4**(6): p. e202000956.
99. Paudel, K.R., et al., *Rutin loaded liquid crystalline nanoparticles inhibit non-small cell lung cancer proliferation and migration in vitro*. Life Sci, 2021. **276**: p. 119436.

100. Mook, O.R., et al., *In situ localization of gelatinolytic activity in the extracellular matrix of metastases of colon cancer in rat liver using quenched fluorogenic DQ-gelatin*. J Histochem Cytochem, 2003. **51**(6): p. 821-9.
101. Eisner, M.D., et al., *An official American Thoracic Society public policy statement: Novel risk factors and the global burden of chronic obstructive pulmonary disease*. Am J Respir Crit Care Med, 2010. **182**(5): p. 693-718.
102. MacNee, W., *Pulmonary and systemic oxidant/antioxidant imbalance in chronic obstructive pulmonary disease*. Proc Am Thorac Soc, 2005. **2**(1): p. 50-60.
103. Paudel, K.R., et al., *Attenuation of Cigarette-Smoke-Induced Oxidative Stress, Senescence, and Inflammation by Berberine-Loaded Liquid Crystalline Nanoparticles: In Vitro Study in 16HBE and RAW264.7 Cells*. Antioxidants (Basel), 2022. **11**(5).
104. Dinarello, C.A., *The interleukin-1 family: 10 years of discovery*. Faseb j, 1994. **8**(15): p. 1314-25.
105. Wang, D., et al., *GDF15: emerging biology and therapeutic applications for obesity and cardiometabolic disease*. Nature Reviews Endocrinology, 2021. **17**(10): p. 592-607.
106. Jiang, G., C.T. Liu, and W.D. Zhang, *IL-17A and GDF15 are able to induce epithelial-mesenchymal transition of lung epithelial cells in response to cigarette smoke*. Exp Ther Med, 2018. **16**(1): p. 12-20.
107. Mueller, T., et al., *Association of the biomarkers soluble ST2, galectin-3 and growth-differentiation factor-15 with heart failure and other non-cardiac diseases*. Clin Chim Acta, 2015. **445**: p. 155-60.
108. Yadav, D.K., et al., *Molecular docking and ADME studies of natural compounds of Agarwood oil for topical anti-inflammatory activity*. Curr Comput Aided Drug Des, 2013. **9**(3): p. 360-70.
109. Wang, S., et al., *Agarwood Essential Oil Ameliorates Restrain Stress-Induced Anxiety and Depression by Inhibiting HPA Axis Hyperactivity*. Int J Mol Sci, 2018. **19**(11).
110. Hu, X., B. Hong, and M. Sun, *Peitu Shengjin Recipe Attenuates Airway Inflammation via the TLR4/NF-kB Signaling Pathway on Chronic Obstructive Pulmonary Disease*. Evid Based Complement Alternat Med, 2022. **2022**: p. 2090478.
111. Novick, D., et al., *Interleukin-18 binding protein: a novel modulator of the Th1 cytokine response*. Immunity, 1999. **10**(1): p. 127-136.

112. Soler Palacios, B., et al., *Growth Hormone Reprograms Macrophages toward an Anti-Inflammatory and Reparative Profile in an MAFB-Dependent Manner*. The Journal of Immunology, 2020: p. ji1901330.
113. Bortner, J.D., Jr., et al., *Proteomic profiling of human plasma by iTRAQ reveals down-regulation of ITI-HC3 and VDBP by cigarette smoking*. J Proteome Res, 2011. **10**(3): p. 1151-9.
114. Pini, A., et al., *Protection from cigarette smoke-induced vascular injury by recombinant human relaxin-2 (serelaxin)*. J Cell Mol Med, 2016. **20**(5): p. 891-902.
115. Duffney, P.F., et al., *Cigarette smoke dampens antiviral signaling in small airway epithelial cells by disrupting TLR3 cleavage*. Am J Physiol Lung Cell Mol Physiol, 2018. **314**(3): p. L505-L513.
116. Kardas, G., et al., *Role of Platelet-Derived Growth Factor (PDGF) in Asthma as an Immunoregulatory Factor Mediating Airway Remodeling and Possible Pharmacological Target*. Front Pharmacol, 2020. **11**: p. 47.
117. Thim, L. and F.E. May, *Structure of mammalian trefoil factors and functional insights*. Cell Mol Life Sci, 2005. **62**(24): p. 2956-73.
118. Wang, C., et al., *Agarwood Extract Mitigates Intestinal Injury in Fluorouracil-Induced Mice*. Biol Pharm Bull, 2019. **42**(7): p. 1112-1119.
119. Wang, C., et al., *Agarwood Alcohol Extract Protects against Gastric Ulcer by Inhibiting Oxidation and Inflammation*. Evid Based Complement Alternat Med, 2021. **2021**: p. 9944685.
120. Zhang, J. and C. Bai, *The Significance of Serum Interleukin-8 in Acute Exacerbations of Chronic Obstructive Pulmonary Disease*. Tanaffos, 2018. **17**(1): p. 13-21.
121. Ko, H.K., et al., *The role of transforming growth factor- β 2 in cigarette smoke-induced lung inflammation and injury*. Life Sci, 2023: p. 121539.
122. Birben, E., et al., *Oxidative stress and antioxidant defense*. World Allergy Organ J, 2012. **5**(1): p. 9-19.
123. Mao, G.E., et al., *Glutathione S-transferase P1 Ile105Val polymorphism, cigarette smoking and prostate cancer*. Cancer Detect Prev, 2004. **28**(5): p. 368-74.
124. Li, T., et al., *Cigarette smoke extract induces airway epithelial cell death via repressing PRMT6/AKT signaling*. Aging (Albany NY), 2020. **12**(23): p. 24301-24317.
125. Kuo, C.L., C.W. Chi, and T.Y. Liu, *The anti-inflammatory potential of berberine in vitro and in vivo*. Cancer Lett, 2004. **203**(2): p. 127-37.

126. DiNicolantonio, J.J., et al., *A nutraceutical strategy for downregulating TGF β signalling: prospects for prevention of fibrotic disorders, including post-COVID-19 pulmonary fibrosis*. *Open Heart*, 2021. **8**(1).
127. Qi, H.W., et al., *Epithelial-to-mesenchymal transition markers to predict response of Berberine in suppressing lung cancer invasion and metastasis*. *J Transl Med*, 2014. **12**: p. 22.
128. Tsai, P.L. and T.H. Tsai, *Hepatobiliary excretion of berberine*. *Drug Metab Dispos*, 2004. **32**(4): p. 405-12.
129. Paudel, K.R., et al., *Berberine-loaded liquid crystalline nanoparticles inhibit non-small cell lung cancer proliferation and migration in vitro*. *Environ Sci Pollut Res Int*, 2022. **29**(31): p. 46830-46847.
130. Chountoulesi, M., et al., *Lyotropic Liquid Crystalline Nanostructures as Drug Delivery Systems and Vaccine Platforms*. *Pharmaceuticals (Basel)*, 2022. **15**(4).
131. Tan, C., S.F. Hosseini, and S.M. Jafari, *Cubosomes and Hexosomes as Novel Nanocarriers for Bioactive Compounds*. *J Agric Food Chem*, 2022. **70**(5): p. 1423-1437.
132. Mehta, M., et al., *Berberine loaded liquid crystalline nanostructure inhibits cancer progression in adenocarcinomic human alveolar basal epithelial cells in vitro*. *J Food Biochem*, 2021. **45**(11): p. e13954.
133. Alnuqaydan, A.M., et al., *Evaluation of the Cytotoxic Activity and Anti-Migratory Effect of Berberine-Phytantriol Liquid Crystalline Nanoparticle Formulation on Non-Small-Cell Lung Cancer In Vitro*. *Pharmaceutics*, 2022. **14**(6).
134. Alnuqaydan, A.M., et al., *Phytantriol-Based Berberine-Loaded Liquid Crystalline Nanoparticles Attenuate Inflammation and Oxidative Stress in Lipopolysaccharide-Induced RAW264.7 Macrophages*. *Nanomaterials (Basel)*, 2022. **12**(23).
135. Jin, Y., et al., *Berberine Suppressed the Progression of Human Glioma Cells by Inhibiting the TGF- β 1/SMAD2/3 Signaling Pathway*. *Integr Cancer Ther*, 2022. **21**: p. 15347354221130303.
136. Sanz-Rodriguez, F., et al., *Endoglin regulates cytoskeletal organization through binding to ZRP-1, a member of the Lim family of proteins*. *J Biol Chem*, 2004. **279**(31): p. 32858-68.
137. Bremnes, R.M., C. Camps, and R. Sirera, *Angiogenesis in non-small cell lung cancer: The prognostic impact of neoangiogenesis and the cytokines VEGF and bFGF in tumours and blood*. *Lung Cancer*, 2006. **51**(2): p. 143-158.

138. Yum, H.Y., et al., *Allergen-induced coexpression of bFGF and TGF- β 1 by macrophages in a mouse model of airway remodeling: bFGF induces macrophage TGF- β 1 expression in vitro*. *Int Arch Allergy Immunol*, 2011. **155**(1): p. 12-22.
139. Zanini, A., et al., *The role of the bronchial microvasculature in the airway remodelling in asthma and COPD*. *Respir Res*, 2010. **11**(1): p. 132.
140. Wang, Y., et al., *Role of inflammatory cells in airway remodeling in COPD*. *Int J Chron Obstruct Pulmon Dis*, 2018. **13**: p. 3341-3348.
141. Fezza, M., et al., *DKK1 promotes hepatocellular carcinoma inflammation, migration and invasion: Implication of TGF- β 1*. *PLoS One*, 2019. **14**(9): p. e0223252.
142. Li, X., et al., *Berberine hydrochloride IL-8 dependently inhibits invasion and IL-8-independently promotes cell apoptosis in MDA-MB-231 cells*. *Oncol Rep*, 2014. **32**(6): p. 2777-88.
143. Liu, L., et al., *Berberine inhibits growth and inflammatory invasive phenotypes of ectopic stromal cells: Imply the possible treatment of adenomyosis*. *J Pharmacol Sci*, 2018. **137**(1): p. 5-11.
144. Li, J., et al., *Berberine hydrochloride inhibits cell proliferation and promotes apoptosis of non-small cell lung cancer via the suppression of the MMP2 and Bcl-2/Bax signaling pathways*. *Oncol Lett*, 2018. **15**(5): p. 7409-7414.
145. Zhang, L.C., et al., *Berberine alleviates dextran sodium sulfate-induced colitis by improving intestinal barrier function and reducing inflammation and oxidative stress*. *Exp Ther Med*, 2017. **13**(6): p. 3374-3382.
146. Poindexter, N.J., et al., *IL-24 is expressed during wound repair and inhibits TGF α -induced migration and proliferation of keratinocytes*. *Exp Dermatol*, 2010. **19**(8): p. 714-22.
147. Sokol, J.P. and W.P. Schiemann, *Cystatin C antagonizes transforming growth factor beta signaling in normal and cancer cells*. *Mol Cancer Res*, 2004. **2**(3): p. 183-95.
148. Tian, M. and W.P. Schiemann, *Preclinical efficacy of cystatin C to target the oncogenic activity of transforming growth factor Beta in breast cancer*. *Transl Oncol*, 2009. **2**(3): p. 174-83.
149. Vyas-Read, S., et al., *Nitric oxide attenuates epithelial-mesenchymal transition in alveolar epithelial cells*. *Am J Physiol Lung Cell Mol Physiol*, 2007. **293**(1): p. L212-21.

150. Wang, Y., et al., *Berberine prevents hyperglycemia-induced endothelial injury and enhances vasodilatation via adenosine monophosphate-activated protein kinase and endothelial nitric oxide synthase*. Cardiovascular Research, 2009. **82**(3): p. 484-492.
151. Huang, C., et al., *Berberine inhibits epithelial-mesenchymal transition and promotes apoptosis of tumour-associated fibroblast-induced colonic epithelial cells through regulation of TGF- β signalling*. Journal of Cell Communication and Signaling, 2020. **14**(1): p. 53-66.
152. Du, H., et al., *Berberine Suppresses EMT in Liver and Gastric Carcinoma Cells through Combination with TGF β R Regulating TGF- β /Smad Pathway*. Oxid Med Cell Longev, 2021. **2021**: p. 2337818.
153. Kim, S., et al., *Berberine Suppresses Cell Motility Through Downregulation of TGF- β 1 in Triple Negative Breast Cancer Cells*. Cell Physiol Biochem, 2018. **45**(2): p. 795-807.
154. Chu, S.C., et al., *Berberine reverses epithelial-to-mesenchymal transition and inhibits metastasis and tumor-induced angiogenesis in human cervical cancer cells*. Mol Pharmacol, 2014. **86**(6): p. 609-23.
155. Sun, Y., et al., *Berberine inhibits glioma cell migration and invasion by suppressing TGF- β 1/COL11A1 pathway*. Biochem Biophys Res Commun, 2022. **625**: p. 38-45.
156. Lieber, M., et al., *A continuous tumor-cell line from a human lung carcinoma with properties of type II alveolar epithelial cells*. Int J Cancer, 1976. **17**(1): p. 62-70.
157. Watanabe, T., et al., *Comparison of lung cancer cell lines representing four histopathological subtypes with gene expression profiling using quantitative real-time PCR*. Cancer Cell International, 2010. **10**(1): p. 2.
158. Schuliga, M., *NF-kappaB Signaling in Chronic Inflammatory Airway Disease*. Biomolecules, 2015. **5**(3): p. 1266-83.
159. Brookes, O., et al., *Co-culture of type I and type II pneumocytes as a model of alveolar epithelium*. PLoS One, 2021. **16**(9): p. e0248798.
160. Arezki, Y., et al., *A Co-Culture Model of the Human Respiratory Tract to Discriminate the Toxicological Profile of Cationic Nanoparticles According to Their Surface Charge Density*. Toxics, 2021. **9**(9).
161. Zamprogno, P., et al., *Second-generation lung-on-a-chip with an array of stretchable alveoli made with a biological membrane*. Communications Biology, 2021. **4**(1): p. 168.

162. Justilien, V. and A.P. Fields, *Utility and applications of orthotopic models of human non-small cell lung cancer (NSCLC) for the evaluation of novel and emerging cancer therapeutics*. *Curr Protoc Pharmacol*, 2013. **62**: p. 14.27.1-14.27.17.
163. Ghorani, V., et al., *Experimental animal models for COPD: a methodological review*. *Tobacco Induced Diseases*, 2017. **15**(1): p. 25.
164. Liu, G., et al., *Adverse roles of mast cell chymase-1 in chronic obstructive pulmonary disease*. *Eur Respir J*, 2022.
165. Stellari, F., et al., *Monitoring inflammation and airway remodeling by fluorescence molecular tomography in a chronic asthma model*. *Journal of Translational Medicine*, 2015. **13**(1): p. 336.
166. Kim, D., Y.S. Lin, and C.L. Haynes, *On-chip evaluation of shear stress effect on cytotoxicity of mesoporous silica nanoparticles*. *Anal Chem*, 2011. **83**(22): p. 8377-82.
167. Hoffman, S.M., et al., *Endoplasmic reticulum stress mediates house dust mite-induced airway epithelial apoptosis and fibrosis*. *Respiratory Research*, 2013. **14**(1): p. 141.

APPENDIX I

Published version of main thesis chapters

CHAPTER 2

Research Paper #1

Anticancer activity of NFκB decoy oligonucleotide-loaded nanoparticles against human lung adenocarcinoma

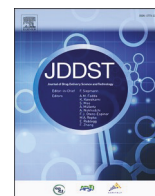
(Kannaujiya VK[#], De Rubis G[#], Paudel KR, Manandhar B, Chellappan DK, Singh SK, MacLoughlin R, Gupta G, Xenaki D, Kumar P, Hansbro PM, Oliver BGG, Wich PR, Dua K. *Anticancer activity of NFκB decoy oligonucleotide-loaded nanoparticles against human lung cancer*, **Journal of Drug Delivery Science and Technology**. 2023 Apr 82; 104328, doi: <https://doi.org/10.1016/j.jddst.2023.104328>.)

[#] Authors contributed equally to this work



Contents lists available at ScienceDirect

Journal of Drug Delivery Science and Technology

journal homepage: www.elsevier.com/locate/jddst

Anticancer activity of NFκB decoy oligonucleotide-loaded nanoparticles against human lung cancer

Vinod Kumar Kannaujiya^{a,b,1}, Gabriele De Rubis^{c,d,1}, Keshav Raj Paudel^e,
Bikash Manandhar^{c,d}, Dinesh Kumar Chellappan^f, Sachin Kumar Singh^{d,g},
Ronan MacLoughlin^{h,i,j}, Gaurav Gupta^{k,l,m}, Dikaia Xenakiⁿ, Pradeep Kumar^o,
Philip Michael Hansbro^e, Brian Gregory George Oliver^{n,p,**}, Peter Richard Wich^{a,b,***},
Kamal Dua^{c,d,*}

^a School of Chemical Engineering, University of New South Wales, Sydney, NSW, 2052, Australia

^b Australian Centre for NanoMedicine, University of New South Wales, Sydney, NSW, 2052, Australia

^c Discipline of Pharmacy, Graduate School of Health, University of Technology Sydney, Sydney, NSW, 2007, Australia

^d Faculty of Health, Australian Research Centre in Complementary and Integrative Medicine, University of Technology Sydney, Ultimo, NSW, 2007, Australia

^e Centre for Inflammation, Centenary Institute and University of Technology Sydney, Faculty of Science, School of Life Sciences, Sydney, NSW, 2007, Australia

^f Department of Life Sciences, School of Pharmacy, International Medical University, Bukit Jalil, 57000, Kuala Lumpur, Malaysia

^g School of Pharmaceutical Sciences, Lovely Professional University, Jalandhar-Delhi GT Road, Phagwara, 144411, Punjab, India

^h Research and Development, Aerogen, IDA Business Park, Dangan, Galway, H91HE94, Ireland

ⁱ School of Pharmacy & Biomolecular Sciences, Royal College of Surgeons in Ireland, D02 YN77, Dublin, Leinster, Ireland

^j School of Pharmacy & Pharmaceutical Sciences, Trinity College, D02 PN40, Dublin, Leinster, Ireland

^k School of Pharmacy, Suresh Gyan Vihar University, Jaipur, 302017, Rajasthan, India

^l Uttaranchal Institute of Pharmaceutical Sciences, Uttaranchal University, Dehradun, 248007, Uttarakhand, India

^m Department of Pharmacology, Saveetha Dental College, Saveetha Institute of Medical & Technical Sciences, Saveetha University, Chennai, 602105, India

ⁿ Woolcock Institute of Medical Research, University of Sydney, Sydney, New South Wales, Australia

^o Wits Advanced Drug Delivery Platform Research Unit, Department of Pharmacy and Pharmacology, School of Therapeutic Sciences, Faculty of Health Sciences, University of the Witwatersrand, Johannesburg, South Africa

^p School of Life Sciences, University of Technology Sydney, Ultimo, NSW, 2007, Australia

ARTICLE INFO

Keywords:

AcDex nanoparticles
Decoy oligodeoxynucleotides
Lung cancer
NSCLC
Migration
Proliferation
NFκB
Pulmonary delivery

ABSTRACT

Non-small cell lung cancer (NSCLC) is among the leading global causes of cancer-related mortality. Current treatment options have limited efficacy and severe adverse effects, underlining the necessity for innovative therapeutic strategies. Among emerging strategies, NFκB inhibition is particularly promising, as NFκB is considered a master regulator of NSCLC pathogenesis. NFκB activity can be efficiently inhibited by double-stranded decoy oligodeoxynucleotides (ODNs). However, therapeutic use of ODNs is strongly limited by enzymatic degradation and poor transport across cell membranes. In this study, we report the encapsulation of a small hydrophilic NFκB decoy ODN into a biodegradable, biocompatible, and acid-responsive dextran-based nanoparticle (NP) system. This formulation has shown excellent encapsulation efficiency (up to 99.5%) with 185 nm average particle size and pH-dependent ODN release at acidic pH. NFκB decoy ODN NPs showed promising anticancer activity, with significant anti-proliferative, anti-migratory, and anti-colony formation activity. These were measured by MTT assay, Boyden chamber and scratch wound healing assays, and crystal violet staining, respectively. Mechanistically, the anti-proliferative effect was exerted through the activation of the expression of key genes regulating apoptosis and necroptosis such as TNF-α, RIPK1, RIPK3, and MLKL. The findings of this study provide the foundations for further investigation of the molecular mechanisms by which NFκB inhibition results in anticancer activity, simultaneously providing proof-of-concept of the therapeutic potential of dextran-based nanoparticles carrying NFκB decoy ODNs against NSCLC.

* Corresponding author. Discipline of Pharmacy, Graduate School of Health, University of Technology Sydney, Sydney, NSW, 2007, Australia.

** Corresponding author. Woolcock Institute of Medical Research, University of Sydney, Sydney, New South Wales, Australia.

*** Corresponding author. School of Chemical Engineering, University of New South Wales, Sydney, NSW, 2052, Australia.

*N) ("#88-&11&DY#n.oliver@uts.edu.au (B.G.G. Oliver), p.wich@unsw.edu.au (P.R. Wich), kamal.dua@uts.edu.au (K. Dua).

¹ These two authors contributed equally to this work.

<https://doi.org/10.1016/j.jddst.2023.104328>

Received 20 November 2022; Received in revised form 28 February 2023; Accepted 2 March 2023

Available online 9 March 2023

1773-2247/© 2023 Elsevier B.V. All rights reserved.

1. Introduction

Across all cancer types, lung cancer (LC) is one of the leading causes of death, with more than 1.7 million LC-related deaths recorded in the world in 2020 [1]. Non-small-cell lung cancer (NSCLC) represents the majority (85%) of LC cases [2]. The five-year survival rate of LC is only 17.8%, lower than that of other main cancers [3]. Besides smoking, other factors causing LC include increasing urbanization and environmental pollution [4].

The current mainstay treatment modalities for LC include surgery [5], chemotherapy [6], radiotherapy [7], targeted therapy [8], and immunotherapy [9,10]. Despite the availability of numerous treatment strategies, a large percentage of patients experience relapse and treatment resistance [9]. This, together with the elevated chemo- and radiation toxicity associated to chemotherapy and radiotherapy [11], demonstrates the urgency for the development of innovative NSCLC treatment strategies with increased efficacy and reduced toxicity [12–14].

Nuclear factor κ B (NF κ B) represents a family of transcription factors that was discovered in 1987 as factors binding to the enhancer of κ immunoglobulins in activated B cells [15]. Since then, NF κ B has been found to have a pivotal role in the transcriptional regulation of a plethora of cellular responses, particularly related to the immune system and inflammation [16]. Besides its role in the immune response, NF κ B is an essential contributor to many cancer hallmarks, as its activation promotes phenomena such as tumour cell proliferation and survival [17], and it is considered the key point of connection between persistent infections, chronic inflammation, and increased cancer risk [18]. In NSCLC, NF κ B is considered a master regulator of cancer pathogenesis and progression, influencing many aspects of this cancer such as proliferation [19], cancer survival [20], cancer cell migration, infiltration and metastasis [21], and epithelial-to-mesenchymal transition (EMT) [22]. Recently, increased NF κ B expression in NSCLC was associated with reduced overall survival and 5-year survival rate, worsening tumour stage, and lymph node metastasis [23]. This supports the potential of targeting and inhibiting NF κ B as an effective approach for LC therapy [24,25], and numerous molecules inhibiting the NF κ B pathway are currently being studied [26]. Despite this, no NF κ B targeting treatment has reached clinical approval for application as cancer therapy.

Among the many possible modalities of NF κ B inhibition for therapeutic purposes, the use of decoy oligodeoxynucleotides (ODNs) represents a viable strategy [27,28]. Decoy ODNs are therapeutic molecules consisting in double-stranded synthetic oligonucleotides with a sequence that mimics the DNA target sequence of the intended transcription factor. As a consequence, the transcription factor binds specifically to the decoy ODN, and fewer copies of the transcription factor are available to bind the target DNA, resulting in the net inhibition of the transcription factor's activity [29]. For this reason, decoy ODNs represent promising tools to finely regulate the activity of specific transcription factors in many diseases [30,31]. In a recent study, for example, the transfection with a NF κ B decoy ODN resulted in strong suppression of the proliferation of the androgen-independent prostate cancer cell line PC-3M, together with induction of apoptosis [32]. Despite the versatility of decoy ODNs, these therapeutic tools have many limitations, including lack of tissue specificity in the case of systemic administration [33] and, importantly, an unfavourable pharmacokinetic profile [27] characterised by two major issues: (1) low cellular permeability due to the large size and presence of negative charges; and (2) instability of the ODN under *in vivo* conditions due to nuclease activity [34]. This results in reduced therapeutic efficacy [27,35,36]. Despite structural ODN modifications such as peptide nucleic acids (PNAs) [37], locked nucleic acids (LNAs) [38] and phosphorothioate-substituted ODNs [33] resulted in increased resistance to degradation, concerns about toxicity, side effects, poor binding efficacy and specificity of these nucleotide derivatives remain [27]. For this reason, there is a need to develop suitable delivery systems for NF κ B decoy delivery to the target

site of action [39].

One potential strategy to efficiently deliver ODN cargo to target cells is represented by the use of advanced nanocarriers allowing pulmonary delivery through nebulization [40]. De Rosa et al. have reported a biodegradable polymer, poly(DL-lactic co-glycolic acid) (PLGA)-based micro spherical particle, for the delivery of NF κ B decoy ODN in RAW 264.7 macrophages, obtaining sustained release of ODN together with inhibition of NF κ B at low concentrations [41]. Similarly, NF κ B ODN-loaded PLGA microspheres were reported to achieve site-specific delivery of ODN in a rat-carrageenin sponge implant model, inhibiting NF κ B activation in chronic inflammation [42].

Polysaccharide-based drug delivery systems have gained a considerable interest due to properties such as biocompatibility, biodegradability, and easy chemical modification [43,44]. Recently, NF κ B/p65 antisense oligonucleotide-loaded chitosan-based nanoparticles (NPs) were reported to achieve an excellent loading efficiency exploiting ionic interactions between cationic chitosan and anionic nucleotides [45]. Similarly, Cohen et al. have reported an acid-responsive acetalated dextran-based nanocarrier for the delivery of siRNA to HeLa-luc cells [46]. Upon cellular uptake, the acetal groups undergo hydrolysis under slightly acidic environments such as those found in lysosomes/late endosomes and, importantly, in the tumour microenvironment [47]. This generates water-soluble dextran material, acetone, and methanol as side product [48]. The hydrolysis of the acetal groups initiates the disassembly of NPs and the controlled release of the payload [49]. Additionally, the dextran side chain was modified with spermine to introduce cationic moieties in the polymer, thus facilitating encapsulation of highly polyanionic siRNA molecules through electrostatic interactions. Furthermore, the cationic nature of spermine-modified acetalated dextran (SpAcDex) NPs has shown enhanced cellular uptake due to the electrostatic interactions occurring with the negatively charged cell membrane [50].

In this study, we encapsulated NF κ B double-stranded decoy ODNs into SpAcDex NPs and evaluated the anticancer activity of this formulation in the human A549 NSCLC cell line. The present study is the first in which an NF κ B decoy ODN is encapsulated within a bio-compatible, acid-responsive delivery system, which allows selective release of the payload in the acidic tumor microenvironment. This has the potential to minimize adverse effects caused by the off-target, aspecific inhibition of NF κ B in healthy cells. The formulation revealed a strong anticancer activity, with significant inhibition of cancer hallmarks including cancer cell proliferation, migration, and ability to form clonal colonies. Mechanistically, the anti-proliferative effect of this formulation was achieved by enhancing the expression of genes mediating apoptosis and necroptosis such as tumor necrosis factor- α (TNF- α), Receptor-interacting serine/threonine-protein kinases 1 and 3 (RIPK1, RIPK3), and Mixed lineage kinase domain-like (MLKL). This study provides proof-of-concept of the suitability of SpAcDex NP-based ODN formulations for the therapeutic inhibition of NF κ B in NSCLC.

2. Materials and methods

2.1. Materials

Dextran (Mw 9–11 kDa, from *Leuconostoc mesenteroides*) was purchased from (Sigma Aldrich). Sodium periodate, 2-Methoxy propene, spermine, Sodium borohydride were purchased from Merck. Water used during particle preparation was adjusted to pH 8 with triethylamine (Sigma Aldrich). All buffers and water used for the preparation of SpAcDex-based NPs were in nuclease free and filtrated through syringe filters (Millex, sterile PES membrane, pore size 0.22 μ m, Merck). Brandon Digital Sonifier 450 (Power: 400 W; Line Voltage: 200–245 @ 50/60 Hz, Sonic Tip Micro Tapered 1/8). Dynamic light scattering (DLS) (Malvern Zetasizer Nano ZS). NF κ B decoy ODN and scramble decoy ODN were purchased from Merck, Bayswater, VIC, Australia MTT (3-[4,5-dimethylthiazol-2-yl]-2,5-diphenyl tetrazolium bromide),

crystal violet, DMSO, H/E staining solutions Dulbecco's Modified Eagle's Medium (DMEM), fetal bovine serum (FBS), and penicillin and streptomycin were purchased from Sigma-Aldrich, St. Louis, MO, USA. All remaining agents and solvents used in experiments involving cell culture were purchased from Sigma-Aldrich unless stated otherwise.

2.2. Synthesis of spermine-functionalized acetalated dextran

The spermine-functionalized acetalated dextran was synthesized over three steps according to literature [46].

Partial Oxidation of Dextran (OxDex): For the synthesis of partially oxidized dextran, dextran (2.0 g, 12.3 mmol) was dissolved in 8.0 mL dd-H₂O. The solution was stirred for 5 h at room temperature after sodium periodate (480 mg, 2.25 mmol) addition. Further, the reaction mixture was dialyzed against dd-H₂O for 3 days using a snakeskin regenerated cellulose membrane with MWCO of 3500 g/mol. After lyophilization, a colourless powder (1.3 g) was obtained, with an aldehyde content of 8.9 ± 0.02 mol aldehyde per 100 mol anhydrous glucose units (AGU) confirmed by BCA assay.

Acetalation of Partially Oxidized Dextran (OxAcDex): The solubility switch from hydrophilic to hydrophobic dextran was obtained as described by *Bachelder* et al. The oxidized dextran (1 g, 6.17 mmol) was dissolved in DMSO (12.0 mL). Further, 2-methoxypropene (2.6 g, 36 mmol) was added slowly after addition of pyridinium *p*-toluenesulfonate (22 mg, 0.088 mmol). The reaction mixture was stirred for 10 min at room temperature followed by reaction quenching with the help of triethylamine (1 mL) [48]. The resulting reaction mixture was precipitated in dd-H₂O pH 8 (100 mL) and isolated by centrifugation (12,000 g, 20 min, 4 °C). The product was further washed 5 times with dd-H₂O pH 8. After lyophilization, the OxAcDex (1.2 g) was obtained as a colorless powder. The obtained product contains 79.1% acetals, where 30.2% are cyclic and 48.9% are acyclic acetals.

Spermine Modification of OxAcDex (SpAcDex): To further modify oxidized acetalated dextran with spermine, the Ox-AcDex (1.0 g, (AGU) 202 g/mol, 5.05 mmol) was dissolved in DMSO (4.5 mL). After addition of spermine (1 g, 5.05 mmol), the reaction mixture was incubated with continuous stirring for 24 h at 40 °C. Afterwards, sodium borohydride (560 mg, 15.2 mmol) was added, and reaction was stirred for additional 24 h at 50 °C. After purification using similar method as mentioned above, the product was lyophilized to obtain a white powder. The degree of functionalization was determined by elementary analysis (1.36% N, 53.46% C and 7.83% H) and resulted in 4.8 mol spermine per 100 mol AGU.

2.3. Transcription factor decoy ODN

Single stranded decoy ODN to double stranded NFκB inhibitor was obtained by annealing. The sequence of sense and antisense oligodeoxynucleotides was annealed in 1 × annealing buffer (20 mM Tris-HCl, 20 mM MgCl₂ and 50 mM NaCl, pH 7.5). The mixture was heated at 80 °C for 5 min and allowed to cool slowly at room temperature overnight.

The sequence of the ODN decoy to NFκB used was.

(1) NFκB decoy ODN sequence

5'-CCTGAAGGGATTTCCCTCC-3'
3'-GGAACCTCCCTAAAGGGAGG-5'

(2) scrambled decoy ODN sequence

5'-TTGCCGTACCTGACTTAGCC-3'
3'-AACGGCATGGACTGAATCGG-5'

2.4. Nanoparticle preparation

ODN-loaded and empty nanoparticles were prepared by a double emulsion method using a probe sonicator. 10 mg spermine-modified acetalated dextran was dissolved in 800 μL dichloromethane (DCM) and 130 μL phosphate-buffered saline (PBS) with and without 121.5 μg annealed ODN was added for loaded and empty nanoparticle formulations, respectively. The first sonication was performed for 10 s followed by addition of 4 mL polyvinyl alcohol (PVA) solution (3% w/w in PBS, 13–27 kDa, 87–89% partially hydrolyzed) on top of primary emulsion. Further, a second sonication was performed for 30 s to achieve a secondary water-in-oil-in-water emulsion. The resulting emulsion was stirred overnight to allow DCM evaporation followed purification by ultracentrifugation (45,000×g, 20 min, 20 °C) and was washed three times with 4.0 mL dd-H₂O (pH 8). Before lyophilization, 50 μL PVA solution (0.3% w/w in dd-H₂O pH 8) was added as cryoprotectant. The particle yield was about 60%, based on the initial spermine-modified dextran material.

2.5. Measurement of particle size and zeta potential

The size of the different dextran-based NP was determined by nanoparticle dynamic light scattering (DLS), using a Malvern Zetasizer Nano ZS. All NP samples were measured in dd-H₂O (pH 8.0) after sonication (Unisonics FXP) for 60 s at 25 °C in triplets. The size calculation was performed with Malvern software. Zeta potential (particle charge) was measured using a clear disposable zeta cell. Three measurements with 20 individual runs each were performed at 25 °C. Particle samples were prepared at concentrations of 0.1 mg/mL in HEPES buffer (25 mM, pH 7.4). The calculation was performed with the Malvern Zetasizer software 6.20. Data shown represent the average zeta potential (standard deviation of distributions of three sequential measurements).

2.6. Scanning electron microscopy (SEM)

Particle shape and morphology were analyzed by scanning electron microscopy (SEM). The freeze-dried Dex(ODN-loaded) NPs dispersed in distilled (1 mg⁻¹ mL) were dried and coated with Pt layer under argon atmosphere. Images of the samples were taken on an FEI Nova Nano SEM 230 FE-SEM at an accelerating voltage of 5.0 kV.

2.7. Determination of ODN loading by RiboGreen assay

An indirect method of quantification was performed to determine the encapsulated double-stranded decoy ODN in double emulsion particles using the Quant-iT™ RiboGreen® assay [51]. Here, particle solution was centrifuged after particle formation and solvent evaporation. The amount of free decoy ODN present in the supernatant was then quantified and compared with the initial concentration of decoy ODN used in particle formulation [52]. The non-encapsulated decoy ODN present in the supernatant was able to react with the RiboGreen® reagent resulting in a fluorescent compound with an emission maximum at 535 nm (λ_{ex} = 485 nm). To determine the decoy ODN content, 10 μL of the supernatant was combined with 90 μL of PBS in a black, flat-bottom 96-well microplate. Meanwhile, the pure double-stranded decoy ODN was diluted in PBS to a concentration that ensured 100% encapsulation. The RiboGreen® reagent was diluted 1:200 with PBS, and 100 μL was added to each well, resulting in a total volume of 200 μL per well. The reaction mixture was then carefully incubated for 5 min in the dark before the fluorescence of the reacted dye was recorded using a Tecan microplate reader. To further verify any presence of free decoy ODN in the nanoparticle pellets, the particles were washed twice with nuclease free pH 8.0 water and ODN content were measured in supernatant. The results were compared with the fluorescence of the theoretical amount of encapsulated decoy ODN using Microsoft Excel to determine total ODN loading. Loading content and encapsulation efficiency was calculated

according to formula as LC and EE.

$$LC \text{ (wt \%)} = \frac{\text{weight of ODN in particle}}{\text{weight of ODN - loaded particle}} \bullet 100\% \quad (1)$$

$$EE \text{ (wt \%)} = \frac{\text{weight of ODN in particle}}{\text{weight of total ODN used in particle formulation}} \bullet 100\% \quad (2)$$

2.8. pH-dependent degradation of SpAcDex particles

Empty particles were suspended in triplicate at a concentration of 0.25 mg/mL in either a 0.3 M acetate buffer (pH 5.5) or PBS (pH 7.4) buffer and incubated at 37 °C under gentle agitation using a MultiTherm shaker (Eppendorf). At various time points, the size distribution of the samples was measured using DLS. For visual observation, the particles were incubated at a concentration of 2.5 mg/mL and were photographed at various time points.

2.9. pH-dependent release of decoy ODN from SpAcDex particles

ODN-loaded particles were incubated at a concentration of 5 mg/mL in either a 0.3 M acetate buffer (pH 5.5) or PBS (pH 7.4) buffer at 37 °C temperature under gentle agitation using a thermo incubator (Eppendorf). At different time interval the aliquots were collected and centrifuged at 10 000 g for 10 min to pellet out insoluble materials, and the supernatant was stored at -20 °C. The release ODN in the supernatant sample was quantified by Quant-iT™ RiboGreen® assay. The amount of ODN in each sample was calculated by fitting the emission to a calibration curve using the Quant-iT™ RiboGreen® assay. For this experiment, all solutions included heparin at 25 mg/mL to disrupt electrostatic interactions between polymer amines and decoy ODN to enable quantification.

2.10. ODN molecular generation and visualization

The double stranded molecular structures of NFκB and scrambled ODNs were generated using the default DNA/RNA builder tool in Avogadro 2.0.8.0 Molecule Editor & Visualizer System [53]. The generated ODN structure was then visualized and scanned using UCSF Chimera 1.14 Molecular Modelling System employing conventional Nucleic Acid Database (NDB) colors and formats [54].

2.11. Cell culture

A549 (human lung epithelial carcinoma) and BEAS-2B (human non-cancerous bronchial epithelial) cell lines (ATCC, USA) were a kind gift from Prof. Alaina Ammit, Woolcock Institute of Medical Research, Sydney, Australia. Cells were cultured in DMEM supplemented with 10% FBS, 1% penicillin and streptomycin, in a humidified 37 °C incubator supplied with 5% CO₂.

2.12. Cell viability assessment - MTT assay

The MTT assay was performed to assess A549 and BEAS-2B cell proliferation and viability as previously described [55,56]. Briefly, 5000 A549 cells/well were seeded in a 96-well plate and, 24 h post attachment, cells were treated with Dex(NFκB-ODN) NPs or Dex (scrambled-ODN) NPs or empty nanoparticles at different concentrations (corresponding to 0.5, 1, 2.5, 5, 10 nM ODN). Twenty-four hours after treatment, MTT solution (20 μL of a 5 mg/mL stock solution MTT in PBS, for a final concentration of 0.5 mg/mL MTT) was added to the wells and the mixture was incubated at 37 °C for 4 h. Successively, the supernatant was removed and 100 μL dimethyl sulphoxide (DMSO) were added to each well to dissolve the formazan crystals. The absorbance of the wells was then read using an UV/VIS spectrophotometer at a wavelength of 540 nm. The percent viability of the cells treated with

either Dex(NFκB-ODN) NPs or Dex(scrambled-ODN) NPs or empty NPs was reported as percentage compared to the control (untreated) group.

2.13. Wound healing assay

The wound healing assay was performed as reported previously [57–59] to assess the anti-migratory activity of the Dex(NFκB-ODN) NPs on A549 cells. Briefly, 3*10⁵ A549 cells/well were seeded into 6-well plates and cultured until confluency. The cell monolayer was scratched using the tip of a sterile 200 μL pipette tip, followed by multiple washing steps with PBS. Images at 0 h time point were taken after PBS washing, then A549 cells were treated with 10 nM Dex(NFκB-ODN) NPs or concentration-matched Dex(scrambled-ODN) NPs for 24 h. The distance between the edges of the scratch before and 24 h after treatment was measured using the IS capture software after imaging with a light microscope at 10× magnification, and the percentage wound closure was reported compared to the control (untreated) group.

2.14. Boyden's chamber assay

To determine A549 cells migration, a modified Boyden's chamber assay was performed as previously described [58,60], using transwell permeable supports (6.5-mm insert 8-μM pore size polycarbonate membrane). First, the lower surface of the membranes was coated with 2.5% gelatin in 1 M acetic acid for 1 h. Subsequently, cells were seeded in the upper chamber at a density of 10⁴ cells/mL in a volume of 200 μL DMEM culture media. The chamber was then placed in a well containing 600 μL DMEM. After attachment, the cells were treated with 10 nM Dex (NFκB-ODN) NPs or concentration-matched Dex(scrambled-ODN) NPs for 24 h, and cells were allowed to migrate for 24 h more after the end of the treatment. Following this, the non-migrated cells remaining in the upper surface of the membrane were removed using cotton swabs, while the cells that successfully migrated reaching the lower surface were fixed in 10% formalin and stained with hematoxylin and eosin. Finally, the cells that had clearly migrated through the pores of the membranes were counted in 5 random fields with a light microscope, with a 20× magnification. Average cells per field of view were then calculated and reported.

2.15. Colony formation assay

The colony formation assay was performed as reported previously [58,61] to test the anti-colony formation activity of Dex(NFκB-ODN) NPs in A549 cells. First, cells were seeded at a density of 500 cells/well into six-well plates. Following adhesion, cells were treated with 10 nM Dex(NFκB-ODN) NPs or concentration-matched Dex(scrambled-ODN) NPs. After colony development (about 2 weeks), the cells were washed with PBS and fixed with 3.7% formaldehyde for 20 min. Successively, cells were washed again with PBS and stained with 0.4% crystal violet, then washed four to five times with PBS. The colonies were finally counted using the ImageJ software.

2.16. Real-time qPCR

The effects of Dex(NFκB-ODN) NPs on the mRNA expression levels of proliferation-related genes were assessed through quantitative real-time PCR (qPCR) as described in a previous study [61]. First, 1.5*10⁵ A549 cells/well were seeded into 6-well plates and left to attach overnight. The following day, cells were treated with 10 nM Dex(NFκB-ODN) NPs or concentration-matched Dex(scrambled-ODN) NPs for 24 h. After the treatment, the cells were lysed with 500 μL TRI reagent (Sigma-Aldrich, Australia). The samples were vortexed for 45 s to ensure complete cell rupture. Successively, 125 μL chloroform (Sigma-Aldrich, Australia) were added and the samples were centrifuged at 12,000 g, 3 °C, for 15 min. The aqueous layer was transferred into fresh tubes and the RNA was precipitated by adding 250 μL ice-cold isopropyl alcohol

(Sigma-Aldrich, Australia). The tubes were then centrifuged at 12,000 g, 3 °C, for 10 min. After centrifugation, the supernatant was removed, and the precipitated RNA pellets were washed twice with 1 mL 75% ethanol (Sigma-Aldrich, Australia), centrifuging the tubes at 8000 g, 4 °C, for 5 min each time. After the second centrifugation, the ethanol was removed, and dried RNA pellets were dissolved in 20 µL nuclease-free water (Sigma-Aldrich, Australia). Nanodrop (Thermo Fisher Scientific, Waltham, MA, USA) was used to determine the concentration and purity of the RNA samples.

The RNA samples were subjected to DNase I (Sigma-Aldrich, Australia) treatment. Successively, 800 ng total RNA was reverse-transcribed to cDNA using the reaction mixture of M-MLV buffer (Thermo Fisher Scientific), random primers (0.5 µg/µL, Thermo Fisher Scientific), dNTPs (10 mM, Thermo Fisher Scientific) and DTT (100 mM, Thermo Fisher Scientific). For the reverse transcription reaction, a thermal cycler (Eppendorf, Hamburg, Germany) was used with the following steps: denaturation (65 °C, 10 min), annealing (25 °C, 10 min), reverse transcription (37 °C, 50 min), and enzyme inactivation (70 °C, 15 min). An amount of 16 ng of cDNA from each sample was then subjected to real-time qPCR using the iTaq Universal SYBR green (BioRad, Hercules, CA, USA) mix and gene-specific primers (forward and reverse, 0.5 µM each, Sigma-Aldrich, Australia). The thermal cycler used was a CFX96 PCR system (BioRad). The real-time qPCR protocol included the following cycles: 95 °C for 30 s (1 cycle), 95 °C for 15 s (50 cycles) and 60 °C for 30 s (1 cycle). The human gene for Glyceraldehyde 3-phosphate dehydrogenase (GAPDH) has been used as a control for normalization.

The sequences of human primers used were as follows.

Gene name	FW sequence	RV sequence
TNF-α	AGGCAGTCAGATCATCTTC	TTATCTCTCAGCTCCAGG
RIPK1	TGATAATACCAGTAGTCTGACG	ACAGTTTTTCCAGTGCTTTC
RIPK3	AACITTCAGAAACCAGATGC	GTTGTATATGTTAACGAGCGG
MLKL	GTGAAGAATGTGAAGACTGG	AAGATTTTCATCCACAGAGGG
GAPDH	TCGGAGTCAACGGATTTC	CAACAATATCCACTTTACCAGAG

2.17. Statistical analysis

The data are represented as mean ± SEM. Statistical analysis was performed by ordinary one-way ANOVA, followed by Tukey multiple comparison test. The software used was GraphPad Prism (v.9.4, GraphPad Software, San Diego, CA, USA). In pairwise comparisons, a two-tailed p-value <0.05 was considered statistically significant. In Fig. 4d, a Mann-Whitney *U* test was performed between the 5 nM and 10 nM Dex(NFκB)

3. Results

3.1. Nanoparticle size and zeta potential

The obtained NPs were visualized and characterized by dynamic light scattering (DLS, Fig. 1a) and scanning electron microscopy (SEM, Fig. 1b). The spherical morphology of the NPs was confirmed by SEM data. Both empty and double stranded decoy ODN loaded particles have shown similar particle diameter distribution, in the range of 150–200 nm. A slight increase in the particle size distribution was observed in loaded particles compared to empty particles. The surface charge of the particles was determined by zeta-potential measurements (Table 1). A positive surface zeta-potential of 12.43 mV was observed for empty nanoparticles due to the presence of protonated amines on the particle surface. The encapsulation of the charged decoy ODN slightly reduced the surface zeta potential (11.83–12.37 mV) which is most likely due to the non-covalent adsorption of a small number of negatively charged decoy ODN on the surface of particles.

Molecular modelling was used to predict the three-dimensional structure of the ODNs, which demonstrated self-assembly into well-defined tubular structures with acidic phosphate groups forming the periphery of the tubular structure and amine groups aligning in the centre (Fig. S1). This is important for efficient encapsulation and loading of the ODNs into spermine-AcDex nanosystems, wherein the amines of the cationic polymer interact with the negatively charged peripheral phosphate groups of the ODNs [62].

3.2. Quantification of decoy ODN loading

An indirect method of quantification was performed to validate the successful encapsulation and quantification of decoy ODN loading [52] using the Quant-iT™ RiboGreen assay. The unloaded decoy ODN present in the supernatant was quantified after centrifugation followed by particle formulation and solvent evaporation. The amount of decoy ODN present in the supernatant represent the total amount of free decoy ODN, which has not been encapsulated in the particles. As the decoy ODN is highly soluble in water, any unencapsulated decoy ODN would stay in

Table 1

Physical characterization of empty, NFκB ODN and scrambled ODN loaded Dex NP.

Particle type	Diameter (nm)	PDI	Zeta-potential/mV
Dex(empty) NP	178 ± 1.0	0.20 ± 0.01	12.4 ± 0.5
Dex(NFκB-ODN) NP	187 ± 1.5	0.23 ± 0.01	11.8 ± 0.3
Dex(scrambled-ODN) NP	182 ± 6.0	0.24 ± 0.03	12.4 ± 0.5

(The data obtained from three replicate DLS measurements are represented as the mean ± standard deviation).

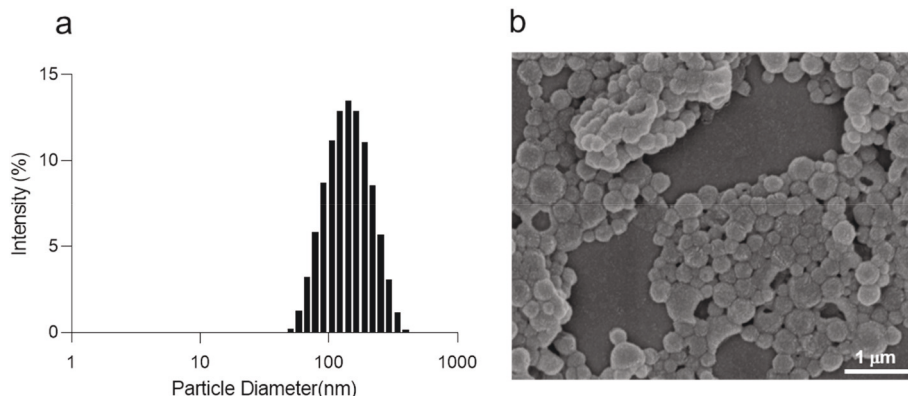


Fig. 1. Characterisation of decoy ODN-Encapsulated dextran NPs. (a) Size distribution obtained by DLS; (b) SEM analysis.

the supernatant. Furthermore, the particle pellets were washed twice with pH 8.0 nuclease-free water and a negligible amount of free decoy ODN was observed in the supernatant, providing confirmation of the successful encapsulation of the decoy ODN. Both NFκB and scrambled decoy ODN have shown a similar encapsulation efficiency of up to 99.5%. Overall, up to 11.89 μg decoy ODNs were encapsulated per mg NPs, as shown in Table 2.

3.3. pH-dependent particle degradation

The decoy ODN was encapsulated into an acid-responsive NPs to prevent the premature release of payload under physiological conditions. Under acidic conditions, the acetal groups present on the SpAcDex backbone undergo rapid hydrolysis, forming a water-soluble dextran, acetone and methanol that leads to particle degradation. To determine the degradation behaviour, the NPs were incubated at 37 °C in PBS buffer at pH 7.4 to simulate the physiological conditions of the blood stream and in acetate buffer at pH 5.5 to mimic the acidic tumour microenvironment. The successful pH-dependent particle degradation at acidic pH was confirmed by DLS measurements (Fig. 2a). The initial increase in particle size (calculated according to number distribution) can be explained by the uncontrolled aggregation of degradation materials and has been observed previously in similar polysaccharide-based nanosystems [63,64]. The degradation can also be detected by visually observing the particle solutions (Fig. 2b). While the typical nanoparticle opaqueness clears under acidic conditions, there was no significant change observed in PBS buffer pH 7.4, indicating the stability of the formulation under physiological conditions.

3.4. pH-dependent decoy ODN release

The decoy ODN-loaded particles were incubated at different pH values similar to the above experiment. The amount of ODNs released from dextran NPs were quantified by using a Quant-iT™ RiboGreen® assay. Heparin was used to prevent the electrostatic interactions between water soluble spermine modified dextran and negatively charged ODN. As expected, a fast release of decoy ODN up to 90% was observed within the first 8 h under acidic conditions [46], while physiological pH 7.4 has shown only a slight release of ODN even after 24 h (Fig. 3). In the first 5 min after incubation, almost 10% ODN release was observed under both conditions, indicating the adsorption of free ODN on the surface of particles due to electrostatic interaction between particle surface amine and ODN during formulation.

3.5. Anti-proliferative activity of NFκB-ODN-NPs in A549 and BEAS-2B cells

The effect of Dex(NFκB-ODN) NPs, Dex(scrambled-ODN) NPs, and empty NPs on the proliferation and viability of A549 and BEAS-2B cells is shown in Fig. 4. Dex(NFκB-ODN) NPs at concentrations of 2.5, 5 and 10 nM significantly reduced the proliferation rate of A549 cells by 13.4%, 27.8% and 37.2%, respectively, compared to control (untreated cells) in the MTT assay (Fig. 4a). Considering that the highest anti-proliferative effect was observed with 10 nM Dex(NFκB-ODN) NPs, this concentration has been used for the subsequent experiments. In comparison, treatment with the Dex(scrambled-ODN) NPs at 10 nM concentration resulted only in a relatively small reduction of cell

Table 2

Quantification of decoy ODN encapsulation.

Particle type	Decoy ODN in μg•mg ⁻¹ NP	Encapsulation efficiency (in %)
Dex(NFκB-ODN) NP	11.89	99.5
Dex(scrambled-ODN) NP	11.88	99.4

viability of 12% (Fig. 4b). To assess the effect of Dex(NFκB-ODN) NPs on the viability of non-cancerous cells, the nanoparticles were tested on BEAS-2B human bronchial epithelial cells. Dex(NFκB-ODN) NPs at concentrations of 1, 2.5, 5 and 10 nM significantly reduced the viability of BEAS-2B cells by 8.5%, 14.3%, 15.1%, and 19.2%, respectively, compared to control (untreated cells) in the MTT assay (Fig. 4d). The effect of 5 nM and 10 nM Dex(NFκB-ODN) NPs on BEAS-2B cell viability was significantly lower than the effect obtained by the same concentration of NPs on A549 cells proliferation (Fig. 4d), indicating the relative safety of these NPs for healthy cells compared to cancer cells. Treatment with Dex(scrambled-ODN) NPs did not result in a significant reduction of BEAS-2B cell viability (Fig. 4e). Finally, treatment with empty Dex NPs resulted in no significant effect on A549 and BEAS-2B cell viability at concentrations ranging between 0.5 and 10 μg/mL (Fig. 4c and f, respectively).

3.6. Effect of Dex(NFκB-ODN) NPs on the expression of apoptosis/necroptosis genes in A549 cells

To provide a mechanistic explanation of the anti-proliferative effects of Dex(NFκB-ODN) NPs on A549 cells, the effect of the nanoparticle formulation on the expression of transcripts encoding for TNF-α, RIPK1, RIPK3, and MLKL was assessed via real-time qPCR (Fig. 5). Dex(NFκB-ODN) NPs at 10 nM concentration induced a significant increase in the expression of RIPK1 (11.3%, Fig. 5a) and MLKL (10.8%, Fig. 5b). A similar trend was observed with the expression of TNF-α and RIPK3, which was induced on average by 4.9-fold (TNF-α, Figs. 5c) and 7.1-fold (RIPK3, Fig. 5d) upon treatment with 10 nM Dex(NFκB-ODN) NPs, without reaching statistical significance. Treatment with Dex (scrambled-ODN) NPs did not result in an increase of the expression of any of the four genes analyzed (Fig. 5a–d).

3.7. Anti-migratory activity of NFκB-ODN-NPs in A549 cells

The effect of Dex(NFκB-ODN) NPs on the migration of A549 cells was assessed by a wound healing assay (Fig. 6) and by a Boyden chamber assay (Fig. 7). Dex(NFκB-ODN) NPs successfully suppressed A549 cell migration in the wound healing assay for 24 h. This treatment has shown 54.3% of migration inhibition compared to the untreated control (Fig. 6a) while the treatment with similar concentration of Dex (scrambled-ODN) NPs has also somewhat suppressed A549 cells migration, although to a lesser extent compared to the Dex(NFκB-ODN) NPs (27.8% compared to untreated control, Fig. 6b).

A similar anti-migratory activity of the Dex(NFκB-ODN) NPs was observed with the transwell chamber assay. In this experiment, the Dex (NFκB-ODN) NPs significantly inhibited A549 cells migration (Fig. 7a) by 43.2% compared to the untreated control (Fig. 7b), while upon treatment with Dex(scrambled-ODN) NPs, no significant inhibition of cells migration was observed as shown in Fig. 7b.

3.8. Anti-colony formation activity of NFκB-ODN-NPs in A549 cells

The anti-colony formation activity of the Dex(NFκB-ODN) NPs in A549 cells was evaluated by colony formation assay after staining with crystal violet. The result of this assay is depicted in Fig. 8, where the Dex (NFκB-ODN) NPs is shown to inhibit colony formation compared to the untreated and Dex(scrambled-ODN) NPs treated cells (Fig. 8a). In particular, treatment with the Dex(NFκB-ODN) NPs resulted in a significantly high inhibition of colony formation up to 42% (Fig. 8b).

4. Discussion

In this study, we have shown the potent anticancer activity of a SpAcDex-based NFκB decoy ODN formulations against an established *in vitro* model of lung cancer, the A549 NSCLC cell line. This anticancer activity was exerted primarily through the inhibition of proliferation,

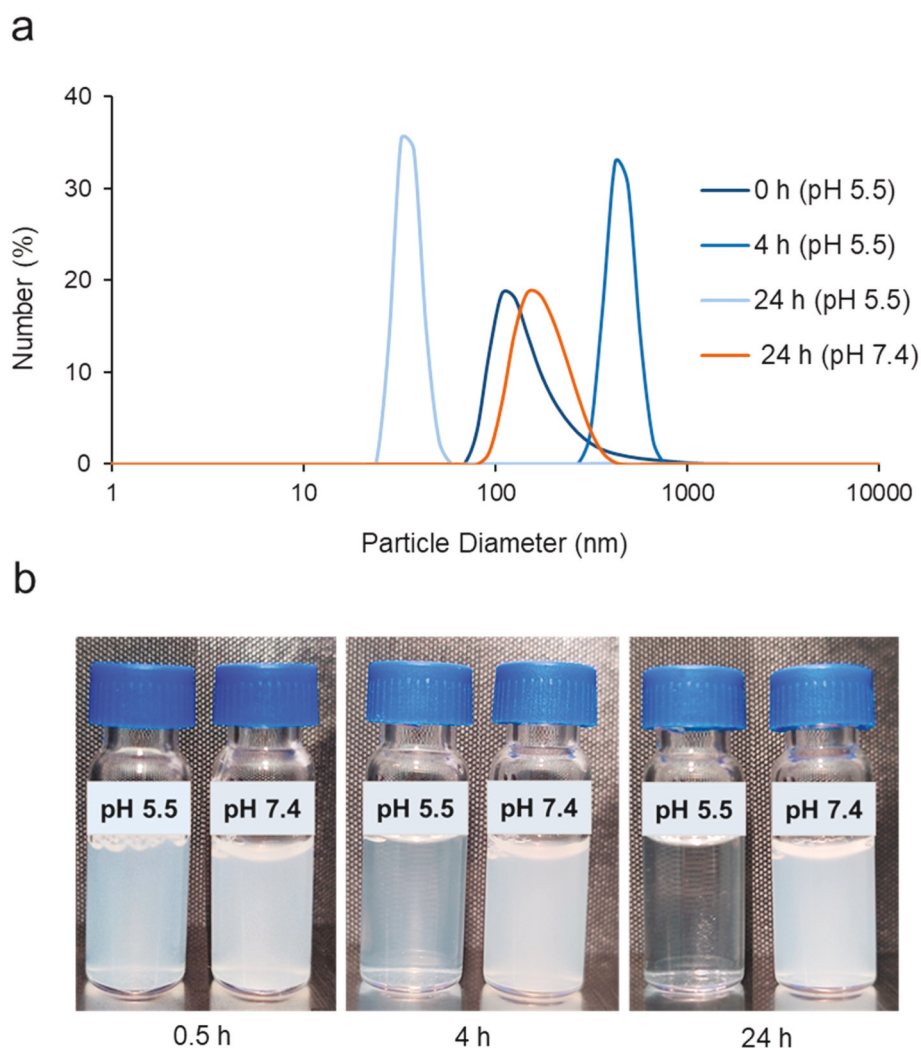


Fig. 2. Particle degradation under pH 5.5 and pH 7.4 (a) DLS data; (b) visual observation.

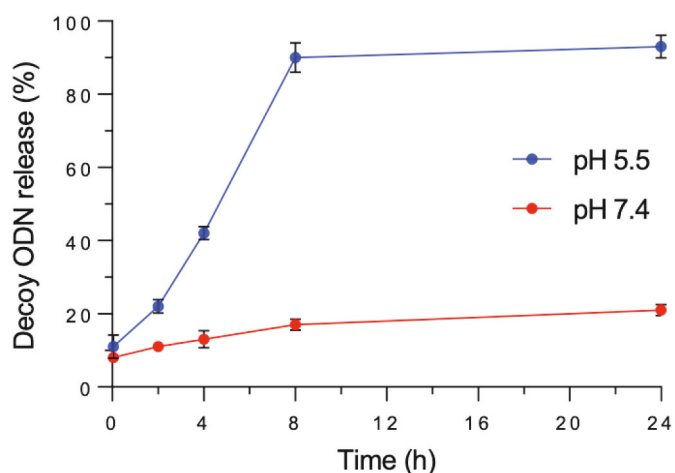


Fig. 3. Decoy ODN release under pH 5.5 and pH 7.4 (Data are presented as means \pm SD (n = 3)).

migration, and colony formation.

Both scrambled and NF κ B decoy ODNs were encapsulated into an acid responsive SpAcDex NPs. The spermine-modified acetalated dextran material was synthesized according to Cohen et al. [46] The

acetal modification of dextran introduces an acid-sensitive functional group to switch the solubility of dextran from hydrophilic to hydrophobic, allowing particle formulation using the emulsion method [49, 65]. These acetalated dextran-based nanocarriers have been effectively used for the delivery of a range of different payloads, including plasmid DNA [66]. To further improve the encapsulation efficiency for small oligonucleotides like siRNA or mRNA, the possibility of additional electrostatic interactions with the phosphate backbone of the RNAs, which is predicted to be exposed on the external surface of dsRNA strands, was provided via functionalization with cationic amines by introducing spermine molecules in the dextran backbone. The spermine modification resulted in an excellent loading of oligonucleotides. The presence of positive charges on the surface of SpAcDex NPs also enhances cellular uptake by improving their interaction with negatively charged cell membranes.

For the particle formulation and ODN encapsulation in spermine-modified acetalated dextran NPs, a double emulsion method was applied [67,68]. The hydrophilic double-stranded decoy ODN dissolved in PBS buffer was added on top of the DCM layer containing spermine-modified acetalated dextran before the first sonication step to encapsulate this hydrophilic payload into the core of the NPs.

After secondary emulsion and solvent evaporation, narrow size distributed nanoparticles were obtained. The free decoy ODN was quantified by analysing the supernatant after centrifugation using a fluorescence-based indirect method with RiboGreen assay. This

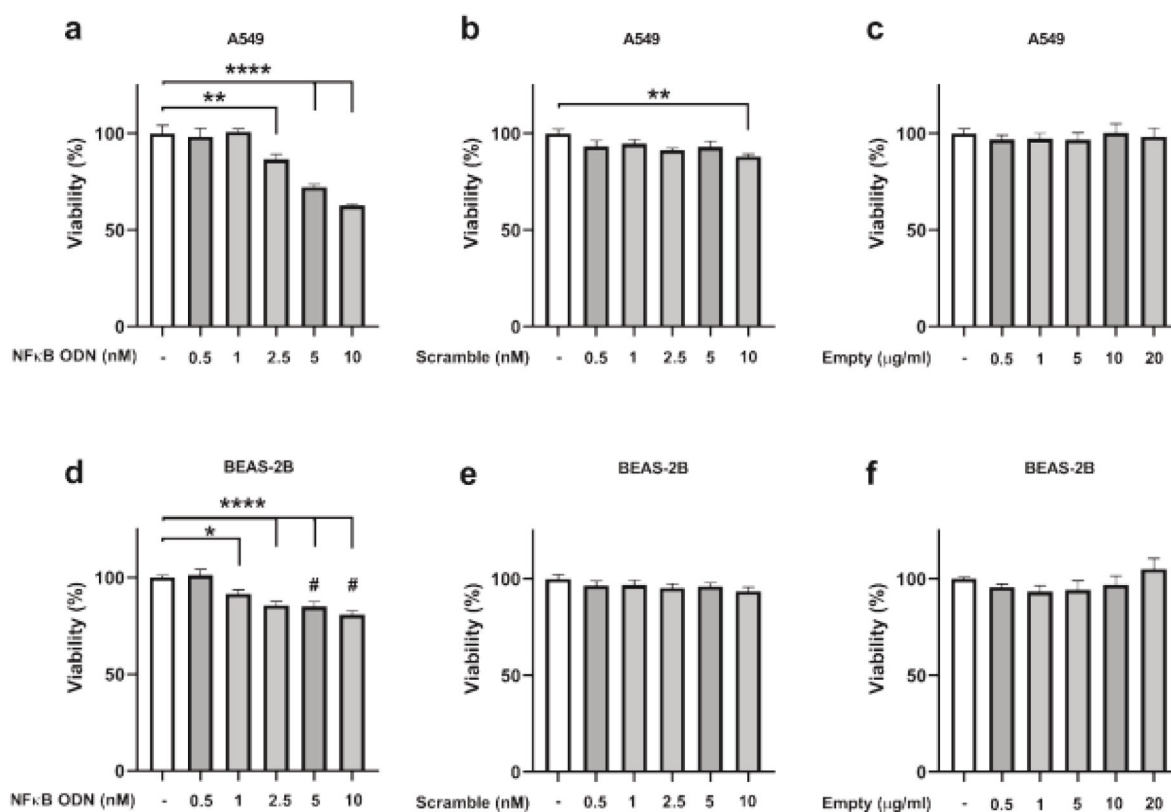


Fig. 4. Anti-proliferative activity by MTT assay: The A549 cells (a–c) and BEAS-2B cells (d–f) were treated with various doses of Dex(NFκB-ODN) NPs (a, d) or Dex (scrambled-ODN) NPs (b, e) or empty NPs (c, f) for 24 h. The values are expressed as average \pm SEM of $n = 3$ independent experiments. Statistical analysis was performed by ordinary one-way ANOVA test. * = $P < 0.05$; ** = $P < 0.01$; **** = $P < 0.0001$ vs control (untreated). In (d), # = $P < 0.05$ vs concentration-matched group on A549 cells as assessed by Mann-Whitney U test.

confirmed the successful encapsulation of decoy ODN in the nanoparticles. A high encapsulation efficiency was observed, which can be attributed to the electrostatic interaction between the cationic component of spermine AcDex material and the negatively charged decoy ODN [46].

The degradation of particles after incubation in acidic conditions was observed as a result of the hydrolysis of acetal groups. This process led to the conversion of the polysaccharide component of the particles back to its water-soluble native form which ultimately leads to particle degradation. The pH-dependence of particle degradation was confirmed using dynamic light scattering (DLS) and visual observations over different time periods. Additionally, the release rate of oligonucleotide (ODN) from loaded particles was determined to be dependent on the pH, with a higher rate of release observed in acidic conditions. The observation of limited decoy ODN released under neutral pH 7.4 over a 24 h period acts as a control and highlights the stability of these particles in normal physiological conditions. This stability is critical for ensuring that the particles remain intact to avoid any unwanted leakage and the protection of loaded decoy ODN from nuclease activity in physiological environments such as the bloodstream or typical extracellular spaces, where neutral pH levels are maintained.

Additionally, these particles have been reported to escape endosomes upon cellular uptake via the proton sponge effect, due to the presence of amine content. Upon endocytosis, the degradation of these particles is triggered by low pH in the endosomal compartment. Furthermore, the buffering of the endosome by spermine content leads to accumulation of counterions (such as Cl^-), which raises the osmotic pressure and causes the endosome to burst [69,70]. This releases the decoy ODN into the cytoplasm, protecting it from degradation by lysosomal enzymes and ensuring its successful delivery [71].

The overall stability of the particles under physiological conditions

reduces the risk of unintended side effects and toxicity, while the acid-triggered release pattern suggests that decoy ODN will only be released in the acidic environment of tumor or endosome/lysosome, which makes this system an attractive candidate for administration of decoy oligonucleotides. The controlled release of decoy ODN from these particles may lead to improved therapeutic outcomes for patients. Next, we tested the anticancer activity of the Dex(NFκB-ODN) NPs formulation against A549 cells. We used A549 cells as an *in vitro* model of NSCLC as this cell line has been extensively characterized and is commonly used in NSCLC studies aimed at investigating mechanisms of action and efficacy of novel experimental anticancer drugs. In particular, the A549 cells are hypotriploid human alveolar basal epithelial cells, with extensive applications as *in vitro* model for lung adenocarcinoma and type II pulmonary epithelial cells [72]. Being cell proliferation and migration/metastasis two hallmarks of cancer progression [73,74], we have investigated these processes in A549 cells by measuring the impact of treatment with Dex(NFκB-ODN) NPs on the cell ability to proliferate, migrate and form colonies.

As shown by the MTT assay, treatment with Dex(NFκB-ODN) NPs significantly inhibited (37.2%) the proliferation of A549 cells in a dose-dependent manner. Furthermore, we have obtained a low (12%), but significant, anti-proliferative activity when treating A549 cells with the 10 nM concentrated Dex(scrambled-ODN) NPs (here 10 nM concentration represents the concentration of ODNs). Considering that this anti-proliferative activity was sensibly lower compared to the value obtained with the concentration-matched Dex(NFκB-ODN) NPs, we performed the subsequent experiments using 10 nM concentrated ODNs. Furthermore, the fact that the anti-proliferative effect with the 10 nM concentrated Dex(scrambled-ODN) NPs was lower compared to the 10 nM Dex(NFκB-ODN) NPs, confirming that the anti-proliferative activity of the Dex(NFκB-ODN) NPs derives specifically from their NFκB-

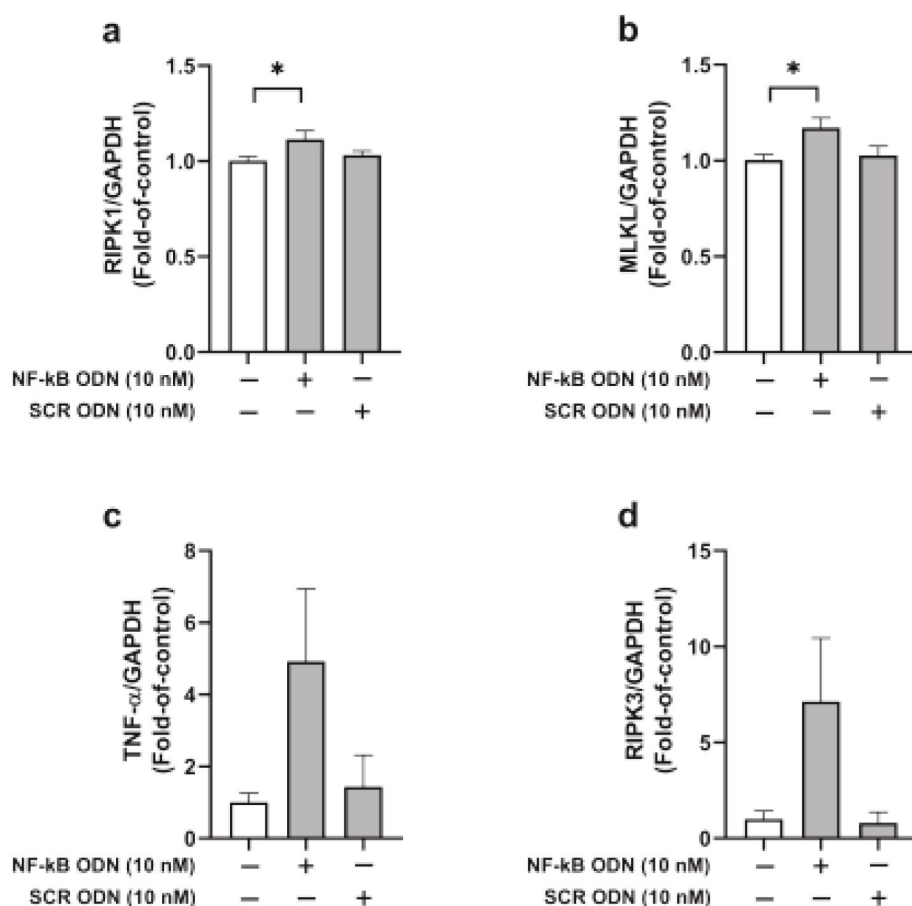


Fig. 5. Effect of Dex(NFκB-ODN) NPs on the expression of apoptosis/necroptosis genes in A549 cells. A549 cells were treated with 10 nM Dex (NFκB-ODN) NPs or Dex(scrambled-ODN) NPs and the relative expression of the following genes was measured with real-time qPCR: RIPK1 (a), MLKL (b), TNF-α(c), and RIPK3 (d). Values are expressed as average ± SEM of n = 3 independent experiments. Statistical analysis was performed by ordinary one-way ANOVA test * = P < 0.05 vs control (untreated).

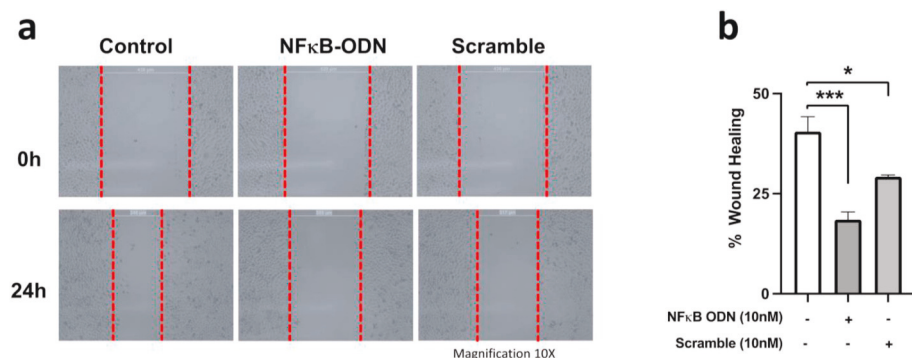


Fig. 6. Anti-migratory activity by wound healing migration assay. The wound was created by scratching, with a sterile pipette tip, a confluent layer of A549 cells. Cells were then treated with 10 nM Dex (NFκB-ODN) NPs or concentration-matched Dex (scrambled-ODN) NPs for 24 h. Photographs were acquired on a light microscope under 10× magnification (a). The distance between the edges of the wounds was measured before treatment (0 h) and after 24 h to calculate the percent wound closure (b). Values are expressed as average ± SEM of n = 3 independent experiments. Statistical analysis was performed by ordinary one-way ANOVA test. * = P < 0.05; *** = P < 0.001 vs control (untreated).

inhibiting action.

To assess the safety of the Dex(NFκB-ODN) NPs, the formulations were tested on non-cancerous BEAS-2B human bronchial epithelial cells. Although Dex(NFκB-ODN) NPs exerted a significant reduction of BEAS-2B cell viability, the relative safety of our formulation is demonstrated by the fact that, at the highest concentrations tested, the impact on BEAS-2B cell viability was significantly lower compared to the impact on A549 cell viability. This suggests that Dex(NFκB-ODN) NPs specifically inhibit the proliferation of cancerous A549 cells.

To assess whether the materials used in the synthesis of the NPs had any toxic effects on cells, empty nanoparticle were tested on both A549 and BEAS-2B cells. Treatment with empty NPs concentrations of up to 20 μg/mL resulted in no significant reduction of cell viability on both cell lines, in accordance with reports showing that the NPs materials have minimal toxicity against most cells at moderate concentrations

[46].

Considering that, in PC-3M androgen-independent prostate cancer cells, the transfection with an NFκB decoy ODN has been reported to induce apoptosis, together with strong suppression of cell proliferation [32], we cannot exclude that, in our experiment, an eventual induction of apoptosis or necroptosis caused by NFκB blockade has at least a partial influence on the reduced metabolic activity reported by the MTT assay. To test this hypothesis, we have assessed the effect of Dex (NFκB-ODN) NPs on the expression of the genes RIPK1, MLKL, TNF-α, and RIPK3, which are collectively considered key mediators of apoptosis and necroptosis [75]. Treatment of A549 cells with Dex(NFκB-ODN) NPs resulted in an overall increased expression of these genes, which reached statistical significance for RIPK1 and MLKL. The fact that Dex (NFκB-ODN) NPs induced a trend of increase of the expression of TNF-α and RIPK3 genes is caused by a relatively higher variability of the

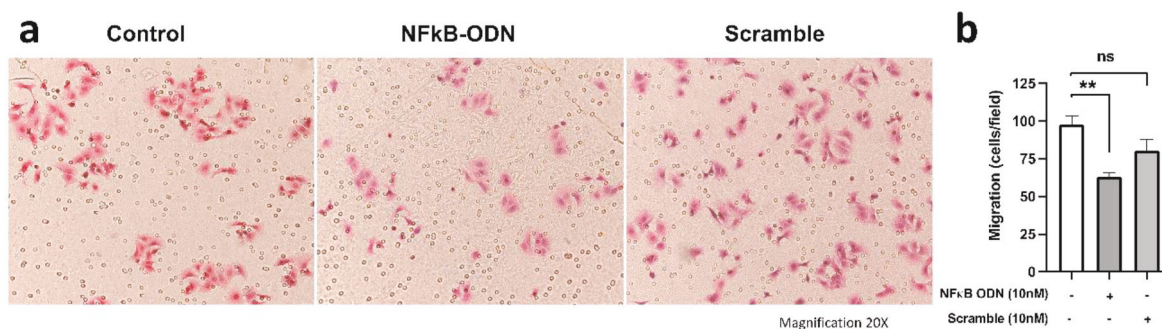


Fig. 7. Anti-migratory activity of Dex(NFκB-ODN) NPs in A549 cells: Transwell chamber assay. A549 cells were seeded in a transwell chamber previously coated with gelatin and treated with 10 nM Dex(NFκB-ODN) NPs or concentration-matched Dex(scrambled-ODN)NPs for 24 h. Subsequently, cells were allowed to migrate through the membrane for additional 24 h. The cells that successfully migrated were then stained with hematoxylin-eosin and imaged under a light microscope (a). The migrated cells were counted in 5 random positions per well under a high-power field (b). Values are expressed as average \pm SEM of $n = 3$ independent experiments. Statistical analysis was performed by ordinary one-way ANOVA test. ns = $P \geq 0.05$; ** = $P < 0.01$ vs control (untreated).

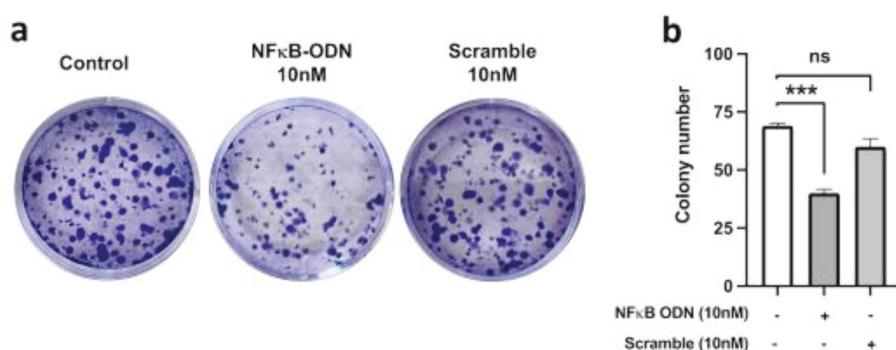


Fig. 8. Anti-colony formation activity of Dex (NFκB-ODN) NPs in A549 cells. A549 cells were seeded at low density in 6-well plates and, after adhesion, treated with 10 nM Dex(NFκB-ODN) NPs or concentration-matched Dex(scrambled-ODN) NPs for 24 h. After colony formation (≈ 2 weeks), cells were stained with crystal violet solution and each individual well was imaged using the light microscope (a). The resulting number of colonies in each well has been counted and is plotted in (b). Values are expressed as average \pm SEM of $n = 3$ independent experiments. Statistical analysis was performed by ordinary one-way ANOVA test. ns = $P \geq 0.05$; ** = $P < 0.01$ vs control (untreated). (For interpretation of the references to color in this figure legend, the reader is referred to the Web version of this article.)

expression of these genes. However, these results collectively confirm that at least part of the anti-proliferative effect of Dex(NFκB-ODN) NPs is caused by the activation of the TNF- α /RIPK1/RIPK3/MLKL pathway which leads to necroptosis.

Furthermore, the inhibition of the NFκB pathway through treatment with the decoy ODN NPs exerted a significant anti-migratory activity, as demonstrated in the wound healing assay as well as in the transwell chamber assay. In the wound healing assay, treatment with Dex (scrambled-ODN) NPs exerted a slight anti-migratory activity, similar to what was observed in the MTT assay. However, a significantly stronger anti-migratory activity was obtained upon treatment with Dex (NFκB-ODN) NPs, which suggests this effect is exerted specifically through the inhibition of NFκB.

The anticancer activity of the Dex(NFκB-ODN) NPs was also supported by the colony formation assay, where a significantly lower number of colonies was formed upon treatment with Dex(NFκB-ODN) NPs compared to Dex(scrambled-ODN) NPs.

Taken together, these results underscore the strong anticancer activity of Dex(NFκB-ODN) NPs, further highlighting the therapeutic potential of NFκB blockage through NP-mediated delivery of decoy ODNs for lung cancer [27,76].

The robustness and relevance of such a treatment approach would enormously benefit from a mechanistic explanation of the pathways through which the Dex(NFκB-ODN) NPs exert their anti-migratory activity. In the modified Boyden's chamber assay, the surface of the chamber was coated with 2.5% gelatin. Considering that gelatin is degraded by matrix metalloproteinases (MMPs) [77], it can be hypothesized that the reduction of the migratory ability of A549 cells obtained upon NFκB inhibition could be caused by the downregulation of MMPs expression and/or activity. This would also be in agreement with the fact that MMPs, including MMP2 and MMP9, are upregulated

upon NFκB activation [78]. Therefore, the assessment of the levels of MMPs via Western blot [58], and/or of their activity through gel zymography [79], could shed further light on the mechanism by which the inhibition of NFκB signalling results in impaired migrating ability. A limitation of our study resides in the fact that only one cell line, A549, has been used to investigate the anticancer activity of Dex(NFκB-ODN) NPs. Although this cell line is a well-established model of LC [72], testing the anticancer activity of Dex(NFκB-ODN) NPs on further human LC cell lines, as well as on animal models of LC, would surely deepen our comprehension of the exact mechanism(s) by which treatment with Dex (NFκB-ODN) NPs exerts its anticancer activity. This would also be useful in expanding the applicability of this treatment strategy against different subtypes of LC, as well as against other types of cancer, thus strongly enhancing its potential therapeutic range.

A point of strength of the present study lies in the great potential for clinical translation of the Dex(NFκB-ODN) NPs. Acetalated dextran, in fact, is an easy-to-synthesize, bio-compatible material derived by the FDA-approved dextran [80], and it is characterised by extreme versatility and tunability of application as drug delivery system [44,65]. The application of Dex(NFκB-ODN) NPs in the treatment of lung diseases such as NSCLC is advantageous due to the possibility of deliver the therapeutic agent via inhalational delivery, which represents a privileged administration route for the direct delivery of drug to the lung tissue. Acetalated dextran nanoparticles are suitable for this application, as they can be formulated as dry powder to be administered via inhalation [46,66,80]. The *in vivo* study of the delivery and efficacy of Dex (NFκB-ODN) NPs would enormously streamline the clinical translation of this formulation.

5. Conclusions

In conclusion, this study strongly supports the feasibility of inhibiting the NF κ B signalling pathway as a therapeutic approach against NSCLC using a cationic dextran-based pH-sensitive delivery system for decoy ODNs. An excellent loading and a controlled release of decoy ODN demonstrated the significance of polysaccharide-based NPs as a novel therapeutic strategy. This resulted in a strong, significant inhibition of three cancer hallmarks: cell proliferation, migration and colony formation. The results of this study provide an innovative direction into the clinical management of lung cancer. Furthermore, these findings represent a blueprint for further medical research and application against lung infectious diseases and other chronic respiratory diseases, providing solid theoretical bases to test similar nanoformulation approaches to enhance the pulmonary delivery of compounds with poor pharmacokinetic properties and bioavailability such as ODNs.

CRedit authorship contribution statement

Vinod Kumar Kannaujiya: Conceptualization, Data curation, Formal analysis, Investigation, Methodology, Writing – review & editing. **Gabriele De Rubis:** Conceptualization, Data curation, Formal analysis, Investigation, Writing – original draft, Writing – review & editing. **Keshav Raj Paudel:** Data curation, Formal analysis, Investigation, Methodology, Writing – review & editing. **Bikash Manandhar:** Data curation, Formal analysis, Investigation, Methodology, Writing – review & editing. **Dinesh Kumar Chellappan:** Methodology. **Sachin Kumar Singh:** Methodology. **Ronan MacLoughlin:** Resources, Methodology. **Gaurav Gupta:** Methodology. **Dikaia Xenaki:** Methodology. **Pradeep Kumar:** Data curation, Formal analysis, Investigation, Methodology. **Philip Michael Hansbro:** Supervision. **Brian Gregory George Oliver:** Conceptualization, Supervision. **Peter Richard Wich:** Supervision, Resources, Conceptualization, Funding acquisition, Methodology, Project administration, Writing – review & editing. **Kamal Dua:** Supervision, Resources, Conceptualization, Funding acquisition, Methodology, Project administration, Writing – review & editing.

Declaration of competing interest

Confirm that there are no interests to declare

Data availability

Data will be made available on request.

Acknowledgments

The authors are thankful to the Graduate School of Health, University of Technology Sydney, Australia. KD is supported by a project grant from the Rebecca L Cooper Medical Research Foundation and the Maridulu Budyari Gumal Sydney Partnership for Health, Education, Research and Enterprise (SPHERE) RSEOH CAG Seed grant, fellowship and extension grant; Faculty of Health MCR/ECR Mentorship Support Grant and UTS Global Strategic Partnerships Seed Funding Scheme. GDR is supported by the UTS International Research Scholarship and the UTS President's Scholarship. KRP is supported by a fellowship from Prevent Cancer Foundation (PCF), Alexandria, Virginia, United States, and the International Association for the Study of Lung Cancer (IASLC), Denver, Colorado, United States. We also thank Maryam Hosseini for her help with SEM imaging.

Appendix A. Supplementary data

Supplementary data to this article can be found online at <https://doi.org/10.1016/j.jddst.2023.104328>.

References

- [1] H. Sung, J. Ferlay, R.L. Siegel, et al., Global cancer statistics 2020: GLOBOCAN estimates of incidence and mortality worldwide for 36 cancers in 185 countries, *Cancer J. Clin. Oncol.* 71 (3) (2021) 209–249.
- [2] V. Malyla, K.R. Paudel, S.D. Shukla, et al., Recent advances in experimental animal models of lung cancer, *Future Med. Chem.* 12 (7) (2020) 567–570.
- [3] M.C.S. Wong, X.Q. Lao, K.F. Ho, W.B. Goggins, S.L.A. Tse, Incidence and mortality of lung cancer: global trends and association with socioeconomic status, *Sci. Rep.* 7 (1) (2017), 14300.
- [4] P. Sharma, M. Mehta, D.S. Dhanjal, et al., Emerging trends in the novel drug delivery approaches for the treatment of lung cancer, *Chem. Biol. Interact.* 309 (2019), 108720.
- [5] M.W. Onaitis, R.P. Petersen, S.S. Balderson, et al., Thoracoscopic lobectomy is a safe and versatile procedure: experience with 500 consecutive patients, *Ann. Surg.* 244 (3) (2006) 420–425.
- [6] J. Klasterky, A. Awada, Milestones in the use of chemotherapy for the management of non-small cell lung cancer (NSCLC), *Crit. Rev. Oncol. Hematol.* 81 (1) (2012) 49–57.
- [7] T.M. Kang, N. Hardcastle, A.K. Singh, et al., Practical considerations of single-fraction stereotactic ablative radiotherapy to the lung, *Lung Cancer* 170 (2022) 185–193.
- [8] S.Y. Liu, S.M. Liu, W.Z. Zhong, Y.L. Wu, Targeted therapy in early stage non-small cell lung cancer, *Curr. Treat. Options Oncol.* (2022), <https://doi.org/10.1007/s11864-022-00994-w>.
- [9] D. Baci, E. Cekani, A. Imperatori, D. Ribatti, L. Mortara, Host-related factors as targetable drivers of immunotherapy response in non-small cell lung cancer patients, *Front. Immunol.* 13 (2022), 914890.
- [10] K.R. Paudel, N. Panth, R. Pangei, et al., Chapter 23 - targeting lung cancer using advanced drug delivery systems, in: K. Dua, P.M. Hansbro, R. Wadhwa, M. Haghi, L.G. Pont, K.A. Williams (Eds.), *Targeting Chronic Inflammatory Lung Diseases Using Advanced Drug Delivery Systems*, Academic Press, 2020, pp. 493–516.
- [11] V. Yazbeck, E. Alesi, J. Myers, M.H. Hackney, L. Cuttino, D.A. Gewirtz, An overview of chemotoxicity and radiation toxicity in cancer therapy, *Adv. Cancer Res.* 155 (2022) 1–27.
- [12] K.R. Paudel, D.K. Chellappan, R. MacLoughlin, T.J.A. Pinto, K. Dua, P.M. Hansbro, Editorial: advanced therapeutic delivery for the management of chronic respiratory diseases, *Front. Med.* 9 (2022), 983583.
- [13] K.R. Paudel, K. Dua, N. Panth, P.M. Hansbro, D.K. Chellappan, Advances in research with rutin-loaded nanoformulations in mitigating lung diseases, *Future Med. Chem.* 14 (18) (2022) 1293–1295.
- [14] V. Malyla, K.R. Paudel, G.D. Rubis, N.G. Hansbro, P.M. Hansbro, K. Dua, Extracellular vesicles released from cancer cells promote tumorigenesis by inducing epithelial to mesenchymal transition via β -catenin signaling, *Int. J. Mol. Sci.* 24 (4) (2023) 3500.
- [15] R. Sen, D. Baltimore, In vitro transcription of immunoglobulin genes in a B-cell extract: effects of enhancer and promoter sequences, *Mol. Cell Biol.* 7 (5) (1987) 1989–1994.
- [16] Q. Zhang, M.J. Lenardo, D. Baltimore, 30 Years of NF- κ B: a blossoming of relevance to human pathobiology, *Cell* 168 (1–2) (2017) 37–57.
- [17] L. Xia, S. Tan, Y. Zhou, et al., Role of the NF κ B-signaling pathway in cancer, *OncoTargets Ther.* 11 (2018) 2063–2073.
- [18] K. Taniguchi, M. Karin, NF- κ B, inflammation, immunity and cancer: coming of age, *Nat. Rev. Immunol.* 18 (5) (2018) 309–324.
- [19] Z. Cai, K.M. Tchou-Wong, W.N. Rom, NF- κ B in lung tumorigenesis, *Cancers* 3 (4) (2011) 4258–4268.
- [20] D.R. Jones, R.M. Broad, L.V. Madrid, A.S. Baldwin Jr., M.W. Mayo, Inhibition of NF- κ B sensitizes non-small cell lung cancer cells to chemotherapy-induced apoptosis, *Ann. Thorac. Surg.* 70 (3) (2000) 930–936, discussion 936–937.
- [21] M. Gao, P.Y. Yeh, Y.S. Lu, W.C. Chang, M.L. Kuo, A.L. Cheng, NF- κ B p50 promotes tumor cell invasion through negative regulation of invasion suppressor gene CRMP-1 in human lung adenocarcinoma cells, *Biochem. Biophys. Res. Commun.* 376 (2) (2008) 283–287.
- [22] M. Kumar, D.F. Allison, N.N. Baranova, et al., NF- κ B regulates mesenchymal transition for the induction of non-small cell lung cancer initiating cells, *PLoS One* 8 (7) (2013), e68597.
- [23] L. Gu, Z. Wang, J. Zuo, H. Li, L. Zha, Prognostic significance of NF- κ B expression in non-small cell lung cancer: a meta-analysis, *PLoS One* 13 (5) (2018), e0198223.
- [24] K.K. Wong, T. Jacks, G. Dranoff, NF- κ B fans the flames of lung carcinogenesis, *Cancer Prev. Res.* 3 (4) (2010) 403–405.
- [25] H. Yu, L. Lin, Z. Zhang, H. Zhang, H. Hu, Targeting NF- κ B pathway for the therapy of diseases: mechanism and clinical study, *Signal Transduct. Targeted Ther.* 5 (1) (2020) 209.
- [26] V. Ramadass, T. Vaiyapuri, V. Tergaonkar, Small molecule NF- κ B pathway inhibitors in clinic, *Int. J. Mol. Sci.* 21 (14) (2020).
- [27] M. Mehta, K.R. Paudel, S.D. Shukla, et al., Recent trends of NF κ B decoy oligodeoxynucleotide-based nanotherapeutics in lung diseases, *J. Contr. Release* 337 (2021) 629–644.
- [28] P.R. Wardwell, R.A. Bader, Immunomodulation of cystic fibrosis epithelial cells via NF- κ B decoy oligonucleotide-coated polysaccharide nanoparticles, *J. Biomed. Mater. Res.* 103 (5) (2015) 1622–1631.
- [29] M.Z. Ahmad, S. Akhter, N. Mallik, M. Anwar, W. Tabassum, F.J. Ahmad, Application of decoy oligonucleotides as novel therapeutic strategy: a contemporary overview, *Curr. Drug Discov. Technol.* 10 (1) (2013) 71–84.
- [30] M.J. Mann, Transcription factor decoys: a new model for disease intervention, *Ann. N. Y. Acad. Sci.* 1058 (2005) 128–139.

- [31] M. Imran, L.A. Jha, N. Hasan, et al., Nanodecoys - future of drug delivery by encapsulating nanoparticles in natural cell membranes, *Int. J. Pharm.* 621 (2022), 121790.
- [32] Y. Fang, H. Sun, J. Zhai, et al., Antitumor activity of NF- κ B decoy oligodeoxynucleotides in a prostate cancer cell line, *Asian Pac. J. Cancer Prev. APJCP* 12 (10) (2011) 2721–2726.
- [33] R. Morishita, J. Higaki, N. Tomita, T. Ogihara, Application of transcription factor "decoy" strategy as means of gene therapy and study of gene expression in cardiovascular disease, *Circ. Res.* 82 (10) (1998) 1023–1028.
- [34] T.D. Dinh, Y. Higuchi, S. Kawakami, F. Yamashita, M. Hashida, Evaluation of osteoclastogenesis via NF- κ B decoy/mannosylated cationic liposome-mediated inhibition of pro-inflammatory cytokine production from primary cultured macrophages, *Pharm. Res. (N. Y.)* 28 (4) (2011) 742–751.
- [35] D. De Stefano, Oligonucleotides decoy to NF- κ B: becoming a reality? *Discov. Med.* 12 (63) (2011) 97–105.
- [36] L. Farahmand, B. Darvishi, A.K. Majidzadeh, Suppression of chronic inflammation with engineered nanomaterials delivering nuclear factor κ B transcription factor decoy oligodeoxynucleotides, *Drug Deliv.* 24 (1) (2017) 1249–1261.
- [37] C. Mischiati, M. Borgatti, N. Bianchi, et al., Interaction of the human NF- κ B p52 transcription factor with DNA-PNA hybrids mimicking the NF- κ B binding sites of the human immunodeficiency virus type 1 promoter, *J. Biol. Chem.* 274 (46) (1999) 33114–33122.
- [38] R. Crinelli, M. Bianchi, L. Gentilini, et al., Transcription factor decoy oligonucleotides modified with locked nucleic acids: an in vitro study to reconcile biostability with binding affinity, *Nucleic Acids Res.* 32 (6) (2004) 1874–1885.
- [39] L. Farahmand, B. Darvishi, A.K. Majidzadeh, Suppression of chronic inflammation with engineered nanomaterials delivering nuclear factor κ B transcription factor decoy oligodeoxynucleotides, *Drug Deliv.* 24 (1) (2017) 1249–1261.
- [40] M. Doroudian, R. Macloughlin, F. Poynton, A. Prina-Mello, S.C. Donnelly, Nanotechnology based therapeutics for lung disease, *Thorax* 74 (10) (2019) 965–976.
- [41] G. De Rosa, M.C. Maiuri, F. Ungaro, et al., Enhanced intracellular uptake and inhibition of NF- κ B activation by decoy oligonucleotide released from PLGA microspheres, *J. Gene Med.* 7 (6) (2005) 771–781.
- [42] D. De Stefano, G. De Rosa, M.C. Maiuri, et al., Oligonucleotide decoy to NF- κ B slowly released from PLGA microspheres reduces chronic inflammation in rat, *Pharmacol. Res.* 60 (1) (2009) 33–40.
- [43] N. Zhang, P.R. Wardwell, R.A. Bader, Polysaccharide-based micelles for drug delivery, *Pharmaceutics* 5 (2) (2013) 329–352.
- [44] P. Prasher, M. Sharma, M. Mehta, et al., Current-status and applications of polysaccharides in drug delivery systems, *Colloid Inter. Sci. Commun.* 42 (2021), 100418.
- [45] L. Ma, C.A. Shen, L. Gao, et al., Anti-inflammatory activity of chitosan nanoparticles carrying NF- κ B/p65 antisense oligonucleotide in RAW264.7 macrophage stimulated by lipopolysaccharide, *Colloids Surf. B Biointerfaces* 142 (2016) 297–306.
- [46] J.L. Cohen, S. Schubert, P.R. Wich, et al., Acid-degradable cationic dextran particles for the delivery of siRNA therapeutics, *Bioconjugate Chem.* 22 (6) (2011) 1056–1065.
- [47] E. Boedtker, S.F. Pedersen, The acidic tumor microenvironment as a driver of cancer, *Annu. Rev. Physiol.* 82 (2020) 103–126.
- [48] E.M. Bachelder, T.T. Beaudette, K.E. Broaders, J. Dashe, J.M. Frechet, Acetal-derivatized dextran: an acid-responsive biodegradable material for therapeutic applications, *J. Am. Chem. Soc.* 130 (32) (2008) 10494–10495.
- [49] S. Wang, F. Fontana, M.A. Shahbazi, H.A. Santos, Acetalated dextran based nano- and microparticles: synthesis, fabrication, and therapeutic applications, *Chem. Commun.* 57 (35) (2021) 4212–4229.
- [50] D. Bamberger, D. Hobernik, M. Konhauser, M. Bros, P.R. Wich, Surface modification of polysaccharide-based nanoparticles with PEG and dextran and the effects on immune cell binding and stimulatory characteristics, *Mol. Pharm.* 14 (12) (2017) 4403–4416.
- [51] K. Shi, J. Xue, Y. Fang, et al., Inorganic kernel-reconstituted lipoprotein biomimetic nanovehicles enable efficient targeting "trojan horse" delivery of STAT3-decoy oligonucleotide for overcoming TRAIL resistance, *Theranostics* 7 (18) (2017) 4480–4497.
- [52] M.N. Centelles, C. Qian, M.A. Campanero, J.M. Irache, New methodologies to characterize the effectiveness of the gene transfer mediated by DNA-chitosan nanoparticles, *Int. J. Nanomed.* 3 (4) (2008) 451–460.
- [53] M.D. Hanwell, D.E. Curtis, D.C. Lonie, T. Vandermeersch, E. Zurek, G.R. Hutchison, Avogadro: an advanced semantic chemical editor, visualization, and analysis platform, *J. Cheminform.* 4 (1) (2012) 17.
- [54] E.F. Pettersen, T.D. Goddard, C.C. Huang, et al., UCSF Chimera—a visualization system for exploratory research and analysis, *J. Comput. Chem.* 25 (13) (2004) 1605–1612.
- [55] H.H. Lee, K.R. Paudel, D.W. Kim, Terminalia chebula fructus inhibits migration and proliferation of vascular smooth muscle cells and production of inflammatory mediators in RAW 264.7, *Evid. Based Complement. Alternat. Med.* (2015), 502182, 2015.
- [56] K.R. Paudel, N. Panth, B. Manandhar, et al., Attenuation of cigarette-smoke-induced oxidative stress, senescence, and inflammation by berberine-loaded liquid crystalline nanoparticles: in vitro study in 16HBE and RAW264.7 cells, *Antioxidants* 11 (5) (2022).
- [57] M.Y. Jun, R. Karki, K.R. Paudel, B.R. Sharma, D. Adhikari, D.W. Kim, Alkaloid rich fraction from Nelumbo nucifera targets VSMC proliferation and migration to suppress restenosis in balloon-injured rat carotid artery, *Atherosclerosis* 248 (2016) 179–189.
- [58] K.R. Paudel, R. Wadhwa, X.N. Tew, et al., Rutin loaded liquid crystalline nanoparticles inhibit non-small cell lung cancer proliferation and migration in vitro, *Life Sci.* 276 (2021), 119436.
- [59] K.R. Paudel, M. Mehta, G.H.S. Yin, et al., Berberine-loaded liquid crystalline nanoparticles inhibit non-small cell lung cancer proliferation and migration in vitro, *Environ. Sci. Pollut. Res. Int.* 29 (31) (2022) 46830–46847.
- [60] R. Wadhwa, K.R. Paudel, L.H. Chin, et al., Anti-inflammatory and anticancer activities of Naringenin-loaded liquid crystalline nanoparticles in vitro, *J. Food Biochem.* 45 (1) (2021), e13572.
- [61] A.M. Alnuqaydan, A.G. Almutary, M. Azam, et al., Evaluation of the cytotoxic activity and anti-migratory effect of berberine-phytantriol liquid crystalline nanoparticle formulation on non-small-cell lung cancer in vitro, *Pharmaceutics* 14 (6) (2022).
- [62] L. Wan, X. Yao, F. Faiola, et al., Coating with spermine-pullulan polymer enhances adenoviral transduction of mesenchymal stem cells, *Int. J. Nanomed.* 11 (2016) 6763–6769.
- [63] B.B. Breitenbach, E. Steiert, M. Konhäuser, et al., Double stimuli-responsive polysaccharide block copolymers as green macrosurfactants for near-infrared photodynamic therapy, *Soft Matter* 15 (6) (2019) 1423–1434.
- [64] C.B. Braga, G. Perli, T.B. Becher, C. Ornelas, Biodegradable and pH-responsive acetalated dextran (Ac-Dex) nanoparticles for NIR imaging and controlled delivery of a platinum-based prodrug into cancer cells, *Mol. Pharm.* 16 (5) (2019) 2083–2094.
- [65] E.M. Bachelder, E.N. Pino, K.M. Ainslie, Acetalated dextran: a tunable and acid-labile biopolymer with facile synthesis and a range of applications, *Chem. Rev.* 117 (3) (2017) 1915–1926.
- [66] J.A. Cohen, T.T. Beaudette, J.L. Cohen, K.E. Broaders, E.M. Bachelder, J.M. Frechet, Acetal-modified dextran microparticles with controlled degradation kinetics and surface functionality for gene delivery in phagocytic and non-phagocytic cells, *Adv. Mater.* 22 (32) (2010) 3593–3597.
- [67] F. Foerster, D. Bamberger, J. Schupp, et al., Dextran-based therapeutic nanoparticles for hepatic drug delivery, *Nanomedicine* 11 (20) (2016) 2663–2677.
- [68] M. Konhauser, V.K. Kannaujiya, E. Steiert, K. Schwicker, T. Schirmeister, P. R. Wich, Co-encapsulation of l-asparaginase and etoposide in dextran nanoparticles for synergistic effect in chronic myeloid leukemia cells, *Int. J. Pharm.* 622 (2022), 121796.
- [69] J. Nguyen, F.C. Szoka, Nucleic acid delivery: the missing pieces of the puzzle? *Acc. Chem. Res.* 45 (7) (2012) 1153–1162.
- [70] S. Mahajan, T. Tang, Polyethylenimine-DNA nanoparticles under endosomal acidification and implication to gene delivery, *Langmuir* 38 (27) (2022) 8382–8397.
- [71] A. Akinc, M. Thomas, A.M. Klibanov, R. Langer, Exploring polyethylenimine-mediated DNA transfection and the proton sponge hypothesis, *J. Gene Med.* 7 (5) (2005) 657–663.
- [72] M. Lieber, B. Smith, A. Szakal, W. Nelson-Rees, G. Todaro, A continuous tumor-cell line from a human lung carcinoma with properties of type II alveolar epithelial cells, *Int. J. Cancer* 17 (1) (1976) 62–70.
- [73] R. Wadhwa, K.R. Paudel, S. Shukla, et al., Epigenetic therapy as a potential approach for targeting oxidative stress-induced non-small-cell lung cancer, in: S. Chakraborti, B.K. Ray, S. Roychoudhury (Eds.), *Handbook of Oxidative Stress in Cancer: Mechanistic Aspects*, Springer Nature Singapore, Singapore, 2022, pp. 1545–1560.
- [74] R. Khursheed, K. Dua, S. Vishwas, et al., Biomedical applications of metallic nanoparticles in cancer: current status and future perspectives, *Biomed. Pharmacother.* 150 (2022), 112951.
- [75] J. Seo, Y.W. Nam, S. Kim, D.-B. Oh, J. Song, Necroptosis molecular mechanisms: recent findings regarding novel necroptosis regulators, *Exp. Mol. Med.* 53 (6) (2021) 1007–1017.
- [76] F.D. Dimitrakopoulos, A.E. Kottorou, M. Kalofonou, H.P. Kalofonos, The fire within: NF- κ B involvement in non-small cell lung cancer, *Cancer Res.* 80 (19) (2020) 4025–4036.
- [77] O.R. Mook, C. Van Overbeek, E.G. Ackema, F. Van Maldegem, W.M. Frederiks, In situ localization of gelatinolytic activity in the extracellular matrix of metastases of colon cancer in rat liver using quenched fluorogenic DQ-gelatin, *J. Histochem. Cytochem.* 51 (6) (2003) 821–829.
- [78] J. Li, G.K. Lau, L. Chen, et al., Interleukin 17A promotes hepatocellular carcinoma metastasis via NF- κ B induced matrix metalloproteinases 2 and 9 expression, *PLoS One* 6 (7) (2011), e21816.
- [79] H. Frankowski, Y.H. Gu, J.H. Heo, R. Milner, G.J. Del Zoppo, Use of gel zymography to examine matrix metalloproteinase (gelatinase) expression in brain tissue or in primary glial cultures, *Methods Mol. Biol.* 814 (2012) 221–233.
- [80] P. Prasher, M. Sharma, S. Kumar Singh, et al., Versatility of acetalated dextran in nanocarriers targeting respiratory diseases, *Mater. Lett.* 323 (2022), 132600.

CHAPTER 3

Research Paper #2




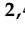





Agarwood oil nanoemulsion attenuates cigarette smoke-induced inflammation and oxidative stress markers in B*Ci*NS1.1 airway epithelial cells

(**De Rubis G**[#], Paudel KR[#], Manandhar B, Singh SK, Gupta G, Malik R, Shen J, Chami A, MacLoughlin R, Chellappan DK, Oliver BGG, Hansbro PM, Dua K. *Agarwood Oil Nanoemulsion Attenuates Cigarette Smoke-Induced Inflammation and Oxidative Stress Markers in B*Ci*-NS1.1 Airway Epithelial Cells*. **Nutrients**. 2023 Feb 17;15(4):1019. doi: 10.3390/nu15041019.)

[#] Authors contributed equally to this work

Article

Agarwood Oil Nanoemulsion Attenuates Cigarette Smoke-Induced Inflammation and Oxidative Stress Markers in BCI-NS1.1 Airway Epithelial Cells

Gabriele De Rubis ^{1,2,†} , Keshav Raj Paudel ^{3,†} , Bikash Manandhar ^{1,2} , Sachin Kumar Singh ^{2,4} , Gaurav Gupta ^{5,6,7}, Raniya Malik ⁸, Jessie Shen ⁸, Aniss Chami ⁹, Ronan MacLoughlin ^{10,11,12} , Dinesh Kumar Chellappan ¹³ , Brian Gregory George Oliver ^{14,15} , Philip Michael Hansbro ^{3,*}  and Kamal Dua ^{1,2,*} 

- ¹ Discipline of Pharmacy, Graduate School of Health, University of Technology Sydney, Sydney, NSW 2007, Australia
 - ² Faculty of Health, Australian Research Centre in Complementary and Integrative Medicine, University of Technology Sydney, Ultimo, NSW 2007, Australia
 - ³ Centre for Inflammation, Centenary Institute and University of Technology Sydney, Faculty of Science, School of Life Sciences, Sydney, NSW 2007, Australia
 - ⁴ School of Pharmaceutical Sciences, Lovely Professional University, Jalandhar-Delhi GT Road, Phagwara 144411, Punjab, India
 - ⁵ School of Pharmacy, Suresh Gyan Vihar University, Jaipur 302017, Rajasthan, India
 - ⁶ Uttaranchal Institute of Pharmaceutical Sciences, Uttaranchal University, Dehradun 248007, Uttarakhand, India
 - ⁷ Department of Pharmacology, Saveetha Institute of Medical and Technical Sciences, Saveetha Dental College, Saveetha University, Tamil Nadu 602105, Chennai, India
 - ⁸ DeAurora Pty Ltd., Dean, VIC 3363, Australia
 - ⁹ Vitex Pharmaceuticals, Eastern Creek, NSW 2766, Australia
 - ¹⁰ Aerogen, IDA Business Park, H91 HE94 Galway, Ireland
 - ¹¹ School of Pharmacy & Biomolecular Sciences, Royal College of Surgeons in Ireland, D02 YN77 Dublin, Ireland
 - ¹² School of Pharmacy & Pharmaceutical Sciences, Trinity College, D02 PN40 Dublin, Ireland
 - ¹³ Department of Life Sciences, School of Pharmacy, International Medical University, Kuala Lumpur 57000, Malaysia
 - ¹⁴ Woolcock Institute of Medical Research, University of Sydney, Sydney, NSW 2037, Australia
 - ¹⁵ School of Life Sciences, University of Technology Sydney, Ultimo, NSW 2007, Australia
- * Correspondence: philip.hansbro@uts.edu.au (P.M.H.); kamal.dua@uts.edu.au (K.D.)
† These two authors have contributed equally.



Citation: De Rubis, G.; Paudel, K.R.; Manandhar, B.; Singh, S.K.; Gupta, G.; Malik, R.; Shen, J.; Chami, A.; MacLoughlin, R.; Chellappan, D.K.; et al. Agarwood Oil Nanoemulsion Attenuates Cigarette Smoke-Induced Inflammation and Oxidative Stress Markers in BCI-NS1.1 Airway Epithelial Cells. *Nutrients* **2023**, *15*, 1019. <https://doi.org/10.3390/nu15041019>

Academic Editors: Adil El Midaoui, Gérard Lizard and Antoni Pons

Received: 11 December 2022

Revised: 14 February 2023

Accepted: 14 February 2023

Published: 17 February 2023



Copyright: © 2023 by the authors. Licensee MDPI, Basel, Switzerland. This article is an open access article distributed under the terms and conditions of the Creative Commons Attribution (CC BY) license (<https://creativecommons.org/licenses/by/4.0/>).

Abstract: Chronic obstructive pulmonary disease (COPD) is an irreversible inflammatory respiratory disease characterized by frequent exacerbations and symptoms such as cough and wheezing that lead to irreversible airway damage and hyperresponsiveness. The primary risk factor for COPD is chronic cigarette smoke exposure, which promotes oxidative stress and a general pro-inflammatory condition by stimulating pro-oxidant and pro-inflammatory pathways and, simultaneously, inactivating anti-inflammatory and antioxidant detoxification pathways. These events cause progressive damage resulting in impaired cell function and disease progression. Treatments available for COPD are generally aimed at reducing the symptoms of exacerbation. Failure to regulate oxidative stress and inflammation results in lung damage. In the quest for innovative treatment strategies, phytochemicals, and complex plant extracts such as agarwood essential oil are promising sources of molecules with antioxidant and anti-inflammatory activity. However, their clinical use is limited by issues such as low solubility and poor pharmacokinetic properties. These can be overcome by encapsulating the therapeutic molecules using advanced drug delivery systems such as polymeric nanosystems and nanoemulsions. In this study, agarwood oil nanoemulsion (agarwood-NE) was formulated and tested for its antioxidant and anti-inflammatory potential in cigarette smoke extract (CSE)-treated BCI-NS1.1 airway basal epithelial cells. The findings suggest successful counteractivity of agarwood-NE against CSE-mediated pro-inflammatory effects by reducing the expression of the pro-inflammatory cytokines IL-1 α , IL-1 β , IL-8, and GDF-15. In addition, agarwood-NE induced the expression of the anti-inflammatory mediators IL-10, IL-18BP, TFF3, GH, VDBP, relaxin-2, IFN- γ ,

and PDGF. Furthermore, agarwood-NE also induced the expression of antioxidant genes such as GCLC and GSTP1, simultaneously activating the PI3K pro-survival signalling pathway. This study provides proof of the dual anti-inflammatory and antioxidant activity of agarwood-NE, highlighting its enormous potential for COPD treatment.

Keywords: agarwood; nanoemulsion; drug delivery; phytoceuticals; nutraceuticals; inflammation; cigarette smoke; chronic obstructive pulmonary disease; inflammation

1. Introduction

Chronic obstructive pulmonary disease (COPD) is a slow-developing, irreversible disease. It represents the third highest cause of death worldwide, causing approximately 3 million deaths per year [1,2]. The principal features of COPD are chronic airway inflammation, remodelling, and irreversible damage of the lung parenchyma, that result in mucus retention and severe airflow limitation that lead to symptoms such as difficulty in breathing, coughing, wheezing, increased chest wall diameter, dyspnea, and progressive and irreversible hyperresponsiveness of the airways [1,3]. COPD is characterized by frequent exacerbations, consisting of the acute worsening of the disease's symptoms. These often require patient hospitalization, resulting in elevated healthcare costs [4]. The main risk factor for COPD is represented by chronic cigarette smoking, which is associated with airway inflammation, oxidative stress, tissue damage, and fibrosis [5,6]. The interplay between chronic inflammation, oxidative stress, and tissue damage is particularly relevant for COPD development [7,8], and cigarette smoke (CS) enhances these processes because it contains several hundreds of compounds with pro-inflammatory and pro-oxidant activities [9].

In the context of inflammation and COPD, CS exposure has been described in several *in vivo* and *in vitro* models to act on broncho-epithelial cells and immune cells such as macrophages, dysregulating many signalling pathways and generally promoting pro-inflammatory, and pro-oxidant states [10]. Effects of CS include the promotion of the release of pro-inflammatory cytokines and mediators such as the interleukins (IL) IL-1 α [11], IL-1 β [12], IL-8 [13], IL-18 [14], and growth/differentiation factor-15 (GDF15) [15], as well as inhibition of the release of anti-inflammatory cytokines such as IL-10 [16]. GDF-15 has also been reported to be a biomarker for COPD [15], and circulating GDF-15 levels have been found to be 2.1-fold higher in COPD patients when compared to healthy subjects [17]. Other anti-inflammatory mediators whose release is impacted by CS include IL-18 binding protein (IL-18BP), growth hormone (GH), and vitamin D binding protein (VDBP). IL-18BP is a protein that acts as a natural IL-18 decoy, blocking the IL-18-mediated inflammatory response [18], and whose expression is reduced in the alveolar macrophages of rats exposed to second-hand smoke [19]. Besides its main activity as a stimulator of tissue growth, cell reproduction, and cell regeneration, GH is known to reprogram macrophages towards an anti-inflammatory, reparative phenotype [20], and chronic exposure to CS has been shown to reduce circulating GH levels [21]. VDBP is endowed with cytokine-like activity and is an important mediator of inflammatory tissue injury [22]. VDBP levels are downregulated in the plasma of cigarette smokers compared to non-smokers [23]. Platelet-derived growth factor (PDGF) is a family of proteins regulating inflammation in the airways. In particular, PDGF-BB has a complex immunomodulatory role in many conditions including asthma, where it was shown to orchestrate lung tissue remodelling [24], and it is known to inhibit inflammatory responses during sepsis through the inhibition of pro-inflammatory cytokines including tumour necrosis factor- α (TNF- α), IL-6, IL-1 β , and IL-8 [25]. Another anti-inflammatory protein with a relevant role in lung health is relaxin-2, which was recently shown, in a guinea pig model of CS exposure, to counteract CS-induced inflammation, remodelling, and tissue damage when administered exogenously [26].

The neuropeptide trefoil factor 3 (TFF3) is expressed by many cells of the respiratory tract and modulates the cytokine-induced secretion of inflammatory mediators [27]. By do-

ing so, it affects airway mucus secretion and is involved in maintaining epithelial integrity and healing after mucosal injury [28]. Expression of TFF3 has been reported to be reduced in a rat model of COPD obtained through exposure to CS [29], and this could potentially contribute to tissue damage caused by CS exposure. Further contribution to tissue damage by CS is caused by the direct induction of airway epithelial cell death, which is mediated by many mechanisms including inhibition of the protein arginine methyltransferase 6 (PRMT6)-phosphatidylinositol 3-kinase (PI3K)-Akt cell survival signalling pathway [30]. Moreover, CS impairs the antiviral response of airway epithelial cells by inhibiting the production of interferon gamma (IFN- γ) [31] and IFN- γ -dependent signalling [32], resulting in further increased susceptibility to infection-associated tissue damage which can, in turn, fuel COPD progression [33].

Another fundamental driving factor of COPD is oxidative stress, which is caused by an imbalance between the production and elimination, through antioxidant detoxification mechanisms, of reactive oxygen species (ROS) [7,34,35]. A fundamental mediator of cellular detoxification is glutathione [36]. This molecule is produced by a biosynthetic pathway whose initial and rate-limiting step is catalysed by the enzyme glutamate-cysteine ligase (GCLC) [37], and it has antioxidant activity as it acts as ROS scavenger [37]. Furthermore, carcinogenic products of tobacco smoke are detoxified upon conjugation with glutathione, and this reaction is catalysed by the enzyme glutathione S-transferase P (GSTP1) [38]. GSTP1 expression is reduced in lung and sputum specimens of patients with severe COPD [39].

Therapeutic approaches against COPD are aimed at improving the symptoms of exacerbations and involve the use of antibiotics, corticosteroids, and bronchodilators [4,40]. However, these treatment strategies are symptomatic, and do not essentially address the underlying cause of the disease. Furthermore, these treatments have several adverse effects including osteoporosis, insomnia, mood swings, and weight gains [4]. For these reasons, there is an unmet need for the development of novel therapeutic strategies allowing the successful, durable pharmacotherapy of COPD with simultaneous minimization of adverse effects.

In the search for novel treatment strategies, a generous source of nutraceuticals or compounds endowed with therapeutic activity is represented by nature, in particular plants [41]. Traditional medicinal plants, for example, are a fundamental source of phytochemical compounds such as berberine [12,42,43], curcumin [44], rutin [45], boswellic acid [46], nobiletin [47] with antioxidant, anti-inflammatory, and anticancer activities. Furthermore, numerous plant extracts of complex composition are reported to have anti-inflammatory and anti-oxidant properties [48–50]. One of such extracts is agarwood oil. Agarwood is a fragrant, dark resinous wood which is derived from the heartwood of trees belonging to the *Aquilaria* species that have been wounded or infested by some species of mould [51], and it has been used in Ayurvedic and Chinese traditional medicine for several centuries [52].

The main active ingredient of agarwood is its essential oil, which can be extracted from agarwood using different techniques [53]. Agarwood essential oil has been extensively studied recently, and many of its chemical components, particularly sesquiterpenes and chromones, have been reported to have strong in vitro and in vivo anti-inflammatory and antioxidant activities [53]. Numerous studies have also demonstrated the anti-inflammatory and antioxidant activities of agarwood oil as a whole, complex mixture [53]. These activities are exerted through many mechanisms including the inhibition of the production and function of proinflammatory cytokines [54,55] and prostaglandins [56,57], increased production of anti-inflammatory cytokines [58], blockade of inflammatory pathways such as NF- κ B [59], and general reduction of oxidative stress and related mediators such as nitric oxide [60]. These studies collectively demonstrate the notable therapeutic potential of agarwood oil in the management of chronic inflammatory diseases such as COPD [53].

Despite the enormous potential of bioactive plant-derived compounds and extracts, their clinical application is severely limited by issues including low solubility, poor bioavail-

ability, and insufficient intestinal absorption [12,45,61–63]. This is particularly true for essential oils such as agarwood oil which, being an oily extract, has very poor water solubility. With the aim of overcoming these limitations, numerous advanced drug delivery systems have been developed. Many of these successful delivery systems involve the encapsulation of therapeutic molecules in polymeric nanosystems such as liquid crystalline nanoparticles and solid lipid nanoparticles [64–66]. To improve the properties of highly lipophilic essential oils and extracts, nanoemulsion systems (NEs) are emerging as advanced drug delivery systems of choice, thanks to their relative ease and low cost of preparation, biocompatibility, and physicochemical stability [67,68]. NEs exist in submicron colloidal particulate systems of size ranging between 20 and 200 nm that are produced through different techniques including ultrasound emulsification, high-pressure homogenization, and microfluidization [67,68].

In this study, the antioxidant and anti-inflammatory activities of a poloxamer 407-based agarwood oil nanoemulsion (agarwood-NE) against an in vitro model of COPD obtained through exposure of BCI-NS1.1 human basal epithelial cells to 5% cigarette smoke extract (CSE) was investigated [12]. The biological activity of agarwood-NE was studied using in vitro experiments relevant to oxidative stress and inflammation pathways. The results of this study confirm the potent, multifaceted anti-inflammatory and antioxidant activities of agarwood oil, providing proof of the enormous potential of agarwood-NE as a therapeutic strategy against chronic inflammatory diseases such as COPD.

2. Methods

2.1. Preparation of Agarwood-NE

Agarwood oil was extracted from *Aquilaria crassna*. The plant material was chopped and ground into powder and left to air dry for 14 days to reduce moist contents. The essential oil was extracted from the dry agarwood powder through supercritical fluid carbon dioxide extraction at 0.005–0.006% per kg of raw agarwood powder. The extraction was performed at a pressure of 22 MPa and a temperature of 47 °C for 2 h, with a carbon dioxide fluid flow rate of 2 L/h. The separation was performed at 8 MPa and 40 °C. The essential oil was characterised by DeAurora Pty Ltd. The essential oil obtained appeared as a transparent, slightly viscous liquid, with a brown colour and a deep woody aroma. The essential oil was soluble in alcohol and fixed oils and had the following composition (Table 1):

Table 1. Composition of the agarwood oil.

Component	Actual %
Valerianol	12.31%
gamma-Eudesmol	8.03%
epi-Cyclocolorenone	3.71%
Nootkatone	3.71%
beta-Eudesmol	3.69%
Methyl phenethyl ketone	3.02%
10-epi-gamma-Eudesmol	2.90%
Hinesol	1.74%
dihydro-Columellarin	1.68%
alpha-Curcumene	0.88%
alpha-Humulene	0.85%
alpha-Bulnesene	0.56%
Selina-4,11-diene	0.45%
Debromofiliformin	0.38%
4,5-di-epi-Aristolochene	0.26%
Elemol	0.25%
alpha-Guaiene	0.16%
alpha-Selinene	0.11%

Agarwood nanoemulsion was prepared using a probe sonication method. Briefly, 200 mg of accurately weighed amount of agarwood oil was taken in a 50 mL Falcon conical tube. In another tube, 50 mg of Poloxamer 407 was dissolved with a required amount of purified distilled water (about 10 mL), and vortexed to ensure complete solubilization of the Poloxamer. The prepared solution was gradually added to the agarwood oil at ambient temperature and vortexed for 1 min. The coarse emulsion formed was subjected to probe sonication for 15 min at 80% amplitude in a 1 Hz on/off cycle to minimize heating. This resulted in the formation of a milky nanoemulsion, which was made up to a final volume of 20 mL by adding purified water. The obtained nanoemulsion was characterized for size and polydispersity index (dynamic light scattering), and morphology (transmission electron microscopy). The nanoemulsion was composed of droplets with spherical morphology, of 180 ± 4.7 nm diameter and 0.36 ± 0.03 polydispersity index.

2.2. Cell Culture and Agarwood-NE Treatment

Minimally immortalized human airway epithelium-derived basal cells (BCiNS1.1) were purchased from R. G. Crystal (Weill Cornell Medical College, New York, NY, USA). These cells were grown in broncho-epithelial basal media (BEBM) (Lonza, New York, NY, USA) supplemented with various growth factors and other supplements, including bovine pituitary extract, insulin, GA-1000 (Gentamicin sulfate-Amphotericin), retinoic acid, transferrin, triiodothyronine, epinephrine, human epidermal growth factor (BEGM Single Quots, Lonza), at 37 °C under humidified condition in the presence of 5% CO₂. For experiments, the cells were seeded onto a 96-well plate (Corning, New York, NY, USA) or a 6-well plate (Corning) at a density of 1×10^4 /well and 2×10^5 /well, respectively. After 80% confluency, the cells were pre-treated for 1 h with agarwood-NE at the concentrations indicated, followed by the treatment of with or without 5% cigarette-smoke extract (CSE) for 24 h.

2.3. Cell Viability

The cell viability of BCiNS1.1 cells was assessed using 3-(4,5-Dimethylthiazol-2-yl)-2,5-diphenyltetrazolium bromide (MTT, Merck, Rahway, NJ, USA), as described previously [69]. The cells were treated with different concentrations of agarwood-NE (10–1000 µg/mL) for 24 h in a 96-well plate. Then, MTT solution (250 µg/mL) was added into each well and incubated for 4 h. After incubation, the media was removed and the coloured formazan crystals formed in the reaction were dissolved with 100 µL dimethyl sulfoxide (DMSO, Merck, Rahway, NJ, USA). The absorbance at a wavelength of 540 nm was read using a POLARstar Omega microplate reader (BMG Labtech, Ortenberg, Germany).

2.4. Real Time-qPCR

The effects of agarwood-NE on mRNA expression levels of inflammation-related and oxidative stress-related genes in CSE-induced BCiNS1.1 cells were determined by real time-qPCR, as described previously [70]. The cells were pre-treated with agarwood-NE at 25 and 50 µg/mL for 1 h, and then treated with or without 5% CSE for 24 h. The cells were then lysed with 500 µL TRI reagent (Merck). A total of 250 µL of chloroform was added and the mixture was centrifuged at $12,000 \times g$, 4 °C, for 15 min. The aqueous phase was pipetted out into new Eppendorf tubes and 500 µL of isopropyl alcohol was added to precipitate the RNA. The tubes were then centrifuged at $12,000 \times g$, room temperature, for 10 min. After centrifugation, the supernatant was removed, and the RNA pellets were washed 2× with 1 mL 75% ethanol. The tubes were centrifuged again at $8000 \times g$, 4 °C, for 5 min. After the second round of centrifugation, the ethanol was removed, and the dry RNA pellets were dissolved in nuclease-free water. Nanodrop (Thermo Fisher Scientific, Waltham, MA, USA) was used to determine the concentration and purity of the RNA.

After subjecting to DNase I (Merck) treatment, 1 µg total RNA was reverse-transcribed to cDNA using the reaction mixture of M-MLV buffer (Thermo Fisher Scientific), random primers (0.5 µg/µL), dNTPs (10 mM), and DTT (100 mM). A thermal cycler (Eppendorf,

Hamburg, Germany) was used in the subsequent steps involving denaturation (65 °C, 10 min), annealing (25 °C, 10 min), reverse transcription (37 °C, 50 min), and enzyme inactivation (70 °C, 15 min). Equal amounts (25 ng) of cDNA were then subjected to real-time qPCR with iTaq Universal SYBR green (BioRad, Hercules, CA, USA) and primers (forward and reverse, 0.5 µM each) using a CFX96 PCR system (BioRad). The real-time qPCR involved thermal cycles of 95 °C for 30 s (1 cycle), 95 °C for 15 s (40 cycles), and 60 °C for 30 s (1 cycle).

The sequences of human primers used were as follows (Table 2):

Table 2. Nucleotidic sequence of the primers used in the Real-time qPCR.

Gene Name	FW Sequence	RV Sequence
IL-8	GCCTCAAGGAAAAGAATCTG	GGATCTACTCTCCAGC
GAPDH	TCGGAGTCAACGGATTG	CAACAATATCCACTTTACCAGAG
GCLC	TTATTAGAGACCCACTGACAC	TTCTCAAAATGGTCAGACTC
GSTP1	TTTCCAGTTCGAGGC	ATAGGCAGGAGGCTTTG
PI3K	GAGTAACAGACTAGCTAGAGAC	AGAAAATCTTTCTCCTGCTC

2.5. Human Cytokine Protein Array

The effects of agarwood-NE on cytokine expression levels in CSE-induced BCI-NS1.1 cells were assessed using a human cytokine protein array kit (R&D Systems, Minneapolis, MN, USA), as described in a previous study [12]. The cells were seeded in 6-well plates as indicated previously and were pre-treated with agarwood-NE at 25 and 50 µg/mL for 1 h, then treated with 5% CSE for 24 h. The cells were lysed using RIPA buffer (ThermoFisher Scientific, Sydney, NSW, Australia) that contained protease and phosphatase inhibitors (Roche Diagnostics GmbH, Mannheim, Germany). Equal amounts (300 µg) of protein were loaded onto human cytokine arrays and incubated overnight at 4 °C. Further incubation with antibodies and reagents were conducted in accordance with the manufacturer's instructions. The protein spots in the array were photographed using the ChemiDoc MP (Bio-Rad, Hercules, CA, USA) and analysed using Image J. (version 1.53c, Bethesda, MD, USA).

2.6. Statistical Analysis

In Figures 1, 2, 5 and 6, the data were expressed as mean ± SEM and statistically analysed using 1-way ANOVA, followed by Dunnett multiple comparison test. A *p*-value of <0.05 was considered significant. In Figures 3 and 4, the individual measurements are indicated together with the mean value of each group.

3. Results

3.1. Identification of an Optimal Concentration of Agarwood-NE for Treatment in CSE-Induced BCI-NS1.1 Cells

To find a safe agarwood-NE concentration for cell treatment, a toxicity study was performed, using the MTT assay to measure cell viability upon exposure of 5% CSE-induced BCI-NS1.1 cells to various concentrations of agarwood-NE. The findings are shown in Figure 1. Treatment with agarwood-NE amounts corresponding to up to 50 µg/mL agarwood oil extract did not result in significant reduction of cell viability (Figure 1). Concentrations of 100, 500, and 1000 µg/mL agarwood oil significantly decreased cell viability by 9.5%, 78.7%, and 97.7%, respectively (Figure 1, *p* < 0.0001 against untreated control). In the subsequent experiments, cells were exposed to the non-toxic concentrations of 25 and 50 µg/mL agarwood-NE.

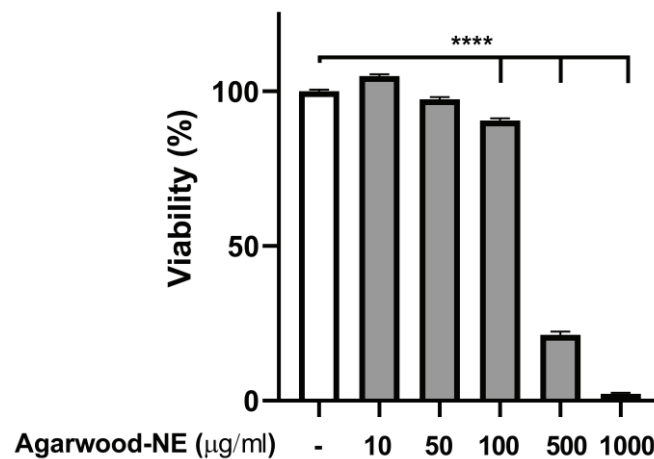


Figure 1. Effect of Agarwood-NE on the cell viability of 5% CSE-induced BCI-NS1.1 cells. BCI-NS1.1 cells were pre-incubated for 1 h in the presence of increasing concentrations of agarwood-NE (10, 50, 100, 500, or 1000 µg/mL), followed by exposure to 5% CSE for 24 h. Upon treatment, MTT assay was used to measure cell viability. Cell viability was normalised as a percentage compared to untreated control. The results are mean \pm SEM of 3 independent experiments (****; $p < 0.0001$).

3.2. Agarwood-NE Inhibits the CSE-Induced Transcription of the Pro-Inflammatory Cytokine IL-8

The anti-inflammatory activity of agarwood-NE was studied on 5% CSE-induced BCI-NS1.1 cells by measuring the mRNA levels of the pro-inflammatory cytokine IL-8. CSE induced a 6.2-fold increase of the transcription of the IL-8 mRNA compared to control (Figure 2, $p < 0.0001$). Treatment with agarwood-NE at 25 and 50 µg/mL concentration resulted in the concentration-dependent reduction of IL-8 mRNA levels by 16.1% and 54.9%, respectively, compared to CSE-treated cells (Figure 2, $p < 0.05$ and $p < 0.0001$, respectively).

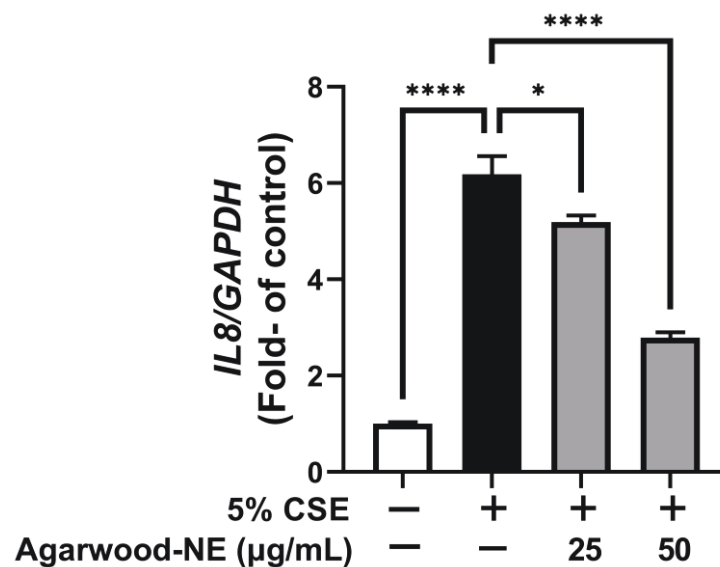


Figure 2. Effect of Agarwood-NE on the CSE-induced transcription of the pro-inflammatory cytokine IL-8. BCI-NS1.1 cells were pre-incubated for 1 h in the presence of 25 and 50 µg/mL agarwood-NE, followed by exposure to 5% CSE for 24 h. The mRNA levels of IL-8 were determined via RT-qPCR. Values are expressed as mean \pm SEM ($n = 4$, *; $p < 0.05$; ****; $p < 0.0001$).

3.3. Agarwood-NE Inhibits the CSE-Induced Protein Expression of Pro-Inflammatory Cytokines and Mediators

The protein levels of the pro-inflammatory cytokines and mediators IL-1 α , IL-1 β , IL-1Ra, and GDF-15 are shown in Figure 3. Exposure of BCI-NS1.1 cells to 5% CSE induced a significant increase in the levels of IL-1 α (1.6-fold, Figure 3A), IL-1 β (1.7-fold, Figure 3B), IL-

1Ra (1.1-fold, Figure 3C), and GDF-15 (1.1-fold, Figure 3D) compared to untreated control. The levels of these proteins were significantly reduced to similar extents upon treatment with the two concentrations of agarwood-NE tested (25 and 50 $\mu\text{g}/\text{mL}$). Upon treatment with 50 $\mu\text{g}/\text{mL}$ agarwood-NE, the levels of IL-1 α were reduced by 54.5% (Figure 3A), while the levels of IL-1 β were reduced by 35.4% ($p < 0.0001$, Figure 3B). Furthermore, treatment with 50 $\mu\text{g}/\text{mL}$ agarwood-NE resulted in a 15.4% reduction of the levels of IL-1Ra (Figure 3C) and in a 45.3% reduction of the levels of GDF-15 (Figure 3D). Although, treatment with 25 $\mu\text{g}/\text{mL}$ agarwood-NE resulted in a slightly lower extent of reduction of the amount of these four cytokines, no statistically significant difference was detected between the two concentrations of agarwood-NE tested in all cases.

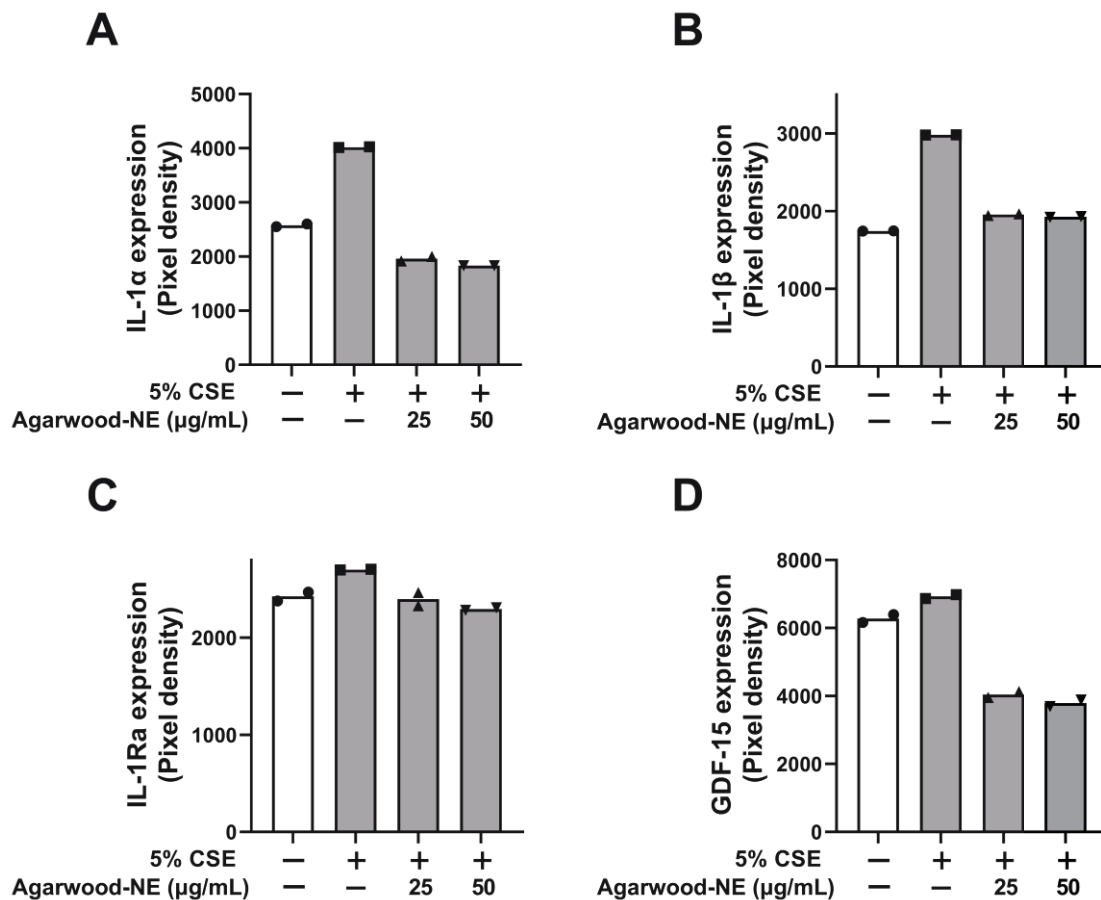


Figure 3. Effect of Agarwood-NE on the CSE-induced production of pro-inflammatory mediators in human cytokine protein array. BCI-NS1.1 cells were pre-incubated for 1 h in the presence of 25 and 50 $\mu\text{g}/\text{mL}$ agarwood-NE, followed by exposure to 5% CSE for 24 h. The protein levels of IL-1 α (A), IL-1 β (B), IL-1Ra (C), and GDF-15 (D) were determined via human cytokine protein array.

3.4. Agarwood-NE Stimulates the CSE-Inhibited Protein Expression of Anti-Inflammatory Cytokines and Mediators

The protein levels of the investigated anti-inflammatory cytokines and mediators are shown in Figure 4. Treatment of BCI-NS1.1 cells with 5% CSE caused a significant reduction of the protein levels of the following cytokines compared to untreated control: IL-10 (13.3%, Figure 4A), IL-18 Bpa (18.9%, Figure 4B), growth hormone (GH, 14.5%, Figure 4C), vitamin D binding protein (VDBP, 7.3%, Figure 4D), relaxin-2 (14.0%, Figure 4E), interferon- γ (IFN- γ , 15.9%, Figure 4F), platelet-derived growth factor (PDGF-BB, 13.3%, Figure 4G), and trefoil factor 3 (TFF3, 17.5%, Figure 4H). Exposure to 50 $\mu\text{g}/\text{mL}$ of agarwood-NE counteracted the effect of CSE treatment, significantly increasing the levels of all these proteins compared to cells treated with 5% CSE only. In particular, the 50 $\mu\text{g}/\text{mL}$ concentration of agarwood-NE increased the levels of IL-10 by 13.1% (Figure 4A) and the levels of IL-18 Bpa by

11.7% (Figure 4B). The levels of GH were increased by 7.0% (Figure 4C) and the levels of VDBP were increased by 7.0% (Figure 4D). Furthermore, upon treatment with 50 $\mu\text{g}/\text{mL}$ agarwood-NE, relaxin-2 levels resulted in an increase by 8.0% (Figure 4E), and the levels of IFN- γ increased by 11.8% (Figure 4F). Finally, 50 $\mu\text{g}/\text{mL}$ agarwood-NE treatment increased the levels of PDGF-BB by 10.6% (Figure 4G) and the levels of TFF3 by 12.7% (Figure 4H). Treatment with 25 $\mu\text{g}/\text{mL}$ agarwood-NE significantly increased the levels of IL-18Bpa (6.8%, Figure 4B), relaxin-2 (8.8%, Figure 4E), and IFN- γ (6.7%, Figure 4F).

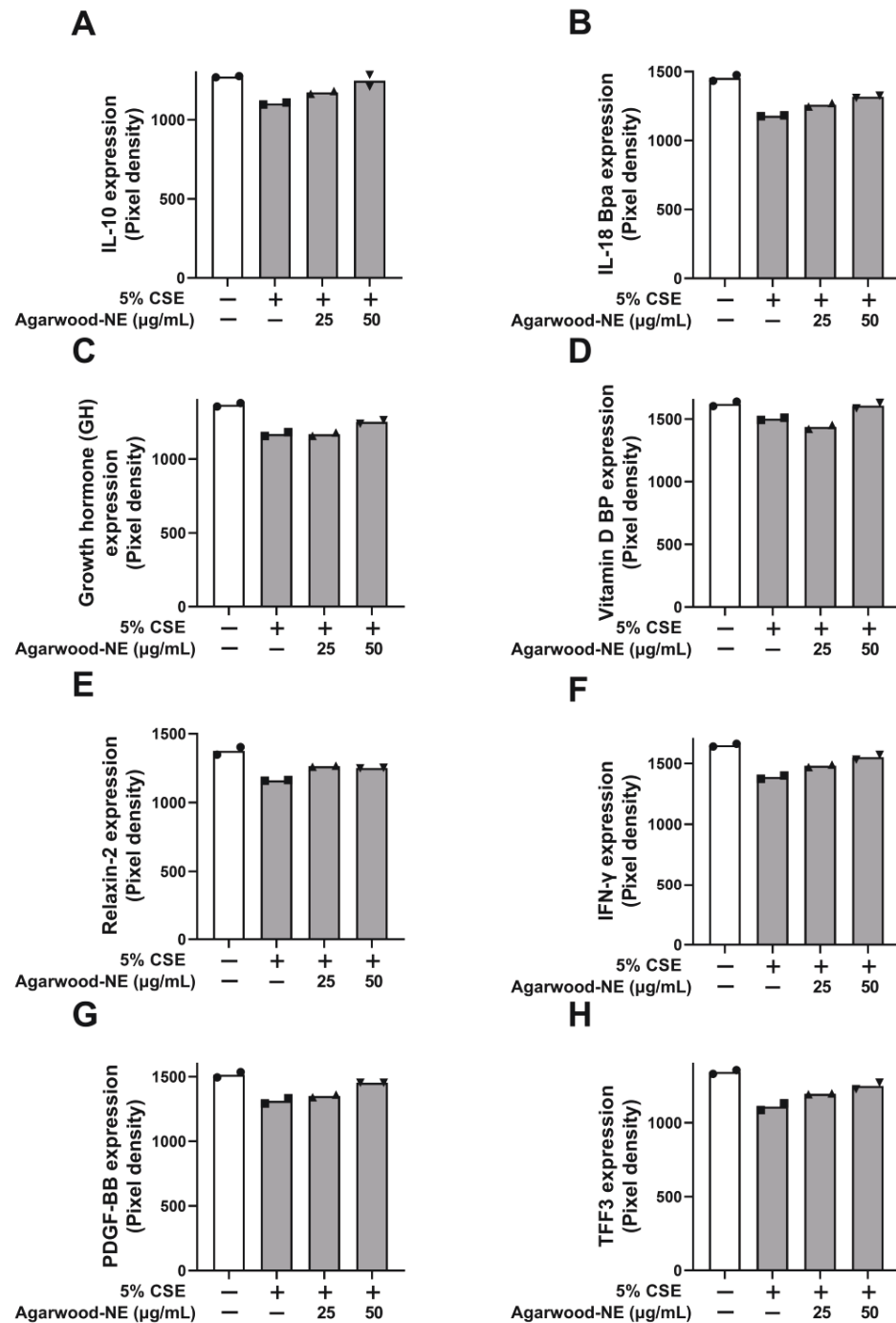


Figure 4. Effect of agarwood-NE on the CSE-inhibited production of anti-inflammatory mediators in human cytokine protein array. BCi-NS1.1 cells were pre-incubated for 1 h in the presence of 25 and 50 $\mu\text{g}/\text{mL}$ agarwood-NE, followed by exposure to 5% CSE for 24 h. The protein levels of IL-10 (A), IL-18Bpa (B), GH (C), VDBP (D), relaxin-2 (E), IFN- γ (F), PDGF-BB (G), and TFF3 (H) were determined via human cytokine protein array.

3.5. Agarwood-NE Stimulates the CSE-Inhibited Transcription of Antioxidant Genes

The antioxidant activity of agarwood-NE was investigated on 5% CSE-induced BCI-NS1.1 cells by measuring the mRNA levels of the genes GCLC and GSTP1 (Figure 5). Compared to the untreated control, CSE induced a 32.7% reduction of the transcription of the GCLC mRNA (Figure 5A, $p < 0.0001$) and a 65.4% reduction of the transcription of the GSTP1 mRNA (Figure 5B, $p < 0.01$). Treatment with agarwood-NE at 50 $\mu\text{g}/\text{mL}$ concentration resulted in a significant 63.6% increase of the mRNA levels of GCLC (Figure 5A, $p < 0.0001$) and in a significant 344.0% increase of the mRNA levels of GSTP1 (Figure 5B, $p < 0.001$), compared to the 5% CSE-treated group. Furthermore, treatment with agarwood-NE at 25 $\mu\text{g}/\text{mL}$ concentration significantly increased the GSTP1 mRNA levels by 138.5% compared to the 5% CSE-treated group (Figure 5B, $p < 0.05$).

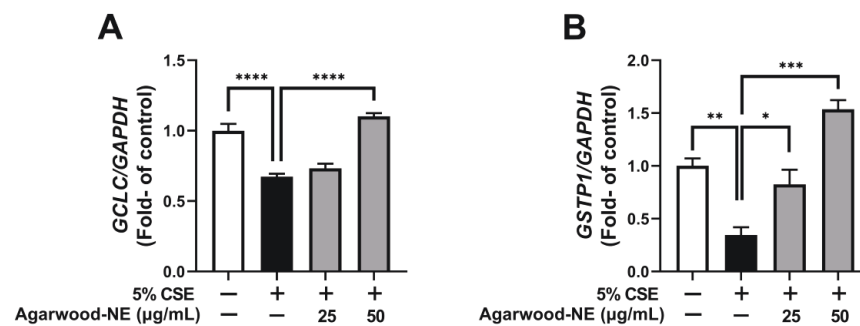


Figure 5. Effect of Agarwood-NE on the CSE-inhibited transcription of antioxidant genes. BCI-NS1.1 cells were pre-incubated for 1 h in the presence of 25 and 50 $\mu\text{g}/\text{mL}$ agarwood-NE, followed by exposure to 5% CSE for 24 h. The mRNA levels of GCLC (A) and GSTP1 (B) were determined via RT-qPCR. Values are expressed as mean \pm SEM ($n = 3-4$, *: $p < 0.05$; **: $p < 0.01$; ***: $p < 0.001$; ****: $p < 0.0001$).

3.6. Agarwood-NE Stimulates the CSE-Inhibited Transcription of the Pro-Survival Gene PI3K

Finally, the effect of agarwood-NE on pro-survival pathways was investigated on 5% CSE-induced BCI-NS1.1 cells by measuring the mRNA levels of the PI3K gene (Figure 6). Exposure of cells to CSE resulted in a significant 31.2% reduction of the PI3K mRNA levels compared to the untreated control group ($p < 0.0001$, Figure 6). Treatment with agarwood-NE at 25 $\mu\text{g}/\text{mL}$ and 50 $\mu\text{g}/\text{mL}$ concentration resulted in a significant, concentration-dependent increase of PI3K mRNA levels by 26.5% and 54.8% ($p < 0.001$ and $p < 0.0001$, respectively), compared to the 5% CSE-treated group (Figure 6).

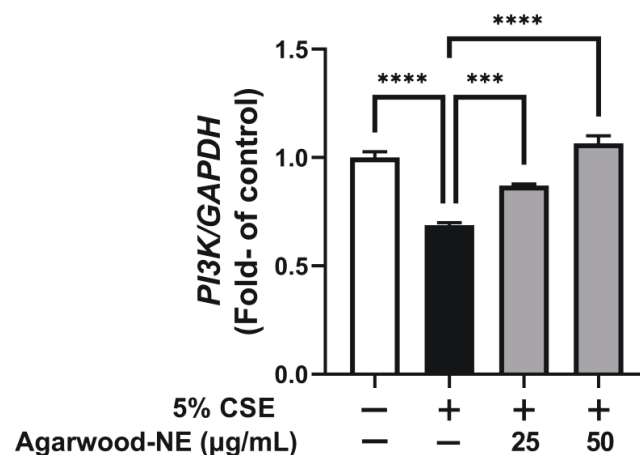


Figure 6. Effect of Agarwood-NE on the CSE-inhibited transcription of the pro-survival gene PI3K. BCI-NS1.1 cells were pre-incubated for 1 h in the presence of 25 and 50 $\mu\text{g}/\text{mL}$ agarwood-NE, followed by exposure to 5% CSE for 24 h. The mRNA levels of PI-3K were determined via RT-qPCR. Values are expressed as mean \pm SEM ($n = 4$, ***: $p < 0.001$; ****: $p < 0.0001$).

4. Discussion

COPD is a progressive inflammatory respiratory disease characterized by chronic lung inflammation that causes irreversible obstruction of the airflow and periodic exacerbations [71–73]. This causes significant medical and financial burden worldwide [74]. Cigarette smoking is the main cause of COPD [75], and it is known to cause inflammation and oxidative stress which, together, play fundamental roles in the pathogenesis of chronic inflammatory diseases such as COPD [76,77]. Current treatment strategies for COPD involve pulmonary rehabilitation, smoke cessation, and pharmacological relief of symptoms through inhalational therapy [78]. Despite this, COPD still represents a leading cause of morbidity and mortality worldwide [79]. This leads to the urgent necessity of novel therapeutic strategies for COPD with increased efficacy and reduced adverse effects. In this context, therapeutic agents embedded with both anti-inflammatory and antioxidant activities would be advantageous, considering the prominent role played by the interaction between oxidative stress and inflammation in COPD.

In the search for novel therapeutic compounds, the natural world is an endless source of inspiration, and many traditional medicinal plants produce molecules embedded with anti-inflammatory and antioxidant properties. These include, for example, berberine [12] and rutin [80]. Complex mixtures such as the essential oils extracted from many plants [81], including agarwood oil [53], are also known for their potent antioxidant and anti-inflammatory properties. Despite all these, the therapeutic application of plant-based compounds is often hampered by issues such as low water solubility, poor bioavailability and, in general, an unfavourable pharmacokinetic profile [12,82]. The use of nanoparticles/carriers-based novel drug delivery systems represents a promising strategy to overcome these limitations [62]. This study reports the potent anti-inflammatory and antioxidant properties of agarwood extract oil formulated in a poloxamer 407-based nanoemulsion on BCI-NS1.1 human basal epithelial cells exposed to 5% CSE.

Cigarette smoke (CS) is known to contain several hundreds of compounds with oxidative, pro-inflammatory, and carcinogenic properties [9], and each puff of cigarette contains 10^{17} oxidant molecules [83]. These molecules promote inflammation, oxidative stress, and tissue damage, which in turn collectively orchestrate the development of COPD [84,85]. The chemicals contained in CS are known to interfere with many different signalling pathways in cells of the lung parenchyma, activating DNA damage responses, inflammation, oxidative stress, and autophagy, ultimately leading to increased cellular senescence, cell death, or cancerous transformation [86–88]. CS induces a pro-inflammatory state by (i) activating pathways that lead to the release of pro-inflammatory cytokines and mediators such as IL-8 [89], IL-1 α [11], IL-1 β [90], and GDF-15 [15]; and (ii) inactivating pathways that lead to the production of anti-inflammatory cytokines and mediators such as IL-10 [16], IL-18BP [19], GH [21], and VDBP [23].

This study reports the anti-inflammatory activity of agarwood-NE which is exerted by counteracting both the aforementioned mechanisms. In particular, the treatment of CSE-induced BCI-NS1.1 with agarwood-NEs significantly reduced the transcription of the gene encoding for IL-8 as well as the levels of IL-1 α and IL-1 β proteins. With regards to IL-1 α and IL-1 β , our findings are in agreement with previous reports where agarwood oil, or single components extracted from it, were found to reduce the expression of these cytokines [53]. This study is the first to report that agarwood oil extract reduces the expression of IL-8. Furthermore, treatment with agarwood-NE resulted in significant reduction of the levels of GDF-15. The fact that GDF-15 plays a role in the induction of cancer epithelial-to-mesenchymal transition (EMT) [15] also suggests the possibility that agarwood-NE may possess anti-cancer or anti-metastatic activity. Considering the importance of EMT as a fundamental process contributing to airway remodelling in inflammatory lung diseases [91], the inhibition of GDF-15 represents a potential mechanism by which agarwood-NE may counteract airway remodelling. IL-1Ra is an anti-inflammatory protein that is released in response to IL-1 β signalling and acts as a negative regulator of IL-1 signalling, with the aim of mitigating hyper-inflammatory states [92]. The fact that the expression of IL-

1Ra is stimulated by CSE fits with its role as a negative “buffer” of IL-1 signalling, and the reduction of its expression obtained by concomitant agarwood-NE treatment may be secondary to the induced downregulation of both IL-1 α and IL-1 β [92].

With regards to the induction of CSE-inactivated anti-inflammatory mediators, treatment with agarwood-NE, particularly at a 50 $\mu\text{g}/\text{mL}$ concentration, successfully increased the levels of IL-10, IL-18BP, GH, and VDBP to levels comparable to those measured prior to exposure to 5% CSE. The induction of IL-10 is consistent with previous reports where agarwood oil was shown to increase IL-10 levels in *in vivo* mice models of intestinal injury [58] and gastric ulcer [59]. This current study is the first to report that agarwood oil induces IL-18BP, GH, and VDBP. Furthermore, this study also reports that treatment of BCI-NS1.1 with 5% CSE significantly decreased the levels of two other anti-inflammatory factors: PDGF-BB and relaxin-2. To the best of our knowledge, this is the first study to report that CSE causes a reduction of the levels of these two proteins. Considering the anti-inflammatory and immunomodulatory activity of both PDGF-BB and relaxin-2, the induction of the expression of these two factors represents another pathway by which agarwood-NE exerts its anti-inflammatory activity, reinforcing its potential against COPD.

Together with the modulation of pro- and anti-inflammatory mediators, another important finding of this study is that treatment with agarwood-NE successfully counteracted the CSE-induced reduction of the levels of mRNAs encoding for GCLC and GSTP1. Considering the fundamental roles played by these two proteins in the synthesis of glutathione (GCLC, [37]) and in its conjugation with tobacco carcinogens (GSTP1, [38]), this study findings suggest that agarwood-NE promotes an anti-oxidant state which, together with its anti-inflammatory activity, makes our formulation suitable as a potential dual antioxidant and anti-inflammatory treatment to counteract these CS-induced processes.

Besides its action on inflammatory and oxidative pathways, the study also shows that another mechanism by which agarwood-NE counteracts the deleterious effects of CS is through the induction of molecular pathways that are actively involved in protecting cells from damage, infection, and death. These include TFF3, IFN- γ , and PI3K. TFF3 participates in the maintenance of epithelial integrity and in mucosal healing [28], and therefore, may play an important role in protecting the lung parenchyma from CS-induced damage. In this study, treatment of BCI-NS1.1 cells with 5% CSE resulted in a reduction of TFF3 levels, which was counteracted upon treatment with agarwood-NE. A similar trend was observed for IFN- γ and PI3K. Considering the critical role of IFN- γ in the activation of antiviral responses, as well as in their modulation to minimize collateral tissue damage [93], the fact that treatment with agarwood-NE increases IFN- γ levels provides a further mechanism by which this formulation exerts its protective activity against CSE-induced damage. Finally, this study report that treatment of BCI-NS1.1 cells with agarwood-NE increases the levels of PI3K transcript. Due to the fact that PI3K mediates a pro-survival signalling pathway [30,94], this may represent another mechanism by which agarwood-NE treatment protects cells from CSE-induced cell death.

Taken together, the findings and observations obtained from this study demonstrate that the agarwood-NE formulation tested is embedded with potent dual antioxidant and anti-inflammatory activities, which is exerted through a pleiotropic action on many different molecular pathways. The molecular pathways activated or inhibited by the treatment with agarwood-NE formulation are summarized in Figure 7.

This underlines the potential of agarwood-NE as a treatment strategy for diseases where inflammation and oxidative stress interact significantly, such as COPD.

Although the promising results shown provide a proof of concept of the effect of agarwood-NE against CSE-induced COPD a limitation of this study is that it only provides information about the effect of agarwood-NE on basal epithelial cells. To increase the reach and scope of the present findings, the effect of agarwood-NE should be tested on different cell lines such as macrophages and other cell lines present in the lung, in order to provide a complete and realistic picture of the multifaceted activity of agarwood-NE against inflammation and oxidative stress. Furthermore, considering the many pathways impacted

by the treatment with agarwood-NE, it would be interesting to investigate the activity of this formulation against other inflammatory diseases such as asthma, and lung cancer. Another exciting future perspective is represented by the investigation of the effect of the agarwood-NE formulation against other processes occurring in COPD, such as remodelling and cellular senescence. Finally, in order to proceed towards clinical translation, this study must be validated further with suitable *in vivo* animal models of COPD.

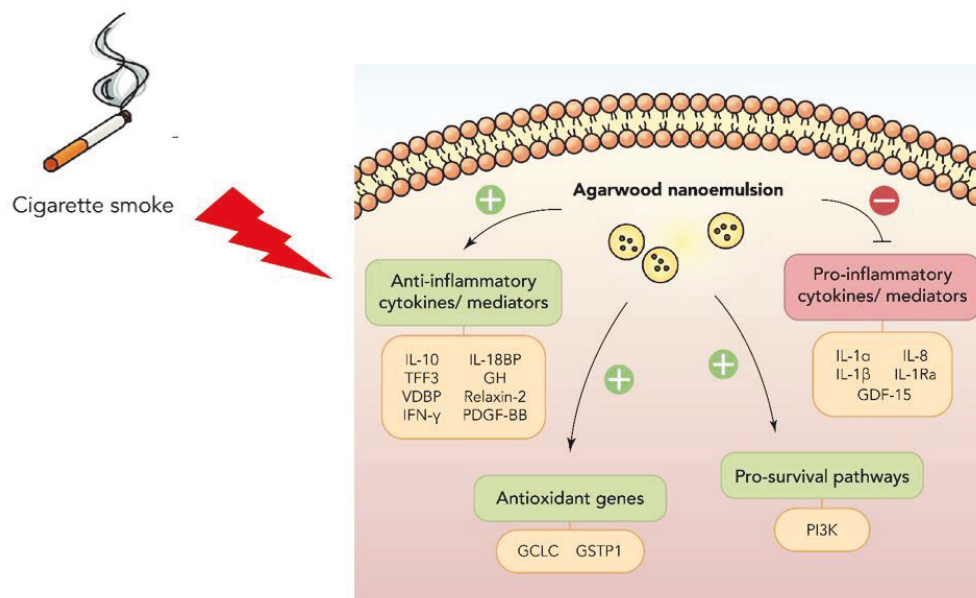


Figure 7. Summary of the anti-inflammatory and antioxidant molecular pathways activated by agarwood-NE to counteract the effect of cigarette smoke extract in BCI-NS1.1 cells.

5. Conclusions

In this study, we demonstrated that agarwood-NE exerts potent *in vitro* anti-inflammatory and antioxidant activities by counteracting several pro-inflammatory and pro-oxidant pathways activated by treatment of BCI-NS1.1 human airway epithelium-derived basal cells with 5% CSE. The results of this study provide proof for the enormous potential of agarwood-NE as dual antioxidant and anti-inflammatory treatment for inflammatory respiratory diseases such as COPD. However, for the results of these studies to be translated into clinic, the findings reported in this study must be validated through further *in vitro* investigation, as well as through *in vivo* pre-clinical studies.

Author Contributions: Conceptualization, G.D.R., K.R.P., K.D., P.M.H. and B.G.G.O.; Methodology, G.D.R., K.R.P., K.D., P.M.H., B.M., D.K.C., S.K.S., R.M. (Raniya Malik), J.S., G.G., R.M. (Ronan MacLoughlin) and A.C.; Formal Analysis, G.D.R., K.R.P. and B.M.; Investigation, G.D.R., K.R.P., B.M., R.M. (Ronan MacLoughlin), R.M. (Raniya Malik), J.S., A.C., G.G. and S.K.S.; Resources, R.M. (Raniya Malik), J.S. and R.M. (Ronan MacLoughlin); Data Curation, G.D.R., K.R.P. and B.M.; Writing—Original Draft Preparation, G.D.R.; Writing—Review and Editing, G.D.R., K.R.P., K.D., P.M.H., B.M., D.K.C., S.K.S., R.M. (Raniya Malik), J.S., G.G., R.M. (Ronan MacLoughlin), A.C. and B.G.G.O.; Supervision, K.D., P.M.H. and B.G.G.O.; Project Administration, K.D. and P.M.H.; Funding Acquisition, K.D. and P.M.H. All authors have read and agreed to the published version of the manuscript.

Funding: The authors are thankful to the Graduate School of Health, University of Technology Sydney, Australia. KD is supported by a project grant from the Rebecca L Cooper Medical Research Foundation and the Maridulu Budyari Gumal Sydney Partnership for Health, Education, Research and Enterprise (SPHERE) RSEOH CAG Seed grant, fellowship and extension grant; Faculty of Health MCR/ECR Mentorship Support Grant and UTS Global Strategic Partnerships Seed Funding Scheme. GDR is supported by the UTS International Research Scholarship and the UTS President's Scholarship. KRP is supported by a fellowship from Prevent Cancer Foundation (PCF) and the International Association for the Study of Lung Cancer (IASLC). The authors would also like to

thank DeAurora Pty Ltd. for providing us with the agarwood oil along with financial support for the project.

Institutional Review Board Statement: Not applicable.

Informed Consent Statement: Not applicable.

Data Availability Statement: The data presented in this study are available on request from the corresponding authors.

Conflicts of Interest: The authors have no conflicts of interest to declare.

References

1. Eapen, M.S.; Myers, S.; Walters, E.H.; Sohal, S.S. Airway inflammation in chronic obstructive pulmonary disease (COPD): A true paradox. *Expert Rev. Respir. Med.* **2017**, *11*, 827–839. [[CrossRef](#)] [[PubMed](#)]
2. Liu, G.; Jarnicki, A.G.; Paudel, K.R.; Lu, W.; Wadhwa, R.; Philp, A.M.; Van Eeckhoutte, H.; Marshall, J.E.; Malyla, V.; Katsifis, A.; et al. Adverse roles of mast cell chymase-1 in chronic obstructive pulmonary disease. *Eur. Respir. J.* **2022**, *60*, 2101431. [[CrossRef](#)] [[PubMed](#)]
3. Vogelmeier, C.F.; Criner, G.J.; Martínez, F.J.; Anzueto, A.; Barnes, P.J.; Bourbeau, J.; Celli, B.R.; Chen, R.; Decramer, M.; Fabbri, L.M.; et al. Global Strategy for the Diagnosis, Management, and Prevention of Chronic Obstructive Lung Disease 2017 Report: GOLD Executive Summary. *Arch. Bronconeumol.* **2017**, *53*, 128–149. [[CrossRef](#)] [[PubMed](#)]
4. Bollmeier, S.G.; Hartmann, A.P. Management of chronic obstructive pulmonary disease: A review focusing on exacerbations. *Am. J. Health Syst. Pharm.* **2020**, *77*, 259–268. [[CrossRef](#)]
5. Mehta, M.; Dhanjal, D.S.; Paudel, K.R.; Singh, B.; Gupta, G.; Rajeshkumar, S.; Thangavelu, L.; Tambuwala, M.M.; Bakshi, H.A.; Chellappan, D.K.; et al. Cellular signalling pathways mediating the pathogenesis of chronic inflammatory respiratory diseases: An update. *Inflammopharmacology* **2020**, *28*, 795–817. [[CrossRef](#)]
6. Lugg, S.T.; Scott, A.; Parekh, D.; Naidu, B.; Thickett, D.R. Cigarette smoke exposure and alveolar macrophages: Mechanisms for lung disease. *Thorax* **2022**, *77*, 94–101. [[CrossRef](#)]
7. Dua, K.; Malyla, V.; Singhvi, G.; Wadhwa, R.; Krishna, R.V.; Shukla, S.D.; Shastri, M.D.; Chellappan, D.K.; Maurya, P.K.; Satija, S.; et al. Increasing complexity and interactions of oxidative stress in chronic respiratory diseases: An emerging need for novel drug delivery systems. *Chemico-Biological Interactions* **2019**, *299*, 168–178. [[CrossRef](#)]
8. Mehta, M.; Paudel, K.R.; Shukla, S.D.; Shastri, M.D.; Satija, S.; Singh, S.K.; Gulati, M.; Dureja, H.; Zaccani, F.C.; Hansbro, P.M.; et al. Rutin-loaded liquid crystalline nanoparticles attenuate oxidative stress in bronchial epithelial cells: A PCR validation. *Future Med. Chem.* **2021**, *13*, 543–549. [[CrossRef](#)]
9. Malyla, V.; Paudel, K.R.; Shukla, S.D.; Donovan, C.; Wadhwa, R.; Pickles, S.; Chimankar, V.; Sahu, P.; Bielefeldt-Ohmann, H.; Bebawy, M.; et al. Recent advances in experimental animal models of lung cancer. *Future Med. Chem.* **2020**, *12*, 567–570. [[CrossRef](#)]
10. Albano, G.D.; Gagliardo, R.P.; Montalbano, A.M.; Profita, M. Overview of the Mechanisms of Oxidative Stress: Impact in Inflammation of the Airway Diseases. *Antioxidants* **2022**, *11*, 2237. [[CrossRef](#)]
11. Milad, N.; Pineault, M.; Lechasseur, A.; Routhier, J.; Beaulieu, M.J.; Aubin, S.; Morissette, M.C. Neutrophils and IL-1 α Regulate Surfactant Homeostasis during Cigarette Smoking. *J. Immunol.* **2021**, *206*, 1923–1931. [[CrossRef](#)]
12. Paudel, K.R.; Panth, N.; Manandhar, B.; Singh, S.K.; Gupta, G.; Wich, P.R.; Nammi, S.; MacLoughlin, R.; Adams, J.; Warkiani, M.E.; et al. Attenuation of Cigarette-Smoke-Induced Oxidative Stress, Senescence, and Inflammation by Berberine-Loaded Liquid Crystalline Nanoparticles: In Vitro Study in 16HBE and RAW264.7 Cells. *Antioxidants* **2022**, *11*, 873. [[CrossRef](#)]
13. Mio, T.; Romberger, D.J.; Thompson, A.B.; Robbins, R.A.; Heires, A.; Rennard, S.I. Cigarette smoke induces interleukin-8 release from human bronchial epithelial cells. *Am. J. Respir. Crit. Care Med.* **1997**, *155*, 1770–1776. [[CrossRef](#)]
14. Kaplanski, G. Interleukin-18: Biological properties and role in disease pathogenesis. *Immunol. Rev.* **2018**, *281*, 138–153. [[CrossRef](#)]
15. Jiang, G.; Liu, C.T.; Zhang, W.D. IL-17A and GDF15 are able to induce epithelial-mesenchymal transition of lung epithelial cells in response to cigarette smoke. *Exp. Ther. Med.* **2018**, *16*, 12–20. [[CrossRef](#)]
16. Hu, X.; Hong, B.; Sun, M. Peitu Shengjin Recipe Attenuates Airway Inflammation via the TLR4/NF- κ B Signaling Pathway on Chronic Obstructive Pulmonary Disease. *Evid. Based Complement. Alternat. Med.* **2022**, *2022*, 2090478. [[CrossRef](#)]
17. Mueller, T.; Leitner, I.; Egger, M.; Haltmayer, M.; Dieplinger, B. Association of the biomarkers soluble ST2, galectin-3 and growth-differentiation factor-15 with heart failure and other non-cardiac diseases. *Clin. Chim. Acta* **2015**, *445*, 155–160. [[CrossRef](#)]
18. Novick, D.; Kim, S.-H.; Fantuzzi, G.; Reznikov, L.L.; Dinarello, C.A.; Rubinstein, M. Interleukin-18 binding protein: A novel modulator of the Th1 cytokine response. *Immunity* **1999**, *10*, 127–136. [[CrossRef](#)]
19. Kratzer, A.; Salys, J.; Nold-Petry, C.; Cool, C.; Zamora, M.; Bowler, R.; Koczulla, A.R.; Janciauskiene, S.; Edwards, M.G.; Dinarello, C.A.; et al. Role of IL-18 in second-hand smoke-induced emphysema. *Am. J. Respir. Cell Mol. Biol.* **2013**, *48*, 725–732. [[CrossRef](#)]
20. Soler Palacios, B.; Nieto, C.; Fajardo, P.; González de la Aleja, A.; Andrés, N.; Dominguez-Soto, Á.; Lucas, P.; Cuenda, A.; Rodríguez-Frade, J.M.; Martínez, A.C.; et al. Growth Hormone Reprograms Macrophages toward an Anti-Inflammatory and Reparative Profile in an MAFB-Dependent Manner. *J. Immunol.* **2020**, *205*, 776–788. [[CrossRef](#)]

21. Tweed, J.O.; Hsia, S.H.; Lutfy, K.; Friedman, T.C. The endocrine effects of nicotine and cigarette smoke. *Trends Endocrinol. Metab.* **2012**, *23*, 334–342. [[CrossRef](#)]
22. Kew, R.R. The Vitamin D Binding Protein and Inflammatory Injury: A Mediator or Sentinel of Tissue Damage? *Front. Endocrinol.* **2019**, *10*, 470. [[CrossRef](#)] [[PubMed](#)]
23. Bortner, J.D., Jr.; Richie, J.P., Jr.; Das, A.; Liao, J.; Umstead, T.M.; Stanley, A.; Stanley, B.A.; Belani, C.P.; El-Bayoumy, K. Proteomic profiling of human plasma by iTRAQ reveals down-regulation of ITI-HC3 and VDBP by cigarette smoking. *J. Proteome. Res.* **2011**, *10*, 1151–1159. [[CrossRef](#)] [[PubMed](#)]
24. Kardas, G.; Daszyńska-Kardas, A.; Marynowski, M.; Brząkalska, O.; Kuna, P.; Panek, M. Role of Platelet-Derived Growth Factor (PDGF) in Asthma as an Immunoregulatory Factor Mediating Airway Remodeling and Possible Pharmacological Target. *Front. Pharmacol.* **2020**, *11*, 47. [[CrossRef](#)] [[PubMed](#)]
25. Wang, M.; Wei, J.; Shang, F.; Zang, K.; Ji, T. Platelet-derived growth factor B attenuates lethal sepsis through inhibition of inflammatory responses. *Int. Immunopharmacol.* **2019**, *75*, 105792. [[CrossRef](#)]
26. Pini, A.; Boccalini, G.; Baccari, M.C.; Becatti, M.; Garella, R.; Fiorillo, C.; Calosi, L.; Bani, D.; Nistri, S. Protection from cigarette smoke-induced vascular injury by recombinant human relaxin-2 (serelaxin). *J. Cell Mol. Med.* **2016**, *20*, 891–902. [[CrossRef](#)]
27. Thim, L.; May, F.E. Structure of mammalian trefoil factors and functional insights. *Cell Mol. Life Sci.* **2005**, *62*, 2956–2973. [[CrossRef](#)]
28. Bijelić, N.; Belovari, T.; Tolušić Levak, M.; Baus Lončar, M. Localization of trefoil factor family peptide 3 (TFF3) in epithelial tissues originating from the three germ layers of developing mouse embryo. *Bosn. J. Basic Med. Sci.* **2017**, *17*, 241–247. [[CrossRef](#)]
29. Li, Y.H.; Zheng, F.J.; Huang, Y.; Zhong, X.G.; Guo, M.Z. Synergistic anti-inflammatory effect of Radix Platycodon in combination with herbs for cleaning-heat and detoxification and its mechanism. *Chin. J. Integr. Med.* **2013**, *19*, 29–35. [[CrossRef](#)]
30. Li, T.; Fanning, K.V.; Nyunoya, T.; Chen, Y.; Zou, C. Cigarette smoke extract induces airway epithelial cell death via repressing PRMT6/AKT signaling. *Aging* **2020**, *12*, 24301–24317. [[CrossRef](#)]
31. Duffney, P.F.; McCarthy, C.E.; Nogales, A.; Thatcher, T.H.; Martinez-Sobrido, L.; Phipps, R.P.; Sime, P.J. Cigarette smoke dampens antiviral signaling in small airway epithelial cells by disrupting TLR3 cleavage. *Am. J. Physiol. Lung Cell Mol. Physiol.* **2018**, *314*, L505–L513. [[CrossRef](#)]
32. Modestou, M.A.; Manzel, L.J.; El-Mahdy, S.; Look, D.C. Inhibition of IFN-gamma-dependent antiviral airway epithelial defense by cigarette smoke. *Respir. Res.* **2010**, *11*, 64. [[CrossRef](#)]
33. Leung, J.M.; Tiew, P.Y.; Mac Aogáin, M.; Budden, K.F.; Yong, V.F.; Thomas, S.S.; Pethe, K.; Hansbro, P.M.; Chotirmall, S.H. The role of acute and chronic respiratory colonization and infections in the pathogenesis of COPD. *Respirology* **2017**, *22*, 634–650. [[CrossRef](#)]
34. Nucera, F.; Mumby, S.; Paudel, K.R.; Dharwal, V.; Di Stefano, A.; Casolaro, V.; Hansbro, P.M.; Adcock, I.M.; Caramori, G. Role of oxidative stress in the pathogenesis of COPD. *Minerva Med.* **2022**, *113*, 370–404. [[CrossRef](#)]
35. Panth, N.; Paudel, K.R.; Parajuli, K. Reactive Oxygen Species: A Key Hallmark of Cardiovascular Disease. *Adv. Med.* **2016**, *2016*, 9152732. [[CrossRef](#)]
36. Ketterer, B.; Coles, B.; Meyer, D.J. The role of glutathione in detoxication. *Environ. Health Perspect.* **1983**, *49*, 59–69. [[CrossRef](#)]
37. Birben, E.; Sahiner, U.M.; Sackesen, C.; Erzurum, S.; Kalayci, O. Oxidative stress and antioxidant defense. *World Allergy Organ. J.* **2012**, *5*, 9–19. [[CrossRef](#)]
38. Mao, G.E.; Morris, G.; Lu, Q.Y.; Cao, W.; Reuter, V.E.; Cordon-Cardo, C.; Dalbagni, G.; Scher, H.I.; De Kernion, J.B.; Zhang, Z.F. Glutathione S-transferase P1 Ile105Val polymorphism, cigarette smoking and prostate cancer. *Cancer Detect. Prev.* **2004**, *28*, 368–374. [[CrossRef](#)]
39. Harju, T.; Mazur, W.; Merikallio, H.; Soini, Y.; Kinnula, V.L. Glutathione-S-transferases in lung and sputum specimens, effects of smoking and COPD severity. *Respir. Res.* **2008**, *9*, 80. [[CrossRef](#)]
40. Putcha, N.; Wise, R.A. Medication Regimens for Managing COPD Exacerbations. *Respir Care* **2018**, *63*, 773–782. [[CrossRef](#)]
41. Allam, V.; Paudel, K.R.; Gupta, G.; Singh, S.K.; Vishwas, S.; Gulati, M.; Gupta, S.; Chaitanya, M.; Jha, N.K.; Gupta, P.K.; et al. Nutraceuticals and mitochondrial oxidative stress: Bridging the gap in the management of bronchial asthma. *Environ. Sci. Pollut. Res. Int.* **2022**, *29*, 62733–62754. [[CrossRef](#)] [[PubMed](#)]
42. Kuo, C.L.; Chi, C.W.; Liu, T.Y. The anti-inflammatory potential of berberine in vitro and in vivo. *Cancer Lett.* **2004**, *203*, 127–137. [[CrossRef](#)] [[PubMed](#)]
43. Mehta, M.; Malya, V.; Paudel, K.R.; Chellappan, D.K.; Hansbro, P.M.; Oliver, B.G.; Dua, K. Berberine loaded liquid crystalline nanostructure inhibits cancer progression in adenocarcinomic human alveolar basal epithelial cells in vitro. *J. Food Biochem.* **2021**, *45*, e13954. [[CrossRef](#)] [[PubMed](#)]
44. Hardwick, J.; Taylor, J.; Mehta, M.; Satija, S.; Paudel, K.R.; Hansbro, P.M.; Chellappan, D.K.; Bebawy, M.; Dua, K. Targeting Cancer using Curcumin Encapsulated Vesicular Drug Delivery Systems. *Curr. Pharm. Des.* **2021**, *27*, 2–14. [[CrossRef](#)]
45. Paudel, K.R.; Wadhwa, R.; Mehta, M.; Chellappan, D.K.; Hansbro, P.M.; Dua, K. Rutin loaded liquid crystalline nanoparticles inhibit lipopolysaccharide induced oxidative stress and apoptosis in bronchial epithelial cells in vitro. *Toxicol. Vitro* **2020**, *68*, 104961. [[CrossRef](#)]
46. Solanki, N.; Mehta, M.; Chellappan, D.K.; Gupta, G.; Hansbro, N.G.; Tambuwala, M.M.; Aa Aljabali, A.; Paudel, K.R.; Liu, G.; Satija, S.; et al. Antiproliferative effects of boswellic acid-loaded chitosan nanoparticles on human lung cancer cell line A549. *Future Med. Chem.* **2020**, *12*, 2019–2034. [[CrossRef](#)]

47. Kim, E.; Kim, Y.J.; Ji, Z.; Kang, J.M.; Wirianto, M.; Paudel, K.R.; Smith, J.A.; Ono, K.; Kim, J.A.; Eckel-Mahan, K.; et al. ROR activation by Nobiletin enhances antitumor efficacy via suppression of IkappaB/NF-kappaB signaling in triple-negative breast cancer. *Cell Death Dis.* **2022**, *13*, 374. [[CrossRef](#)]
48. Rodríguez-Yoldi, M.J. Anti-Inflammatory and Antioxidant Properties of Plant Extracts. *Antioxidants* **2021**, *10*, 921. [[CrossRef](#)]
49. Kim, T.M.; Paudel, K.R.; Kim, D.W. Eriobotrya japonica leaf extract attenuates airway inflammation in ovalbumin-induced mice model of asthma. *J. Ethnopharmacol.* **2020**, *253*, 112082. [[CrossRef](#)]
50. Lee, H.H.; Paudel, K.R.; Kim, D.W. Terminalia chebula Fructus Inhibits Migration and Proliferation of Vascular Smooth Muscle Cells and Production of Inflammatory Mediators in RAW 264.7. *Evid. Based Complement. Alternat. Med.* **2015**, *2015*, 502182. [[CrossRef](#)]
51. Liu, Y.; Chen, H.; Yang, Y.; Zhang, Z.; Wei, J.; Meng, H.; Chen, W.; Feng, J.; Gan, B.; Chen, X.; et al. Whole-tree agarwood-inducing technique: An efficient novel technique for producing high-quality agarwood in cultivated Aquilaria sinensis trees. *Molecules* **2013**, *18*, 3086–3106. [[CrossRef](#)]
52. Wang, S.; Yu, Z.; Wang, C.; Wu, C.; Guo, P.; Wei, J. Chemical Constituents and Pharmacological Activity of Agarwood and Aquilaria Plants. *Molecules* **2018**, *23*. [[CrossRef](#)]
53. Alamil, J.M.R.; Paudel, K.R.; Chan, Y.; Xenaki, D.; Panneerselvam, J.; Singh, S.K.; Gulati, M.; Jha, N.K.; Kumar, D.; Prasher, P.; et al. Rediscovering the Therapeutic Potential of Agarwood in the Management of Chronic Inflammatory Diseases. *Molecules* **2022**, *27*, 3038. [[CrossRef](#)]
54. Peng, D.-Q.; Yu, Z.-X.; Wang, C.-H.; Gong, B.; Liu, Y.-Y.; Wei, J.-H. Chemical Constituents and Anti-Inflammatory Effect of Incense Smoke from Agarwood Determined by GC-MS. *Int. J. Anal. Chem.* **2020**, *2020*, 4575030. [[CrossRef](#)]
55. Yadav, D.K.; Mudgal, V.; Agrawal, J.; Maurya, A.K.; Bawankule, D.U.; Chanotiya, C.S.; Khan, F.; Thul, S.T. Molecular docking and ADME studies of natural compounds of Agarwood oil for topical anti-inflammatory activity. *Curr. Comput. Aided Drug Des.* **2013**, *9*, 360–370. [[CrossRef](#)]
56. Chitre, T.; Bhutada, P.; Nandakumar, K.; Somani, R.; Miniyar, P.; Mundhada, Y.; Gore, S.; Jain, K. Analgesic and anti-inflammatory activity of heartwood of Aquilaria agallocha in laboratory animals. *Pharmacol. Online* **2007**, *1*, 288–298.
57. Zheng, H.; Gao, J.; Man, S.; Zhang, J.; Jin, Z.; Gao, W. The protective effects of Aquilariae Lignum Resinatum extract on 5-Fluorouracil-induced intestinal mucositis in mice. *Phytomedicine* **2019**, *54*, 308–317. [[CrossRef](#)]
58. Wang, C.; Wang, S.; Peng, D.; Yu, Z.; Guo, P.; Wei, J. Agarwood Extract Mitigates Intestinal Injury in Fluorouracil-Induced Mice. *Biol. Pharm. Bull.* **2019**, *42*, 1112–1119. [[CrossRef](#)]
59. Wang, C.; Peng, D.; Liu, Y.; Wu, Y.; Guo, P.; Wei, J. Agarwood Alcohol Extract Protects against Gastric Ulcer by Inhibiting Oxidation and Inflammation. *Evid. Based. Complement. Alternat. Med.* **2021**, *2021*, 9944685. [[CrossRef](#)]
60. Hamouda, A.F. A biochemical study of agarwood on methanol injection in rat. *J. Drug Alcohol Res.* **2019**, *8*, 1–14.
61. Liu, C.S.; Zheng, Y.R.; Zhang, Y.F.; Long, X.Y. Research progress on berberine with a special focus on its oral bioavailability. *Fitoterapia* **2016**, *109*, 274–282. [[CrossRef](#)] [[PubMed](#)]
62. Ng, P.Q.; Ling, L.S.C.; Chellian, J.; Madheswaran, T.; Panneerselvam, J.; Kunnath, A.P.; Gupta, G.; Satija, S.; Mehta, M.; Hansbro, P.M.; et al. Applications of Nanocarriers as Drug Delivery Vehicles for Active Phytoconstituents. *Curr. Pharm. Des.* **2020**, *26*, 4580–4590. [[CrossRef](#)] [[PubMed](#)]
63. Chan, Y.; Mehta, M.; Paudel, K.R.; Madheswaran, T.; Panneerselvam, J.; Gupta, G.; Su, Q.P.; Hansbro, P.M.; MacLoughlin, R.; Dua, K.; et al. Versatility of liquid crystalline nanoparticles in inflammatory lung diseases. *Nanomedicine* **2021**, *16*, 1545–1548. [[CrossRef](#)] [[PubMed](#)]
64. Paudel, K.R.; Chellappan, D.K.; MacLoughlin, R.; Pinto, T.J.A.; Dua, K.; Hansbro, P.M. Editorial: Advanced therapeutic delivery for the management of chronic respiratory diseases. *Front. Med.* **2022**, *9*, 983583. [[CrossRef](#)] [[PubMed](#)]
65. Paudel, K.R.; Dua, K.; Panth, N.; Hansbro, P.M.; Chellappan, D.K. Advances in research with rutin-loaded nanoformulations in mitigating lung diseases. *Future Med. Chem.* **2022**, *14*, 1293–1295. [[CrossRef](#)]
66. Clarence, D.D.; Paudel, K.R.; Manandhar, B.; Singh, S.K.; Devkota, H.P.; Panneerselvam, J.; Gupta, V.; Chitranshi, N.; Verma, N.; Saad, S.; et al. Unravelling the Therapeutic Potential of Nano-Delivered Functional Foods in Chronic Respiratory Diseases. *Nutrients* **2022**, *14*, 3828. [[CrossRef](#)]
67. Jaiswal, M.; Dudhe, R.; Sharma, P.K. Nanoemulsion: An advanced mode of drug delivery system. *3 Biotech* **2015**, *5*, 123–127. [[CrossRef](#)]
68. Dupuis, V.; Cerbu, C.; Witkowski, L.; Potarniche, A.V.; Timar, M.C.; Żychska, M.; Sabliov, C.M. Nanodelivery of essential oils as efficient tools against antimicrobial resistance: A review of the type and physical-chemical properties of the delivery systems and applications. *Drug Deliv.* **2022**, *29*, 1007–1024. [[CrossRef](#)]
69. Alnuqaydan, A.M.; Almutary, A.G.; Azam, M.; Manandhar, B.; Yin, G.H.S.; Yen, L.L.; Madheswaran, T.; Paudel, K.R.; Hansbro, P.M.; Chellappan, D.K.; et al. Evaluation of the Cytotoxic Activity and Anti-Migratory Effect of Berberine-Phytantriol Liquid Crystalline Nanoparticle Formulation on Non-Small-Cell Lung Cancer In Vitro. *Pharmaceutics* **2022**, *14*, 1119. [[CrossRef](#)]
70. Wadhwa, R.; Paudel, K.R.; Chin, L.H.; Hon, C.M.; Madheswaran, T.; Gupta, G.; Panneerselvam, J.; Lakshmi, T.; Singh, S.K.; Gulati, M.; et al. Anti-inflammatory and anticancer activities of Naringenin-loaded liquid crystalline nanoparticles in vitro. *J. Food Biochem.* **2021**, *45*, e13572. [[CrossRef](#)]
71. King, P.T. Inflammation in chronic obstructive pulmonary disease and its role in cardiovascular disease and lung cancer. *Clin. Transl. Med.* **2015**, *4*, 68. [[CrossRef](#)]

72. Chellappan, D.K.; Yee, L.W.; Xuan, K.Y.; Kunalan, K.; Rou, L.C.; Jean, L.S.; Ying, L.Y.; Wie, L.X.; Chellian, J.; Mehta, M.; et al. Targeting neutrophils using novel drug delivery systems in chronic respiratory diseases. *Drug Dev. Res.* **2020**, *81*, 419–436. [[CrossRef](#)]
73. Paudel, K.R.; Dharwal, V.; Patel, V.K.; Galvao, I.; Wadhwa, R.; Malya, V.; Shen, S.S.; Budden, K.F.; Hansbro, N.G.; Vaughan, A.; et al. Role of Lung Microbiome in Innate Immune Response Associated With Chronic Lung Diseases. *Front. Med.* **2020**, *7*, 554. [[CrossRef](#)]
74. May, S.M.; Li, J.T. Burden of chronic obstructive pulmonary disease: Healthcare costs and beyond. *Allergy Asthma Proc.* **2015**, *36*, 4–10. [[CrossRef](#)]
75. Eisner, M.D.; Anthonisen, N.; Coultas, D.; Kuenzli, N.; Perez-Padilla, R.; Postma, D.; Romieu, I.; Silverman, E.K.; Balmes, J.R. An official American Thoracic Society public policy statement: Novel risk factors and the global burden of chronic obstructive pulmonary disease. *Am. J. Respir. Crit. Care Med.* **2010**, *182*, 693–718. [[CrossRef](#)]
76. Biswas, S.K. Does the Interdependence between Oxidative Stress and Inflammation Explain the Antioxidant Paradox? *Oxid. Med. Cell Longev.* **2016**, *2016*, 5698931. [[CrossRef](#)]
77. Chellappan, D.K.; Dharwal, V.; Paudel, K.R.; Jha, N.K.; MacLoughlin, R.; Oliver, B.G.; Dua, K. Mitochondrial dysfunctions associated with chronic respiratory diseases and their targeted therapies: An update. *Future Med. Chem.* **2021**, *13*, 1249–1251. [[CrossRef](#)]
78. Watson, A.; Wilkinson, T.M.A. Digital healthcare in COPD management: A narrative review on the advantages, pitfalls, and need for further research. *Ther. Adv. Respir. Dis.* **2022**, *16*, 17534666221075493. [[CrossRef](#)]
79. Alqahtani, J.S. Prevalence, incidence, morbidity and mortality rates of COPD in Saudi Arabia: Trends in burden of COPD from 1990 to 2019. *PLoS ONE* **2022**, *17*, e0268772. [[CrossRef](#)]
80. Devkota, H.P.; Paudel, K.R.; Khanal, S.; Baral, A.; Panth, N.; Adhikari-Devkota, A.; Jha, N.K.; Das, N.; Singh, S.K.; Chellappan, D.K.; et al. Stinging Nettle (*Urtica dioica* L.): Nutritional Composition, Bioactive Compounds, and Food Functional Properties. *Molecules* **2022**, *27*, 5219. [[CrossRef](#)]
81. Zhao, Q.; Zhu, L.; Wang, S.; Gao, Y.; Jin, F. Molecular mechanism of the anti-inflammatory effects of plant essential oils: A systematic review. *J. Ethnopharmacol.* **2022**, *301*, 115829. [[CrossRef](#)] [[PubMed](#)]
82. Raman, S.; Murugaiyah, V.; Parumasivam, T. *Andrographis paniculata* Dosage Forms and Advances in Nanoparticulate Delivery Systems: An Overview. *Molecules* **2022**, *27*, 6164. [[CrossRef](#)] [[PubMed](#)]
83. MacNee, W. Pulmonary and systemic oxidant/antioxidant imbalance in chronic obstructive pulmonary disease. *Proc. Am. Thorac. Soc.* **2005**, *2*, 50–60. [[CrossRef](#)] [[PubMed](#)]
84. Pahwa, R.; Goyal, A.; Jialal, I. *Chronic Inflammation*; StatPearls Publishing: Treasure Island, FL, USA, 2022.
85. Hussain, T.; Tan, B.; Yin, Y.; Blachier, F.; Tossou, M.C.; Rahu, N. Oxidative Stress and Inflammation: What Polyphenols Can Do for Us? *Oxid. Med. Cell Longev.* **2016**, *2016*, 7432797. [[CrossRef](#)]
86. Nyunoya, T.; Mebratu, Y.; Contreras, A.; Delgado, M.; Chand, H.S.; Tesfaigzi, Y. Molecular processes that drive cigarette smoke-induced epithelial cell fate of the lung. *Am. J. Respir. Cell Mol. Biol.* **2014**, *50*, 471–482. [[CrossRef](#)]
87. Paudel, K.R.; Mehta, M.; Shukla, S.D.; Panth, N.; Chellappan, D.K.; Dua, K.; Hansbro, P. Advancements in nanotherapeutics targeting senescence in chronic obstructive pulmonary disease. *Nanomedicine* **2022**. [[CrossRef](#)]
88. Nucera, F.; Hansbro, P.M.; Paudel, K.R.; Casolaro, V.; Appanna, R.; Kirkham, P.; Adcock, I.M.; Caramori, G. Chapter 14—Role of autoimmunity in the pathogenesis of chronic obstructive pulmonary disease and pulmonary emphysema. In *Translational Autoimmunity*; Rezaei, N., Ed.; Academic Press: Cambridge, MA, USA, 2022; Volume 3, pp. 311–331.
89. Ma, W.J.; Sun, Y.H.; Jiang, J.X.; Dong, X.W.; Zhou, J.Y.; Xie, Q.M. Epoxyeicosatrienoic acids attenuate cigarette smoke extract-induced interleukin-8 production in bronchial epithelial cells. *Prostaglandins Leukot. Essent. Fatty Acids* **2015**, *94*, 13–19. [[CrossRef](#)]
90. Pauwels, N.S.; Bracke, K.R.; Dupont, L.L.; Van Pottelberge, G.R.; Provoost, S.; Vanden Berghe, T.; Vandenabeele, P.; Lambrecht, B.N.; Joos, G.F.; Brusselle, G.G. Role of IL-1 α and the Nlrp3/caspase-1/IL-1 β axis in cigarette smoke-induced pulmonary inflammation and COPD. *Eur. Respir. J.* **2011**, *38*, 1019–1028. [[CrossRef](#)]
91. Feng, K.N.; Meng, P.; Zou, X.L.; Zhang, M.; Li, H.K.; Yang, H.L.; Li, H.T.; Zhang, T.T. IL-37 protects against airway remodeling by reversing bronchial epithelial-mesenchymal transition via IL-24 signaling pathway in chronic asthma. *Respir. Res.* **2022**, *23*, 244. [[CrossRef](#)]
92. Hurme, M.; Santtila, S. IL-1 receptor antagonist (IL-1Ra) plasma levels are co-ordinately regulated by both IL-1Ra and IL-1beta genes. *Eur. J. Immunol.* **1998**, *28*, 2598–2602. [[CrossRef](#)]
93. Lee, A.J.; Ashkar, A.A. The Dual Nature of Type I and Type II Interferons. *Front. Immunol.* **2018**, *9*, 2061. [[CrossRef](#)]
94. Pungsrinont, T.; Kallenbach, J.; Baniahmad, A. Role of PI3K-AKT-mTOR Pathway as a Pro-Survival Signaling and Resistance-Mediating Mechanism to Therapy of Prostate Cancer. *Int. J. Mol. Sci.* **2021**, *22*, 1088. [[CrossRef](#)]

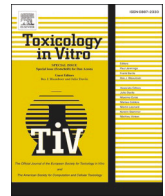
Disclaimer/Publisher’s Note: The statements, opinions and data contained in all publications are solely those of the individual author(s) and contributor(s) and not of MDPI and/or the editor(s). MDPI and/or the editor(s) disclaim responsibility for any injury to people or property resulting from any ideas, methods, instructions or products referred to in the content.

CHAPTER 4

Research Paper #3

Berberine-loaded engineered nanoparticles attenuate TGF- β -induced remodelling features in human bronchial epithelial cells

(**De Rubis G**, Paudel KR, Liu G, Agarwal V, MacLoughlin R, de Jesus Andreoli Pinto T, Singh SK, Adams J, Nammi S, Chellappan DK, Oliver BGG, Hansbro PM, Dua K. Berberine-loaded engineered nanoparticles attenuate TGF- β -induced remodelling in human bronchial epithelial cells. **Toxicology In Vitro**. 2023 92:105660. doi: 10.1016/j.tiv.2023.105660)



Berberine-loaded engineered nanoparticles attenuate TGF- β -induced remodelling in human bronchial epithelial cells

Gabriele De Rubis^{a,b}, Keshav Raj Paudel^c, Gang Liu^c, Vipul Agarwal^d, Ronan MacLoughlin^{e,f,g}, Terezinha de Jesus Andreoli Pinto^h, Sachin Kumar Singh^{b,i}, Jon Adams^b, Srinivas Nammi^j, Dinesh Kumar Chellappan^k, Brian Gregory George Oliver^{l,m}, Philip Michael Hansbro^c, Kamal Dua^{a,b,n,*}

^a Discipline of Pharmacy, Graduate School of Health, University of Technology Sydney, Sydney, NSW 2007, Australia

^b Faculty of Health, Australian Research Centre in Complementary and Integrative Medicine, University of Technology Sydney, Ultimo, NSW 2007, Australia

^c Centre for Inflammation, Centenary Institute and University of Technology Sydney, Faculty of Science, School of Life Sciences, Sydney, NSW 2007, Australia

^d Cluster for Advanced Macromolecular Design (CAMD), School of Chemical Engineering, University of New South Wales, Sydney, NSW 2052, Australia

^e Aerogen, IDA Business Park, H91 HE94 Galway, Connacht, Ireland

^f School of Pharmacy & Biomolecular Sciences, Royal College of Surgeons in Ireland, D02 YN77 Dublin, Leinster, Ireland

^g School of Pharmacy & Pharmaceutical Sciences, Trinity College, D02 PN40 Dublin, Leinster, Ireland

^h Department of Pharmacy, Faculty of Pharmaceutical Sciences, University of São Paulo, São Paulo, Brazil

ⁱ School of Pharmaceutical Sciences, Lovely Professional University, Phagwara, Punjab, India

^j School of Science, Western Sydney University, Penrith, NSW 2751, Australia

^k Department of Life Sciences, School of Pharmacy, International Medical University, Bukit Jalil, 57000 Kuala Lumpur, Malaysia

^l Woolcock Institute of Medical Research, The University of Sydney, Sydney, NSW, Australia

^m School of Life Sciences, University of Technology Sydney, Ultimo, NSW 2007, Australia

ⁿ Uttarakhand Institute of Pharmaceutical Sciences, Uttarakhand University, Dehradun, India

ARTICLE INFO

Editor: Dr. Martin Leonard

Keywords:

Asthma
COPD
Lung cancer
Airway remodelling
TGF- β
Berberine
Phytoceuticals
Liquid crystalline nanoparticles

ABSTRACT

Airway remodelling occurs in chronic respiratory diseases (CRDs) such as asthma and chronic obstructive pulmonary disease (COPD). It is characterized by aberrant activation of epithelial repair, excessive extracellular matrix (ECM) deposition, epithelial-to-mesenchymal transition (EMT), and airway obstruction. The master regulator is Transforming Growth Factor- β (TGF- β), which activates tissue repair, release of growth factors, EMT, increased cell proliferation, and reduced nitric oxide (NO) secretion. Due to its fundamental role in remodelling, TGF- β is an emerging target in the treatment of CRDs. Berberine is a benzylisoquinoline alkaloid with antioxidant, anti-inflammatory, and anti-fibrotic activities whose clinical application is hampered by poor permeability. To overcome these limitations, in this study, berberine was encapsulated in monoolein-based liquid crystalline nanoparticles (BM-LCNs). The potential of BM-LCNs in inhibiting TGF- β -induced remodelling features in human bronchial epithelial cells (BEAS-2B) was tested. BM-LCNs significantly inhibited TGF- β -induced migration, reducing the levels of proteins upregulated by TGF- β including endoglin, thrombospondin-1, basic fibroblast growth factor, vascular-endothelial growth factor, and myeloperoxidase, and increasing the levels of cystatin C, a protein whose expression was downregulated by TGF- β . Furthermore, BM-LCNs restored baseline NO levels downregulated by TGF- β . The results prove the *in vitro* therapeutic efficacy of BM-LCNs in counteracting TGF- β -induced remodelling features. This study supports the suitability of berberine-loaded drug delivery systems to counteract airway remodelling, with potential application as a treatment strategy against CRDs.

1. Introduction

Chronic respiratory diseases (CRDs) are a heterogeneous group of

diseases affecting the airways and other lung structures and including asthma, chronic obstructive pulmonary disease (COPD), occupational lung diseases, pulmonary hypertension, idiopathic pulmonary fibrosis,

* Corresponding author at: Discipline of Pharmacy, Graduate School of Health, University of Technology Sydney, Sydney, NSW 2007, Australia.

E-mail address: kamal.dua@uts.edu.au (K. Dua).

<https://doi.org/10.1016/j.tiv.2023.105660>

Received 1 March 2023; Received in revised form 5 July 2023; Accepted 14 August 2023

Available online 15 August 2023

0887-2333/© 2023 Elsevier Ltd. All rights reserved.

and others (Labaki and Han, 2020; Tan et al., 2022; Prasher et al., 2022a). Lung cancer (LC), particularly non-small cell lung cancer (NSCLC), is often considered a CRD as well (Bratova et al., 2020). The main aetiological factor associated with the development of these diseases is cigarette smoking through the exposure to the thousands of toxic chemicals in tobacco smoke, which promote a chronic pro-inflammatory and pro-oxidant state that further prompts disease progression (Dua et al., 2019; Lugg et al., 2022; Kc et al., 2022). CRDs, particularly asthma, COPD, and LC, are among the leading causes of mortality and morbidity worldwide, and their global burden is significant (Viegi et al., 2020). According to recent data, in 2017–2019, COPD caused about 3.3 million deaths annually (Safiri et al., 2022), while about 500,000 yearly deaths were associated with asthma (Viegi et al., 2020). Overall, LC is one of the deadliest types of cancer, with 1.7 million deaths attributed to LC globally in 2020, a trend that is currently increasing (Sung et al., 2021). Although less frequent compared to other CRDs, idiopathic pulmonary fibrosis (IPF) is a chronic, progressive disease characterized by the irreversible scarring of the lung's interstitial framework with a median survival of 3–5 years if untreated (Martinez et al., 2017).

Current therapeutic approaches for CRDs include pharmacological and non-pharmacological strategies. These are severely limited and, in the case of asthma, IPF and COPD, aim at improving and managing disease symptoms rather than tackling the underlying disease mechanisms (Martinez et al., 2017; Porsbjerg, 2023; Riley and Sciruba, 2019). Despite showing some efficacy, the currently available pharmacotherapies for CRDs are limited by severe side effects (Martinez et al., 2017; Celli et al., 2008; Leuppi et al., 2013). With regards to LC, therapeutic approaches include various combinations of surgical removal, radiotherapy, chemotherapy, and immunotherapy, depending on the tumor stage (Kumbhar et al., 2022). Chemotherapies are all limited by severe organ toxicity, adverse effects, as well as by the eventual development of cancer multidrug resistance (Kumbhar et al., 2022; Yazbeck et al., 2022; Li et al., 2022). This underlines the need to develop novel therapeutics with improved treatment outcomes and reduced adverse effects. In this context, developing treatment strategies tackling one or more cellular and molecular mechanisms shared by different diseases would be advantageous.

A fundamental feature shared between all these CRDs is the progressive radical deterioration and alteration of the structure of the respiratory tract, also termed airway remodelling (Dhanjal et al., 2022; Grzela et al., 2016; Mehta et al., 2020). Structural transformations in airway remodelling include subepithelial fibrosis, infiltration of immune cells, disruption of epithelial cell layers, excessive mucus secretion, excessive production of matrix metalloproteinases (MMPs), and thickening of the basement membrane due to excessive collagen deposition (Liu et al., 2021). This leads to severe airway obstruction (Dhanjal et al., 2022; Mehta et al., 2020; Doerner and Zuraw, 2009). The thickening of the basement membrane is caused by the presence of an excessive number of highly synthetic myofibroblasts, which express alpha-smooth muscle actin (α -SMA) (Doerner and Zuraw, 2009). Epithelial-to-mesenchymal transition (EMT) of lung epithelial cells, which acquire increased proliferative and migratory capacity, is considered an important source of myofibroblasts contributing to airway remodelling (Doerner and Zuraw, 2009; Iwano et al., 2002; Pain et al., 2014).

One of the master regulators of tissue remodelling, particularly in the airways, is transforming growth factor-beta (TGF- β) (Pain et al., 2014; Gupta et al., 2021; Aschner and Downey, 2016). TGF- β is a multifunctional cytokine present in three different isoforms: TGF- β 1, TGF- β 2, and TGF- β 3, with partially overlapping biological activities (Massagué, 2008; Huang et al., 2014). TGF- β is secreted in an inactive form called large latent complex (LLC), in which the functional protein is bound to the latency-associated peptide (LAP) and other proteins (Aschner and Downey, 2016; Liu et al., 2019). The LLC is primarily localized in the ECM and it functions as a reservoir of inactive TGF- β (Aschner and Downey, 2016). The active form of TGF- β is released following different stimuli, including temperature spikes, acidification of the

microenvironment, oxidative stress, proteolysis, and integrin binding (Aschner and Downey, 2016). Thrombospondin-1 and MMPs are among the main proteins activating TGF- β , and the fact that these proteins are upregulated by TGF- β itself represents an important positive feedback mechanism enhancing TGF- β activation (Crawford et al., 1998; Yu and Stamenkovic, 2000). Upon binding to its receptor, TGF- β regulates the expression of a plethora of target genes mainly through the canonical TGF- β /Smad pathway, in which Smad proteins are phosphorylated and translocated into the nucleus, where they act as transcription factors (Huse et al., 2001). Many other proteins are involved in the regulation and action of TGF- β signalling in airway remodelling and EMT. These include growth factors such as the vascular endothelial growth factor (VEGF), which is a known inducer of lung remodelling (Lee et al., 2004) and whose secretion is enhanced by TGF- β in airway smooth muscle cells (Shin et al., 2009), as well as the basic fibroblast growth factor (bFGF), which is co-expressed with TGF- β in the lung of ovalbumin (OVA)-induced mice (Yum et al., 2011) and induces angiogenesis associated to remodelling in asthma and COPD (Zanini et al., 2010). Other proteins involved in TGF- β -induced remodelling and EMT include myeloperoxidase (Wang et al., 2018), and endoglin, which is associated with the TGF- β receptors and affects TGF- β responses (Guerrero-Esteo et al., 2002). TGF- β signalling is also controlled by negative regulators such as cystatin C (Sokol and Schiemann, 2004).

An important mechanism through which TGF- β induces EMT in alveolar epithelial cells is through the reduction of baseline nitric oxide (NO) levels (Vyas-Read et al., 2007). NO, in fact, is a critical factor that attenuates EMT, and TGF- β reduces its baseline production in the injured lung through the inhibition of the endothelial NO synthase (eNOS) (Vyas-Read et al., 2007) and other enzymes involved in NO production such as soluble guanylate cyclase (sGC) and cGMP-dependent protein kinase I (PKGI) (Bachiller et al., 2010).

Physiologically, TGF- β plays a pleiotropic role in lung health and development. Its activity is fundamental in lung organogenesis, and in the regulation of homeostatic alveolar epithelial growth, differentiation, and EMT (Saito et al., 2018). Due to its fundamental role in lung homeostasis, dysregulation of TGF- β signalling is common in many diseases where tissue remodelling plays a relevant role, including CRDs (Saito et al., 2018; Takizawa et al., 2001). Considering its function as a promoter of EMT in healthy cells, dysregulation of TGF- β signalling is also an important factor contributing to increased cell migration and invasion in many types of cancer, including LC, where it is recognised as the most potent inducer of EMT (Saito et al., 2018). Interestingly, increased levels of TGF- β have been detected in the airways of COPD, asthma, and LC patients, as well as tobacco smokers (Saito et al., 2018; Takizawa et al., 2001).

The multifaceted role played by TGF- β in CRDs makes it a valuable pharmacological target (Gupta et al., 2021). In the quest for novel pharmacological strategies to treat respiratory disorders, plant-derived molecules, also known as phytochemicals, are an endless source of inspiration (Paudel et al., 2022a). In this context, one promising phytochemical is berberine, an isoquinoline alkaloid found in barberry, tree turmeric, and other plants (Kuo et al., 2004; Paudel et al., 2022b). Berberine is widely known for its potent antioxidant, anti-inflammatory, and anticancer properties (Paudel et al., 2022b; Alnuqaydan et al., 2022a; Alnuqaydan et al., 2022b; Mehta et al., 2021; Paudel et al., 2022c), and it also exerts antifibrotic activity in the lungs, heart, liver, pancreas and kidneys of rodents (DiNicolantonio et al., 2021). In the lung, in particular, the antifibrotic activity of berberine is exerted through the suppression of nuclear factor- κ B (NF- κ B)-induced TGF- β activation (Chitra et al., 2013). Furthermore, berberine was shown to counteract TGF- β -induced EMT *in vitro* on A549 human NSCLC cells (Qi et al., 2014).

Despite its promising biological activity, the clinical use of berberine, similarly to that of other phytochemicals, is currently limited by its poor solubility and permeability which, together with a high rate of hepatobiliary excretion, translates into poor oral bioavailability and

unfavourable pharmacokinetics (Yin et al., 2008; Tsai and Tsai, 2004). To overcome these limitations, encapsulation of phytochemicals within advanced, nanoparticle (NP)-based drug delivery systems is an advantageous strategy (Paudel et al., 2022a; Paudel et al., 2022d; Khurshed, 2022). This allows to drastically increase the solubility, permeability, and stability of the encapsulated molecules, improving their bioavailability and pharmacokinetic properties (Gupta et al., 2021; Paudel et al., 2022a; Devkota et al., 2022; Clarence et al., 2022). Among the many available classes of nanoformulations, liquid crystalline nanoparticles (LCNs) are particularly versatile in the treatment of pulmonary diseases (Chan et al., 2021). Our research team has worked extensively with berberine-loaded LCNs, demonstrating their superior *in vitro* anticancer activity against A549 lung cancer cells (Alnuqaydan et al., 2022b; Mehta et al., 2021; Paudel et al., 2022c), as well as a potent antioxidant, anti-inflammatory, and anti-senescence activity in cigarette smoke-induced BCI-NS1.1 human airway basal cells (Paudel et al., 2022b; Paudel et al., 2022e) and antioxidant and anti-inflammatory activity in lipopolysaccharide (LPS)-induced mouse RAW264.7 macrophages (Alnuqaydan et al., 2022a).

In the present work, we tested a monoolein-based berberine LCN formulation (BM-LCNs) against a model of airway remodelling and EMT obtained by stimulating BEAS-2B human bronchial epithelial cells with TGF- β (Doerner and Zuraw, 2009). We show that BM-LCNs significantly attenuate the functional and molecular features associated with TGF- β -induced remodelling and EMT. This study highlights the enormous potential of nanoparticle-based drug delivery systems in enhancing the use of phytochemicals for the treatment of lung diseases, providing proof of the applicability of BM-LCNs as a potential therapeutic agent tackling the aberrant airway remodelling process that drives the pathogenesis of CRDs.

2. Materials and methods

2.1. Formulation and physicochemical characterisation of BM-LCNs

Berberine hydrochloride (Cat. #B3251), monoolein (Cat. #CRM44893), and poloxamer 407 (Cat. #16758) were purchased from Sigma-Aldrich, Australia, and were used for the preparation of BM-LCNs. BM-LCNs were formulated using the ultrasonication method, and characterized for physicochemical characteristics such as particle size, polydispersity index, zeta potential, entrapment efficiency, morphology, and *in vitro* release, as reported in a previous study (Paudel et al., 2022c). Briefly, 200 mg monoolein were melted at 70 °C in a glass vial. Poloxamer 407 (20 mg) was dissolved in 4.8 mL deionized water and heated to 70 °C in a glass vial. Berberine powder (5 mg) was added to the melted monoolein and vortexed until completely dissolved. Then, the poloxamer 407 solution was added to the berberine-monoolein solution until formation of a coarse dispersion. The coarse dispersion was finally subjected to size reduction using a probe sonicator, using an amplitude of 80 for 5 min, with 5-s-on and 5-s-off cycles.

2.2. Cell culture

The human bronchial epithelial cells (BEAS-2B, ATCC #CRL-9609) were a kind gift from Professor Alaina Ammit (Woolcock Institute of Medical Research, Sydney, NSW, Australia). These cells were used at passages between 15 and 25 throughout the study, and were cultured at 37 °C in Dulbecco's Modified Eagle Medium (DMEM, Sigma-Aldrich, Australia, Cat. #D6046) supplemented with 5% fetal bovine serum (Sigma-Aldrich, Australia, Cat. #F9423), 100 unit/ml penicillin and 100 μ g streptomycin (Pen-Strep solution, Sigma-Aldrich Australia, Cat. #P4333) in a humidified atmosphere containing 5% CO₂.

2.3. Cell viability assay - MTT

The MTT cell viability assay was performed as reported in a previous

study (Alnuqaydan et al., 2022a). The BEAS-2B cells were seeded at a density of 5000 cells/well in a transparent, clear-bottom 96-well plate and left to attach overnight. The following day, the cells were incubated in the presence of 5 ng/mL human TGF- β 1 (R&D Systems Biotechnology, Minnesota, USA, Cat. # 754BH005), at 37 °C for 24 h. The cells were then incubated for 24 more hours in the presence of BM-LCN concentrations ranging between 0 and 10 μ M or with empty LCNs at dilutions representative to the BM-LCNs concentrations tested. Then, 250 μ g/mL MTT ((3-(4,5-dimethylthiazol-2-yl)-2,5-diphenyl tetrazolium bromide, Sigma-Aldrich, Australia, Cat. #M2003) was added to each well and incubated at 37 °C for further 4 h. Upon incubation, the supernatant was removed, and the formed formazan crystals were dissolved using 100 μ L dimethyl sulfoxide (DMSO, Sigma-Aldrich, Australia, Cat. #D8418). The absorbance was read at 570 nm wavelength using a TECAN Infinite M1000 plate reader (Tecan Trading AG, Switzerland).

2.4. Cell viability assay – Trypan blue staining

The impact of BM-LCNs on cell viability has also been assessed using Trypan Blue staining, similarly to how reported in a previous study (Paudel et al., 2022c). Briefly, 10,000 cells/well were seeded in a 48-well plate and left to attach overnight. The following day, the cells were incubated in the presence of 5 ng/mL human TGF- β 1, at 37 °C for 24 h. The cells were then incubated for 24 more hours in the presence of BM-LCN concentrations ranging between 0 and 10 μ M. After incubation, the cells were treated with 300 μ L 1 \times Trypsin-EDTA solution (Sigma-Aldrich, Australia, Cat. # T4299), incubating at 37 °C for 2 min to allow cell detachment. The trypsin was then inactivated by adding 300 μ L FBS-supplemented DMEM, and the cells were centrifuged at 500 xg, for 5 min, at room temperature. The cell pellet was then resuspended in 20 μ L FBS-supplemented DMEM and mixed at a 1:1 ratio with 0.4% Trypan Blue solution (ThermoFisher Scientific, Australia, Cat. #15250061). The number of live cells/mL was counted using a Neubauer Improved haemocytometer, using a light microscope at 10 \times magnification.

2.5. Wound healing assay

To assess the anti-migratory activity of BM-LCNs on TGF- β -stimulated BEAS-2B cells, the wound healing assay was performed. Briefly, 100,000 BEAS-2B cells/well were seeded into 6-well plates and incubated at 37 °C overnight. The following day, the cell monolayer was scratched using the tip of a sterile 200 μ L pipette tip, and the wells were washed five times with sterile PBS (Sigma-Aldrich, Australia, Cat. #P3813). The cells were then incubated in the presence of 5 ng/mL TGF- β 1 alone or in the presence of 5 ng/mL TGF- β 1 and 0.5 μ M BM-LCNs for up to 48 h. The distance between the edges of the scratch was measured under a light microscope, at 10 \times magnification, at 0, 24, and 48 h time points. The percentage of wound closure was normalized as a percentage compared to the control (untreated) group.

2.6. Human cytokine protein array

The effect of BM-LCNs on the expression of cytokines and other proteins in TGF- β -induced BEAS-2B cells was studied using the Proteome Profiler Human XL Cytokine Array Kit (R&D Systems, Minneapolis, MN, USA, Cat. #ARY022B), as described previously (Paudel et al., 2022b). The cells were seeded in a 6-well plate at a density of 100,000 cells/well and left to attach overnight. The following day, the cells were incubated in the presence of 5 ng/mL TGF- β 1 and incubated at 37 °C for 24 h. The cells were then incubated for another 24 h in the presence of 0.5 μ M BM-LCNs. Following incubation, the cells were lysed with 500 μ L RIPA buffer (ThermoFisher Scientific, Australia, Cat. #89900) supplemented with protease inhibitor tablets (Roche Diagnostics GmbH, Mannheim, Germany, Cat. #11697498001). An amount of 300 μ g of proteins from each experimental group was loaded onto each array and incubated overnight at 4 °C. The further incubation steps with antibodies and

chemiluminescent reagents were performed following the manufacturer's instructions. The arrays were photographed using a ChemiDoc MP (Bio-Rad, Hercules, CA, USA) and the pixel density for each spot was analysed with ImageJ (version 1.53c, Bethesda, MD, USA).

2.7. NO levels determination with Griess reagent

The relative levels of NO released by BEAS-2B cells in the culture supernatants were determined using the modified Griess reagent (Sigma-Aldrich, Australia, Cat. #G4410). The cells were seeded in a 6-well plate at a density of 100,000 cells/well and left to attach overnight. The following day, the cells were incubated in the presence of 5 ng/mL TGF- β 1 and incubated at 37 °C for 24 h. The cells were then incubated for another 24 h in the presence of 0.5 μ M BM-LCNs. Following incubation, the culture supernatants were collected, and 100 μ L of the supernatants were added to a clear-bottom, transparent 96-well plate. The supernatants were mixed in a 1:1 ratio with the Griess reagent and the plates were incubated for 30 min at room temperature in dark. The relative NO levels were determined using a TECAN Infinite M1000 plate reader (Tecan Trading AG, Switzerland) by measuring the absorbance at 540 nm. Unconditioned cell culture media was used as a blank, and its absorbance was subtracted from the absorbance of each sample. Relative NO levels were reported as a percent change compared to the untreated group.

2.8. Statistical analysis

The data are presented as mean \pm SEM. The data were analysed by ordinary one-way ANOVA, followed by Tukey multiple comparison test, using GraphPad Prism (v.9.4, GraphPad Software, San Diego, CA, USA). A two-tailed of p -value < 0.05 was considered statistically significant for pairwise comparisons.

3. Results

3.1. Identification of an optimal concentration of BM-LCNs for treating TGF- β -stimulated BEAS-2B cells

To find a non-lethal BM-LCNs concentration to treat BEAS-2B cells, the MTT assay and the Trypan Blue assay were performed to assess the cell viability following treatment of TGF- β -induced BEAS-2B cells with increasing BM-LCNs concentrations. The results are shown in Fig. 1a (MTT assay) and Fig. 1b (Trypan Blue assay). Furthermore, the toxicity of empty LCNs on BEAS-2B cells was tested through MTT assay (Fig. 1c). Treatment with BM-LCNs concentrations of 0.25 and 0.5 μ M resulted in a slight, not statistically significant, reduction in cell viability of 4.5% and 12.8%, respectively (Fig. 1a, $p > 0.05$ against the TGF- β -treated group for both groups). At higher concentrations of 1, 2.5, 5, and 10 μ M, treatment with BM-LCNs caused a significant reduction of cell viability of 28.0%, 29.4%, 26.5%, and 51.9%, respectively (Fig. 1, $p < 0.0001$ against the TGF- β -treated group for all groups). In the Trypan Blue assay, treatment with BM-LCNs concentrations of 0.25 and 0.5 μ M resulted in a slight, not statistically significant, increase in cell viability of 0.8% and 1.5%, respectively (Fig. 1b, $p > 0.05$ against the TGF- β -treated group for both groups). At higher concentrations of 1, 2.5, 5, and 10 μ M, treatment with BM-LCNs caused a significant reduction of cell viability of 18.1% ($p < 0.01$ against the TGF- β -treated group), 30.2% ($p < 0.001$ against the TGF- β -treated group), 54.7% ($p < 0.0001$ against the TGF- β -treated group), and 89.4% ($p < 0.0001$ against the TGF- β -treated group), respectively (Fig. 1b). The highest non-toxic BM-LCNs concentration resulted to be 0.5 μ M across both assays, and this concentration was used to treat cells in the following experiments. Furthermore, treatment of BEAS-2B cells with empty LCNs used at a concentration corresponding to 0.25, 0.5, and 1 μ M BM-LCNs resulted in a slight, not significant, reduction in cell viability (of 1.4%, 1.6%, and 4.2% respectively ($p > 0.05$ against the untreated group, Fig. 1c). Treatment with higher concentrations of empty LCNs, corresponding to 2.5, 5, and 10 μ M BM-

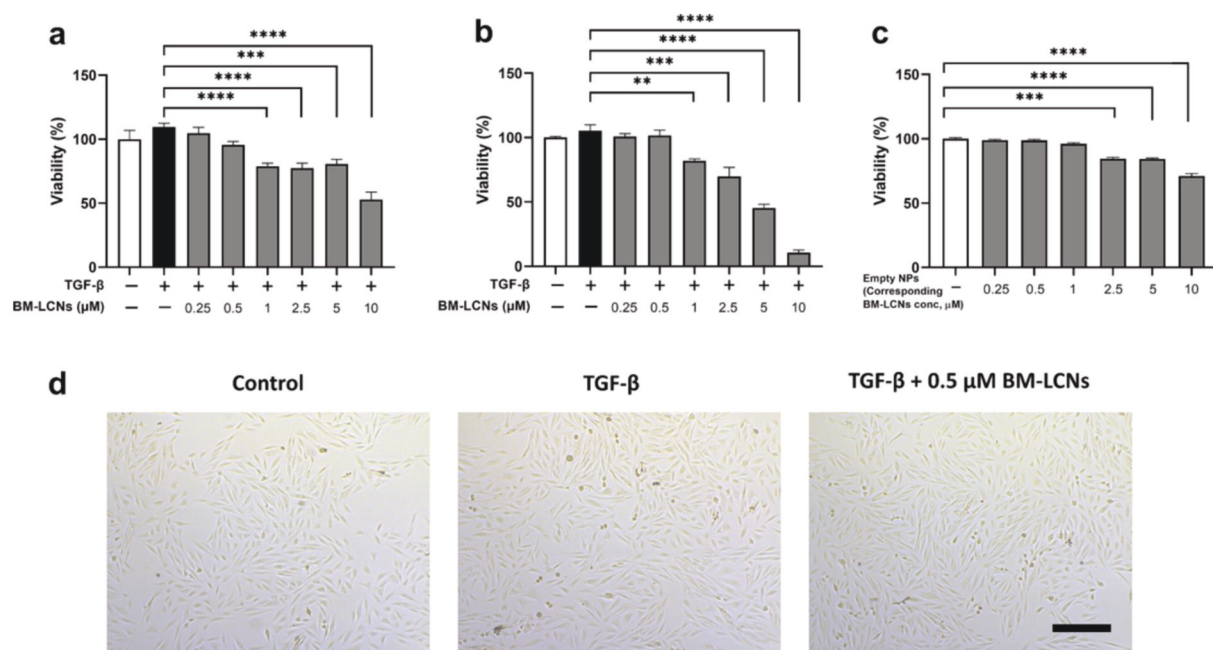


Fig. 1. Impact of BM-LCNs treatment on the cell viability and morphology of TGF- β -induced BEAS-2B. BEAS-2B cells were incubated for 24 h in the presence of 5 ng/mL TGF- β and for a further 24 h with increasing concentrations of BM-LCNs (0.25, 0.5, 1, 2.5, 5, 10 μ M, Fig. 1a, b). Subsequently, the MTT assay (a) or the Trypan Blue assay (b) was performed to assess cell viability. BEAS-2B cells were incubated for 24 h in the presence of increasing empty LCN concentrations, corresponding to 0.25, 0.5, 1, 2.5, 5, 10 μ M BM-LCNs, and the MTT assay was performed to assess cell viability (c). The BEAS-2B cell morphology upon treatment with TGF- β alone or with TGF- β and 0.5 μ M BM-LCNs is shown in (d). Scale bar = 300 μ m. The results in (a-c) were normalized as a percentage compared to untreated control and indicated as mean \pm SEM ($n = 3$, **: $p < 0.01$; ***: $p < 0.001$; ****: $p < 0.0001$ with one-way ANOVA test). (For interpretation of the references to colour in this figure legend, the reader is referred to the web version of this article.)

LCNs, resulted in a significant reduction of cell viability of 15.8% ($p < 0.001$ against the untreated group), 16.5% ($p < 0.0001$ against the untreated group), and 27.9% 16.5% ($p < 0.0001$ against the untreated group), respectively (Fig. 1c). Treatment with either TGF- β alone or with TGF- β and 0.5 μ M BM-LCNs did not result in significant changes in the cells' morphology (Fig. 1d).

3.2. Anti-migratory activity of BM-LCNs in TGF- β -induced BEAS-2B cells

The effect of treatment with 0.5 μ M BM-LCNs on the migratory capacity of TGF- β -induced BEAS-2B cells was assessed through the wound healing assay after 24 and 48 h of treatment (Fig. 2a and b, respectively). At the 24 h time, the percentage of wound closure of the untreated group was 36.3% (Fig. 2a). Treatment with TGF- β resulted in a significant 42% increase in the percentage of wound closure compared to the untreated group (percentage wound closure of 51.5%, $p < 0.0001$, Fig. 2a). Simultaneous treatment with BM-LCNs reversed the effect of TGF- β , resulting in a significantly lower percent wound closure similar to the

untreated group (34.8%, $p < 0.0001$ vs TGF- β -induced group, Fig. 2a). At the 48 h time point, the percentage of wound closure of the untreated group was 65.5% (Fig. 2b), and treatment with TGF- β resulted in a significant 18% increase in the percentage of wound closure compared to the untreated group (percentage wound closure of 77.3%, $p < 0.01$, Fig. 2b). Simultaneous treatment with BM-LCNs reversed the effect of TGF- β , resulting in a significantly lower percent of wound closure which was similar to the untreated group (63.0%, $p < 0.01$ vs TGF- β -induced group, Fig. 2b). Representative figures of the cells at the indicated time points are shown in Fig. 2c.

3.3. BM-LCNs counteract the protein expression signature induced by TGF- β

The relative protein levels of endoglin, basic FGF, myeloperoxidase, thrombospondin-1, VEGF, myeloperoxidase, and cystatin C are shown in Fig. 3, as detected using the Human XL Cytokine Protein Array. Treatment with 0.5 μ M BM-LCNs counteracted the action of TGF- β by

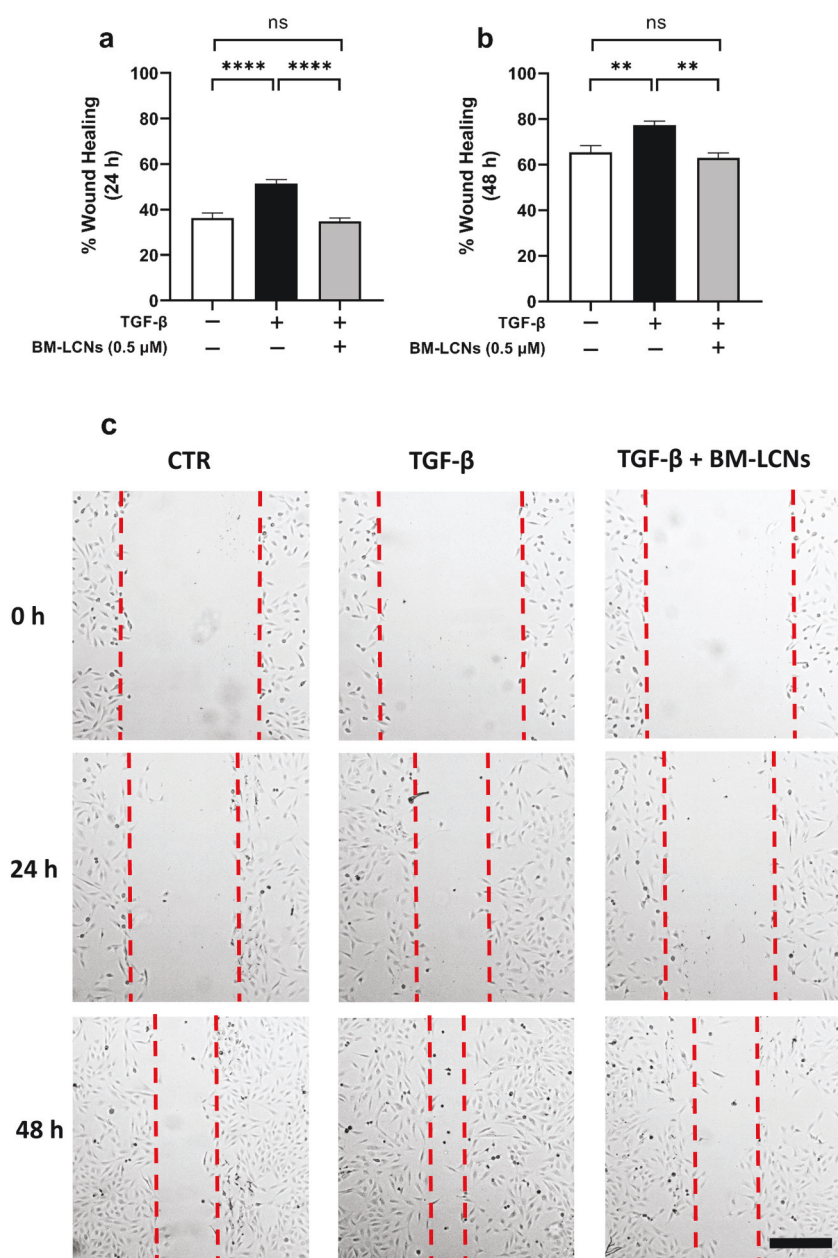


Fig. 2. Anti-migratory activity of BM-LCNs in TGF- β -induced BEAS-2B cells. The wound was created by scratching, with a sterile pipette tip, a layer of BEAS-2B cells. Cells were then treated with 5 ng/mL TGF- β 1 with or without the presence of 0.5 μ M BM-LCNs. Photographs were acquired using a light microscope at 10 \times magnification. The distance between the edges of the wounds was measured before treatment (0 h) and after 24 h (a) and 48 h (b) incubation in order to calculate the percent wound closure. Representative pictures of the cells at the indicated time points are shown in (c). Magnification: 10 \times ; Scale bar = 300 μ m. Values are expressed as mean \pm SEM ($n = 3$; ns: $p > 0.05$; **: $p < 0.01$; ****: $p < 0.0001$ with one-way ANOVA test).

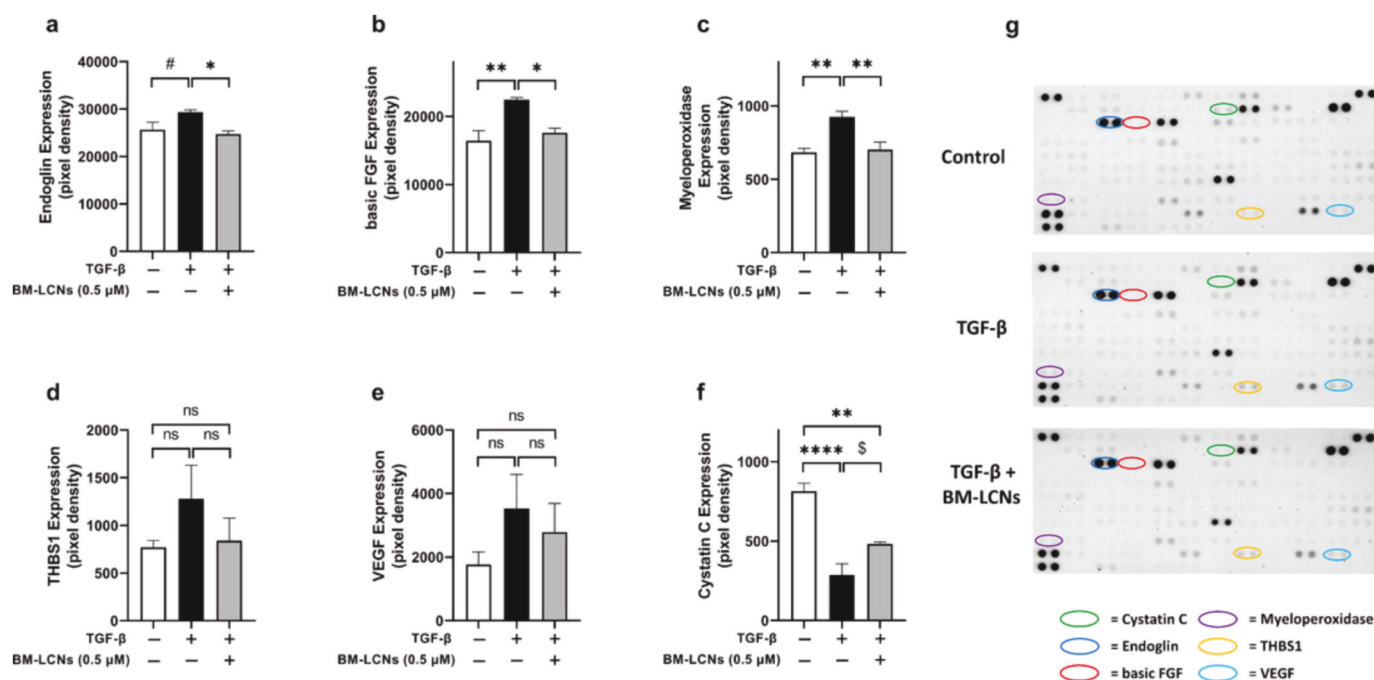


Fig. 3. BM-LCNs counteract the expression patterns of proteins induced by TGF- β . BEAS-2B cells were treated with 5 ng/mL TGF- β 1 for 24 h with or without a successive 24 h treatment with 0.5 μ M BM-LCNs. The relative protein expression levels of endoglin (a), basic FGF (b), myeloperoxidase (c), thrombospondin-1 (THBS1) (d), VEGF (e), and cystatin C (f) were determined using the Human XL Cytokine Protein Array. A representative array for each group is shown in (g). Values in (a-f) are expressed as mean \pm SEM ($n = 4$, *: $p < 0.05$; **: $p < 0.01$; ****: $p < 0.0001$; #: $p = 0.07$; \$: $p = 0.053$ with one-way ANOVA test).

reducing the expression of endoglin, basic FGF, myeloperoxidase, thrombospondin-1, and VEGF (Fig. 3a to 3e, respectively), which are induced by TGF- β , as well as by partially restoring the expression of cystatin C, which is suppressed by TGF- β (Fig. 3f). A representative array for each experimental group is shown in Fig. 3g. In particular, treatment of BEAS-2B cells with TGF- β resulted in a nearly statistically significant increase in the signal intensity correlated to the levels of endoglin (1.14-fold, $p = 0.07$, Fig. 3a), as well as a statistically significant increase in the signal of basic FGF (1.37-fold, $p < 0.01$, Fig. 3b), and myeloperoxidase (1.35-fold, $p < 0.05$, Fig. 3c). Simultaneous treatment with BM-LCNs resulted in a significant reduction of the signal intensity for all these proteins. The signal corresponding to endoglin was reduced by 15.7% ($p < 0.05$, Fig. 3a), the signal corresponding to basic FGF was reduced by 21.6% ($p < 0.05$, Fig. 3b), and the signal corresponding to myeloperoxidase was reduced by 24.0% ($p < 0.01$, Fig. 3c). A similar trend, although not statistically significant, was observed for thrombospondin-1 (THBS1) and VEGF. Upon treatment with TGF- β , THBS1 signal was increased by 1.58-fold and VEGF signal was increased by 2-fold (Fig. 3d and e, respectively, $p > 0.05$). Treatment with BM-LCNs reduced the signal related to the expression of these proteins by 34.4% ($p > 0.05$, Fig. 3d) and 21.2% ($p > 0.05$, Fig. 3e), respectively. With regards to cystatin C, its expression was significantly reduced by 65% upon treatment with TGF- β ($p < 0.0001$, Fig. 3f). Treatment with BM-LCNs resulted in a 1.68-fold increase in the signal correlated to cystatin C ($p = 0.053$, Fig. 3f).

3.4. BM-LCNs restore baseline levels of NO

The effect of BM-LCNs on NO production in BEAS-2B cells was assessed by measuring NO levels in the cell culture supernatant using the Griess reagent. The results are shown in Fig. 4. Treatment of BEAS-2B cells with TGF- β resulted in a significant 36.4% reduction of the NO levels compared to untreated group ($p < 0.01$, Fig. 4). The subsequent treatment with BM-LCNs restored the secretion of NO to the same levels as the untreated group ($p < 0.01$ against the TGF- β -treated group, Fig. 4). No statistically significant difference was observed between the

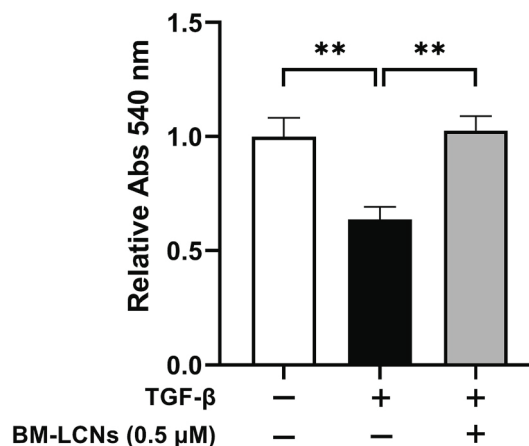


Fig. 4. BM-LCNs restore baseline levels of NO. BEAS-2B cells were treated with 5 ng/mL TGF- β 1 for 24 h with or without a successive 24 h treatment with 0.5 μ M BM-LCNs. The NO levels in the cell culture supernatant were determined using the Griess reagent and measuring the absorbance at 540 nm. The values indicated are mean \pm SEM ($n = 3$; **: $p < 0.01$ with one-way ANOVA test).

untreated group and the TGF- β + BM-LCNs treated group (Fig. 4).

4. Discussion

CRDs are among the leading causes of morbidity and mortality worldwide, causing substantial medical and economic burdens (Viegi et al., 2020). Cigarette smoking is considered to be among the main causative factors for this heterogeneous group of diseases due to the fact that it results in the exposure of the respiratory system to thousands of different noxious chemicals, promoting chronic inflammation, oxidative stress, and consequentially severe tissue damage (Malyla et al., 2020; Nucera et al., 2022a; Nucera et al., 2022b). Traditional therapies for CRDs are mainly aimed at improving disease symptoms, and they are

often ineffective at restoring the destroyed airways and lung parenchyma (Wang et al., 2020). Furthermore, the currently available pharmacological strategies for these ailments are hampered by severe side effects (Celli et al., 2008). This is particularly true in the case of LC due to the elevated toxicity of the currently used chemotherapeutic drugs (Yazbeck et al., 2022).

A common feature shared between the CRDs is the process of airway remodelling, consisting of radical structural changes occurring in both the large and small airways and contributing to severe airway obstruction (Mehta et al., 2020; Gupta et al., 2021). The main structural alterations in airway remodelling include EMT of epithelial layers, excessive collagen and mucus secretion, and thickening of the basement membrane. These processes are orchestrated by TGF- β , whose expression and signalling are aberrant in virtually all CRDs (Aschner and Downey, 2016; Prasher et al., 2022b). In this context, a therapeutic agent tackling the TGF- β signalling would be advantageous. It would find widespread clinical application as a therapy for all diseases where tissue remodelling and fibrosis play a fundamental role (Walton et al., 2017).

The plant world represents an endless source of inspiration for novel compounds, collectively termed phytochemicals or nutraceuticals, with the most disparate pharmacological activities (Paudel et al., 2022a). Many phytochemicals are known to downregulate TGF- β signalling and therefore show great promise in treating CRDs and fibrotic disorders (DiNicolantonio et al., 2021). One of these compounds is berberine, which has been shown to suppress TGF- β expression and signalling and subsequent cell motility, proliferation, and EMT *in vitro* in many types of cancer (Huang et al., 2020; Du et al., 2021; Kim et al., 2018; Chu et al., 2014; Jin et al., 2022; Sun et al., 2022) and is embedded with potent multi-organ antifibrotic activity *in vivo* (DiNicolantonio et al., 2021). Despite its potent biological activity, the clinical application of berberine is limited by a poor pharmacokinetic profile, mainly deriving from its scarce permeability. This results in the necessity to administer large doses of berberine to achieve therapeutic efficacy, with an increased risk of adverse effects (Yin et al., 2008). To overcome this important obstacle to the clinical application of berberine and other phytochemicals, several types of advanced drug delivery systems are currently being developed (Gupta et al., 2021; Paudel et al., 2022a).

The present study shows that berberine encapsulated in a liquid crystalline nanoparticle formulation attenuates some of the TGF- β -induced remodelling features in BEAS-2B human bronchial epithelial cells. In particular, treatment of TGF- β -induced BEAS-2B cells with BM-LCNs significantly reduced the cells' increased motility up to 48 h of treatment, as assessed through wound healing assay, resulting in an extent of migration that was comparable to that observed in the untreated group. This is in accordance with previous reports showing, in different cell systems, that berberine is capable of inhibiting cell migration (Paudel et al., 2022c; Jin et al., 2022).

The protein array experiment revealed fundamental mechanistic insights about the pathways impacted by berberine in counteracting TGF- β action. Endoglin is a known interactor of TGF- β receptors I and II. It is an auxiliary component of the TGF- β signalling machinery capable of modulating the downstream signalling (Guerrero-Esteo et al., 2002). Among its different functions, endoglin is known to regulate actin cytoskeletal organization in endothelial cells, and this could contribute to the increased angiogenesis observed in tissue remodelling (Sanz-Rodriguez et al., 2004). The present study is the first to report that berberine treatment results in the downregulation of endoglin levels, restoring them to levels compared to untreated cells. Other factors activated upon TGF- β signalling and contributing to various aspects of tissue remodelling, including angiogenesis, are thrombospondin-1, VEGF, and bFGF. In this study, treatment with BM-LCNs reduced the expression of these proteins to levels comparable to the untreated group. Besides being among the main activator factors of latent TGF- β , thrombospondin-1 is involved in physiological tissue repair and pathologic fibrosis in TGF- β -dependent and independent pathways

(Sweetwyne and Murphy-Ullrich, 2012). The present study is the first to report that berberine inhibits the expression of thrombospondin-1.

With regards to VEGF and bFGF, these two cytokines are known to mediate TGF- β -induced remodelling and angiogenesis in various diseases, including asthma and COPD (Yum et al., 2011; Zanini et al., 2010; Wang et al., 2018). Furthermore, these two cytokines are considered among the most important inducers of angiogenesis in cancers such as NSCLC (Bremnes et al., 2006). The finding that BM-LCNs counteract the TGF- β -induced upregulation of these proteins are in accordance with reports showing that berberine (i) suppresses the expression of bFGF in breast cancer cells, and (ii) downregulates the expression of VEGF in hepatocellular carcinoma cells, concomitantly inhibiting their angiogenic potential (Jie et al., 2011).

Myeloperoxidase is mainly produced by neutrophils and other body cells (Khan et al., 2018), and it plays a pivotal role in airway inflammation and tissue remodelling in diseases such as COPD (Wang et al., 2018). In the present study, berberine significantly counteracted the TGF- β -induced increase in myeloperoxidase expression in BEAS-2B cells. This is in accordance with a study where berberine was shown to alleviate dextran sulfate sodium (DSS)-induced colitis in mice through the reduction of inflammation and oxidative stress, which was exerted *via* mechanisms including the downregulation of myeloperoxidase levels (Zhang et al., 2017).

Treatment of BEAS-2B cells with TGF- β further resulted in the downregulation of Cystatin C protein expression. This is a negative regulator of TGF- β signalling (Sokol and Schiemann, 2004). Administration of Cystatin C, in particular, has been shown to have preclinical efficacy against the oncogenic activity of TGF- β in an *in vivo* model of breast cancer (Tian and Schiemann, 2009). In the present study, BM-LCNs partially restored the TGF- β -induced downregulation of the expression of Cystatin C, further highlighting the potent activity of BM-LCNs in inhibiting TGF- β signalling.

Nitric oxide (NO) plays a fundamental role in preserving the epithelial phenotype of lung epithelial cells by preventing EMT (Vyas-Read et al., 2007). In this context, one of the mechanisms by which TGF- β induces EMT is the reduction of endogenous NO production *via* the downregulation and inhibition of eNOS (Vyas-Read et al., 2007), sGC, and PKGI (Bachiller et al., 2010). In the present study, treatment of TGF- β -induced BEAS-2B cells with BM-LCNs significantly counteracted the effect of TGF- β , restoring the baseline NO production to levels comparable to the untreated group. An increased NO production induced by berberine was shown in a study by Wang et al. (2009), in which treatment of high-fat-diet and streptozotocin-induced diabetic rats with berberine resulted in increased eNOS expression and, concomitantly, higher NO levels (Wang et al., 2009). Interestingly, in a previous report, treatment of lipopolysaccharide (LPS)-stimulated RAW264.7 mouse macrophages with a similar berberine-LCN formulation resulted in a significant reduction of the elevated NO levels induced by LPS, which was exerted through the downregulation of the expression of the inducible NO synthase (iNOS) (Alnuqaydan et al., 2022a). This shows proof of the multifaceted, context-dependent biological activity of berberine, that promotes physiological levels of NO and a generally healthy cell phenotype through its potent anti-inflammatory, antioxidant, and anti-fibrotic properties. The findings reported in this study are summarized in the Graphical Abstract of the present manuscript.

An important advantage of the present study is that BM-LCNs significantly counteracted TGF- β -induced remodelling features at an equivalent berberine concentration of 0.5 μ M. This concentration is substantially lower (10- to 600-fold) compared to the average concentration range of free berberine powder that was shown to be active in counteracting TGF- β -induced features in previous reports (5–300 μ M) (Huang et al., 2020; Du et al., 2021; Kim et al., 2018; Chu et al., 2014; Jin et al., 2022; Sun et al., 2022). Although these mentioned studies were performed on different cell lines and with different experimental setups, this strong discrepancy in active berberine concentration reflects the fact that nanoparticle-based drug delivery systems such as LCNs

allow improved delivery of the therapeutic cargo, with resulting lower doses necessary to achieve a significant therapeutic effect. This is in agreement with previous reports from our research team showing that encapsulating phytochemicals in LCNs or other nanoparticle-based delivery systems resulted in potent activity at lower concentrations than the free molecule (Paudel et al., 2022b; Alnuqaydan et al., 2022a; Paudel et al., 2020; Chang et al., 2017; Solanki et al., 2020).

Despite the promising activity of BM-LCNs in counteracting TGF- β -induced remodelling features, the present study is not exempt from limitations. The main limitation is that these study findings are reported only on TGF- β -induced BEAS-2B bronchial epithelial cells, which represent a rather simplistic *in vitro* model of airway remodelling that does not account for the totality of the cellular and molecular mechanisms involved. Despite the fact that epithelial cell proliferation is one of the key factors driving airway remodelling (Liu et al., 2021), and that TGF- β signalling plays a central role in this process (Halwani et al., 2011), the lung, like any other organ, is composed of different cell types that, together, orchestrate its function in health and disease. Airway remodelling itself is an extremely complex process, which involves several other cell types as well as other pro-fibrotic factors that work in synergism with TGF- β (Zhang et al., 1999). Similar studies performed on other cell types, such as alveolar epithelial cells, endothelial cells, and macrophages, would provide a more complete picture of the true potential of BM-LCNs in counteracting TGF- β -mediated aberrant airway remodelling. In this context, the use of *in vitro* models consisting of the co-culture of different cell lines (Zhang et al., 1999; Osei et al., 2020), especially in conjunction with microfluidic (Zeng et al., 2022) and “airway-on-a-chip” devices (Bennet et al., 2021), would provide a more accurate and detailed depiction of the airway remodelling process. Furthermore, to allow the translation of these *in vitro* results to the clinic, BM-LCNs should be tested on suitable animal models of asthma, COPD, and pulmonary fibrosis.

5. Conclusions

This study highlights the potent activity of BM-LCNs in counteracting TGF- β -induced remodelling features in human bronchial epithelial cells. This activity is exerted through the inhibition of TGF- β -induced cell migration, by regulating the expression of several cytokines and mediators dysregulated by treatment with TGF- β , and by restoring physiological baseline NO levels. The findings reported in this manuscript provide further proof of the multifaceted applicability of BM-LCNs as a potential therapy for CRDs where aberrant tissue remodelling plays a pivotal role. However, in order to achieve clinical translation, the results of this finding must be further confirmed and validated by investigating the effect of BM-LCNs on more complex *in vitro* systems, as well as on *in vivo* models of CRDs.

Funding

The authors are thankful to the Graduate School of Health, University of Technology Sydney, Australia. KD is supported by a project grant from the Rebecca L Cooper Medical Research Foundation and the Maridulu Budyari Gumal Sydney Partnership for Health, Education, Research and Enterprise (SPHERE) RSEOH CAG Seed grant, fellowship and extension grant; Faculty of Health MCR/ECR Mentorship Support Grant and UTS Global Strategic Partnerships Seed Funding Scheme. The authors would also like to thank Uttaranchal University for their seed grant. GDR is supported by the UTS International Research Scholarship, the UTS President's Scholarship, and by the Triple I Clinical Academic Group CAG) Secondment / Exchange Program grant. KRP is supported by a fellowship from Prevent Cancer Foundation (PCF) and the International Association for the Study of Lung Cancer (IASLC). GL is supported by CREATE Hope Scientific Fellowship from Lung Foundation Australia.

Declaration of Competing Interest

The authors have no conflict of interest to declare.

Data availability

The data presented in this study are available on request from the corresponding authors.

References

- Alnuqaydan, A.M., et al., 2022a. Phytantriol-based Berberine-loaded liquid crystalline nanoparticles attenuate inflammation and oxidative stress in lipopolysaccharide-induced RAW264.7 macrophages. *Nanomaterials (Basel)* 12 (23).
- Alnuqaydan, A.M., et al., 2022b. Evaluation of the cytotoxic activity and anti-migratory effect of Berberine-Phytantriol liquid crystalline nanoparticle formulation on non-small-cell lung Cancer *in vitro*. *Pharmaceutics* 14 (6).
- Aschner, Y., Downey, G.P., 2016. Transforming growth factor- β : master regulator of the respiratory system in health and disease. *Am. J. Respir. Cell Mol. Biol.* 54 (5), 647–655.
- Bachiller, P.R., Nakanishi, H., Roberts Jr., J.D., 2010. Transforming growth factor-beta modulates the expression of nitric oxide signaling enzymes in the injured developing lung and in vascular smooth muscle cells. *Am. J. Phys. Lung Cell. Mol. Phys.* 298 (3), L324–L334.
- Bennet, T.J., et al., 2021. Airway-on-A-Chip: designs and applications for lung repair and disease. *Cells* 10 (7).
- Bratova, M., et al., 2020. Non-small cell lung Cancer as a chronic disease - a prospective study from the Czech TULUNG registry. *In Vivo* 34 (1), 369–379.
- Bremnes, R.M., Camps, C., Sirera, R., 2006. Angiogenesis in non-small cell lung cancer: the prognostic impact of neoangiogenesis and the cytokines VEGF and bFGF in tumours and blood. *Lung Cancer* 51 (2), 143–158.
- Celli, B.R., et al., 2008. Effect of pharmacotherapy on rate of decline of lung function in chronic obstructive pulmonary disease: results from the TORCH study. *Am. J. Respir. Crit. Care Med.* 178 (4), 332–338.
- Chan, Y., et al., 2021. Versatility of liquid crystalline nanoparticles in inflammatory lung diseases. *Nanomedicine (London)* 16 (18), 1545–1548.
- Chang, H.L., et al., 2017. Naringenin inhibits migration of lung cancer cells via the inhibition of matrix metalloproteinases-2 and -9. *Exp. Ther. Med.* 13 (2), 739–744.
- Chitra, P., et al., 2013. Berberine attenuates bleomycin induced pulmonary toxicity and fibrosis via suppressing NF- κ B dependant TGF- β activation: a biphasic experimental study. *Toxicol. Lett.* 219 (2), 178–193.
- Chu, S.C., et al., 2014. Berberine reverses epithelial-to-mesenchymal transition and inhibits metastasis and tumor-induced angiogenesis in human cervical cancer cells. *Mol. Pharmacol.* 86 (6), 609–623.
- Clarence, D.D., et al., 2022. Unravelling the therapeutic potential of Nano-delivered functional foods in chronic respiratory diseases. *Nutrients* 14 (18).
- Crawford, S.E., et al., 1998. Thrombospondin-1 is a major activator of TGF-beta1 *in vivo*. *Cell* 93 (7), 1159–1170.
- Devkota, H.P., et al., 2022. Phytochemicals and their Nanoformulations targeted for pulmonary diseases. In: *Advanced Drug Delivery Strategies for Targeting Chronic Inflammatory Lung Diseases*. Springer, pp. 95–106.
- Dhanjal, D.S., et al., 2022. Concepts of advanced therapeutic delivery systems for the management of remodeling and inflammation in airway diseases. *Future Med. Chem.* 14 (4), 271–288.
- DiNicolantonio, J.J., et al., 2021. A nutraceutical strategy for downregulating TGF β signalling: prospects for prevention of fibrotic disorders, including post-COVID-19 pulmonary fibrosis. *Open Heart* 8 (1).
- Doerner, A.M., Zuraw, B.L., 2009. TGF- β 1 induced epithelial to mesenchymal transition (EMT) in human bronchial epithelial cells is enhanced by IL-1 β but not abrogated by corticosteroids. *Respir. Res.* 10 (1), 100.
- Du, H., et al., 2021. Berberine suppresses EMT in liver and gastric carcinoma cells through combination with TGF β R regulating TGF- β /Smad pathway. *Oxidative Med. Cell. Longev.* 2021, 2337818.
- Dua, K., et al., 2019. Increasing complexity and interactions of oxidative stress in chronic respiratory diseases: an emerging need for novel drug delivery systems. *Chem. Biol. Interact.* 299, 168–178.
- Grzela, K., et al., 2016. Airway remodeling in chronic obstructive pulmonary disease and asthma: the role of matrix Metalloproteinase-9. *Arch. Immunol. Ther. Exp.* 64 (1), 47–55.
- Guerrero-Esteo, M., et al., 2002. Extracellular and cytoplasmic domains of endoglin interact with the transforming growth factor-beta receptors I and II. *J. Biol. Chem.* 277 (32), 29197–29209.
- Gupta, G., et al., 2021. Advanced drug delivery approaches in managing TGF- β -mediated remodeling in lung diseases. *Nanomedicine (London)* 16 (25), 2243–2247.
- Halwani, R., et al., 2011. Role of transforming growth factor- β in airway remodeling in asthma. *Am. J. Respir. Cell Mol. Biol.* 44 (2), 127–133.
- Huang, C., et al., 2020. Berberine inhibits epithelial-mesenchymal transition and promotes apoptosis of tumour-associated fibroblast-induced colonic epithelial cells through regulation of TGF- β signalling. *J. Cell Commun. Signal.* 14 (1), 53–66.
- Huang, T., Schor, S.L., Hinck, A.P., 2014. Biological activity differences between TGF- β 1 and TGF- β 3 correlate with differences in the rigidity and arrangement of their component monomers. *Biochemistry* 53 (36), 5737–5749.

- Huse, M., et al., 2001. The TGF beta receptor activation process: an inhibitor-to-substrate-binding switch. *Mol. Cell* 8 (3), 671–682.
- Iwano, M., et al., 2002. Evidence that fibroblasts derive from epithelium during tissue fibrosis. *J. Clin. Invest.* 110 (3), 341–350.
- Jie, S., et al., 2011. Berberine inhibits angiogenic potential of Hep G2 cell line through VEGF down-regulation in vitro. *J. Gastroenterol. Hepatol.* 26 (1), 179–185.
- Jin, Y., et al., 2022. Berberine suppressed the progression of human glioma cells by inhibiting the TGF- β 1/SMAD2/3 signaling pathway. *Integr. Cancer Ther.* 21, p. 15347354221130303.
- Kc, B.B., et al., 2022. Prevalence and factors associated with tobacco use among high school students. *J. Nepal Health Res Counc* 20 (2), 310–315.
- Khan, A.A., Alsahli, M.A., Rahmani, A.H., 2018. Myeloperoxidase as an active disease biomarker: recent biochemical and pathological perspectives. *Med. Sci. (Basel)* 6 (2).
- Khurshheed, R., et al., 2022. Expanding the arsenal against pulmonary diseases using surface-functionalized polymeric micelles: breakthroughs and bottlenecks. *Nanomedicine (London)* 17 (12), 881–911.
- Kim, S., et al., 2018. Berberine suppresses cell motility through downregulation of TGF- β 1 in triple negative breast Cancer cells. *Cell. Physiol. Biochem.* 45 (2), 795–807.
- Kumbhar, P., et al., 2022. Inhalation delivery of repurposed drugs for lung cancer: approaches, benefits and challenges. *J. Control. Release* 341, 1–15.
- Kuo, C.L., Chi, C.W., Liu, T.Y., 2004. The anti-inflammatory potential of berberine in vitro and in vivo. *Cancer Lett.* 203 (2), 127–137.
- Labaki, W.W., Han, M.K., 2020. Chronic respiratory diseases: a global view. *Lancet Respir. Med.* 8 (6), 531–533.
- Lee, C.G., et al., 2004. Vascular endothelial growth factor (VEGF) induces remodeling and enhances TH2-mediated sensitization and inflammation in the lung. *Nat. Med.* 10 (10), 1095–1103.
- Leuppi, J.D., et al., 2013. Short-term vs conventional glucocorticoid therapy in acute exacerbations of chronic obstructive pulmonary disease: the REDUCE randomized clinical trial. *Jama* 309 (21), 2223–2231.
- Li, C., Qiu, Y., Zhang, Y., 2022. Research Progress on therapeutic targeting of Cancer-associated fibroblasts to tackle treatment-resistant NSCLC. *Pharmaceuticals (Basel)* 15 (11).
- Liu, G., et al., 2019. Fibulin-1c regulates transforming growth factor- β activation in pulmonary tissue fibrosis. *JCI Insight* 5 (16).
- Liu, G., et al., 2021. Therapeutic targets in lung tissue remodeling and fibrosis. *Pharmacol. Ther.* 225, 107839.
- Lugg, S.T., et al., 2022. Cigarette smoke exposure and alveolar macrophages: mechanisms for lung disease. *Thorax* 77 (1), 94–101.
- Malyla, V., et al., 2020. Recent advances in experimental animal models of lung cancer. *Future Med. Chem.* 12 (7), 567–570.
- Martinez, F.J., et al., 2017. Idiopathic pulmonary fibrosis. *Nat. Rev. Dis. Primers* 3, 17074.
- Massagué, J., 2008. TGF β in Cancer. *Cell* 134 (2), 215–230.
- Mehta, M., et al., 2020. Incipient need of targeting airway remodeling using advanced drug delivery in chronic respiratory diseases. *Future Med. Chem.* 12 (10), 873–875.
- Mehta, M., et al., 2021. Berberine loaded liquid crystalline nanostructure inhibits cancer progression in adenocarcinomic human alveolar basal epithelial cells in vitro. *J. Food Biochem.* 45 (11), e13954.
- Nucera, F., et al., 2022a. Role of oxidative stress in the pathogenesis of COPD. *Minerva Med.* 113 (3), 370–404.
- Nucera, F., et al., 2022b. Chapter 14 - role of autoimmunity in the pathogenesis of chronic obstructive pulmonary disease and pulmonary emphysema. In: Rezaei, N. (Ed.), *Translational Autoimmunity*. Academic Press, pp. 311–331.
- Osei, E.T., Booth, S., Hackett, T.L., 2020. What have in vitro co-culture models taught us about the contribution of epithelial-mesenchymal interactions to airway inflammation and remodeling in asthma? *Cells* 9 (7).
- Pain, M., et al., 2014. Tissue remodelling in chronic bronchial diseases: from the epithelial to mesenchymal phenotype. *Eur. Respir. Rev.* 23 (131), 118–130.
- Paudel, K.R., et al., 2020. Rutin loaded liquid crystalline nanoparticles inhibit lipopolysaccharide induced oxidative stress and apoptosis in bronchial epithelial cells in vitro. *Toxicol. in Vitro* 68, 104961.
- Paudel, K.R., et al., 2022a. Nanomedicine and medicinal plants: emerging symbiosis in managing lung diseases and associated infections. *EXCLI J.* 21, 1299–1303.
- Paudel, K.R., et al., 2022b. Attenuation of cigarette-smoke-induced oxidative stress, senescence, and inflammation by berberine-loaded liquid crystalline nanoparticles: in vitro study in 16HBE and RAW264.7 cells. *Antioxidants (Basel)* 11 (5).
- Paudel, K.R., et al., 2022c. Berberine-loaded liquid crystalline nanoparticles inhibit non-small cell lung cancer proliferation and migration in vitro. *Environ. Sci. Pollut. Res.* 29 (31), 46830–46847.
- Paudel, K.R., et al., 2022d. Advanced Therapeutic Delivery for the Management of Chronic Respiratory Diseases. *Frontiers Media SA*, p. 983583.
- Paudel, K.R., et al., 2022e. Advancements in nanotherapeutics targeting senescence in chronic obstructive pulmonary disease. *Nanomedicine (London)* 17 (23), 1757–1760.
- Porsbjerg, C., et al., 2023. Asthma. *Lancet*. 401 (10379), 858–873.
- Prasher, P., et al., 2022a. Advances and applications of dextran-based nanomaterials targeting inflammatory respiratory diseases. *J. Drug Deliv. Sci. Technol.* 74, 103598.
- Prasher, P., et al., 2022b. Targeting mucus barrier in respiratory diseases by chemically modified advanced delivery systems. *Chem. Biol. Interact.* 365, 110048.
- Qi, H.W., et al., 2014. Epithelial-to-mesenchymal transition markers to predict response of Berberine in suppressing lung cancer invasion and metastasis. *J. Transl. Med.* 12, 22.
- Riley, C.M., Sciruba, F.C., 2019. Diagnosis and outpatient Management of Chronic Obstructive Pulmonary Disease: a review. *Jama* 321 (8), 786–797.
- Safiri, S., et al., 2022. Burden of chronic obstructive pulmonary disease and its attributable risk factors in 204 countries and territories, 1990-2019: results from the global burden of disease study 2019. *Bmj* 378, e069679.
- Saito, A., Horie, M., Nagase, T., 2018. TGF- β signaling in lung health and disease. *Int. J. Mol. Sci.* 19 (8), 2460.
- Sanz-Rodriguez, F., et al., 2004. Endoglin regulates cytoskeletal organization through binding to ZRP-1, a member of the Lim family of proteins. *J. Biol. Chem.* 279 (31), 32858–32868.
- Shin, J.H., et al., 2009. TGF-beta effects on airway smooth muscle cell proliferation, VEGF release and signal transduction pathways. *Respirology* 14 (3), 347–353.
- Sokol, J.P., Schiemann, W.P., 2004. Cystatin C antagonizes transforming growth factor beta signaling in normal and cancer cells. *Mol. Cancer Res.* 2 (3), 183–195.
- Solanki, N., et al., 2020. Antiproliferative effects of boswellic acid-loaded chitosan nanoparticles on human lung cancer cell line A549. *Future Med. Chem.* 12 (22), 2019–2034.
- Sun, Y., et al., 2022. Berberine inhibits glioma cell migration and invasion by suppressing TGF- β 1/COL11A1 pathway. *Biochem. Biophys. Res. Commun.* 625, 38–45.
- Sung, H., et al., 2021. Global Cancer statistics 2020: GLOBOCAN estimates of incidence and mortality worldwide for 36 cancers in 185 countries. *CA Cancer J. Clin.* 71 (3), 209–249.
- Sweetwyne, M.T., Murphy-Ullrich, J.E., 2012. Thrombospondin1 in tissue repair and fibrosis: TGF- β -dependent and independent mechanisms. *Matrix Biol.* 31 (3), 178–186.
- Takizawa, H., et al., 2001. Increased expression of transforming growth factor-beta1 in small airway epithelium from tobacco smokers and patients with chronic obstructive pulmonary disease (COPD). *Am. J. Respir. Crit. Care Med.* 163 (6), 1476–1483.
- Tan, C.L., et al., 2022. Unravelling the molecular mechanisms underlying chronic respiratory diseases for the development of novel therapeutics via in vitro experimental models. *Eur. J. Pharmacol.* 919, 174821.
- Tian, M., Schiemann, W.P., 2009. Preclinical efficacy of cystatin C to target the oncogenic activity of transforming growth factor Beta in breast cancer. *Transl. Oncol.* 2 (3), 174–183.
- Tsai, P.L., Tsai, T.H., 2004. Hepatobiliary excretion of berberine. *Drug Metab. Dispos.* 32 (4), 405–412.
- Viegi, G., et al., 2020. Global burden of chronic respiratory diseases. *J. Aerosol. Med. Pulm. Drug Deliv.* 33 (4), 171–177.
- Vyas-Read, S., et al., 2007. Nitric oxide attenuates epithelial-mesenchymal transition in alveolar epithelial cells. *Am. J. Phys. Lung Cell. Mol. Phys.* 293 (1), L212–L221.
- Walton, K.L., Johnson, K.E., Harrison, C.A., 2017. Targeting TGF- β mediated SMAD signaling for the prevention of fibrosis. *Front. Pharmacol.* 8, 461.
- Wang, C., et al., 2009. Ameliorative effect of berberine on endothelial dysfunction in diabetic rats induced by high-fat diet and streptozotocin. *Eur. J. Pharmacol.* 620 (1–3), 131–137.
- Wang, M.Y., et al., 2020. Current therapeutic strategies for respiratory diseases using mesenchymal stem cells. *MedComm* 2 (3), 351–380.
- Wang, Y., et al., 2018. Role of inflammatory cells in airway remodeling in COPD. *Int. J. Chron. Obstruct. Pulmon. Dis.* 13, 3341–3348.
- Yazbeck, V., et al., 2022. An overview of chemotoxicity and radiation toxicity in cancer therapy. *Adv. Cancer Res.* 155, 1–27.
- Yin, J., Xing, H., Ye, J., 2008. Efficacy of berberine in patients with type 2 diabetes mellitus. *Metabolism* 57 (5), 712–717.
- Yu, Q., Stamenkovic, I., 2000. Cell surface-localized matrix metalloproteinase-9 proteolytically activates TGF-beta and promotes tumor invasion and angiogenesis. *Genes Dev.* 14 (2), 163–176.
- Yum, H.Y., et al., 2011. Allergen-induced coexpression of bFGF and TGF- β 1 by macrophages in a mouse model of airway remodeling: bFGF induces macrophage TGF- β 1 expression in vitro. *Int. Arch. Allergy Immunol.* 155 (1), 12–22.
- Zanini, A., et al., 2010. The role of the bronchial microvasculature in the airway remodelling in asthma and COPD. *Respir. Res.* 11 (1), 132.
- Zeng, Y., et al., 2022. An open microfluidic coculture model of fibroblasts and eosinophils to investigate mechanisms of airway inflammation. *Front. Bioeng. Biotechnol.* 10, 993872.
- Zhang, L.C., et al., 2017. Berberine alleviates dextran sodium sulfate-induced colitis by improving intestinal barrier function and reducing inflammation and oxidative stress. *Exp. Ther. Med.* 13 (6), 3374–3382.
- Zhang, S., et al., 1999. Growth factors secreted by bronchial epithelial cells control myofibroblast proliferation: an in vitro co-culture model of airway remodeling in asthma. *Lab. Investig.* 79 (4), 395–405.

APPENDIX II

Additional publications relevant to thesis work

1) Research Paper: Phytantriol-Based Berberine-Loaded Liquid Crystalline Nanoparticles Attenuate Inflammation and Oxidative Stress in Lipopolysaccharide-Induced RAW264.7 Macrophages









Status: Published in the journal **Nanomaterials**

Citation: Alnuqaydan AM, Almutary AG, Azam M, Manandhar B, **De Rubis G**, Madheswaran T, Paudel KR, Hansbro PM, Chellappan DK, Dua K. *Phytantriol-Based Berberine-Loaded Liquid Crystalline Nanoparticles Attenuate Inflammation and Oxidative Stress in Lipopolysaccharide-Induced RAW264.7 Macrophages*. **Nanomaterials (Basel)**. 2022 Dec 5;12(23):4312. doi: 10.3390/nano12234312.

Contribution: I contributed to the conception and planning of the study, as well as performed part of the experiments and contributed to the writing and revision process of the manuscript

Article

Phytantriol-Based Berberine-Loaded Liquid Crystalline Nanoparticles Attenuate Inflammation and Oxidative Stress in Lipopolysaccharide-Induced RAW264.7 Macrophages

Abdullah M. Alnuqaydan ^{1,*}, Abdulmajeed G. Almutary ¹, Mohd Azam ², Bikash Manandhar ^{3,4}, Gabriele De Rubis ^{3,4}, Thiagarajan Madheswaran ⁵, Keshav Raj Paudel ⁶, Philip M. Hansbro ⁶, Dinesh Kumar Chellappan ⁷ and Kamal Dua ^{3,4}

¹ Department of Medical Biotechnology, College of Applied Medical Sciences, Qassim University, Buraidah 51452, Saudi Arabia

² Department of Medical Laboratories, College of Applied Medical Sciences, Qassim University, Buraidah 51452, Saudi Arabia

³ Discipline of Pharmacy, Graduate School of Health, University of Technology Sydney, Sydney, NSW 2007, Australia

⁴ Faculty of Health, Australian Research Centre in Complementary & Integrative Medicine, University of Technology Sydney, Ultimo, NSW 2007, Australia

⁵ Department of Pharmaceutical Technology, School of Pharmacy, International Medical University, Kuala Lumpur 57000, Malaysia

⁶ Centre for Inflammation, Faculty of Science, School of Life Sciences, Centenary Institute and University of Technology Sydney, Sydney, NSW 2007, Australia

⁷ Department of Life Sciences, School of Pharmacy, International Medical University, Kuala Lumpur 57000, Malaysia

* Correspondence: ami.alnuqaydan@qu.edu.sa



Citation: Alnuqaydan, A.M.;

Almutary, A.G.; Azam, M.;

Manandhar, B.; De Rubis, G.;

Madheswaran, T.; Paudel, K.R.;

Hansbro, P.M.; Chellappan, D.K.;

Dua, K. Phytantriol-Based Berberine-

Loaded Liquid Crystalline

Nanoparticles Attenuate

Inflammation and Oxidative Stress in

Lipopolysaccharide-Induced

RAW264.7 Macrophages.

Nanomaterials **2022**, *12*, 4312. <https://doi.org/10.3390/nano12234312>

Academic Editor: Zili Sideratou

Received: 25 October 2022

Accepted: 30 November 2022

Published: 5 December 2022

Publisher's Note: MDPI stays neutral with regard to jurisdictional claims in published maps and institutional affiliations.



Copyright: © 2022 by the authors. Licensee MDPI, Basel, Switzerland. This article is an open access article distributed under the terms and conditions of the Creative Commons Attribution (CC BY) license (<https://creativecommons.org/licenses/by/4.0/>).

Abstract: Inflammation and oxidative stress are interrelated processes that represent the underlying causes of several chronic inflammatory diseases that include asthma, cystic fibrosis, chronic obstructive pulmonary disease (COPD), allergies, diabetes, and cardiovascular diseases. Macrophages are key initiators of inflammatory processes in the body. When triggered by a stimulus such as bacterial lipopolysaccharides (LPS), these cells secrete inflammatory cytokines namely TNF- α that orchestrate the cellular inflammatory process. Simultaneously, pro-inflammatory stimuli induce the upregulation of inducible nitric oxide synthase (iNOS) which catalyzes the generation of high levels of nitric oxide (NO). This, together with high concentrations of reactive oxygen species (ROS) produced by macrophages, mediate oxidative stress which, in turn, exacerbates inflammation in a feedback loop, resulting in the pathogenesis of several chronic inflammatory diseases. Berberine is a phytochemical embedded with potent in vitro anti-inflammatory and antioxidant properties, whose therapeutic application is hindered by poor solubility and bioavailability. For this reason, large doses of berberine need to be administered to achieve the desired pharmacological effect, which may result in toxicity. Encapsulation of such a drug in liquid crystalline nanoparticles (LCNs) represents a viable strategy to overcome these limitations. We encapsulated berberine in phytantriol-based LCNs (BP-LCNs) and tested the antioxidant and anti-inflammatory activities of BP-LCNs in vitro on LPS-induced mouse RAW264.7 macrophages. BP-LCNs showed potent anti-inflammatory and antioxidant activities, with significant reduction in the gene expressions of TNF- α and iNOS, followed by concomitant reduction of ROS and NO production at a concentration of 2.5 μ M, which is lower than the concentration of free berberine concentration required to achieve similar effects as reported elsewhere. Furthermore, we provide evidence for the suitability for BP-LCNs both as an antioxidant and as an anti-inflammatory agent with potential application in the therapy of chronic inflammatory diseases.

Keywords: berberine; liquid crystalline nanoparticles; inflammation; oxidative stress; macrophages; LPS; advanced drug delivery; chronic inflammatory diseases

1. Introduction

Inflammation is a complex physiological reaction occurring in various tissues in response to a plethora of endogenous and exogenous stimuli, that may include pathogens such as viruses and bacteria, as well as exposure to toxic chemicals, allergens, and radiations [1]. Physiologically, the primary aim of inflammation is to eliminate the initial damaging stimulus. However, prolonged and dysregulated inflammation eventually leads to chronic inflammatory diseases such as diabetes, cardiovascular diseases, arthritis, joint diseases, allergies, and chronic respiratory diseases. Among these asthma, chronic obstructive pulmonary disease (COPD), and lung cancer are of utmost significance [2–5]. Therefore, chronic inflammation constitutes to be the main etiological factor for a wide range of diseases. Inflammation is mediated by different classes of inflammatory cells. Among these, macrophages and neutrophils take part in the initiation of the inflammatory cascade, and hence play significant roles in the pathogenesis of the aforementioned pathophysiological features through the secretion of various inflammatory mediators that may include the inflammatory cytokines tumor necrosis factor- α (TNF- α), Interleukin 6 (IL-6), and IL-1 β [6,7]. It is well known that lipopolysaccharides (LPS), a bacterial toxin generally found in the cell membrane of Gram-negative bacteria cause exacerbated inflammatory cascade primarily in cells including macrophages [8,9].

Oxidative stress is a pathogenic mechanism that results when the balance between the generation of oxidative agents, namely reactive oxygen species (ROS), reactive nitrogen intermediates (RNI), and their elimination through biological antioxidants, other defense mechanisms has been compromised [10–12]. ROS and RNI are physiologically produced by cells and, at low concentrations, function as important mediators and signaling molecules involved in the maintenance of cell homeostasis, and oxidative stress. Accumulation of these species leads to the damage of cellular components such as DNA, lipids, and proteins [1]. For this reason, oxidative stress is a potent inducer of inflammation, and it is known to exacerbate inflammatory processes, leading to the aggravation of chronic inflammatory diseases [1,10,13]. Moreover, proinflammatory triggers such as LPS are known to induce the generation of high levels of ROS and nitric oxide (NO) in macrophages and in other inflammatory cells [14,15]. NO is one of the principal RNI which is generated by macrophages, and other inflammatory cells, upon activation of the inducible NO synthase (iNOS). iNOS is a key enzyme that is mediated by macrophages in the inflammatory cascade [16]. ROS are highly unstable chemical species that are known to attack NO and convert it into peroxynitrite, a toxic intermediate that causes apoptosis in many cell types, further exacerbating the severity of inflammation [14].

Considering the extent of the cross-talk between inflammation and oxidative stress, these two processes are tightly interrelated and, together, play pivotal roles in the pathogenesis of chronic diseases [17]. The strictly interdependent relationship between oxidative stress and inflammation has been recently proposed as a possible explanation for the “antioxidant paradox”, which is referred to the observation that dietary administration of large doses of antioxidants is often ineffective in the prevention or treatment of diseases where the disease pathogenesis is heavily influenced by oxidative stress [17,18]. To address this concern, the use of compounds endowed with both antioxidant and anti-inflammatory properties could be beneficial.

A valuable source for potential therapeutic agents, in this context, is represented by natural sources such as traditional medicinal plants, which have provided several promising novel phytochemical compounds such as rutin [19], boswellic acids [20], curcumin [21], and nobiletin to name a few [22]. Berberine, an isoquinoline alkaloid molecule extracted from the root, stem bark, and rhizomes of plants belonging to the genus *Berberis*, is widely known for its antioxidant, anti-inflammatory, and anticancer properties [23–30]. It has also been shown to improve the lipid and glucose profile when administered in association with silymarin, thus promoting cardiometabolic health [31].

Despite the encouraging beneficial activities of berberine against many illnesses, its therapeutic application, similar to that of many other promising phytochemicals, is severely

limited by issues such as poor oral bioavailability and limited intestinal absorption, which hamper in vivo efficacy and clinical translation [32–34]. A valuable approach to overcome these limitations is to employ advanced drug delivery methods, such as encapsulation of therapeutic molecules in advanced nanoparticle (NP)-based systems [35]. Among the many currently available advanced nanoformulations, liquid crystalline nanoparticle (LCNs) based delivery represents a highly versatile tool with the substantial capability of enhancing the bioavailability and stability of therapeutic moieties [36]. In this context, our research group has recently demonstrated significant in vitro anticancer action of berberine-loaded LCN formulation against non-small-cell lung cancer (NSCLC) cells [37,38]. Furthermore, we showed that a berberine-phytantriol LCN formulation possessed strong in vitro cytotoxic and anti-migratory activity against NSCLC [39]. In another study, we showed that berberine-loaded LCNs were highly effective in attenuating oxidative stress, senescence, and inflammation triggered by cigarette smoke in an in vitro model of COPD obtained by exposing mouse macrophage cells (RAW264.7) and human broncho-epithelial cells (16HBE) to cigarette smoke extract [40].

In the current study, we explored the protective activity of the berberine-phytantriol LCN formulation (BP-LCN) against LPS-induced inflammation and oxidative stress on mouse RAW264.7 macrophages. We demonstrate that BP-LCNs significantly reduce LPS-induced ROS production, along with the upregulation of the pro-inflammatory cytokines TNF- α , IL-6, and IL-1 β . Furthermore, BP-LCNs were found to reduce LPS-induced iNOS expression, with a concomitant reduction of NO production. The results of our study confirm the dual antioxidant/anti-inflammatory activity of berberine, providing valuable proof of the applicability of berberine-loaded LCNs as a therapeutic agent in chronic inflammatory conditions.

2. Materials and Methods

2.1. Cell Culture and Formulation Aspects of BP-LCNs

A Dulbecco's modified Eagle's medium (DMEM) (Lonza, Basel, Switzerland) was employed to culture the procured RAW 264.7 mouse macrophages (ATCC, Manassas, VA, USA). The entire process was performed in a humidified incubator. The incubator was monitored at a temperature of 37 °C with 5% CO₂. Furthermore, the medium also contained 5% (v/v) foetal bovine serum (FBS) (Lonza, Basel, Switzerland) along with 1% (v/v) penicillin-streptomycin (Lonza, Basel, Switzerland). The experiments were carried out in the DMEM both in the presence and absence of berberine-phytantriol LCNs maintained at a temperature of 37 °C with 5% CO₂. BP-LCN formulations were prepared as described previously [39].

2.2. Cell Viability Determination

The determination of cell viability was conducted in RAW 264.7 cells using MTT reagent (3-(4,5-Dimethylthiazol-2-yl)-2,5-diphenyltetrazolium bromide, Sigma-Aldrich, St. Louis, MO, USA) as described previously [41]. Briefly, seeding of the RAW 264.7 cells was carried out at a density of 20,000 cells/well in a clear-bottomed, transparent 96-welled plate. This mixture was incubated at 37 °C for a duration of 24 h. Subsequently, these cells were incubated for 1 h in the presence of lipopolysaccharide (LPS) obtained from *Escherichia coli* (with a final concentration of 1 μ g/mL, Merck, Kenilworth, NJ, USA). An additional 24 h incubation was allowed for the cells both with and without the BP-LCNs. Finally, the working concentrations employed were 0.5, 1.0, 2.5, 5.0, or 10.0 μ M. Subsequently, to the wells, 250 μ g/mL MTT reagent was incorporated. The mixture was then incubated further for 4 h, after which the supernatant was removed with caution. Dimethyl sulfoxide (DMSO) (Merck, Kenilworth, NJ, USA) was employed to solubilize the developed formazan crystals. This was followed by measuring the absorbance levels of the mixture. The wavelength employed was 540 nm. The entire operation was performed with a POLARstar Omega microplate reader (BMG Labtech, Ortenberg, Germany).

2.3. Determination of ROS Generation

Generation of cellular ROS was determined with 2',7'-dihydrodichlorofluorescein diacetate (DCF-DA, Merck, Kenilworth, NJ, USA) using a fluorescence plate reader and fluorescence microscopy, as described previously [40].

2.3.1. ROS Determination by Fluorescence Plate Reader

A black 96-welled plate (Greiner Bio-One GmbH, Frickenhausen, Germany) was employed to seed the RAW264.7 cells. The cells were seeded for a 24 h duration. Subsequently, these cells were subjected to preincubation for 1 h with LPS (final concentration 1 µg/mL). The mixture was then incubated with or without BP-LCNs for a period of 24 h with an eventual concentration of 1.0 or 2.5 µM respectively. This was followed by a 30-min incubation at room temperature under a dark condition in the presence of DCF-DA (final concentration 10 µM). The fluorescence intensity was determined at an excitation wavelength of 488 nm. The emission wavelength employed was 525 nm. The entire operation was performed with a FLUOstar Omega (BMG LABTECH Pty Ltd., Victoria, Australia).

2.3.2. ROS Determination by Fluorescence Microscopy

RAW264.7 cells were grown on a coverslip of a 6-welled plate (Greiner Bio-One GmbH). Post overnight incubation, the cells were preincubated with 1 µg/mL LPS for 1 h. This was followed by the incubation for 24 h with or without BP-LCNs (1.0 or 2.5 µM respectively). This was followed by washing of the cells with phosphate-buffered saline (PBS, 2X washes). The mixture was subsequently subjected to incubation with 10 µM of DCF-DA in dark at room temperature for a duration of 30 min. Then PBS was used to wash the cells (2X) and the fluorescence images were captured at 20× magnification using a fluorescence microscope (Zeiss Axio Imager Z2, Oberkochen, Germany).

2.4. Determination of NO Production with Griess Reagent

The levels of NO secretion by RAW264.7 was determined using a modified Griess reagent (Merck). A transparent, clear-bottom 96-well plate was employed for seeding the RAW264.7 cells. A total of 24 h after incubation, the cells were subjected to pre-incubation for 1 h with 1 µg/mL LPS, which was then incubated for 24 h with or without the BP-LCNs (1.0 or 2.5 µM respectively). The culture supernatants were then collected, and 150 µL of the supernatant was added onto a clear bottom, transparent 96-well plate and treated with Griess reagent (1:1 (v/v) ratio). The samples were then subjected to incubation for 30 min duration at room temperature in dark conditions. The relative levels of NO in the form of nitrite were recorded by measuring the absorbance at 540 nm (excitation wavelength) using a TECAN Infinite M1000 plate reader (Tecan Trading AG, Männedorf, Switzerland). The absorbance of the blank (unconditioned cell culture media) was subtracted from the absorbance of each sample and variations of NO levels were reported as percentages compared to the control (untreated) group.

2.5. Real-Time Quantitative Polymerase Chain Reaction (PCR)

The experiment was performed with 6-well plates which were used to grow the RAW264.7 cells. After reaching 80% confluency, preincubation was carried out with LPS (1 µg/mL) for a duration of 1 h. The mixture was then incubated for 24 h both with and without BP-LCNs (2.5 µM). Subsequently, PBS was used to wash the cells (2X), and were lysed using the TRI reagent (Merck). The next step involved the total isolation of RNA [39]. The purity and the concentration of RNA were measured by Nanodrop One (Thermo Fisher Scientific, North Ryde, NSW, Australia).

A quantitative reverse transcription PCR technique was employed to measure the mRNA levels [38]. Briefly, the mixture was subjected to DNase treatment with a DNase I kit (Merck), 1 µg of RNA was used to synthesize cDNA by reverse transcription using a Mastercycler Nexus GSX1 thermal cycler (Eppendorf, Hamburg, Germany) via subsequent steps of denaturation (65 °C, 15 min) and annealing (25 °C, 10 min). After this, reverse transcrip-

tion at 37 °C for 50 min was performed followed by the inactivation of enzymes at 70 °C, for 15 min were performed. The reaction mix contained random primers (500 ng/μL), dNTPs (10 mM), MMLV reaction buffer (1×), and DTT (100 mM). Real-time qPCR was conducted on 25 ng cDNA with a CFX96 real-time PCR detection system (Bio-Rad, Hercules, CA, USA) using iTaq Universal SYBR Green supermix (1×, Bio-Rad, Hercules, CA, USA) and 0.5 μM of each of the forward and reverse primers for TNF-α (Forward: TCTGTC-TACTGAACTTCGGGGTGA; Reverse: TTGTCTTTGAGATCCATGCCGTT), IL-1β (Forward: TGGGATCCTCTCCAGCCAAGC; Reverse: AGCCCTTCATCTTTTGGGGTCCG), IL-6 (Forward: AGAAAACAATCTGAACTTCCAGAGAT; Reverse: GAAGACCAGAG-GAAATTTTCAATAGG), iNOS (Forward: AGCGAGGAGCAGGTGGAAGACT; Reverse: CCATAGGAAAAGACTGCACCGAA), and HPRT (Forward: AGCCAGACTTTTGTG-GATTGAA; Reverse: CAACTTGCGCTCATCTTAGGCTTT).

2.6. Statistical Analysis

All data were presented as Mean ± SEM. To check for normal distribution of data, the data points for each group were plotted on a histogram and visually inspected. Upon visual confirmation of normal distribution, data were analyzed by 1-way ANOVA, followed by Dunnett multiple comparisons test, using GraphPad Prism (v.9.4, GraphPad Software, San Diego, CA, USA). The pairwise comparisons of a 2-tailed *p*-value < 0.05 were considered statistically significant.

3. Results

3.1. Determination of Optimum Dose of BP-LCNs for Treatment in LPS-Induced RAW 264.7 Cells

The MTT assay results showed that BP-LCNs did not induce cell toxicity on LPS-induced RAW 264.7 cells up to a concentration of 2.5 μM (Figure 1). However, the cell viability of RAW 264.7 cells decreased significantly when they were incubated in the presence of BP-LCNs at 5 and 10 μM (Figure 1, *p* < 0.0001 for both against the control). Hence, the non-toxic doses of 1.0 and/or 2.5 μM BP-LCNs were used in the subsequent experiments.

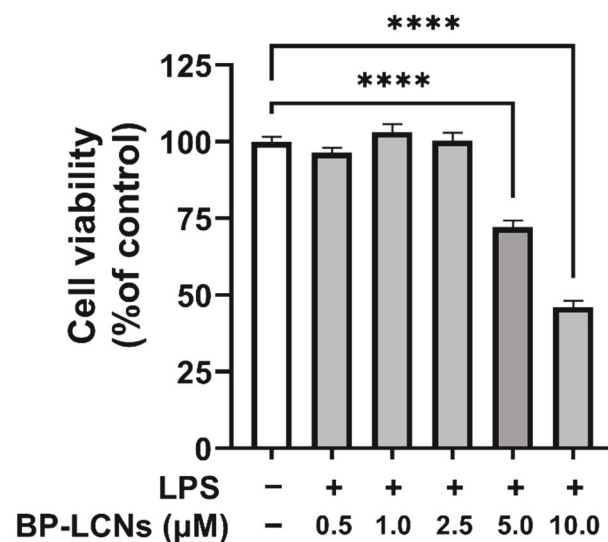


Figure 1. Effect of BP-LCNs on the cell viability of LPS-induced RAW 264.7 cells. RAW 264.7 cells were pre-incubated for 1 h in the presence of LPS (final concentration 1 μg/mL), then incubated for 24 h in the absence or presence of BP-LCNs (final concentration 0.5, 1.0, 2.5, 5.0 or 10.0 μM). MTT reagent was added to each well, the cells were incubated for a further 4 h and the formazan crystals were dissolved in DMSO. The cell viability was determined by measuring absorbance at 540 nm with a microplate reader and the cell viability was normalized as a percentage of control cells. The results are Mean ± SEM of three independent experiments (**** *p* < 0.0001).

3.2. BP-LCNs Inhibit ROS Generation in a Dose-Dependent Manner

The anti-oxidative potential of BP-LCNs was assessed by measuring ROS levels in LPS-induced RAW 264.7 cells. The LPS induction increased oxidative stress by 38% increase in ROS production (Figure 2A, $p < 0.0001$ against control). The ROS levels were not affected by BP-LCNs at a concentration of 1 μM (Figure 2A). However, the inclusion of BP-LCNs at a concentration of 2.5 μM decreased ROS production by 10% (Figure 2A, $p < 0.0001$ against cells treated with LPS alone). The increase in ROS production by LPS induction was apparent due to the increased fluorescence of DCF-DA in LPS-induced RAW 264.7 cells (Figure 2B). As observed in the fluorescence images, the inclusion of BP-LCNs in the incubation inhibited LPS-induced NO production at both 1.0 and 2.5 μM concentrations (Figure 2B).

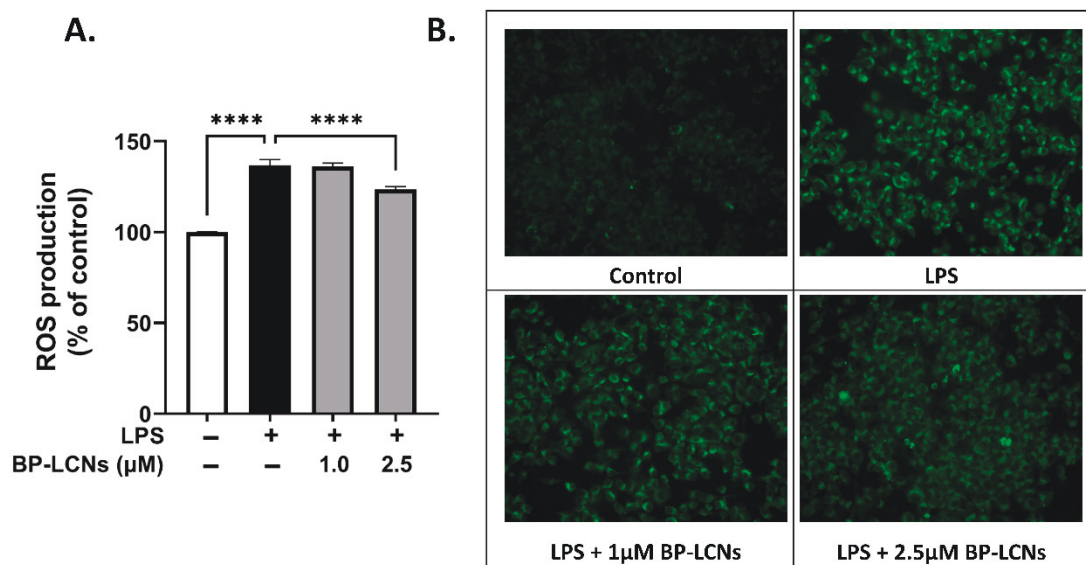


Figure 2. Effect of BP-LCNs on LPS-induced ROS production in RAW 264.7 cells. RAW 264.7 cells were pre-incubated for 1 h in the presence of LPS (final concentration 1 $\mu\text{g}/\text{mL}$), then incubated for 24 h in the absence or presence of BP-LCNs (final concentration 1.0 or 2.5 μM). The ROS generation was determined semi-quantitatively and qualitatively by measuring the fluorescence intensity of DCF-DA using a fluorescence plate reader (A) and fluorescence microscopy (B). The values in (A) represent the Mean \pm SEM of three independent experiments (**** $p < 0.0001$).

3.3. BP-LCNs Inhibit NO Generation

The potential of BP-LCNs to inhibit NO production was assessed by measuring NO levels in the culture supernatant and mRNA levels of iNOS in LPS-induced RAW 264.7 cells. LPS induction increased NO production 3.3-fold (Figure 3A, $p < 0.0001$ against control). The inclusion of BP-LCNs at concentrations of 1 μM and 2.5 μM significantly decreased NO production by 32% (Figure 3A, $p < 0.001$ against control) and 46% (Figure 3A, $p < 0.0001$ against control), respectively.

The underlying mechanism may be explained by BP-LCNs-mediated regulation of iNOS gene expression in LPS-induced RAW 264.7 cells. The mRNA levels of LPS-treated RAW 264.7 cells increased by 23-fold compared to the control (Figure 3B, $p < 0.0001$). However, the inclusion of BP-LCNs in the incubation decreased the iNOS mRNA levels by 0.92-fold compared to LPS alone-treated RAW 264.7 cells (Figure 3B, $p < 0.0001$). The iNOS mRNA levels in BP-LCNs-treated RAW 264.7 cells were comparable to the values of the control cells (Figure 3B).

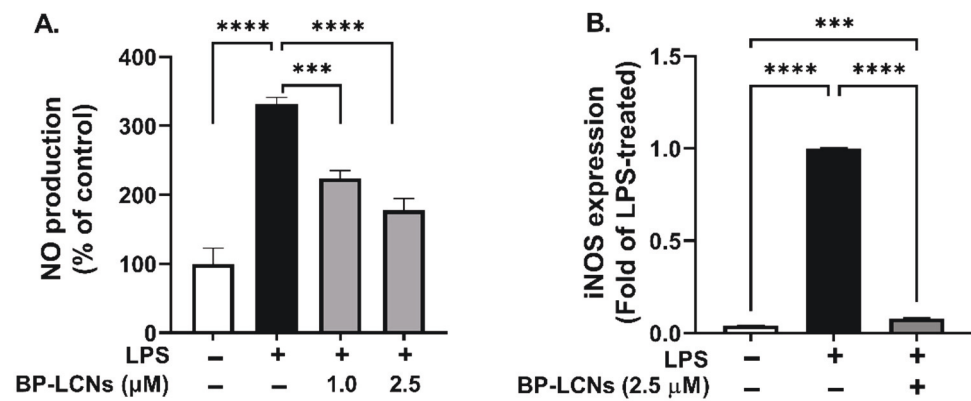


Figure 3. Effect of BP-LCNs on LPS-induced NO production and iNOS mRNA expression in RAW 264.7 cells. RAW 264.7 cells were pre-incubated for 1 h in the presence of LPS (final concentration 1 $\mu\text{g}/\text{mL}$), then incubated for 24 h in the absence or presence of BP-LCNs (final concentration 1.0 or 2.5 μM). The NO production in the culture supernatant was determined by using Griess reagent and measuring the absorbance with a fluorescence plate reader (A). The mRNA levels of iNOS (B) were determined by RT-qPCR as described in Materials and Methods Section 2.5. The values in (A,B) are Mean \pm SEM of three independent experiments (** $p < 0.001$; **** $p < 0.0001$).

3.4. BP-LCNs Inhibit mRNA Levels of the Pro-Inflammatory Cytokines TNF- α , IL-6, and IL-1 β

The anti-inflammatory potential of BP-LCNs was assessed on LPS-induced RAW 264.7 cells by measuring the mRNA levels of pro-inflammatory cytokines TNF- α , IL-6, and IL-1 β . The LPS induction in RAW 264.7 cells significantly increased the mRNA levels of these cytokines compared to the control (Figure 4, $p < 0.0001$). The inclusion of BP-LCNs in the incubation significantly decreased the mRNA levels of these cytokines compared to the control (Figure 4A–C, $p < 0.0001$ against LPS-only treated cells). Thus, the LPS-induced increase in the mRNA level of these cytokines was significantly inhibited in the presence of BP-LCNs, suggesting a strong anti-inflammatory potential of BP-LCNs. The LPS-induced mRNA levels of TNF- α were decreased by BP-LCNs to levels comparable to the control cells (Figure 4A).

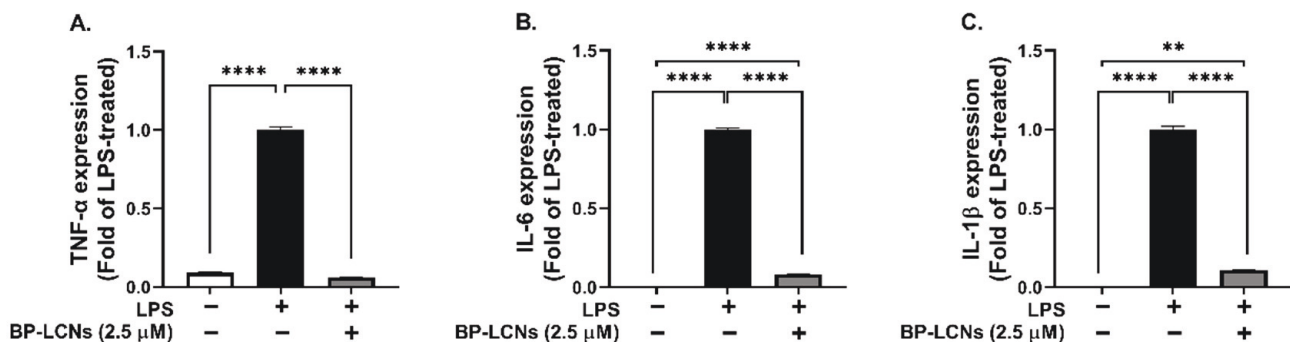


Figure 4. Effect of BP-LCNs on mRNA expression of LPS-induced pro-inflammatory cytokines TNF- α (A), IL-6 (B), and IL-1 β (C) in RAW 264.7 cells. RAW 264.7 cells were pre-incubated for 1 h in the presence of LPS (final concentration 1 $\mu\text{g}/\text{mL}$), then incubated for 24 h in the absence or presence of BP-LCNs (final concentration 2.5 μM). Total RNA was extracted using TRI reagent, cDNA synthesized by reverse transcription, and mRNA levels for TNF- α , IL-6, and IL-1 β were determined by quantitative PCR with SYBR green. The values shown are Mean \pm SEM of three independent experiments (** $p < 0.01$; **** $p < 0.0001$).

4. Discussion

Inflammation and oxidative stress are two intimately interrelated processes that represent fundamental aetiological factors for many chronic inflammatory diseases. One of the many pathways that initiate inflammatory responses involves the stimulation of macrophages with the bacterial molecule LPS, which initiates a signaling cascade mediated by the toll-like receptor 4 (TLR4). This activates downstream signaling pathways resulting, among many outcomes, in increased secretion of pro-inflammatory cytokines, increased ROS production, as well as increased iNOS expression that, in turn, generates higher levels of NO [14].

Here, we demonstrated significant anti-inflammatory and antioxidant activity of BP-LCNs in LPS-induced RAW264.7 mouse macrophages, which was mediated by inhibition of the transcription of the pro-inflammatory cytokines TNF- α , IL-6, and IL-1 β , as well as through reduction of ROS production, inhibition of iNOS expression and subsequent reduction of LPS-induced NO production.

Despite the many demonstrated clinical benefits, berberine is characterized by very low water solubility [42]. This, together with the fact that it is poorly absorbed by the gastrointestinal tract, results in its characteristic poor bioavailability (0.68% in rats) [43], which severely hampers its therapeutic use. Poor solubility and relatively low bioavailability are common characteristics across a wide range of medicinally active phytochemicals [44]. Due to these limitations, high doses of berberine should be administered to achieve the relevant pharmacological activity, but this might not be feasible due to the possibility of toxic effects, which are more evident when using pure berberine compared to plant extracts or plant fractions containing it [45]. For this reason, the use of nanotechnology-based innovative drug delivery technologies involving the encapsulation of berberine in LCNs is a viable strategy to improve its physicochemical properties, enhancing its therapeutic efficacy and potency.

In this study, BP-LCNs demonstrated anti-inflammatory and antioxidant activity when used at an equivalent berberine concentration of 2.5 μ M. The low effective berberine concentration needed to exert this effect is concordant with our previous study, in which we demonstrated that berberine encapsulated in LCNs has significant dose-dependent antioxidant activity at concentrations ranging between 1 and 5 μ M, and anti-inflammatory and anti-senescence activity at 5 μ M, on both RAW264.7 and 16HBE human bronchoepithelial cells exposed to cigarette smoke extract [40]. In comparison, a similar anti-inflammatory effect was reported when using concentrations of free berberine powder between 10 and 100 μ M [25,30,46]. This represents a clear demonstration of the advantages of formulating poorly soluble molecular moieties in advanced drug delivery systems such as LCNs to overcome common limitations affecting many phytochemicals. Taken together with our previous results [40], the findings reported in the present study demonstrate how berberine-encapsulated LCNs are capable of counteracting inflammation and oxidative stress induced by different stimuli, namely cigarette smoke, and LPS. This inspires further research to provide a mechanistic explanation of the molecular pathways impacted by berberine that lead to its therapeutic activity. In particular, it would be interesting to investigate whether these activities are exerted by impacting signaling pathways such as NF- κ B, MAPKinase, and the NLRP3 inflammasome pathway. These investigations will represent the core of our future studies on the characterization of the therapeutic activity of BP-LCNs.

Although we observed promising antioxidant and anti-inflammatory activity of BP-LCNs, a limitation of our study lies in the fact that we only investigated the expression of TNF- α , IL-6, and IL-1 β mRNA to assess the anti-inflammatory activity of BP-LCNs. Although the inhibitory effect of berberine on these fundamental cytokines is in agreement with studies from our laboratory and other research groups [40,47,48], it would be useful to extend these findings to better understand the effect of our BP-LCNs on other cytokines and pro- and anti-inflammatory mediators. Another limitation lies in the fact that the experiments were entirely performed *in vitro*. To complement our findings, it would be

interesting to investigate the activity of BP-LCNs in preclinical animal models of diseases for which inflammation and oxidative stress represent an important aetiological factor such as cancer, cardiovascular diseases, arthritis, chronic respiratory diseases, and others. Considering the versatility of LCNs as drug delivery systems for inflammatory lung diseases, which allow direct lung delivery of therapeutic moieties via inhalation [36], it would be particularly interesting to test the *in vivo* activity of our BP-LCNs on animal models of chronic respiratory diseases such as asthma [49,50] and COPD [51].

Despite this limitation, this study suggests that encapsulation of berberine in LCNs has potent dual antioxidant and anti-inflammatory activity at relatively low berberine concentrations, resulting in improved physicochemical characteristics and potentially reduced toxic effects.

5. Conclusions

Our study demonstrates the advantages of the LCN-based formulation of berberine, which exerted potent *in vitro* anti-inflammatory and antioxidant activity in LPS-induced RAW246.7 macrophages at lower concentrations compared to free berberine. These effects were mediated by inhibition of TNF- α , IL-6, IL-1 β , and iNOS gene expression and simultaneous reduction of ROS and NO production. In conclusion, these results provide proof of the validity of BP-LCNs as a new candidate for further development as a therapeutic strategy for chronic inflammatory diseases. However, to allow translation into clinical practice, these findings need to be validated by preclinical and clinical studies.

Author Contributions: A.M.A., A.G.A., M.A. and K.D. developed the research hypotheses and visualization process for this project. G.D.R., B.M. and K.R.P. designed the experiments, and also performed data acquisition, and statistical analyses. D.K.C., G.D.R., K.R.P. and T.M. were directly involved in development of BP-LCN formulations. P.M.H. reviewed/edited the manuscript. All authors have read and agreed to the published version of the manuscript.

Funding: The authors would like to gratefully acknowledge the Qassim University represented by the Deanship of Scientific Research for the financial support towards this research (ID Number: 10169-camsl-2020-1-3-I) during the academic year 1441 AH/2020 AD.

Institutional Review Board Statement: Not Applicable.

Informed Consent Statement: Not Applicable.

Data Availability Statement: Data may be made available on request from the corresponding author.

Acknowledgments: The authors would like to gratefully acknowledge the Qassim University represented by the Deanship of Scientific Research for the financial support towards this research (ID Number: 10169-camsl-2020-1-3-I) during the academic year 1441 AH/2020 AD. The authors would also like to acknowledge Kris Rogers (Graduate School of Health, UTS) for his consultation to the statistical analysis.

Conflicts of Interest: The authors declare no conflict of interest.

Abbreviations

BP-LCNs: Berberine-Phytantriol Liquid Crystalline Nanoparticles; COPD: Chronic Obstructive Pulmonary Disease; DCF-DA: 2',7'-dihydrodichlorofluorescein diacetate; DMEM: Dulbecco's modified Eagle's medium; DMSO: dimethyl sulfoxide; IL: Interleukin; iNOS: Inducible Nitric Oxide Synthase; LCN: Liquid Crystalline Nanoparticles; LPS: Lipopolysaccharide; NO: Nitric Oxide; NSCLC: non-small-cell lung cancer; RNI: reactive nitrogen intermediates; ROS: Reactive Oxygen Species; TNF- α : Tumour Necrosis Factor- α ; TLR4: Toll-Like Receptor 4.

References

1. Hussain, T.; Tan, B.; Yin, Y.; Blachier, F.; Tossou, M.C.; Rahu, N. Oxidative Stress and Inflammation: What Polyphenols Can Do for Us? *Oxid. Med. Cell Longev.* **2016**, *2016*, 7432797. [[CrossRef](#)]
2. Pahwa, R.; Goyal, A.; Jialal, I. Chronic Inflammation. In *StatPearls*; StatPearls Publishing Copyright © 2022; StatPearls Publishing LLC: Treasure Island, FL, USA, 2022.
3. Paudel, K.R.; Kim, D.-W. Microparticles-Mediated Vascular Inflammation and its Amelioration by Antioxidant Activity of Baicalin. *Antioxidants* **2020**, *9*, 890. [[CrossRef](#)]
4. Kim, T.-M.; Paudel, K.R.; Kim, D.-W. Eriobotrya japonica leaf extract attenuates airway inflammation in ovalbumin-induced mice model of asthma. *J. Ethnopharmacol.* **2019**, *253*, 112082. [[CrossRef](#)]
5. Wadhwa, R.; Paudel, K.R.; Shukla, S.; Shastri, M.; Gupta, G.; Devkota, H.P.; Chellappan, D.K.; Hansbro, P.M.; Dua, K. Epigenetic Therapy as a Potential Approach for Targeting Oxidative Stress-Induced Non-Small-Cell Lung Cancer. In *Handbook of Oxidative Stress in Cancer: Mechanistic Aspects*; Springer: Singapore, 2020; pp. 1–16.
6. Zhang, J.M.; An, J. Cytokines, inflammation, and pain. *Int. Anesthesiol. Clin.* **2007**, *45*, 27–37. [[CrossRef](#)]
7. Chellappan, D.K.; Yee, L.W.; Xuan, K.Y.; Kunalan, K.; Rou, L.C.; Jean, L.S.; Ying, L.Y.; Wie, L.X.; Chellian, J.; Mehta, M.; et al. Targeting neutrophils using novel drug delivery systems in chronic respiratory diseases. *Drug Dev. Res.* **2020**, *81*, 419–436. [[CrossRef](#)]
8. Takeuchi, O.; Akira, S. Pattern recognition receptors and inflammation. *Cell* **2010**, *140*, 805–820. [[CrossRef](#)]
9. Paudel, K.R.; Karki, R.; Kim, D.W. Cepharanthine inhibits in vitro VSMC proliferation and migration and vascular inflammatory responses mediated by RAW264.7. *Toxicol. In Vitro* **2016**, *34*, 16–25. [[CrossRef](#)]
10. Dua, K.; Malya, V.; Singhvi, G.; Wadhwa, R.; Krishna, R.V.; Shukla, S.D.; Shastri, M.D.; Chellappan, D.K.; Maurya, P.K.; Satija, S.; et al. Increasing complexity and interactions of oxidative stress in chronic respiratory diseases: An emerging need for novel drug delivery systems. *Chemico-Biol. Interact.* **2019**, *299*, 168–178. [[CrossRef](#)]
11. Nucera, F.; Mumby, S.; Paudel, K.R.; Dharwal, V.; Di Stefano, A.; Casolaro, V.; Hansbro, P.M.; Adcock, I.M.; Caramori, G. Role of oxidative stress in the pathogenesis of COPD. *Minerva Med.* **2022**, *113*, 370–404. [[CrossRef](#)]
12. Panth, N.; Paudel, K.R.; Parajuli, K. Reactive Oxygen Species: A Key Hallmark of Cardiovascular Disease. *Adv. Med.* **2016**, *2016*, 9152732. [[CrossRef](#)]
13. Mehta, M.; Paudel, K.R.; Shukla, S.D.; Shastri, M.D.; Satija, S.; Singh, S.K.; Gulati, M.; Dureja, H.; Zacconi, F.C.; Hansbro, P.M.; et al. Rutin-loaded liquid crystalline nanoparticles attenuate oxidative stress in bronchial epithelial cells: A PCR validation. *Future Med. Chem.* **2021**, *13*, 543–549. [[CrossRef](#)]
14. Paudel, K.R.; Wadhwa, R.; Mehta, M.; Chellappan, D.K.; Hansbro, P.M.; Dua, K. Rutin loaded liquid crystalline nanoparticles inhibit lipopolysaccharide induced oxidative stress and apoptosis in bronchial epithelial cells in vitro. *Toxicol. In Vitro* **2020**, *68*, 104961. [[CrossRef](#)]
15. Lee, H.H.; Paudel, K.R.; Kim, D.W. Terminalia chebula Fructus Inhibits Migration and Proliferation of Vascular Smooth Muscle Cells and Production of Inflammatory Mediators in RAW 264.7. *Evid. Based Complement. Alternat. Med.* **2015**, *2015*, 502182.
16. McNeill, E.; Crabtree, M.J.; Sahgal, N.; Patel, J.; Chuaiphichai, S.; Iqbal, A.J.; Hale, A.B.; Greaves, D.R.; Channon, K.M. Regulation of iNOS function and cellular redox state by macrophage Gch1 reveals specific requirements for tetrahydrobiopterin in NRF2 activation. *Free Radic. Biol. Med.* **2015**, *79*, 206–216. [[CrossRef](#)]
17. Biswas, S.K. Does the Interdependence between Oxidative Stress and Inflammation Explain the Antioxidant Paradox? *Oxid. Med. Cell Longev.* **2016**, *2016*, 5698931. [[CrossRef](#)]
18. Halliwell, B. The antioxidant paradox: Less paradoxical now? *Br. J. Clin. Pharmacol.* **2013**, *75*, 637–644. [[CrossRef](#)]
19. Paudel, K.R.; Wadhwa, R.; Tew, X.N.; Lau, N.J.X.; Madheswaran, T.; Panneerselvam, J.; Zeeshan, F.; Kumar, P.; Gupta, G.; Anand, K.; et al. Rutin loaded liquid crystalline nanoparticles inhibit non-small cell lung cancer proliferation and migration in vitro. *Life Sci.* **2021**, *276*, 119436. [[CrossRef](#)]
20. Solanki, N.; Mehta, M.; Chellappan, D.K.; Gupta, G.; Hansbro, N.G.; Tambuwala, M.M.; Aljabali, A.A.; Paudel, K.R.; Liu, G.; Satija, S.; et al. Antiproliferative effects of boswellic acid-loaded chitosan nanoparticles on human lung cancer cell line A549. *Future Med. Chem.* **2020**, *12*, 2019–2034. [[CrossRef](#)]
21. Hardwick, J.; Taylor, J.; Mehta, M.; Satija, S.; Paudel, K.R.; Hansbro, P.M.; Chellappan, D.K.; Bebawy, M.; Dua, K. Targeting Cancer using Curcumin Encapsulated Vesicular Drug Delivery Systems. *Curr. Pharm. Des.* **2021**, *27*, 2–14. [[CrossRef](#)]
22. Kim, E.; Kim, Y.J.; Ji, Z.; Kang, J.M.; Wirianto, M.; Paudel, K.R.; Smith, J.A.; Ono, K.; Kim, J.A.; Eckel-Mahan, K.; et al. ROR activation by Nobiletin enhances antitumor efficacy via suppression of IkappaB/NF-kappaB signaling in triple-negative breast cancer. *Cell Death Dis.* **2022**, *13*, 374. [[CrossRef](#)]
23. Kuo, C.L.; Chi, C.W.; Liu, T.Y. The anti-inflammatory potential of berberine in vitro and in vivo. *Cancer Lett.* **2004**, *203*, 127–137. [[CrossRef](#)]
24. Li, Z.; Geng, Y.-N.; Jiang, J.-D.; Kong, W.-J. Antioxidant and anti-inflammatory activities of berberine in the treatment of diabetes mellitus. *Evid. Based Complement. Alternat. Med.* **2014**, *2014*, 289264. [[CrossRef](#)]
25. Mo, C.; Wang, L.; Zhang, J.; Numazawa, S.; Tang, H.; Tang, X.; Han, X.; Li, J.; Yang, M.; Wang, Z.; et al. The crosstalk between Nrf2 and AMPK signal pathways is important for the anti-inflammatory effect of berberine in LPS-stimulated macrophages and endotoxin-shocked mice. *Antioxid. Redox Signal.* **2014**, *20*, 574–588. [[CrossRef](#)]

26. El-Wahab, A.E.A.; Ghareeb, D.A.; Sarhan, E.E.; Abu-Serie, M.M.; El Demellawy, M.A. In vitro biological assessment of *Berberis vulgaris* and its active constituent, berberine: Antioxidants, anti-acetylcholinesterase, anti-diabetic and anticancer effects. *BMC Complement. Altern. Med.* **2013**, *13*, 218. [[CrossRef](#)]
27. Ni, L.; Li, Z.; Ren, H.; Kong, L.; Chen, X.; Xiong, M.; Zhang, X.; Ning, B.; Li, J. Berberine inhibits non-small cell lung cancer cell growth through repressing DNA repair and replication rather than through apoptosis. *Clin. Exp. Pharmacol. Physiol.* **2022**, *49*, 134–144. [[CrossRef](#)]
28. Tew, X.N.; Lau, N.J.X.; Chellappan, D.K.; Madheswaran, T.; Zeeshan, F.; Tambuwala, M.M.; Aljabali, A.A.; Balusamy, S.R.; Perumalsamy, H.; Gupta, G.; et al. Immunological axis of berberine in managing inflammation underlying chronic respiratory inflammatory diseases. *Chem. Biol. Interact.* **2020**, *317*, 108947. [[CrossRef](#)]
29. Ma, J.; Chan, C.-C.; Huang, W.-C.; Kuo, M.-L. Berberine Inhibits Pro-inflammatory Cytokine-induced IL-6 and CCL11 Production via Modulation of STAT6 Pathway in Human Bronchial Epithelial Cells. *Int. J. Med. Sci.* **2020**, *17*, 1464–1473. [[CrossRef](#)]
30. Gong, M.; Duan, H.; Wu, F.; Ren, Y.; Gong, J.; Xu, L.; Lu, F.; Wang, D. Berberine Alleviates Insulin Resistance and Inflammation via Inhibiting the LTB4-BLT1 Axis. *Front. Pharmacol.* **2021**, *12*, 722360. [[CrossRef](#)]
31. Fogacci, F.; Grassi, D.; Rizzo, M.; Cicero, A. Metabolic effect of berberine-silymarin association: A meta-analysis of randomized, double-blind, placebo-controlled clinical trials. *Phytother. Res.* **2019**, *33*, 862–870. [[CrossRef](#)]
32. Battu, S.K.; Repka, M.A.; Maddineni, S.; Chittiboyina, A.; Avery, M.; Majumdar, S. Physicochemical characterization of berberine chloride: A perspective in the development of a solution dosage form for oral delivery. *AAPS PharmSciTech* **2010**, *11*, 1466–1475. [[CrossRef](#)]
33. Liu, C.-S.; Zheng, Y.-R.; Zhang, Y.-F.; Long, X.-Y. Research progress on berberine with a special focus on its oral bioavailability. *Fitoterapia* **2016**, *109*, 274–282. [[CrossRef](#)]
34. Spinozzi, S.; Colliva, C.; Camborata, C.; Roberti, M.; Ianni, C.; Neri, F.; Calvarese, C.; Lisotti, A.; Mazzella, G.; Roda, A. Berberine and its metabolites: Relationship between physicochemical properties and plasma levels after administration to human subjects. *J. Nat. Prod.* **2014**, *77*, 766–772. [[CrossRef](#)]
35. Ng, P.Q.; Ling, L.S.C.; Chellian, J.; Madheswaran, T.; Panneerselvam, J.; Kunnath, A.P.; Gupta, G.; Satija, S.; Mehta, M.; Hansbro, P.M.; et al. Applications of Nanocarriers as Drug Delivery Vehicles for Active Phytoconstituents. *Curr. Pharm. Des.* **2020**, *26*, 4580–4590. [[CrossRef](#)]
36. Chan, Y.; Mehta, M.; Paudel, K.R.; Madheswaran, T.; Panneerselvam, J.; Gupta, G.; Su, Q.P.; Hansbro, P.M.; MacLoughlin, R.; Dua, K.; et al. Versatility of liquid crystalline nanoparticles in inflammatory lung diseases. *Nanomedicine* **2021**, *16*, 1545–1548. [[CrossRef](#)]
37. Mehta, M.; Malyala, V.; Paudel, K.R.; Chellappan, D.K.; Hansbro, P.M.; Oliver, B.G.; Dua, K. Berberine loaded liquid crystalline nanostructure inhibits cancer progression in adenocarcinomic human alveolar basal epithelial cells in vitro. *J. Food Biochem.* **2021**, *45*, e13954. [[CrossRef](#)]
38. Paudel, K.R.; Mehta, M.; Yin, G.H.S.; Yen, L.L.; Malyala, V.; Patel, V.K.; Panneerselvam, J.; Madheswaran, T.; MacLoughlin, R.; Jha, N.K.; et al. Berberine-loaded liquid crystalline nanoparticles inhibit non-small cell lung cancer proliferation and migration in vitro. *Environ. Sci. Pollut. Res. Int.* **2022**, *29*, 46830–46847. [[CrossRef](#)]
39. Alnuqaydan, A.M.; Almutary, A.G.; Azam, M.; Manandhar, B.; Yin, G.H.S.; Yen, L.L.; Madheswaran, T.; Paudel, K.R.; Hansbro, P.M.; Chellappan, D.K.; et al. Evaluation of the Cytotoxic Activity and Anti-Migratory Effect of Berberine-Phytantriol Liquid Crystalline Nanoparticle Formulation on Non-Small-Cell Lung Cancer In Vitro. *Pharmaceutics* **2022**, *14*, 1119. [[CrossRef](#)]
40. Paudel, K.R.; Panth, N.; Manandhar, B.; Singh, S.K.; Gupta, G.; Wich, P.R.; Nammi, S.; MacLoughlin, R.; Adams, J.; Warkiani, M.E.; et al. Attenuation of Cigarette-Smoke-Induced Oxidative Stress, Senescence, and Inflammation by Berberine-Loaded Liquid Crystalline Nanoparticles: In Vitro Study in 16HBE and RAW264.7 Cells. *Antioxidants* **2022**, *11*, 873. [[CrossRef](#)]
41. Manandhar, B.; Kim, H.J.; Rhyu, D.Y. Caulerpa okamurae extract attenuates inflammatory interaction, regulates glucose metabolism and increases insulin sensitivity in 3T3-L1 adipocytes and RAW 264.7 macrophages. *J. Integr. Med.* **2020**, *18*, 253–264. [[CrossRef](#)]
42. Singh, M.; Bhowal, R.; Vishwakarma, R.; Chopra, D. Assessing the impact on aqueous solubility of berberine chloride via co-crystallization with different stoichiometric ratios of pyromellitic dianhydride. *J. Mol. Struct.* **2020**, *1200*, 127086. [[CrossRef](#)]
43. Chen, W.; Miao, Y.-Q.; Fan, D.-J.; Yang, S.-S.; Lin, X.; Meng, L.-K.; Tang, X. Bioavailability study of berberine and the enhancing effects of TPGS on intestinal absorption in rats. *AAPS PharmSciTech* **2011**, *12*, 705–711. [[CrossRef](#)] [[PubMed](#)]
44. Selby-Pham, S.N.B.; Miller, R.B.; Howell, K.; Dunshea, F.; Bennett, L.E. Physicochemical properties of dietary phytochemicals can predict their passive absorption in the human small intestine. *Sci. Rep.* **2017**, *7*, 1931. [[CrossRef](#)] [[PubMed](#)]
45. Singh, N.; Sharma, B. Toxicological Effects of Berberine and Sanguinarine. *Front. Mol. Biosci.* **2018**, *5*, 21. [[CrossRef](#)] [[PubMed](#)]
46. Bae, Y.A.; Cheon, H.G. Activating transcription factor-3 induction is involved in the anti-inflammatory action of berberine in RAW264.7 murine macrophages. *Korean J. Physiol. Pharmacol.* **2016**, *20*, 415–424. [[CrossRef](#)] [[PubMed](#)]
47. Zhang, H.; Shan, Y.; Wu, Y.; Xu, C.; Yu, X.; Zhao, J.; Yan, J.; Shang, W. Berberine suppresses LPS-induced inflammation through modulating Sirt1/NF- κ B signaling pathway in RAW264.7 cells. *Int. Immunopharmacol.* **2017**, *52*, 93–100. [[CrossRef](#)] [[PubMed](#)]
48. Zhai, L.; Huang, T.; Xiao, H.T.; Wu, P.G.; Lin, C.Y.; Ning, Z.W.; Zhao, L.; Kwan, H.Y.A.; Hu, X.J.; Wong, H.L.X.; et al. Berberine Suppresses Colonic Inflammation in Dextran Sulfate Sodium-Induced Murine Colitis Through Inhibition of Cytosolic Phospholipase A2 Activity. *Front. Pharmacol.* **2020**, *11*, 576496. [[CrossRef](#)]

49. Kim, R.Y.; Horvat, J.C.; Pinkerton, J.W.; Starkey, M.R.; Essilfie, A.T.; Mayall, J.R.; Nair, P.M.; Hansbro, N.G.; Jones, B.; Haw, T.J.; et al. MicroRNA-21 drives severe, steroid-insensitive experimental asthma by amplifying phosphoinositide 3-kinase-mediated suppression of histone deacetylase 2. *J. Allergy Clin. Immunol.* **2017**, *139*, 519–532. [[CrossRef](#)]
50. Feng, K.-N.; Meng, P.; Zou, X.-L.; Zhang, M.; Li, H.-K.; Yang, H.-L.; Li, H.-T.; Zhang, T.-T. IL-37 protects against airway remodeling by reversing bronchial epithelial-mesenchymal transition via IL-24 signaling pathway in chronic asthma. *Respir. Res.* **2022**, *23*, 244. [[CrossRef](#)]
51. Beckett, E.L.; Stevens, R.L.; Jarnicki, A.G.; Kim, R.Y.; Hanish, I.; Hansbro, N.G.; Deane, A.; Keely, S.; Horvat, J.C.; Yang, M.; et al. A new short-term mouse model of chronic obstructive pulmonary disease identifies a role for mast cell tryptase in pathogenesis. *J. Allergy Clin. Immunol.* **2013**, *131*, 752–762. [[CrossRef](#)]

2) Research Paper: Extracellular Vesicles Released from Cancer Cells Promote Tumorigenesis by Inducing Epithelial to Mesenchymal Transition via β -Catenin Signaling

Status: Published in the **International Journal of Molecular Sciences**

Citation: Malya V, Paudel KR, **De Rubis G**, Hansbro NG, Hansbro PM, and Dua K. *Extracellular Vesicles Released from Cancer Cells Promote Tumorigenesis by Inducing Epithelial to Mesenchymal Transition via β -Catenin Signaling*. **International Journal of Molecular Sciences** 2023, 24(4), 3500; <https://doi.org/10.3390/ijms24043500>

Contribution: I conceived, planned, and performed part of the experiments, and contributed to the final revision of the manuscript



Article

Extracellular Vesicles Released from Cancer Cells Promote Tumorigenesis by Inducing Epithelial to Mesenchymal Transition via β -Catenin Signaling

Vamshikrishna Malyla ^{1,2,†}, Keshav Raj Paudel ^{2,†} , Gabriele De Rubis ¹ , Nicole G. Hansbro ², Philip M. Hansbro ^{2,3,*} and Kamal Dua ^{1,2,3,*}

¹ Discipline of Pharmacy, Graduate School of Health, University of Technology Sydney, Sydney, NSW 2007, Australia

² Centre for Inflammation, Faculty of Science, School of Life Sciences, Centenary Institute and University of Technology Sydney, Sydney, NSW 2007, Australia

³ Australian Research Centre in Complementary and Integrative Medicine, Faculty of Health, University of Technology Sydney, Ultimo, NSW 2007, Australia

* Correspondence: philip.hansbro@uts.edu.au (P.M.H.); kamal.dua@uts.edu.au (K.D.)

† These authors contributed equally to this work.

Abstract: Lung cancer is the leading cause of cancer-related deaths globally, in part due to a lack of early diagnostic tools and effective pharmacological interventions. Extracellular vesicles (EVs) are lipid-based membrane-bound particles released from all living cells in both physiological and pathological states. To understand the effects of lung-cancer-derived EVs on healthy cells, we isolated and characterized EVs derived from A549 lung adenocarcinoma cells and transferred them to healthy human bronchial epithelial cells (16HBE14o). We found that A549-derived EVs carry oncogenic proteins involved in the pathway of epithelial to mesenchymal transition (EMT) that are regulated by β -catenin. The exposure of 16HBE14o cells to A549-derived EVs resulted in a significant increase in cell proliferation, migration, and invasion via upregulating EMT markers such as E-Cadherin, Snail, and Vimentin and cell adhesion molecules such as CEACAM-5, ICAM-1, and VCAM-1, with concomitant downregulation of EpCAM. Our study suggests a role for cancer-cell-derived EVs to induce tumorigenesis in adjacent healthy cells by promoting EMT via β -catenin signaling.

Keywords: lung cancer; extracellular vesicles; tumorigenesis; β -catenin signaling; biomarkers; EMT



Citation: Malyla, V.; Paudel, K.R.; Rubis, G.D.; Hansbro, N.G.; Hansbro, P.M.; Dua, K. Extracellular Vesicles Released from Cancer Cells Promote Tumorigenesis by Inducing Epithelial to Mesenchymal Transition via β -Catenin Signaling. *Int. J. Mol. Sci.* **2023**, *24*, 3500. <https://doi.org/10.3390/ijms24043500>

Academic Editor: Petra Wise

Received: 8 January 2023

Revised: 17 January 2023

Accepted: 20 January 2023

Published: 9 February 2023



Copyright: © 2023 by the authors. Licensee MDPI, Basel, Switzerland. This article is an open access article distributed under the terms and conditions of the Creative Commons Attribution (CC BY) license (<https://creativecommons.org/licenses/by/4.0/>).

1. Introduction

EVs are lipid-based membrane-bound particles released from every living cells in both physiological as well as pathological states [1]. EVs carry numerous physiological biomolecules, such as DNA, RNA, lipids, and proteins, and therefore play a key role in cell-to-cell communication [1–4]. Based on the mechanism of biogenesis, size, characteristic surface markers such as CD63+/CD81+ and Annexin V, and method of collection, EVs are broadly divided into two subtypes: either small EVs (sEVs) or exosomes that are <100–200 nm, or medium to large EVs (m/IEVs) which are >200nm [1]. EVs have been extensively studied in the past couple of decades, and the importance of EVs lies primarily in the transport of physiological biomolecules from parent cells to recipient cells [5]. Cancer-cell-derived EVs can also play an important role in cell–cell communication, however, this remains incompletely defined, particularly in the context of tumorigenesis [6–9]. At the same time, there is a paucity of effective pre-clinical models to study disease pathophysiology which contributes to even now a poor understanding of the disease [10–12]. As a result, lung cancer has a very low five-year survival rate of around 15%, and an estimated 1.9 million cases are predicted to result in 0.6 million deaths in the United States alone in 2022 [13–15].

Cancer-cell-derived EVs (C-EVs) carry different biomarkers to their originating parent cells. As C-EVs are found in various biofluids, they can potentially serve as a diagnostic tool for cancer. For example, cancer markers such as CD91, CD317, and epidermal growth factor receptor (EGFR) are detected as membrane proteins on C-EVs, and a panel of 12 miRNAs was detected in EVs as RNA markers [6,7]. C-EVs also have the capacity to induce tumorigenesis in recipient cells by transferring oncogenic cargo; for example, mutant beta-catenin in EVs derived from colorectal cancer can activate WNT signaling in recipient cells [8]. Moreover, C-EVs are known to interact with different cell types such as endothelial cells and immune cells and are found in different organs such as the lymph nodes and bone marrow, wherein the capacity to induce tumorigenesis can have serious deleterious consequences for the individual [16–19]. Therefore, a better understanding of C-EVs not only helps in the detection of lung cancer via biomarker identification, but also helps in understanding tumorigenesis, and therefore may contribute to the design of effective therapeutic interventions.

Epithelial–mesenchymal transition (EMT) is a series of processes whereby epithelial cells lose their defining phenotype and gain mesenchymal characteristics, and which is a key driver of cancer metastasis [20]. Identification of EMT can be conducted by analyzing the changes in expression of well-characterized epithelial markers such as E-Cadherin and β -catenin and mesenchymal markers such as Vimentin, Snail, and N-Cadherin [21]. These molecules are also significant because they can promote tumorigenesis by enhancing migration and proliferation, eventually leading to metastasis [22].

Until now, the effects of lung C-EVs on healthy recipient cells is not well characterized. To interrogate the role of lung C-EVs in tumorigenesis, and to evaluate their use as biomarkers for lung cancer, we isolated medium C-EVs released from lung adenocarcinoma cells (A549) into the culture supernatant and characterized them by three well-established methods: flow cytometry (for surface markers), Western blot (for protein markers), and diffraction light scattering (for size). Then, we profiled the A549 C-EVs by protein array to reveal novel markers and studied the potential of these lung C-EVs to induce tumorigenesis in healthy human bronchial epithelial cells.

2. Results

2.1. Isolation and Characterization of EVs

Isolation of medium EVs was performed as reported [23] and is described in Figure 1A. Determining the size of EVs is critical, prior to performing any downstream analysis. For this, we performed dynamic light scattering (DLS) on both A549- and 16HBE14o-derived EVs and found that both EVs are in the size range of medium EVs (>200–1000 nm). Size distribution of A549 EVs was measured in triplicate and the Z Average was 392.2 nm, whereas the 16HBE14o EVs' Z average was 300 nm. In addition, data show that isolated EVs are pure, with no peaks in the lower or higher range of medium EVs, and the polydispersity index was around 0.5 and 0.4, indicating favorable polydispersity of EVs. After analyzing size, we characterized the EVs by the commonly known marker tetraspanin CD63 [24]. We observed that CD63 was detected in A549 EVs but not in the cells, which further confirms that we isolated bona fide EVs (Figure 1C). EVs are made up of a lipid membrane, so characterizing the membrane lipids is another way to confirm EVs. We performed Annexin V-FITC staining of phosphatidylserine (PS) on EVs and visualized the EVs by microscopy (Figure 1D). Annexin V binding to PS is reversible and calcium-dependent. We therefore assessed Annexin V binding to A549 and 16HBE14o EVs by flow cytometry in the presence and absence of calcium and confirmed that the fluorescent signal is abrogated in the absence of calcium.

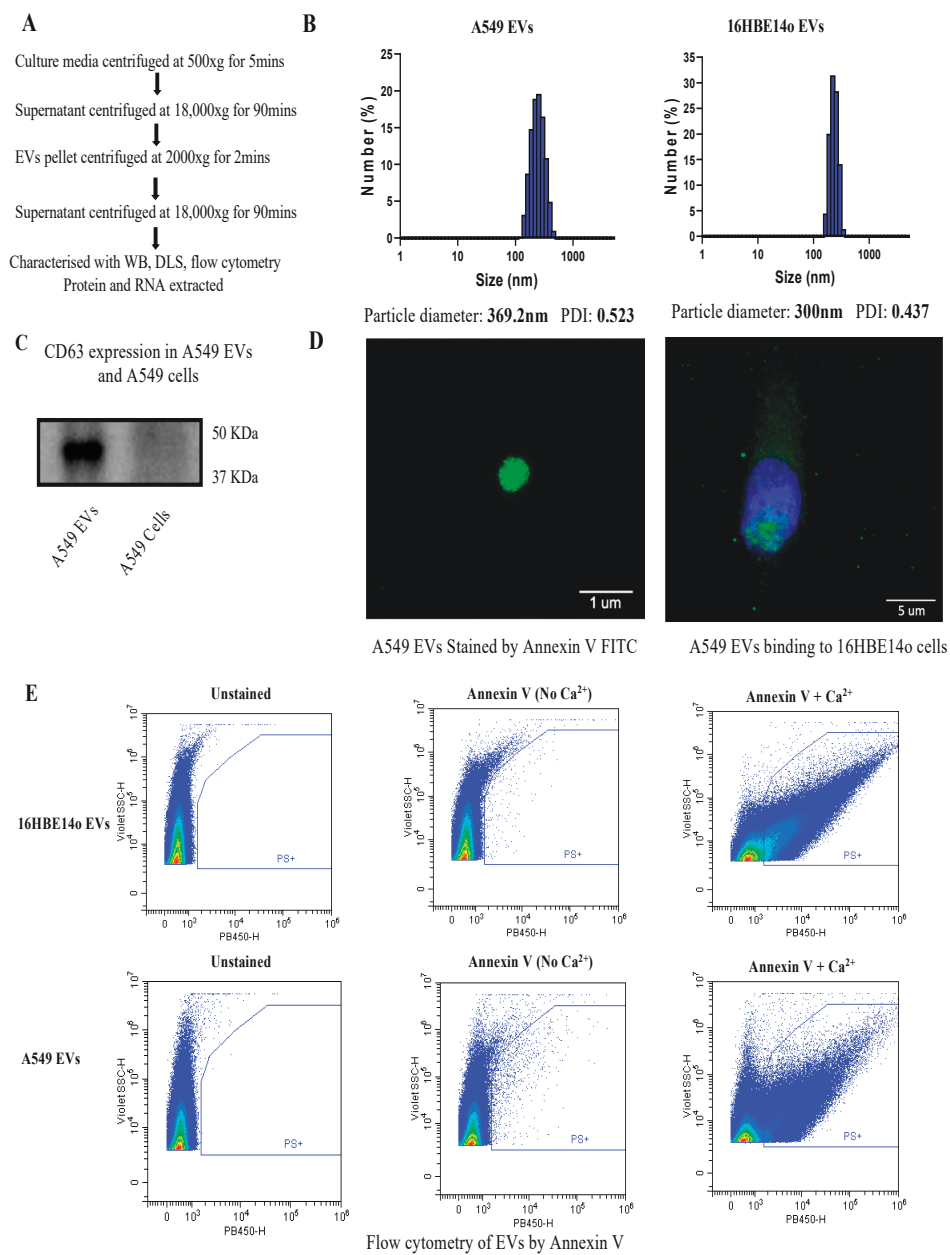


Figure 1. Isolation and characterization of EVs. (A) Flowchart showing the isolation of A549 and 16HBE14o EVs by high-speed centrifugation. (B) Size distribution of A549 and 16HBE14o EVs by DLS indicating both EVs are in the size range of medium EVs (>200–1000 nm). (C) Characterization of protein expression of tetraspanin marker CD63 on A549 EVs using Western blot. (D) Annexin V-FITC staining of EVs. Green fluorescence signal indicates positive staining of Annexin V-FITC for PS (**left panel**) and A549 EVs binding to 16HBE14o cells (**right panel**); nucleus was stained with DAPI (blue) and images were taken with an SP8 microscope at 100× magnification under oil immersion of EVs alone and at 40× magnification for cells with EVs. (E) Representative dot-plots of the flow cytometric analysis of PS exposure. Five micrograms of EVs enriched from the supernatant of 16HBE14o cells (**top row**) and A549 cells (**bottom row**) was stained with Annexin V-V450 in the presence of calcium (**right column**) to detect PS surface exposure. Unstained samples (**left column**) were analyzed to control for eventual sample autofluorescence. Staining in the absence of calcium (**middle column**) was performed to control for specific Annexin V binding.

2.2. Profiling A549 EVs for Oncogenic Protein Expression and Effects on Cell Migration, Invasion, and Proliferation

Profiling of EVs is crucial before performing any downstream functional analysis. We conducted an oncology protein array to measure 84 major cancer-related proteins in both A549 cells and A549 EVs and found that EpCAM, EGFR, Dkk-1, Galectine-3, Endostatin, E-Cadherin, FGF basic, Vimentin, and progranulin are the top nine hits (Figure 2A). EpCAM is highly expressed in EVs relative to their parental cells, a finding that we further validated by WB (Figure 2B). We examined the expression of EpCAM in publicly available lung cancer data and found that EpCAM is highly upregulated in LC (<https://lce.biohpc.swmed.edu/>, accessed on 2 July 2022).

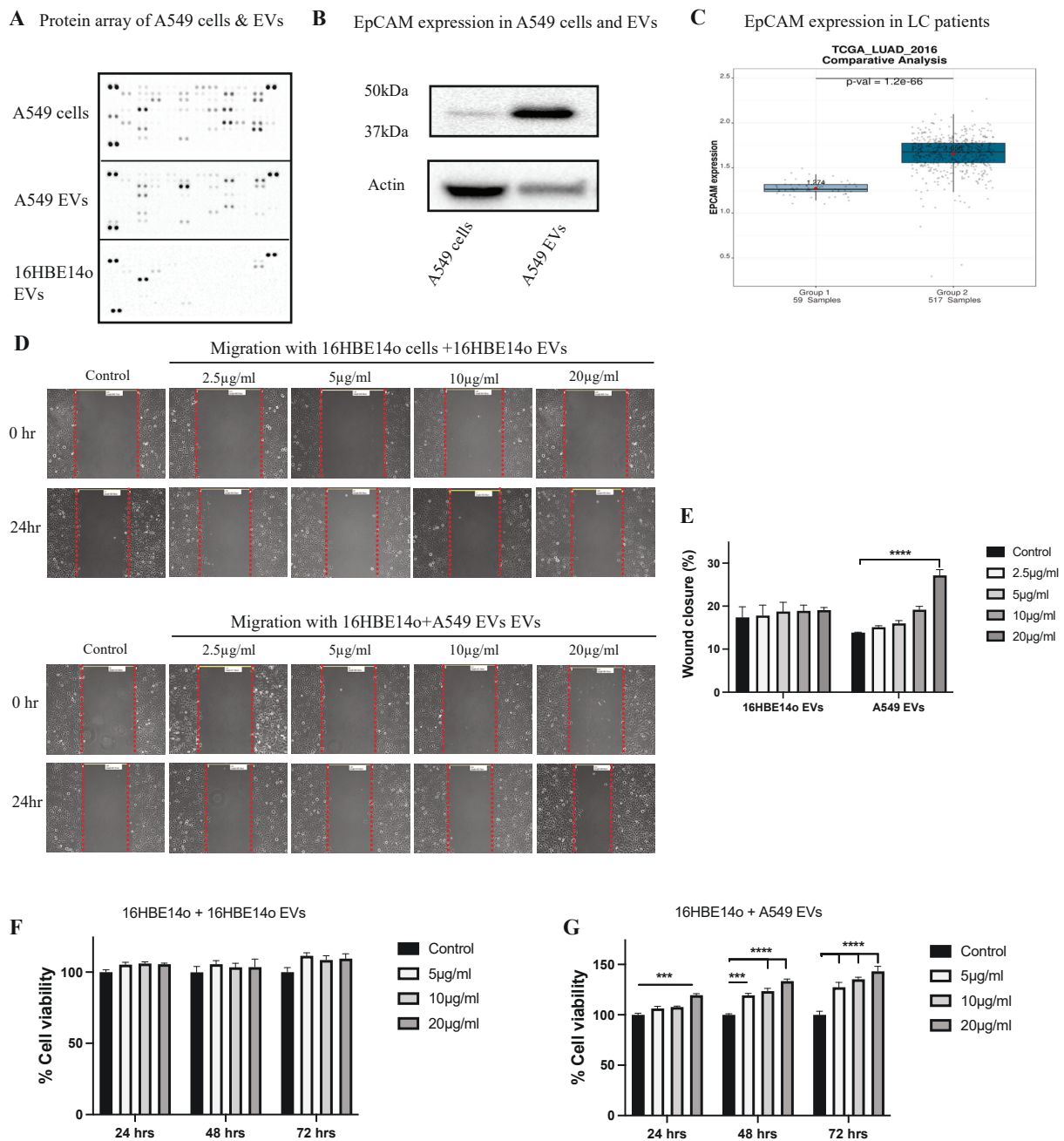


Figure 2. Cont.

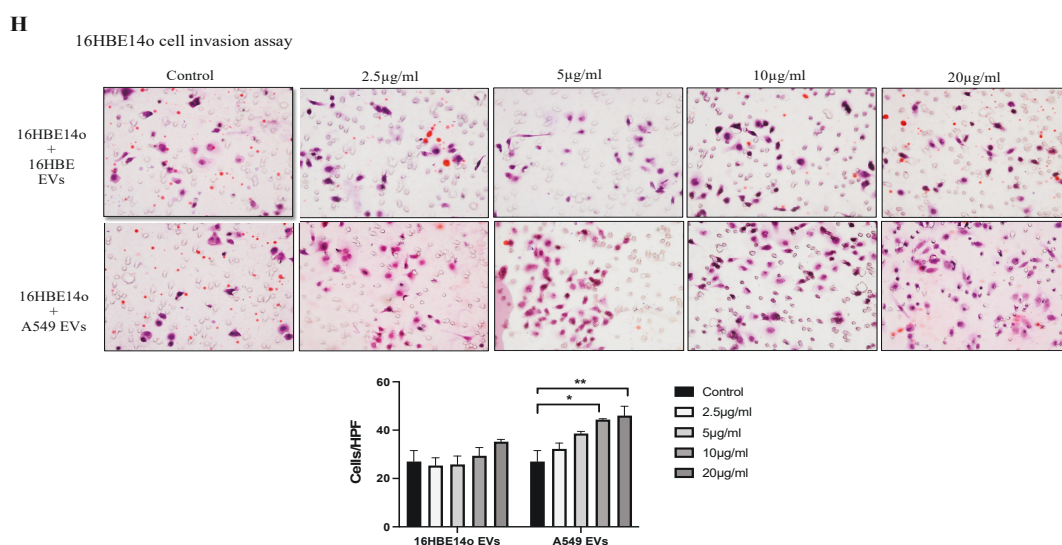


Figure 2. A549 EVs induced tumorigenesis in healthy 16HBE14o cells. (A) Human oncology array of A549 cell, A549 EV, and healthy and C-EVs recipient cell protein expression. (B) EpCAM protein expression (Western blot) in A549 cells and EVs showing EpCAM is highly encapsulated in A549 EVs. (C) EpCAM gene expression analyzed from publicly available LC database. (D) The 16HBE14o cell migration included by A549 EVs. Images were taken at 10× magnification. (E) The distance between the two edges of scratch was measured at 0 and 24 h. Data were analyzed using a one-way ANOVA: **** $p < 0.001$ vs. control. (F,G) Proliferation activity of A549EVs by MTT cell viability assay. Data analyzed using a one-way ANOVA: *** $p < 0.001$, **** $p \leq 0.0001$ vs. control. (H) Invasion activity of A549 and 16HBE14o EVs was measured using Boyden's chamber assay with 16HBE14o cells after 24 h. It was found that 10 and 20 µg/mL of A549 EVs showed invasion compared to control. Values are expressed as mean \pm SEM ($n = 3$ independent experiments) and statistical differences were assessed by one-way ANOVA: * $p \leq 0.05$, ** $p \leq 0.01$.

We then assessed the effects of EVs on the migration capacity of 16HBE14o cells. Treatment of 16HBE14o cells with 20 µg/mL protein-equivalent A549 EVs significantly increased cell migration (Figure 2E), whereas no significant change in migration was observed when 16HBE14o cells were treated with 16HBE14o EVs. Cell proliferation assays were performed on 16HBE14o cells treated with A549 EVs and 16HBE14o EVs over 0, 24, 48, and 72 h (Figure 2F,G), and it was found that A549 EVs significantly increased proliferation at 5, 10, and 20 µg/mL of protein equivalent EVs in a dose-dependent fashion. No significant change in proliferation was observed when cells were treated with 16HBE14o EVs. Similar results were observed in an invasion assay with 10 and 20 µg/mL A549 EVs. These functional assays clearly indicate that C-EVs induced tumorigenesis in healthy cells.

2.3. Understanding the Mechanism of A549-EV-Induced Tumorigenesis

To further investigate the mechanism, it is clearly essential to validate the tumorigenesis potential of A549 EVs to induce migration, proliferation, and invasion. We again performed an oncology array on the recipient cells (16HBE14o) (Figure 3A). Our analysis revealed that EpCAM is highly enriched in A549 EVs, and when we treat 16HBE14o cells with A549 EVs, EpCAM can be utilized by the recipient cells (Figure 3B), which was further confirmed by Western blot analysis (Figure 3C). Moreover, the oncology array of the 16HBE14o cells indicated a significant rise of other oncogenic cell adhesion molecules, such as carcinoembryonic antigen-related cell adhesion molecule5 (CEACAM-5), intercellular adhesion molecule-1 (ICAM-1) [25], vascular cell adhesion molecule 1 (VCAM-1), E-Cadherin (epithelial marker) [26], Snail [27], and Vimentin (mesenchymal marker) [28]. Thus, recipient cells exposed to A549 EVs have higher expression of EMT markers, which may promote tumorigenesis.

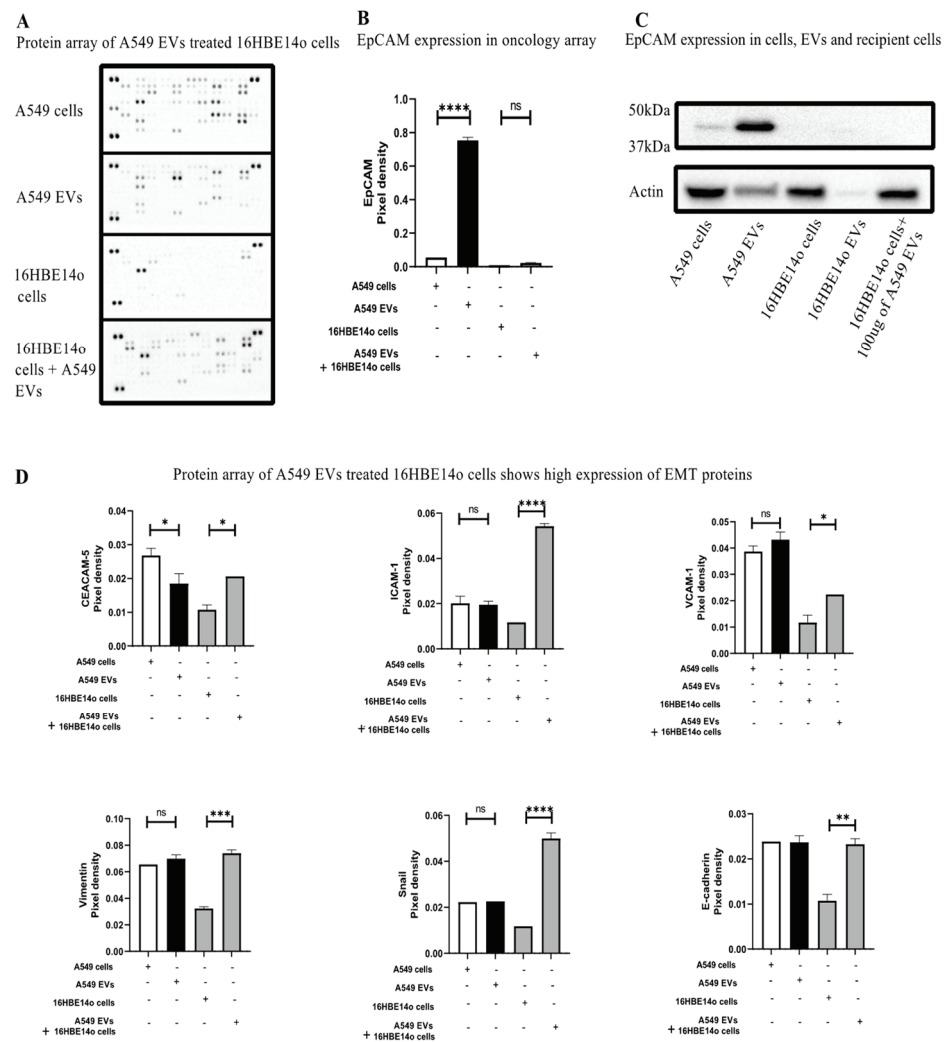


Figure 3. A549 EVs induced tumorigenesis in healthy cells by upregulating EMT markers (A) An oncology array of cancer markers upregulated in A549 cells and EVs, 16HBE14o cells and A549 EVs treated 16HBE14o cells shows a high amount of cancer markers was observed on the treated cells. (B) EpCAM, which is highly expressed in EVs has been utilized by the healthy cells, as observed by measuring the pixel density of EpCAM among the groups by Image J Fiji (version 1.53). Statistical analysis was done using a One-way ANOVA $*** p \leq 0.0001$. (C) EpCAM expression in the recipient cells was further confirmed by western blot. (D) An oncology array shows a significant upregulation of various EMT markers on the recipient cells like CEACAM5, ICAM1, VCAM1, Vimentin, Snail1, and E-cadherin. Pixel density was measured using Image J Fiji and significant differences were evaluated using a One-Way ANOVA ns = non-significant, $* p > 0.05$, $** p \leq 0.05$, $*** p \leq 0.01$, $**** p < 0.001$.

2.4. Understating the Location, Encapsulation, and Uptake of EpCAM

Initially, we performed flow cytometric analysis of EpCAM on the surface of healthy 16HBE14o and A549 cells and detected EpCAM on the A549 cells, which indicates that during membrane shredding EpCAM was encapsulated in the EVs (Figure 4A). Flow cytometric analysis of A549 EVs could not detect EVs on the surface, which suggests EpCAM was internalized by the EVs (Figure 4B). Further Western blot analysis of the recipient cells after treatment with A549 EVs at different timepoints (4, 8, 16, and 32 h) showed that, surprisingly, EpCAM seems to be most detected in the recipient cells before 4 h (Figure 4C). Overall, the EpCAM location indicates it is a transmembrane protein on A549 cells, and that it has been encapsulated by A549 EVs as well as been transferred by healthy 16HBE14o cells (Figure 4D).

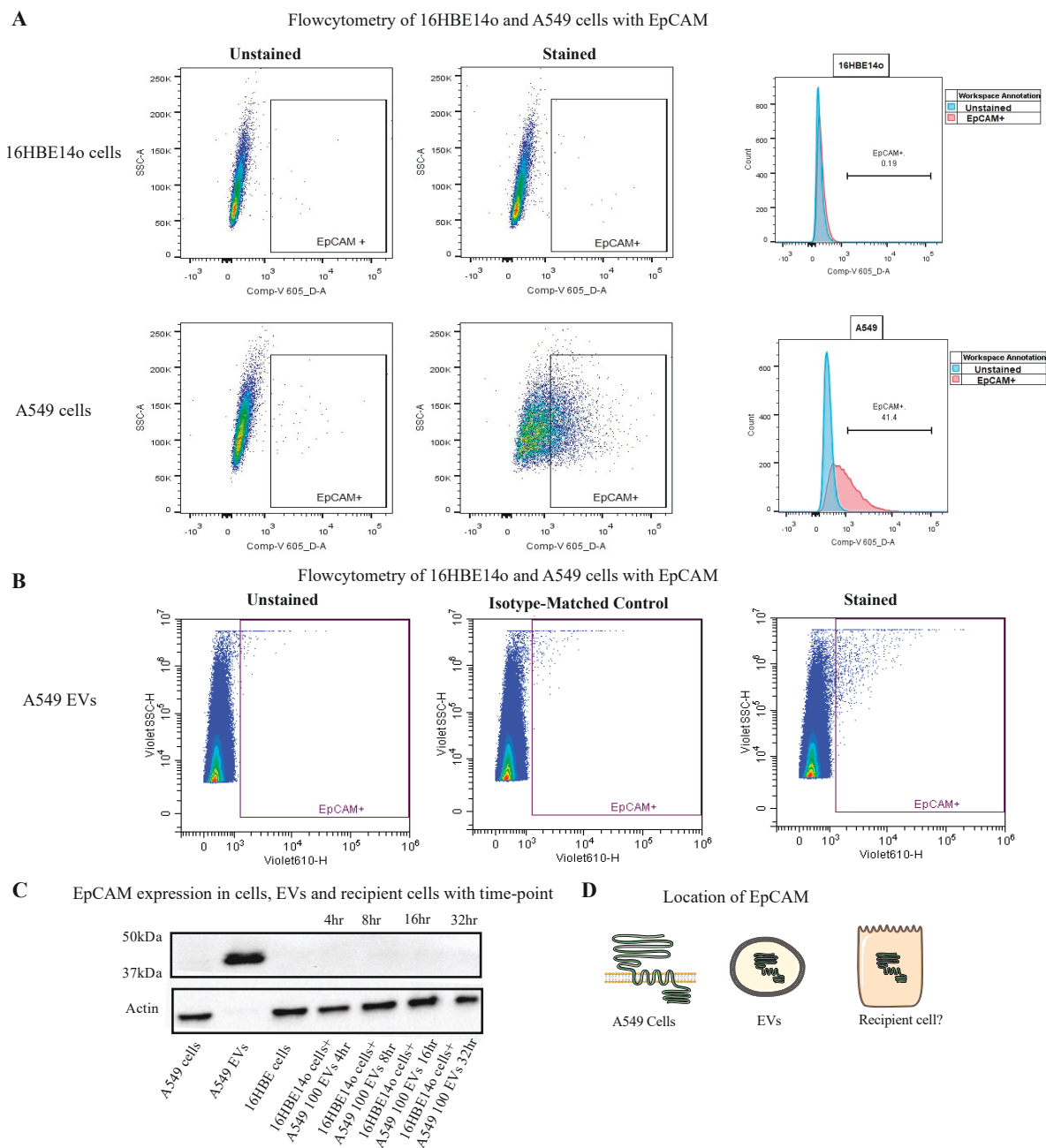


Figure 4. (A) To understand the localisation of EpCAM, flow cytometric analysis was performed on 16HBE14o (upper row) and A549 cells (lower row): 41.4 % of A449 cells stain positive for EpCAM at the surface. (B) Flow cytometric analysis of A549 EVs with EpCAM indicating that EpCAM was encapsulated inside the EVs. (C) Immunoblotting was performed with EpCAM on the recipient cells at 4, 8, 16, and 32 h timepoints. (D) Schematic overview of EpCAM location and utilisation.

3. Materials and Methods

3.1. Cell Culture

Lung adenocarcinoma cell line A549 purchased from ATCC, USA was obtained as a kind gift from Woolcock Institute of Medical Research, Sydney. A549 cells were grown in a Roswell Park Memorial Institute (RPMI) media (Sigma Aldrich, St. Louis, MI, USA) containing 5% heat-inactivated fetal bovine serum (FBS) (Novogen, North Mackay, Australia), 1% penicillin, and streptomycin (Gibco, Waltham, MA, USA) and were maintained in a humidified atmosphere of 5% CO₂ at 37 °C. All EVs collected from A549 cells were from A549 passage number 20–25 for p consistency. In addition, 16HBE14o-human normal

(healthy) bronchial epithelial cells (passage 10–15) were provided by Ling Bi from Charles Perkins Centre—The University of Sydney, Australia, and grown in DMEM supplemented with 10% heat-inactivated FBS and 100 IU/mL penicillin and 100 µg/mL streptomycin in a humidified atmosphere of 5% CO₂ at 37 °C. Cells were constantly checked for mycoplasma contamination and all experiments were conducted in mycoplasma-negative cells. FBS may contain exosomes that may result in false-positive results during characterization, therefore we performed all experiments in exosome-depleted media. For this, FBS was spun using a Beckman Coulter ultracentrifuge at 100,000× *g* for 18 h [29]. The supernatant was collected, leaving the exosome pellet in the bottom of the tube. The collected FBS was used to prepare 5% or 10% FBS media, referred to as exosome-depleted media [29].

3.2. Collection and Isolation of EVs

A density of 10×10^6 A549 cells were seeded in 12 T-175 flasks. The following day, media were discarded before washing twice with PBS and media were replenished with fresh exosome-depleted media. After 72 h, the supernatant was collected and centrifuged at $500 \times g$ for 5 min to remove any dead cells or cell debris, then supernatant was centrifuged again at high speed ($18,000 \times g$) for 90 min at 4 °C, and the pellet-containing EVs were resuspended and washed in serum-free media and further centrifuged for 2 min at $2000 \times g$ to remove any debris. Finally, the supernatant was further centrifuged for 30 min at $18,000 \times g$ and 4 °C and the final pellet containing EVs was resuspended in 1 mL PBS and stored at –80 °C for downstream analysis [23]. The 16HBE14o cells were seeded at a density of 10×10^6 into six T-175 flasks. The following day, media were discarded followed by washing twice with PBS, and media were replenished with fresh exosome-depleted media. As healthy cells do not release the same amount of EVs as cancer cells do, we had to stimulate the 16HBE14o cells with lipopolysaccharides (LPS; 1 µg/mL) obtained from *Pseudomonas aeruginosa*. Stimulating healthy cells with LPS to induce the release of significant amounts of EVs is a well-established protocol referred to by many studies [30]. After 48 h of stimulation, media were collected and centrifuged similarly to A549 EVs.

3.3. Particle Size Distribution by Dynamic Light Scattering

A small volume of the EV fraction was obtained from A549 and 16HBE14o EVs and further diluted in PBS. Particle size and zeta potential were measured using Zetasizer Nano ZS equipped with He-Ne 633 nm laser light source and a reading was measured at 25 °C in a size range of 0.3–10,000 nm diameter size.

3.4. Protein Extraction from EVs, Whole Cell Lysate, and Protein Quantification

RIPA buffer containing phosphatase and protease inhibitor cocktail (Roche, USA) was added to the EV pellet followed by vortex and incubation on ice for 15 min. The EVs were then sonicated at 30% amplitude three times for 2 s, before being incubated again on ice for an additional 15 min. Then, the lysate was then centrifuged for 30 min at $18,000 \times g$ and 4 °C, before the supernatant was collected, and the protein concentration quantified using a Pierce™ BCA Protein Array Kit (Thermo fisher Scientific, Waltham, MA, USA).

A549 and 16HBE14o cells grown in 6-well plates were allowed to reach approximately 80% confluence before the media were removed, and the cells washed with ice-cold PBS and RIPA lysis buffer containing phosphatase inhibitor cocktail were added. Using a cell scraper, cells were scraped, and the lysate transferred to 1.5 mL tubes followed by incubation on ice for 15 min. The lysate was then sonicated at 30% amplitude three times for 2 s followed by incubation on ice for another 15 min. Finally, the lysate was centrifuged at $12,000 \times g$ for 15 min at 4 °C, before the supernatant was collected, and protein concentration quantified using a Pierce™ BCA Protein Array Kit.

3.5. Western Blotting

Equal amounts of extracted protein were loaded for SDS-PAGE and transferred to PVDF membrane for immunoblotting. After an overnight incubation with primary

antibody (Anti-CD63 (ab193349) and Anti-EpCAM (epithelial cell adhesion molecule) (ab223582) at 1:1000 and 1:1500 dilution, respectively, at 4 °C and anti-mouse secondary IgG antibody for CD63 and Anti-rabbit IgG for EpCAM), images were taken using a chemiDoc imaging system. The blots were then stripped with stripping buffer and blocked with 1% BSA, incubated with beta Actin (ab8226) at a 1:10,000 dilution for 2 h at room temperature, washed 3 times with TBST buffer followed by an incubation with anti-mouse secondary antibody (1:10,000 dilutions), and imaged using a chemiDoc.

3.6. Immunofluorescence

Freshly isolated EVs were seeded onto collagen-coated slides and stained with Annexin V-FITC (BD Bioscience) for 2 h along with Annexin V binding buffer and images were taken by confocal microscopy (SP8). Images were analyzed using ImageJ. 1×10^5 . Then, 16HBE14o cells were seeded onto collagen-coated glass slides and allowed to attach for 6 h. A549 EVs were stained with Annexin V-FITC and seeded onto 16HBE14o cells and allowed to attach for 4 h. ProLong™ Gold antifade mountant was then used for staining the nucleus and microscopic images were taken by confocal microscopy at 40× magnification.

3.7. Flow Cytometry

An amount of 5 µg of A549 and 16HBE14o EVs was analyzed by flow cytometry. Both EVs were stained with V450 Annexin V (BD Horizon™ catalog No. 560506) for 30 min in the dark. Unstained samples were used as a negative control. Initially, 5 µg of unstained samples were run to determine the concentration of EVs for flow cytometry based on the gating strategy. EVs stained with Annexin V were run in the presence or absence of calcium, as Annexin V binding can be determined only in the presence of calcium. Unstained A549 cells and EVs were used as negative controls to establish the gating strategy. A549 EVs and cells stained for EpCAM were then run and plotted for EpCAM binding.

3.8. Protein Array of EVs and Cells

Protein from A549 cells, A549 EVs, 16HBE14o cells, and 16HBE14o cells treated with A549 EVs were isolated as previously mentioned, and equal amounts (600 µg) of protein were loaded to perform an oncology array (R&D Systems, Minneapolis, MN, USA) following the manufacturer's protocol (<https://www.rndsystems.com>, accessed on 10 January 2022). Data were analyzed using Image J by measuring the pixel density.

3.9. Migration (Scratch Wound Healing Assay)

The 16HBE14o cells were plated in a six-well plate at a density of 2×10^4 cells per well. The following day, cells were washed twice with PBS. A vertical straight scratch at the center of the plate was made with a sterile 200 µL pipette tip followed by washing at least 3 times to remove unattached cells. Then, 2 mL of cell culture media was added and images of each well at three different positions (up, middle, and down) were taken at 10× magnification. Baseline images were taken at T = 0 before EVs from A549 cells were treated with increasing protein concentrations of 1 µg/mL, 2.5 µg/mL, 5 µg/mL, 10 µg/mL, and 20 µg/mL. The plates were then incubated at 37 °C for 24 h or 48 h. Images of all wells were then taken again at 10× magnification.

3.10. MTT Cell Proliferation Assay

In a 96-well plate, 16HBE14o cells were seeded at a density of 2500 cells per well for 72 h, 5000 cells for 48 h, and 10,000 cells for 24 h. The following day, the media were discarded and any unadhered cells were removed by washing with PBS. Cells were treated with or without proliferation inducers at different concentrations and incubated for 24 h, 48 h, and 72 h depending on the experimental time course. MTT solution was added at 0.5 mg/mL in 100 µL of culture media per well and incubated for 4 h. Media were then

discarded and 100 μ L of DMSO was added to dissolve the formazan. The absorbance was then measured at 562 nm using a microplate reader (BMG Labtech, Carbine Way, Australia).

3.11. Cell Invasion Assay

To determine the effect of EVs on the invasion capacity of 16HBE14o cells, we performed a modified Boyden's chamber assay using EVs derived from either healthy or cancer cells. We used 24 transwell permeable supports (6.5 mm insert, 8 μ M pore size polycarbonate membrane), precoated on the lower surface of the membranes with 2.5% gelatin in 1 M acetic acid for 1 h. The 16HBE14o cells were seeded in the upper chamber (200 cells/well in 200 μ L of DMEM), and inserts were then placed in a well containing 600 μ L of DMEM. Cells were allowed to adhere and then treated with A549- or 16HBE14o-derived EVs (0, 2.5, 5, 10, or 20 μ g/mL) and incubated for 24 h. The cells from the upper transwell surface were removed by cotton swabs, and the membrane was cut and fixed in 10% formalin and stained with hematoxylin and eosin. Cells that had crossed the pores of the membrane to the lower surface were counted in 5 random fields (magnification 20 \times), and cell invasion was calculated as average cells per field of view [31].

3.12. Statistical Analysis

The values are represented as mean \pm SEM. Graph Pad Prism (version 9.3) was used to perform statistical analyses. Statistical comparisons were conducted by unpaired, two-tailed Student's *t* test for two groups and one-way ANOVA for more than two groups. A value of $p < 0.05$ was considered statistically significant.

4. Discussion

EVs have the capacity to alter the phenotype of recipient cells from healthy to malignant when internalized by the healthy cell. This is primarily mediated by the transfer of oncogenic proteins and RNA present in cancer-cell-derived EVs [8,32]. However, it remains unknown how exactly they are internalized and how they develop a cancer-related phenotype in terms of the mechanistic and molecular regulation of pathways in the recipient cell. This study provides further understanding of how C-EVs induce a tumor-like phenotype in healthy bronchial epithelial cells, mostly at the protein level.

We initially focused on the isolation of A549 and 16HBE14o medium-sized EVs by separating them from sEVs and large oncosomes, which is critical before any further downstream analysis can be conducted [33]. According to the *Minimal information for studies of extracellular vesicles 2018 (MISEV2018)* guidelines [1], isolated EVs should be characterized by at least two well-established methods [26]. In our study, we initially characterized EVs by DLS, confirming a size consistent with medium EVs, then verified protein expression of tetraspanin CD63 as an EV marker using Western blot. Furthermore, we performed flow cytometric analysis and microscopy for phosphatidylserine surface staining using Annexin V (Figure 1) [29].

We analyzed the oncogenic proteins which are encapsulated in A549 EVs and found that EpCAM, EGFR, Dkk-1, Galectine-3, Endostatin, E-Cadherin, FGF basic, Vimentin, and progranulin were the top nine hits on the oncology blot. Interestingly, all these proteins are connected to the WNT/ β -catenin signaling pathway. Among them, DKK1 and Endostatin are downregulators of this pathway [34–42]. To see the effect of these oncogenic proteins within the EVs, we treated healthy bronchial epithelial cells with A549 EVs and elevated changes in the oncogenic activity of the healthy cells by using assays for cell migration, invasion, and proliferation. Interestingly, we found a significant increase in the cell proliferation, migration, and invasion activity in the recipient healthy cells (16HBE14o) (Figure 2).

Furthermore, we performed an oncology array on the EV-treated recipient cells and found that the highly expressed protein on A549 EVs, EpCAM, was efficiently transferred to healthy cells [43], a finding that we further confirmed by WB (Figure 3). The use of EpCAM in recipient cells is already demonstrated in the literature, where EpCAM is cleaved

by β -catenin, leading to activation of EMT and further leading to tumorigenesis [44,45]. In contrast, we saw a significant increase in other oncogenic cell adhesion molecules including CEACAM-5, ICAM-1 [25], and VCAM-1 [46], epithelial markers such as E-Cadherin [26], as well as mesenchymal markers such as Snail [27] and Vimentin [28] in the recipient cells. Interestingly, all these markers are part of the EMT and mainly regulated by β -catenin signaling, but our findings suggest for the first time that C-EVs can activate EMT markers in healthy cells, leading to tumorigenesis [47–54] (Figure 5). Overall, the use of a β -catenin pathway inhibitor could be a potential therapy for C-EV-induced tumorigenesis/metastasis, and detection of these EV markers in biological fluids can be a potential diagnostic application.

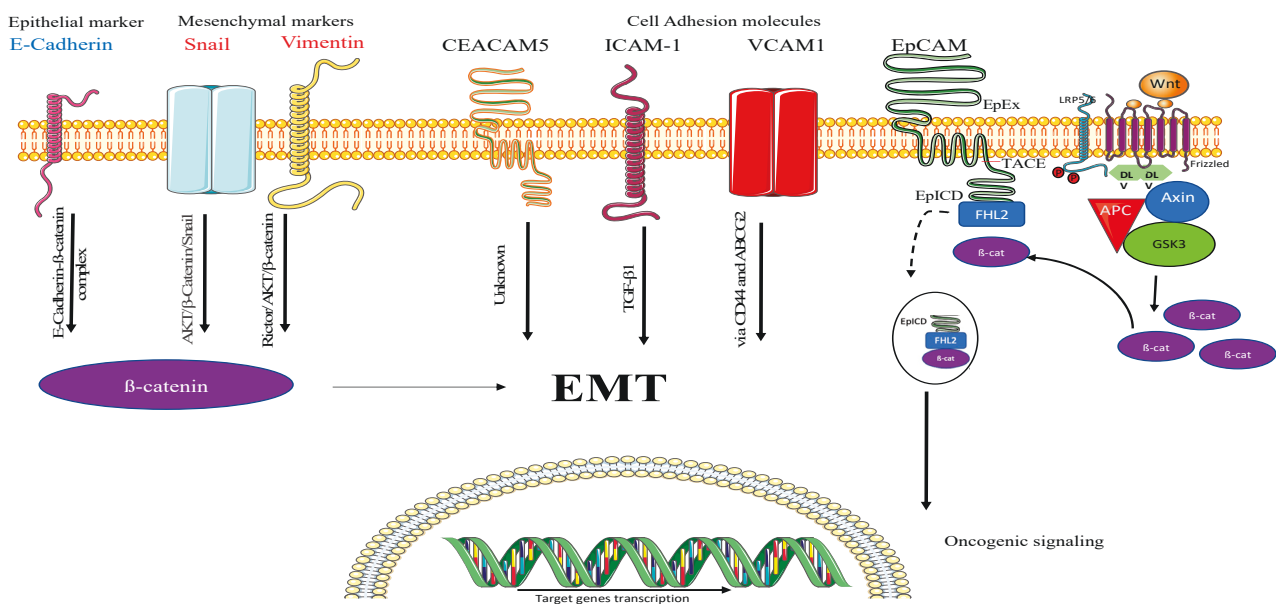


Figure 5. Predicted mechanism of tumorigenesis. (From left) Epithelial marker E-Cadherin was found on recipient cells, which is known to form a complex with β -catenin and can thereby promote EMT. Mesenchymal markers such as Snail and Vimentin further support our hypothesis, which are known to interact with β -catenin via AKT/ β -Catenin/Snail and Rictor/AKT/ β -catenin complexes, respectively. Cell adhesion molecules are surface proteins involved in cell–cell communication, and CEACAM-5 is known to induce tumorigenesis, but its exact role is still unknown in terms of EMT. ICAM-1 is known to induce EMT by regulating TGF- β 1. Another cell adhesion molecule, VCAM-1, is known to induce EMT via CD44 and ABCG2 expression. Finally, EpCAM is taken up by the recipient cells, utilized by breaking down of EpCAM by tumor necrosis factor α -converting enzyme (TACE), which is known as EpICD, which merges with four-and-a-half LIM domain protein 2 (FHL2) forming a complex with β -catenin and further activates oncogenic signaling.

5. Conclusions

Overall, we have shown how different EMT signaling proteins induce tumorigenic changes in a healthy cell, namely by increasing cell migration, proliferation, and invasive potential. In addition, the highly expressed protein EpCAM was completely taken up by healthy cells, as they could not be detected by an oncology array or Western blot, indicating some proteins are directly utilized by cells following their uptake. Interestingly, many EMT and cell adhesion molecule related proteins were detected on the recipient cells (Figure 5), which suggests they are enhancing tumorigenesis by regulating β -catenin and eventually EMT. Thus, this study gives further evidence that cancer cell EVs carry oncogenic proteins which are actively taken up by healthy cells to induce tumorigenesis. Finally, this study helps in better understanding EMT induced by C-EVs. The validation of these findings with an inhibitor could be a potential therapy for LC.

Author Contributions: Conceptualization, V.M., K.R.P., P.M.H. and K.D.; methodology, V.M., K.R.P., P.M.H. and K.D.; validation, V.M., G.D.R. and K.R.P.; formal analysis, V.M., G.D.R. and K.R.P.; investigation, V.M. and K.R.P.; data curation, V.M., G.D.R. and K.R.P.; writing—original draft preparation, V.M.; writing—review and editing, V.M., K.D., P.M.H., K.R.P., G.D.R. and N.G.H.; visualization, V.M. and K.R.P.; supervision, K.D., P.M.H. and K.R.P.; project administration, V.M., K.D., P.M.H. and K.R.P.; funding acquisition, K.D. and P.M.H. All authors have read and agreed to the published version of the manuscript.

Funding: Philip M. Hansbro would like to acknowledge the support from Cancer Council NSW, National Health and Medical Research Council and University of Technology Sydney, Australia. Kamal Dua is supported by project grants from the Rebecca L Cooper Medical Research Foundation and the fellowship from Maridulu Budyari Gumal—Sydney Partnership for Health Education, Research and Enterprise (SPHERE). Vamshikrishna Malya is supported by an international research scholarship by UTS. Keshav Raj Paudel and Philip M. Hansbro are supported by a joint fellowship from the Prevent Cancer Foundation and the International Association for the Study of Lung Cancer Foundation, USA.

Institutional Review Board Statement: Not applicable.

Informed Consent Statement: Not applicable.

Data Availability Statement: The data presented in this study are available in the manuscript.

Conflicts of Interest: The authors declare no conflict of interest.

References

1. Théry, C.; Witwer, K.W.; Aikawa, E.; Alcaraz, M.J.; Anderson, J.D.; Andriantsitohaina, R.; Antoniou, A.; Arab, T.; Archer, F.; Atkin-Smith, G.K. Minimal information for studies of extracellular vesicles 2018 (MISEV2018): A position statement of the International Society for Extracellular Vesicles and update of the MISEV2014 guidelines. *J. Extracell. Vesicles* **2018**, *7*, 1535750. [[CrossRef](#)] [[PubMed](#)]
2. Valadi, H.; Ekström, K.; Bossios, A.; Sjöstrand, M.; Lee, J.J.; Lötvall, J.O. Exosome-mediated transfer of mRNAs and microRNAs is a novel mechanism of genetic exchange between cells. *Nat. Cell Biol.* **2007**, *9*, 654–659. [[CrossRef](#)] [[PubMed](#)]
3. Thakur, B.K.; Zhang, H.; Becker, A.; Matei, I.; Huang, Y.; Costa-Silva, B.; Zheng, Y.; Hoshino, A.; Brazier, H.; Xiang, J. Double-stranded DNA in exosomes: A novel biomarker in cancer detection. *Cell Res.* **2014**, *24*, 766–769. [[CrossRef](#)] [[PubMed](#)]
4. Taylor, J.; Bebawy, M. Proteins regulating microvesicle biogenesis and multidrug resistance in cancer. *Proteomics* **2019**, *19*, 1800165. [[CrossRef](#)] [[PubMed](#)]
5. Yáñez-Mó, M.; Siljander, P.R.-M.; Andreu, Z.; Bedina Zavec, A.; Borràs, F.E.; Buzas, E.I.; Buzas, K.; Casal, E.; Cappello, F.; Carvalho, J. Biological properties of extracellular vesicles and their physiological functions. *J. Extracell. Vesicles* **2015**, *4*, 27066. [[CrossRef](#)]
6. Rabinowits, G.; Gerçel-Taylor, C.; Day, J.M.; Taylor, D.D.; Kloecker, G.H. Exosomal microRNA: A diagnostic marker for lung cancer. *Clin. Lung Cancer* **2009**, *10*, 42–46. [[CrossRef](#)]
7. Jakobsen, K.R.; Paulsen, B.S.; Bæk, R.; Varming, K.; Sorensen, B.S.; Jørgensen, M.M. Exosomal proteins as potential diagnostic markers in advanced non-small cell lung carcinoma. *J. Extracell. Vesicles* **2015**, *4*, 26659. [[CrossRef](#)]
8. Kalra, H.; Gangoda, L.; Fonseka, P.; Chitti, S.V.; Liem, M.; Keerthikumar, S.; Samuel, M.; Boukouris, S.; Al Saffar, H.; Collins, C. Extracellular vesicles containing oncogenic mutant β -catenin activate Wnt signalling pathway in the recipient cells. *J. Extracell. Vesicles* **2019**, *8*, 1690217. [[CrossRef](#)]
9. Krishn, S.R.; Salem, I.; Quaglia, F.; Naranjo, N.M.; Agarwal, E.; Liu, Q.; Sarker, S.; Kopenhaver, J.; McCue, P.A.; Weinreb, P.H. The $\alpha\beta 6$ integrin in cancer cell-derived small extracellular vesicles enhances angiogenesis. *J. Extracell. Vesicles* **2020**, *9*, 1763594. [[CrossRef](#)]
10. Malya, V.; Paudel, K.R.; Shukla, S.D.; Donovan, C.; Wadhwa, R.; Pickles, S.; Chimankar, V.; Sahu, P.; Bielefeldt-Ohmann, H.; Bebawy, M. Recent advances in experimental animal models of lung cancer. *Future Med. Chem.* **2020**, *12*, 567–570. [[CrossRef](#)]
11. Herbst, R.S.; Morgensztern, D.; Boshoff, C. The biology and management of non-small cell lung cancer. *Nature* **2018**, *553*, 446–454. [[CrossRef](#)]
12. Brozos-Vázquez, E.M.; Díaz-Peña, R.; García-González, J.; León-Mateos, L.; Mondelo-Macia, P.; Peña-Chilet, M.; López-López, R. Immunotherapy in nonsmall-cell lung cancer: Current status and future prospects for liquid biopsy. *Cancer Immunol. Immunother.* **2021**, *70*, 1177–1188. [[CrossRef](#)]
13. Bray, F.; Ferlay, J.; Soerjomataram, I.; Siegel, R.L.; Torre, L.A.; Jemal, A. Global cancer statistics 2018: GLOBOCAN estimates of incidence and mortality worldwide for 36 cancers in 185 countries. *CA A Cancer J. Clin.* **2018**, *68*, 394–424. [[CrossRef](#)]
14. Engholm, G.; Ferlay, J.; Christensen, N.; Bray, F.; Gjerstorff, M.L.; Klint, Å.; Køtlum, J.E.; Ólafsdóttir, E.; Pukkala, E.; Storm, H.H. NordCAN—a Nordic tool for cancer information, planning, quality control and research. *Acta Oncol.* **2010**, *49*, 725–736. [[CrossRef](#)]
15. Siegel, R.L.; Miller, K.D.; Fuchs, H.E.; Jemal, A. Cancer statistics, 2022. *CA Cancer J. Clin.* **2022**, *72*, 7–33. [[CrossRef](#)]

16. Al-Nedawi, K.; Meehan, B.; Kerbel, R.S.; Allison, A.C.; Rak, J. Endothelial expression of autocrine VEGF upon the uptake of tumor-derived microvesicles containing oncogenic EGFR. *Proc. Natl. Acad. Sci. USA* **2009**, *106*, 3794–3799. [[CrossRef](#)]
17. Baj-Krzyworzeka, M.; Szatanek, R.; Weglarczyk, K.; Baran, J.; Zembala, M. Tumour-derived microvesicles modulate biological activity of human monocytes. *Immunol. Lett.* **2007**, *113*, 76–82. [[CrossRef](#)]
18. Hood, J.L.; San, R.S.; Wickline, S.A. Exosomes Released by Melanoma Cells Prepare Sentinel Lymph Nodes for Tumor Metastasis-Melanoma Exosome Preparation of Lymph Nodes for Metastasis. *Cancer Res.* **2011**, *71*, 3792–3801. [[CrossRef](#)]
19. Peinado, H.; Alečković, M.; Lavotshkin, S.; Matei, I.; Costa-Silva, B.; Moreno-Bueno, G.; Hergueta-Redondo, M.; Williams, C.; García-Santos, G.; Ghajar, C.M. Melanoma exosomes educate bone marrow progenitor cells toward a pro-metastatic phenotype through MET. *Nat. Med.* **2012**, *18*, 883–891. [[CrossRef](#)]
20. Chen, T.; You, Y.; Jiang, H.; Wang, Z.Z. Epithelial–mesenchymal transition (EMT): A biological process in the development, stem cell differentiation, and tumorigenesis. *J. Cell. Physiol.* **2017**, *232*, 3261–3272. [[CrossRef](#)]
21. Xu, S.; Zhan, M.; Wang, J. Epithelial-to-mesenchymal transition in gallbladder cancer: From clinical evidence to cellular regulatory networks. *Cell Death Discov.* **2017**, *3*, 17069. [[CrossRef](#)]
22. Lamouille, S.; Xu, J.; Derynck, R. Molecular mechanisms of epithelial–mesenchymal transition. *Nat. Rev. Mol. Cell Biol.* **2014**, *15*, 178–196. [[CrossRef](#)] [[PubMed](#)]
23. Jaiswal, R.; Luk, F.; Dalla, P.V.; Grau, G.E.R.; Bebawy, M. Breast cancer-derived microparticles display tissue selectivity in the transfer of resistance proteins to cells. *PLoS ONE* **2013**, *8*, e61515. [[CrossRef](#)] [[PubMed](#)]
24. Jankovičová, J.; Sečová, P.; Michalková, K.; Antalíková, J. Tetraspanins, More than Markers of Extracellular Vesicles in Reproduction. *Int. J. Mol. Sci.* **2020**, *21*, 7568. [[CrossRef](#)] [[PubMed](#)]
25. Morishita, Y.; Watanabe, M.; Nakazawa, E.; Ishibashi, K.; Kusano, E. The interaction of LFA-1 on mononuclear cells and ICAM-1 on tubular epithelial cells accelerates TGF- β 1-induced renal epithelial-mesenchymal transition. *PLoS ONE* **2011**, *6*, e23267. [[CrossRef](#)] [[PubMed](#)]
26. Schmalhofer, O.; Brabletz, S.; Brabletz, T. E-cadherin, β -catenin, and ZEB1 in malignant progression of cancer. *Cancer Metast. Rev.* **2009**, *28*, 151–166. [[CrossRef](#)]
27. Liu, T.; Yu, J.; Ge, C.; Zhao, F.; Miao, C.; Jin, W.; Su, Y.; Geng, Q.; Chen, T.; Xie, H. B-Cell Receptor-Associated Protein 31 Promotes Metastasis via AKT/ β -Catenin/Snail Pathway in Hepatocellular Carcinoma. *Front. Mol. Biosci.* **2021**, *8*, 278. [[CrossRef](#)]
28. Ding, Y.; Lv, C.; Zhou, Y.; Zhang, H.; Zhao, L.; Xu, Y.; Fan, X. Vimentin loss promotes cancer proliferation through up-regulating Rictor/AKT/ β -catenin signaling pathway. *Exp. Cell Res.* **2021**, *405*, 112666. [[CrossRef](#)]
29. Shelke, G.V.; Lässer, C.; Ghossein, Y.S.; Lötvall, J. Importance of exosome depletion protocols to eliminate functional and RNA-containing extracellular vesicles from fetal bovine serum. *J. Extracell. Vesicles* **2014**, *3*, 24783. [[CrossRef](#)]
30. Paudel, K.R.; Kim, D.-W. Microparticles-mediated vascular inflammation and its amelioration by antioxidant activity of baicalin. *Antioxidants* **2020**, *9*, 890. [[CrossRef](#)]
31. Paudel, K.R.; Mehta, M.; Yin, G.H.S.; Yen, L.L.; Malyla, V.; Patel, V.K.; Panneerselvam, J.; Madheswaran, T.; MacLoughlin, R.; Jha, N.K. Berberine-loaded liquid crystalline nanoparticles inhibit non-small cell lung cancer proliferation and migration in vitro. *Environ. Sci. Pollut. Res.* **2022**, *29*, 46830–46847. [[CrossRef](#)]
32. Wu, F.; Yin, Z.; Yang, L.; Fan, J.; Xu, J.; Jin, Y.; Yu, J.; Zhang, D.; Yang, G. Smoking Induced Extracellular Vesicles Release and Their Distinct Properties in Non-Small Cell Lung Cancer. *J. Cancer* **2019**, *10*, 3435–3443. [[CrossRef](#)]
33. Jaiswal, R.; Johnson, M.S.; Pokharel, D.; Krishnan, S.R.; Bebawy, M. Microparticles shed from multidrug resistant breast cancer cells provide a parallel survival pathway through immune evasion. *BMC Cancer* **2017**, *17*, 104. [[CrossRef](#)]
34. Zhou, F.Q.; Qi, Y.M.; Xu, H.; Wang, Q.Y.; Gao, X.S.; Guo, H.G. Expression of EpCAM and Wnt/ β -catenin in human colon cancer. *Genet. Mol. Res.* **2015**, *14*, 4485–4494. [[CrossRef](#)]
35. Singh, G.; Hossain, M.M.; Bhat, A.Q.; Ayaz, M.O.; Bano, N.; Eachkoti, R.; Dar, M.J. Identification of a cross-talk between EGFR and Wnt/beta-catenin signaling pathways in HepG2 liver cancer cells. *Cell Signal* **2021**, *79*, 109885. [[CrossRef](#)]
36. Zhou, J.; Jiang, J.; Wang, S.; Xia, X. DKK1 inhibits proliferation and migration in human retinal pigment epithelial cells via the Wnt/ β -catenin signaling pathway. *Exp. Ther. Med.* **2016**, *12*, 859–863. [[CrossRef](#)]
37. Sant’ana, J.M.; Chammas, R.; Liu, F.T.; Nonogaki, S.; Cardoso, S.V.; Loyola, A.M.; de Faria, P.R. Activation of the Wnt/beta-catenin signaling pathway during oral carcinogenesis process is not influenced by the absence of galectin-3 in mice. *Anticancer Res.* **2011**, *31*, 2805–2811.
38. Zhang, X.; Yang, M.; Shi, H.; Hu, J.; Wang, Y.; Sun, Z.; Xu, S. Reduced E-cadherin facilitates renal cell carcinoma progression by WNT/ β -catenin signaling activation. *Oncotarget* **2017**, *8*, 19566–19576. [[CrossRef](#)]
39. Wu, T.; Duan, X.; Hu, T.; Mu, X.; Jiang, G.; Cui, S. Effect of endostatin on Wnt pathway of stem-like cells in bladder cancer in tumor microenvironment. *Mol. Biol. Rep.* **2020**, *47*, 3937–3948. [[CrossRef](#)]
40. Wang, X.; Zhu, Y.; Sun, C.; Wang, T.; Shen, Y.; Cai, W.; Sun, J.; Chi, L.; Wang, H.; Song, N. Feedback activation of basic fibroblast growth factor signaling via the Wnt/ β -catenin pathway in skin fibroblasts. *Front. Pharmacol.* **2017**, *8*, 32. [[CrossRef](#)]
41. Yang, S.; Liu, Y.; Li, M.-Y.; Ng, C.S.; Yang, S.-I.; Wang, S.; Zou, C.; Dong, Y.; Du, J.; Long, X. FOXP3 promotes tumor growth and metastasis by activating Wnt/ β -catenin signaling pathway and EMT in non-small cell lung cancer. *Mol. Cancer* **2017**, *16*, 1–12. [[CrossRef](#)] [[PubMed](#)]
42. Tian, R.; Li, Y.; Yao, X. PGRN Suppresses Inflammation and Promotes Autophagy in Keratinocytes Through the Wnt/ β -Catenin Signaling Pathway. *Inflammation* **2016**, *39*, 1387–1394. [[CrossRef](#)] [[PubMed](#)]

43. Jachin, S.; Bae, J.S.; Sung, J.J.; Park, H.S.; Jang, K.Y.; Chung, M.J.; Kim, D.G.; Moon, W.S. The role of nuclear EpICD in extrahepatic cholangiocarcinoma: Association with β -catenin. *Int. J. Oncol.* **2014**, *45*, 691–698. [[CrossRef](#)]
44. Warneke, V.; Behrens, H.; Haag, J.; Krüger, S.; Simon, E.; Mathiak, M.; Ebert, M.; Röcken, C. Members of the EpCAM signalling pathway are expressed in gastric cancer tissue and are correlated with patient prognosis. *Br. J. Cancer* **2013**, *109*, 2217–2227. [[CrossRef](#)]
45. Denzel, S.; Maetzel, D.; Mack, B.; Eggert, C.; Bähr, G.; Gires, O. Initial activation of EpCAM cleavage viacell-to-cell contact. *BMC Cancer* **2009**, *9*, 402. [[CrossRef](#)] [[PubMed](#)]
46. Zhang, D.; Bi, J.; Liang, Q.; Wang, S.; Zhang, L.; Han, F.; Li, S.; Qiu, B.; Fan, X.; Chen, W.; et al. VCAM1 Promotes Tumor Cell Invasion and Metastasis by Inducing EMT and Transendothelial Migration in Colorectal Cancer. *Front. Oncol.* **2020**, *10*, 1066. [[CrossRef](#)]
47. Wegwitz, F.; Lenfert, E.; Gerstel, D.; von Ehrenstein, L.; Einhoff, J.; Schmidt, G.; Logsdon, M.; Brandner, J.; Tiegs, G.; Beauchemin, N.; et al. CEACAM1 controls the EMT switch in murine mammary carcinoma in vitro and in vivo. *Oncotarget* **2016**, *7*, 63730–63746. [[CrossRef](#)]
48. Bui, T.M.; Wiesolek, H.L.; Sumagin, R. ICAM-1: A master regulator of cellular responses in inflammation, injury resolution, and tumorigenesis. *J. Leukoc. Biol.* **2020**, *108*, 787–799. [[CrossRef](#)]
49. Basu, S.; Cheriyaundath, S.; Ben-Ze'ev, A. Cell-cell adhesion: Linking Wnt/ β -catenin signaling with partial EMT and stemness traits in tumorigenesis. *F1000Research* **2018**, *7*. [[CrossRef](#)]
50. Wong, S.H.M.; Fang, C.M.; Chuah, L.H.; Leong, C.O.; Ngai, S.C. E-cadherin: Its dysregulation in carcinogenesis and clinical implications. *Crit. Rev. Oncol. Hematol.* **2018**, *121*, 11–22. [[CrossRef](#)]
51. Satelli, A.; Li, S. Vimentin in cancer and its potential as a molecular target for cancer therapy. *Cell Mol. Life Sci.* **2011**, *68*, 3033–3046. [[CrossRef](#)]
52. Wang, Y.; Shi, J.; Chai, K.; Ying, X.; Zhou, B.P. The Role of Snail in EMT and Tumorigenesis. *Curr. Cancer Drug Targets* **2013**, *13*, 963–972. [[CrossRef](#)]
53. Valenta, T.; Hausmann, G.; Basler, K. The many faces and functions of β -catenin. *EMBO J.* **2012**, *31*, 2714–2736. [[CrossRef](#)]
54. Le Bras, G.F.; Taubenslag, K.J.; Andl, C.D. The regulation of cell-cell adhesion during epithelial-mesenchymal transition, motility and tumor progression. *Cell Adh. Migr.* **2012**, *6*, 365–373. [[CrossRef](#)]

Disclaimer/Publisher's Note: The statements, opinions and data contained in all publications are solely those of the individual author(s) and contributor(s) and not of MDPI and/or the editor(s). MDPI and/or the editor(s) disclaim responsibility for any injury to people or property resulting from any ideas, methods, instructions or products referred to in the content.

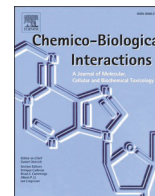
3) Literature Review: Short Chain Fatty Acids: Fundamental mediators of the gut-lung axis and their involvement in pulmonary diseases

Status: Published in the journal **Chemico-Biological Interactions**

Citation: Ashique S[#], **De Rubis G**[#], Sirohi E, Mishra N, Rihan M, Garg A, Reyes RJ, Manandhar B, Bhatt S, Jha NK, Singh TG, Gupta G, Singh SK, Chellappan DK, Paudel KR, Hansbro PM, Oliver BG, Dua K. *Short Chain Fatty Acids: Fundamental mediators of the gut-lung axis and their involvement in pulmonary diseases*. **Chemico-Biological Interactions**. 2022 Dec 1;368:110231. doi: 10.1016/j.cbi.2022.110231.

[#] = authors have contributed equally to this work

Contribution: In this review, I am involved as co-first author together with Sumel Ashique. Mr Ashique and I wrote this review in conjunction and coordinated the revision process.



Review Article

Short Chain Fatty Acids: Fundamental mediators of the gut-lung axis and their involvement in pulmonary diseases

Sumel Ashique^{a,1}, Gabriele De Rubis^{b,c,1}, Ekta Sirohi^a, Neeraj Mishra^d, Mohd Rihan^e, Ashish Garg^f, Ruby-Jean Reyes^g, Bikash Manandhar^{b,c}, Shvetank Bhatt^h, Niraj Kumar Jha^{i,j,k}, Thakur Gurjeet Singh^l, Gaurav Gupta^{m,n,o}, Sachin Kumar Singh^{b,p}, Dinesh Kumar Chellappan^q, Keshav Raj Paudel^r, Philip M. Hansbro^{r,s}, Brian G. Oliver^{s,t}, Kamal Dua^{b,c,*}

^a Department of Pharmacy, Bharat Institute of Technology (BIT), School of Pharmacy, Meerut, UP 250103, India

^b Discipline of Pharmacy, Graduate School of Health, University of Technology Sydney, NSW 2007, Australia

^c Faculty of Health, Australian Research Centre in Complementary and Integrative Medicine, University of Technology Sydney, Ultimo, Australia

^d Department of Pharmaceutics, Amity Institute of Pharmacy, Amity University Madhya Pradesh (AUMP), Gwalior, MP 474005, India

^e Department of Pharmacology, National Institute of Pharmaceutical Education and Research (NIPER), S.A.S. Nagar, Punjab 160062, India

^f Department of P.G. Studies and Research in Chemistry and Pharmacy, Rani Durgavati University, Jabalpur, MP 482001, India

^g Faculty of Health, University of Technology Sydney, Ultimo, Australia

^h School of Pharmacy, Dr. Vishwanath Karad MIT World Peace University, Pune-411038, Maharashtra, India

ⁱ Department of Biotechnology, School of Engineering & Technology (SET), Sharda University, Greater Noida, Uttar Pradesh 201310, India

^j Department of Biotechnology, School of Applied & Life Sciences (SALS), Uttarakhand University, Dehradun 248007, India

^k Department of Biotechnology Engineering and Food Technology, Chandigarh University, Mohali, 140413, India

^l Chitkara College of Pharmacy, Chitkara University, 140401, Punjab, India

^m School of Pharmacy, Suresh Gyan Vihar University, Jaipur, Rajasthan, India

ⁿ Department of Pharmacology, Saveetha Dental College, Saveetha Institute of Medical and Technical Sciences, Saveetha University, Chennai, India

^o Uttarakhand Institute of Pharmaceutical Sciences, Uttarakhand University, Dehradun, India

^p School of Pharmacy and Pharmaceutical Science, Lovely Professional University, India

^q Department of Life Sciences, School of Pharmacy, International Medical University, Bukit Jalil, Kuala Lumpur 57000, Malaysia

^r Centre for Inflammation, Centenary Institute and University of Technology Sydney, Faculty of Science, School of Life Sciences, Sydney, NSW 2007, Australia

^s School of Life Sciences, University of Technology Sydney, Ultimo, NSW 2007, Australia

^t Woolcock Institute of Medical Research, University of Sydney, Sydney, New South Wales, Australia



ARTICLE INFO

Keywords:

Short-chain fatty acids
Gut microbiota metabolites
Gut-lung axis
Respiratory diseases
Potential therapeutics

ABSTRACT

The human microbiota is fundamental to correct immune system development and balance. Dysbiosis, or microbial content alteration in the gut and respiratory tract, is associated with immune system dysfunction and lung disease development. The microbiota's influence on human health and disease is exerted through the abundance of metabolites produced by resident microorganisms, where short-chain fatty acids (SCFAs) represent the fundamental class. SCFAs are mainly produced by the gut microbiota through anaerobic fermentation of dietary fibers, and are known to influence the homeostasis, susceptibility to and outcome of many lung diseases. This article explores the microbial species found in healthy human gastrointestinal and respiratory tracts. We investigate factors contributing to dysbiosis in lung illness, and the gut-lung axis and its association with lung diseases, with a particular focus on the functions and mechanistic roles of SCFAs in these processes. The key focus of this review is a discussion of the main metabolites of the intestinal microbiota that contribute to host-pathogen interactions: SCFAs, which are formed by anaerobic fermentation. These metabolites include propionate, acetate, and butyrate, and are crucial for the preservation of immune homeostasis. Evidence suggests that SCFAs prevent infections by directly affecting host immune signaling. This review covers the various and intricate ways through which SCFAs affect the immune system's response to infections, with a focus on pulmonary diseases including chronic obstructive pulmonary diseases, asthma, lung cystic fibrosis, and tuberculosis. The findings reviewed

* Corresponding author. Discipline of Pharmacy, Graduate School of Health, University of Technology Sydney, NSW, 2007, Australia.

E-mail address: kamal.dua@uts.edu.au (K. Dua).

¹ These two authors contributed equally.

suggest that the immunological state of the lung may be indirectly influenced by elements produced by the gut microbiota. SCFAs represent valuable potential therapeutic candidates in this context.

Abbreviations

ACE2	Angiotensin-Converting Enzyme 2	SCFAs	short-chain fatty acids
ARDS	acute respiratory distress syndrome	TB	Tuberculosis
BALF	bronchoalveolar lavage fluid	TNF- α	Tumor necrosis factor-alpha
CF	Cystic Fibrosis	AHR	Aryl-hydrocarbon receptor
COPD	Chronic Obstructive Lung Disease	TMPRSS2	Transmembrane protease, serine 2
CXCL10	C-X-C motif chemokine ligand 10	Treg	Regulatory T Lymphocyte
DC	Dendritic Cell	VLCKD	very-low-calorie ketogenic diet
FFA	Free Fatty Acid	P-gp	P-glycoprotein
GIT	gastrointestinal tract	SMCT	Sodium-bound Monocarboxylate Transporter
GPCR	G-protein Coupled Receptor	ICSs	Inhaled corticosteroids
HDAC	Histone deacetylase	LTD4	Leukotriene D4
ILCs	Innate Lymphoid Cells	ADR- β 2	Adrenoceptor β 2
IL-x	Interleukin x	AR	adrenergic receptor
LPS	lipopolysaccharide	GR	glucocorticoid receptor
MACs	microbiota-accessible carbohydrates	LABA	long-acting β -agonist
MCT	Monocarboxylate Transporter	LAMA	long-acting muscarinic receptor antagonists
NF- κ B	Nuclear Factor-kappa B	SABA	short-acting β -agonists
PPAR γ	peroxisome proliferator-activated receptor-gamma	SAMA	short-acting muscarinic receptor antagonists
		OR51E2	Olfactory receptor 51E2

1. - Introduction

The human gut flora plays an important role for maintaining the body's immune system. This includes shielding from inflammatory states during viral infections of the mucosae. Metabolites produced by the gut flora have fundamental roles in the response to acute and chronic diseases, as these molecules alter the immunological activities occurring in many organs including the lungs and the brain [1,2].

The microbiota is made up of living microorganisms located inside or on the surface of the body. The skin and mucosal tissues such as the pulmonary, vaginal, oral, nasal, and importantly, gastrointestinal mucosa, are colonized by trillions of viruses, fungi, and bacteria, which live in symbiotic association with the host. In the gastrointestinal tract (GIT), these species reach exceptional densities for mutual benefit with the host organism [1,2]. Within the GIT, and in particular the colon, small chain fatty acids (SCFAs) such as acetate, propionate, and butyrate, are produced by bacterial fermentation of dietary fibers, and are fundamental mediators of the communication between the gut and the brain within the gut-brain axis [3].

Despite its fundamental role in human health, the gut microbiota has seen an increase of interest in research only in the last 20 years. The microbiota collaborates with the host system to maintain tissue and immunological homeostasis, carrying out a variety of beneficial functions for the body, including the production of metabolites through fermentation of dietary components. Furthermore, the gut microbiota has a pivotal role in warding off infections, modulating metabolic, endocrine, and immune systems, and influencing drug absorption and metabolism [4]. The importance of the gut microbiota's influence on local health homeostasis, as well as its influence on illnesses, is recently becoming more well-known [5]. Historically, of the many existing inter-organ relations, the gut-brain axis has been more widely investigated than the new and emerging research interest of the gut-lung axis. Although the role of SCFAs produced in the gut in the modulation of neurochemical pathways through the gut-brain axis has been thoroughly characterized [3], little is known about the role of these molecules in the gut-lung axis. In this review, we will discuss the fundamental

role of the gut microbiome in influencing respiratory diseases through the gut-lung axis. In particular, considering the regulatory function of SCFAs in the gut-brain axis [3], we showcase the current knowledge on the effects of SCFAs in many lung diseases including influenza, COVID-19, cystic fibrosis, tuberculosis, asthma, Chronic Obstructive Pulmonary Disease (COPD) and lung cancer.

Previous studies demonstrating a link between altered gut microbiota and airway illness provided the first proof of gut-lung cross talk. Greater vulnerability to allergies and lung infections was linked to the dysbiosis caused by the use of antibiotics or by chronic illness [6]. Because respiratory infections have such a significant global impact on morbidity and mortality, it is crucial to comprehend the corresponding susceptibility mechanisms with the aim of developing novel, more potent treatments. According to the most recent studies, SCFAs reduce the frequency and severity of lung infections. The mechanisms of action by which SCFAs exert these actions are quite complicated, and depending on the circumstances, their effects might vary greatly. For the creation of suitable pharmacological methods based on, for instance, Free Fatty Acid Receptor (FFAR) agonism, a deeper understanding of the biological characteristics of SCFAs is required [7]. SCFAs are potential therapeutic candidates in this context. Patients who suffer from digestive system issues have lower SCFA levels and are more likely to develop lung conditions [8]. However, there is disagreement about the origin, levels, and immediate effects of SCFAs on the lungs. Only a few studies have demonstrated that the lung microbiota can synthesize SCFAs, and the majority of study data points to the gut microbiota as the main source of SCFA production. As a result of (i) insufficient substrates, and (ii) the scarce presence of SCFAs in the lungs, Trompette and colleagues hypothesized that lung-resident bacteria do not significantly contribute to the formation of SCFAs [9]. Therefore, SCFAs made by the gut microbiota are capable of exerting systemic effects, particularly on circulating immune cells or bone marrow progenitor cells which then, directly and indirectly, affect the lung compartment. SCFAs have a wide spectrum of immunomodulatory properties and have frequently been examined in the context of lung infections. Furthermore, intestinal inflammation is decreased and the integrity of the intestinal barrier is increased by the microbial synthesis of SCFAs, notably butyrate, in the

gut, thus reducing leakage and bacterial translocation [10].

2. - The gut-lung axis

The gut-lung axis, represented in Fig. 1, is defined as the interrelation between the two organ systems in immunological homeostasis and the physiological mechanisms through which this influences disease susceptibility, and is influenced by the health and functioning status of the intestinal microbiota. Each person's metabolic phenotype is modulated by their specific microbiome's composition, which in turn has a significant impact on biochemistry and disease susceptibility [11]. The host's systemic immunity and competence to moderate or control inflammation is affected by the gut microbiota composition [12]. For example, intestinal dysbiosis mediates pulmonary immune response dysregulation, with concomitant activation of inflammatory mediators such as T cells, eventually resulting in increased mortality from respiratory infections [13]. This immune dysregulation can be caused by microbial compounds absorbed from the gut mucosal tissue, which are transported in the lungs and bind to pulmonary receptors, resulting in the activation of immune cells [14].

2.1. - The gut-lung axis, the gut microbiome, SCFAs and respiratory ailments

Despite their physical distinction, the gastrointestinal and respiratory tracts have a common embryogenesis and many structural similarities, suggesting that the two locations, although separated, may interact in a variety of ways. Both the gut and the lungs, which have strong mucosal defensive systems against germs, exhibit similar microbial colonization properties in the early stages of life. The gut-lung axis represents the interactions between the gut and lungs, as many studies have revealed that the intestines and lungs communicate with one another via microbial and immunological processes to accomplish a two-way, reciprocal control [15]. The human microbiome's commensal bacterial mass is mainly concentrated in the gut, and in particular in the colon. These microorganisms produce a plethora of metabolites that function in aiding the digestion process, and also modulate the immune

system, thereby indirectly influencing inflammation. These metabolites are capable of exerting systemic effects because they are absorbed by the GIT and can easily reach circulation [16]. There is a bidirectional connection occurring between the lungs and the digestive tract known as the gut-lung axis [17]. This axis is associated with lung diseases, these are known to impact the digestive system and vice versa [18,19]. This inter-organ connection is enabled by the gut microbiome [20] which, through anaerobic fermentation of dietary fibers such as resistant starch, pectin, and cellulose [21], produces a multitude of metabolites, particularly SCFAs. The SCFAs are anti-inflammatory chemicals embedded with immunomodulatory functions including inhibition of chemotaxis and adhesion of immune cells, as well as induction of the expression of anti-inflammatory cytokines and stimulation of apoptosis in immune cells [22]. SCFA concentrations are reduced in individuals with intestinal problems, rendering them more susceptible to lung ailments [23]. This makes SCFAs potential medication candidates in this context. It is well known that SCFAs produced in the gut are able to reach systemic circulation and are transported to different organs [24]. Nevertheless, considering the lung microbiome's fundamental role in regulating the innate immune responses associated with chronic lung diseases [25], the production of SCFAs directly from the lung microbiota cannot be completely ruled out. The multifaceted role of SCFAs in lung immunology is summarized in Fig. 2.

3. - Immunomodulatory mechanisms of action of SCFAs and interplay between receptors

The fundamental role of SCFAs is to reduce intestinal pH and promote mucin synthesis, therefore preventing the development and adhesion of harmful bacteria, enhancing epithelial integrity, and enhancing host systemic immunity [26]. SCFAs may increase the number and functioning of T regulatory (Treg), T helper (Th) 1, and Th17 effector cells by inhibiting histone deacetylase enzymes (HDACs), hence reducing excessive inflammatory and immunological responses in gastrointestinal and airway diseases [27,28]. SCFAs may access the systemic circulation via both passive diffusion and active transport [29], the latter being mediated notably by transporters such as

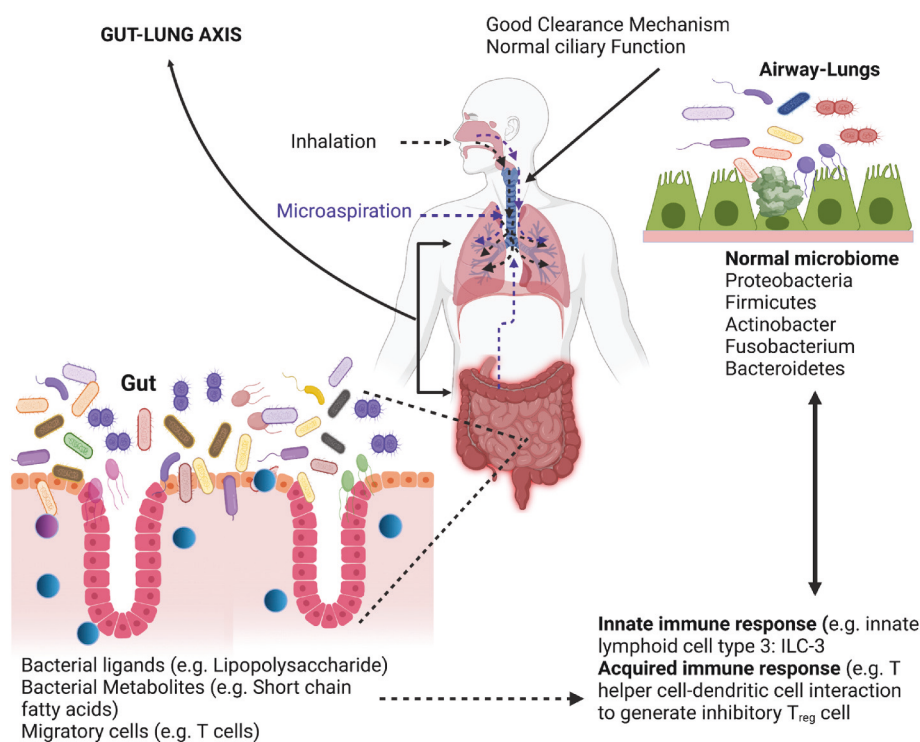


Fig. 1. - The gut-lung axis. Through the exposure of structural ligands such as lipopolysaccharide (LPS) and/or peptidoglycan and the production of secreted metabolites such as short-chain fatty acids (SCFAs), a healthy gut microbiota supports homeostatic local immune responses. Circulating lymphocytes' activity is affected by ingested metabolites and invader microbes, which helps control systemic immune responses. The usual microbiota-derived signals are altered when the gut microbiota is disrupted, such as during an illness or antibiotic exposure, and this impacts the immune response. Dysbiosis of the gut microbiota in adults can result in systemic inflammation and the proliferation of opportunistic infections, which can induce chronic inflammation at distal locations. This can happen, for instance, as a result of exposure to tobacco smoke. These general principles describe the function of the microbiota in the gut-lung crosstalk.

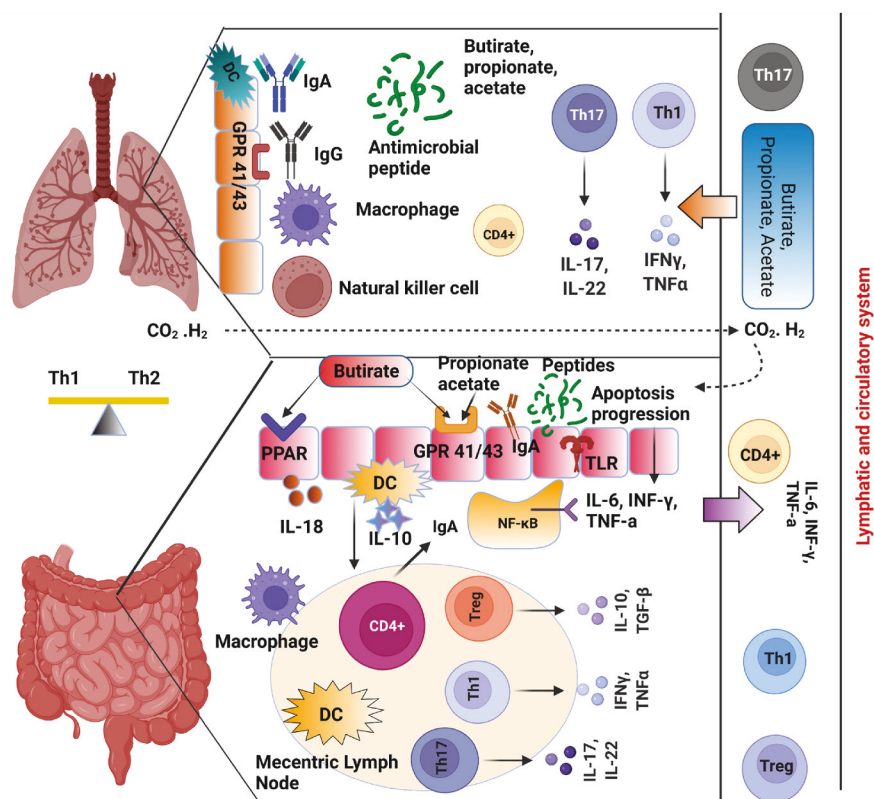


Fig. 2. Paradigm: Regulating role of SCFAs in lung immunology.

GPR43 and GPR41 are G-protein coupled receptors responsive to butyrate, propionate, and acetate. Butyrate also interacts with GPR109A or peroxisome proliferation activating receptors (PPAR- γ). All the SCFAs modulate the activity of Treg lymphocytes, impacting the production and release of regulatory cytokines (IL-10, TGF- α , INF- γ , IL-6), via influencing the activity of the transcription factor NF- κ B on dendritic cells (DC). The gut-lungs axis is interlinked thanks to the circulation of regulating cytokines, as well as SCFAs, between the gut and the lungs. This messenger circulation occurs via the blood and lymphatic systems. Reduction in SCFAs correlates to the activation of Th-2 cells, which is accompanied by a rise, in particular, of IgE levels, as well as the activation of mast cells, and basophils, and eosinophils. As a consequence of these factors, bronchial hyper-reactivity or asthma will develop.

monocarboxylate transporter 1 and 4 (MCT1, MCT4) and sodium-bound monocarboxylate transporter 1 and 2 (SMCT1, SMCT2) [30].

SCFAs have been shown to interact with distinct receptors, including the G-protein-coupled receptors (GPCRs) GPR43 and GPR41, also referred to as FFA2 or FFA3 respectively [31], as well as GPR109a [32]. Immune cells, including lymphocytes, monocytes, and neutrophils, specifically exhibit GPR43 [33], while GPR41 is more widely expressed in many tissues, including adipose tissue, pancreas, spleen, and lymph nodes [26,28], with different SCFAs having different affinities for the two receptors [28]. Another important biological action of SCFAs is that of HDAC inhibitors, which is particularly exerted by butyrate [34,35]. HDAC inhibition in turn suppresses lipopolysaccharide (LPS)-induced nitric oxide synthesis via inducible Nitric Oxide Synthase (iNOS) and the release of LPS-induced proinflammatory cytokines (IL-6, IL-12) [30,36]. Furthermore, the anti-inflammatory effect of butyrate is linked to a decrease in the activity of the Nuclear Factor-kappa B (NF- κ B) signaling pathway, coupled with the stimulation of the production of anti-inflammatory cytokines such as IL-10 by mononuclear cells such as neutrophils [29,30,37]. SCFAs have anti-inflammatory and immunomodulatory attributes, and they are involved in the recruitment, differentiation and activation of neutrophils, dendritic cells (DCs), monocytes, macrophages and T cells [38]. SCFAs inhibit dendritic cells, macrophages, and monocytes maturation by suppressing their ability to recognize antigens and generate pro-inflammatory cytokines including IL-12 and TNF- α [38]. Further studies demonstrated that SCFAs can have either anti-inflammatory or pro-inflammatory effects on lung cells, depending on the type of cells tested or the SCFA concentration. This suggests that, based on the cell type and the specific chemical environment, SCFAs can serve as pro- or anti-inflammatory chemicals [39].

Finally, SCFA synthesis induced by high-fiber intake has been shown to influence bone marrow hematopoiesis, speeding up the production of macrophages and DC precursors and then seeding the lungs with highly phagocytic DCs [23,40]. By decreasing immune cell migration and

proliferation, various types of cytokines, and causing apoptosis, SCFAs may reduce inflammation. All the studies mentioned in this section so far showcase the potent anti-inflammatory properties of SCFAs. Further to this, it is believed that illnesses connected to immunological and metabolic abnormalities are caused by significant variations in SCFA concentrations in blood or different organs. For this reason, gut microorganisms may have both positive and negative impacts on health. In order to prevent and treat diseases through the administration of SCFAs, it may be crucial to determine the right SCFA concentrations required to maintain a normal immune system and metabolism [41]. Among SCFAs, butyric acid is particularly renowned for its anti-inflammatory activity, as it alleviates excessive inflammation and lowers oxidative stress levels in a variety of diseases, including respiratory viral infections [42]. It is interesting to note that short-chain fatty acids (SCFAs) can have opposing pro- and anti-inflammatory effects on the host's inflammatory response. This is caused by the fact that SCFAs have various binding receptors. According to a study, SCFAs target the activation of free fatty acid receptors (FFARs) 2 and 3 on macrophages and neutrophils to reduce the expression of IL-8 during airway inflammation, which helps the host's health. The receptors GPR43, GPR41, GPR109a, and OR51E2 are all stimulated by SCFAs. In this sense, propionate, acetate, and butyrate are typically the activators of GPR43. Furthermore, butyrate and propionate are capable of activating GPR41 [43]. Acetate and propionate are known to stimulate the Olfr-78 receptor, while butyrate and hydroxybutyrate can activate the GPR109a receptor [44]. Angiotensin-like protein 4 (ANGPTL4/FIAF), which is involved in controlling lipid metabolism in gut bacteria and accumulation of adipose tissue in intestinal adenocarcinoma, is also stimulated by SCFAs, and it plays a role in the activation of peroxisome proliferator-activated receptors γ (PPAR- γ) [45]. Adipocytes, immunological cells, and gut epithelial cells are the main cell types that express GPR43. The lymph node cells, adipocytes, splenocytes, big intestinal lamina propria cells, bone marrow cells, peripheral nervous system, and polymorphonuclear

leukocytes are just a few of the human cells that express GPR41. Dendritic cells, macrophages, monocytes, and neutrophils are immune cells that reside in intestinal epithelial cells and express GPR109a [46]. SCFA-sensing GPRs regulate everything from metabolism to the immune system and neuronal signaling. To understand how these receptors specifically interact within cells, more research is needed. Due to the high levels of SCFA in the intestine, it is anticipated that these receptors will be highly activated in intestinal tissues. By stimulating the FFAR pathway, the SCFA acetate also prevents mouse and human monocytes from secreting tumor necrosis factor (TNF) after exposure to LPS [47]. The SCFA butyrate reduces the levels of pro-inflammatory factors (inducible NOS, TNF, MCP-1, and IL-6) in macrophages by interacting with and activating the free fatty acid receptor 3 (FFAR3/GPR41). These findings suggest that the potent anti-inflammatory properties of SCFAs are mainly reliant on free fatty acids 2 and 3 receptors (FFAR2/3). Their agonist activity on FFAR2 and FFAR3 receptors is the rationale for the potential of SCFAs as pharmacological treatment [48]. Table 1 summarizes the main receptors for SCFAs, their tissues of expression, and their functions [49–54].

4. - SCFAs: protective role against COPD

The presence of SCFAs in sputum provides confirmation of the presence of a connection between the gut and the lungs [55,56]. In this context, it is worth noting that SCFAs can modulate metabolic programming in LPS-exposed alveolar macrophages, which assists in the maintenance of the lung immunometabolism [57]. COPD is characterized by defective epithelial barrier function in the bronchial epithelium, leading, among many issues, to progressive airflow limitation [58]. COPD's main risk factor is cigarette smoke exposure, which causes substantial impairment of tight junction integrity in the lung [59]. In a recent study, the SCFAs propionate and butyrate were shown to restore the barrier function of human bronchial airway epithelial cells compromised by house dust mite [60]. This underlines potential clinical applications of SCFAs in restoring bronchial epithelial functionality in diseases such as COPD [61]. In an *in vivo* study, increased cecal levels of SCFAs caused by a whey peptide-based enteral diet were correlated to attenuation of emphysema, one of the pathological hallmarks of COPD [62]. In general, considering the strong link between diet and gut microbiome composition, and the important role of the gut microbiome in the production of SCFAs, the nature of nutrition and relative SCFA abundance has been hypothesized to be linked with the development of the clinically heterogeneous course of COPD. In a recent study, the composition of the gut microbiome of COPD patients has been compared with that of healthy volunteers, and a *Prevotella*-dominated gut enterotype, associated with relatively lower fecal levels of SCFAs, was observed in COPD patients [63]. Furthermore, in the same study, overall lower levels of SCFAs were determined in Stage III-IV COPD compared to Stage I-II COPD and healthy volunteers [64]. Consistent with this, another study reported higher levels of SCFAs in the breath condensate

of COPD patients compared to healthy volunteers [65]. Finally, Mao et al. showed, in an *in vivo* study in rats with COPD induced by cigarette smoke exposure and LPS injection, that the Bufe Jianpi formula, a traditional Chinese medicine, altered the gut microbiota composition, resulting in increased SCFA levels. This was correlated with improved pulmonary function and reduced lung inflammation [65]. These studies collectively highlight a protective role of SCFAs against COPD, which is summarized in Fig. 3.

5. - SCFAs: potential role in reducing asthma

SCFAs have been identified as a crucial connection between gut microbiota, nutrition, and asthma etiology [66]. As a consequence, SCFAs have emerged as intriguing therapeutic candidates for the reduction of pro-inflammatory reactions in the lungs in asthma [67]. The effects of SCFAs in lung infections are summarized in Fig. 4. Many gut microbial metabolites serve as important modulators of the interplay between gut microbiota composition alterations and variation of host epigenetic markers [68]. In particular, SCFAs generated by the gut microbiota are known to act as epigenetic modulators through the induction of variations in DNA methylation as well as histone modifications [69]. SCFAs are known to regulate the host's immunological homeostasis, which is required for the recruitment and/or growth of colonic regulatory T cells (Tregs) [70]. Treg malfunction contributes to the collapse of the immune system's ability to regulate an overactive Th2 response, which can progress to allergic asthma [71]. Butyrate enhances Treg and DC differentiation by engaging GPCRs such as FFA receptors (FFA2 & FFA3), thus exerting its activity as HDAC inhibitor [72]. Furthermore, butyrate alleviates gut inflammation by limiting NF- κ B-mediated B-cell activation in the intestine or triggering expression modulation of peroxisome proliferator-activated receptor-gamma (PPAR γ) [73]. Butyrate was found to exert anti-asthma activity by blocking the production of GATA binding protein 3 (GATA3) and other pro-inflammatory cytokines in human lung Group 2 innate lymphoid cells (ILCs) [74]. Many host activities, including fetal immunological development, are influenced by the transplacental action of gut bacterial metabolites. These metabolites operate as vital mediators of the host homeostasis, modulating functions including immunological regulation, inflammation, epigenetic alterations, and energy generation [75,76]. A significant category of metabolites implicated in immune regulation, SCFAs produced from microbiota-accessible carbohydrates (MACs), has received a lot of study interest. T cells are indirectly influenced by short-chain fatty acids generated by maternal gut bacteria to create a tolerogenic immunological milieu in the offspring. GPR41/FFA3, GPR43/FFA2, and GPR109a are the three G protein-coupled receptors that SCFAs bind to. By interacting with GPR43 and directly inhibiting HDAC, SCFAs have an apoptotic effect on neutrophils and eosinophils [32]. Butyrate and propionate have been demonstrated to modulate dendritic cell activity individually by reducing T lymphocyte activation [77]. The same route was discovered to be active in colonic

Table 1
Identified receptors for short-chain fatty acids.

Receptor	Ligand	Location	Function after activation	Ref
GPR41 (free fatty acid receptor 3, FFAR3)	acetate, propionate, butyrate	large intestine lamina propria cells, spleen cells, lymph nodes, bone marrow, adipocytes	metabolism, inflammation and immunity	[49]
GPR43 (free fatty acid receptor 2, FFAR2)	acetate, propionate, butyrate	digestive tract epithelial cells, immune system cells, adipocytes in adipose tissue	metabolism, inflammation and immunity	[50]
GPR109A (hydroxycarboxylic acid receptor 2, HCA2)	niacin, ketone bodies, β -hydroxybutyric acids, butyrate	Large intestinal epithelium, macrophages, monocytes, dendritic cells, neutrophils, and adipocytes	metabolism, cancer and immunity	[51]
GPR109A (hydroxycarboxylic acid receptor 2, HCA2)	acetate, propionate	neurons, enteroendocrine cells, the epithelium of the large intestine, renal arteries, smooth muscles of blood vessels	Regulating blood pressure	[52]
PPAR γ (Peroxisome proliferator-activated receptors γ)	propionate, butyrate	large intestine adenocarcinoma cells	Stimulate the synthesis of angiotensin-like protein	[53]
Aryl-hydrocarbon receptor (AHR)	butyrate	Treg, dendritic cells, stem Cells, Breg	Immunity	[54]

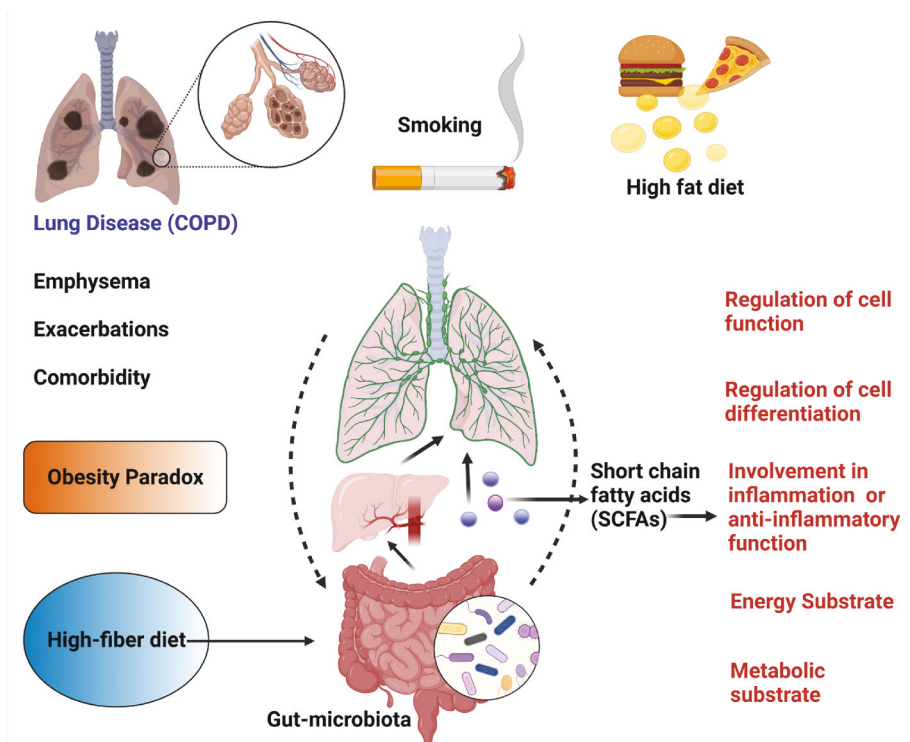


Fig. 3. - Role of SCFAs in COPD. Short-chain fatty acids are revealed to be involved in biological processes connected to chronic obstructive pulmonary disease (COPD), exerting a protective effect against the main COPD features. These effects are mediated by the known anti-inflammatory effect of SCFAs.

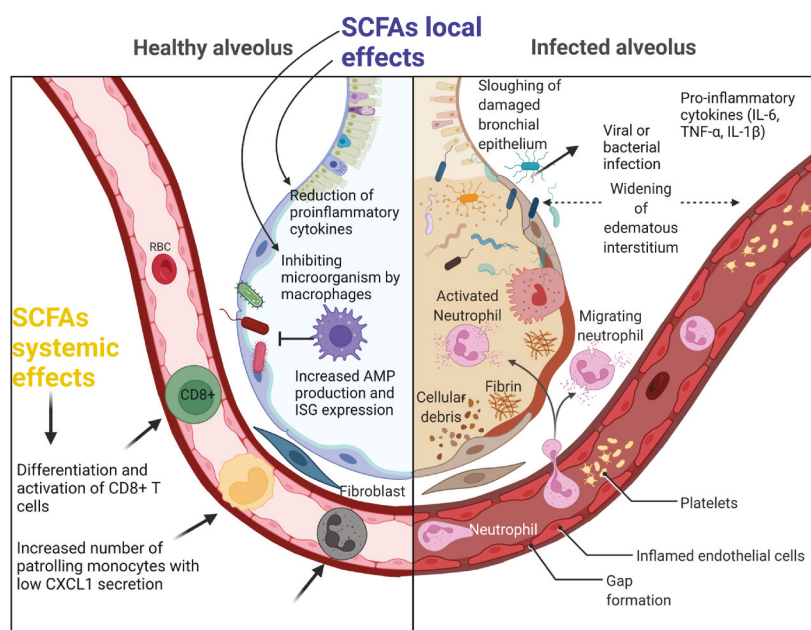


Fig. 4. SCFAs: protective effects in lung infections. SCFAs have the ability to modify the immune response on both a systemic and a local level, and this enhances pathogen clearance while reducing tissue damage caused by elevated inflammation. Locally, SCFAs act as anti-inflammatory mediators, minimizing inflammatory damage, while systemically SCFAs stimulate the differentiation of CD8⁺ T cells and increase the levels of patrolling monocytes. This results in an increased pathogen clearance.

inflammatory reactions [78]. Additionally, butyrate activates the niacin receptor GPR109a, and mice lacking GPR109a have fewer T cells producing IL-10 [79]. A protective Th1 phenotype and tolerogenic immune profile are produced by regulatory T cells, which may help prevent the onset of asthma [33]. Introduced Tregs decrease existing illness and prevent disease progression in mouse models of allergic airway inflammation [80]. Treg populations and functions are directly

impacted by SCFAs. Foxp3 and IL-10 expression in these cells increases, along with colonic Treg formation, as a result of acetate and propionate treatment [81]. SCFAs influence T cells both directly and indirectly, generating a tolerogenic immunological profile with elevated Treg numbers and activity [82]. Increased maternal dietary MACs have been shown to be related with a reduction in the severity of allergic airway inflammation in the offspring by Trompette et al. [83] and Thorburn

et al. [80]. These studies have indicated a potential target for therapies to lessen the burden of respiratory disorders like asthma by showing a relationship between mother dietary MACs, prenatal exposure to SCFAs, and offspring asthma; however, more clinical investigations are necessary. Overall, these studies underline a potential role for SCFAs in reducing asthma inflammation.

6. - SCFAs and gut microbiota: impact on lung cancer

Lung cancer is one of the world's most devastating diseases, having one of the highest rates of morbidity and mortality across all cancers [84]. The interaction between the lungs and gut microbiota exerted through the gut-lung axis is known to influence lung cancer pathogenesis [15]. Kirshcner et al. demonstrated that the composition of the intestinal microbiota and the fecal levels of metabolites such as SCFAs are altered in cancer patients [85]. SCFAs are an important source of energy for gut epithelial cells, and they exert several beneficial functions in the gut including strengthening intestinal barrier integrity, reducing inflammation, and avoiding translocation of bacteria. In cancer, as well as metabolic abnormalities, an intestinal decrease in SCFA synthesis, together with a drop in SCFA-producing bacteria counts and gut dysbiosis, are often observed [86]. Lung cancer has been linked to reduced numbers of *Bifidobacterium* or *Actinobacteria* and enhanced populations of *Enterococcus* spp. in the gut microbiota [87]. Furthermore, perturbation of the gut microbiota's normal functioning has been shown to influence lung cancer progression [88]. Numerous studies have demonstrated the existence of a relationship between alterations in the gut microbiome and lung cancer, particularly with regards to the impact of these alterations on treatment outcome [89]. In a recent study, patients with lung cancer were found to have lower levels of *Enterobacter*, *Faecalibacterium*, *Kluyvera*, *Dialister* and *Escherichia-Shigella* and greater levels of *Veillonella*, *Bacteroides* and *Fusobacterium* compared to healthy controls [90]. An aberrant composition of the gut microbiota may lead to resistance to immune checkpoint inhibitor therapy. Since lung cancer patients frequently have lower levels of *Akkermansia muciniphila*, another microorganism responsible for the production of SCFAs [91], supplementing the diet with these bacteria may improve immune responses to checkpoint inhibitors [92]. It has also been postulated that extraintestinal malignancies, such as breast cancer, are influenced by the gut microbiome [93].

From a mechanistic point of view, SCFAs present in the gut or other organs have been shown to minimize carcinogenesis through the suppression of cancer cell growth and migration. This effect is exerted through HDAC repression and triggering of apoptosis, and provides the rationale for the potential of SCFAs in the treatment and prevention of gastrointestinal or lung malignancies [94]. In terms of anticancer activity, the majority of SCFA studies primarily concentrated on butyrate and propionate. In a recent study, treatment with sodium butyrate resulted in an increase of miR-3935 expression, which inhibited the proliferation and migration of A549 lung adenocarcinoma epithelial cells [95]. In another study, propionate was shown to induce cell cycle arrest and apoptosis in the H1299 and H1703 lung cancer cell lines through increased p21 and decreased expression of survivin, providing insight into the potential of propionate in lung cancer therapy [96]. Conversely, treatment of lung cancer cells with sodium butyrate was shown to increase STAT-3 expression levels, as well as its phosphorylation, resulting in the stabilization of the *ABCB1* mRNA, with subsequent increase in P-glycoprotein (P-gp, the product of the *ABCB1* gene) levels [71]. Considering the fundamental role of P-gp as mediator of cancer chemoresistance [97], this represents a potential limitation of the use of butyrate in cancer therapy.

Considering the studies showcased in this section, the gut-lung axis' role in lung cancer development and etiology, as well as the potential for its alteration as a therapeutic strategy for lung cancer, would benefit from further research.

7. - SCFAs: impact on SARS-CoV-2

The outbreak of the COVID-19 pandemic caused a worldwide threat to human health. The 2019 novel coronavirus (SARS-CoV-2) causing COVID-19 is highly contagious and can infect individuals by entry through the nose. Angiotensin-Converting Enzyme 2 (ACE2), a protein that is fundamental for SARS-CoV-2 infection, is most abundant in the nasal passages [98]. People with hypertension are at high risk for coronavirus disease 2019 (COVID-19) and tend to experience gastrointestinal symptoms, indicating that disrupted gut-lung communications may be partly to blame for this illness' multi-organ symptoms, including its cardiovascular manifestations [99]. This concept is supported by a previous study investigating spontaneously hypertensive rats, which showed higher expression of ACE2 and Transmembrane protease, serine 2 (TMPRSS2, another molecule which is fundamental for SARS-CoV-2 infection) in their gut epithelial cells compared to normal rats [100]. In humans, a significant quantity of SARS-CoV-2 viral genetic material was found in the anal swab of almost 40% of SARS-CoV-2 patients, and a number of patients complained of nausea, vomiting, and diarrhea [101, 102]. Since the microbiota is thought to be the biggest risk factor for the development of severe disease outcomes, the involvement of the gut in the pathophysiology of COVID-19 has not been thoroughly investigated. The small intestine of humans contains mature enterocytes that express membrane ACE2, and SARS-CoV-2 may infect those cells thanks to the help of the proteases TMPRSS2 and TMPRSS4 [103]. Enteric ACE2 integrity/functionality may be significantly reduced as a result of enterocyte infection with SARS-CoV-2 (Zang et al., 2020). Angiotensin (Ang) II and other renin-angiotensin system constituents are upregulated when ACE2 expression declines [104]. Elevated Ang II levels can alter metabolomics and gut microbial composition in a sex-specific way [105]. Given that certain COVID-19 patients have intestinal dysbiosis, it is possible that SARS-CoV-2 infection of enterocytes modifies the gut microbiota [106]. Patients with SARS-CoV-2 infection also demonstrated a decline in the relative abundances of the butyrate-producing bacteria, *Faecalibacterium prausnitzii* and *Bifidobacterium bifidum* [107]. Butyrate is a SCFA that controls the renewal and integrity of the epithelial barrier function, which in turn affects the proliferation and differentiation of epithelial intestinal cells [108]. Another investigation highlighted that patients with COVID-19 had considerably decreased fecal amounts of SCFAs and L-isoleucine both before and after COVID-19 infection had resolved, and correlated this condition with higher C-X-C motif chemokine ligand 10 (CXCL10), NT-proB-type natriuretic peptide, and C-reactive protein levels as well as disease severity [109]. This study highlighted the potential use of SCFAs as a treatment to reduce COVID-19 mortality and susceptibility to SARS-CoV-2 infection. A further study by Takabayashi et al. has shown that nasal inflammation might reduce a person's vulnerability to the SARS-CoV-2 virus [110]. In particular, COVID-19 patients with rhinosinusitis, or nasal irritation, have a lower risk of hospitalization, and this is correlated with lower ACE2 expression. Furthermore, it was explored the impact of SCFAs on ACE2 expression in the nasal cavity, and its effect on SARS-CoV-2 infection, finding that SCFAs blocked dsRNA-inducible ACE2 expression, potentially reducing susceptibility to SARS-CoV-2 infection.

SARS-CoV-2 infection prevention and treatment approaches that take gastroenterology and the intestinal microbiota into account have attracted a lot of interest recently. As proven by existing indirect evidence, changing the composition of the gut flora and its metabolites represents a promising therapeutic possibility for preventing and treating COVID-19. As possible SARS-CoV-2 therapeutic targets, certain intestinal bacteria that decrease intestinal ACE2 expression have also been proposed [111]. It has been suggested that a high-fiber diet may modify the ratio of *Firmicutes* and *Bacteroidetes*, and this may increase the amount of SCFAs in the gut and blood, resulting in a reduction of lung damage caused by infection with respiratory syncytial viruses [112]. Many other metabolites of the symbiotic gut flora have an influence on the host immunity in addition to SCFAs [82].

Considering that the high mortality observed among the elderly and people with chronic diseases affected by COVID-19 is caused by the development of acute respiratory distress syndrome (ARDS) [113], it is crucial to develop preventive dietary methods that enable at-risk patients to generate optimal immune responses. In this context, the literature discussed in this section provides rationale that using a diet that causes increased SCFA synthesis may be a suitable approach to enhance the development of a more competent immune system. The mechanism by which SCFAs inhibit binding of SARS-CoV-2 and entry into the target cells is shown in Fig. 5.

8. - SCFAs: impact on influenza

According to recent research, SCFAs serve as a bridge between the airways, the gut, and the bone marrow [23]. These molecules were detected in the lungs in small quantities, suggesting that the lung microbiome does not produce large quantities, and therefore the SCFAs do not build up in the lung tissue. For this reason, SCFAs may not have a direct role in the lungs but, as discussed earlier, their role can be indirect, as they can be transported into the bone marrow where they exert their immunomodulatory action. Successively, immune cells produced in the bone marrow upon SCFAs influence may relocate to the lungs, promoting immunological balance [83,114,115]. With regards to influenza, SCFAs have been shown to control Ly6c-negative patrolling monocyte hematopoiesis and improve CD8⁺ T cell functionality through the activation of GPR41, thus providing protection against influenza virus infection [96]. Furthermore, it has been shown that butyrate can activate GPR109A, stimulating differentiation of Treg cells and cells that produce IL-10 and IL-18 [79]. Finally, in a recent study, the perturbation of the gut microbiota occurring in influenza was shown to lead to a reduced production of the SCFA acetate, and this affected the capacity of alveolar macrophages to destroy bacteria responsible for bacterial superinfection occurring during influenza [116]. Supplementation with acetate resulted in the activation of the Free Fatty Acid Receptor 2 (FFAR2) SCFA receptor, with subsequent reduction of local and systemic bacterial loads [116].

9. - SCFAs: pro-inflammatory impact on lung cystic fibrosis

Aerobic microorganisms are found to thrive in oxygenated environments, and for this reason, they are most abundant in the lungs. These microorganisms have received the greatest attention among the components of the lung microbiota. In chronic lung disorders such as cystic fibrosis (CF), the airway microenvironment becomes hypoxic [117], whereas anaerobic bacteria benefit to thrive in such conditions [118]. Anaerobic microbes are increasingly found in airway CF fluids as individuals age [119]. CF bronchial brushings, bronchoalveolar lavage (BAL) and supernatants from anaerobic bacterial cultures were investigated to determine whether these bacteria released mediators that induce airway inflammation. This study showed that SCFAs, secreted by anaerobic bacteria in CF patients' lungs, trigger the production of IL-8 (IL-8/CXCL8, the main inflammatory mediator in lung illness), with the impact being more prominent in CF than in healthy bronchial epithelium [114]. Mechanistically, bronchial epithelial cells expressed both the SCFA receptors GPR41 and GPR43, and inhibiting GPR41 dramatically lowered SCFA-induced IL-8 production [119]. In an effort to comprehend why the SCFA receptor GPR41 was up-regulated in CF epithelial cells, Ghorbani and colleagues addressed pathways that are known to be dysregulated in CF in their findings [42]. Ghorbani and colleagues, similarly to Mirkovic and colleagues, showed that SCFAs stimulate the production of pro-inflammatory cytokines from bronchial epithelial cells, including granulocyte colony stimulating factor, granulocyte-macrophage colony stimulating factor, and IL-6 [42]. This research also revealed a relationship between SCFAs and airway neutrophils in CF patients, suggesting that enhanced neutrophil recruitment into CF lungs results from SCFA-induced IL-8 release [42]. Additionally, this latter study demonstrated that elevated SCFA levels are indicative of decreased nitric oxide production and that SCFAs affect *Pseudomonas aeruginosa* growth, pointing to a complex relationship between anaerobic bacteria and the prevalent CF pathogen [42].

10. - SCFA: impact on infective respiratory diseases

The host's immune system is directly influenced by the microbial communities, which also produce soluble mediators that the host may be

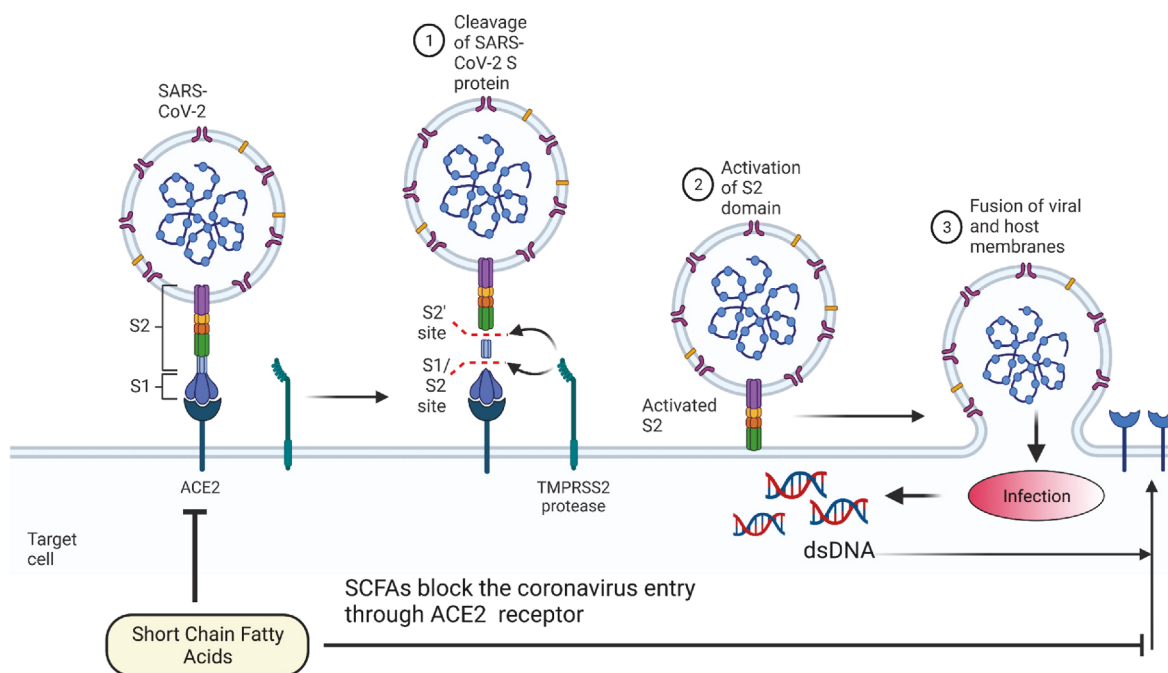


Fig. 5. – Protective Effects of SCFAs against SARS-CoV-2 infection. SCFAs block the ACE2 receptor, inhibiting the binding of SARS-CoV-2 and viral entry, and blocks the dsRNA-inducible expression of the ACE2 receptor.

able to detect. This has been shown to have a substantial role in affecting the immune system of the gut [21]. Butyrate, propionate, and acetate, the three main SCFAs, are effective in preventing respiratory tract infections. According to research by Haak et al., patients who underwent allogeneic hematopoietic stem cell transplantation had a lower chance of getting viral lower respiratory tract infections when there was a large concentration of butyrate-producing bacteria in their feces [120]. Butyrate's protective effect is not restricted to viruses, as it was found to be effective in extending the lifespan of mice infected with *Klebsiella pneumoniae* [121]. Furthermore, acetate prevented mice from contracting the respiratory syncytial virus, reducing lung viral load and inflammation [122]. Another report also suggested that acetate reduced bacterial load and inflammation levels by activating FFAR2, thereby protecting against *Klebsiella pneumoniae* infection [122]. Acetate was also found to offer protection against subsequent lung infections via enhancing alveolar macrophages' capacity to fight bacteria, thus increasing mice's survival time [123]. Collectively, these reports indicate how gut microbial metabolites can protect against infectious respiratory illnesses.

11. - SCFAs: Impact on Tuberculosis

Several studies have highlighted the importance of the gut microbiota in the protection, development, and treatment of chronic respiratory illnesses, including tuberculosis (TB) [124–126]. The microbiota primarily affects the function of specific immune cell subsets by producing bacteriocins that directly inhibit *Mycobacterium tuberculosis* growth, and influence the anti-TB drugs' pharmacokinetics and bioavailability, thus influencing TB prevention, pathogenesis, and treatment [117]. All of these compounds, including propionate and butyrate, are transported to the lungs where they may reduce IL-17 synthesis, depress Th1 immunity, and boost the number of T regulatory cells, all of which may have an impact on how *M. tuberculosis* infection develops [127–129]. Indole propionic acid, another product of the gut microbiota, may disrupt *M. tuberculosis*' ability to produce tryptophan and so directly impede its development [130].

12. - Conclusions

This review focused on various mechanisms by which an abundantly studied class of bacterial metabolites, SCFAs, may influence lung immunological homeostasis. By extension, SCFAs contribute to numerous lung diseases, including lung cancer, COVID-19, COPD, asthma, CF, TB, and other infectious diseases. The studies analyzed in this review provide a strong rationale for the potential therapeutic application of SCFAs, as well as the role of SCFA-producing bacteria, in the prevention and treatment of lung diseases. The exact composition of the microbiota and the type of diet both synergistically affect SCFA production. In this sense, altering one's diet to increase the content of non-digestible fibres represents a potential strategy that can influence both the course and the outcome of the lung diseases discussed in this review. It should be mentioned that many of the benefits of a diet high in dietary fibers may be related to several other dietary components, including minerals and vitamins, in addition to the microbial fermentation of these fibers leading to the generation of SCFAs in the gut. Numerous studies that stress the significance of various dietary components have confirmed these findings. The intricate molecular mechanisms of action of SCFAs demand advanced experimental and clinical verification. In this sense, future studies investigating the role of SCFAs in the clinically diverse progression of the lung illnesses discussed in this review may hold promise. Because respiratory infections have such a significant global impact on morbidity and mortality, it is crucial to comprehend the corresponding susceptibility mechanisms and to develop novel treatments [131]. According to the most recent studies highlighted in this review, SCFAs have the potential to reduce the frequency and severity of infections, in particular through their pleiotropic

regulatory effect on immune homeostasis. For this reason, the direct use and administration of SCFAs as therapeutic agents represent a valid therapeutic option for diseases in which the maintenance of a correct immune homeostasis is fundamental. Finally, the development of more efficient therapeutic intervention programs that are better suited to unique illness course trajectories will be made possible by a greater knowledge of the intricate mechanisms of action by which SCFAs exert their multifaceted activity.

Declaration of competing interest

The authors declare that they have no known competing financial interests or personal relationships that could have appeared to influence the work reported in this paper.

Data availability

Data will be made available on request.

Acknowledgements

The authors are thankful to the Graduate School of Health, University of Technology Sydney, Australia. KD is supported by a project grant from the Rebecca L Cooper Medical Research Foundation and the Maridulu Budyari Gumal Sydney Partnerships for Health, Education, Research and Enterprise (SPHERE) RSEOH CAG Seed grant, fellowship and extension grant; Faculty of Health MCR/ECR Mentorship Support Grant and UTS Global Strategic Partnerships Seed Funding Scheme. GDR is supported by the UTS International Research Scholarship and the UTS President's Scholarship. KRP is supported by a fellowship from Prevent Cancer Foundation (PCF) and the International Association for the Study of Lung Cancer (IASLC).

References

- [1] L.V. Hooper, D.R. Littman, A.J. Macpherson, Interactions between the microbiota and the immune system, *Science* 336 (6086) (2012) 1268–1273.
- [2] D. Erny, A.L. Hrabě De Angelis, M. Prinz, Communicating systems in the body: how microbiota and microglia cooperate, *Immunology* 150 (1) (2017) 7–15.
- [3] Y.P. Silva, A. Bernardi, R.L. Frozza, The role of short-chain fatty acids from gut microbiota in gut-brain communication, *Front. Endocrinol.* 11 (2020) 25.
- [4] N.W. Palm, M.R. De Zoete, R.A. Flavell, Immune-microbiota interactions in health and disease, *Clin. Immunol.* 159 (2) (2015) 122–127.
- [5] L. Chiu, T. Bazin, M.E. Truchetet, T. Schaeveerbecke, L. Delhaes, T. Pradeu, Protective microbiota: from localized to long-reaching Co-immunity, *Front. Immunol.* 8 (2017) 1678.
- [6] A. Cait, M.R. Hughes, F. Antignano, J. Cait, P.A. Dimitriu, K.R. Maas, L. A. Reynolds, L. Hacker, J. Mohr, B.B. Finlay, C. Zaph, Microbiome-driven allergic lung inflammation is ameliorated by short-chain fatty acids, *Mucosal Immunol.* 11 (3) (2018) 785–795.
- [7] V. Sencio, A. Barthelemy, L.P. Tavares, M.G. Machado, D. Soulard, C. Cuinat, C. M. Queiroz-Junior, M.L. Noordine, S. Salomé-Desnoize, L. Deryuter, B. Foligne, Gut dysbiosis during influenza contributes to pulmonary pneumococcal superinfection through altered short-chain fatty acid production, *Cell Rep.* 30 (9) (2020) 2934–2947.
- [8] A.T. Dang, B.J. Marsland, Microbes, metabolites, and the gut–lung axis, *Mucosal Immunol.* 12 (4) (2019) 843–850.
- [9] A. Trompette, E.S. Gollwitzer, K. Yadava, A.K. Sichelstiel, N. Sprenger, C. Ngombu, C. Blanchard, T. Junt, L.P. Nicod, N.L. Harris, B.J. Marsland, Gut microbiota metabolism of dietary fiber influences allergic airway disease and hematopoiesis, *Nature Med* 20 (2) (2014) 159–166.
- [10] J.Y. Yoo, M. Groer, S.V. Dutra, A. Sarkar, D.I. McSkimming, Gut microbiota and immune system interactions, *Microorganisms* 8 (10) (2020) 1587.
- [11] J.K. Nicholson, I.D. Wilson, Opinion: understanding 'global' systems biology: metabolomics and the continuum of metabolism, *Nat. Rev. Drug Discov.* 2 (8) (2003) 668–676.
- [12] C. Abraham, J.H. Cho, IL-23 and autoimmunity: new insights into the pathogenesis of inflammatory bowel disease, *Annu. Rev. Med.* 60 (2009) 97–110.
- [13] M.H. Grayson, L.E. Camarda, S.A. Hussain, et al., Intestinal microbiota disruption reduces regulatory T cells and increases respiratory viral infection mortality through increased IFN γ production, *Front. Immunol.* 9 (2018) 1587.
- [14] G.L.V. De Oliveira, C.N.S. Oliveira, C.F. Pinzan, L.V.V. De Salis, C.R.B. Cardoso, Microbiota modulation of the gut-lung Axis in COVID-19, *Front. Immunol.* 12 (2021), 635471.

- [15] Y. Zhao, Y. Liu, S. Li, et al., Role of lung and gut microbiota on lung cancer pathogenesis, *J. Cancer Res. Clin. Oncol.* 147 (8) (2021) 2177–2186.
- [16] B. Wang, M. Yao, L. Lv, Z. Ling, L. Li, The human microbiota in health and disease, *Engineering* 3 (1) (2017) 71–82.
- [17] K.F. Budden, S.L. Gellatly, D.L. Wood, et al., Emerging pathogenic links between microbiota and the gut-lung axis, *Nat. Rev. Microbiol.* 15 (1) (2017) 55–63.
- [18] S. Keely, P.M. Hansbro, Lung-gut cross talk: a potential mechanism for intestinal dysfunction in patients with COPD, *Chest* 145 (2) (2014) 199–200.
- [19] M. Fricker, B.J. Goggins, S. Mateer, et al., Chronic cigarette smoke exposure induces systemic hypoxia that drives intestinal dysfunction, *JCI Insight* 3 (3) (2018).
- [20] S. Anand, S.S. Mande, Diet, microbiota and gut-lung connection, *Front. Microbiol.* 9 (2018) 2147.
- [21] D. Parada Venegas, M.K. De La Fuente, G. Landskron, et al., Short chain fatty acids (SCFAs)-Mediated gut epithelial and immune regulation and its relevance for inflammatory bowel diseases, *Front. Immunol.* 10 (2019) 277.
- [22] W. Ratajczak, A. Rył, A. Mizerski, K. Walczakiewicz, O. Sipak, M. Laszczyńska, Immunomodulatory potential of gut microbiome-derived short-chain fatty acids (SCFAs), *Acta Biochim. Pol.* 66 (1) (2019) 1–12.
- [23] A.T. Dang, B.J. Marsland, Microbes, metabolites, and the gut–lung axis, *Mucosal Immunol.* 12 (4) (2019) 843–850.
- [24] J.H. Cummings, E.W. Pomare, W.J. Branch, C.P. Naylor, G.T. Macfarlane, Short chain fatty acids in human large intestine, portal, hepatic and venous blood, *Gut* 28 (10) (1987) 1221–1227.
- [25] K.R. Paudel, V. Dharwal, V.K. Patel, et al., Role of lung microbiome in innate immune response associated with chronic lung diseases, *Front. Med.* 7 (2020) 554.
- [26] S. Fukuda, H. Toh, K. Hase, et al., Bifidobacteria can protect from enteropathogenic infection through production of acetate, *Nature* 469 (7331) (2011) 543–547.
- [27] E.E. Hull, M.R. Montgomery, K.J. Leyva, HDAC inhibitors as epigenetic regulators of the immune system: impacts on cancer therapy and inflammatory diseases, *BioMed Res. Int.* 2016 (2016) 1–15, 8797206.
- [28] M. Li, B. Van Esch, G.T.M. Wagenaar, J. Garssen, G. Folkerts, Henricks PaJ, Pro- and anti-inflammatory effects of short chain fatty acids on immune and endothelial cells, *Eur. J. Pharmacol.* 831 (2018) 52–59.
- [29] R. Ranjbar, S.N. Vahdati, S. Tavakoli, R. Khodaie, H. Behboudi, Immunomodulatory roles of microbiota-derived short-chain fatty acids in bacterial infections, *Biomed. Pharmacother.* 141 (2021), 111817.
- [30] S. Sivaprakasam, Y.D. Bhutia, S. Yang, V. Ganapathy, Short-chain fatty acid transporters: role in colonic homeostasis, *Compr. Physiol.* 8 (1) (2017) 299–314.
- [31] E.M. Sturm, E. Knuplez, G. Marsche, Role of short chain fatty acids and apolipoproteins in the regulation of eosinophilia-associated diseases, *Int. J. Mol. Sci.* 22 (9) (2021).
- [32] M. Aoyama, J. Kotani, M. Usami, Butyrate and propionate induced activated or non-activated neutrophil apoptosis via HDAC inhibitor activity but without activating GPR-41/GPR-43 pathways, *Nutrition* 26 (6) (2010) 653–661.
- [33] E. Le Poul, C. Loison, S. Struyf, et al., Functional characterization of human receptors for short chain fatty acids and their role in polymorphonuclear cell activation, *J. Biol. Chem.* 278 (28) (2003) 25481–25489.
- [34] M. Jardou, R. Lawson, Supportive therapy during COVID-19: the proposed mechanism of short-chain fatty acids to prevent cytokine storm and multi-organ failure, *Med. Hypotheses* 154 (2021), 110661.
- [35] P.V. Chang, L. Hao, S. Offermanns, R. Medzhitov, The microbial metabolite butyrate regulates intestinal macrophage function via histone deacetylase inhibition, *Proc. Natl. Acad. Sci. U. S. A.* 111 (6) (2014) 2247–2252.
- [36] J. He, P. Zhang, L. Shen, et al., Short-chain fatty acids and their association with signalling pathways in inflammation, glucose and lipid metabolism, *Int. J. Mol. Sci.* 21 (17) (2020).
- [37] K. Meijer, P. De Vos, M.G. Priebe, Butyrate and other short-chain fatty acids as modulators of immunity: what relevance for health? *Curr. Opin. Clin. Nutr. Metab. Care* 13 (6) (2010) 715–721.
- [38] R. Corrêa-Oliveira, J.L. Fachi, A. Vieira, F.T. Sato, M.A. Vinolo, Regulation of immune cell function by short-chain fatty acids, *Clin Transl Immunology* 5 (4) (2016) e73.
- [39] S. Rutting, D. Xenaki, M. Malouf, et al., Short-chain fatty acids increase TNF α -induced inflammation in primary human lung mesenchymal cells through the activation of p38 MAPK, *Am. J. Physiol. Lung Cell Mol. Physiol.* 316 (1) (2019) L157–L174.
- [40] K. Liu, G.D. Victora, T.A. Schwickert, et al., In vivo analysis of dendritic cell development and homeostasis, *Science* 324 (5925) (2009) 392–397.
- [41] A. Woting, M. Blaut, The intestinal microbiota in metabolic disease, *Nutrients* 8 (4) (2016) 202.
- [42] K. Nk, P. Patil, S.K. Bhandary, et al., Is Butyrate a Natural Alternative to Dexamethasone in the Management of CoVID-19? *F1000Res*, vol. 10, 2021, p. 273.
- [43] A.J. Brown, S.M. Goldsworthy, A.A. Barnes, M.M. Eilert, L. Tcheang, D. Daniels, A.I. Muir, M.J. Wigglesworth, I. Kinghorn, N.J. Fraser, N.B. Pike, The Orphan G protein-coupled receptors GPR41 and GPR43 are activated by propionate and other short chain carboxylic acids, *J. Biol. Chem.* 278 (13) (2003) 11312–11319.
- [44] J.L. Pluznick, R.J. Protzko, H. Gevorgyan, Z. Peterlin, A. Sipos, J. Han, I. Brunet, L.X. Wan, F. Rey, T. Wang, S.J. Firestein, Olfactory receptor responding to gut microbiota-derived signals plays a role in renin secretion and blood pressure regulation, *Proc. Natl. Acad. Sci. USA* 110 (11) (2013) 4410–4415.
- [45] S. Alex, K. Lange, T. Amolo, J.S. Grinstead, A.K. Haakonsson, E. Szalowska, A. Koppen, K. Mudde, D. Haenen, S.A. Al-Lahham, H. Roelofsén, Short-chain fatty acids stimulate angiotensin-like 4 synthesis in human colon adenocarcinoma cells by activating peroxisome proliferator-activated receptor γ , *MCB (Mol. Cell. Biol.)* 33 (7) (2013) 1303–1316.
- [46] A. Koh, F. De Vadder, P. Kovatcheva-Datchary, F. Bäckhed, From dietary fiber to host physiology: short-chain fatty acids as key bacterial metabolites, *Cell* 165 (6) (2016) 1332–1345.
- [47] R. Masui, M. Sasaki, Y. Funaki, N. Ogasawara, M. Mizuno, A. Iida, S. Izawa, Y. Kondo, Y. Ito, Y. Tamura, K. Yanamoto, G protein-coupled receptor 43 moderates gut inflammation through cytokine regulation from mononuclear cells, *Inflamm. Bowel Dis.* 19 (13) (2013) 2848–2856.
- [48] H. Ohira, Y. Fujioka, C. Katagiri, R. Mamoto, M. Aoyama-Ishikawa, K. Amako, Y. Izumi, S. Nishiumi, M. Yoshida, M. Usami, M. Ikeda, Butyrate attenuates inflammation and lipolysis generated by the interaction of adipocytes and macrophages, *J. Atherosclerosis Thromb.* 20 (5) (2013) 425–442.
- [49] A.J. Brown, S.M. Goldsworthy, A.A. Barnes, M.M. Eilert, L. Tcheang, D. Daniels, A.I. Muir, M.J. Wigglesworth, I. Kinghorn, N.J. Fraser, N.B. Pike, The Orphan G protein-coupled receptors GPR41 and GPR43 are activated by propionate and other short chain carboxylic acids, *J. Biol. Chem.* 278 (13) (2003) 11312–11319.
- [50] I. Kimura, K. Ozawa, D. Inoue, T. Imamura, K. Kimura, T. Maeda, K. Terasawa, D. Kashiwara, K. Hirano, T. Tani, T. Takahashi, The gut microbiota suppresses insulin-mediated fat accumulation via the short-chain fatty acid receptor GPR43, *Nat. Commun.* 4 (1) (2013) 1–2.
- [51] L. Macia, J. Tan, A.T. Vieira, K. Leach, D. Stanley, S. Luong, M. Maruya, C. Ian McKenzie, A. Hijikata, C. Wong, L. Binge, Metabolite-sensing receptors GPR43 and GPR109A facilitate dietary fiber-induced gut homeostasis through regulation of the inflammasome, *Nat. Commun.* 6 (1) (2015) 1–5.
- [52] J.L. Pluznick, Gut microbiota in renal physiology: focus on short-chain fatty acids and their receptors, *Kidney Int.* 90 (6) (2016) 1191–1198.
- [53] S. Alex, K. Lange, T. Amolo, J.S. Grinstead, A.K. Haakonsson, E. Szalowska, A. Koppen, K. Mudde, D. Haenen, S.A. Al-Lahham, H. Roelofsén, Short-chain fatty acids stimulate angiotensin-like 4 synthesis in human colon adenocarcinoma cells by activating peroxisome proliferator-activated receptor γ , *Mol. Cell Biol.* 33 (7) (2013) 1303–1316.
- [54] E.C. Rosser, C.J. Piper, D.E. Matei, P.A. Blair, A.F. Rendeiro, M. Orford, D. G. Alber, T. Krausgruber, D. Catalan, N. Klein, J.J. Manson, Microbiota-derived metabolites suppress arthritis by amplifying aryl-hydrocarbon receptor activation in regulatory B cells, *Cell Metabol.* 31 (4) (2020) 837–851.
- [55] P. Ghorbani, P. Santhakumar, Q. Hu, et al., Short-chain fatty acids affect cystic fibrosis airway inflammation and bacterial growth, *Eur. Respir. J.* 46 (4) (2015) 1033–1045.
- [56] M.D. Ardatskaia, V.V. Shevtsov, A.N. Zhakot, et al., [Microflora metabolites of different habitats in bronchopulmonary diseases], *Eksp Klin Gastroenterol* (3) (2014) 46–54.
- [57] Q. Liu, X. Tian, D. Maruyama, M. Arjomandi, A. Prakash, Lung immune tone via gut-lung axis: gut-derived LPS and short-chain fatty acids' immunometabolic regulation of lung IL-1 β , FFAR2, and FFAR3 expression, *Am. J. Physiol. Lung Cell Mol. Physiol.* 321 (1) (2021) L65–L78.
- [58] A.D. Lopez, K. Shibuya, C. Rao, et al., Chronic obstructive pulmonary disease: current burden and future projections, *Eur. Respir. J.* 27 (2) (2006) 397–412.
- [59] A.C. Schamberger, N. Mise, J. Jia, et al., Cigarette smoke-induced disruption of bronchial epithelial tight junctions is prevented by transforming growth factor- β , *Am. J. Respir. Cell Mol. Biol.* 50 (6) (2014) 1040–1052.
- [60] L.B. Richards, M. Li, G. Folkerts, Henricks PaJ, J. Garssen, B. Van Esch, Butyrate and propionate restore the cytokine and house dust mite compromised barrier function of human bronchial airway epithelial cells, *Int. J. Mol. Sci.* 22 (1) (2020).
- [61] K. Tomoda, K. Kubo, K. Dairiki, et al., Whey peptide-based enteral diet attenuated elastase-induced emphysema with increase in short chain fatty acids in mice, *BMC Pulm. Med.* 15 (1) (2015) 64.
- [62] S. Kotlyarov, Role of short-chain fatty acids produced by gut microbiota in innate lung immunity and pathogenesis of the heterogeneous course of chronic obstructive pulmonary disease, *Int. J. Mol. Sci.* 23 (9) (2022).
- [63] N. Li, Z. Dai, Z. Wang, et al., Gut microbiota dysbiosis contributes to the development of chronic obstructive pulmonary disease, *Respir. Res.* 22 (1) (2021) 274.
- [64] T.M. Karavaeva, M.V. Maksimenya, P.P. Tereshkov, I.N. Gaimolenko, T. A. Medvedeva, A.A. Parshina, [Long-chain fatty acids and short-chain fatty acids in exhaled breath condensate of patients with chronic obstructive pulmonary disease], *Biomed. Khim.* 67 (2) (2021) 169–174.
- [65] J. Mao, Y. Li, Q. Bian, et al., The Bufeijianpi formula improves mucosal immune function by remodeling gut microbiota through the SCFAs/GPR43/NLRP3 pathway in chronic obstructive pulmonary disease rats, *Int. J. Chronic Obstr. Pulm. Dis.* 17 (2022) 1285–1298.
- [66] D. Ríos-Covián, P. Ruas-Madiedo, M. Argolles, M. Gueimonde, C.G. De Los Reyes-Gavilán, N. Salazar, Intestinal short chain fatty acids and their link with diet and human health, *Front. Microbiol.* 7 (2016) 185.
- [67] W. Barcik, R.C.T. Boutin, M. Sokolowska, B.B. Finlay, The role of lung and gut microbiota in the pathology of asthma, *Immunology* 52 (2) (2020) 241–255.
- [68] J. Miro-Blanch, O. Yanes, Epigenetic regulation at the interplay between gut microbiota and host metabolism, *Front. Genet.* 10 (2019) 638.
- [69] H.S. Lee, The interaction between gut microbiome and nutrients on development of human disease through epigenetic mechanisms, *Genomics Inform* 17 (3) (2019) e24.
- [70] S. Steinmeyer, K. Lee, A. Jayaraman, R.C. Alaniz, Microbiota metabolite regulation of host immune homeostasis: a mechanistic missing link, *Curr. Allergy Asthma Rep.* 15 (5) (2015) 24.

- [71] S.T. Zhao, C.Z. Wang, Regulatory T cells and asthma, *J. Zhejiang Univ. - Sci. B* 19 (9) (2018) 663–673.
- [72] M. Kespohl, N. Vachharajani, M. Luu, et al., The microbial metabolite butyrate induces expression of Th1-associated factors in CD4(+) T cells, *Front. Immunol.* 8 (2017) 1036.
- [73] F. Indrio, S. Martini, R. Francavilla, et al., Epigenetic matters: the link between early nutrition, microbiome, and long-term health development, *Front. Pediatr.* 5 (2017) 178.
- [74] G. Lewis, B. Wang, P. Shafiei Jahani, et al., Dietary fiber-induced microbial short chain fatty acids suppress ILC2-dependent airway inflammation, *Front. Immunol.* 10 (2019) 2051.
- [75] J.K. Nicholson, E. Holmes, J. Kinross, et al., Host-gut microbiota metabolic interactions, *Science* 336 (6086) (2012) 1262–1267.
- [76] E. Holmes, J.V. Li, J.R. Marchesi, J.K. Nicholson, Gut microbiota composition and activity in relation to host metabolic phenotype and disease risk, *Cell Metabol.* 16 (5) (2012) 559–564.
- [77] A.L. Millard, P.M. Mertes, D. Ittelet, F. Villard, P. Jeannesson, J. Bernard, Butyrate affects differentiation, maturation and function of human monocyte-derived dendritic cells and macrophages, *Clin. Exp. Immunol.* 130 (2) (2002) 245–255.
- [78] N. Singh, M. Thangaraju, P.D. Prasad, et al., Blockade of dendritic cell development by bacterial fermentation products butyrate and propionate through a transporter (Slc5a8)-dependent inhibition of histone deacetylases, *J. Biol. Chem.* 285 (36) (2010) 27601–27608.
- [79] N. Singh, A. Gurav, S. Sivaprakasam, et al., Activation of Gpr109a, receptor for niacin and the commensal metabolite butyrate, suppresses colonic inflammation and carcinogenesis, *Immunity* 40 (1) (2014) 128–139.
- [80] A.N. Thorburn, P.M. Hansbro, Harnessing regulatory T cells to suppress asthma: from potential to therapy, *Am. J. Respir. Cell Mol. Biol.* 43 (5) (2010) 511–519.
- [81] P.M. Smith, M.R. Howitt, N. Panikoff, et al., The microbial metabolites, short-chain fatty acids, regulate colonic Treg cell homeostasis, *Science* 341 (6145) (2013) 569–573.
- [82] M.G. Rooks, W.S. Garrett, Gut microbiota, metabolites and host immunity, *Nat. Rev. Immunol.* 16 (6) (2016) 341–352.
- [83] A. Trompette, E.S. Gollwitzer, K. Yadava, et al., Gut microbiota metabolism of dietary fiber influences allergic airway disease and hematopoiesis, *Nat. Med.* 20 (2) (2014) 159–166.
- [84] H. Sung, J. Ferlay, R.L. Siegel, et al., Global cancer statistics 2020: GLOBOCAN estimates of incidence and mortality worldwide for 36 cancers in 185 countries, *CA A Cancer J. Clin.* 71 (3) (2021) 209–249.
- [85] S. Kirschner, N. Deutz, C. Hermann, M. Engelen, Plasma short-chain fatty acid (SCFA) concentrations are related to cognition and adipose tissue mass but not muscle function in older adults, *Current Developments in Nutrition* 6 (Supplement_1) (2022), 33–33.
- [86] Q. Yang, J. Ouyang, F. Sun, J. Yang, Short-chain fatty acids: a soldier fighting against inflammation and protecting from tumorigenesis in people with diabetes, *Front. Immunol.* 11 (2020), 590685.
- [87] D. Zhang, S. Li, N. Wang, H.Y. Tan, Z. Zhang, Y. Feng, The cross-talk between gut microbiota and lungs in common lung diseases, *Front. Microbiol.* 11 (2020) 301.
- [88] H. Zhuang, L. Cheng, Y. Wang, et al., Dysbiosis of the gut microbiome in lung cancer, *Front. Cell. Infect. Microbiol.* 9 (2019) 112.
- [89] Q. Gui, H. Li, A. Wang, et al., The association between gut butyrate-producing bacteria and non-small-cell lung cancer, *J. Clin. Lab. Anal.* 34 (8) (2020), e23318.
- [90] W.Q. Zhang, S.K. Zhao, J.W. Luo, et al., Alterations of fecal bacterial communities in patients with lung cancer, *Am J Transl Res* 10 (10) (2018) 3171–3185.
- [91] Z. Li, G. Hu, L. Zhu, et al., Study of growth, metabolism, and morphology of *Akkermansia muciniphila* with an in vitro advanced bionic intestinal reactor, *BMC Microbiol.* 21 (1) (2021) 61.
- [92] B. Routy, E. Le Chatelier, L. Derosa, et al., Gut microbiome influences efficacy of PD-1-based immunotherapy against epithelial tumors, *Science* 359 (6371) (2018) 91–97.
- [93] M.F. Fernández, I. Reina-Pérez, J.M. Astorga, A. Rodríguez-Carrillo, J. Plaza-Díaz, L. Fontana, Breast cancer and its relationship with the microbiota, *Int. J. Environ. Res. Publ. Health* 15 (8) (2018).
- [94] T.O. Keku, S. Dulal, A. Deveaux, B. Jovov, X. Han, The gastrointestinal microbiota and colorectal cancer, *Am. J. Physiol. Gastrointest. Liver Physiol.* 308 (5) (2015) G351–G363.
- [95] X. Xiao, Y. Cao, H. Chen, Profiling and characterization of microRNAs responding to sodium butyrate treatment in A549 cells, *J. Cell. Biochem.* 119 (4) (2018) 3563–3573.
- [96] K. Kim, O. Kwon, T.Y. Ryu, et al., Propionate of a microbiota metabolite induces cell apoptosis and cell cycle arrest in lung cancer, *Mol. Med. Rep.* 20 (2) (2019) 1569–1574.
- [97] C. Karthika, R. Sureshkumar, M. Zehravi, et al., Multidrug resistance of cancer cells and the vital role of P-glycoprotein, *Life* 12 (6) (2022).
- [98] W. Ni, X. Yang, D. Yang, et al., Role of angiotensin-converting enzyme 2 (ACE2) in COVID-19, *Crit. Care* 24 (1) (2020) 422.
- [99] R.K. Sharma, B.R. Stevens, A.G. Obukhov, et al., ACE2 (Angiotensin-Converting enzyme 2) in cardiopulmonary diseases: ramifications for the control of SARS-CoV-2, *Hypertension* 76 (3) (2020) 651–661.
- [100] J. Li, E.M. Richards, E.M. Handberg, C.J. Pepine, M.K. Raizada, Butyrate regulates COVID-19-relevant genes in gut epithelial organoids from normotensive rats, *Hypertension* 77 (2) (2021) e13–e16.
- [101] W. Chen, Y. Lan, X. Yuan, et al., Detectable 2019-nCoV viral RNA in blood is a strong indicator for the further clinical severity, *Emerg. Microb. Infect.* 9 (1) (2020) 469–473.
- [102] K. Kotfis, K. Skonieczna-Żydecka, COVID-19: gastrointestinal symptoms and potential sources of SARS-CoV-2 transmission, *Anaesthesiol. Intensive Ther.* 52 (2) (2020) 171–172.
- [103] R. Zang, M.F. Gomez Castro, B.T. Mccune, et al., TMPRSS2 and TMPRSS4 promote SARS-CoV-2 infection of human small intestinal enterocytes, *Sci Immunol* 5 (47) (2020).
- [104] S. Beyerstedt, E.B. Casaro, B. Rangel É, COVID-19: angiotensin-converting enzyme 2 (ACE2) expression and tissue susceptibility to SARS-CoV-2 infection, *Eur. J. Clin. Microbiol. Infect. Dis.* 40 (5) (2021) 905–919.
- [105] M.U. Cheema, J.L. Pluznick, Gut microbiota plays a central role to modulate the plasma and fecal metabolomes in response to angiotensin II, *Hypertension* 74 (1) (2019) 184–193.
- [106] S. Gu, Y. Chen, Z. Wu, et al., Alterations of the gut microbiota in patients with coronavirus disease 2019 or H1N1 influenza, *Clin. Infect. Dis.* 71 (10) (2020) 2669–2678.
- [107] Y.K. Yeoh, T. Zuo, G.C.-Y. Lui, et al., Gut microbiota composition reflects disease severity and dysfunctional immune responses in patients with COVID-19, *Gut* 70 (4) (2021) 698–706.
- [108] A.M. Valdes, J. Walter, E. Segal, T.D. Spector, Role of the gut microbiota in nutrition and health, *BMJ* 361 (2018) k2179.
- [109] F. Zhang, Y. Wan, T. Zuo, et al., Prolonged impairment of short-chain fatty acid and L-isoleucine biosynthesis in gut microbiome in patients with COVID-19, *Gastroenterology* 162 (2) (2022) 548–561, e544.
- [110] T. Takabayashi, K. Yoshida, Y. Imoto, R.P. Schleimer, S. Fujieda, Regulation of the expression of SARS-CoV-2 receptor angiotensin-converting enzyme 2 in nasal mucosa, *Am J Rhinol Allergy* 36 (1) (2022) 115–122.
- [111] T. Zuo, F. Zhang, G.C.Y. Lui, et al., Alterations in gut microbiota of patients with COVID-19 during time of hospitalization, *Gastroenterology* 159 (3) (2020) 944–955, e948.
- [112] G. Den Besten, K. Van Eunen, A.K. Groen, K. Venema, D.J. Reijngoud, B. M. Bakker, The role of short-chain fatty acids in the interplay between diet, gut microbiota, and host energy metabolism, *J. Lipid Res.* 54 (9) (2013) 2325–2340.
- [113] C. Wu, X. Chen, Y. Cai, et al., Risk factors associated with acute respiratory distress syndrome and death in patients with coronavirus disease 2019 pneumonia in wuhan, China, *JAMA Intern. Med.* 180 (7) (2020) 934–943.
- [114] A. Trompette, E.S. Gollwitzer, C. Pattaroni, et al., Dietary fiber confers protection against flu by shaping Ly6c(-) patrolling monocyte hematopoiesis and CD8(+) T cell metabolism, *Immunity* 48 (5) (2018) 992–1005, e1008.
- [115] M. Kopf, C. Schneider, S.P. Nobs, The development and function of lung-resident macrophages and dendritic cells, *Nat. Immunol.* 16 (1) (2015) 36–44.
- [116] V. Sencio, A. Barthelemy, L.P. Tavares, et al., Gut dysbiosis during influenza contributes to pulmonary pneumococcal superinfection through altered short-chain fatty acid production, *Cell Rep.* 30 (9) (2020) 2934–2947, e2936.
- [117] D. Worlitzsch, R. Tarran, M. Ulrich, et al., Effects of reduced mucus oxygen concentration in airway *Pseudomonas* infections of cystic fibrosis patients, *J. Clin. Invest.* 109 (3) (2002) 317–325.
- [118] M.M. Tunney, T.R. Field, T.F. Moriarty, et al., Detection of anaerobic bacteria in high numbers in sputum from patients with cystic fibrosis, *Am. J. Respir. Crit. Care Med.* 177 (9) (2008) 995–1001.
- [119] B. Mirković, M.A. Murray, G.M. Lavelle, et al., The role of short-chain fatty acids, produced by anaerobic bacteria, in the cystic fibrosis airway, *Am. J. Respir. Crit. Care Med.* 192 (11) (2015) 1314–1324.
- [120] B.W. Haak, E.R. Littmann, J.L. Chaubard, et al., Impact of gut colonization with butyrate-producing microbiota on respiratory viral infection following allo-HCT, *Blood* 131 (26) (2018) 2978–2986.
- [121] K. Chakraborty, M. Raundhal, B.B. Chen, et al., The mito-DAMP cardiolipin blocks IL-10 production causing persistent inflammation during bacterial pneumonia, *Nat. Commun.* 8 (2017), 13944.
- [122] K.H. Antunes, J.L. Fachi, R. De Paula, et al., Microbiota-derived acetate protects against respiratory syncytial virus infection through a GPR43-type 1 interferon response, *Nat. Commun.* 10 (1) (2019) 3273.
- [123] I. Galvão, L.P. Tavares, R.O. Corrêa, et al., The metabolic sensor GPR43 receptor plays a role in the control of *Klebsiella pneumoniae* infection in the lung, *Front. Immunol.* 9 (2018) 142.
- [124] T.W. Hand, The role of the microbiota in shaping infectious immunity, *Trends Immunol.* 37 (10) (2016) 647–658.
- [125] S.D. Shukla, K.F. Budden, R. Neal, P.M. Hansbro, Microbiome effects on immunity, health and disease in the lung, *Clin Transl Immunology* 6 (3) (2017) e133.
- [126] D.N. O'dwyer, R.P. Dickson, B.B. Moore, The lung microbiome, immunity, and the pathogenesis of chronic lung disease, *J. Immunol.* 196 (12) (2016) 4839–4847.
- [127] S. Namasivayam, A. Sher, M.S. Glickman, M.F. Wiperman, The microbiome and tuberculosis: early evidence for cross talk, *mBio* 9 (5) (2018).
- [128] E. Lachmandas, C.N. Van Den Heuvel, M.S. Damen, M.C. Cleophas, M.G. Netea, R. Van Crevel, Diabetes mellitus and increased tuberculosis susceptibility: the role of short-chain fatty acids, *J. Diabetes Res.* 2016 (2016) 1–15, 6014631.
- [129] L.N. Segal, J.C. Clemente, Y. Li, et al., Anaerobic bacterial fermentation products increase tuberculosis risk in antiretroviral-drug-treated HIV patients, *Cell Host Microbe* 21 (4) (2017) 530–537, e534.
- [130] D.A. Negatu, Y. Yamada, Y. Xi, et al., Gut Microbiota Metabolite Indole Propionic Acid Targets Tryptophan Biosynthesis in *Mycobacterium tuberculosis*, *mBio* 10 (2) (2019).
- [131] M.G. Machado, V. Sencio, F. Trottein, Short-chain fatty acids as a potential treatment for infections: a closer look at the lungs, *Infect. Immun.* 89 (9) (2021) e00188-21.

4) Literature Review: Tackling the cytokine storm using advanced drug delivery in allergic airway disease

Status: Published in **Journal of Drug Delivery Science and Technology**

Citation: Patel VK, Vishwas S, Kumar R, **De Rubis G**, Shukla SD, Paudel KR, Manandhar B, Singh TG, Chellappan DK, Gulati M, Kaur IP, Allam VSRR, Hansbro PM, Oliver BG, MacLoughlin R, Singh SK, Dua K. *Tackling the cytokine storm using advanced drug delivery in allergic airway disease*. **Journal of Drug Release Science and Technology. Journal of Drug Delivery Science and Technology.** 2023 Apr 82: 104366. doi: <https://doi.org/10.1016/j.jddst.2023.104366>

Contribution: I contributed to the preparation of this collaborative review, specifically on sections related to the clinical trials in which novel drug delivery systems have been evaluated against asthma. Furthermore, I have contributed to the final manuscript revision process and in addressing some of the reviewers' comments.



Review article

Tackling the cytokine storm using advanced drug delivery in allergic airway disease



Vyoma K. Patel^{a,b,c}, Sukriti Vishwas^d, Rajan Kumar^d, Gabriele De Rubis^{a,b}, Shakti D. Shukla^{a,b}, Keshav Raj Paudel^e, Bikash Manandhar^{a,b}, Thakur Gurjeet Singh^f, Dinesh Kumar Chellappan^g, Monica Gulati^{b,d}, Indu Pal Kaur^h, Venkata Sita Rama Raju Allamⁱ, Philip M. Hansbro^e, Brian G. Oliver^{j,k}, Ronan MacLoughlin^{l,m,n}, Sachin Kumar Singh^{b,d,**}, Kamal Dua^{a,b,o,*}

^a Discipline of Pharmacy, Graduate School of Health, University of Technology Sydney, P.O. Box 123 Broadway, Ultimo, NSW, 2007, Australia

^b Faculty of Health, Australian Research Centre in Complementary and Integrative Medicine, University of Technology Sydney, Ultimo, NSW, 2007, Australia

^c School of Clinical Medicine, Faculty of Medicine and Health, University of New South Wales, Sydney, NSW, 2052, Australia

^d School of Pharmaceutical Sciences, Lovely Professional University, Phagwara, Punjab, India

^e Centre for Inflammation, Centenary Institute and University of Technology Sydney, School of Life Sciences, Faculty of Science, Sydney, NSW, 2007, Australia

^f Chitkara College of Pharmacy, Chitkara University, Punjab, 140401, India

^g Department of Life Sciences, School of Pharmacy, International Medical University, Bukit Jalil, Kuala Lumpur, 57000, Malaysia

^h University Institute of Pharmaceutical Sciences, Panjab University, Chandigarh, 160014, India

ⁱ Department of Medical Biochemistry and Microbiology, Uppsala University, Uppsala, Sweden

^j School of Life Sciences, Faculty of Science, University of Technology Sydney, Ultimo, NSW, Australia

^k Woolcock Institute of Medical Research, University of Sydney, Sydney, NSW, Australia

^l Aerogen Ltd., IDA Business Park, Dangan, Galway, H91 HE94, Ireland

^m School of Pharmacy & Biomolecular Sciences, Royal College of Surgeons in Ireland, Dublin, D02 YN77, Ireland

ⁿ School of Pharmacy & Pharmaceutical Sciences, Trinity College, Dublin, D02 PN40, Ireland

^o Uttaranchal Institute of Pharmaceutical Sciences, Uttaranchal University, Dehradun, 248007, India

ARTICLE INFO

Keywords:

Asthma

Cytokines

Drug delivery systems

Clinical trials

ABSTRACT

Asthma is one of the leading causes of mortality worldwide presenting a huge socio-economic burden with rising morbidity and mortality rates. It is a chronic inflammatory airway disease that is eminent with multiple epidemiological and pathophysiological features such as over production of pro-inflammatory cytokines that triggers an uncontrolled aberrant inflammatory response known as 'cytokine storm'. This phenomenon interferes with the signalling and production of cytokines over time leading to the progression of disease and the development of complications that lead to fatal consequences in many individuals. Targeting this overproduction and signalling of cytokines may prove a promising approach to develop novel cytokine specific therapies in the treatment of asthma. This review discusses on the various pharmacological strategies, recent advancements in drug delivery systems and significant findings from clinical trials that may have a potential to outweigh the limitations of the current therapies in the treatment of asthma.

1. Introduction

The prevalence and burden of chronic respiratory diseases (CRDs), especially asthma and chronic obstructive pulmonary disease (COPD), are constantly accelerating worldwide. Notably, the report on the global burden of disease highlights that about 545 million individuals develop

a chronic respiratory condition on an average. This accounts for approximately 3.9 million deaths annually [1]. Moreover, over the past years, CRDs have accounted towards a huge proportion of disability-adjusted life years globally, with an 18% increase [1]. In Australia, both COPD and asthma, along with lung cancer feature in the top ten leading causes of diseases [2]. In 2020-21, the prevalence of

* Corresponding author. Discipline of Pharmacy, Graduate School of Health, University of Technology Sydney, P.O. Box 123 Broadway, Ultimo, NSW, 2007, Australia.

** Corresponding author. School of Pharmaceutical Sciences, Lovely Professional University, Phagwara, Punjab, India.

W[- + Å#&1, % %Z&in.16030@lpu.co.in (S.K. Singh), Kamal.Dua@uts.edu.au (K. Dua).

<https://doi.org/10.1016/j.jddst.2023.104366>

Received 14 November 2022; Received in revised form 6 March 2023; Accepted 12 March 2023

Available online 20 March 2023

1773-2247/© 2023 Elsevier B.V. All rights reserved.

asthma and COPD were reported to be 10.7% and 1.5% respectively among individuals of all ages [3]. Understandably, the prevalence of COPD has now increased to 5.2% in people aged >75 years. In Australia, asthma-related deaths remain exceptionally high (417 deaths in 2020) when compared worldwide. Both asthma and COPD are categorised as chronic respiratory diseases that require lifelong patient-centric management of symptoms resulting in an enormous health as well as economic burden on patient as well as on the healthcare system [2].

Asthma is a rather common but heterogeneous chronic condition, and unfortunately, it is often inadequately controlled in most patients [4]. For example, only 1 in 3 Australians has a scripted asthma action plan or uses asthma-related medications recurrently [5]. This further complicates the disease presentation and management, and often leads to accelerated progression of disease. Hence, there is a critical need for novel strategies for managing asthma. Furthermore, asthma affects individuals of all ages, although the presentation of disease may vary depending upon the exposure to allergens, racial background, gender, diet, and other indicators such as socio-economic status [6]. Asthma may present differently in individuals and is categorised based on clinical symptoms and immunological characteristics of the disease. The symptoms of asthma include shortness of breath, chest tightness, coughing and wheezing. Allergic asthma exacerbates in response to exposure to non-specific environmental stimuli, including infectious (microbes) and non-infectious (mould, dust mite, and pollen) triggers, in addition to host genetic makeup [7]. These intrinsic and extrinsic triggers lead to aberrant inflammatory response that may result in the exacerbation of asthma symptoms, resulting in severe and deleterious consequences such as hospitalisation and increased risk of morbidity. Mild-to-moderate asthma is primarily characterised by a T-helper cell type-2-mediated inflammation developing due to heightened responses to common allergens. The major cell types involved in type-2 asthma are mast cells, Th2 cells, basophils, eosinophils, group 2 innate lymphoid cells (ILC2s), and IgE-producing B cells [8]. Moreover, prolonged exposure to these common allergens and resulting persistent inflammation further leads to myofibroblast infiltration, leading to remodeling of the airway epithelium. This results in increased mucus secretion, hypertrophy of airway smooth muscle, and significant increase in collagen deposition [8]. This causes the airways to become increasingly more responsive to aeroallergen provocation, and this leads to the characteristic 'wheezing' and obstructed airflow. An extensive amount of scientific research has progressed the understanding of the underlying inflammatory mechanisms and the development of new therapies in asthma management.

Asthma can be categorised into different phenotypes, depending on the observable characteristics, which primarily relies on the clinical presentation of the disease; or endotypes, depending on the distinct underlying disease mechanisms that are taken into consideration [9]. These are rather complex and represent the heterogeneous and varying outcomes of host-environment interactions [7]. Based on the cells activated during inflammation, asthma can be categorised into neutrophilic, eosinophilic, or paucigranulocytic (in which no increased numbers of neutrophils or eosinophils are observed). A combination of clinical symptoms and cellular and molecular, are utilised to categorise the asthma sub-types, as well as to determine the treatment strategies for individuals with asthma. In this review, we summarise the key inflammatory pathways activated in asthma, and we explore the potential approaches, including recent drug delivery techniques, to mitigate the inflammation-induced lung damage in asthma.

2. Pathophysiology of asthma

The pathogenesis of asthma involves the interaction between inflammation and remodeling of the airways of the lungs, resulting in airway hyperresponsiveness (AHR) [10]. AHR is the major feature of asthma, leading to an exaggerated bronchoconstrictor response to various environmental stimuli such as allergens (infectious and

non-infectious), farm dust, microbiomes, air pollutants, and other chemicals. The hyperresponsiveness of the bronchial airways alters the integrity of the inner wall of the lung epithelium, which is maintained by the contraction and relaxation of smooth muscles and elastic fibers, in response to the inflammatory mediators, thus resulting in excessive narrowing of the airways [11]. Asthma diminishes the lung function in an accelerated manner, which in severe and chronic cases, causes an irreversible airflow obstruction via airway remodeling. AHR involves multiple and complex mechanisms, including increased histamine production from mast cells, inflammation, loss of airway contractility, and increased thickness of the inner wall, causing difficulty in breathing [8, 12]. The interplay between innate and adaptive cells and mediators in type 2 inflammation underpins the pathophysiology of asthma as discussed below (Fig. 1). Moreover, airway inflammation is a characteristic feature of asthma and involves an early phase of initiation involving sensitisation of immunoglobulin E (IgE), released by plasma cells, to environmental allergens and pollutants. The serum IgE is elevated and binds to mast cells and basophils [8,13]. Mast cells then de-granulate to release cytokines such as histamine, prostaglandins, and leukotrienes, which in turn causes the contraction of airway smooth muscle resulting in airway constriction [7,8].

Th2 lymphocytes play an important role in the exacerbation of airway inflammation [14]. The antigen-presenting dendritic cells in the airways process the allergens into small peptides and presents them to naïve T cells via major histocompatibility complex (MHC) class II molecules [14]. This leads to differentiation of the T cells to Th2 phenotype, which produce a series of pro-inflammatory cytokines such as interleukin (IL)-3, IL-4, IL-5, IL-6, IL-8, IL-9, IL-13, as well as granulocyte macrophage-colony stimulating factor (GM-CSF), proteases, reactive oxygen species (ROS) and prostaglandins. This phenomenon is also known as 'cytokine storm' [8,15–18]. These cytokines subsequently stimulate localisation of dendritic cells (DCs), type 2 innate lymphoid cells (ILC2s), basophils, eosinophils, mast cells, and alternatively activated macrophages (AAMs) that promote adaptive Th2 immunity via induction of ox40L (is also known as tumour necrosis factor super family member 4 and is ligand for ox40 that is expressed by many antigen-presenting cells such as T cells, natural killer (NK) cells and lymphocytes) [19] and suppression of IL-12, particularly in DCs [20–22]. This leads to bronchoconstriction and inflammation. Notably, a prior exposure to allergens can dampen the epithelial cell response leading to an upregulation of tumour necrosis factor acute induced protein-3 (TNFAIP-3), which further suppresses the activity of nuclear factor- κ B (NF- κ B) in epithelial cells (Fig. 1). This aberrant inflammatory response eventually leads to airway remodeling - a complex clinical feature of asthma that involves long term disruption and modification of airway architecture. This significantly contributes to AHR and lung function decline [23,24]. Airway remodeling is characterised by epithelial damage, ciliary dysfunction, extracellular matrix deposition, and increased epithelial-to-mesenchymal transition (EMT), causing permanent airflow obstruction [8,23–26]. This further leads to inefficient adhesion of bronchial epithelial cells to the airway wall thus, leading to infiltration of airway smooth muscle cells and thickening of the airway walls due to migration of bronchial epithelial cells [27]. At this stage, further release of a wider range of cytokines such as TNF- α , IL1- β , IL-6, IL-13 IL-17 and ROS via interactions between eosinophils and mast cells further amplifies inflammatory response and oxidative stress. This leads to an irreversible airflow obstruction and lung function decline [8,26,28]. Although the pathophysiology of asthma, airway inflammation and remodeling, including subsequent cytokine release, have been well documented in the literature, this dogma is predominantly translated from only murine models of asthma. Nevertheless, further research is essential to determine the effects of inhibiting the cytokine response, being that is a key player in both airway inflammation and remodeling in asthma. Targeting the release of this wider repertoire of cytokines may have the potential to dramatically improve symptoms and disease burden in asthmatic patients.

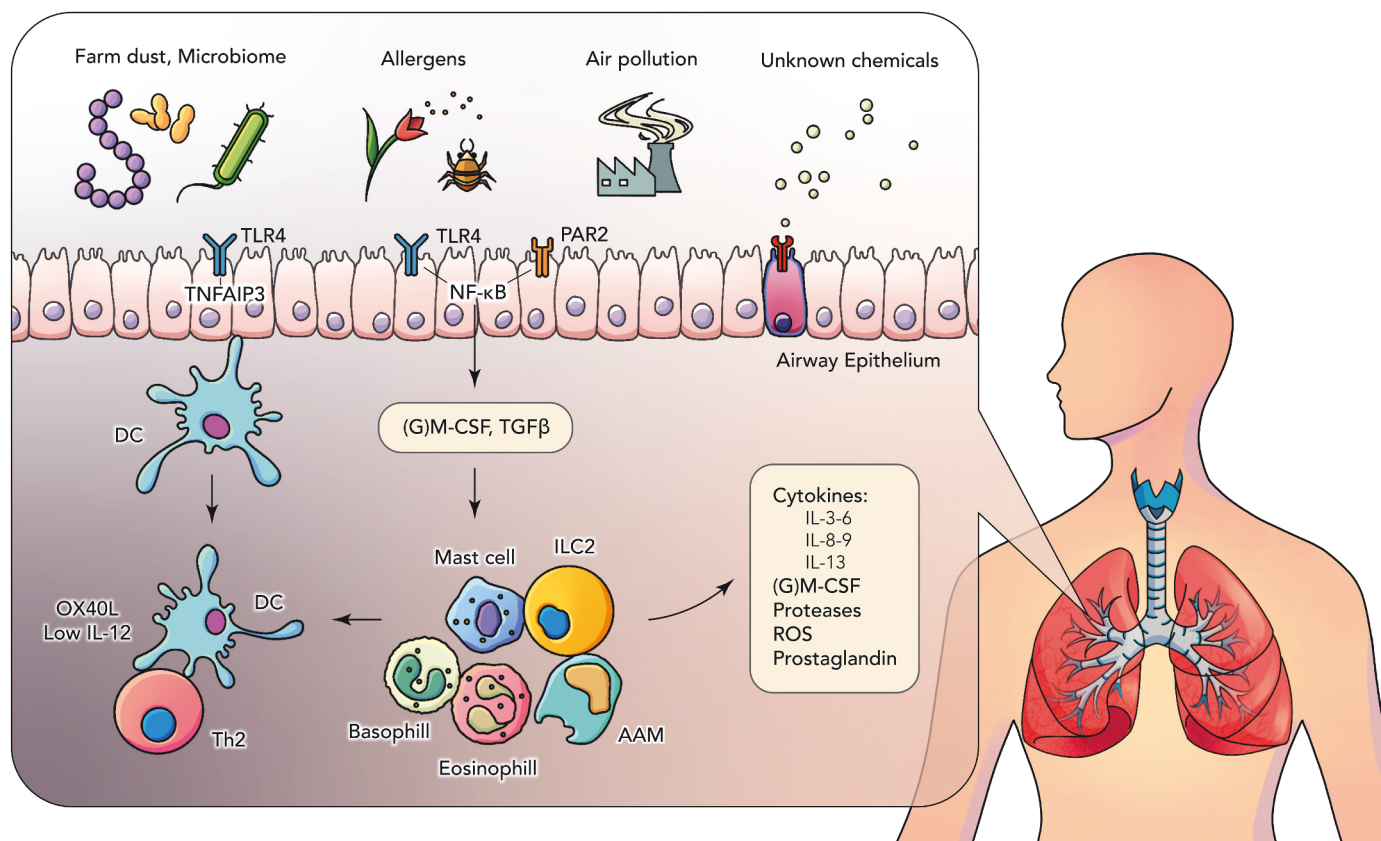


Fig. 1. Schematic representation of asthma pathophysiology

Upon exposure to various allergens several inflammatory cells, cytokines and mediators are recruited or activated, producing acute effects on the airway epithelium –such as bronchoconstriction, mucus secretion, plasma leakage, together with airway remodeling leading to fibrosis of sub-epithelium, angiogenesis and narrowing airway smooth muscles. Abbreviations: TLR – Toll like receptor; DC – dendritic cell; IL–interleukin; GMCSF – Granulocyte macrophage colony-stimulating factor; TNFAIP3 – Tumour Necrosis Factor Alpha Induced Protein 3; NFκB – Nuclear factor kappa B; ROS- reactive oxygen species; Th2 – T helper cell type 2; TGF-β – Transforming growth factor beta; PAR2 - Protease activated receptor 2; AAM – alternative activated macrophages; ILC2 - type 2 innate lymphoid cells.

3. Current therapies to treat asthma and their limitations

Although there is no proper cure for asthma, the overall aim is to effectively manage and control the symptoms that are associated with the disease, such as inflammation, exacerbations, airway narrowing, mucus production that are associated with the disease, and to improve the quality of life of the patients [29]. The current treatment strategies employed in the treatment of asthma are mainly focussed on reducing symptoms for the two key clinical features of asthma explicitly, inflammation and bronchoconstriction via anti-inflammatory agents (commonly, inhaled corticosteroids) and bronchodilators. Targeting inflammation is a key success factor to the long-term management of asthma, and identifying various inflammatory targets implied with the disease is fundamental. Treatment strategies against these targets to surrogate the inflammation result in better outcomes when compared to targeting bronchodilation [30]. The conventional anti-inflammatory therapy that is widely recommended by the global clinical guidelines includes the use of the inhaled corticosteroids (ICS) [31]. ICS therapy is a key treatment for asthmatics that reduces an inflammation either by inducing apoptosis or by reducing infiltration of the inflammatory cells such as eosinophils, mast cells and T cells thereby preventing the exacerbations and improving the lung function to further reduce morbidity and mortality associated to asthma [32,33].

Although ICS are effective in the treatment of asthma, unwanted adverse effects associated with long-term treatment include weight gain, development of cataract and glaucoma, osteoporosis, hyperglycaemia, and drug-associated diabetes, and skin diseases associated with the long-term treatment limit the use of ICS [32]. In addition to the adverse

effects, the compliance with ICS is very poor as this therapy does not cure asthma, and the symptoms usually persist upon treatment discontinuation. Interestingly, about 5–10% asthmatics respond poorly to this conventional therapy due to altered and unstable expression of glucocorticoid receptor and nuclear translocation failure of the corticoids-receptor complex that ultimately leads to steroid resistance, highlighting the necessity to develop alternative anti-inflammatory therapies that can treat the disease effectively. Moreover, oxidative stress in severe asthma further mediates various mechanisms including impairment of the histone deacetylase-2 (HDAC2) and activation of p38 mitogen activated protein kinase (MAPK), and this which results in the amplification of the inflammatory response and the reduction of the anti-inflammatory response to the steroids [34].

Targeting bronchoconstriction is another significant strategy in asthma treatment, and bronchodilators are highly necessary to relieve bronchoconstriction, enabling to relax the smooth muscle especially in acute episodes of asthma. Bronchodilators including the fast-acting β₂-agonists, such as albuterol, short-acting anticholinergics, such as ipratropium bromide, and long acting β₂-agonists (LABAs) such as salmeterol and formoterol, are currently used either alone or in combination with the ICS for the effective management of asthma [31,35]. Although advancements in research have led to the development of ultra-long acting β₂-agonists such as indacaterol, carmoterol, milveterol, poor adherence and associated adverse effects such as sympathomimetic effects i.e., anxiety, tremors, tachycardia, and cholinergic blocking effects i.e., xerostomia, limit the usage of this class of drugs [32,36].

The use of biologics represents another approach for the treatment of asthma associated with allergic conditions. Blockade of IgE with

omalizumab and targeting IL-5 cytokine with antibodies such as mepolizumab, reslizumab and benralizumab, and IL-4 cytokine with duplizumab acts on various pathways to prevent IgE binding to receptors on mast cells. Moreover, blockade of IL-5 cytokine from binding to its receptor and activating apoptosis of eosinophils are reported to be reasonably effective particularly in cases of severe asthma [31,37,38]. Several experiments have been trailed by the administration of the Th1 cytokines like interferon (IF)- α , β , γ , and IL-12 to suppress the Th2 asthmatic responses. However, due to adverse effects and the lack of efficacy, this strategy has not progressed further [39]. The existing biologics mainly targets the Th2 asthmatic response, although there are other Th2 lower asthmatic endotypes that are not fully characterised. Biologics targeting these endotypes that are specific to the airway neutrophilia were proven to be unsuccessful. Therefore, the current research aim to target the wider repertoire of the cytokines such as TNF- α , IL1- β , IL-6, IL-17 which may affect airway neutrophilia of the Th2 lower asthmatic endotypes [40]. Furthermore, the crossover and overlap of different pathways in asthma and the high cost of the treatment limit the effective usage of these biologics effectively in asthma treatment [37].

Alternative therapeutic approaches include the use of leukotriene modifiers such as montelukast and the 5-lipoxygenase inhibitor zileuton that act as anti-inflammatory and bronchodilators have also been recommended for use in combination with LABAs or ICS to treat asthma [33]. Similarly, phosphodiesterase inhibitors such as theophylline and roflumilast have also shown beneficial effects in inhibiting inflammation in murine models and clinical studies [31,32]. Furthermore, inhibiting the kinases particularly, phosphoinositide-3-kinase (PI3K) - that regulates the expression of chemotactic and inflammatory genes (PI3K γ), and reduces the corticosteroid response (PI3K δ) - may also aid as an alternative to the ICS therapy [31,33]. However, these inhibitors possess a narrow therapeutic index and hold potential adverse effects that are associated with multiple inhibitory homeostatic pathways. Finally, the use of nutraceuticals as supplements has also shown some efficacy in the treatment of asthma. However, poor drug distribution and lack of efficacy have further led researchers to find alternate strategies to these therapies [41,42]. Despite the development of various therapeutic strategies, a better understanding of the asthma pathogenesis is highly essential to develop alternative therapies that can selectively target mechanistic pathways using novel drug delivery methods with minimal adverse effects and enhanced efficacy.

4. Pharmacological strategies and recent advancements in nano-drug delivery for targeting asthma

Nano-drug delivery systems are the latest trends in drug delivery science that are rapidly growing in the present era. Particles in the nanoscale range are used for diagnosis as well as to deliver therapeutic agents to the targeted sites in a controlled manner. The major benefit of nanotechnology is that it allows to treat chronic diseases could be treated though site-specific, and target-oriented delivery systems. Nanotechnology is used to deliver several therapeutic moieties including biological agents, chemotherapeutic agents, and immunotherapeutic agents to treat various diseases [43].

Nanoparticles (NPs) as therapeutic agents provide more benefits than conventional drugs in the management of respiratory diseases. These benefits of NPs include uniform drug distribution, dissolution rate, macromolecule delivery, enhanced solubility, sustained release, appropriate cell internalisation, and targeted delivery of drug molecules to the required site. With the help of targeted delivery, local drug concentration could be improved in the lungs, and this may enhance the therapeutic efficacy of drugs in lungs for the treatment of asthma [44, 45].

The pulmonary route is advantageous for locally acting drugs and bioactives that are used to treat lung diseases because it reduces adverse effects associated with systemic administration. It is also a possible route for the administration of drugs to achieve systemic effects, since it offers

a large surface area for drug absorption, a weak epithelial barrier, and efficient blood circulation, resulting in the direct and rapid entrance of medications into the bloodstream [46]. Pulmonary administration is crucial for the efficient delivery of drugs to the lungs as NPs travel a considerable distance from the nasal canal to the lung alveoli. Throughout this process of drug delivery, NPs should overcome several obstacles, including pulmonary barriers [47]. Various type of nano delivery systems developed to treat asthma are shown in Fig. 2A and the mechanistic illustration of pulmonary drug targeting using nano-formulations into the lung are presented in Fig. 2B and C.

A list of a key studies implicating role and development of various NPs in treatment of asthma is summarised in Table 1.

4.1. Inorganic metallic NPs

Inorganic metallic NPs have been reported as very good therapeutic, diagnostic, sensor, and imaging agents for the treatment of asthma. There are various types of inorganic metallic NPs including gold, platinum, zinc, cerium, and silver NPs [48,49]. Recently, these materials have been extensively utilised in biomedical applications, primarily for cell and biomolecule labelling. Metallic NPs may be employed as antioxidants due to their capacity to lower ROS levels and reduce their potential. Since oxidative stress plays a key role in progression of asthma and metallic NPs such as gold and silver NPs conjugated with antioxidants have been shown to enhance drug absorption at the target site and thus, reduce the progression of asthma [44,49].

Interestingly, a study conducted by Serra et al., reported that gold NPs administered intranasally in a mice model of asthma attenuated glucocorticoid (GC) resistance in asthma via administration through intranasal route in a mice model. For the induction of asthma, ovalbumin was administered through intranasal route once a week for nine weeks. Moreover, another study has reported that gold NPs can attenuate the levels of biomarkers such as nuclear factor erythroid 2-related factor 2 (NRF2), histone deacetylase 2 (HDAC2), thiobarbituric acid reactive substances (TBARS), and PI3K δ , which play a critical role in mediating oxidative stress. These findings indicate that the gold NPs possess a potential to reduce the level of oxidative stress and inflammation by attenuating these asthmatic biomarkers [50]. The mechanistic pathways of gold NPs against lung inflammation especially in asthma are presented in Fig. 3.

Interestingly, studies have shown that gold NPs exhibited good cellular permeability and reached the target site rapidly due to their small particle size, 2-3 nm [51,52]. Indeed, Barreto et al., demonstrated the efficacy of gold NPs administered via intranasal route in asthmatic mice and showed that gold NPs reduced airway hyper-reactivity, lung remodeling, and inflammation upon induction with ovalbumin [53]. Park et al., reported that the intranasal delivery of silver NPs to treat asthma in ovalbumin-induced asthmatic mice led to increase in the levels of various cytokines such as IL-5, IL-6, IL-13, and nuclear factor kappa light chain enhancer of activated B cells (NF κ B) as well as ROS. By enhancing the levels of these potential biomarkers, ovalbumin increased the degree of inflammation and oxidative stress. Various biochemical parameters have been analysed to evaluate the antioxidant and anti-inflammatory effects of silver NPs against ovalbumin-induced oxidative stress. The results showed that silver NPs reduced the levels of IL-5, IL-6, IL-13, NF κ B and ROS [54]. Jang et al., developed silver NPs and analysed their inhibitory effects on mucus hypersecretion in allergic airway inflammation in female BALBc mice [55]. The findings showed that intranasal administration of silver NPs significantly reduced the elevated levels of VEGF, PI3K, hypoxia-inducible factor (HIF)-1, and phosphorylated-Akt levels, as well as mucosal glycoprotein expression (Muc5ac) in lung tissues [55].

4.2. Polymeric NPs

In recent years, polymeric NPs have gained substantial attention

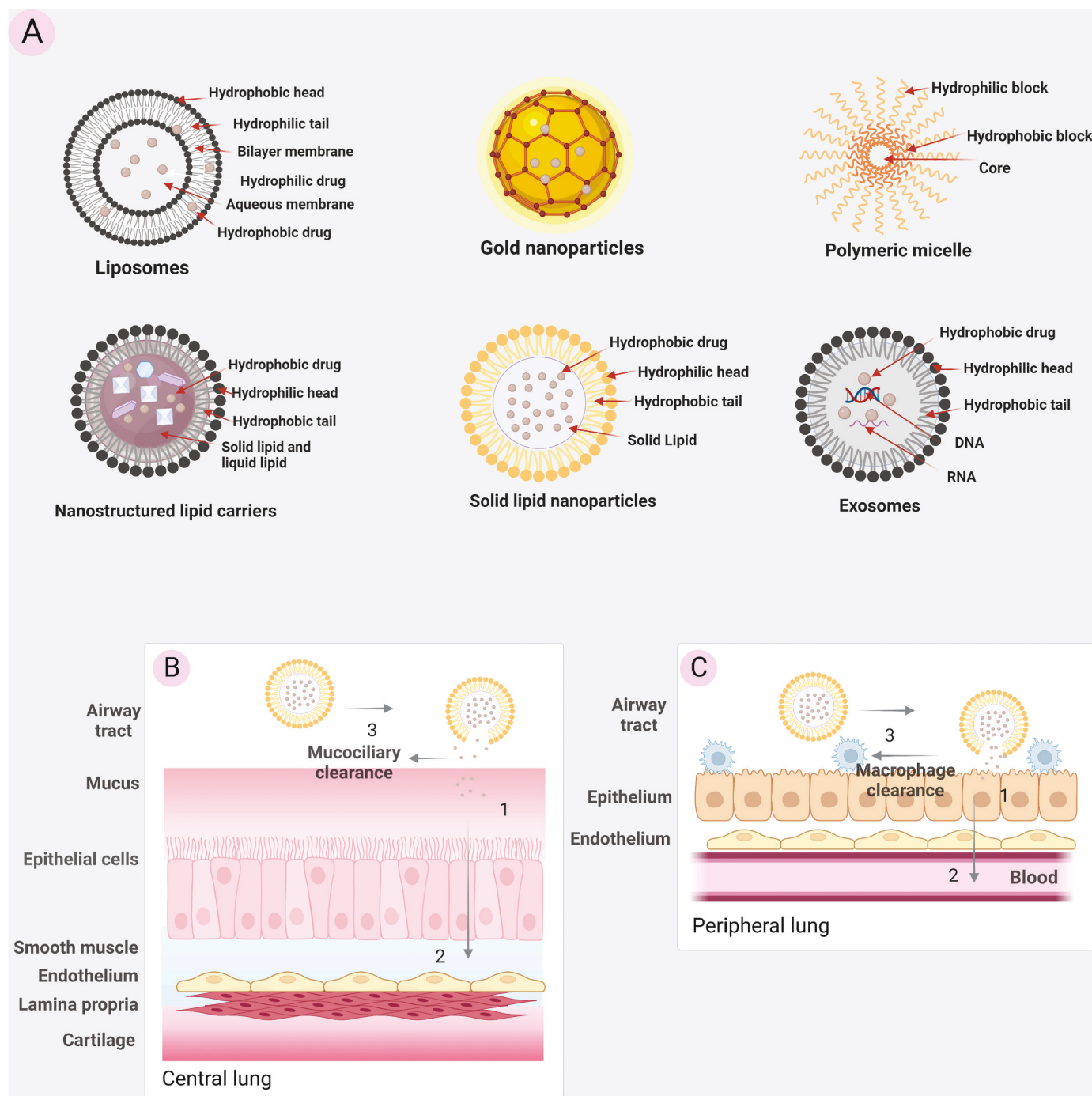


Fig. 2. Nanoformulations and their delivery to lung

(A) Various nanoformulations explored to treat asthma. Delivery of drug in section (B) the central lung and (C) peripheral lung nanoparticles (NPs) circumvent the pulmonary barriers (such as mucociliary clearance and macrophage clearance) and get absorbed as well as internalised into the cells. After being absorbed, they enter the blood.

owing to their compact size [56,57]. Properties of polymeric NPs are categorised based on their capability for controlled release, ability to shield biologically active drugs and other chemicals from the environment, and their capacity to enhance bioavailability and therapeutic index of conjugated drug [58]. Various studies have reported that polymeric NPs alone, as well as those conjugated with drugs can enhance drug delivery to the pulmonary route and increase drug potency.

A study conducted in 2022 by Ullah et al., reported an enhanced pulmonary delivery of montelukast when loaded into polymeric NPs.

The optimised polymeric NPs prepared by the ionic gelation were reported to have average particle size range, zeta potential, and polydispersity index (PDI) of 220 nm–383 nm, -11 mV–22 mV, and 0.50, respectively. To evaluate physical and chemical properties as well as purity of the developed polymeric NPs, differential scanning calorimetry (DSC) and Fourier transform infrared spectroscopy (FTIR) studies were performed. Polymeric NPs significantly increased potency and pulmonary delivery of montelukast conjugated with them as that of raw montelukast [59]. Another study conducted in 2021 by Jin et al., showed that NPs loaded with berberine exhibited a beneficial effect in a

Table 1
Role of different NPs in targeting and drug delivery for asthma.

No.	Formulation	Route of administrations	Animals or/and cell lines	Inducing agent	Outcomes	References
Inorganic metallic NPs						
1.	PEGylated and Citrated gold NPs	Intranasal	Mice	Ovalbumin	<ul style="list-style-type: none"> It provided anti-inflammatory effects by attenuating IL-1β Inhibited airway hyperreactivity and inflammatory infiltrates 	[107]
2.	Titanium dioxide NPs	Intranasal	Mice	Ovalbumin	<ul style="list-style-type: none"> Titanium dioxide NPs activated level of transient receptor potential vanilloids (TRPVs) and TRPV P 2 \times 7 Secreted neuromediators that cause airway inflammation and exacerbate asthma 	[108]
3.	Silica dioxide NPs	Intranasal	Mice	Ovalbumin	<ul style="list-style-type: none"> Enhanced mRNA expression Attenuated level of thioredoxin-interacting protein, NLRP3 inflammasome, and IL-1β proteins 	[109]
4.	Zinc oxide NPs	Intranasal	Mice	Ovalbumin	<ul style="list-style-type: none"> Reduced airway inflammation Enhanced Th2 cytokine 	[110]
5.	Zinc oxide NPs	Intranasal	Mice	Ovalbumin	<ul style="list-style-type: none"> Reduced IL-4, IL-5, and IL-13 	[111]
NPs						
6.	Carbon black NPs	Intranasal	Mice	Ovalbumin	<ul style="list-style-type: none"> Attenuated airway hyperreactivity, Reduced remodeling Produced antiinflammation Inhibited IL4-, IL-6, IL-13, IL-1β and TNF-α Alleviated level of IL-10 	[112]
7.	Conjugated α alumina NPs with vasoactive intestinal peptide (VIP)	Intranasal	Mice	Ovalbumin	<ul style="list-style-type: none"> α-alumina NPs prevented enzymatic denaturation of VIP in the respiratory tract Attenuated numbers of eosinophils, Th2 cytokines, serum IgE level and hyperresponsiveness 	[113]
8.	DNA NPs mediated thymulin gene therapy	Intranasal	Mice	Ovalbumin	<ul style="list-style-type: none"> Attenuated pro-inflammatory cytokines such as IL-13, eosinophiles Mitigated lung remodeling, airway inflammation and leading Improved pulmonary mechanics Attenuated collagen deposition 	[114]
9.	Bilirubin NPs	Intravenous	Mice	Ovalbumin	<ul style="list-style-type: none"> Ameliorated level of Th2-related infection in lungs during allergic inflammation 	[115]
Liposomes						
10.	Salbutamol sulphate	Intraperitoneal	Rats and guinea pig	Ovalbumin	<ul style="list-style-type: none"> Enhanced encapsulation efficiency by 70% in rats Reduced the risk of asthma in guinea pigs 	[116]
Solid lipid NPs						
11.	Curcumin	Intraperitoneal	Rats	Ovalbumin	<ul style="list-style-type: none"> Enhanced bioavailability by 26 folds as compared to naïve curcumin Attenuated airway hyperresponsiveness Reduced expression of T-helper-2-type cytokines like IL-4, IL-5 and IL-13 Offers antioxidant effects and helped in decreasing levels of ROS 	[117]
12.	Curcumin	Intraperitoneal	Mice	LPS	<ul style="list-style-type: none"> Attenuated the pro-inflammatory mediator such as IL-6, IL-1β and TNF-α Augmented the level of cytokine IL-10 by ELISA Inhibited the expression of TLR4, TLR2, and TNF-α in lymph node tissues 	[118]
13.	CCR3 antagonists (R321 peptide)	Intranasal	Mice	Eotaxin	<ul style="list-style-type: none"> Inhibited the level of eosinophiles Blocked airway hyperresponsiveness 	[119]
Exosomes						
14.	Exosomal miRNA	Intranasal	Human	–	<ul style="list-style-type: none"> Attenuated the level of various cytokinin such as IL-13 and TNF-α 	[120]
15.	B-cell-derived exosomes	Intraperitoneal	Mice	Ovalbumin	<ul style="list-style-type: none"> Enhanced the levels of various cytokinin such as IL-4, IL-5, and IL-13 Attenuated levels of IFN-γ, and TNF-α 	[121]

house dust mite (HDM) model of asthma in mice. NPs were prepared with polylactic-co-glycolic acid (PLGA) and polyethylene glycol (PEG) that were coated with platelet membranes (PM). These NPs were then administered intranasally, and the resulting therapeutic outcome was evaluated. The formed NPs without PM were found to be of 280 nm in size, and after coating with PM, the size of NPs increased up to 400 nm. The surface charge of the NPs was found to be 0 mV and -23 mV in case of NPs with and without PM coating, respectively. The berberine loading percentage significantly increased from 8.1% to 81.02% after

encapsulation and coating resulted in a sustained release of berberine. The cellular uptake of the NPs was evaluated on the A549 human adenocarcinoma cell line and was observed that, when the cell line was in normal conditions, there was no difference between the uptake of the uncoated and PM coated NPs. However, when the cell line was treated with house dust mite (HDM), the uptake of PM-coated NPs was higher than uncoated NPs. Further analysis showed that PM-coated NPs enhanced the expression of cytokine IL-12 and decreased the expression of IL-13 and IL-4, demonstrating the role of PM coating in treating

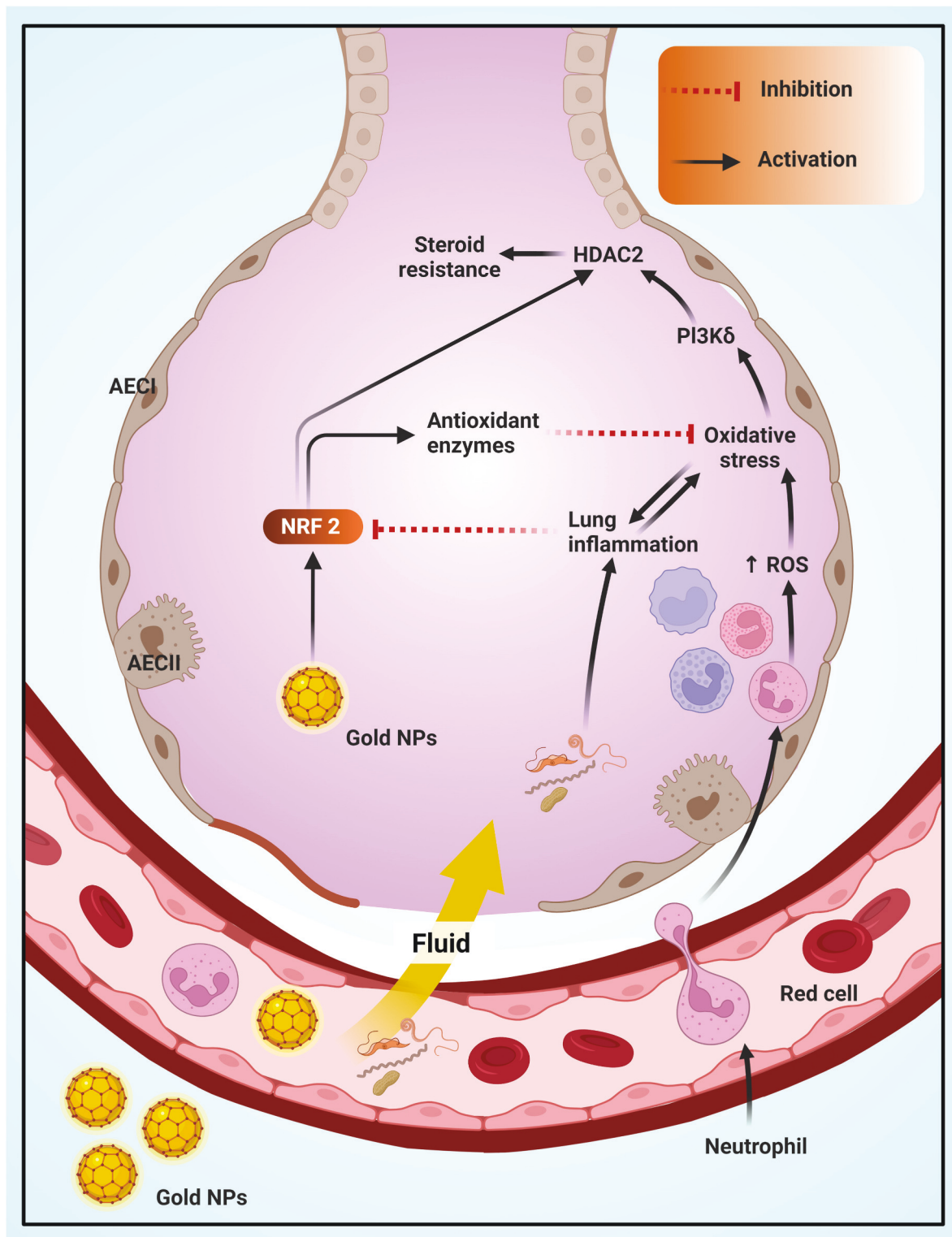


Fig. 3. Effects of gold nanoparticles (NPs) against asthma

Gold NPs decreased the expression of NRF2, HDAC2, and PI3K. The results indicated that the gold NPs lowered the levels of oxidative stress and inflammation in asthmatic biomarkers. Abbreviations: NRF2 - nuclear factor erythroid 2-related factor 2; HDAC2 - Histone deacetylase 2; PI3K - Phosphoinositide 3-kinases. (For interpretation of the references to colour in this figure legend, the reader is referred to the Web version of this article.)

inflammation [60].

Matsuo et al., showed the beneficial effect of polymeric NPs, prepared using poly (D, L-lactic acid (PLA) homopolymers, polyethylene glycol (PEG), diethanolamine, acetone, and a blend of PLA-PEG, and conjugated with betamethasone (BP), in a murine model of asthma. The

evaluation of particle size and drug loading was performed using dynamic light scattering (DLS) method and high-performance liquid chromatography (HPLC). Importantly, it was revealed that BP conjugated with NPs was detectable in the lungs up to a week from the day of administration compared to BP alone that was undetectable after 24 h

post-administration. Importantly, the findings from this study demonstrated that BP conjugated NPs significantly reduced the inflammation and the release of IL-13 and IL-14 upon intravenous administration when compared with BP alone [61].

4.3. Chitosan-based NPs

Chitosan-based NPs are highly biodegradable, biocompatible, and stable in nature, that are soluble in aqueous acidic solutions and can regulate the release of active substances [62]. Chitosan is a mucopolysaccharide found abundantly in the cell walls of several fungal species [63]. Wang et al., reported the successful development and evaluation of the chitosan-based NPs of baicalein and their efficacy in altering the pathology of asthma in ovalbumin-induced asthma mouse model. This study used glyceryl monooleate, P407, anhydrous ethanol, gelucire 44/14, and trimethyl chitosan for the development of the NPs. The particle size of the developed NPs was reported to be 285 ± 25 nm with negative zeta potential of -10.5 mV, whereas drug loading and encapsulation efficiency were 74.2% and 96.1%, respectively, with enhanced drug release in drug-loaded NPs compared to encapsulated NPs. While evaluating the efficacy of these NPs against asthma, it was observed that both loaded and encapsulated NPs significantly increased IL-12 levels and decreased IL-5 levels when compared to the non-treatment group [64]. Dhayanandamoorthy et al., have reported anti-asthmatic effects of hyaluronic acid-decorated and ferulic acid-loaded chitosan NPs (HAFACNPs) against ovalbumin-induced asthma in mice. Intranasal administration of HAFACNPs aerosols significantly attenuated the level of various cytokines such as IL-5, IL-13, TNF- α , and IFN- γ in addition to the attenuation of airway resistance, eosinophil infiltration and serum IgE levels [65].

4.4. Dendrimers

Dendrimers are radially symmetric, homogeneous, monodispersed systems that are structurally similar in appearance as that of tree branches. They consist of a core structure that is made up of a central atom or group of atoms [66]. Branches of dendrimers also known as "dendrons," are developed from this core structure by several chemical processes [66].

Nasr et al., successfully developed, and characterised beclomethasone dipropionate (BDP)- loaded polyamidoamine (PAMAM) dendrimers. To characterise the optimised BDP-loaded dendrimers, drug solubility in various buffers having different pH and *in vitro* drug release were evaluated. Three different nebulisers: Aeroneb Pro® (actively vibrating mesh), Pari LC® Sprint (air-jet), and Omron Micro Air® (passively vibrating-mesh) were used to evaluate aerosol formulation properties. Drug release study revealed that only 35% drug was released from the dendrimer loaded with the drug after 8 h successfully representing a sustained release pattern of the drug from the formulation.

Importantly, dendrimers are classified based on their growth process and generation number, such as G0.5, G1, G2, G3, G4, and G5 [67]. When a generation 3 (G3) was used as a model dendrimer it was observed that the amount of BDP complexed with the dendrimers was increased upon increasing the pH from 5 to 7.4, and the maximum solubility was found at pH 9.8. In contrast, there was no difference in the solubility of the uncoated BDP upon change in pH. Moreover, it was also observed that the generation of dendrimer has no impact on the aerosol's output, however, higher aerosol output was observed in Pari LC® Sprint nebuliser compared to the Aeroneb Pro device, but this was not statistically significant ($p > 0.05$) [68].

4.5. Microspheres

Microspheres are very small particles that are spherical in shape and have an average particle size lies in the range of 1–100 μ m. These can be prepared by several techniques such as coacervation, coprecipitation,

solvent dispersion, emulsification, and spray freeze-drying technique [69,70].

A study conducted by Nagaraja et al., reported the successful development of microspheres of salbutamol using spray drying. The microspheres (developed with PLGA and PEG) loaded with salbutamol were administered through the intravenous route and its anti-asthma potential was evaluated on A547 cell line. The percentage yield and encapsulation efficiency of microspheres were found to be $86\% \pm 0.4\%$ and $72\% \pm 0.8\%$, respectively. The particle size of the optimised microspheres was found to be 8.24 μ m. The developed salbutamol microspheres showed sustained release action as compared to salbutamol alone. Interestingly, MTT assay demonstrated that salbutamol entrapped in the microsphere was less toxic compared to salbutamol alone, thus implying the relative safety of the developed NPs [70].

4.6. Liposomes

Liposomes are commonly used drug delivery systems that employ microscopic spherical-shaped vesicles composed of cholesterol and non-toxic natural phospholipids [71]. Liposomes possess several biomedical applications owing to their nano size and hydrophobicity [71,72]. A study conducted by Ng et al., demonstrated significant anti-inflammatory activity of liposomes in a lipopolysaccharide (LPS)-induced *in vitro* asthma model that employed the BCI-NS1.1 minimally immortalized human airway epithelial cell line. These liposomes were prepared by lipid hydration technique and were loaded with curcumin. The optimised liposomes showed an average vesicle size and zeta potential of 271.3 ± 3.06 nm and -61.0 mV, respectively. During biochemical studies, various inflammation parameters were analysed. Curcumin-loaded liposomes significantly attenuated IL-6, IL-8, IL-1 β , and TNF α levels as compared to naïve curcumin. Curcumin-loaded liposomes were found to be five times more potent than naïve curcumin [73].

Xiao et al., reported bergenin-loaded cationic liposomes (designed by thin film dispersion technique) for the treatment of asthma. Optimised liposomes showed a vesicle size and zeta potential of 158.33 ± 5.88 nm, and $+24.51 \pm 0.51$ mV respectively. The bergenin-loaded liposomes showed 3.33-fold more potential when compared with naïve bergenin. This study reported that bergenin loaded liposomes minimised inflammatory activities and enhanced the balance between T helper 1 cytokines and T helper 2 cytokines [74,75].

4.7. Polymeric micelles (PMs)

PMs are one of the most viable nanocarriers for delivery of a drug through the pulmonary route. The small size of PMs increases the solubility of lipophilic drugs and aids in preventing pulmonary macrophage clearance [76]. Importantly, PMs can improve the drug release properties and facilitate lung targeting. The alteration of polymers with ligands targeting receptors on the surface of alveoli could promote absorption of medicines, diffusion via the epithelium, and cellular uptake, thereby enhancing their bioavailability. Eventually, the administered drug doses may be decreased by effectively targeting the drug to lungs, which significantly increases patient compliance [77].

Peng and co-workers have formulated anti-high affinity immunoglobulin epsilon receptor subunit gamma (Fc ϵ RI) fragment antigen binding (Fab)-loaded celastrol micelles against allergic inflammation. *In vitro* analysis revealed that the drug-loaded micellar formulation exhibited greater cellular uptake and cytotoxicity towards the human basophil cell line KU812. During the *in vivo* study, it was observed that the celastrol micelles got accumulated in the lungs and caused a significant decrease in IgE, histamine, Th2 cytokines such as IL-4, IL-5, TNF- α , as well as eosinophil infiltration and mucus formation [78]. Yoo et al., have developed hydroxybenzyl alcohol incorporated polyoxalate (HPOX) micelles, prepared by using conventional single emulsion technique, against airway inflammatory diseases in ovalbumin-induced

asthmatic rats. Importantly, intratracheal administration of HPOX micelles reduced not only the action of inflammatory cells but also, demonstrated antioxidant and anti-inflammatory action as they reduced levels of ROS, IL-1 β , COX-2, and inducible nitric oxide synthetase (iNOS) in lungs [79].

4.8. Exosomes

Exosomes are small extracellular vesicles that are released by virtually every cell type and possess an excellent capacity to deliver drugs at a target site rapidly. In addition, exosomes also have several benefits over other inorganic and organic carriers, including high transmission efficiency, and minimal immunogenicity [80–83].

Various studies have shown that intranasal administration of M2 macrophage-derived exosomes (M2 Φ -Exos) in ovalbumin-induced asthmatic mice inhibited the expression of various cytokines such as IL6, IL1 β , TNF- α and monocyte chemoattractant protein-1 (MCP-1) [84]. Another study conducted by Shang et al., reported the anti-inflammatory effects of adipose-derived stem cell (ADSC)-exosomes administered intravenously for the treatment of asthma in mice via intravenous route. The results of biochemical studies revealed that adipose-derived stem cell (ADSC)-exosomes significantly reduced iNOS, TNF-, and IFN- expression, simultaneously increasing the expression of anti-inflammatory cytokine IL-10 [85].

4.9. Solid lipid NPs (SLNs)

SLNs are novel drug delivery systems that are generally spherical in shape, with an average diameter of 10–1000 nm. SLNs are categorised as colloidal NPs that contain a lipid drug carrier (prepared by solid lipid, surfactants, and water.) They provide good drug loading capacity and remarkable physical stability [86,87]. SLNs have several biomedical applications as they enhance the drug solubility and bioavailability. They offer controlled drug release, improve drug targeting, and offer flexibility of administration through numerous routes, including parenteral, oral, pulmonary, and topical [87].

Lv et al., reported the therapeutic benefits of rhynchophylline-loaded within SLNs. The purpose of developing this system was to enhance the therapeutic efficacy of rhynchophylline for the treatment of allergic asthma. SLNs were prepared by solvent injection method and showed an average particle size, zeta potential and drug entrapment efficiency of 62.06 ± 1.62 nm, -6.53 ± 0.04 mV, and $82.6 \pm 1.8\%$, respectively. On days 0, 14, 28, and 42, mice were subcutaneously injected with 20 μ g of ovalbumin mixed with 1 mg aluminium hydroxide. From days 21–42, mice were administered with aerosol of 1% ovalbumin (w/v) for the induction of allergic asthma. Rhynchophylline-loaded within SLNs at the dose of 20 mg/kg significantly attenuated the levels of airway remodeling markers such as mucus gland hyperplasia and collagen deposition, oxidative stress, and airway inflammation. By inhibiting the p38 signalling pathway, it also increased the expression of suppressor of cytokine signalling 1. These findings suggested that rhynchophylline loaded SLNs showed improved response compared with the free drug [88]. Li et al., developed curcumin loaded SLNs in the form dry powder inhaler (DPI) for the treatment of asthma in mice. Curcumin loaded SLNs were prepared by microemulsion method and solidification was done by spray-drying techniques. Ovalbumin was administered to produce asthma in mice. Curcumin SLNs DPI showed a sustained-release action during *in vitro* release studies and there was no evidence for acute toxicity of this formulation found in mice. Curcumin's SLNs DPI significantly ameliorated the airway inflammatory response of the airway and the severity of pulmonary congestion in mice [89].

4.10. Nanostructured lipid carriers (NLCs)

The second generation of SLNs are reported as NLCs. NLCs are preferred over other lipid formulations due to their increased physical

stability, drug loading capacity, enhanced oral bioavailability, and modulated drug release profile. Interestingly, Gadhe et al., have reported the anti-asthmatic potential of montelukast-loaded NLCs, where NLCs were prepared by the melt emulsification homogenization technique and exhibited an average particle size and encapsulation efficiency of 181.4 ± 6.5 nm and $96.13 \pm 0.98\%$, respectively. Montelukast-loaded NLCs enhanced the oral bioavailability by 1.43-fold as compared to naïve montelukast [90].

5. Gene therapy for asthma

As the existing therapeutic approaches for asthma management are outdated, and a considerable patient population is developing steroid-resistant asthma, researchers are now focusing on the promising aspect of gene therapy for asthma [91]. *In vitro* studies have demonstrated that the usage of the decoy oligodeoxynucleotide (ODN) inhibiting NF κ B can attenuate airway inflammation by inhibiting the expression of LPS-induced cytokines such as IL-6 and IL-8 in IB3-1 human bronchial epithelial cells [92,93]. In an ovalbumin-induced rat asthma model, the ODN specific for signal transducer and activator of transcription (STAT) family members 1 and 3 were found to decrease the characteristic features of allergic inflammation as revealed by a decrease in the bronchoalveolar lavage fluid (BALF) count of eosinophils and T lymphocytes. Similarly, the protein expression of CD40 in the lung tissue was significantly attenuated by STAT ODN [94].

Using the nanotechnology approach, it is now possible to formulate gene-loaded nanotherapeutics such as NF κ B ODN to target chronic respiratory diseases, including asthma [95]. Ungaro et al., developed a sustained release decoy ODN to NF κ B using poly(lactic-co-glycolic) acid (PLGA), and an "adjuvant" hydrophilic polymer polyethylenimine (PEI) as a carrier. These respirable particles delivering ODN to NF κ B were tested for their efficacy to inhibit the expression of cytokines IL-8 and mucus-secreting gene *MUC2* in LPS-induced airway epithelial cells. It was observed that ODN to NF κ B results in an extended inhibition of IL-8 and *MUC2* expression *in vitro*, compared to the naked decoy ODN, in human bronchial epithelial cells and human epithelial pulmonary cells, respectively [96].

Nanoparticle-based thymulin gene therapy can reverse the primary features of allergic asthma in a mice model induced by ovalbumin [97]. A single dose intratracheal administration of plasmids encoding biologically active thymulin analog showed enhanced penetration of the airway mucus barrier [97]. After three weeks of thymulin treatment, it was observed that the chronic airway inflammation measured in terms of BALF eosinophil and lymphocytes counts, immune cells recruiting chemokines such as CCL11, CXCL1, CCL17, and pro-and anti-inflammatory mediators such as IL-4, IL-13, IL-10 were significantly decreased compared to only ovalbumin (without thymulin treatment) group. Similarly, the airway remodeling factors such as vascular endothelial growth factor (VEGF) and transforming growth factor-beta (TGF- β) were significantly decreased. Likewise, the dysregulated levels of lymphocyte mediators such as IL-13 and IL-10 and macrophage polarization marker Foxp3 and Arginase were normalised by a single dose of thymulin-loaded nanoparticles. Furthermore, in a methacholine challenge assessment, more pronounced airway resistance and dynamic compliance were observed in asthmatic mice lungs while improved in the thymulin nanoparticles group [97].

Another study conducted by Gavitt et al. investigated the GATA binding protein 3 (GATA3) peptide DNzyme nucleic acid nanocapsules (pep Dz-NANs) for *in vivo* efficacy in asthma. In this study, HDM antigen was administered intranasally for five days/week for five weeks to induce allergic asthma in mice and intranasal pep Dz-NANs at a dose of 25 nM, 125 nM, 250 nM, and 1250 nM. On the site of airway inflammation, the high level of matrix metalloproteinase-9 (MMP9), a proteolytic enzyme can cleave the pep Dz NAN to individual DNzyme-surfactant conjugates for intracellular gene regulation of *GATA3*. Interestingly, mice treated with pep Dz-NANs reduced the severity of

HDM-induced allergic lung inflammation as shown by a decrease in BALF eosinophil count. This study thus suggests that peptide-based GATA3 Dz-NANs could be a promising approach to decrease the severity of asthma symptoms [98].

Kumar et al., showed that in an ovalbumin-induced mice model of allergic asthma, the chitosan-based interferon- γ (IFN- γ) plasmid DNA nanoparticles can reduce the inflammation and airway reactivity [99]. Mechanistically, it was demonstrated that intranasal administration of 10 μ g chitosan IFN- γ nanoparticles before intraperitoneal injection of ovalbumin decreased the antigen-presenting capacity of dendritic cells isolated from lung and lymph nodes, as evident from the reduction in CD80 and CD86 expression. Likewise, chitosan IFN- γ nanoparticles remarkably reduced the population of CD11c⁺b⁺ dendritic cells in lymph nodes, indicating that endogenous IFN- γ expression may immunomodulate dendritic cell migration and activation. Furthermore, there was a reduction of IFN- γ production and apoptosis of ovalbumin-specific CD8⁺ T cells (isolated from mice) cultured *in vitro* in the presence of ovalbumin [100].

Researchers have established that c-kit, a proto-oncogene in dendritic cells, plays a crucial role in the development of allergic asthma by regulating T helper cell differentiation [101]. Wu et al., found that intranasal administration of siRNA nanoparticles targeting c-kit can suppress the features of allergic asthma in an ovalbumin-induced mouse model. In this study, the intranasal administration of 35 μ g/day of siRNA for 3 consecutive days (Day 21–23 after ovalbumin sensitisation) significantly downregulated the expression of the *c-kit* gene and suppressed mucus secretion and eosinophil infiltration in the BALF. Additionally, *c-kit* siRNA inhibited the generation of stem cell factor (a ligand of c-kit), IL-4, and IL-5, while there were no changes in interferon- γ (IFN- γ) levels, suggesting the therapeutic potential of siRNA-based nanoparticles to manage allergic asthma [102]. Taken together, these studies have clearly highlighted the immense beneficial biological activity of gene therapy for the effective management of asthma, which could be a promising alternative to current treatment options such as β_2 agonists and ICS.

6. Clinical trials and studies using advanced drug delivery systems to target asthma

Despite the growing body of evidence showcasing the enormous potential of advanced drug delivery systems in pulmonary diseases, most of the clinical studies so far have focused on the treatment of malignancies [43], and a limited number of clinical studies are currently in progress or have completed to assess the efficacy of these drug delivery systems against asthma. The clinical studies identified are summarised in Table 2.

Interestingly, a clinical study showed that liposomes possess a potential to be used as an advanced delivery system to entrap and deliver *D. pteronyssinus* allergens that are used as antigen vaccination approaches against asthma [103]. In this case, liposome encapsulation of the antigen was used to exploit the depot effect and the increased antigen delivery to lymphatic vessels and lymph nodes that are characteristic of liposome-based formulations administered through subcutaneous injections [103]. This vaccination approach proved successful in protecting mild asthma patients from the worsening of symptoms that usually occurs upon dust mite exposure [103].

Notably, a phase II clinical trial demonstrated safety, efficacy, and tolerability of QbG10 (i.e., bacteriophage Qbeta-derived virus-like particle loaded with the bacterial oligonucleotide CpG-motif G10), administered subcutaneously (NCT00890734). QbG10 is identified to stimulate the immune system towards a protective Th1-mediated response *via* stimulation of toll-like receptor (TLR-9). This study showed that treatment with QbG10 achieved continued control of asthma upon steroid reduction in patients under treatment with moderate or high doses of inhalational steroids [45].

Allergic bronchopulmonary aspergillosis (ABPA) is an infrequent

Table 2
Clinical trials using advanced drug delivery systems to target asthma.

Clinical Trials	Drug and Drug Delivery Method	Outcomes	Clinical Trial Identifier	References
Pre-Phase I	Liposome-entrapped <i>D. Pteronyssinus</i> vaccination	Formulation protects mild asthma patients from worsening of symptoms following dust mite exposure	N/A	[103]
Phase I	Salbutamol Sulphate entrapped in niosome-based nanoparticles	Niosome-based formulation resulted in sustained, controlled pulmonary release of salbutamol sulphate compared to classical formulation	NCT03059017	[49]
Phase II	Virus-like nanoparticles loaded with bacterial oligonucleotide CpG-motif G10	Formulation was effective in controlling asthma upon steroid reduction in patients on moderate or high-dose inhalational steroids	NCT00890734	[45]
Phase II	Nebulised Liposomal Amphotericin B (Ambisome®)	Formulation failed to show a reduced risk of severe ABPA clinical exacerbations when used as maintenance treatment. Positive secondary outcomes (reduction of immunoglobulin-E and Aspergillus precipitins) achieved.	NCT02273661	[104]

complication of ailments such as chronic asthma and cystic fibrosis [46]. Notably, Godet et al., reported that inhalational treatment with nebulised liposomal amphotericin B (LAmB) was effective and induced durable improvements in a patient with uncontrolled ABPA [47]. Despite this finding, a Phase II clinical trial (NCT02273661) performed by the same research group failed to show a reduced risk of severe ABPA clinical exacerbations upon maintenance therapy with nebulised liposomal amphotericin-B (Ambisome®) [104]. Nevertheless, some positive secondary outcomes such as significant reduction of immunoglobulin-E and *Aspergillus* precipitins were achieved in the treatment group, providing a platform for further investigation in the field [104].

Arafa et al., had successfully developed niosome-based nanovesicles entrapping salbutamol sulphate (SS) for the treatment of asthma with potential for packaging into a metered dose inhaler (MDI) meeting the US Pharmacopoeia aerosol guidelines [105]. The relative bioavailability of this formulation was compared with that of a classical SS MDI formula in a Phase I clinical trial (NCT03059017). Administration of the niosome-based formulation resulted in sustained, controlled pulmonary release of SS to maintain therapeutic drug levels [49].

7. Conclusion

Over the last few years our understanding of the pathophysiology of

asthma, especially the role of cytokines, has undergone a paradigm shift. Primarily, asthma is recognised as a Th2-mediated cell disorder, and this dogma has been predominantly translated from mouse models of asthma that led to development of several type-2 targeted therapeutic agents specifically to reduce frequency of exacerbations in patients who are on conventional therapy. However, not all patients demonstrate improvement in symptoms, and this is due to the heterogeneity of cytokine pathways and mechanisms that drive the disease. This has led to the development of cytokine targeting drug delivery systems as well as clinical trials as we discussed in this review. However, despite the growing body of research that illustrates enormous potential of advanced drug delivery systems in pulmonary diseases, most of the clinical research so far has focused on the treatment of malignancies, and very few clinical studies are currently in progress or completed to assess the efficacy of these drug delivery systems against asthma that have a pleotropic effect on specific cytokines. The bottlenecks associated with the clinical translation of advanced drug delivery systems are manufacturing of such systems in bulk quantity, biological barriers, safety, government regulated protocols, and overall cost-effectiveness as compared to currently available treatments. The maintenance of the integrity of nanoparticles in terms of their size, homogeneity and release behaviour with batch-to-batch consistency and reproducibility during scale-up has always been a challenging task. Despite, industries have taken several initiatives in this area with approaches such as six sigma (i. e., process that uses statistics and data analysis to analyse and reduce errors in medication non-adherence [106]) and quality by design, for understanding of key manufacturing attributes affecting physicochemical properties of formulations however, a complete control on the variables still requires further elucidation.

To overcome the biological barriers such as inter-individual heterogeneity of tissue barriers, immune system, cellular uptake, and intracellular trafficking in repose to disease, a good correlation between disease pathology and inter-individual heterogeneity is crucial. The understanding of physicochemical behaviour of advanced drug delivery systems *in vivo* and strategies for overcoming biological barriers for achieving better targeting of drugs to diseased tissue and restriction in their build-up in non-specific organs should be tailored. Unfortunately, limited attention has been paid towards correlations between behaviour of advanced drug delivery systems and patients' biology. In our opinion, this could also be one of the prime reasons for the failure of such formulations during clinical trials. These biological barriers could be an important deterrent for pharmaceutical industries for investing on advanced drug delivery systems. Hence, it is important to comprehensively evaluate the preclinical data in terms of therapeutic efficacy, safety, biodistribution, and pharmacokinetics in appropriate animal models and correlate them with human physiology. Furthermore, for achieving reproducible results, the studies should be done on multiple animal models rather than depending on the trial done on a single animal model. This is very important as the animals decipher only correlation with human physiology. Using multiple animal models to understand the safety and efficacy of the formulation will reduce the chances of failure of formulation's performance during correlation of preclinical and clinical data.

Advanced drug delivery systems are always associated with clinical toxicities. The sponsors must ensure the safety of developed delivery systems prior to their clinical use. A careful monitoring of excipients used and their safety, as well as the stability of the formulations during their production should be performed. Such practices would assist the sponsors in reducing the risk of product failure due to regulatory objections related to their toxicity or instability. The knowledge of biological activity and toxicity associated with active pharmaceutical ingredients, excipients, and their advanced drug delivery, as well as their interaction with biological components, helps in predicting the toxicity of formulations. Furthermore, the influence of drug release rate on target and off-target concentrations of bioavailable drug could also help in predicting their safety and toxicity. In addition, conducting

specialized toxicity studies in suitable animal models can provide additional in the assessment of both short-term and long-term toxicity.

Nevertheless, ongoing developments in gene therapy, drug delivery systems and clinical trials will further unravel the complexity of asthma leading to improved therapies that can target specific or multiple cytokine pathways underlying pathophysiological asthma traits.

Ethics approval

Not applicable.

Author contributions

VKP formatted and compiled the manuscript. VKP, SV, RK, SDS, KRP, GDR, BM, DKC, VSRA, PMH, BGO, RML and KD contributed to manuscript writing and proof reading; VKP, DKC, SV, RK and SKS prepared the figures. All authors approved the content of the manuscript.

Funding

This research did not receive any specific grant from funding agencies in the public, commercial, or not-for-profit sectors.

Consent to participate

Not applicable.

Consent to for publication

Not applicable.

Declaration of competing interest

None.

Data availability

No data was used for the research described in the article.

Acknowledgements

The authors are thankful to the Graduate School of Health, University of Technology Sydney, Australia. KD is supported by a project grant from the Rebecca L Cooper Medical Research Foundation and the Maridulu Budyari Gungal Sydney Partnership for Health, Education, Research and Enterprise (SPHERE) RSEOH CAG Seed grant, fellowship, and extension grant; Faculty of Health MCR/ECR Mentorship Support Grant and UTS Global Strategic Partnerships Seed Funding Scheme. KD is supported by a project funding from the Uttaranchal University to undertake respiratory research. GDR is supported by the UTS International Research Scholarship and the UTS President's Scholarship. KRP is supported by a fellowship from Prevent Cancer Foundation (PCF) and the International Association for the Study of Lung Cancer (IASLC).

References

- [1] Collaborators GBDCRD, Prevalence and attributable health burden of chronic respiratory diseases, 1990-2017: a systematic analysis for the Global Burden of Disease Study 2017, *Lancet Respir. Med.* 8 (6) (2020) 585–596.
- [2] Australian Bureau of Statistics, A, ABS Website, 2020-21. (Accessed 18 January 2023).
- [3] [Internet] Australian Bureau of Statistics, ABS Website, 2020, p. 21.
- [4] M.D. Shastri, W.C. Chong, K. Dua, G.M. Peterson, R.P. Patel, M.Q. Mahmood, et al., Emerging concepts and directed therapeutics for the management of asthma: regulating the regulators, *Inflammopharmacology* 29 (1) (2021) 15–33.
- [5] [Internet] Australian Bureau of Statistics, Asthma, ABS Website, 2020, p. 21.
- [6] R. Beasley, A. Semprini, E.A. Mitchell, Risk factors for asthma: is prevention possible? *Lancet* 386 (9998) (2015) 1075–1085.

- [7] A. Papi, C. Brightling, S.E. Pedersen, H.K. Reddel, Asthma. *Lancet*. 391 (10122) (2018) 783–800.
- [8] J.V. Fahy, Type 2 inflammation in asthma—present in most, absent in many. *Nat. Rev. Immunol.* 15 (1) (2015) 57–65.
- [9] M.E. Kuruvilla, F.E. Lee, G.B. Lee, Understanding asthma phenotypes, endotypes, and mechanisms of disease. *Clin. Rev. Allergy Immunol.* 56 (2) (2019) 219–233.
- [10] G.G. King, A. James, L. Harkness, P.A.B. Wark, Pathophysiology of severe asthma: we've only just started. *Respirology* 23 (3) (2018) 262–271.
- [11] A. Bush, Pathophysiological mechanisms of asthma. *Front Pediatr* 7 (2019) 68.
- [12] S.T. Holgate, S. Wenzel, D.S. Postma, S.T. Weiss, H. Renz, P.D. Sly, Asthma. *Nat Rev Dis Primers*. 1 (2015), 15025.
- [13] B. Burrows, F.D. Martinez, M. Halonen, R.A. Barbee, M.G. Cline, Association of asthma with serum IgE levels and skin-test reactivity to allergens. *N. Engl. J. Med.* 320 (5) (1989) 271–277.
- [14] S.T. Holgate, Innate and adaptive immune responses in asthma. *Nat. Med.* 18 (5) (2012) 673–683.
- [15] J. Ghaffari, A.R. Rafiei, A. Ajami, M. Mahdavi, B. Hoshjar, Serum interleukins 6 and 8 in mild and severe asthmatic patients, is it difference? *Caspian J. Intern. Med.* 2 (2) (2011) 226–228.
- [16] H. Yssel, H. Groux, Characterization of T cell subpopulations involved in the pathogenesis of asthma and allergic diseases. *Int. Arch. Allergy Immunol.* 121 (1) (2000) 10–18.
- [17] R. Dworski, Oxidant stress in asthma. *Thorax* 55 (Suppl 2) (2000) S51–S53.
- [18] R.S. Peebles Jr., Prostaglandins in asthma and allergic diseases. *Pharmacol. Ther.* 193 (2019) 1–19.
- [19] S. Balan, K.J. Radford, N. Bhardwaj, Unexplored horizons of cDC1 in immunity and tolerance. *Adv. Immunol.* 148 (2020) 49–91.
- [20] R.G. Klein Wolterink, A. Kleijnjan, M. van Nimwegen, I. Bergen, M. de Bruijn, Y. Levani, et al., Pulmonary innate lymphoid cells are major producers of IL-5 and IL-13 in murine models of allergic asthma. *Eur. J. Immunol.* 42 (5) (2012) 1106–1116.
- [21] R.R. Ricardo-Gonzalez, S.J. Van Dyken, C. Schneider, J. Lee, J.C. Nussbaum, H. E. Liang, et al., Tissue signals imprint ILC2 identity with anticipatory function. *Nat. Immunol.* 19 (10) (2018) 1093–1099.
- [22] S.J. Van Dyken, J.C. Nussbaum, J. Lee, A.B. Molofsky, H.E. Liang, J.L. Pollack, et al., A tissue checkpoint regulates type 2 immunity. *Nat. Immunol.* 17 (12) (2016) 1381–1387.
- [23] J. St-Laurent, C. Bergeron, N. Page, C. Couture, M. Lavolette, L.P. Boulet, Influence of smoking on airway inflammation and remodelling in asthma. *Clin. Exp. Allergy* 38 (10) (2008) 1582–1589.
- [24] G. Varricchi, S. Ferri, J. Pepys, R. Poto, G. Spadaro, E. Nappi, et al., Biologics and airway remodeling in severe asthma. *Allergy* 77 (12) (2022) 3538–3552.
- [25] S.L. Limb, K.C. Brown, R.A. Wood, R.A. Wise, P.A. Eggleston, J. Tonascia, et al., Irreversible lung function deficits in young adults with a history of childhood asthma. *J. Allergy Clin. Immunol.* 116 (6) (2005) 1213–1219.
- [26] K.R. Bartemes, H. Kita, Dynamic role of epithelium-derived cytokines in asthma. *Clin. Immunol.* 143 (3) (2012) 222–235.
- [27] D.C. Doering, J. Solway, Airway smooth muscle in the pathophysiology and treatment of asthma. *J. Appl. Physiol.* 114 (7) (2013) 834–843 (1985).
- [28] M. Kudo, Y. Ishigatsubo, I. Aoki, Pathology of asthma. *Front. Microbiol.* 4 (2013) 263.
- [29] J.C. de Groot, A. ten Brinke, E.H.D. Bel, Management of the patient with eosinophilic asthma: a new era begins. *ERJ Open Res.* 1 (1) (2015), 00024–2015.
- [30] A. Papi, F. Blasi, G.W. Canonica, L. Morandi, L. Richeldi, A. Rossi, Treatment strategies for asthma: reshaping the concept of asthma management. *Allergy Asthma Clin. Immunol.* 16 (2020) 75.
- [31] P.J. Barnes, New therapies for asthma: is there any progress? *Trends Pharmacol. Sci.* 31 (7) (2010) 335–343.
- [32] I. Sulaiman, J.C.W. Lim, H.L. Soo, J. Stanslas, Molecularly targeted therapies for asthma: current development, challenges and potential clinical translation. *Pulm. Pharmacol. Therapeut.* 40 (2016) 52–68.
- [33] N.A. Hanania, Targeting airway inflammation in asthma: current and future therapies. *Chest* 133 (4) (2008) 989–998.
- [34] Y. Marandi, N. Farahi, G.S. Hashjin, Asthma: beyond corticosteroid treatment. *Arch. Med. Sci.* 9 (3) (2013) 521–526.
- [35] M. Cazzola, A. Segreti, M.G. Matera, Novel bronchodilators in asthma. *Curr. Opin. Pulm. Med.* 16 (1) (2010).
- [36] K. Sunkara, M. Mehta, S. Satija, D.S. Dhanjal, P. Sharma, S.D. Shukla, et al., An introduction to respiratory diseases and an emerging need for efficient drug delivery systems, in: D.K. Chellappan, K. Pabreja, M. Faiyazuddin (Eds.), *Advanced Drug Delivery Strategies for Targeting Chronic Inflammatory Lung Diseases*, Springer Singapore, Singapore, 2022, pp. 1–24.
- [37] S. Quirce, E. Phillips-Angles, J. Domínguez-Ortega, P. Barranco, Biologics in the treatment of severe asthma. *Allergol. Immunopathol.* 45 (2017) 45–49.
- [38] H.J. Jin, Biological treatments for severe asthma. *Yeungnam Univ J Med* 37 (4) (2020) 262–268.
- [39] P.M. Hansbro, G.E. Kaiko, P.S. Foster, Cytokine/anti-cytokine therapy - novel treatments for asthma? *Br. J. Pharmacol.* 163 (1) (2011) 81–95.
- [40] R. Tan, M.F. Liew, H.F. Lim, B.P. Leung, W.S.F. Wong, Promises and challenges of biologics for severe asthma. *Biochem. Pharmacol.* 179 (2020), 114012.
- [41] V. Allam, D.K. Chellappan, N.K. Jha, M.D. Shastri, G. Gupta, S.D. Shukla, et al., Treatment of chronic airway diseases using nutraceuticals: mechanistic insight. *Crit. Rev. Food Sci. Nutr.* (2021) 1–15.
- [42] V. Allam, K.R. Paudel, G. Gupta, S.K. Singh, S. Vishwas, M. Gulati, et al., Nutraceuticals and mitochondrial oxidative stress: bridging the gap in the management of bronchial asthma. *Environ. Sci. Pollut. Res. Int.* (42) (2022) 62733–62754.
- [43] A. Ahmad, Pharmacological strategies and recent advancement in nano-drug delivery for targeting asthma. *Life* 12 (4) (2022).
- [44] M.J. Alvarez, S. Echechipia, B. Garcia, A.I. Tabar, S. Martin, P. Rico, et al., Liposome-entrapped D. pteronyssinus vaccination in mild asthma patients: effect of 1-year double-blind, placebo-controlled trial on inflammation, bronchial hyperresponsiveness and immediate and late bronchial responses to the allergen. *Clin. Exp. Allergy* 32 (11) (2002) 1574–1582.
- [45] K.M. Beeh, F. Kannies, F. Wagner, C. Schilder, I. Naudts, A. Hammann-Haenni, et al., The novel TLR-9 agonist QbG10 shows clinical efficacy in persistent allergic asthma. *J. Allergy Clin. Immunol.* 131 (3) (2013) 866–874.
- [46] R. Agarwal, V. Muthu, I.S. Sehgal, S. Dhooria, K.T. Prasad, A.N. Aggarwal, Allergic bronchopulmonary aspergillosis. *Clin. Chest Med.* 43 (1) (2022) 99–125.
- [47] C. Godet, J.C. Meurice, F. Roblot, C. Kauffmann-Lacroix, M. Verdaguier, J.P. Frat, et al., Efficacy of nebulised liposomal amphotericin B in the attack and maintenance treatment of ABPA. *Eur. Respir. J.* 39 (5) (2012) 1261–1263.
- [48] C. Godet, F. Couturaud, S. Marchand-Adam, C. Pison, F. Gagnadoux, E. Blanchard, et al., Nebulised liposomal amphotericin-B as maintenance therapy in allergic bronchopulmonary aspergillosis: a randomised, multicentre trial. *Eur. Respir. J.* 59 (6) (2022).
- [49] M.G. Arafal, B.M. Ayoub, Bioavailability study of niosomal salbutamol sulfate in metered dose inhaler: controlled pulmonary drug delivery. *J. Aerosol Med. Pulm. Drug Deliv.* 31 (2) (2018) 114–115.
- [50] M.F. Serra, A.C. Cotias, A.S. Pimentel, A.C.S. Arantes, A.L.A. Pires, M. Lanzetti, et al., Gold nanoparticles inhibit steroid-insensitive asthma in mice preserving histone deacetylase 2 and NRF2 pathways. *Antioxidants* 11 (9) (2022).
- [51] S. Barua, S. Mitrugotri, Challenges associated with penetration of nanoparticles across cell and tissue barriers: a review of current status and future prospects. *Nano Today* 9 (2) (2014) 223–243.
- [52] R. Gupta, B. Rai, Effect of size and surface charge of gold nanoparticles on their skin permeability: a molecular dynamics study. *Sci. Rep.* 7 (2017), 45292.
- [53] E. Barreto, M.F. Serra, R.V. Dos Santos, C.E. Dos Santos, J. Hickmann, A.C. Cotias, et al., Local administration of gold nanoparticles prevents pivotal pathological changes in murine models of atopic asthma. *J. Biomed. Nanotechnol.* 11 (6) (2015) 1038–1050.
- [54] H.S. Park, K.H. Kim, S. Jang, J.W. Park, H.R. Cha, J.E. Lee, et al., Attenuation of allergic airway inflammation and hyperresponsiveness in a murine model of asthma by silver nanoparticles. *Int. J. Nanomed.* 5 (2010) 505–515.
- [55] S. Jang, J.W. Park, H.R. Cha, S.Y. Jung, J.E. Lee, S.S. Jung, et al., Silver nanoparticles modify VEGF signaling pathway and mucus hypersecretion in allergic airway inflammation. *Int. J. Nanomed.* 7 (2012) 1329–1343.
- [56] K.S. Soppimath, T.M. Aminabhavi, A.R. Kulkarni, W.E. Rudzinski, Biodegradable polymeric nanoparticles as drug delivery devices. *J. Contr. Release* 70 (1–2) (2001) 1–20.
- [57] S. Vishwas, S.K. Singh, M. Gulati, A. Awasthi, R. Khursheed, L. Corrie, et al., Harnessing the therapeutic potential of fisetin and its nanoparticles: journey so far and road ahead. *Chem. Biol. Interact.* 356 (2022), 109869.
- [58] A. Zielinska, F. Carreiro, A.M. Oliveira, A. Neves, B. Pires, D.N. Venkatesh, et al., Polymeric nanoparticles: production, characterization, toxicology and ecotoxicology. *Molecules* 25 (16) (2020).
- [59] F. Ullah, K.U. Shah, S.U. Shah, A. Nawaz, T. Nawaz, K.A. Khan, et al., Synthesis, characterization and in vitro evaluation of chitosan nanoparticles physically admixed with lactose microspheres for pulmonary delivery of montelukast. *Polymers* 14 (17) (2022).
- [60] H. Jin, J. Li, M. Zhang, R. Luo, P. Lu, W. Zhang, et al., Berberine-loaded biomimetic nanoparticles attenuate inflammation of experimental allergic asthma via enhancing IL-12 expression. *Front. Pharmacol.* 12 (2021), 724525.
- [61] Y. Matsuo, T. Ishihara, J. Ishizaki, K. Miyamoto, M. Higaki, N. Yamashita, Effect of betamethasone phosphate loaded polymeric nanoparticles on a murine asthma model. *Cell. Immunol.* 260 (1) (2009) 33–38.
- [62] R. Pangestuti, S.K. Kim, Neuroprotective properties of chitosan and its derivatives. *Mar. Drugs* 8 (7) (2010) 2117–2128.
- [63] U. Garg, S. Chauhan, U. Nagaich, N. Jain, Current advances in chitosan nanoparticles based drug delivery and targeting. *Adv. Pharmaceut. Bull.* 9 (2) (2019) 195–204.
- [64] D. Wang, E. Mehrabi Nasab, S.S. Athari, Study effect of Baicalein encapsulated/loaded Chitosan-nanoparticle on allergic Asthma pathology in mouse model. *Saudi J. Biol. Sci.* 28 (8) (2021) 4311–4317.
- [65] Y. Dhayanandamoorthy, M.G. Antoniraj, C.A.B. Kandregula, R. Kandasamy, Aerosolized hyaluronic acid decorated, ferulic acid loaded chitosan nanoparticle: a promising asthma control strategy. *Int. J. Pharm.* 591 (2020), 119958.
- [66] E. Abbasi, S.F. Aval, A. Akbarzadeh, M. Milani, H.T. Nasrabadi, S.W. Joo, et al., Dendrimers: synthesis, applications, and properties. *Nanoscale Res. Lett.* 9 (1) (2014) 247.
- [67] N. Shao, Y. Su, J. Hu, J. Zhang, H. Zhang, Y. Cheng, Comparison of generation 3 polyamidoamine dendrimer and generation 4 polypropyleneimine dendrimer on drug loading, complex structure, release behavior, and cytotoxicity. *Int. J. Nanomed.* 6 (2011) 3361–3372.
- [68] M. Nasr, M. Najlah, A. D'Emanuele, A. Elhissi, PAMAM dendrimers as aerosol drug nanocarriers for pulmonary delivery via nebulization. *Int. J. Pharm.* 461 (1–2) (2014) 242–250.
- [69] Y. Su, B. Zhang, R. Sun, W. Liu, Q. Zhu, Q. Zhang, et al., PLGA-based biodegradable microspheres in drug delivery: recent advances in research and application. *Drug Deliv.* 28 (1) (2021) 1397–1418.

- [70] N. SreeHarsha, K.N. Venugopala, A.B. Nair, T.S. Roopashree, M. Attimarad, J. G. Hiremath, et al., An efficient, lung-targeted, drug-delivery system to treat asthma via microparticles, *Drug Des. Dev. Ther.* 13 (2019) 4389–4403.
- [71] P. Liu, G. Chen, J. Zhang, A review of liposomes as a drug delivery system: current status of approved products, regulatory environments, and future perspectives, *Molecules* 27 (4) (2022).
- [72] A. Akbarzadeh, R. Rezaei-Sadabady, S. Davaran, S.W. Joo, N. Zarghami, Y. Hanifehpour, et al., Liposome: classification, preparation, and applications, *Nanoscale Res. Lett.* 8 (1) (2013) 102.
- [73] Z.Y. Ng, J.Y. Wong, J. Panneerselvam, T. Madheswaran, P. Kumar, V. Pillay, et al., Assessing the potential of liposomes loaded with curcumin as a therapeutic intervention in asthma, *Colloids Surf. B Biointerfaces* 172 (2018) 51–59.
- [74] H. Lin, P. Wang, W. Zhang, H. Yan, H. Yu, L. Yan, et al., Novel combined preparation and investigation of bergenin-loaded albumin nanoparticles for the treatment of acute lung injury: in vitro and in vivo evaluations, *Inflammation* 45 (1) (2022) 428–444.
- [75] X. Shi, M. Xu, K. Luo, W. Huang, H. Yu, T. Zhou, Anticancer activity of bergenin against cervical cancer cells involves apoptosis, cell cycle arrest, inhibition of cell migration and the STAT3 signalling pathway, *Exp. Ther. Med.* 21 (6) (2021) 653.
- [76] M. Ghezzi, S. Pescina, C. Padula, P. Santi, E. Del Favero, L. Cantu, et al., Polymeric micelles in drug delivery: an insight of the techniques for their characterization and assessment in biorelevant conditions, *J. Contr. Release* 332 (2021) 312–336.
- [77] R. Khurshid, K.R. Paudel, M. Gulati, S. Vishwas, N.K. Jha, P.M. Hansbro, et al., Expanding the arsenal against pulmonary diseases using surface-functionalized polymeric micelles: breakthroughs and bottlenecks, *Nanomedicine* 17 (12) (2022) 881–911.
- [78] X. Peng, J. Wang, X. Li, L. Lin, G. Xie, Z. Cui, et al., Targeting mast cells and basophils with anti-FcεpsilonR1alpha fab-conjugated celastrol-loaded micelles suppresses allergic inflammation, *J. Biomed. Nanotechnol.* 11 (12) (2015) 2286–2299.
- [79] D. Yoo, K. Guk, H. Kim, G. Khang, D. Wu, D. Lee, Antioxidant polymeric nanoparticles as novel therapeutics for airway inflammatory diseases, *Int. J. Pharm.* 450 (1–2) (2013) 87–94.
- [80] R.M. Johnstone, M. Adam, J.R. Hammond, L. Orr, C. Turbide, Vesicle formation during reticulocyte maturation. Association of plasma membrane activities with released vesicles (exosomes), *J. Biol. Chem.* 262 (19) (1987) 9412–9420.
- [81] D.M. Pegtel, S.J. Gould, Exosomes, *Annu Rev Biochem.* 88 (2019) 487–514.
- [82] Y. Ye, X. Zhang, F. Xie, B. Xu, P. Xie, T. Yang, et al., An engineered exosome for delivering sgRNA: Cas9 ribonucleoprotein complex and genome editing in recipient cells, *Biomater. Sci.* 8 (10) (2020) 2966–2976.
- [83] S. Vishwas, R. Kumar, R. Khurshid, A.K. Ramanunni, R. Kumar, A. Awasthi, et al., Expanding arsenal against neurodegenerative diseases using quercetin based nanoformulations: breakthroughs and bottlenecks, *Curr. Neuropharmacol.* 21 (2022).
- [84] C. Li, C. Deng, T. Zhou, J. Hu, B. Dai, F. Yi, et al., MicroRNA-370 carried by M2 macrophage-derived exosomes alleviates asthma progression through inhibiting the FGF1/MPK/STAT1 axis, *Int. J. Biol. Sci.* 17 (7) (2021) 1795–1807.
- [85] Y. Shang, Y. Sun, J. Xu, X. Ge, Z. Hu, J. Xiao, et al., Exosomes from mmu_circ_0001359-modified ADSCs attenuate airway remodeling by enhancing FoxO1 signaling-mediated M2-like macrophage activation, *Mol. Ther. Nucleic Acids* 19 (2020) 951–960.
- [86] S.J. Guo, C.G. Ma, Y.Y. Hu, G. Bai, Z.J. Song, X.Q. Cao, Solid lipid nanoparticles for phytosterols delivery: the acyl chain number of the glyceride matrix affects the arrangement, stability, and release, *Food Chem.* 394 (2022), 133412.
- [87] B. Mukherjee Sc, L. Mondal, B.S. Satapathy, S. Sengupta, L. Dutta, A. Choudhury, D. Mandal, Multifunctional Drug Nanocarriers Facilitate More Specific Entry of Therapeutic Payload into Tumors and Control Multiple Drug Resistance in Cancer, 2016.
- [88] C. Lv, H. Li, H. Cui, Q. Bi, M. Wang, Solid lipid nanoparticle delivery of rhynchophylline enhanced the efficiency of allergic asthma treatment via the upregulation of suppressor of cytokine signaling 1 by repressing the p38 signaling pathway, *Bioengineered* 12 (1) (2021) 8635–8649.
- [89] N. Li, X. Li, P. Cheng, P. Yang, P. Shi, L. Kong, et al., Preparation of curcumin solid lipid nanoparticles loaded with flower-shaped lactose for lung inhalation and preliminary evaluation of cytotoxicity in vitro, *Evid Based Complement Alternat. Med.* 2021 (2021), 4828169.
- [90] A. Patil-Gadhe, V. Pokharkar, Montelukast-loaded nanostructured lipid carriers: part I oral bioavailability improvement, *Eur. J. Pharm. Biopharm.* 88 (1) (2014) 160–168.
- [91] J. Al-Kouba, A.N. Wilkinson, M.R. Starkey, R. Rudraraju, R.B. Werder, X. Liu, et al., Allergen-encoding bone marrow transfer inactivates allergic T cell responses, alleviating airway inflammation, *JCI Insight* 2 (11) (2017).
- [92] D. De Stefano, F. Ungaro, C. Giovino, A. Polimeno, F. Quaglia, R. Carnuccio, Sustained inhibition of IL-6 and IL-8 expression by decoy ODN to NF-kappaB delivered through respirable large porous particles in LPS-stimulated cystic fibrosis bronchial cells, *J. Gene Med.* 13 (4) (2011) 200–208.
- [93] V. Bezzerri, M. Borgatti, E. Nicolis, I. Lampronti, M.C. Dehecchi, I. Mancini, et al., Transcription factor oligodeoxynucleotides to NF-kappaB inhibit transcription of IL-8 in bronchial cells, *Am. J. Respir. Cell Mol. Biol.* 39 (1) (2008) 86–96.
- [94] A. Luhrmann, T. Tschernig, H. von der Leyen, M. Hecker, R. Pabst, A.H. Wagner, Decoy oligodeoxynucleotide against STAT transcription factors decreases allergic inflammation in a rat asthma model, *Exp. Lung Res.* 36 (2) (2010) 85–93.
- [95] M. Mehta, K.R. Paudel, S.D. Shukla, V. Allam, V.K. Kannaujia, N. Panth, et al., Recent trends of NfkappaB decoy oligodeoxynucleotide-based nanotherapeutics in lung diseases, *J. Contr. Release* 337 (2021) 629–644.
- [96] F. Ungaro, D. De Stefano, C. Giovino, A. Masuccio, A. Miro, R. Sorrentino, et al., PEI-engineered respirable particles delivering a decoy oligonucleotide to NF-kappaB: inhibiting MUC2 expression in LPS-stimulated airway epithelial cells, *PLoS One* 7 (10) (2012), e46457.
- [97] A.L. da Silva, G.P. de Oliveira, N. Kim, F.F. Cruz, J.Z. Kitoko, N.G. Blanco, et al., Nanoparticle-based thymulin gene therapy therapeutically reverses key pathology of experimental allergic asthma, *Sci. Adv.* 6 (24) (2020), eay7973.
- [98] T.D. Gavitt, A.K. Hartmann, S.S. Sawant, A.B. Mara, S.M. Szczepanek, J.L. Rouge, A GATA3 targeting nucleic acid nanocapsule for in vivo gene regulation in asthma, *ACS Nano* 15 (7) (2021) 11192–11201.
- [99] M. Kumar, X. Kong, A.K. Behera, G.R. Hellermann, R.F. Lockey, S.S. Mohapatra, Chitosan IFN-gamma-pDNA nanoparticle (CIN) therapy for allergic asthma, *Genet. Vaccine Ther.* 1 (1) (2003) 3.
- [100] X. Kong, G.R. Hellermann, W. Zhang, P. Jena, M. Kumar, A. Behera, et al., Chitosan interferon-gamma nanogene therapy for lung disease: modulation of T-cell and dendritic cell immune responses, *Allergy Asthma Clin. Immunol.* 4 (3) (2008) 95–105.
- [101] N. Krishnamoorthy, T.B. Oriss, M. Paglia, M. Fei, M. Yarlagadda, B. Vanhaesebroeck, et al., Activation of c-Kit in dendritic cells regulates T helper cell differentiation and allergic asthma, *Nat. Med.* 14 (5) (2008) 565–573.
- [102] W. Wu, H. Chen, Y.M. Li, S.Y. Wang, X. Diao, K.G. Liu, Intranasal sirna targeting c-kit reduces airway inflammation in experimental allergic asthma, *Int. J. Clin. Exp. Pathol.* 7 (9) (2014) 5505–5514.
- [103] M.J. Alvarez, S. Echechupía, B. García, A.I. Tabar, S. Martín, P. Rico, et al., Liposome-entrapped D. pteronyssinus vaccination in mild asthma patients: effect of 1-year double-blind, placebo-controlled trial on inflammation, bronchial hyperresponsiveness and immediate and late bronchial responses to the allergen, *Clin. Exp. Allergy* 32 (11) (2002) 1574–1582.
- [104] C. Godet, F. Couturaud, S. Marchand-Adam, C. Pison, F. Gagnadoux, E. Blanchard, et al., Nebulised liposomal amphotericin-B as maintenance therapy in allergic bronchopulmonary aspergillosis: a randomised, multicentre trial, *Eur. Respir. J.* 59 (6) (2022).
- [105] M.G. Arafa, B.M. Ayoub, Nano-vesicles of salbutamol sulphate in metered dose inhalers: formulation, characterization and in vitro evaluation, *Int. J. Appl. Pharm.* 9 (6) (2017) 100–105.
- [106] B. Vrijens, A Six Sigma framework to successfully manage medication adherence, *Br. J. Clin. Pharmacol.* 85 (8) (2019) 1661–1663.
- [107] A.J. Omlor, D.D. Le, J. Schlicker, M. Hannig, R. Ewen, S. Heck, et al., Local effects on airway inflammation and systemic uptake of 5 nm PEGylated and citrated gold nanoparticles in asthmatic mice, *Small* 13 (10) (2017).
- [108] B.G. Kim, M.K. Park, P.H. Lee, S.H. Lee, J. Hong, M.M.M. Aung, et al., Effects of nanoparticles on neuroinflammation in a mouse model of asthma, *Respir. Physiol. Neurobiol.* 271 (2020), 103292.
- [109] J.W. Ko, N.R. Shin, L. Je-Oh, T.Y. Jung, C. Moon, T.W. Kim, et al., Silica dioxide nanoparticles aggravate airway inflammation in an asthmatic mouse model via NLRP3 inflammasome activation, *Regul. Toxicol. Pharmacol.* 112 (2020), 104618.
- [110] K.L. Huang, H.L. Chang, F.M. Tsai, Y.H. Lee, C.H. Wang, T.J. Cheng, The effect of the inhalation of and topical exposure to zinc oxide nanoparticles on airway inflammation in mice, *Toxicol. Appl. Pharmacol.* 384 (2019), 114787.
- [111] K.L. Huang, Y.H. Lee, H.I. Chen, H.S. Liao, B.L. Chiang, T.J. Cheng, Zinc oxide nanoparticles induce eosinophilic airway inflammation in mice, *J. Hazard Mater.* 297 (2015) 304–312.
- [112] R. Deng, P. Ma, B. Li, Y. Wu, X. Yang, Development of allergic asthma and changes of intestinal microbiota in mice under high humidity and/or carbon black nanoparticles, *Ecotoxicol. Environ. Saf.* 241 (2022), 113786.
- [113] S.S. Athari, Z. Pourpak, G. Folkerts, J. Garssen, M. Moin, I.M. Adcock, et al., Conjugated Alpha-Alumina nanoparticle with vasoactive intestinal peptide as a Nano-drug in treatment of allergic asthma in mice, *Eur. J. Pharmacol.* 791 (2016) 811–820.
- [114] A.L. da Silva, S.V. Martini, S.C. Abreu, S. Samary Cdos, B.L. Diaz, S. Fernezlian, et al., DNA nanoparticle-mediated thymulin gene therapy prevents airway remodeling in experimental allergic asthma, *J. Contr. Release* 180 (2014) 125–133.
- [115] D.E. Kim, Y. Lee, M. Kim, S. Lee, S. Jon, S.H. Lee, Bilirubin nanoparticles ameliorate allergic lung inflammation in a mouse model of asthma, *Biomaterials* 140 (2017) 37–44.
- [116] X. Chen, W. Huang, B.C. Wong, L. Yin, Y.F. Wong, M. Xu, et al., Liposomes prolong the therapeutic effect of anti-asthmatic medication via pulmonary delivery, *Int. J. Nanomed.* 7 (2012) 1139–1148.
- [117] W. Wang, R. Zhu, Q. Xie, A. Li, Y. Xiao, K. Li, et al., Enhanced bioavailability and efficiency of curcumin for the treatment of asthma by its formulation in solid lipid nanoparticles, *Int. J. Nanomed.* 7 (2012) 3667–3677.
- [118] J. Wang, H. Wang, R. Zhu, Q. Liu, J. Fei, S. Wang, Anti-inflammatory activity of curcumin-loaded solid lipid nanoparticles in IL-1beta transgenic mice subjected to the lipopolysaccharide-induced sepsis, *Biomaterials* 53 (2015) 475–483.
- [119] M. Grozdanovic, K.G. Laffey, H. Abdelkarim, B. Hitchinson, A. Harjith, H. G. Moon, et al., Novel peptide nanoparticle-biased antagonist of CCR3 blocks

- eosinophil recruitment and airway hyperresponsiveness, *J. Allergy Clin. Immunol.* 143 (2) (2019) 669–680 e12.
- [120] B. Levanen, N.R. Bhakta, P. Torregrosa Paredes, R. Barbeau, S. Hiltbrunner, J. L. Pollack, et al., Altered microRNA profiles in bronchoalveolar lavage fluid exosomes in asthmatic patients, *J. Allergy Clin. Immunol.* 131 (3) (2013) 894–903.
- [121] N. Almqvist, A. Lonnqvist, S. Hultkrantz, C. Rask, E. Telemo, Serum-derived exosomes from antigen-fed mice prevent allergic sensitization in a model of allergic asthma, *Immunology* 125 (1) (2008) 21–27.

5) Editorial: Modernizing traditional medicine: nanoparticle-based drug delivery systems to improve the delivery of phytoceuticals in managing chronic respiratory diseases

Status: Accepted as an Editorial in the 2023 Newsletter of the Controlled Release Society – Indian Chapter (CRSIC). It will be available online at the following link: <https://crsic.org/newsetters/>

Citation: **De Rubis G**, Paudel KR, Dua K. *Modernizing traditional medicine: nanoparticle-based drug delivery systems to improve the delivery of phytoceuticals in managing chronic respiratory diseases*. **Controlled Release Society, Indian Chapter (CRSIC) – 2023 Newsletter**

Contribution: I prepared the first draft of the editorial and contributed to the further revision and editing processes

Modernizing traditional medicine: nanoparticle-based drug delivery systems to improve the delivery of phytochemicals in managing chronic respiratory diseases

Gabriele De Rubis^{1,2}, Keshav Raj Paudel³, Kamal Dua^{1,2*}

¹Faculty of Health, Australian Research Centre in Complementa

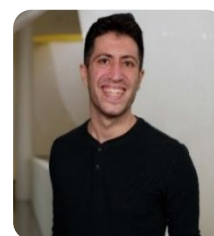
ry & Integrative Medicine, University of Technology Sydney, 2007, Ultimo, Australia

²Discipline of Pharmacy, Graduate School of Health, University of Technology Sydney, Sydney, NSW 2007, Australia

³Centre for Inflammation, Centenary Institute and University of Technology Sydney, Faculty of Science, School of Life Sciences, Sydney, NSW 2007, Australia

Email*: Kamal.Dua@uts.edu.au

Chronic respiratory diseases (CRDs), including asthma, chronic obstructive pulmonary disease (COPD), cystic fibrosis (CF), and lung cancer (LC), currently represent a major global public health challenge due to their high incidence rate and mortality rate, which keep increasing on account of the limitations of currently available treatment approaches [1]. Considering the pivotal role played by the interaction between inflammation and oxidative stress in the pathogenesis of CRDs, a substantial amount of research is currently being conducted with the aim of identifying novel compounds endowed with dual anti-inflammatory and antioxidant activity [2]. In this context, traditional medicinal plants represent an invaluable source of molecules, or phytochemicals, with great potential for the treatment of CRDs [3]. Examples of such phytochemicals with demonstrated anti-inflammatory, antioxidant, and anticancer properties, and a generally greater safety profile compared to conventional medicines, include molecules such as berberine, curcumin, rutin, naringenin, and celastrol [3], as well as complex extracts and essential oils such as Agarwood oil [4]. Despite the enormous potential of these compounds in the treatment of CRDs, their clinical application is currently hampered by their generally poor aqueous solubility, which translates into poor oral bioavailability and intestinal absorption and, in general, an unfavourable pharmacokinetic profile [5]. To overcome these limitations, a variety of nanoparticle (NP)-based advanced drug delivery systems are currently being developed, and the emerging symbiosis between nanotechnology and phytochemicals is set to revolutionize the way we treat CRDs [6]. These systems include liposomes, lipidic micelles, dendrimers, solid lipid nanoparticles (SLNs), nanoemulsions, liquid crystalline nanoparticles, and others, and they all share one common feature: the therapeutic moiety is encapsulated within nano-sized structures, of size between 1 and 1000 nm, which allow improved delivery of the therapeutic cargo by increasing its solubility and chemical stability, as well as by improving cell targeting and internalization [5]. Nanoparticle-based drug delivery systems are particularly



Gabriele De Rubis



Keshav Raj Paudel



Kamal Dua

suitable for lung diseases due to the possibility of developing formulations for inhalational delivery which are advantageous because they allow targeted lung delivery with reduced side effects associated with systemic administration [7]. In the next section, a selection of recent *in vitro* studies highlighting the enormous potential of advanced nanoparticle-based systems for the improved delivery of phytochemicals such as berberine, curcumin, rutin, naringenin, boswellic acid, and celastrol, in the treatment of CRDs is discussed.

Nanoparticle-based formulations for improved delivery of phytochemicals in lung diseases

Berberine is an isoquinoline alkaloid extracted from the roots, bark, and rhizomes of *Berberis* plants. Paudel et al. (2022) developed a monoolein-poloxamer 407-based liquid crystalline nanoparticles (LCN) formulation encapsulating berberine (BM-LCNs) and tested it on A549 human non-small cell lung cancer (NSCLC) cells, revealing a potent *in vitro* anticancer activity that was exerted through inhibition of cancer hallmarks such as proliferation, migration, colony formation, and epithelial-to-mesenchymal transition (EMT) [8]. Mechanistically, the anticancer activity of BM-LCNs was shown to be exerted through the downregulation of the expression of proteins fundamental for cancer progression such as heme oxygenase -1 (HO-1), C-X-C Motif Chemokine Ligand 8 (CXCL-8), and Chemokine (C-C motif) ligand 20 (CCL-20) [9]. Alnuqaydan et al. (2022) developed a similar, phytantriol-based, LCN formulation encapsulating berberine (BP-LCNs), which significantly inhibited A549 cell proliferation and migration by regulating cell survival pathways at both the transcriptional level, *via* the stimulation of the transcription of oncosuppressor genes such as *P53* and *PTEN* and downregulation of oncogenes such as *KRT18*; and the post-transcriptional level, *via* the downregulation of proteins involved in

cancer cell migration and proliferation such as DKK1 and CAPG [10]. These berberine-loaded LCN formulations were also successfully tested against *in vitro* models of inflammatory diseases. BM-LCNs were shown to attenuate cigarette smoke-induced inflammation, oxidative stress, and senescence, in an *in vitro* COPD model generated by exposing 16HBE human bronchial epithelial cells and RAW264.7 macrophages to cigarette smoke extract, by inhibiting reactive oxygen species (ROS) production and by reducing the expression of numerous inflammation, senescence, and oxidative stress-related genes and proteins [11]. Similarly, BP-LCNs significantly attenuated features of inflammation and oxidative stress in lipopolysaccharide (LPS)-induced RAW264.7 macrophages *via* the transcriptional downregulation of pro-inflammatory cytokines such as tumor necrosis factor- α (TNF- α) and the interleukins (IL) IL-6 and IL-1 β , as well as through inhibition of ROS and nitric oxide (NO) production [12]. Importantly, in all the aforementioned studies where berberine-loaded LCNs were tested, the equivalent berberine concentrations needed to achieve therapeutic effects (1-5 μ M) was always lower than the concentration of free berberine powder necessary to achieve comparable activity as reported in literature [12].

Another molecule with potent antioxidant, anti-inflammatory, and anticancer properties is curcumin, which is extracted from turmeric (*Curcuma longa*). Numerous studies have demonstrated the potential of encapsulating curcumin in nanodelivery systems for the treatment of respiratory diseases [13]. Ng *et al.* (2018) developed and characterized a liposome-based formulation encapsulating curcumin, and tested its efficacy against LPS-induced inflammation on BCI-NS1.1 immortalized human small airway cells, obtaining a potent anti-inflammatory effect at a concentration of 1 μ g/mL liposomal curcumin through the reduction of the

expression of pro-inflammatory cytokines involved in the pathogenesis of asthma such as IL-6, IL-8, IL-1 β and TNF- α [14]. A niosome-based curcumin formulation was developed and characterised by Wong *et al.* (2020). This formulation showed similar anti-inflammatory activity against LPS-induced BCI-NS1.1 cell at a 5 $\mu\text{g}/\text{mL}$ equivalent curcumin concentration [15]. More recently, Awasthi *et al.* (2022) applied high pressure homogenisation and probe sonication to formulate and optimize nanostructured lipid carriers (NLCs) loaded with mesalamine and curcumin (Mes-Cur NLCs) [16]. The obtained Mes-Cur NLCs showed strong *in vitro* anti-inflammatory activity against LPS-induced RAW264.7 macrophages obtained through reduction of NO production, concomitantly with minimal toxicity in fibroblast and keratinocyte cell lines, supporting the suitability of this formulation in the treatment of inflammatory diseases [16].

Rutin is a polyphenol extracted from many plant sources, including *Eucalyptus spp.* (Myrtaceae), *Ruta graveolens L.* (Rutaceae), and *Canna indica L.* (Cannaceae), embedded with a variety of biological activities including anticancer, antioxidant, and anti-inflammatory [17]. Paudel *et al.* (2021) tested a monoolein-based LCN formulation encapsulating rutin *in vitro* against A549 lung cancer cells, demonstrating a potent anticancer activity that was exerted through induction of apoptosis, inhibition of cell proliferation and migration, and downregulation of the expression of matrix metalloproteinases (MMPs) such as MMP-9 [18]. Interestingly, in this study, the IC₅₀ of rutin-LCNs was 35.44 μM , and the anti-migratory activity of this formulation was observed at concentrations as low as 20 μM . These concentrations correspond to about one-tenth of the concentration of free rutin needed to achieve a similar effect on A549 cells as reported in another study [18, 19], strongly supporting the advantage of encapsulating phytochemicals such as rutin in

nanocarriers to improve their delivery. The same formulation was tested by Paudel *et al.* (2020) on LPS-induced BEAS-2B human bronchial epithelial cells, where it achieved potent antioxidant and anti-inflammatory activities *via* the reduction of ROS and NO production, as well as anti-apoptotic activity, at low equivalent rutin concentrations of 3-5 μM . Similarly, to what was mentioned in the previous study, the equivalent rutin concentration necessary to achieve this biological effect was lower compared to the active free rutin concentration reported in other studies [20]. In a follow-up study, Mehta *et al.* (2021) provided further mechanistic explanation of the antioxidant activity of this rutin-LCN formulation, demonstrating that rutin-LCNs significantly downregulates the expression of the pro-oxidant genes, NADPH oxidase (*Nox*)-4 and *Nox*-2B, simultaneously upregulating the expression of the antioxidant genes, NADPH quinone oxidoreductase-1 (*NQO1*) and γ -glutamyl cysteine synthetase catalytic subunit (*GCLC*), in LPS-induced BEAS-2B cells [21].

Wadhwa *et al.* (2021) developed and characterised a monoolein-based LCN formulation encapsulating naringenin, a bioactive flavonoid abundantly found in the fruits of plants belonging to the citrus family [22]. This formulation was shown to have potent *in vitro* anti-inflammatory and anticancer activity. The anti-inflammatory activity of this formulation was exerted *via* the inhibition of the LPS-induced production of IL-6, IL-8, IL-1 β and TNF- α in BCI-NS1.1 cells, which was significant at an extremely low dose of 10 nM naringenin [22], whereas the anticancer activity was demonstrated through the inhibition of A549 lung cancer cell proliferation, migration, colony formation, and MMP-9 expression and functional activation [22]. The IC₅₀ obtained with naringenin-LCNs against A549 cell proliferation was 579.62 nM, substantially low compared to the 25-300 μM free naringenin powder reported in a previous study [23],

again highlighting the advantage of encapsulating poorly soluble phytochemicals within nanoparticle-based delivery systems [22].

A chitosan-based nanoparticle formulation encapsulating boswellic acid, a triterpene isolated from the gum resin of *Boswellia* trees, was developed and characterized by Solanki *et al* (2020) [24]. This formulation showed potent anticancer activity, with an IC₅₀ of 17.29 μM that was lower compared to the IC₅₀ of free boswellic acid (29.59 μM) due to enhanced cellular uptake of the encapsulated drug [24].

Finally, Chan *et al.* (2021) developed and characterized a monoolein-based LCN formulation encapsulating celastrol, a bioactive molecule extracted from the traditional Chinese medicine herb *Tripterygium wilfordii* [25]. The formulation showed significant anti-inflammatory activity *via* the inhibition of LPS-induced IL-1β production in LPS stimulated BCI-NS1.1 cells, highlighting the suitability of this system as potential treatment strategy against lung inflammatory diseases.

Conclusions

The scientific studies showcased in this report clearly highlight the extreme timeliness and relevance of nanoparticle-based drug delivery systems as a means to improve the delivery of natural molecules, phytochemicals, with known biological activity but whose clinical use is limited by poor solubility and disadvantageous pharmacokinetics. In the reports discussed, the encapsulation of therapeutic molecules in nanoparticle systems nearly universally resulted in potent biological activity at lower concentrations compared to the free drug. This allows achieving significant anticancer, antioxidant, or anti-inflammatory activity with comparatively low doses of drug, potentially reduced incidences of adverse effects, and subsequent improvement of patients' quality of life. This, together with the compatibility of many of these nanocarrier-

based formulations with inhalational delivery systems, is set to provide a new, invaluable tool, in the clinical management of CRDs, with the potential to revolutionise the way we treat these diseases and providing benefits to the lung clinics.

References

1. Tan, C.L., et al., Unravelling the molecular mechanisms underlying chronic respiratory diseases for the development of novel therapeutics via in vitro experimental models. *European Journal of Pharmacology*, 2022. 919: p. 174821.
2. Dua, K., et al., Increasing complexity and interactions of oxidative stress in chronic respiratory diseases: An emerging need for novel drug delivery systems. *Chemico-Biological Interactions*, 2019. 299: p. 168-178.
3. Clarence, D.D., et al., Unravelling the Therapeutic Potential of Nano-Delivered Functional Foods in Chronic Respiratory Diseases. *Nutrients*, 2022. 14(18).
4. Alamil, J.M.R., et al., Rediscovering the Therapeutic Potential of Agarwood in the Management of Chronic Inflammatory Diseases. *Molecules*, 2022. 27(9).
5. Ng, P.Q., et al., Applications of Nanocarriers as Drug Delivery Vehicles for Active Phytoconstituents. *Current Pharmaceutical Design*, 2020. 26(36): p. 4580-4590.
6. Paudel, K.R., et al., Nanomedicine and medicinal plants: Emerging symbiosis in managing lung diseases and associated infections. *Excli journal*, 2022. 21: p. 1299-1303.
7. Kumbhar, P., et al., Inhalation delivery of repurposed drugs for lung cancer: Approaches, benefits and challenges. *Journal of Controlled Release*, 2022. 341: p. 1-15.
8. Paudel, K.R., et al., Berberine-loaded liquid crystalline nanoparticles inhibit non-small cell lung cancer proliferation and migration in vitro. *Environmental Science and Pollution Research International*, 2022. 29(31): p. 46830-46847.
9. Mehta, M., et al., Berberine loaded liquid crystalline nanostructure inhibits cancer progression in adenocarcinomic human alveolar basal epithelial cells in vitro. *Journal of Food Biochemistry*, 2021. 45(11): p. e13954.
10. Alnuqaydan, A.M., et al., Evaluation of the Cytotoxic Activity and Anti-Migratory Effect of Berberine-Phytantriol Liquid Crystalline Nanoparticle Formulation on Non-Small-Cell Lung Cancer In Vitro. *Pharmaceutics*, 2022. 14(6).
11. Paudel, K.R., et al., Attenuation of Cigarette-Smoke-Induced Oxidative Stress, Senescence, and Inflammation by Berberine-Loaded Liquid

- Crystalline Nanoparticles: In Vitro Study in 16HBE and RAW264.7 Cells. *Antioxidants* (Basel), 2022. 11(5).
12. Alnuqaydan, A.M., et al., Phytantriol-Based Berberine-Loaded Liquid Crystalline Nanoparticles Attenuate Inflammation and Oxidative Stress in Lipopolysaccharide-Induced RAW264.7 Macrophages. *Nanomaterials* (Basel), 2022. 12(23).
 13. Chellappan, D.K., et al., Vesicular Systems Containing Curcumin and Their Applications in Respiratory Disorders - A Mini Review. *Pharmaceutical Nanotechnology*, 2017. 5(4): p. 250-254.
 14. Ng, Z.Y., et al., Assessing the potential of liposomes loaded with curcumin as a therapeutic intervention in asthma. *Colloids and Surfaces B: Biointerfaces*, 2018. 172: p. 51-59.
 15. Jin-Ying, W., et al., Curcumin-loaded niosomes downregulate mRNA expression of pro-inflammatory markers involved in asthma: an in vitro study. *Nanomedicine* (Lond), 2020. 15(30): p. 2955-2970.
 16. Awasthi, A., et al., Novel Nanostructured Lipid Carriers Co-Loaded with Mesalamine and Curcumin: Formulation, Optimization and In Vitro Evaluation. *Pharmaceutical Research*, 2022. 39(11): p. 2817-2829.
 17. Paudel, K.R., et al., Advances in research with rutin-loaded nanoformulations in mitigating lung diseases. *Future Medicinal Chemistry*, 2022. 14(18): p. 1293-1295.
 18. Paudel, K.R., et al., Rutin loaded liquid crystalline nanoparticles inhibit non-small cell lung cancer proliferation and migration in vitro. *Life Sciences*, 2021. 276: p. 119436.
 19. ben Sghaier, M., et al., Rutin inhibits proliferation, attenuates superoxide production and decreases adhesion and migration of human cancerous cells. *Biomedicine & Pharmacotherapy*, 2016. 84: p. 1972-1978.
 20. Paudel, K.R., et al., Rutin loaded liquid crystalline nanoparticles inhibit lipopolysaccharide induced oxidative stress and apoptosis in bronchial epithelial cells in vitro. *Toxicology In Vitro*, 2020. 68: p. 104961.
 21. Mehta, M., et al., Rutin-loaded liquid crystalline nanoparticles attenuate oxidative stress in bronchial epithelial cells: a PCR validation. *Future Medicinal Chemistry*, 2021. 13(6): p. 543-549.
 22. Wadhwa, R., et al., Anti-inflammatory and anticancer activities of Naringenin-loaded liquid crystalline nanoparticles in vitro. *Journal of Food Biochemistry*, 2021. 45(1): p. e13572.
 23. Chang, H.L., et al., Naringenin inhibits migration of lung cancer cells via the inhibition of matrix metalloproteinases-2 and -9. *Experimental and Therapeutic Medicine*, 2017. 13(2): p. 739-744.
 24. Solanki, N., et al., Antiproliferative effects of boswellic acid-loaded chitosan nanoparticles on human lung cancer cell line A549. *Future Medicinal Chemistry*, 2020. 12(22): p. 2019-2034.
 25. Chan, Y., et al., Celastrol-loaded liquid crystalline nanoparticles as an anti-inflammatory intervention for the treatment of asthma. *International Journal of Polymeric Materials and Polymeric Biomaterials*, 2021. 70(11): p. 754-763.

Jumbled Word

(Answer Key on Page 66)

1. ROAEOITEORLTNPC
2. TERIAPUMMYNOH
3. OGIFAUTINM
4. RIORAPPCEOMDHL
5. ZFINAEUNIRL
6. FPMTIESOERIN
7. TNOGIRPSLDAAN
8. LYAIPXHSANA
9. HOAPMRSOCGAIENCM
10. OTAVEGNTRSIRETE

6) Editorial: Nanomedicine and medicinal plants: Emerging symbiosis in managing lung diseases and associated infections








Status: Published in the **EXCLI Journal**

Citation: Paudel KR, **De Rubis G**, Panth N, Singh SK, Chellappan DK, Hansbro PM, Dua K. *Nanomedicine and medicinal plants: Emerging symbiosis in managing lung diseases and associated infections*. **EXCLI J.** 2022 Oct 27;21:1299-1303. doi: 10.17179/excli2022-5376.

Contribution: I contributed to the writing and revisions of the manuscript draft

Letter to the editor:

NANOMEDICINE AND MEDICINAL PLANTS: EMERGING SYMBIOSIS IN MANAGING LUNG DISEASES AND ASSOCIATED INFECTIONS

Keshav Raj Paudel¹, Gabriele De Rubis^{2,3}, Nisha Panth¹, Sachin Kumar Singh⁴,
Dinesh Kumar Chellappan⁵, Philip Michael Hansbro^{1*}, Kamal Dua^{2,3*}

¹ Centre of Inflammation, Centenary Institute and University of Technology Sydney; Faculty of Science, School of Life Sciences, University of Technology Sydney, Sydney 2007, Australia

² Discipline of Pharmacy, Graduate School of Health, University of Technology Sydney, Sydney, NSW 2007, Australia

³ Faculty of Health, Australian Research Centre in Complementary & Integrative Medicine, University of Technology Sydney, 2007, Ultimo, Australia

⁴ School of Pharmacy and Pharmaceutical Sciences, Lovely Professional University, Phagwara, Punjab 144411, India

⁵ Department of Life Sciences, School of Pharmacy, International Medical University, Bukit Jalil 57000, Kuala Lumpur, Malaysia

* **Corresponding authors:** Dr. Kamal Dua, Discipline of Pharmacy, Graduate School of Health, University of Technology Sydney, Sydney, NSW 2007, Australia.

E-mail: Kamal.Dua@uts.edu.au

Prof. Philip M. Hansbro, Centre of Inflammation, Centenary Institute and University of Technology Sydney, Faculty of Science, School of Life Sciences, University of Technology Sydney, Sydney 2007, Australia. E-mail: philip.hansbro@uts.edu.au

<https://dx.doi.org/10.17179/excli2022-5376>

This is an Open Access article distributed under the terms of the Creative Commons Attribution License (<http://creativecommons.org/licenses/by/4.0/>).

Pulmonary diseases refer to a broad category of diseases (both acute and chronic) related to the lungs that include asthma, acute lung injury, chronic obstructive pulmonary disease (COPD), pulmonary hypertension, pulmonary fibrosis, and lung cancer. These diseases affect a significant percentage of the global population (Paudel et al., 2021a). Medicinal plants are gaining massive attention as promising therapeutics in alleviating respiratory diseases (Chan et al., 2021a; Prasher et al., 2020). Advanced drug delivery systems have become well-established, with nanotechnology in particular, which has taken on new significance as an emerging field in the management of inflammatory lung diseases (Devkota et al., 2021; Manandhar et al., 2022).

Nanotechnology involves the formulation, characterization, and application of materials such as therapeutics and diagnostics that exist in the nanoscale range of 1 to 100 nm. As these nanostructures are in the size range or in the scale comparable to biological moieties, they may be engineered with nanotechnology for use in medical applications. The aim of nanomedicine is to utilize the physiochemical characteristics of potential nanomaterials in a way that favors

diagnosis and treatment of various respiratory diseases (Kim et al., 2010). In recent years, the concept of advanced therapeutic delivery systems using nanomedicine as a powerful tool in the management of lung diseases and associated infections has been rapidly progressing. The pathophysiological features of lung diseases, particularly airway remodeling and airway inflammation may be effectively targeted using novel drug delivery systems that generally include the active drug moiety loaded in nanocarriers such as dendrimers, lipid micelles, liposomes, polymeric nanoparticles, solid-lipid nanoparticles (SLN), and liquid crystalline nanoparticles (LCN) (Dhanjal et al., 2022). These nanocarriers offer versatility in the management of lung diseases as observed through the findings from various *in vitro* experiments (example: human healthy and cancerous bronchoepithelial cell line, and macrophages) and *in vivo* experiments (example: urethane induced lung cancer bearing mice) (Chan et al., 2021b). Recent research trends have also highlighted the promising aspect of decoy oligonucleotides (such as NFκB) based nanomedicines in the management of lung diseases (Mehta et al., 2021a). In the section below, we have highlighted the protective role of medicinal plants/single compound-based nanomedicines identified from several *in vivo* and *in vitro* studies showcasing their mechanisms and promising aspects of nanomedicine in managing lung diseases.

Wang et al. (2013) formulated curcumin-loaded solid lipid nanoparticles for the treatment of mice bearing human lung cancer (A549 cells) xenografts and compared their activity with plain/pure curcumin powder. Daily intraperitoneal injection of SLN-curcumin administered 5 days/week for 19 days at a dose of 200 mg/kg body weight resulted in the accumulation of curcumin both in the lung and in the tumor (detected by HPLC analysis). Interestingly, the inhibition of tumor growth by SLN-curcumin was 3.5-fold higher (69.3 %) compared to plain curcumin (19.5 %). The findings from the flow cytometry analysis and TUNEL staining (that analyzes DNA fragments during apoptosis) revealed that the reduction in tumor growth was because of apoptosis (but not necrosis) of tumor cells. In a similar way, the inhibition of tumor proliferation marker Ki67 was higher (33.9 %) with SLN-curcumin compared to the plain curcumin (20.0 %) (Wang et al., 2013). On the other hand, chitosan encapsulation of curcumin was found to enhance the bioavailability and tissue retention of the formulation leading to an improved efficacy in preventing benzo[a]pyrene (a potent carcinogen) induced lung cancer in Swiss albino mice (Vijayakurup et al., 2019). Apart from lung cancer, curcumin-SLN was also found to exert enhanced bioavailability and efficacy against allergic asthma induced by ovalbumin in a mice model by suppression of airway hyperresponsiveness, inflammatory cell infiltration, inhibition of cytokine expression particularly, IL-4 and IL-13 in bronchoalveolar lavage fluid (BALF) compared to the asthma (ovalbumin only) group. The anti-asthmatic activity of curcumin-SLN was superior to the plain/pure curcumin-treated group (Wang et al., 2012).

A self-assembled polyjuglanin (a type of flavonoid found in walnut husks) nanoparticles loaded with chemotherapeutic agents such as doxorubicin and anti-Kras siRNA were formulated by Wen et al. (2017) who investigated the efficacy of the nanoparticles to attenuate tumor growth in a BALB/c nude mice inoculated with lung cancer cell line; A569 and H69. The prepared nanoparticles significantly reduced tumor proliferation by inhibiting Ki-67 expression and thereby induced apoptosis of tumor cells. Comparatively, the anticancer activity of nanoparticles was better than free doxorubicin suggesting juglanin as a potent chemosensitizer (Wen et al., 2017).

Resveratrol-loaded lipid-core nanocapsules were designed by interfacial deposition of biodegradable polymers for oral delivery (5 mg/kg) to test their biological activity against acute lung injury model in A/J mice induced with lipopolysaccharide (LPS). Comparisons of efficacy of resveratrol-loaded nanocapsules were made with unloaded nanocapsules or free resveratrol. Interestingly, there was a notable reduction in LPS-induced leukocyte accumulation in the

BALF, whereas the unloaded nanocapsules did not show any significant changes with leukocyte count compared to the LPS group. Only resveratrol-loaded but not unloaded nanocapsules or free resveratrol improved the impaired lung function (lung elastance) due to LPS treatment. In a similar way, the production of pro-inflammatory cytokines such as IL-6, KC, MIP-1 α , MIP-2, MCP-1 and RANTES in lung tissue were inhibited significantly by resveratrol-loaded but not unloaded nanocapsules. Furthermore, only resveratrol-loaded nanocapsules reduced malondialdehyde (a marker of oxidative stress) and superoxide dismutase (an antioxidant enzyme that upregulates to compensate the oxidative stress due to LPS). LPS binds to the TLR4 receptor and provokes the activation of ERK and PI3K/Akt pathways leading to gene transcription and proinflammatory cytokine production. Only resveratrol-loaded nanocapsules reduced the protein expression of phosphorylated-ERK and phosphorylated-AKT (de Oliveira et al., 2019).

Various phytochemicals have been designed using the nanotechnology approach to test their efficacy *in vitro* in various cell lines of respiratory systems. Naringenin is a bioflavonoid with diverse beneficial activity against chronic respiratory disease, however, its poor water solubility and bioavailability have limited its use (Chin et al., 2020). Wadhwa et al. recently designed the LCNs of naringenin and studied the anti-inflammatory potential of the nanoformulation in LPS induced inflammation in human airway epithelium cells (BCi-NS1.1). The findings revealed that naringenin-loaded LCNs significantly reduced the expression of inflammatory genes; IL-6, IL-1 β , IL-8 and TNF- α . The anti-inflammatory potency of naringenin-LCNs were similar to standard commercially available anti-inflammatory drug fluticasone propionate (Wadhwa et al., 2021). Apart from their anti-inflammatory activity, phytochemical-loaded LCNs are also found to possess antioxidant activity in *in vitro* settings. A recent study has demonstrated the antioxidant activity of nanoparticles loaded with another bioflavonoid, rutin. Rutin-loaded LCNs in LPS-stimulated oxidative stress model were studied using a human bronchial epithelial cell line (BEAS-2B). The authors revealed that a low dose of rutin-LCNs (compared to a high dose of rutin pure compound in another similar study) drastically reduced the generation of reactive oxygen species and nitric oxide production that have further led to the inhibition of BEAS-2B apoptosis (Paudel et al., 2020). The antioxidative activity of rutin-loaded LCNs was due to the upregulation of antioxidant genes Gclc and Nqo-1 and the downregulation of Nox2B and Nox4 (Mehta et al., 2021b). Likewise, rutin-loaded LCNs showed potent anti-cancer activity against the lung cancer cell line A549 by inhibiting cell proliferation, migration, colony formation and by inducing apoptosis of A549 cells (Paudel et al., 2021b). The anticancer activity of another potent plant alkaloid, berberine, when loaded in LCNs, was revealed to be due to the inhibition of CXCL-8, CCL-20 and HO-1 gene expressions that play an important role in cancer cell proliferation and migration (Mehta et al., 2021c). Apart from LCNs, chitosan nanoparticles are excellent carriers of active drug moieties. In this aspect, boswellic acid-loaded chitosan nanoparticles have reportedly shown remarkable cytotoxicity in A549 cells. In comparison to the IC₅₀ value of 29.59 μ M for free drug (boswellic acid), the IC₅₀ value of boswellic acid loaded chitosan nanoparticles was 17.29 μ M which explains the potency of nanoparticles over free drug (Solanki et al., 2020).

Curcumin was loaded into polyvinylpyrrolidone nanoparticles by Yen et al.(2013) to study its beneficial role in TNF- α -treated lung epithelial cells. The overexpression of ICAM-1, reactive oxygen species production and cell adhesion were reported to be ameliorated by curcumin nanoparticles. Mechanistically, the antioxidant activity of curcumin nanoparticles was due to the inhibition of p47 (phox) and MAPKs/AP-1 pathways (Yen et al., 2013). *Pseudomonas aeruginosa* and *Staphylococcus aureus* are common pathogens that attack lungs resulting in pneumonia and other respiratory complications. A hybrid ofloxacin and eugenol (also referred as clove oil) co-loaded chitosan-SLNs were formulated by Rodenak-Kladniew et al. (2019) that

were found to possess enhanced antimicrobial activity against *P. aeruginosa* and *S. aureus*. While the free and nano-encapsulated ofloxacin showed minimum inhibitory concentration (MIC) below 1.0 µg/ml, the MIC values shown by ofloxacin and eugenol co-loaded chitosan-SLN were 6.1- to 16.1-folds less than free and nano-encapsulated ofloxacin. When the nanoparticles were tagged with a fluorescent label, the ability of nanoparticles to interact with the bacterial cell membrane was observed suggesting potent antimicrobial activity of the clove oil (Rodenak-Kladniew et al., 2019).

Although plenty of clinical trials involving phytochemicals have been conducted and investigated for their potential to be used in clinical practice for the management of chronic respiratory diseases, the number of clinical trials involving phytochemicals designed with a nanotechnology approach is very limited. Considering the immense potential of phytochemicals, there is an excellent platform for researchers in the field of nanomedicine/nanotechnology to test such candidate drugs by formulating them into various forms of nanomedicine with enhanced physiochemical properties to generate favorable biological activity against lung disease and associated infections.

The various highlighted recent case studies demonstrate and support the amalgamation of nanotechnology with phytochemicals. The nanoscale encapsulation of therapeutic moieties obtained from medicinal plants has proven to be beneficial with the help of nanocarrier-based systems that have provided a new direction to pulmonary clinics.

REFERENCES

- Chan Y, Mehta M, Paudel KR, Madheswaran T, Panneerselvam J, Gupta G, et al. Versatility of liquid crystalline nanoparticles in inflammatory lung diseases. *Nanomedicine (Lond)*. 2021b;16:1545-48.
- Chan Y, Raju Allam VSR, Paudel KR, Singh SK, Gulati M, Dhanasekaran M, et al. Nutraceuticals: unlocking newer paradigms in the mitigation of inflammatory lung diseases. *Crit Rev Food Sci Nutr*. 2021a;1-31;epub ahead of print.
- Chin LH, Hon CM, Chellappan DK, Chellian J, Madheswaran T, Zeeshan F, et al. Molecular mechanisms of action of naringenin in chronic airway diseases. *Eur J Pharmacol*. 2020;879:173139.
- de Oliveira MTP, de Sa Coutinho D, Tenorio de Souza E, Staniscuaski Guterres S, Pohlmann AR, Silva PMR, et al. Orally delivered resveratrol-loaded lipid-core nanocapsules ameliorate LPS-induced acute lung injury via the ERK and PI3K/Akt pathways. *Int J Nanomedicine*. 2019;14:5215-28.
- Devkota HP, Paudel KR, Jha NK, Gupta PK, Singh SK, Chellappan DK, et al. Applications of drug-delivery systems targeting inflammasomes in pulmonary diseases. *Nanomedicine (Lond)*. 2021;16:2407-10.
- Dhanjal DS, Sharma P, Mehta M, Tambuwala MM, Prasher P, Paudel KR, et al. Concepts of advanced therapeutic delivery systems for the management of remodeling and inflammation in airway diseases. *Future Med Chem*. 2022.
- Kim BY, Rutka JT, Chan WC. *Nanomedicine*. *N Engl J Med*. 2010;363:2434-43.
- Manandhar B, Paudel KR, Panth N, Hansbro P, Oliver BG, Dua K. Applications of extracellular vesicles as a drug-delivery system for chronic respiratory diseases. *Nanomedicine (Lond)*. 2022;17:817-20.
- Mehta M, Paudel KR, Shukla SD, Allam V, Kannaujia VK, Panth N, et al. Recent trends of NFκB decoy oligodeoxynucleotide-based nanotherapeutics in lung diseases. *J Control Release*. 2021a;337:629-44.
- Mehta M, Paudel KR, Shukla SD, Shastri MD, Satija S, Singh SK, et al. Rutin-loaded liquid crystalline nanoparticles attenuate oxidative stress in bronchial epithelial cells: a PCR validation. *Future Med Chem*. 2021b;13:543-49.
- Mehta M, Malya V, Paudel KR, Chellappan DK, Hansbro PM, Oliver BG, et al. Berberine loaded liquid crystalline nanostructure inhibits cancer progression in adenocarcinomic human alveolar basal epithelial cells in vitro. *J Food Biochem*. 2021c;45(11):e13954.

- Paudel KR, Wadhwa R, Mehta M, Chellappan DK, Hansbro PM, Dua K. Rutin loaded liquid crystalline nanoparticles inhibit lipopolysaccharide induced oxidative stress and apoptosis in bronchial epithelial cells in vitro. *Toxicol In Vitro*. 2020;68:104961.
- Paudel KR, Jha SK, Allam V, Prasher P, Gupta PK, Bhattacharjee R, et al. Recent advances in chronotherapy targeting respiratory diseases. *Pharmaceutics*. 2021a;13(12):2008.
- Paudel KR, Wadhwa R, Tew XN, Lau NJX, Madheswaran T, Panneerselvam J, et al. Rutin loaded liquid crystalline nanoparticles inhibit non-small cell lung cancer proliferation and migration in vitro. *Life Sci*. 2021b;276:119436.
- Prasher P, Sharma M, Mehta M, Paudel KR, Satija S, Chellappan DK, et al. Plants derived therapeutic strategies targeting chronic respiratory diseases: Chemical and immunological perspective. *Chem Biol Interact*. 2020;325:109125.
- Rodenak-Kladniew B, Scioli Montoto S, Sbaraglini ML, Di Ianni M, Ruiz ME, Talevi A, et al. Hybrid Ofloxacin/eugenol co-loaded solid lipid nanoparticles with enhanced and targetable antimicrobial properties. *Int J Pharm*. 2019;569:118575.
- Solanki N, Mehta M, Chellappan DK, Gupta G, Hansbro NG, Tambuwala MM, et al. Antiproliferative effects of boswellic acid-loaded chitosan nanoparticles on human lung cancer cell line A549. *Future Med Chem*. 2020;12:2019-34.
- Vijayakurup V, Thulasidasan AT, Shankar GM, Retnakumari AP, Nandan CD, Somaraj J, et al. Chitosan encapsulation enhances the bioavailability and tissue retention of curcumin and improves its efficacy in preventing B[a]P-induced lung carcinogenesis. *Cancer Prev Res (Phila)*. 2019;12:225-36.
- Wadhwa R, Paudel KR, Chin LH, Hon CM, Madheswaran T, Gupta G, et al. Anti-inflammatory and anticancer activities of Naringenin-loaded liquid crystalline nanoparticles in vitro. *J Food Biochem*. 2021;45(1):e13572.
- Wang P, Zhang L, Peng H, Li Y, Xiong J, Xu Z. The formulation and delivery of curcumin with solid lipid nanoparticles for the treatment of on non-small cell lung cancer both in vitro and in vivo. *Mater Sci Eng C Mater Biol Appl*. 2013;33:4802-8.
- Wang W, Zhu R, Xie Q, Li A, Xiao Y, Li K, et al. Enhanced bioavailability and efficiency of curcumin for the treatment of asthma by its formulation in solid lipid nanoparticles. *Int J Nanomedicine*. 2012;7:3667-77.
- Wen ZM, Jie J, Zhang Y, Liu H, Peng LP. A self-assembled polyjuglanin nanoparticle loaded with doxorubicin and anti-Kras siRNA for attenuating multidrug resistance in human lung cancer. *Biochem Biophys Res Commun*. 2017;493:1430-7.
- Yen FL, Tsai MH, Yang CM, Liang CJ, Lin CC, Chiang YC, et al. Curcumin nanoparticles ameliorate ICAM-1 expression in TNF-alpha-treated lung epithelial cells through p47 (phox) and MAPKs/AP-1 pathways. *PLoS One*. 2013;8(5):e63845.

7) Editorial: The versatility of 18 β -glycyrrhetic acid in attenuating pulmonary inflammatory disorders.

Status: Published in the **EXCLI Journal**

Citation: Mohamad MSB, Reyes RJ, **De Rubis G**, Paudel KR, Hansbro PM, Dua K, Chellappan DK. *The versatility of 18 β -glycyrrhetic acid in attenuating pulmonary inflammatory disorders.* **EXCLI J**, 22, 188–190. <https://doi.org/10.17179/excli2023-5845>

Contribution: I contributed to the writing and revisions of the manuscript draft

Letter to the editor:

THE VERSATILITY OF 18B-GLYCYRRHETINIC ACID IN ATTENUATING PULMONARY INFLAMMATORY DISORDERS

Mohamad Siddiq Bin Mohamad^{1,2} , Ruby-Jean Reyes^{2,3} , Gabriele De Rubis^{2,3} ,
Keshav Raj Paudel⁴ , Philip Michael Hansbro⁴ , Kamal Dua^{2,3,5} ,
Dinesh Kumar Chellappan^{6,*} 

- ¹ School of Postgraduate Studies, International Medical University, Bukit Jalil 57000, Kuala Lumpur, Malaysia
- ² Faculty of Health, Australian Research Center in Complementary & Integrative Medicine, University of Technology Sydney, 2007, Ultimo, Australia
- ³ Discipline of Pharmacy, Graduate School of Health, University of Technology Sydney, Sydney, NSW 2007, Australia
- ⁴ Center of Inflammation, Centenary Institute and University of Technology Sydney, Faculty of Science, School of Life Sciences, Sydney 2007, Australia
- ⁵ Uttaranchal Institute of Pharmaceutical Sciences, Uttaranchal University, Dehradun 248007, India
- ⁶ Department of Life Sciences, School of Pharmacy, International Medical University, Bukit Jalil 57000, Kuala Lumpur, Malaysia

* **Corresponding author:** Dr Dinesh Kumar Chellappan, Department of Life Sciences, School of Pharmacy, International Medical University, Bukit Jalil 57000, Kuala Lumpur, Malaysia. E-mail: dinesh_kumar@imu.edu.my

<https://dx.doi.org/10.17179/excli2023-5845>

This is an Open Access article distributed under the terms of the Creative Commons Attribution License (<http://creativecommons.org/licenses/by/4.0/>).

Pulmonary inflammatory disorders encompass a diverse spectrum of diseases including asthma, chronic obstructive pulmonary diseases, lung fibrosis, lung infection, and lung cancer. Inflammation is a physiological response occurring in the human body whenever there is a threat in the form of an infection as well as a non-infectious, harmful damage, activating a myriad of cellular mechanisms that eventually ends with tissue repair. Inflammation in the lung normally occurs as a response to threats such as allergens, infective agents, irritants and, sometimes, tumors. However, excessive inflammation may progress past the tissue repair stage, further leading to deleterious effects, and advancing to pulmonary inflammatory disorders (Moldoveanu et al., 2009).

An estimated 300 million people worldwide suffer from asthma. The World Health Organization (WHO) has estimated that 250,000 asthma fatalities are reported globally each year, along with a loss of 15 million disability-adjusted life-years (Bateman et al., 2008). Lung cancer is one of the most commonly diagnosed malignancies and the biggest cause of cancer-related deaths globally, with an estimated 2.2 million new cases and 1.79 million deaths each year (Ferlay et al., 2021). This shows the alarming and scale of impact posed by pulmonary inflammatory disorders on human health globally, which needs to be addressed imminently.

Fortunately, there are growing trends in applying naturally derived materials to produce medicine to treat pulmonary inflammatory disorders more efficiently. Among these naturally derived materials, 18 β -glycyrrhetic acid (18 β -Gly) is gaining notable attention and importance. 18 β -Gly is a pentacyclic triterpenoid metabolite hydrolyzed from glycyrrhizic acid of the licorice plant (Ming and Yin, 2013). It is suitable for a wide range of potential clinical uses due to its broad spectrum of anti-oxidative, anti-inflammatory, and anti-neoplastic actions (Kowalska and Kalinowska-Lis, 2019). Thus, 18 β -Gly may offer promising medicinal treatment to combat life-threatening diseases such as pulmonary inflammatory disorders.

In recent years, numerous research articles have drawn attention to the potential pharmacological use of 18 β -Gly. In the section below, we highlight the anti-inflammatory effects of 18 β -Gly from *in vivo* studies. Liu et al. (2022) conducted a study to evaluate the potential of 18 β -Gly as an anti-inflammatory therapeutic using an ovalbumin (OVA)-induced asthma mouse model. The result showed that 18 β -Gly significantly attenuated inflammation and enhanced lung function of these asthmatic mouse models. Moreover, 18 β -Gly blocked the OVA-induced phosphorylation of nuclear factor kappa-light-chain-enhancer of activated B cells (NF- κ B) in the lungs of mice. Finally, 18 β -Gly also elevated the nuclear factor erythroid 2-related factor 2 (Nrf2) and heme oxygenase-1 (HO-1) expression. This study concluded that 18 β -Gly posed as a viable treatment option for asthma (Liu et al., 2022). In another study by Kim et al. (2017), the mechanism of action of 18 β -Gly in counteracting airway inflammation was investigated. The study indicated that 18 β -Gly is able to inhibit RAR-related orphan receptor gamma (ROR γ t), signal transducer and activator of transcription 6 (STAT6), GATA binding protein 3 (GATA-3) pathways as well as upregulate forkhead box P3 (Foxp3) transcription, resulting in the suppression of interleukin (IL)-5, IL-13, and immunoglobulin E production. 18 β -Gly also protects against oxidative stress by suppressing MH-S alveolar macrophage cells ability to generate reactive oxygen species (ROS) (Kim et al., 2017). These studies strengthen the potential of 18 β -Gly as a viable novel anti-inflammatory agent.

Furthermore, 18 β -Gly also exhibits anti-neoplastic actions, confirmed by recent *in-vivo* research studies. Luo et al. (2021) conducted a study to assess the anti-neoplastic effects of 18 β -Gly on A549 lung cancer cells (Luo et al., 2021). wherein this study, 18 β -Gly showed a significant cytotoxic effect exerted through mitochondria-dependent apoptosis, G2/M cell cycle arrest, as well as migration inhibition through ROS/mitogen-activated protein kinases (MAPK)/signal transducer and activator of transcription 3 (STAT3)/NF- κ B signaling pathways in A549 cells with no apparent side effects. This places 18 β -Gly as a desired alternative option to treat lung cancer. Moreover, Huang et al. (2014) discovered that 18 β -Gly prevents non-small cell lung cancer cells proliferation through thromboxane synthase (TxAS) inhibition as well as extracellular signal-regulated kinase/cAMP responsive element binding protein (ERK/CREB) signaling initiation (Huang et al., 2014). This indicates that 18 β -Gly has potential for non-small cell lung cancer prevention and treatment.

Despite the numerous research studies investigating the therapeutic potential of 18 β -Gly, this molecule possesses unfavorable physicochemical characteristics such as poor bioavailability and low water solubility (Hao et al., 2010). These characteristics prevents the application of 18 β -Gly as a conventional treatment in clinical practice. In recent years, there has been a rapid progression of nanotechnology which, applied to the advanced delivery of phytochemicals, is helping to improve the bioavailability of many of these molecules. Considering the great therapeutic potential shown by 18 β -Gly, nanotechnology is widely acknowledged as a promising platform for researchers to formulate it into various types of nano-formulation that can improve bioavailability while maintaining the therapeutic potential of 18 β -Gly. This in turn will help to create viable options to treat lung cancer and pulmonary inflammatory diseases more efficiently. The recent research studies highlighted above demonstrate the significant potential of

18 β -Gly in treating pulmonary inflammatory disorders. The application of nanotechnology to create nano-based carriers for 18 β -Gly will help to revolutionize treatment for pulmonary inflammatory disorders.

Conflict of interest

The authors declare that they have no conflict of interest.

REFERENCES

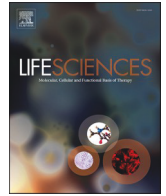
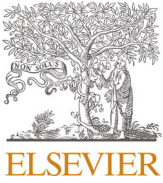
- Bateman ED, Hurd SS, Barnes PJ, Bousquet J, Drazen JM, FitzGerald JM, et al. Global strategy for asthma management and prevention: GINA executive summary. *Eur Respir J*. 2008;31(1):143-78.
- Ferlay J, Colombet M, Soerjomataram I, Parkin DM, Piñeros M, Znaor A, et al. Cancer statistics for the year 2020: An overview. *Int J Cancer*. 2021;149:778-89.
- Hao J, Sun Y, Wang Q, Tong X, Zhang H, Zhang Q. Effect and mechanism of penetration enhancement of organic base and alcohol on Glycyrrhetic acid in vitro. *Int J Pharm*. 2010;399:102-8.
- Huang RY, Chu YL, Huang QC, Chen XM, Jiang ZB, Zhang X, et al. 18 β -Glycyrrhetic acid suppresses cell proliferation through inhibiting thromboxane synthase in non-small cell lung cancer. *PLoS One*. 2014;9(4):e93690.
- Kim SH, Hong JH, Lee JE, Lee YC. 18 β -Glycyrrhetic acid, the major bioactive component of *Glycyrrhizae Radix*, attenuates airway inflammation by modulating Th2 cytokines, GATA-3, STAT6, and Foxp3 transcription factors in an asthmatic mouse model. *Environ Toxicol Pharmacol*. 2017;52:99-113.
- Kowalska A, Kalinowska-Lis U. 18 β -Glycyrrhetic acid: its core biological properties and dermatological applications. *Int J Cosmet Sci*. 2019;41:325-31.
- Liu J, Xu Y, Yan M, Yu Y, Guo Y. 18 β -Glycyrrhetic acid suppresses allergic airway inflammation through NF- κ B and Nrf2/HO-1 signaling pathways in asthma mice. *Sci Rep*. 2022;12(1):3121.
- Luo YH, Wang C, Xu WT, Zhang Y, Zhang T, Xue H, et al. 18 β -Glycyrrhetic acid has anti-cancer effects via inducing apoptosis and G2/M cell cycle arrest, and inhibiting migration of A549 lung cancer cells. *Oncotargets Ther*. 2021;14:5131-44.
- Ming LJ, Yin ACY. Therapeutic effects of glycyrrhizic acid. *Nat Prod Commun*. 2013;8(3):415-8.
- Moldoveanu B, Otmishi P, Jani P, Walker J, Sarmiento X, Guardiola J, et al. Inflammatory mechanisms in the lung. *J Inflamm Res*. 2009;2:1-11.

8) Research Paper: Cigarette smoking induces lung cancer tumorigenesis via upregulation of the WNT/ β -catenin signaling pathway.

Status: Published in **Life Sciences**

Citation: Malya V, Paudel KR, **De Rubis G**, Hansbro NG, Hansbro PM, Dua K. *Cigarette smoking induces lung cancer tumorigenesis via upregulation of the WNT/ β -catenin signaling pathway*. **Life Sciences**. 2023 Aug 1;326:121787. doi: 10.1016/j.lfs.2023.121787

Contribution: I contributed to the experiments, manuscript writing, and revisions of the manuscript draft



Cigarette smoking induces lung cancer tumorigenesis *via* upregulation of the WNT/ β -catenin signaling pathway

Vamshikrishna Malya^{a,b,c}, Keshav Raj Paudel^b, Gabriele De Rubis^{a,c}, Nicole G. Hansbro^b, Philip M. Hansbro^{b,*}, Kamal Dua^{a,b,c,*}

^a Discipline of Pharmacy, Graduate School of Health, University of Technology Sydney, Sydney, NSW 2007, Australia

^b Centre for Inflammation, Faculty of Science, School of Life Sciences, Centenary Institute and University of Technology Sydney, Sydney, NSW 2007, Australia

^c Faculty of Health, Australian Research Centre in Complementary and Integrative Medicine, University of Technology Sydney, Ultimo, NSW 2007, Australia

ARTICLE INFO

Keywords:

Extracellular vesicles
Cigarette smoke
Tumorigenesis
Lung cancer
WNT/ β -catenin signaling

ABSTRACT

Lung cancer has the highest mortality rate compared to any other cancer worldwide, and cigarette smoking is one of the major etiological factors. How cigarette smoke (CS) induces tumorigenesis in healthy cells is still not completely understood. In this study, we treated healthy human bronchial epithelial cells (16HBE14o) with 1 % cigarette smoke extract (CSE) for one week. The CSE exposed cells showed upregulation of WNT/ β -catenin pathway genes like *WNT3*, *DLV3*, *AXIN* and *β -catenin*, 30 oncology proteins were found to be upregulated after CSE treatment. Further, we explored whether the role of extracellular vesicles (EVs) obtained from CSE exposed cells can induce tumorigenesis. We observed that CSE EVs induced migration of healthy 16HBE14o cells by upregulation of various oncology proteins in recipient cells like AXL, EGFR, DKK1, ENG, FGF2, ICAM1, HMOX1, HIF1a, SERPINE1, SNAIL, HGFR, PLAU which are related to WNT signaling, epithelial mesenchymal transition (EMT) and Inflammation, whereas inflammatory marker, GAL-3 and EMT marker, VIM were downregulated. Moreover, β -catenin RNA was found in CSE EVs, upon treatment of these EVs to healthy cells, the β -catenin gene level was decreased in recipient cells compared to healthy 16HBE14o cells, indicating the utilisation of β -catenin RNA in healthy cells. Overall, our study suggests that CS treatment can induce tumorigenesis of healthy cells by upregulating WNT/ β -catenin signaling *in vitro* and human lung cancer patients. Therefore targeting the WNT/ β -catenin signaling pathway is involved in tumorigenesis inhibition of this pathway could be a potential therapeutic approach for cigarette smoke induced lung cancer.

1. Introduction

Cigarette smoke (CS) exposure accounts for 90 % of lung cancer in men and 70–80 % in females (LC) cases [1,2]. For the remaining % of people with LC, the cause is likely due to other factors such as pre-existing lung diseases such as chronic obstructive pulmonary disease (COPD), genetic, environmental, viral, and hormonal factors [3,4]. In 2020, 2.2 million new cases and 1.7 million mortalities were attributed to lung cancer [5]. LC is the most complicated lifestyle-related cancer with a poor diagnosis and prognosis [6]. Moreover, there is a lack of promising early diagnostic markers and the current therapeutic approach cannot significantly improve the overall survival rate [7–9]. It is widely accepted that cigarette smoking is the primary risk factor, but how cigarette carcinogens contribute to LC is not elucidated [10,11].

It is estimated that nearly 7000 chemicals are generated from CS, out of which >60 are reported to be carcinogens, like polyaromatic hydrocarbons (PAH), benzo[a]pyrene, and nitrosamine derived compound 4-(methylnitrosamino)-1-(3-pyridyl)-1-butanone (NNK) [12–14]. Generally, these carcinogens are metabolised by phase 1 detoxifying enzymes such as cytochrome *p*420, which adds an oxygen atom to make them water soluble to be excreted from the body [15]. PAH are highly active compounds that are metabolised by cytochrome *p*450 enzymes, but regular smoking can lead to accumulation in the body; these potent PAH carcinogens can bind to DNA and form DNA adducts leading to a process called metabolic activation, which may lead to mutations in the tumor protein (TP53) gene [16,17] as well as mutation mainly in 12 codons of Kirsten rat sarcoma viral oncogene homolog (KRAS) and Epidermal growth factor receptor (EGFR) [18,19]. Thus, balancing the deactivation and formation of DNA adducts determine the progression of LC.

* Corresponding authors at: Centre for Inflammation, Faculty of Science, School of Life Sciences, Centenary Institute and University of Technology Sydney, Sydney, NSW 2007, Australia.

E-mail addresses: philip.hansbro@uts.edu.au (P.M. Hansbro), Kamal.dua@uts.edu.au (K. Dua).

<https://doi.org/10.1016/j.lfs.2023.121787>

Received 8 March 2023; Received in revised form 8 May 2023; Accepted 15 May 2023

Available online 19 May 2023

0024-3205/© 2023 Published by Elsevier Inc.

Abbreviations

LC	lung cancer	GAPDH	Glyceraldehyde-3-Phosphate Dehydrogenase
CS	cigarette smoke	AXL	AXL receptor tyrosine kinase
16HBE14o	healthy human broncho epithelial cell	DKK1	Dickkopf
CSE	cigarette smoke extract	CTSD	Cathepsin D
COPD	chronic obstructive pulmonary disease	CTSB	Cathepsin D
PAH	polyaromatic hydrocarbons	CAPG	Capping Actin Protein Gelsolin Like
NNK	4-(methylnitrosamino)-1-(3-pyridyl)-1-butanone	ENG	Endoglin
KRAS	Kirsten rat sarcoma viral oncogene homolog	ENO2	Enolase
TP53	tumor protein	ERBB5	erythroblastic oncogene B
DNA	Deoxyribonucleic acid	FGF2	Fibroblast Growth Factor 2
miRNA	micro Ribonucleic acid	ICAM1	Intercellular Adhesion Molecule 1
nAChRs	Nicotinic acetylcholine receptors	HMOX1	Heme Oxygenase 1
β -ARs	β -Adrenergic receptors	HIF1a	Hypoxia-inducible factor
cAMP	adenylyl cyclase and cyclic	MET	MET Proto-Oncogene
NF- κ B	nuclear factor- κ B	Receptor	Tyrosine Kinase
NSCLC	non-small cell lung cancer	CAG	Cytosine Adenine Guanine
WNT	Wingless	GAL-3	Galectin-3
FBS	foetal bovine serum	FOXC1	Forkhead Box C1
DMEM	Dulbecco's modified eagle medium	FOXC2	Forkhead Box C1
IL	interleukin	MSLN	Mesothelin
COX2	cyclooxygenase2	PGDFA	Platelet Derived Growth Factor Subunit A
PBS	Phosphate buffered saline	SPP1	Secreted Phosphoprotein 1
DLS	Dynamic light scattering	GRN	Granulin Precursor
RIPA	Radioimmunoprecipitation assay buffer	SERPINB5	serine protease inhibitor B5
TEM	Transmission electron microscopy	SERPINE1	serine protease inhibitor E1
		SNAIL	Zinc finger protein SNAI1
		VIM	Vimentin

Therefore, the excretion of these carcinogens is critical in preventing tumorigenesis.

Besides the DNA mutations, CS dysregulates various carcinogenic pathways like Nicotinic acetylcholine receptors (nAChRs) signaling as nicotine binds to various α and β subunits of nAChRs and interrupts ion influxes. It is already known that this pathway is upregulated in LC [20,21]. NNK and nicotine binding to $\alpha 7$ subunit of nAChRs can activate phosphoinositide 3-kinases/protein kinase B signaling pathway [22,23]. Along with nAChRs, nicotine and other carcinogens are reported to bind to β -Adrenergic receptors (β -ARs), leading to β -ARs mediated signaling, causing increased cell proliferation of epithelial cells. This can lead to adenylyl cyclase and cyclic (cAMP) signaling leading to LC [24–26]. Besides the cancer pathways, inflammatory pathways are crucial for the LC progression [27]. For example, the nuclear factor- κ B (NF- κ B) pathway has a role in inducing the production of pro-inflammatory markers like interleukin (IL)-6, IL-8, and cyclooxygenase (COX2) and influence cancer progression by recruiting neutrophils and macrophages [28–31]. Other pathways dysregulated by cigarette smoking are Notch signaling and embryogenesis pathways like Hedgehog and WNT/ β -catenin [32–34]. WNT/ β -catenin signaling is an evolutionarily conserved signal transduction pathway that helps in cell-to-cell communication and aids in maintaining cell proliferation, cell polarity, cell homeostasis, embryogenesis, and cancer [35–37]. Mutations or over-activation of these pathways leads to various human diseases, including cancer [38]. WNT/ β -catenin signaling is widely studied in colon cancer. However, its role in LC is not fully elucidated [39,40].

Extracellular vesicles (EVs) are tiny particles released from all cells in the human body and don't have the capability to divide. Based on the size, EVs are categorised into medium EVs (> 200 nm) and small EVs (< 200 nm) [41]. These EVs carry a lot of functional molecules like proteins, RNAs, DNA, and lipids [42–44]. The packages of different cargo into EVs depend on the cell of EVs origin and diseased condition [45,46]. The EVs are mediators in cell-to-cell communication and help maintain homeostasis in the body [42]. Researchers have recently tried to validate if the tumors derived EVs stimulate tumorigenesis in healthy recipient

cells by transferring oncogenic material like miRNA and oncogenic proteins to healthy cells [34,47,48]. Therefore, further understanding the role of cancer-derived EVs helps understand tumorigenesis pathways and find effective diagnostic and prognostic tools, as these EVs are primarily released into the biological fluids [49,50].

It is recently known that cigarette smoke can induce changes in EV composition and release, but their role is not entirely understood [51]. However, few reports highlight that smoking enhances EV release and plays a crucial role in the pathogenesis of non-small cell lung cancer (NSCLC) [34,52,53]. This study investigated how CSE treatment to healthy bronchial epithelial cells can impact WNT/ β -catenin signaling pathways and how the CSE treatment derived EVs can induce tumorigenesis in healthy 16HBE14o cells.

2. Materials and methods

2.1. EVs depletion from foetal bovine serum

As commercially available foetal bovine serum (FBS) contains small EVs, removing the small EVs from FBS is essential while performing an *in vitro* experiment with the EVs [49]. In our study, to deplete the exosomes from FBS, the heat inactivated FBS was initially centrifuged at 18,000g for 90mins to remove any medium size EVs present in the FBS. Soon after, the supernatant was centrifuged for 12 h at 100,000g, maintaining 4 °C to remove small EVs pellets at the bottom. The supernatant passed through a 0.22 μ m filter. These small EVs depleted FBS were used for culturing the human normal bronchial epithelial cells (16HBE14o) [54].

2.2. Cell culture

Healthy human bronchial epithelial cells (16HBE14o) were cultured as previously mentioned [34].

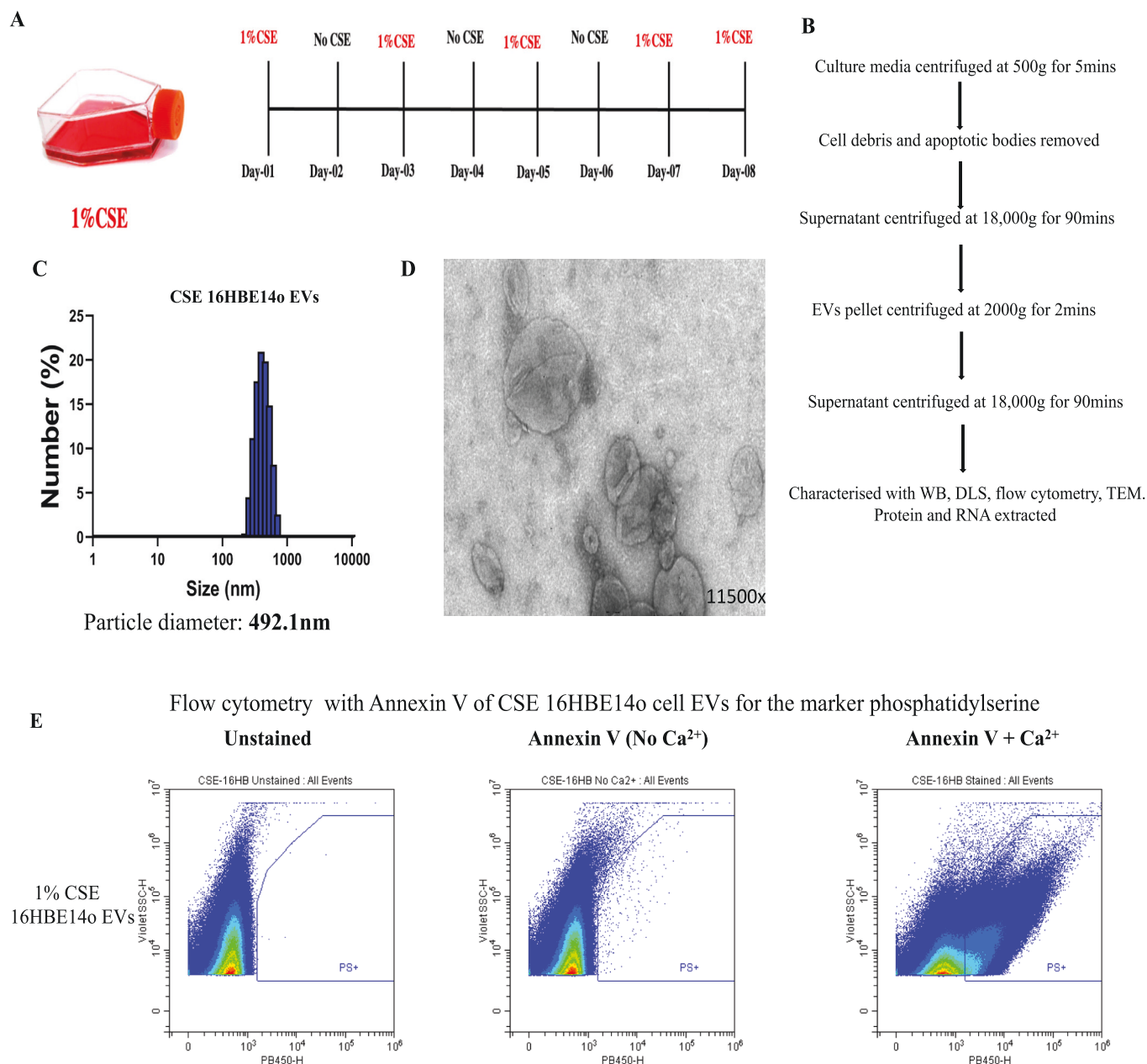


Fig. 1. Isolation and characterisation of 1 % CSE EVs. 1A) Healthy 16HBE14o cells were treated with 1 % CSE for 8 days. 1B) Flow chart of CSE EVs isolation process 1C) DLS of CSE EVs found to be in the range of medium EVs with an average particle diameter of 492.1 nm. 1D) TEM image of CSE EVs, cup shaped EVs indicate the dehydration of EVs during sample preparation, 11,500 \times magnification. 1E) Representative dot-plots from flow cytometric analysis of phosphatidylserine exposure. Unstained CSE EV samples (left) analysed as control for autofluorescence, staining in the absence of Calcium (middle) was performed to control for specific Annexin V binding, stained with Annexin V in the presence of Calcium (right) to detect phosphatidylserine surface exposure.

2.3. Cigarette smoke extract(CSE) preparation

CSE was generated by a custom built smoking device where one research cigarette (Reference Cigarette 3R4F, University of Kentucky) was lit and drawn manually into 10 ml of PBS through silicon tubing. This 10 ml extract was considered 100 % cigarette smoke extract and filtered through a 0.22 μ m filter to sterilise it. The CSE was then diluted in low glucose DMEM media based on the usage percentage. CSE was prepared fresh before the start of any experiment [55,56].

2.4. Exposing cells to CSE

A density of 2×10^6 of 16HBE14o cells were seeded into multiple T-175 flasks using small EVs depleted low glucose DMEM media (as

described in Section 2.1). Next day, discard the media and wash cells with PBS to remove any unattached or dead cells. Freshly prepared 1 % CSE was added to the cells on Monday and left for 24 h. The following day media was replaced with fresh media (without CSE). This cycle continued daily until Friday. On Friday, cells were treated with 1 % CSE and left over the weekend and on Monday, media was collected to isolate CSE EVs (Fig. 1A). Along with the CSE EVs, 1 % CSE treated cells were harvested for protein and RNA extraction ($n = 5$ biological replicates).

2.5. Isolation of EVs

1 % CSE treated supernatant was collected and centrifuged as discussed previously, the final pellet containing CSE EVs was resuspended

Table 1
WNT/ β -catenin signaling human primer sequences.

Gene name	Forward	Reverse	Ref Seq ID
<i>CTNNB1</i>	CTTGAATGAGACTGCTG	AGAGTAAAAGAACGATAGC	NM_001904
<i>DVL3</i>	ATGTCACTCAACATCATCAC	CCTTCATGATAGAGCCAATG	NM_004423
<i>AXIN1</i>	CCGACCTTANATGAAGATGAG	CAGGATCCATACCTGAACCTC	NM_003502
<i>WNT3</i>	CTGTGACTCGCATCATAAG	ATGTGGTCCAGGATAGTC	NM_030753
<i>GAPDH</i>	ACAGTCAGCCGATCTTCT	GACCAAAATCCGTTGACTCCGA	NM_008085

in 1 ml PBS and stored at -80°C for characterisation and downstream protein or RNA extraction (Fig. 1B) [34,46].

2.6. Dynamic light scattering

1 % CSE treated 16HBE14o EVs size and polydispersity index were measured using dynamic light scattering (DLS). A small portion of the EV fraction was diluted in PBS, equilibrated to 37°C , and DLS was measured using a 1 cm path length cuvette. DLS measurements were recorded in triplicates using Zetasizer Nano ZS equipped with a He-Ne 633 nm laser light source and readings measured at 25°C in a size range of 0.3–10,000 nm. The Zeta average diameter of 1 % CSE treated EVs was 492.1 ($n = 6$ biological replicates and 3 technical replicates) [34].

2.7. Protein extraction and quantification

200 μl of CSE EVs suspension was centrifuged as described above to isolate EVs.

Radioprecipitation assay buffer (RIPA) buffer containing phosphatase and protease inhibitor cocktail was added to the CSE EVs followed by vortexing and incubation on ice for 15mins. The mix was then sonicated at 30 % amplitude three times for 2 s and incubated again on ice for an additional 15mins. The lysate was then centrifuged for 30mins at 18,000 g and 4°C , and the supernatant collected. The process for extracting proteins from cells is similar except the protein lysate was centrifuged for 12,000 g at 4°C for 10mins and the protein concentration was quantified using a Pierce™ BCA Protein Array Kit (Thermo Scientific) [34].

2.8. Flow cytometry

5 μg of CSE 16HBE14o EVs were analysed by flow cytometry. EVs stained with V450 annexin V (BD Horizon™ catalogue No. 560506) for 30mins without light. 5 μg of unstained samples were run to identify the concentration of EVs for flow and accordingly gating strategy was made. Annexin V stained EVs were run with and without Calcium, as annexin V binds to EVs only with Calcium ($n = 3$ biological replicates) [34].

2.9. Transmission electron microscopy (TEM)

EV samples were suspended in PBS on carbon coated copper grids (Mesh 200) (GSAU200F-50, ProSciTech) and left to attach for 1 h. The EVs were then fixed onto the grid with 1 % glutaraldehyde, washed with Milli-Q water and negatively stained with 1.5 % uranyl acetate and dried overnight in desiccator images were taken the following day using a Tecnai T20 is a 200 kV TEM TWIN electron microscope ($n = 3$ biological replicates) [57].

2.10. Protein array of CSE EVs and cells

Protein from 16HBE14o cells, 1 % CSE treated 16HBE14o cells, 1 % CSE treated 16HBE14o EVs and CSE EVs treated healthy 16HBE14o cells were isolated and equal amounts (600 μg) were used to run the oncology array as per the manufacturer's instructions (<https://www.rndsystems.com>). Blots are imaged using the Biorad imaging platform. Data was analysed by measuring pixel density in ImageJ software [34,55,58].

2.11. Migration (scratch wound) assay

16HBE14o cells were seeded in a 6-well plate at 2×10^4 cells per well and incubated for 24 h. Following day media was removed and washed twice with PBS. A 200ul yellow pipette tip was used to make a vertical scratch and washed 3 times with PBS to remove unattached cells. 9 images of each well taken at $10\times$ at zero hours. Cells were then treated with 0, 5, 10 and 20 μg protein equivalent of 1 % CSE 16HBE14o EVs and the migration length measured 24 and 48 h later ($n = 5$ biological replicates and 9 technical replicates) [34,59,60].

2.12. RNA extractions and assessment of gene expression level by real-time PCR

RT-PCR was performed as previously mentioned [34] with genes related to WNT/ β -catenin signaling pathway Table 1.

The quantitative expression of the genes was calculated through $2^{-\Delta\Delta\text{Ct}}$, corresponding to the house keeping gene GAPDH. The relative abundance was calculated with the help of untreated control [34].

2.13. Statistical analysis

Data are presented as mean \pm SEM. Statistical analyses were performed using one-way ANOVA for multiple comparisons and t-test for two group comparisons using the Graph Pad Prism software (version 9.3). Statistical significance was accepted at $p < 0.05$.

3. Results

3.1. CSE treatment and characterisation of EVs

To determine whether treating healthy 16HBE14o cells with CSE over time can induce any cancer-like phenotype, we have optimised the concentration of CSE to 1 % so that there is a gradual induction of tumorigenesis. 1 % CSE was treated just over a period of eight days and EVs were collected as shown from day 7&8(48 h) (Fig. 1A) [56]. The isolation of medium size EVs (200-1000 nm) involves very well established multiple centrifugation steps (Fig. 1B) [50]. According to the guidelines [36], the EVs are characterised by at least three different methods. Among these methods, we used DLS for size distribution. We observed that EVs were in the size range of medium EVs (>200 -1000 nm) with no contamination from small EVs (<200 nm), indicating the purity of EVs with an average particle size of Z Average is 492.1 nm (Fig. 1C).

Transmission electron microscopy (TEM) is often used to visualise EVs and to determine EVs from non-EVs material. Traditionally, EVs resemble a cup-shape in TEM images due to a dehydration phase during sample preparation [51]. We also found cup-shaped EVs with no additional non-EV material (Fig. 1D). Another characterisation technique of EVs is identification with a marker that is important in the context of biological properties. As EVs contain lipid membranes, characterising via membrane lipids is another way to confirm EVs. We have carried out Annexin V staining of phosphatidylserine (PS) on EVs [52]. The process of membrane shedding releases EVs and therefore PS is carried with medium EVs [53]. Annexin V is known to bind to PS only in a Calcium dependent manner [49,53]. Therefore, we have visualised PS by flow

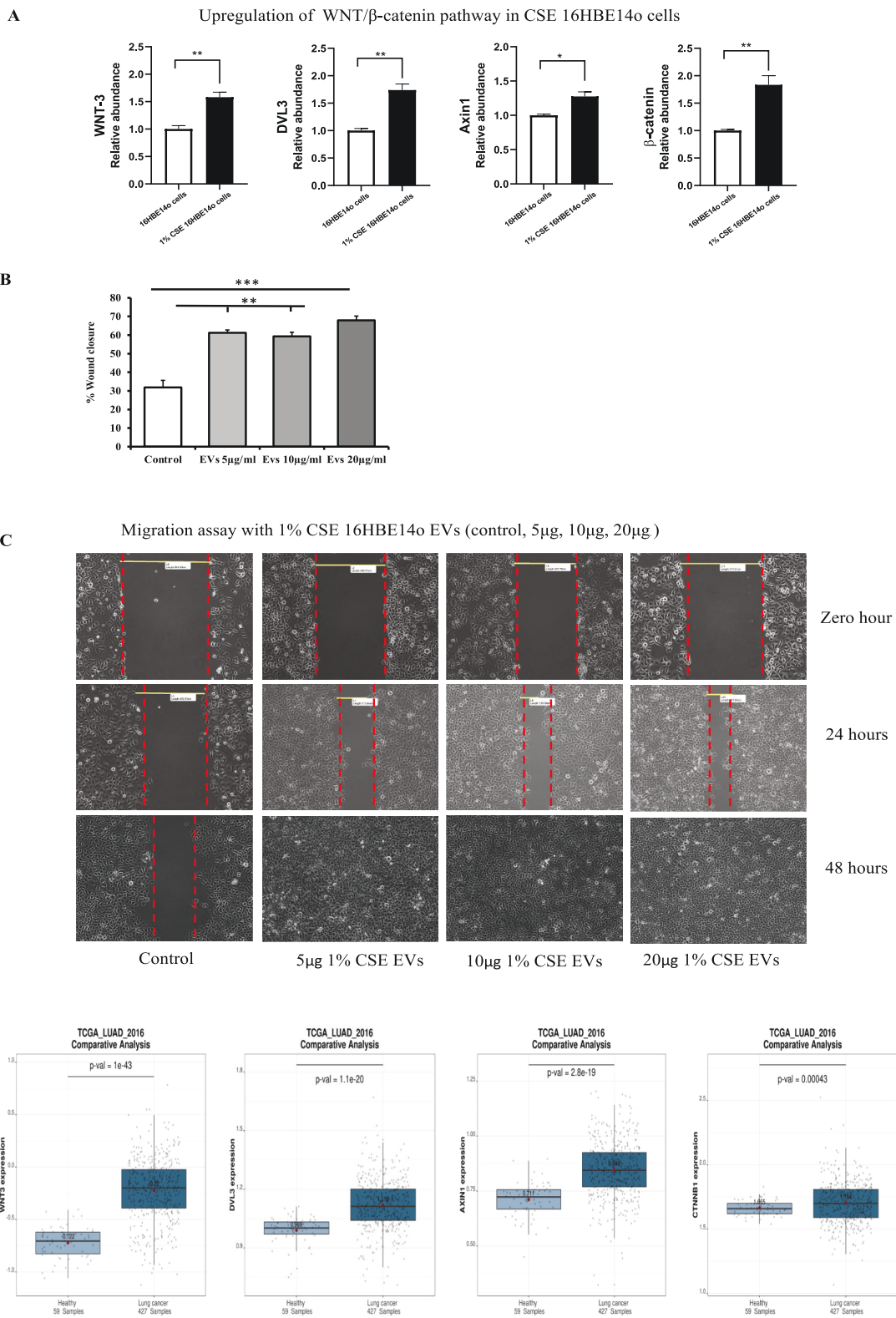


Fig. 2. CSE EVs induced Migration in healthy cells. 2A) 16HBE14o cells treated with CSE had expressed high levels of WNT/ β -catenin RNA levels including *WNT3*, *DVL3*, *Axin1* and β -catenin. *t*-test was performed $** P \leq 0.01$, $* P < 0.05$ vs control. 2B) Healthy 16HBE14o cells treated with 1% CSE EVs showed significant Migration compared to the control. Data were analysed using an ANOVA and % wound closure was calculated. $** P \leq 0.01$, $*** p < 0.001$. 2C) Microscopic images of wound closure induced by CSE EVs at 5 μ g, 10 μ g, and 20 μ g protein equivalent of EVs compared to control. Images were taken at 0 h, 24 h, and 48 h. 100% of wound closure was achieved by 48 h at all concentrations. Images were taken at 10 \times magnification. 2D) Comparative analysis of healthy lung tissue vs lung tumors in smokers of *WNT3*, *DVL3*, *Axin1* and β -catenin.

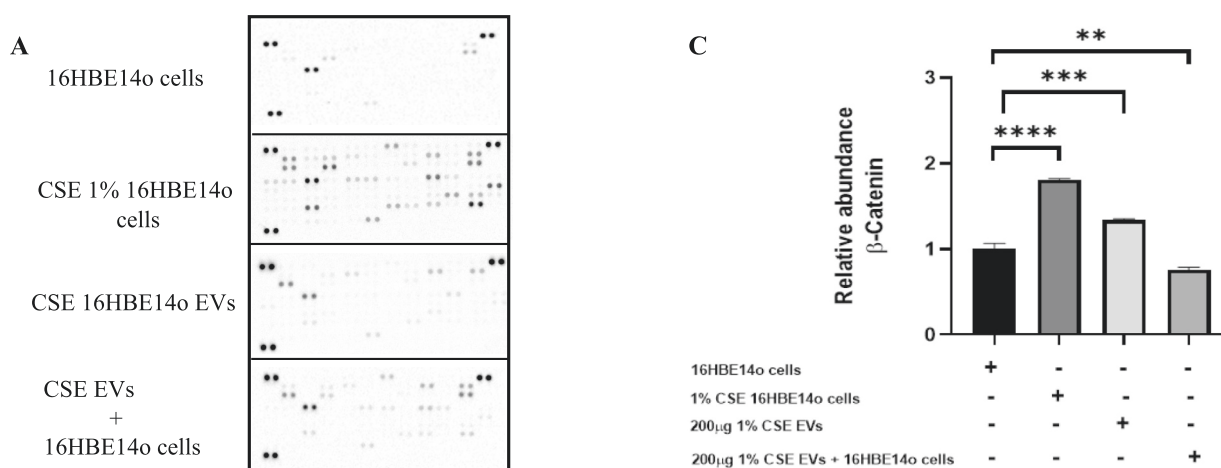


Fig. 3. CSE-treated 16HBE14o cells-derived EVs induced tumorigenesis protein and gene expression in healthy bronchial epithelial cells. 3A) Oncology array blots of healthy 16HBE14o cells, CSE exposed 16HBE14o cells, CSE induced 16HBE14o-derived EVs, and EVs treated to the healthy 16HBE14o cells. 3B) Pixel density graphs of oncology array showing cancer markers expressed in healthy 16HBE14o cells, CSE exposed 16HBE14o cells, CSE induced 16HBE14o-derived EVs and recipient cells, analysis was done with one-way ANOVA. ns = non-significant $** P \leq 0.01$, $***p < 0.001$, $****p < 0.0001$. 3C) Gene expression of β -catenin in healthy 16HBE14o cells, CSE treated 16HBE14o cells, 200 μ g of CSE induced 16HBE14o-derived EVs and EVs treated recipient 16HBE14o cells after 48 h. Relative abundance was measured with respect to *GAPDH* gene. Analysis was done with one-way ANOVA. $** P \leq 0.01$, $***p < 0.001$, $****p < 0.0001$.

cytometry and confirmed the binding of Annexin V in the presence and absence of Calcium (Fig. 1E).

3.2. Upregulation of WNT/ β -catenin pathway genes and CSE induced tumorigenesis

Treatment of 16HBE14o cells with 1 % CSE for 8 days (every alternative days for 6 days) induced upregulation of WNT/ β -catenin pathway genes such as *WNT3*, Dishevelled Segment Polarity Protein 3 (*DVL3*) a key molecule in binding to the cell surface and propagating actions of WNT based signals [54], and *Axin1* a vital component of the β -catenin destruction complex which regulates the activity β -catenin [55] (the critical component of tumorigenesis and EMT) (Fig. 2A). Furthermore, we validated these findings with publicly available datasets of lung cancer (Fig. 2E) and compared healthy lung tissue in smokers with lung tumor tissue of smokers, indicating similar observations in *WNT3*, *DVL3*, *Axin1* and β -catenin. This further confirms that CS induces upregulation of the WNT/ β -catenin pathway [56] (<https://lce.biohpc.swmed.edu/>, accessed on 15 June 2022). We performed an oncology array of 84 cancer proteins from CSE treated cells and EVs and CSE EVs treated healthy 16HBE14o cells. We found 30 oncogenic proteins such as AXL, EGFR, DKK1, CTSD, CTSB, CAPG, ENG, ENO2, ERBB5, FGF2, ICAM1, HMOX1, HIF1a, MET, CAG, GAL-3, FOXC1, FOXC2, IL-8, MSLN, PGDFA, TP53, P27, SPP1, GRN, SERPINB5, SERPINE1, SNAIL, VIM, PLAU. All of these are related to cancer induced inflammation, β -catenin regulators and EMT (Fig. 2B). Among these proteins, a few of the oncogenic proteins are encapsulated in CSE derived EVs like AXL, EGFR, DKK1, CTSD, ENG, ICAM1, IL-8, SPP1, GRN, SERPINE (Fig. 2B). This led us to treat healthy cells with these EVs to determine whether these can induce tumorigenic features in healthy cells. To validate this, we performed scratch wound/migration assays using different concentrations of CSE EVs and found that there was a significant amount of wound closure after 24 h and by 48 h there was 100 % wound closure (Fig. 2C and D).

3.3. WNT/ β -catenin pathway in recipient cells (in vitro)

To further understand the tumorigenesis induced by CSE induced 16HBE14o-derived EVs, we performed an oncology array on recipient cells. We again performed an oncology array on CSE EVs treated 16HBE14o cells. We found that AXL, EGFR, DKK1, CD105, Progranulin,

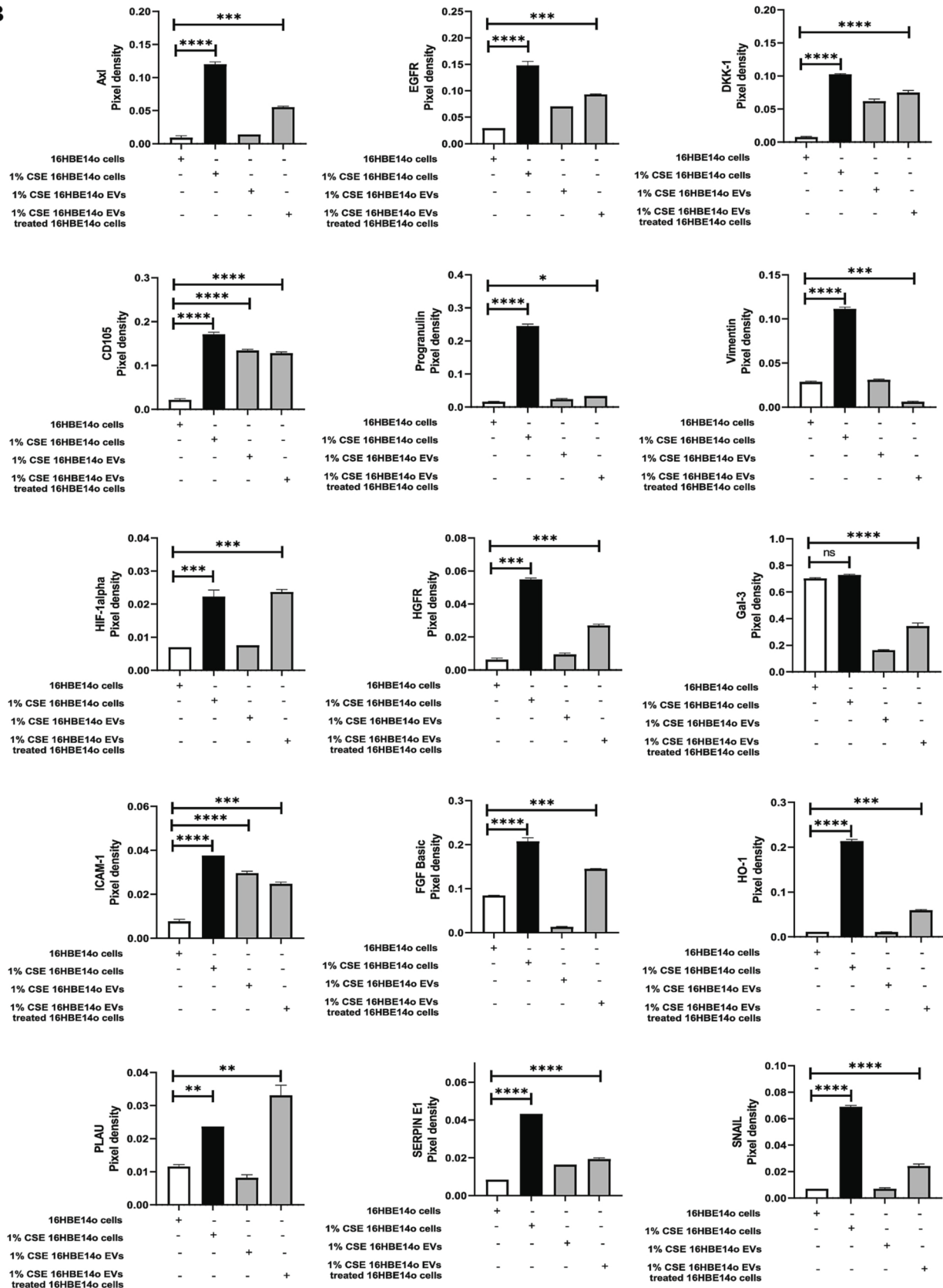
HIF1a, FGF2, ICAM1, HMOX1, HGFR, SERPINE1, SNAIL and PLAU oncology proteins were upregulated in CSE EVs treated healthy 16HBE14o cells indicating that CSE EVs can induce tumorigenesis (Fig. 3A&B). Also, vimentin and Gal-3, which are usually upregulated in cancer, are downregulated compared to the healthy cells, which need further investigation [61,62]. Among the cargo carried by EVs from parent/originating cells, RNA is one of them [57]. As EVs are known to carry RNA in them [57]. We also performed RT-qPCR on healthy cells, CSE treated cells and EVs as well as recipient cells (3C). Interestingly, we found that the main component of the WNT/ β -catenin pathway, β -catenin itself, had its RNA packaged into the CSE EVs. The treated cells utilised the RNA from CSE EVs indicating that β -catenin could have been translated into protein in the recipient cells (Fig. 3C).

4. Discussion

Cigarette smoke significantly contribute to tumorigenesis and the mechanism underlying this response remains poorly understood [63]. A few studies indicate that planar aromatics in cigarette smoke can form DNA adducts leading to mutations and cancer [64]. To further understand the role of cigarette smoke-induced lung cancer progression, we have treated CSE at 1 % for eight days and isolated characterised the EVs by shape using TEM, by size using DLS, and by EVs marker Annexin V using flow cytometry to demonstrate the purity and quality of the EVs collected.

We found that treatment with 1 % CSE for one week increased upregulation of WNT/ β -catenin signaling genes such as *WNT3*, *DVL3*, *AXIN1* and β -catenin in 16HBE14o cells and similar findings were observed in human lung cancer patients. In a healthy scenario when WNT signaling is not activated (Fig. 4A) β -catenin is degraded by the Axin complex via phosphorylation [65]. However, in the presence of WNT signaling (Fig. 4B) the Axin complex moves towards the membrane leaving inhibition of axin complex mediated phosphorylation. This leads to the accumulation of free β -catenin and results in the activation/expression of various oncogenic and WNT genes [66]. Exactly how CSE induces the expression of this pathway is still not known. We found that CSE treatment induced expression of β -catenin, and the RNA of β -catenin was found in the EVs. In addition, our protein oncology array demonstrated the expression of various inflammation and EMT related proteins in CSE treated cells. Interestingly, a few of them were found in the CSE

B



5(6A7A)4Ä'3(2).

EVs, that lead us to investigate whether treatment of healthy epithelial cells with CSE EVs could induce tumorigenesis by transferring oncogenic proteins and RNA to the healthy cells.

We performed a scratch wound healing assay to further understand whether the CSE induced 16HBE14o derived EVs carrying oncogenic protein and β -catenin RNA can induce tumorigenesis. We observed that

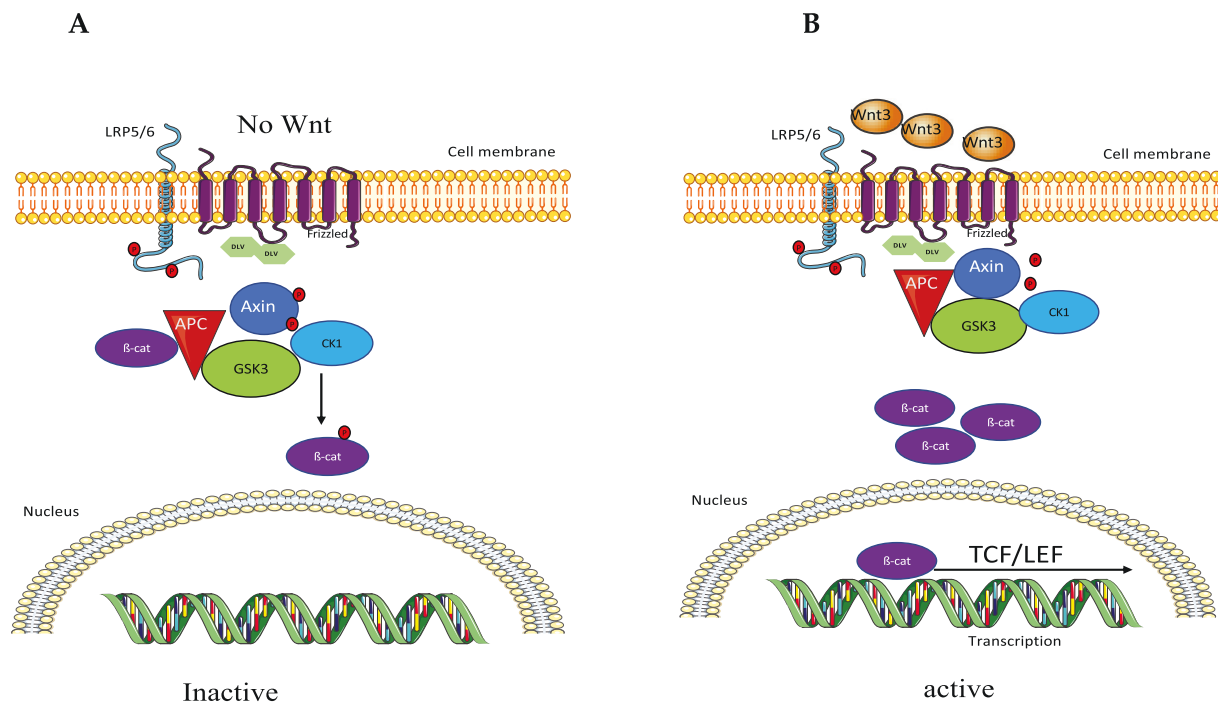


Fig. 4. WNT/ β -catenin pathway in the presence and absence of WNT signal. 4A) in the absence of WNT signal, β -catenin is phosphorylated by the Axin complex leading to the degradation of β -catenin. 4B) In the presence of WNT signal, Axin complex localises to the cell membrane and halts the degradation of β -catenin, leading to various downstream effects. Abbreviation: LRP5/6: Low-density lipoprotein receptors, DLV; Dishevelled, Axin: Axis Inhibition, APC: adenomatous polyposis coli, GSK3: Glycogen synthase kinase 3, CK1: Casein kinase 1, β -cat: β -catenin, TCF/LEF T-cell factor/lymphoid enhancer factor.

treatment of CSE induced 16HBE140 derived EVs has significantly induced cell migration (as revealed by wound closure after 48 h), indicating the transfer of protein and RNA cargo to healthy cells. In terms of RNA, CSE EVs containing β -catenin RNA have been taken by recipient cells. Whether the EVs RNA has been transcribed to protein still needs to be explored. To understand the tumorigenesis induced by CSE induced 16HBE140 derived EVs in the context of proteins, an oncology protein array was performed on recipient healthy cells. The cancer related inflammatory proteins like HMOX1, HIF1a, ENG, FGF2, were upregulated in recipient 16HBE140 cells whereas GAL3 is downregulated. Cell adhesion molecule ICAM and EMT inducer Snail were upregulated whereas EMT inducer Vimentin was downregulated. WNT/ β -catenin pathway endogenous inhibitor DKK1, and other markers like AXL, EGFR, HGFR, SERPINE1, PLAU were expressed in the recipient cells. Overall, our finding suggests that CSE induced 16HBE140 derived EVs induce tumorigenesis by a multitude of factors through WNT/ β -catenin signaling.

Despite the role of WNT and β -catenin in lung cancer, our results further suggest that CS is a critical factor in regulating the WNT/ β -catenin pathway. Additionally, our *in-vitro* and publicly available lung cancer data confirm the high expression of EMT regulator protein β -catenin, which is known to interact with TCF-LEF (Fig. 4B), which activates various cancer-related pathways, specially EMT molecule E-cadherin [67]. Further, β -catenin forms β -catenin-E-cadherin complex causing the release of tight epithelial junctions leading to metastasis, also β -catenin induce tumorigenesis by suppression of of tumor suppressor gene adenomatous polyposis coli, inducing cell proliferation and cancer cell growth [68,69]. Therefore, we can conclude from this study that CS induces upregulation of WNT/ β -catenin pathway, contributing to tumorigenesis. Despite the upregulation of the pathway, how carcinogens contribute to the upregulation and whether this is inducing mutation in WNT/ β -catenin pathway is yet to be validated.

5. Conclusion

Overall, this study indicates that CSE treatment of healthy bronchial epithelial cells can result in tumorigenesis by inducing various inflammatory and WNT/ β -catenin signaling pathways in both *in-vitro* and LC patients. Further, the EVs released by these cells can carry similar markers readily taken up by healthy cells and undergo tumorigenesis. Migration assays confirmed this *via* regulation of WNT/ β -catenin pathway in healthy cells. Furthermore, this study provides evidence that studying CS induced EVs that contain inflammatory and WNT signaling molecules (in EVs) can be a potential therapeutic target and diagnostic marker for detection of CS induced lung cancer. Despite these findings, the mechanistic approach of how CS induced the upregulation of the pathway and the use of the inhibitors as a potential therapy in LC needs to be investigated. This needs to be further investigated in preclinical models of lung cancer to study if CS induce LC by upregulation of the tumorigenesis *via* WNT/ β -catenin pathway pathway. In conclusion, the study of EVs in biofluids such as blood, and the use of WNT pathway inhibitors for smoking induced LC could be an early diagnostic and therapy, respectively for LC.

CRediT authorship contribution statement

Conceptualisation, VM, KD, PMH; methodology, software, validation, formal analysis, investigation, VM, GDR; writing—original draft preparation, VM; writing-review and editing, VM, NGH, KRP, PM.H, KD; supervision, KD, KRP, and PMH. All authors have read and agreed to the published version of the manuscript.

Funding

Philip M. Hansbro would like to acknowledge the support from Cancer Council NSW, National Health and Medical Research Council (NHMRC 1079187, 1175134) and University of Technology Sydney, Australia. Kamal Dua is supported by project grants from the Rebecca L

Cooper Medical Research Foundation and the fellowship from Maridulu Budyari Gumal—Sydney Partnership for Health Education, Research and Enterprise (SPHERE). Vamshikrishna Malyla is supported by international research scholarship by UTS. Keshav Raj Paudel and Philip M. Hansbro are supported by a joint fellowship from the Prevent Cancer Foundation (PCF), Alexandria, Virginia, United States, and the International Association for the Study of Lung Cancer (IASLC) Foundation, Denver, Colorado, United States.

Institutional review board statement

Not applicable.

Informed consent statement

Not applicable.

Declaration of competing interest

No competing interest to declare

Data availability

The data presented in this study are available on request from the corresponding author.

References

1. T. Walser, et al., Smoking and lung cancer: the role of inflammation, *Proc. Am. Thorac. Soc.* 5 (8) (2008) 811–815.
2. G.W. Warren, K.M. Cummings, Tobacco and lung cancer: risks, trends, and outcomes in patients with cancer, *American Society of Clinical Oncology Educational Book* 33 (1) (2013) 359–364.
3. T. Zhang, et al., Genomic and evolutionary classification of lung cancer in never smokers, *Nat. Genet.* 53 (9) (2021) 1348–1359.
4. G.A. Rivera, H. Wakelee, Lung cancer in never smokers, *Lung cancer and personalized medicine: current knowledge and therapies* (2016) 43–57.
5. WCRF. Lung cancer statistics. 2020 [cited 2023 10/4/2023]; Available from: <https://www.wcrf.org/cancer-trends/lung-cancer-statistics/#:~:text=Latest%20lung%20cancer%20data,of%20lung%20cancer%20in%202020>.
6. V. Malyla, et al., Recent advances in experimental animal models of lung cancer, *Future Med. Chem.* 12 (7) (2020) 567–570.
7. K.R. Paudel, et al., Targeting lung cancer using advanced drug delivery systems, in: *Targeting Chronic Inflammatory Lung Diseases Using Advanced Drug Delivery Systems*, Elsevier, 2020, pp. 493–516.
8. N. Solanki, et al., Antiproliferative effects of boswellic acid-loaded chitosan nanoparticles on human lung cancer cell line A549, *Future Med. Chem.* 12 (22) (2020) 2019–2034.
9. R. Wadhwa, et al., Epigenetic therapy as a potential approach for targeting oxidative stress-induced non-small-cell lung cancer, *Handbook of Oxidative Stress in Cancer: Mechanistic Aspects* (2020) 1–16.
10. J. Malhotra, et al., Risk factors for lung cancer worldwide, *Eur. Respir. J.* 48 (3) (2016) 889–902.
11. G. De Rubis, et al., Agarwood oil Nanoemulsion attenuates cigarette smoke-induced inflammation and oxidative stress markers in BGI-NS1.1 airway epithelial cells, *Nutrients* 15 (4) (2023).
12. S.S. Hecht, Tobacco carcinogens, their biomarkers and tobacco-induced cancer, *Nat. Rev. Cancer* 3 (10) (2003) 733–744.
13. S.S. Hecht, D.K. Hatsukami, Smokeless tobacco and cigarette smoking: chemical mechanisms and cancer prevention, *Nat. Rev. Cancer* 22 (3) (2022) 143–155.
14. Zheng, H.-C. and Y. Takano, NNK-induced lung tumors: a review of animal model. *Journal of oncology*, 2011. 2011.
15. K. Luo, et al., Cigarette smoking enhances the metabolic activation of the polycyclic aromatic hydrocarbon phenanthrene in humans, *Carcinogenesis* 42 (4) (2021) 570–577.
16. W.M. Baird, L.A. Hooven, B. Mahadevan, Carcinogenic polycyclic aromatic hydrocarbon-DNA adducts and mechanism of action, *Environ. Mol. Mutagen.* 45 (2–3) (2005) 106–114.
17. B. Moorthy, C. Chu, D.J. Carlin, Polycyclic aromatic hydrocarbons: from metabolism to lung cancer, *Toxicol. Sci.* 145 (1) (2015) 5–15.
18. N. Masykura, et al., Impact of smoking on frequency and spectrum of K-RAS and EGFR mutations in treatment naive Indonesian lung cancer patients, *Lung Cancer: Targets and Therapy* (2019) 57–66.
19. A.M. Varghese, et al., Lungs don't forget: comparison of the KRAS and EGFR mutation profile and survival of collegiate smokers and never smokers with advanced lung cancers, *J. Thorac. Oncol.* 8 (1) (2013) 123–125.
20. H.M. Schuller, Is cancer triggered by altered signalling of nicotinic acetylcholine receptors? *Nat. Rev. Cancer* 9 (3) (2009) 195–205.
21. Y. Zheng, et al., Nicotine stimulates human lung cancer cell growth by inducing fibronectin expression, *Am. J. Respir. Cell Mol. Biol.* 37 (6) (2007) 681–690.
22. J. Tsurutani, et al., Tobacco components stimulate Akt-dependent proliferation and NFκB-dependent survival in lung cancer cells, *Carcinogenesis* 26 (7) (2005) 1182–1195.
23. West, K.A., et al., Rapid Akt activation by nicotine and a tobacco carcinogen modulates the phenotype of normal human airway epithelial cells. *J. Clin. Invest.*, 2003. 111(1): p. 81–90.
24. H.M. Schuller, et al., The tobacco-specific carcinogen 4-(methylnitrosamino)-1-(3-pyridyl)-1-butanone is a β-adrenergic agonist and stimulates DNA synthesis in lung adenocarcinoma via β-adrenergic receptor-mediated release of arachidonic acid, *Cancer Res.* 59 (18) (1999) 4510–4515.
25. H.M. Schuller, Mechanisms of smoking-related lung and pancreatic adenocarcinoma development, *Nat. Rev. Cancer* 2 (6) (2002) 455–463.
26. H.M. Schuller, The impact of smoking and the influence of other factors on lung cancer, *Expert Review of Respiratory Medicine* 13 (8) (2019) 761–769.
27. M. Mehta, et al., Cellular signalling pathways mediating the pathogenesis of chronic inflammatory respiratory diseases: an update, *Inflammopharmacology* 28 (2020) 795–817.
28. C.A. Martey, et al., Cigarette smoke induces cyclooxygenase-2 and microsomal prostaglandin E2 synthase in human lung fibroblasts: implications for lung inflammation and cancer, *Am. J. Phys. Lung Cell. Mol. Phys.* 287 (5) (2004) L981–L991.
29. M. Nishikawa, et al., Superoxide mediates cigarette smoke-induced infiltration of neutrophils into the airways through nuclear factor-κ B activation and IL-8 mRNA expression in guinea pigs in vivo, *Am. J. Respir. Cell Mol. Biol.* 20 (2) (1999) 189–198.
30. S.-R. Yang, et al., IKKα causes chromatin modification on pro-inflammatory genes by cigarette smoke in mouse lung, *Am. J. Respir. Cell Mol. Biol.* 38 (6) (2008) 689–698.
31. D.K. Chellappan, et al., Targeting neutrophils using novel drug delivery systems in chronic respiratory diseases, *Drug Dev. Res.* 81 (4) (2020) 419–436.
32. G. Chiappara, et al., Cigarette smoke upregulates Notch-1 signaling pathway and promotes lung adenocarcinoma progression, *Toxicol. Lett.* 355 (2022) 31–40.
33. H. Lemjabbar-Alaoui, et al., Wnt and hedgehog are critical mediators of cigarette smoke-induced lung cancer, *PLoS One* 1 (1) (2006), e93.
34. V. Malyla, et al., Extracellular vesicles released from Cancer cells promote tumorigenesis by inducing epithelial to mesenchymal transition via β-catenin signaling, *Int. J. Mol. Sci.* 24 (4) (2023) 3500.
35. C.Y. Logan, R. Nusse, The Wnt signaling pathway in development and disease, *Annu. Rev. Cell Dev. Biol.* 20 (2004) 781–810.
36. M. Majidinia, et al., The roles of Wnt/β-catenin pathway in tissue development and regenerative medicine, *J. Cell. Physiol.* 233 (8) (2018) 5598–5612.
37. T. Sidrat, et al., Wnt/β-catenin pathway-mediated PPARδ expression during embryonic development differentiation and disease, *Int. J. Mol. Sci.* 22 (4) (2021) 1854.
38. Z. Steinhart, S. Angers, Wnt signaling in development and tissue homeostasis, *Development* 145 (11) (2018) p. dev146589.
39. D.J. Stewart, Wnt signaling pathway in non-small cell lung cancer, *JNCI: Journal of the National Cancer Institute* 106 (1) (2014).
40. E. Flores-Hernández, et al., Canonical and non-canonical Wnt signaling are simultaneously activated by Wnts in colon cancer cells, *Cell. Signal.* 72 (2020), 109636.
41. C. Théry, et al., Minimal information for studies of extracellular vesicles 2018 (MISEV2018): a position statement of the International Society for Extracellular Vesicles and update of the MISEV2014 guidelines, *Journal of extracellular vesicles* 7 (1) (2018) 1535750.
42. M. Yáñez-Mó, et al., Biological properties of extracellular vesicles and their physiological functions, *Journal of extracellular vesicles* 4 (1) (2015) 27066.
43. K.R. Paudel, D.W. Kim, Microparticles-mediated vascular inflammation and its amelioration by antioxidant activity of Baicalin, *Antioxidants (Basel)* 9 (9) (2020).
44. B. Manandhar, et al., Applications of extracellular vesicles as a drug-delivery system for chronic respiratory diseases, *Nanomedicine (Lond)* 17 (2022) 1–4.
45. M. Record, et al., Extracellular vesicles: lipids as key components of their biogenesis and functions, *J. Lipid Res.* 59 (8) (2018) 1316–1324.
46. R. Jaiswal, et al., Microparticle conferred microRNA profiles-implications in the transfer and dominance of cancer traits, *Mol. Cancer* 11 (2012) 1–13.
47. Y. Fujita, Y. Yoshioka, T. Ochiya, Extracellular vesicle transfer of cancer pathogenic components, *Cancer Sci.* 107 (4) (2016) 385–390.
48. W. Hu, et al., Comprehensive landscape of extracellular vesicle-derived RNAs in cancer initiation, progression, metastasis and cancer immunology, *Mol. Cancer* 19 (2020) 1–23.
49. G. De Rubis, S.R. Krishnan, M. Bebawy, Liquid biopsies in cancer diagnosis, monitoring, and prognosis, *Trends Pharmacol. Sci.* 40 (3) (2019) 172–186.
50. S. Rajeev Krishnan, et al., A liquid biopsy to detect multidrug resistance and disease burden in multiple myeloma, *Blood Cancer Journal* 10 (3) (2020) 37.
51. T. Corsello, et al., Cigarette smoke condensate exposure changes RNA content of extracellular vesicles released from small airway epithelial cells, *Cells* 8 (12) (2019) 1652.
52. A. Paramanatham, et al., Extracellular vesicle (EVs) associated non-coding RNAs in lung cancer and therapeutics, *Int. J. Mol. Sci.* 23 (21) (2022) 13637.
53. W. Li, et al., Liquid biopsy in lung cancer: significance in diagnostics, prediction, and treatment monitoring, *Mol. Cancer* 21 (1) (2022) 25.

- [54] G.V. Shelke, et al., Importance of exosome depletion protocols to eliminate functional and RNA-containing extracellular vesicles from fetal bovine serum, *Journal of extracellular vesicles* 3 (1) (2014) 24783.
- [55] K.R. Paudel, et al., Attenuation of cigarette-smoke-induced oxidative stress, senescence, and inflammation by berberine-loaded liquid crystalline nanoparticles: in vitro study in 16HBE and RAW264. 7 cells, *Antioxidants* 11 (5) (2022) 873.
- [56] J.S. Bourgeois, et al., The bioavailability of soluble cigarette smoke extract is reduced through interactions with cells and affects the cellular response to CSE exposure, *PLoS One* 11 (9) (2016), e0163182.
- [57] L.G. Rikkert, et al., Quality of extracellular vesicle images by transmission electron microscopy is operator and protocol dependent, *Journal of extracellular vesicles* 8 (1) (2019) 1555419.
- [58] K.R. Paudel, et al., Berberine-loaded liquid crystalline nanoparticles inhibit non-small cell lung cancer proliferation and migration in vitro, *Environ. Sci. Pollut. Res.* 29 (31) (2022) 46830–46847.
- [59] R. Wadhwa, et al., Anti-inflammatory and anticancer activities of Naringenin-loaded liquid crystalline nanoparticles in vitro, *J. Food Biochem.* 45 (1) (2021), e13572.
- [60] K.R. Paudel, et al., Rutin loaded liquid crystalline nanoparticles inhibit non-small cell lung cancer proliferation and migration in vitro, *Life Sci.* 276 (2021), 119436.
- [61] Z. Chen, Z. Fang, J. Ma, Regulatory mechanisms and clinical significance of vimentin in breast cancer, *Biomed. Pharmacother.* 133 (2021), 111068.
- [62] Y. Guo, et al., Roles of galectin-3 in the tumor microenvironment and tumor metabolism, *Oncol. Rep.* 44 (5) (2020) 1799–1809.
- [63] W.A. Pryor, et al., Fractionation of aqueous cigarette tar extracts: fractions that contain the tar radical cause DNA damage, *Chem. Res. Toxicol.* 11 (5) (1998) 441–448.
- [64] R. Goldman, et al., Smoking increases carcinogenic polycyclic aromatic hydrocarbons in human lung tissue, *Cancer Res.* 61 (17) (2001) 6367–6371.
- [65] S. Amit, et al., Axin-mediated CKI phosphorylation of beta-catenin at Ser 45: a molecular switch for the Wnt pathway, *Genes Dev.* 16 (9) (2002) 1066–1076.
- [66] B.T. MacDonald, K. Tamai, X. He, Wnt/beta-catenin signaling: components, mechanisms, and diseases, *Dev. Cell* 17 (1) (2009) 9–26.
- [67] W.K. Kim, et al., β -Catenin activation down-regulates cell-cell junction-related genes and induces epithelial-to-mesenchymal transition in colorectal cancers, *Sci. Rep.* 9 (1) (2019) 18440.
- [68] P. Polakis, The oncogenic activation of β -catenin, *Curr. Opin. Genet. Dev.* 9 (1) (1999) 15–21.
- [69] B.M. Gumbiner, Regulation of cadherin-mediated adhesion in morphogenesis, *Nat Rev Mol Cell Biol* 6 (8) (2005) 622–634.

9) Research Paper: Berberine nanostructures attenuate β -catenin, a key component of epithelial mesenchymal transition in lung adenocarcinoma.

Status: Published in **Naunyn-Schmiedeberg's Archives of Pharmacology**

Citation: Malyla V, **De Rubis G**, Paudel KR, Chellappan DK, Hansbro NG, Hansbro PM, Dua K. *Berberine nanostructures attenuate β -catenin, a key component of epithelial mesenchymal transition in lung adenocarcinoma.* **Naunyn-Schmiedeberg's Archives of Pharmacology.** 2023 Jun 2. doi: 10.1007/s00210-023-02553-y

Contribution: I contributed to the experiments, manuscript writing, and revisions of the manuscript draft



Berberine nanostructures attenuate β -catenin, a key component of epithelial mesenchymal transition in lung adenocarcinoma

Vamshikrishna Malyla^{1,2,3} · Gabriele De Rubis^{1,3} · Keshav Raj Paudel^{2,4} · Dinesh Kumar Chellappan⁵ · Nicole G. Hansbro^{2,4} · Philip M. Hansbro^{2,4} · Kamal Dua^{1,2,3}

Received: 27 March 2023 / Accepted: 23 May 2023
© The Author(s) 2023

Abstract

Lung cancer (LC) is the leading cause of cancer-related deaths globally. It accounts for more than 1.9 million cases each year due to its complex and poorly understood molecular mechanisms that result in unregulated cell proliferation and metastasis. β -Catenin is a developmentally active protein that controls cell proliferation, metastasis, polarity and cell fate during homeostasis and aids in cancer progression via epithelial–mesenchymal transition. Therefore, inhibition of the β -catenin pathway could attenuate the progression of LC. Berberine, an isoquinoline alkaloid which is known for its anti-cancer and anti-inflammatory properties, demonstrates poor solubility and bioavailability. In our study, we have encapsulated berberine into liquid crystalline nanoparticles to improve its physiochemical functions and studied if these nanoparticles target the β -catenin pathway to inhibit the human lung adenocarcinoma cell line (A549) at both gene and protein levels. We observed for the first time that berberine liquid crystalline nanoparticles at 5 μ M significantly attenuate the expression of the β -catenin gene and protein. The interaction between berberine and β -catenin was further validated by molecular simulation studies. Targeting β -catenin with berberine nanoparticles represents a promising strategy for the management of lung cancer progression.

Keywords Berberine · Nano-formulations · WNT/ β -catenin signalling pathway · Molecular simulation · Lung cancer

Introduction

Lung cancer (LC) is the leading cause of cancer-related deaths globally, accounting for more than 1.9 million cases

each year. This is due to a lack of early diagnostic tools and effective pharmacological interventions, as well as high prevalence rates of cigarette smoking. Understanding the pathology of LC is vital for developing novel diagnostic and therapeutic interventions (Siegel, et al. 2022; Solanki et al. 2020). One of the primary reasons for the increasing number of lung cancer cases is the lack of effective diagnostic and therapeutic approaches. Understanding the molecular mechanisms responsible for lung cancer pathogenesis, and improving strategies to inhibit specific pathways at the molecular level, could aid in controlling tumorigenesis and metastasis (Malyla et al. 2020). Current approaches for the management of LC include chemotherapy, immunotherapy, targeted therapy, radiation therapy and surgical removal of lung tumour (Paudel et al. 2020; Wadhwa, et al. 2020). With regard to chemotherapy, the major drawbacks of the currently available synthetic drug molecules are poor bioavailability and off-target effects (Cui et al. 2018). Alternatively, there is a growing interest in natural product-derived phytoconstituents, which represent a promising option for the therapeutic targeting of LC. Berberine is an isoquinoline alkaloid abundantly found in

✉ Philip M. Hansbro
Philip.Hansbro@uts.edu.au

✉ Kamal Dua
Kamal.Dua@uts.edu.au

¹ Discipline of Pharmacy, Graduate School of Health, University of Technology Sydney, Sydney, NSW 2007, Australia

² Centre for Inflammation, Centenary Institute, Sydney, Sydney, NSW 2050, Australia

³ Australian Research Centre in Complementary and Integrative Medicine, Faculty of Health, University of Technology Sydney, Ultimo, NSW 2007, Australia

⁴ Faculty of Science, University of Technology Sydney, Sydney, NSW 2007, Australia

⁵ Department of Life Sciences, School of Pharmacy, International Medical University, Bukit Jalil 57000, Kuala Lumpur, Malaysia

the stems, barks and roots of plants belonging to the genus *Berberis*, which is widely known for its anti-cancer and anti-inflammatory properties (Li et al. 2014; Mehta et al. 2021). Berberine has shown to inhibit non-small cell lung cancer (NSCLC) growth through repression of DNA repair and replication (Ni et al. 2022) and through induction of apoptosis (Chen et al. 2022; Chen et al. 2019; Li et al. 2018), as well as through inhibition of proliferation and colony formation capacity (Chen et al. 2020). Furthermore, berberine prevents LC by inhibiting EMT-promoting macrophages overexpressing the protein arginine deaminase 4 (PADI4) (Gu et al. 2022), and it reduces LC cell expression of PD-L1, thus facilitating antitumor immune response (Liu et al. 2020). Despite the promising anti-cancer activity and enormous potential, the major drawbacks of berberine, and many other plant-derived active principles, are low bioavailability and limited bio-absorption, which limit their in vivo efficacy and therapeutic use (Battu et al. 2010). A viable strategy to overcome these drawbacks, particularly for lung and respiratory diseases that allow the administration of drugs through inhalation, is represented by the encapsulation of active principles in advanced nanoparticles/nanocarrier systems (Doroudian et al. 2019). Liquid crystalline nanoparticles (LCNPs), among many emerging nanoparticle-based delivery systems, have been gaining momentum as nanocarrier systems for antioxidant and anti-cancer drugs as they increase the drug's stability, bio-adhesiveness, sustained release properties, bioavailability, drug loading capacity and physicochemical stability (Paudel, et al. 2022). Recent studies have demonstrated the potent in vitro anti-cancer activity of berberine-loaded LCNPs, with an inhibitory effect on the proliferation, colony formation, migration and invasion capacity of NSCLC cells (Mehta et al. 2021; Alnuqaydan, et al. 2022; Paudel et al. 2022). Mechanistically, these effects are mediated by the inhibition of the expression of EMT-related proteins (Snail, P27 and vimentin) and migration and proliferation-related proteins such as BCLx, galectin-3 and survivin (Paudel et al. 2022), as well as by the upregulation of the mRNA levels of tumour suppressors PTEN and p53 downregulation of the oncogene KRT18 (Alnuqaydan, et al. 2022). Furthermore, berberine LCNPs downregulate the expression of inflammation/oxidative stress-related cytokines such as CCL20, CXCL-8 and HO-1 (Mehta et al. 2021).

Although berberine-loaded LCNPs represent a valuable option in the treatment of LC, further research is still needed to completely characterise the pathways that are affected by this treatment which results in such a promising anti-cancer activity. WNT/ β -catenin is a developmentally active signal transduction pathway that controls cell proliferation, metastasis, polarity and cell fate during homeostasis (Zhang and Wang 2020). In a normal state, the β -catenin destruction complex generally recruits dishevelled (DVL), a scaffolding

protein which activates the Axin complex (glycogen synthase kinase 3 (GSK3), casein kinase 1 (CK1) and adenomatous polyposis coli (APC)). This complex attenuates β -catenin. However, during pathological states, WNT markers bind to a transmembrane frizzled receptor, destabilising the β -catenin destruction complex. This would further leads to the accumulation of β -catenin in the cytoplasm. The accumulated β -catenin translocates to the nucleus, resulting in the activation of various oncogenic pathways that regulate the transcription factors in the T cell factor/lymphoid enhancer factor family (TCF/LEF) as well as the epithelial–mesenchymal transition (EMT)-related genes (Fig. 3) (Anthony et al. 2020; Cadigan and Waterman 2012). β -Catenin has a multifaceted role. It is a component of the cadherin-based cell–cell communication system, which helps in maintaining polarity and regulating tight junctions (Meng and Takeichi 2009). In cancer, polarised epithelial cells change their morphology to a mesenchymal phenotype through a process called EMT (Thiery, et al. 2009), which is a key process in embryogenesis and cancer. This process is controlled by β -catenin through regulation of EMT molecules such as cadherins (Heuberger and Birchmeier 2010), Twist family BHLH transcription factor (Twist) (Li and Zhou 2011), Snail1, slug (Stemmer, V.d., et al. 2008), and zinc finger E-box binding homeobox 1 (ZEB1) (Sánchez-Tilló et al. 2011). Therefore, β -catenin is a key agent in cancer progression and EMT, and inhibition of this system could suppress the pathogenesis and attenuate the progression of LC (Valenta et al. 2012).

In this study, we show that treatment of human adenocarcinoma cells (A549) with berberine LCNPs significantly reduced the expression of WNT/ β -catenin pathway markers β -catenin and Axin1 at a low concentration of 5 μ M berberine. Furthermore, we have identified, through docking studies and molecular dynamics simulations, a putative binding site for berberine on β -catenin. This study provides further proof of the improved solubility and stability of berberine which is encapsulated in LCNs as a novel therapeutic approach against LC, shedding light on a previously unexplored mechanism by which berberine-loaded LCNs exerted anti-cancer activity.

Materials

Berberine hydrochloride, monoolein (MO) and poloxamer 407 (P407) were purchased from Sigma Chemical Co, Germany. Spectra/Por dialysis membrane bags (dialysis tubing 238 cellulose membrane; molecular-weight-cut-off: 14,000 g/mol) were purchased from Sigma-Aldrich, USA. Culture media and reagents were of analytical and molecular grade and were used without any further purification.

Methods

Cell culture

A549 adenocarcinoma human alveolar basal epithelial cell line (ATCC, USA) was obtained as a gift from Prof. Alaina Ammit, Woolcock Institute of Medical Research, Sydney, Australia. The cells were grown in a RPMI media (Sigma-Aldrich, USA) containing 5% foetal bovine serum (Novogen, Australia), 1% penicillin and streptomycin (Gibco, New York) and were maintained at 37 °C in an incubator with 5% CO₂. Cells were constantly checked for mycoplasma contamination, and all experiments were conducted in mycoplasma-negative cells.

Preparation of berberine-loaded liquid crystal nanoparticles (LCNPs)

Berberine-loaded liquid crystalline nanoparticles were formulated as previously reported, using the ultrasonication technique (Paudel 2022). Briefly, 5 mg berberine was completely dissolved in 200 mg melted MO at 70 °C. This berberine–MO mixture was then mixed with the surfactant solution (20 mg P407 dissolved in 4.8 mL water), obtaining a coarse dispersion. This dispersion was size-reduced using a probe sonicator (Labsonic® P, Sartorius, Germany), with the amplitude maintained at 80, and 5-s on and 5-s off-cycles for 5 min. This resulted in the production of 1 mg/mL berberine-loaded MO-LCNPs, with a lipid content of 40 mg/mL and a lipid:surfactant ratio of 1:10 w/w (Wadhwa et al. 2021).

Cytotoxicity (cell proliferation) assay of berberine LCNPs (BBR LCNPs) in A549 cells

A549 cells were plated in a 6-well plate at a density of 2×10^5 cells/well. Cells were treated with or without 5 µM of BBR LCNPs for 24 h. The dose of 5 µM of BBR LCNPs was decided from our previously published study showing significant anti-proliferative (MTT assay) and anti-migratory activity of berberine against the A549 cell line at that concentration (Paudel 2022).

RNA extraction and assessment of gene expression level by real-time PCR

RNA was extracted using the TRIzol® method. Extracted RNA was reverse transcribed to cDNA using a high-capacity DNA reverse transcription kit (Applied Biosystems, RI, USA). Real-time PCR analysis was performed using TaqMan primers and probes (Applied Biosystems) to measure the relative expression of genes CTTNB1 (forward

primer: CTTGGAATGAGACTGCTG; reverse primer: AGA GTGAAAAGAACGATAGC), Axin1 (forward primer: CCG ACCTTANATGAAGATGAG; reverse primer: CAGGAT CCATACCTGAACTC). The quantitative expression of these genes was calculated through the $2^{-\Delta\text{-Ct}}$ method and was compared to the respective reference gene (GAPDH). The relative transcript abundance in the treated groups was calculated by comparing the treated groups with untreated controls (Wadhwa et al. 2021).

Immunofluorescence (IF)

Coverslips were sterilised and coated with placenta collagen (Sigma cat. no. C5533) for 30 min and washed twice with 1 ml 1×PBS to allow cell adhesion. Then, 2×10^5 A549 cells were seeded on the cover slip and placed in a 6-well plate. The following day, cells were treated with 5 µM BBR LCNPs for 24 h. The media was then removed, and cells were washed with sterile 1×PBS. Cells were fixed with ice-cold methanol for 20 min, followed by blocking with 2% bovine serum albumin (BSA) for 1 h at room temperature. The cells were then incubated with anti-beta catenin (ab32572) antibody at 1:250 dilution overnight at 4 °C, followed by incubation with goat anti-rabbit IgG H&L Alexa Fluor® 647 (ab150083) for 1 h at room temperature (1:500 dilution), protected from light. Finally, the slides were cover slipped with DAPI fluoromount G (ProSciTech). The microscopic images at random fields were then captured with a fluorescence microscope (Zeiss microscope, Germany) at 40× magnification (Paudel and Kim 2020).

Protein extraction and quantification

RIPA buffer (Sigma-Aldrich) containing phosphatase and protease inhibitor cocktail (Roche, USA) was added to the 6-well plates containing treated and untreated cells, and the lysate was collected in a microcentrifuge tube. Proteins were extracted from lysed cells upon vortex treatment and incubation on ice for 15 min. Soon after, the mixture was sonicated at 30% amplitude, 3 times for 2 s. The mixture was then incubated again on ice for an additional 15 min. The lysate was then centrifuged for 30 min at 18,000 g at 4 °C. Finally, the supernatant was collected, and the proteins were quantified using a Pierce™ BCA Protein Array Kit (Thermo Scientific) following the manufacturer's instructions (Wadhwa et al. 2021).

Immunoblotting

Equal amounts of the extracted proteins were loaded on SDS-PAGE gels and transferred to a PVDF membrane. The membrane was blocked with 5% BSA and incubated

with primary rabbit anti-beta catenin antibody (ab 32,572) at a 1:7500 dilution overnight at 4 °C, followed by incubation with goat anti-rabbit IgG at a 1:10,000 dilution for 1 h. Images were acquired using a ChemiDoc imaging system. Then, the membrane was stripped and blocked again with 5% BSA. It was then incubated with mouse anti-beta actin antibody (ab8226) at 1:10,000 dilution at room temperature for 3 h followed. After this, the membrane was incubated with anti-mouse IgG at 1:10,000 dilution, and images were again acquired using a ChemiDoc imaging system (whole blots were added in the supplementary file). The densitometric analysis of proteins was performed by quantifying pixel density using ImageJ software.

Statistical analysis

The values are represented as mean \pm SEM. GraphPad Prism (version 9.3) was used to perform statistical analyses. Statistical comparisons were done by unpaired, two-tailed student's *t*-test. A value of $p < 0.05$ was considered statistically significant.

Molecular docking study

For the molecular docking study, the three-dimensional structure of human beta catenin (PDB ID: 1JDH) and berberine (PubChem CID 2353) was retrieved from the Protein Data Bank (PDB) and PubChem, respectively (Graham et al. 2001; Berman et al. 2000; Kim et al. 2016). Before molecular docking, the protein structure was prepared by adding hydrogens, optimising geometry and minimising energy with the protein preparation wizard of Schrodinger (Sastry et al. 2013). Similarly, the ligand geometry was optimised with the LigPrep module of Schrodinger (Sastry et al. 2013). The molecular docking study was performed using Vina wizard of PyRx software (Dallakyan and Olson 2015). The grid was generated around the β -catenin residues Phe253, His260, Asn261, Leu264, Asn290, Lys292, Phe293, Ile296, Asp299, Gln302, Tyr306, Gly307, Lys312, Lys335, Arg342, Lys345, Val346, Arg376, Arg386, Asn387, Asp390, Gly422, Ser425, Asn426, Cys429, Asn430, Lys435, Arg469, His470, Ser473, Arg474, Lys508, Gly512, Asn516 and Leu519. These residues were selected because they were reported to be involved in the interaction between β -catenin and human TCF4, in a study in which the β -catenin-hTcf4 complex was characterised through X-Ray crystallography (Graham et al. 2001). The coordinates of X, Y and Z were set to 73.8, -19.75 and -15.46, respectively. The exhaustiveness of the algorithm is set to 8. After molecular docking, the top docking pose of the ligand was selected based on the docking score and subjected to molecular dynamics simulation.

Molecular dynamics study

The molecular dynamics (MD) simulation was run using the Desmond software (Bowers, et al. 2006). For MD simulation, the system was prepared by adding water and neutralised by the addition of sodium and chloride ions. The berberine- β -catenin complex was hydrated in an orthorhombic box using a three-point water model (TIP3P) (Bowers, et al. 2006). The implicit solvent system was used to represent solvent. After that, the system was energy minimised. Finally, the minimised system was subjected to 50 ns of MD simulations in isothermal-isobaric ensemble (NPT) at high temperature. Fifty ns of MD simulations were deemed sufficient for the MD simulation, considering the high-temperature settings, the use of the implicit solvent system and the fact that the backbone chains of carbon atoms showed stability throughout the 50 ns. The final trajectory was analysed with manual inputs and root mean square deviation (RMSD), protein-ligand contact histogram, protein-ligand contact diagram and root mean square fluctuation (RMSF) calculated using the simulation interaction diagram utility of maestro.

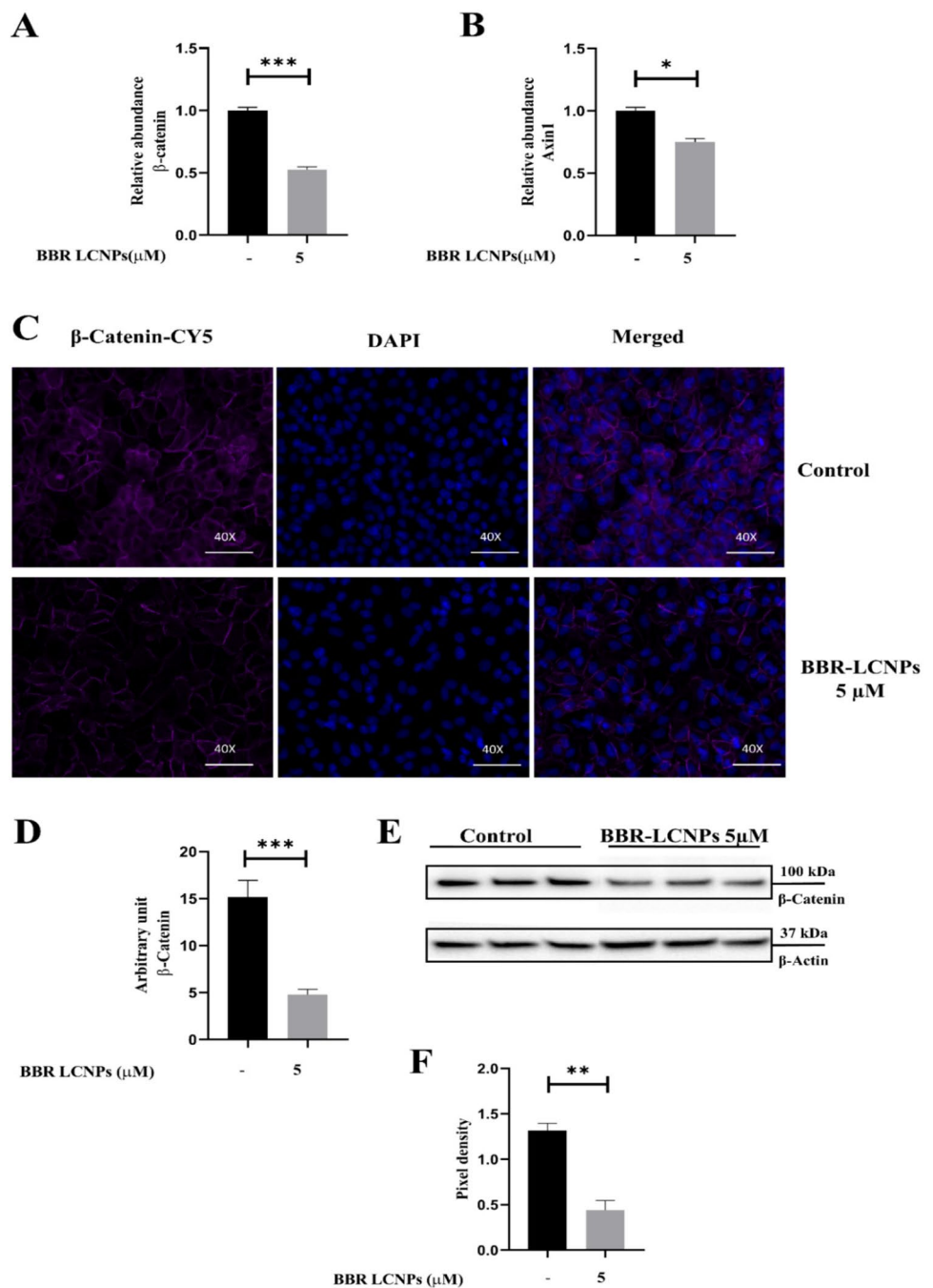
MMGBSA energy calculation

After MD simulation, to estimate the binding affinity of the berberine- β -catenin complex, the binding-free energy (dG_{Bind}) was estimated using the thermal_mmgbsa.py script of Schrodinger (Genheden and Ryde 2015). The calculation was performed on 100 complexes obtained by extracting every 10th frame from the last 10 ns of the stable trajectory. After MMGBSA calculation, an average binding-free energy was reported.

Results

Based on the cytotoxicity studies reported in our previously published work on the effect of BBR LCNPs on A549 cells, we identified 5 μM as the optimal concentration for anti-cancer activity of the formulation. This is validated by anti-proliferative, anti-migratory and colony formation assays (Wadhwa et al. 2021). Based on these data, we proceeded with 5 μM BBR LCNPs as an optimal concentration for studying the effect of these NPs on β -catenin activity. To begin with, we initially validated the activity of the formulation at the transcript level using RT-PCR. In this experiment, a 24-h treatment of A549 cells with BBR LCNPs at 5 μM resulted in a significant downregulation of β -catenin (Fig. 1A) and Axin1 (Fig. 1B), the key components of the WNT/ β -catenin pathway, as compared to untreated control (only A549 cells). BBR LCNs decreased β -catenin expression to 0.5-fold and Axin1 expression to approximately 0.7-fold. This made us

Fig. 1 Effect of BBR LCNPs in the reduction of WNT/ β -catenin pathway genes β -catenin and Axin1. After 24-h treatment of A549 cells with BBR LCNPs, the expression of WNT/ β -catenin pathway genes was assessed via RT-PCR, IF and immunoblotting. **A** β -Catenin expression, RT-PCR. **B** Axin1 expression, RT-PCR. The values are represented as mean \pm SEM of 3 independent experiments, * p < 0.05, *** p < 0.001. **C** Immunofluorescence staining for β -catenin under 40 \times magnification. **D** Fluorescence quantification with ImageJ Fiji. The values represent mean \pm SEM of 3 independent experiments, *** p < 0.001. **E** β -Catenin expression, immunoblotting. **F** Pixel density quantification of immunoblotting with ImageJ Fiji. The values represent mean \pm SEM of 3 independent experiments, ** p \leq 0.01



to look the activity at the protein level, and we performed an immunofluorescence assay to quantify β -catenin protein expression. As shown in Fig. 1C, a 24-h treatment of A549 cells with BBR LCNPs at 5 μ M resulted in a significant decrease in the intensity of the β -catenin fluorescence signal. The quantification of fluorescence intensity showed that BBR LCNP treatment decreased the β -catenin intensity by tenfold (Fig. 1D). A similar trend was observed with western blotting (Fig. 1E). Overall, BBR LCNPs had reduced the expression of β -catenin at both transcript and protein levels. To further understand the putative region where BBR binds

to β -catenin, we performed molecular docking and molecular dynamic simulation studies.

The molecular docking study was performed to explore the best binding pose of berberine with β -catenin. Among all the generated poses of berberine, the best pose exhibited a binding energy of -6.4 kcal/mol in the human TCF4 binding site. To assess the stability of berberine in its predicted binding site, a molecular dynamics simulation was performed. Molecular dynamics simulations represent a robust tool to understand the behaviour of protein–ligand complexes in dynamic conditions. As observed from the

RMSD plot (Fig. 2A), β -catenin remained stable throughout the 50-ns simulation (root mean square deviation 4.17 Å). The maximum RMSF was shown by residues 543–558 of β -catenin (Fig. 2B). The ligand berberine remained stable in the human T cell transcription factor-4 (HTCF-4) binding site for the first 10 ns of simulation time, after which it left the binding site and occupied a site far away from the HTCF-4 binding site, where it remained stable for the remainder of the simulation period (Fig. 2D). At its binding site, berberine remained stable by interacting majorly with hydrophobic residues Pro373, Leu644, Ala652, Ala656, Leu659 and Phe660 via hydrophobic interactions and to a lesser extent with Glu334, Gln375, Thr653, Met662 and Ser663 via water bridges (Fig. 2C). Moreover, berberine exhibited an average free energy of binding (dG_Bind) of -26.82 kcal/mol (Table 1). Berberine was observed binding to β -catenin predominantly

Table 1 The energy components of free energy of binding of berberine– β -catenin complex calculated with MMGBSA programme

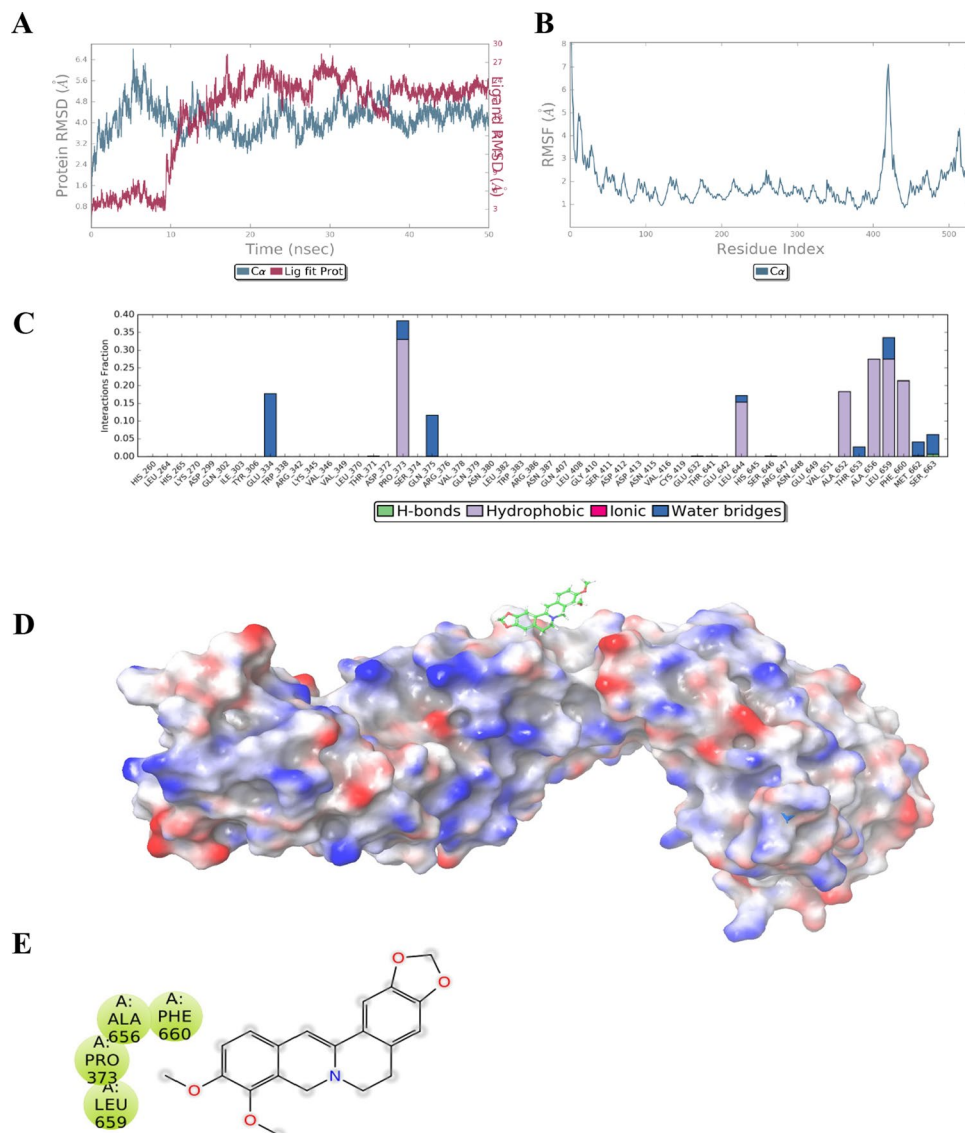
Average dG_Bind	Average dG_Bind_Coulomb	Average dG_Bind_Lipophilic	Average dG_Bind_vdW	Average dG_Bind_Hbond
-26.82	-2.46	-16.52	-17.41	-0.11

via lipophilic (-16.52 kcal/mol) and van der Waals (-17.41 kcal/mol) interactions.

Discussion

Although berberine possesses several therapeutic activities, it is a very hydrophobic molecule with a poor solubility of ~ 2.0 mg/mL resulting in low oral bioavailability

Fig. 2 Molecular docking and simulation studies with berberine and β -catenin. **A** Root mean square deviation (RMSD) indicates the stability of β -catenin with berberine. **B** Root mean square fluctuation (RMSF) plot of berberine– β -catenin complex. **C** Berberine– β -catenin contact summary calculated from the last 10 ns of the stable trajectory. **D** Surface representation of the HTCF-4 binding site of berberine with β -catenin. **E** Two-dimensional representation of the residues of β -catenin surrounding berberine



(Battu et al. 2010). To achieve potent biological activity, berberine should be administered in high doses. However, administration of high doses might not be favourable due to its toxicity in healthy/normal cells. In a published study, Wu Ke et al. have shown that treatment with pure berberine powder at 10 μM concentration in DMSO resulted in significant inhibition of the WNT/ β -catenin pathway in HCT116 colon cancer cells (Wu et al. 2012). To overcome these drawbacks of poor solubility and improved activity at lower concentrations, in this study, we encapsulated BBR in LCNPs and found that at 5 μM (half dose compared to Wu Ke et al. was sufficient to inhibit WNT/ β -catenin pathway's key component β -catenin at both the transcript and protein levels). This demonstrates the advantage of employing berberine-encapsulated LCNPs rather than pure berberine powder for improved activity at lower doses. Furthermore, in a previous study, we have shown that the physicochemical parameters of our BBR LCNP formulation (in terms of particle size, polydispersity index, in vitro release and entrapment efficiency) were significantly favourable (Paudel 2022).

The WNT/ β -catenin pathway is a key activator of various genes related to EMT and cancer, including LC (Valenta et al. 2012; Stewart 2014). The inhibition of the key EMT regulator β -catenin can be crucial in understanding the progression of LC. Previously, we found a

significant reduction of EMT markers like Snail, P27 and vimentin in LC. However, the effect of the formulation on β -catenin remains unknown (Paudel 2022). In the present study, treatment of BBR LCNPs to human lung adenocarcinoma cells (A549) significantly reduced the expression of the WNT/ β -catenin pathway markers β -catenin and Axin1 at transcript level and β -catenin at protein level at a concentration of just 5 μM , which is two times lower than previously reported studies (Albring et al. 2013). The inhibition of Axin1, a key component of the APC destruction complex which regulates and stabilises β -catenin, represents a further way to inhibit the WNT/ β -catenin pathway (Fig. 3A and B) (Jiang et al. 2018). This data provides proof that BBR LCNPs inhibit β -catenin via the canonical WNT/ β -catenin pathway.

Although, among the chemicals used to formulate the LCNPs, no component was specifically reported to have anti-cancer activity, treatment of cancer cells with LCNPs would provide proof of any eventual contributing biological activity mediated by the LCNPs itself, further confirming that the anti-cancer action is mediated by the berberine itself. This will be assessed in future studies in vivo setting which currently are in progress in our laboratory.

Molecular docking studies suggest that berberine binds to β -catenin at the human TCF4 binding site and

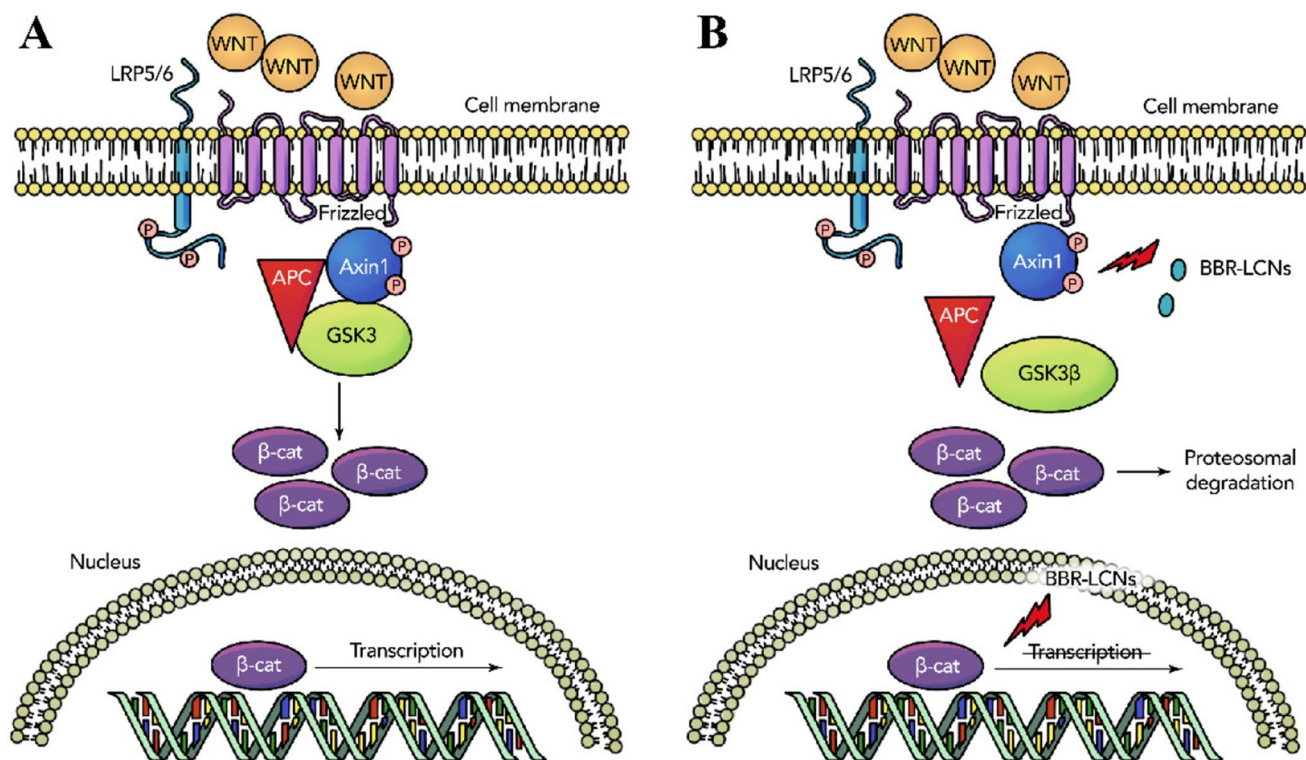


Fig. 3 Predicted molecular mechanism of action of BBR LCNPs on A549 cells. **A** The normal state of WNT/ β -catenin pathway is shown, where binding of WNT molecules leads to the activation

of β -catenin resulting in tumorigenesis. **B** Inhibition of AXIN1 and β -catenin by BBR LCNPs is shown

interacts with various amino acids via hydrophobic and water bridges with amino acids such as Phe660, which is critical for the binding of β -catenin to TCF inhibitors (Graham et al. 2002). Park et al. identified Ser663 as the amino acid where phosphorylation of β -catenin takes place. This event is vital for transcriptional regulation. As a result, the interaction of berberine with these residues may be critical for berberine's β -catenin inhibitory effect (Park et al. 2012).

Conclusions and future perspectives

In conclusion, natural product-derived phytochemicals can be a potential alternative for lung cancer treatment, as they assist to overcome the drawbacks that exist with synthetic anti-cancer drugs such as high cost, adverse reactions and unfavourable effects on the immune system. However, the use of natural phytochemicals such as berberine also has limitations such as poor solubility and low bioavailability. Therefore, the use of nanotechnology and advanced drug delivery approaches to design LCNPs loaded with berberine has improved its physicochemical properties resulting in improved efficacy. The potent anti-cancer activity of this innovative therapeutic tool, obtained through the suppression of β -catenin by BBR LCNPs at a low dose of 5 μ M, at both protein and gene levels is highly promising and requires further mechanistic understanding. Molecular dynamics studies found that BBR binds at Ser663, which is required for phosphorylation of β -catenin. This indicates that BBR might inhibit the phosphorylation of β -catenin at protein level. Future directions of this research should include further characterisation of the detailed in vitro mechanistic effects, as well as the validation of BBR LCNPs in pre-clinical animal models of LC. Furthermore, the clinical application of this promising nanoparticle-based therapeutic approach would benefit from the assessment of its suitability as a pulmonary drug delivery system.

Abbreviations APC: Adenomatous polyposis coli; BBR: Berberine; BSA: Bovine serum albumin; CK1: Casein kinase 1; CTNNB1: Catenin beta 1; DAPI: 4',6-Diamidino-2-phenylindole; DMSO: Dimethyl sulfoxide; DVL: Dishevelled; EMT: Epithelial-mesenchymal transition; GAPDH: Glyceraldehyde 3-phosphate dehydrogenase; GSK3: Glycogen synthase kinase 3; hTCF-4: Human T cell transcription factor-4; IF: Immunofluorescence; LC: Lung cancer; LNP: Liquid crystalline nanoparticle; MD: Molecular dynamics; MMG-BSA: Molecular mechanics with generalised born and surface area solvation; MO: Monoolein; MTT: 3-(4,5-Dimethylthiazol-2-yl)-2,5-diphenyltetrazolium bromide; P407: Poloxamer 407; PADI4: Protein arginine deaminase 4; PBS: Phosphate-buffered saline; RIPA buffer: Radioimmunoprecipitation assay buffer; RMSD: Root mean square deviation; RMSF: Root mean square fluctuation; SDS-PAGE: Sodium dodecyl sulphate-polyacrylamide gel electrophoresis; TCF/LEF: T cell factor/

lymphoid enhancer factor family; TIP3P: Three-point water model; ZEB1: Zinc finger E-box binding homeobox 1

Supplementary information The online version contains supplementary material available at <https://doi.org/10.1007/s00210-023-02553-y>.

Acknowledgements The authors would like to thank and acknowledge the Discipline of Pharmacy, Graduate School of Health, University of Technology Sydney, NSW, Australia; the International Medical University, Kuala Lumpur, Malaysia; and the Centenary Institute, NSW, Australia. We would like to Acknowledge Harshita Tiwari from CSIR-Indian Institute of Integrative Medicine for helping us with molecular simulation studies.

Authors contributions Conceptualisation, VM, PMH, and KD; methodology, VM; validation, VM; formal analysis, VM; investigation, VM; data curation, VM; writing, original draft preparation, VM; writing, review and editing, VM, KD, PMH, KRP, DKC, GDR, and NGH; visualisation, VM; supervision, KD, PMH, and KRP; project administration, KD, NGH, and PMH; and funding acquisition, KD and PMH. All authors have read and agreed to the published version of the manuscript. The authors declare that all data were generated in-house and that no paper mill was used.

Funding Open Access funding enabled and organized by CAUL and its Member Institutions. Philip M. Hansbro would like to acknowledge the support from Cancer Council NSW, the National Health and Medical Research Council and the University of Technology Sydney, Australia. Kamal Dua is supported by project grants from the Rebecca L Cooper Medical Research Foundation and the fellowship from Maridulu Budyari Gumal — Sydney Partnership for Health Education, Research and Enterprise (SPHERE). Kamal Dua, Philip M Hansbro and Keshav Raj Paudel would like to acknowledge the funding support from Maridulu Budyari Gumal - The Sydney Partnership for Health, Education, Research and Enterprise - (TRIPLE I CAG SECONDMENT / EXCHANGE). Vamshikrishna Malyla is supported by an international research scholarship by UTS. Keshav Raj Paudel is supported by a fellowship from the Prevent Cancer Foundation (PCF), Alexandria, Virginia, United States, and the International Association for the Study of Lung Cancer Foundation, Denver, Colorado, United States.

Data availability All the data will be available upon request.

Declarations

Ethical approval No human/animal ethical approved required for this study.

Competing interests The authors declare no competing interests.

Open Access This article is licensed under a Creative Commons Attribution 4.0 International License, which permits use, sharing, adaptation, distribution and reproduction in any medium or format, as long as you give appropriate credit to the original author(s) and the source, provide a link to the Creative Commons licence, and indicate if changes were made. The images or other third party material in this article are included in the article's Creative Commons licence, unless indicated otherwise in a credit line to the material. If material is not included in the article's Creative Commons licence and your intended use is not permitted by statutory regulation or exceeds the permitted use, you will need to obtain permission directly from the copyright holder. To view a copy of this licence, visit <http://creativecommons.org/licenses/by/4.0/>.

References

- Albring KF et al (2013) Berberine acts as a natural inhibitor of Wnt/ β -catenin signaling—Identification of more active 13-arylalkyl derivatives. *BioFactors* 39(6):652–662
- Alnuqaydan AM et al (2022) Evaluation of the cytotoxic activity and anti-migratory effect of berberine-phytantriol liquid crystalline nanoparticle formulation on non-small-cell lung cancer in vitro. *Pharmaceutics* 14(6)
- Anthony CC et al (2020) Nuclear regulation of Wnt/ β -catenin signaling: it's a complex situation. *Genes* 11(8):886
- Battu SK, Repka MA, Maddineni S, Chittiboyina AG, Avery MA, Majumdar S (2010) Physicochemical characterization of Berberine Chloride: a perspective in the development of a solution dosage form for oral delivery. *AAPS PharmSciTech* 11(3):1466–1475. <https://doi.org/10.1208/s12249-010-9520-y>
- Berman HM et al (2000) The Protein Data Bank. *Nucleic Acids Res* 28(1):235–242
- Bowers KJ et al (2006) Scalable algorithms for molecular dynamics simulations on commodity clusters. in SC'06: Proceedings of the 2006 ACM/IEEE Conference on Supercomputing. IEEE
- Cadigan KM, Waterman ML (2012) TCF/LEFs and Wnt signaling in the nucleus. *Cold Spring Harb Perspect Biol* 4(11):a007906
- Chen QQ et al (2019) Berberine induces apoptosis in non-small-cell lung cancer cells by upregulating miR-19a targeting tissue factor. *Cancer Manag Res* 11:9005–9015
- Chen J et al (2020) Berberine chloride suppresses non-small cell lung cancer by deregulating Sin3A/TOP2B pathway in vitro and in vivo. *Cancer Chemother Pharmacol* 86(1):151–161
- Chen Q et al (2022) Berberine induces non-small cell lung cancer apoptosis via the activation of the ROS/ASK1/JNK pathway. *Ann Transl Med* 10(8):485
- Cui Q, Yang DH, and Chen ZS (2018) Special issue: natural products: anticancer and beyond. *Molecules*, 23(6)
- Dallakyan S, Olson AJ (2015) Small-molecule library screening by docking with PyRx. *Methods Mol Biol* 1263:243–250
- Doroudian M et al (2019) Nanotechnology based therapeutics for lung disease. *Thorax* 74(10):965–976
- Genheden S, Ryde U (2015) The MM/PBSA and MM/GBSA methods to estimate ligand-binding affinities. *Expert Opin Drug Discov* 10(5):449–461
- Graham TA et al (2001) Tcf4 can specifically recognize β -catenin using alternative conformations. *Nat Struct Biol* 8(12):1048–1052
- Graham TA et al (2002) The crystal structure of the beta-catenin/ICAT complex reveals the inhibitory mechanism of ICAT. *Mol Cell* 10(3):563–571
- Gu W et al (2022) Berberine regulates PADI4-related macrophage function to prevent lung cancer. *Int Immunopharmacol* 110:108965
- Heuberger J, Birchmeier W (2010) Interplay of cadherin-mediated cell adhesion and canonical Wnt signaling. *Cold Spring Harb Perspect Biol* 2(2):a002915
- Jiang J et al (2018) C9orf140, a novel Axin1-interacting protein, mediates the negative feedback loop of Wnt/ β -catenin signaling. *Oncogene* 37(22):2992–3005
- Kim S et al (2016) PubChem Substance and Compound databases. *Nucleic Acids Res* 44(D1):D1202–D1213
- Li J, Zhou BP (2011) Activation of β -catenin and Akt pathways by Twist are critical for the maintenance of EMT associated cancer stem cell-like characters. *BMC Cancer* 11(1):1–11
- Li Z et al (2014) Antioxidant and anti-inflammatory activities of berberine in the treatment of diabetes mellitus. *Evid Based Complement Alternat Med* 2014:289264
- Li J et al (2018) Berberine hydrochloride inhibits cell proliferation and promotes apoptosis of non-small cell lung cancer via the suppression of the MMP2 and Bcl-2/Bax signaling pathways. *Oncol Lett* 15(5):7409–7414
- Liu Y et al (2020) Berberine diminishes cancer cell PD-L1 expression and facilitates antitumor immunity via inhibiting the deubiquitination activity of CSN5. *Acta Pharm Sin B* 10(12):2299–2312
- Malyla V et al (2020) Recent advances in experimental animal models of lung cancer. *Future Med Chem* 12(7):567–570
- Mehta M et al (2021) Berberine loaded liquid crystalline nanostructure inhibits cancer progression in adenocarcinomic human alveolar basal epithelial cells in vitro. *J Food Biochem* 45(11):e13954
- Meng W, Takeichi M (2009) Adherens junction: molecular architecture and regulation. *Cold Spring Harb Perspect Biol* 1(6):a002899
- Ni L et al (2022) Berberine inhibits non-small cell lung cancer cell growth through repressing DNA repair and replication rather than through apoptosis. *Clin Exp Pharmacol Physiol* 49(1):134–144
- Park MH et al (2012) Phosphorylation of β -catenin at serine 663 regulates its transcriptional activity. *Biochem Biophys Res Commun* 419(3):543–549
- Paudel KR et al (2020) Targeting lung cancer using advanced drug delivery systems. Targeting chronic inflammatory lung diseases using advanced drug delivery systems. Elsevier, pp 493–516
- Paudel KR et al (2022) Berberine-loaded liquid crystalline nanoparticles inhibit non-small cell lung cancer proliferation and migration in vitro. *Environ Sci Pollut Res Int* 29(31):46830–46847
- Paudel KR et al (2022) Berberine-loaded liquid crystalline nanoparticles inhibit non-small cell lung cancer proliferation and migration in vitro. *Environ Sci Pollut Res Int*
- Paudel KR, and Kim DW (2020) Microparticles-mediated vascular inflammation and its amelioration by antioxidant activity of baicalin. *Antioxidants (Basel)* 9(9)
- Paudel KR, et al (2022) Attenuation of cigarette-smoke-induced oxidative stress, senescence, and inflammation by berberine-loaded liquid crystalline nanoparticles: in vitro study in 16HBE and RAW264.7 cells. *Antioxidants (Basel)* 11(5)
- Sánchez-Tilló E et al (2011) β -catenin/TCF4 complex induces the epithelial-to-mesenchymal transition (EMT)-activator ZEB1 to regulate tumor invasiveness. *Proc Natl Acad Sci* 108(48):19204–19209
- Sastry GM et al (2013) Protein and ligand preparation: parameters, protocols, and influence on virtual screening enrichments. *J Comput Aided Mol Des* 27(3):221–234
- Siegel RL et al (2022) Cancer statistics, 2022. CA: a cancer journal for clinicians
- Solanki N et al (2020) Antiproliferative effects of boswellic acid-loaded chitosan nanoparticles on human lung cancer cell line A549. *Future Med Chem* 12(22):2019–2034
- Stemmer Vd et al (2008) Snail promotes Wnt target gene expression and interacts with β -catenin. *Oncogene* 27(37): 5075–5080
- Stewart DJ (2014) Wnt signaling pathway in non-small cell lung cancer. *J Natl Cancer Inst* 106(1): djt356
- Thiery JP et al (2009) Epithelial-mesenchymal transitions in development and disease. *cell* 139(5) 871–890
- Valenta T, Hausmann G, Basler K (2012) The many faces and functions of β -catenin. *EMBO J* 31(12):2714–2736
- Wadhwa R et al (2021) Anti-inflammatory and anticancer activities of naringenin-loaded liquid crystalline nanoparticles in vitro. *J Food Biochem* 45(1):e13572
- Wadhwa R et al (2020) Epigenetic therapy as a potential approach for targeting oxidative stress-induced non-small-cell lung cancer. *Handbook of Oxidative Stress in Cancer: Mechanistic Aspects*, 1–16
- Wu K et al (2012) Berberine inhibits the proliferation of colon cancer cells by inactivating Wnt/ β -catenin signaling. *Int J Oncol* 41(1):292–298
- Zhang Y, Wang X (2020) Targeting the Wnt/ β -catenin signaling pathway in cancer. *J Hematol Oncol* 13(1):165

Publisher's note Springer Nature remains neutral with regard to jurisdictional claims in published maps and institutional affiliations.

10) Research Paper: Zerumbone-incorporated liquid crystalline nanoparticles inhibit proliferation and migration of non-small-cell lung cancer in vitro.

Status: Published in **Naunyn-Schmiedeberg's Archives of Pharmacology**

Citation: Manandhar B, Paudel KR, Clarence DD, **De Rubis G**, Madheswaran T, Panneerselvam J, Zacconi FC, Williams KA, Pont LG, Warkiani ME, MacLoughlin R, Oliver BG, Gupta G, Singh SK, Chellappan DK, Hansbro PM, Dua K. *Zerumbone-incorporated liquid crystalline nanoparticles inhibit proliferation and migration of non-small-cell lung cancer in vitro*. **Naunyn-Schmiedeberg's Archives of Pharmacology**. 2023 Jul 13. doi: 10.1007/s00210-023-02603-5

Contribution: I contributed to the experiments, manuscript writing, and revisions of the manuscript draft



Zerumbone-incorporated liquid crystalline nanoparticles inhibit proliferation and migration of non-small-cell lung cancer in vitro

Bikash Manandhar · Keshav Raj Paudel · Dvya Delilaa Clarence · Gabriele De Rubis · Thiagarajan Madheswaran · Jithendra Panneerselvam, et al. [full author details at the end of the article]

Received: 14 May 2023 / Accepted: 25 June 2023
© The Author(s) 2023

Abstract

Lung cancer is the second most prevalent type of cancer and is responsible for the highest number of cancer-related deaths worldwide. Non-small-cell lung cancer (NSCLC) makes up the majority of lung cancer cases. Zerumbone (ZER) is natural compound commonly found in the roots of *Zingiber zerumbet* which has recently demonstrated anti-cancer activity in both in vitro and in vivo studies. Despite their medical benefits, ZER has low aqueous solubility, poor GI absorption and oral bioavailability that hinders its effectiveness. Liquid crystalline nanoparticles (LCNs) are novel drug delivery carrier that have tuneable characteristics to enhance and ease the delivery of bioactive compounds. This study aimed to formulate ZER-loaded LCNs and investigate their effectiveness against NSCLC in vitro using A549 lung cancer cells. ZER-LCNs, prepared in the study, inhibited the proliferation and migration of A549 cells. These inhibitory effects were superior to the effects of ZER alone at a concentration 10 times lower than that of free ZER, demonstrating a potent anti-cancer activity of ZER-LCNs. The underlying mechanisms of the anti-cancer effects by ZER-LCNs were associated with the transcriptional regulation of tumor suppressor genes *P53* and *PTEN*, and metastasis-associated gene *KRT18*. The protein array data showed downregulation of several proliferation associated proteins such as AXL, HER1, PGRN, and BIRC5 and metastasis-associated proteins such as DKK1, CAPG, CTSS, CTSB, CTSD, and PLAU. This study provides evidence of potential for increasing the potency and effectiveness of ZER with LCN formulation and developing ZER-LCNs as a treatment strategy for mitigation and treatment of NSCLC.

Keywords Zerumbone · Liquid crystalline nanoparticles · Non-small-cell lung cancer · A549 lung cancer cells · Cell proliferation · Cell migration

Abbreviations

ZER Zerumbone
LCN Liquid crystalline nanoparticle

Introduction

Lung cancer represents one of the deadliest respiratory diseases that accounted for 1.7 million deaths worldwide in 2020 (Sung et al. 2021). Non-small-cell lung cancer

(NSCLC) comprises of the majority of the cases (~85% of lung cancer cases) (Malya et al. 2020). Conventional treatment strategies for NSCLC face limitations of disease relapse occurrences, resistance to chemotherapeutic treatment (Baci et al. 2022; Li et al. 2022), and elevated toxicity resulting from chemotherapy and radiotherapy (Kumbhar et al. 2022; Yazbeck et al. 2022).

There is an emerging interest in nanotechnological applications for delivering anti-cancer drugs to achieve a higher drug specificity and therapeutic efficacy. Liquid crystalline nanoparticles (LCNs) have unique structural properties that can add benefits to anti-cancer therapy by providing high capacity of loading lipophilic and hydrophilic drugs, low toxicity, controlled release, non-toxic degradation, biodegradable matrix, low cost and ease of scale up for topical, oral, and intravenous drug administration (Jain et al. 2012; Pardeike et al. 2009).

Bikash Manandhar and Keshav Raj Paudel have equal contribution as first author.

✉ Dinesh Kumar Chellappan
dinesh_kumar@imu.edu.my

Extended author information available on the last page of the article

The LCNs also provide the added benefits of site-specific drug delivery system, modulated drug release, and long-term stability (Muller et al. 2002). Nanotechnology and LCNs have been successfully employed to incorporate and deliver several plant-derived phytochemicals, including berberine (Alnuqaydan et al. 2022; Mehta et al. 2021; Paudel et al. 2022), curcumin (Clarence et al. 2022; Sharma et al. 2021), rutin (Paudel et al. 2021), naringenin (Wadhwa et al. 2021), boswellic acid (Solanki et al. 2020), and agarwood oil (Alamil et al. 2022) to improve their therapeutic potency and efficacy.

Zerumbone (ZER) is a bioactive compound isolated from the *Zingiber zerumbet* (Girisa et al. 2019) that has previously shown to exert potent anti-inflammatory (Su et al. 2021), anti-oxidant (Sidahmed et al. 2015), and anti-cancer activities (Foong et al. 2018; Ghasemzadeh et al. 2017; Rahman et al. 2014). ZER can induce apoptosis in A549 lung cancer cells and enhance cisplatin treatment efficacy in vitro (Hu et al. 2014). ZER can also inhibit proliferation of lung cancer cells in vivo mouse models (Kim et al. 2009). However, its medicinal applications are hindered by its poor aqueous solubility and bioavailability. With incorporation into LCN drug delivery system, ZER has potential for its development as an alternative anti-cancer therapy that can effectively inhibit lung cancer proliferation and migration as well as resolve the issues of drug toxicity, adverse effects, and treatment resistance that are apparent with the conventional therapy. In the present study, ZER was formulated into a monoolein-based LCNs, and the resulting ZER-loaded LCNs (ZER-LCNs) were characterized for physicochemical properties including mean size, entrapment efficiency and in vitro release of ZER. The anti-cancer potential of ZER-LCNs was then tested in vitro in human A549 adenocarcinoma cell line in comparison with that of free ZER.

The results of this study provide substantial evidence of the advantages and feasibility of encapsulating poorly soluble bioactive molecule ZER in LCNs-based nano drug delivery systems for improving their anti-cancer potency and efficacy against NSCLC.

Materials and methods

Materials

ZER (MW218.3) was purchased from Funakoshi Co., Ltd (originally produced by Adipogen Life Science, Japan), Monoolein (MO, 1-oleoyl-rac-glycerol, MW 356.55 g/mol, purity 99.5%), Poloxamer 407 (P407),

and phosphate buffered saline (PBS) containing 137 mM sodium chloride, 2.7 mM potassium chloride, and 10 mM phosphate buffer were purchased from Merck (Kenilworth, NJ, USA). Ultrapure water and reverse-osmosis (RO) purified water were used in several studies. All the solvents and reagents used in the study were of analytical research grade.

Preparation and characterization of ZER-LCNs

Solubility analysis of ZER

For the solubility analysis, 10 mg of ZER was added with 1 mL of methanol to obtain a concentration of 10000 µg/mL. This was then further diluted with methanol to obtain concentrations of 10, 20, 30, 40, 50, 60, 70, and 80 µg/mL. The concentration of soluble ZER in these samples was determined by measuring their absorbance at a wavelength (λ) of 249 nm using the UV-Vis. The optical density (OD) values of the samples were then plotted against their concentration and the R² value (greater than 0.99) as well as the graph equation was obtained.

Preparation of ZER-LCN formulation

The ZER-LCN formulation was prepared by the ultrasonification method, with the formulation composition, as specified in Table 1. The method was conducted by briefly heating MO at 60 °C in a water bath. ZER was then added into the glass vial containing the molten MO, then gently shaken until it was completely dissolved. Simultaneously, P407 was added to water and heated at 60 °C in a water bath. After a brief period, the P407 that was dissolved in the water was added to the ZER-MO mixture. After this, the coarse dispersion obtained was subjected to size reduction by sonication for 5 min and using the ultrasonic cell pulverizer (Labsonic® P; Sartorius) at amplitude 80 and repeated cycles of 5 s on and 5 s off.

Table 1 Formulation composition of blank LCNs and ZER-LCNs

Formulation code	Formulation composition (%w/w)			
	MO	P407	Distilled water	ZER
Blank-LCN	4.00	0.40	95.60	0.00
ZER-LCN	4.00	0.40	95.58	0.02

Entrapment efficiency

0.1 mL of ZER-LCN was added to 0.9 mL of methanol to obtain 10 mL of sample. The absorbance of total ZER (free ZER+ZER entrapped in LCNs) in the sample was measured using the UV-Vis method at $\lambda=249$ nm. The concentration of total ZER in the sample was calculated by comparing the absorbance against the standard curve obtained from the solubility analysis. In order to obtain the concentration of free ZER (non-entrapped ZER) in the ZER-LCN formulation, 2 mL of the sample was transferred to the Amicon Ultra-4 centrifugal filter device (molecular-weight-cut off: 10,000 g/mol; Merck Millipore Ltd., Cork, Ireland), and centrifuged for 15 min at 2800xg, 25 °C to separate the free drug from ZER-LCNs. The supernatant was collected, and the absorbance was measured using the UV-Vis method at $\lambda=249$ nm. The concentration of free ZER in the supernatant was calculated by comparing the absorbance against the standard curve obtained from solubility analysis. The entrapment efficiency (%EE) was calculated using the following equation.

$$\%EE = (\text{Total ZER concentration} - \text{Free ZER concentration}) / \text{Total ZER concentration} \times 100\%$$

In vitro release study

The release profiles of ZER from ZER-LCN formulations were observed using the static dialysis method dialysis tubing cellulose membrane; molecular-weight-cut-off: 14,000 g/mol; Merck). By using the quantification of absorbance, the amount of drug released was tested while being immersed in PBS (pH7.4). The dialysis bags were soaked in water prior to use and were then filled with 1 mL of ZER-LCN sample before being clamped at both ends and submerged in 20 mL of PBS (pH 7.4) in a 50 mL centrifuge tube. The samples in the centrifuge tubes were then submerged into a water-bath at 37 °C (SW22 Julabo, shaken horizontally at 50 strokes per min), thus mimicking the intestinal milieu. Then, 1 mL of each sample was drawn from the tubes at intervals 1, 2, 3, 6, 9, 12, and 24 h. Every time 1 mL of sample was drawn, the same volume was replenished with PBS to ensure that the volume is remained constant. The concentration of ZER in the drawn samples was quantified by measuring absorbance using UV-spectrometry and comparing against the standard curve (Fig. 1).

The cumulative released percentage of ZER was calculated using the equation:

$$\text{Cumulative drug release (\%)} = (C_i V + V_e (C_{9i} - 1) + C_{(i-2)} + \dots + C_1) / T \times 100\%$$

Absorbance against Concentration (mcg) of Zerumbone at 249nm

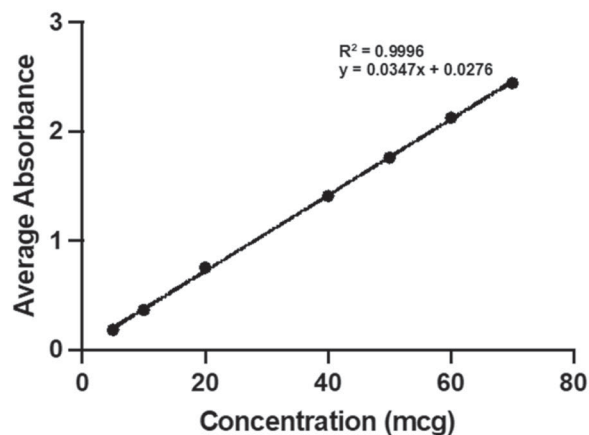


Fig. 1 Graph of absorbance against concentration of Zerumbone

Where, C_i represents the 'i'th sampling concentration of ZER ($\mu\text{g}/\text{mL}$), V is the total the volume of release medium (mL), V_e is the sampling volume (mL), and T is the total mass of ZER present in nanoparticles (μg).

Cell culture and treatment

Human lung carcinoma A549 cells (ATCC, Manassas, VA, USA) was kindly gifted by Prof. Alaina Ammit (Woolcock Institute of Medical Research, Sydney, Australia). The cells were cultured in low-glucose Dulbecco's Modified Eagle's Medium (DMEM, Lonza, Basel, Switzerland), 5% (v/v) fetal bovine serum (Lonza) and 1% (v/v) antibiotic mix of penicillin and streptomycin (Lonza) in a humidified incubator. The incubator was maintained with 5% CO_2 at 37 °C. The in vitro experiments were carried out by treating A549 cells with ZER or ZER-LCNs at the indicated doses for 24 h.

Cell proliferation assay

A549 cell proliferation was measured using 3-(4,5-dimethylthiazol-2-yl)-2,5-diphenyl tetrazolium bromide (MTT, Merck), as previously described (Manandhar et al. 2020). Briefly, the cells were incubated for 24 h in the absence or presence of ZER-LCNs (1, 2.5, 5, 7.5, or 10 μM) or ZER (1, 5, 10, 25, or 50 μM). MTT (250 $\mu\text{g}/\text{mL}$) was added, and the plate was incubated for 4 h. The supernatant was discarded and 100 μL dimethyl sulfoxide (Merck) was added to

dissolve the purple formazan crystals. The absorbance was measured at 540 nm excitation wavelength with the help of TECAN Infinite M1000 plate reader (Tecan Trading AG, Männedorf, Switzerland). The cell proliferation was measured as % cell viability relative to control.

Colony formation assay

Colony formation assay was performed as previously described (Alnuqaydan et al. 2022). Briefly, A549 cells were plated at a density of 500 cells per well in 6-well plates and cultured at 37 °C for two weeks in the absence or presence of 50 µM ZER or 5 µM ZER-LCNs, with repeated replenishment of the media every 48 h. The cells were washed with PBS and fixed at room temperature for 20 minutes with 3.7% (v/v) formaldehyde. After three washes with PBS, the cells were stained with 0.4% crystal violet (Merck). The cells were washed again three times with PBS. The individual wells were photographed from the bottom side of the plates.

Wound healing assay

The impact of ZER and ZER-LCNs on A549 cell migration was evaluated using a wound healing experiment. A549 cells were seeded at a density of 2.5×10^5 /well in 6-well plates and cultured until fully confluent. The cell monolayer was scratched with the tip of a sterile pipette to create a wound. After washing the cells with PBS to remove floating cells, the cells were cultured at 37 °C for 24 h with or without ZER (50 µM) or ZER-LCNs (2.5 or 5 µM). At 0 and 24 h of incubation, images were captured using a phase contrast microscope equipped with a 10× objective lens. The wound closure was determined as a percentage (%) of the change in wound width between 0 h and 24 h relative to that at 0 h.

Trans-well chamber migration assay

The A549 cell migration was also evaluated using a trans-well chamber migration assay as described previously (Pau-del et al. 2022).

Reverse transcriptase-quantitative polymerase chain reaction (RT-qPCR)

After 24 h of incubation of A549 cells in the presence or absence of ZER (50 µM) or ZER-LCNs (2.5 or 5 µM), the cells were washed twice with PBS and lysed with TRI reagent (Merck). The total RNA isolation was conducted as previously described (Alnuqaydan et al. 2022). The RNA purity and concentration was determined using Nanodrop One (Thermo Fisher Scientific). The RNA was reverse transcribed to synthesize cDNA and qPCR was performed to determine the mRNA levels of genes of interest (Alnuqaydan

et al. 2022). The forward and reverse primers for genes encoding tumor protein 53 (*P53*, forward: ACCTATGGA AACTACTTCCTG; reverse: ACCATTGTTCAATATCGT CC), phosphatase and tensin homolog (*PTEN*, forward: GGCTAAGTGAAGATGACAATC; reverse: GTTACTCCC TTTTGTCTCTG), keratin 18 (*KRT18*, forward: GGAAGT AAAAGGCCTACAAG; reverse: GTACTTGTCTAGCTC CTCTC), and glyceraldehyde-3-phosphate dehydrogenase (*GAPDH*, forward: TCGGAGTCAACGGATTTG; reverse: CAACAATATCCACTTTACCAGAG) were procured from Merck.

Proteome profiler human oncology array

After 24 h of incubation of A549 cells with or without ZER (50 µM) or ZER-LCNs (2.5 or 5 µM), the proteins were extracted with RIPA buffer ((Roche Diagnostics, Basel, Switzerland). The proteins were quantified by bicinchoninic acid (BCA) assay using Pierce BCA protein assay kit (Thermo Fisher). Three hundred micrograms protein per group was used to assess the expression of oncology-related proteins using proteome profiler human XL oncology array kit (R&D Systems, Minneapolis, MN), according to the manufacturer's instructions. The protein signals in the array were photographed using the ChemDoc MP imaging system (Bio-Rad, Hercules, CA, USA). The Image J software (version 1.53c, Bethesda, MD, USA) was used to analyze the pixel densities of the protein signals.

Statistical analysis

The data are presented as mean \pm S.E.M and statistical analyses were performed by one-way ANOVA, followed by Dunnett's multiple comparison tests using GraphPad Prism software (version 9.4, San Diego, CA, USA). A *p*-value of less than 0.05 was considered statistically significant.

Results

Characterization of ZER-LCN formulation

Based on the solubility analysis, it was found that the λ_{max} for ZER was at 249 nm. After which a concentration against absorbance study was conducted and a graph was developed from it which indicated that the absorbance increased in a linear concentration dependent manner as observed in Fig. 1. The linear equation of $y = 0.0347x + 0.0276$ and an R^2 value of 0.9996 was obtained from the graph which indicates that there is a strong and significant correlation.

The prepared ZER-LCNs was a white-pigmented viscous liquid. As seen in Fig. 2, the TEM analysis which functioned to show the surface morphology of the

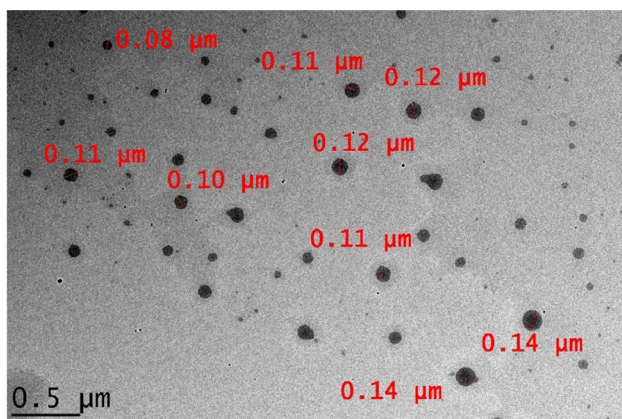


Fig. 2 The analysis of the surface morphologies as visualized on the transmission electron microscopy (Hitachi HT7700 high resolution TEM; Hitachi, Chiyoda, Tokyo, Japan). Scale bar 0.5 μm

formulation showed that the LCNs without ZER had clear cuboidal particles and the similar morphological results were observed when ZER was added into the LCNs. Both samples showed less than 200 nm in size, which indicated positive results to the mean particles size measurement as the smaller the particle size, the better the targeting ability of the drug delivery system.

The mean diameter of ZER-LCN was determined to be $180.6 \pm 3 \text{ nm}$ with all formulations showing a narrow PDI of less than 0.4 while also being negatively charged. Adding on to that, high entrapment efficiency was also observed for the ZER-LCN formulation at $90.63 \pm 0.13\%$ together with a prolonged release over a duration of 24 h. Besides that, the results for the in vitro release test shown in Fig. 3 suggested that the ZER-LCN formulation had a greater amount of drug release in comparison to the free ZER. It was also observed and confirmed that ZER-LCN was also able to produce a drug release over a prolonged period, which in this study was up to 24 h. However, it was observed that there was an initial quick and rapid release which was eventually

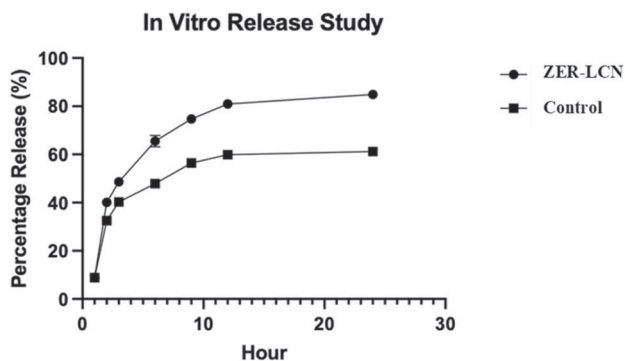


Fig. 3 The in vitro release study of free ZER (control) and ZER-LCNs

followed by a plateau at about slightly more than 80% in the ZER-LCN in comparison to the free ZER which plateaued at around 60%.

Effects of ZER and ZER-LCNs on cell proliferation of A549 cells

ZER did not show inhibitory effect on the cell proliferation of A549 cells up to a concentration of 50 μM . ZER-LCNs, on the other hand, exerted $\sim 45\%$ inhibition of A549 cell proliferation at a dose of 5 μM (Fig. 4, $p < 0.0001$ compared to the control). The inhibition of cell proliferation by ZER-LCNs increased up to $\sim 90\%$ at doses of 7.5 and 10 μM (Fig. 4, $p < 0.0001$ for both compared to the control). ZER at 50 μM and ZER-LCNs at 2.5 or 5 μM were used for subsequent experiments to evaluate their anti-cancer potential on A549 cells.

ZER-LCNs reduced colony formation of A549 cells

The crystal violet staining of the A549 cell colonies clearly demonstrates the anti-proliferative activities of both ZER (50 μM) and ZER-LCNs (5 μM), as compared to the control (Fig. 2). The representative well images visibly depict a modest decrease in the number of cell colonies in ZER-treated cells while almost no colonies in ZER-LCNs-treated cells (Fig. 5), suggesting a greater

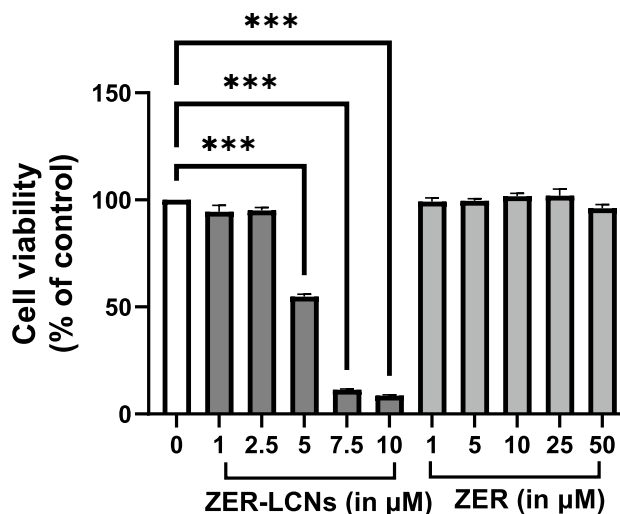
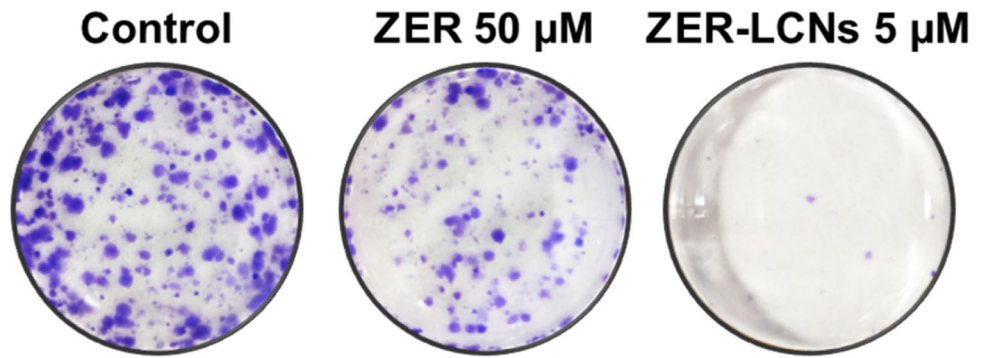


Fig. 4 Anti-proliferative effects of ZER and ZER-LCNs in A549 cells. A549 cells were treated with or without ZER-LCNs (1, 2.5, 5, 7.5, or 10 μM) or ZER (1, 5, 10, 25, or 50 μM) for 24 h, followed by incubation with MTT. The purple formazan crystals formed were dissolved with DMSO and the absorbance was measured with microplate reader. The data in the figure are mean \pm SEM of 3 independent experiments. **** $p < 0.0001$

Fig. 5 Effect of ZER and ZER-LCNs on colony formation of A549 cells. After seeding A549 cells in 6-well plate, they were cultured for 2 weeks in the absence or presence of 50 μM ZER or 5 μM ZER-LCNs. The cell colonies were stained with crystal violet and photographed. The figure shows representative images from 3 independent experiments

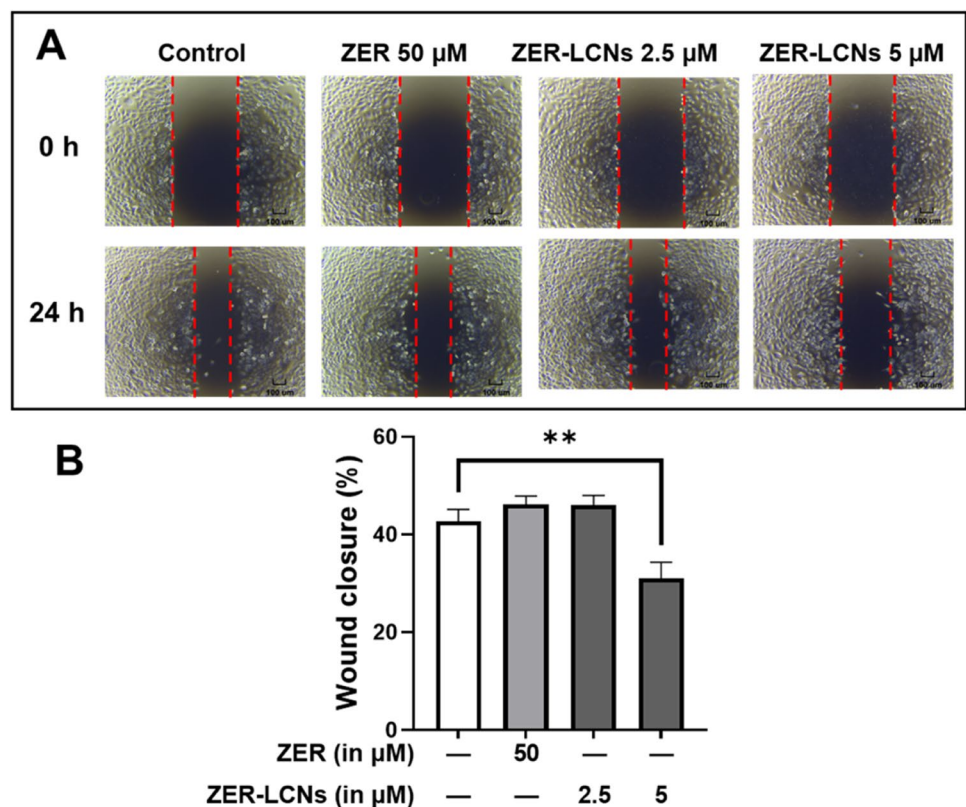


potency of nanoparticle formulation of ZER compared to free ZER.

ZER-LCNs inhibited wound closure in A549 cells

The images from wound healing assay show no difference in the closure of wound in A549 cells treated with ZER (50 μM) or ZER-LCNs (2.5 μM) (Fig. 6A). However, there is a visible inhibition of wound closure in A549 cells treated with ZER-LCNs at 5 μM concentration (Fig. 6A). The quantification of % wound closure is consistent with the representative images, with ~27% inhibition of wound closure in 5 μM ZER-LCNs-treated A549 cells as compared to the control (Fig. 6B, $p < 0.01$).

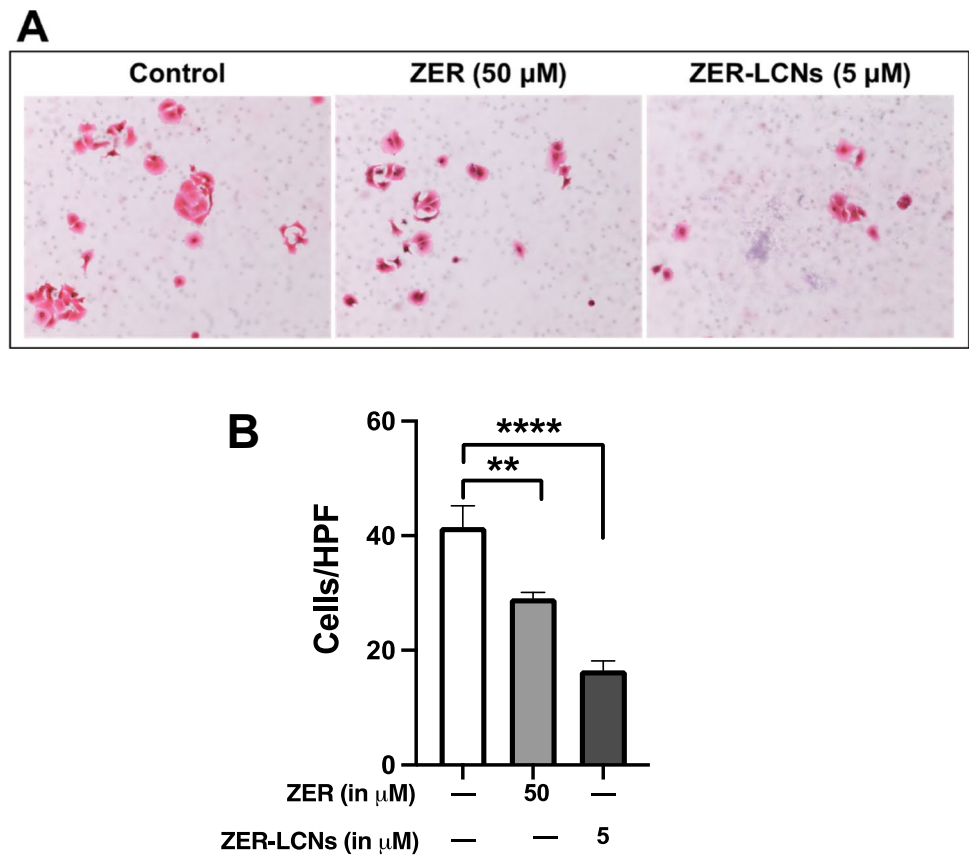
Fig. 6 Wound healing effect of ZER and ZER-LCNs in A549 cells. Wound was scratched on the monolayer of fully confluent A549 cells, then the cells were cultured for 24 h in the absence or presence of 50 μM ZER, 2.5 μM ZER-LCNs, or 5 μM ZER-LCNs. The images were acquired at 0 h and 24 h of treatment with a phase contrast microscope at 4 \times magnification. **A** representative images from 3 independent experiments. **B** % wound closure after 24 h of incubation with or without ZER-LCNs. Data in **B** is expressed as mean \pm SEM of 3 independent experiments. $**p < 0.01$



ZER-LCNs decreased the migration of A549 cells in a trans-well chamber

The visual observation of images from trans-well chamber assay showed decreased number of A549 cell migration when treated with 50 μM ZER or 5 μM ZER-LCNs compared to the control (Fig. 7A). This is also consistent with the decreased number of migrated cells in both 50 μM ZER-treated group (Fig. 7B, $p < 0.01$ against the control) and 5 μM ZER-LCNs (Fig. 7B, $p < 0.0001$ against the control). Fifty micromolar ZER and 5 μM ZER-LCNs decreased cell migration by ~32% and ~60%, respectively (Fig. 7B), suggesting a greater anti-migratory potential of ZER-LCNs compared to the free ZER.

Fig. 7 Effect of ZER and ZER-LCNs on migration of A549 cells in a trans-well chamber. The cells seeded in a trans-well chamber was treated with/without 50 μM ZER or 5 μM ZER-LCNs for 24 h to allow cell migration. Migrated cells in the lower compartment were stained with staining solution of hematoxylin and eosin and microscopic images were taken at 20 \times magnification. **A** representative images from 3 independent experiments. **B** The number of cells, and the data are expressed as mean \pm SEM of 3 independent experiments. $**p < 0.01$, $****p < 0.0001$



ZER-LCNs increased P53 and PTEN mRNA expression and decreased KRT18 mRNA expression

Analysis of mRNA levels with RT-qPCR showed that 5 μM ZER-LCNs upregulates the transcription of tumor suppressor genes *P53* and *PTEN* (Fig. 8A–B, $p < 0.0001$ for both against the control) and downregulates transcription of metastasis-associated *KRT18* (Fig. 8C, $p < 0.001$). Fifty

micromolar ZER and 2.5 μM ZER-LCNs did not show such effects (Fig. 8A–C).

ZER-LCNs downregulated proteins-associated with cancer cell proliferation

Treatment of A549 cells with ZER-LCNs significantly downregulated the protein expression of AXL receptor

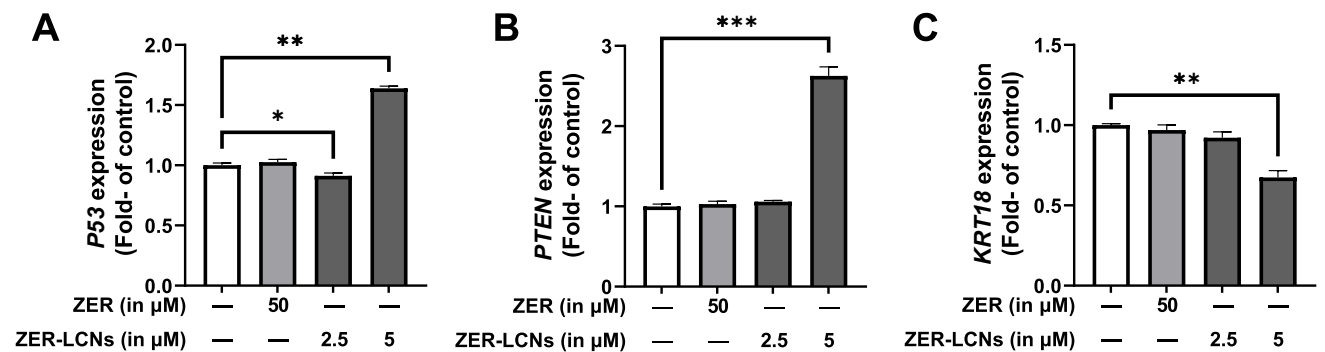


Fig. 8 Regulation of mRNA levels *P53*, *PTEN*, and *KRT18* by ZER and ZER-LCNs. A549 cells were treated with 50 μM ZER, 2.5 μM ZER-LCNs, or 5 μM ZER-LCNs for 24 h. Total RNA was extracted, cDNA synthesized, and mRNA levels were determined with qPCR.

The figure shows the mRNA levels of *P53* (A), *PTEN* (B) and *KRT18* (C), normalized against the levels of *GAPDH*. Data are expressed as mean \pm SEM of 3 independent experiments. $*p < 0.05$, $***p < 0.001$, $****p < 0.0001$

tyrosine kinase (AXL), epidermal growth factor receptor (HER1), progranulin (PGRN), and baculoviral IAP repeat containing 5 (BIRC5) at both 2.5 and 5 μM concentrations (Fig. 9A–D), while ZER only downregulated the protein expression of AXL (Fig. 9A, $p < 0.05$ compared to control). This shows that the regulatory activity of ZER-LCNs on expression of proteins associated with cancer cell proliferation was far superior compared to ZER (Fig. 9A–D).

ZER-LCNs downregulated proteins-associated with cancer cell migration

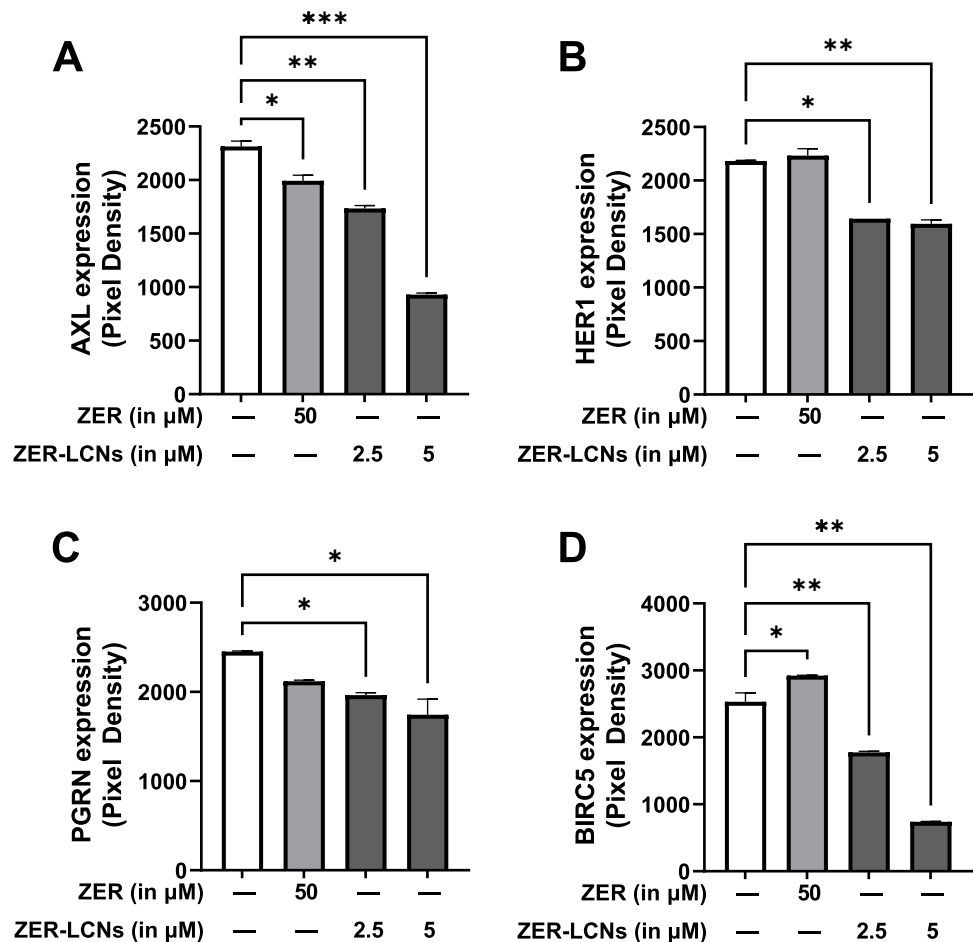
Both 2.5 and 5 μM doses of ZER-LCNs significantly downregulated the protein expression of dickkopf1 (DKK1), actin capping protein, gelsolin like (CAPG), cathepsin S (CTSS), cathepsin B (CTSB), and cathepsin D (CTSD), as compared to the control (Fig. 10A–E), while only 5 μM ZER-LCNs could downregulate the protein expression of urokinase-type plasminogen activator (PLAU) (Fig. 10F, $p < 0.05$ against the control). ZER-treated A549 cells also showed downregulation of DKK1, CAPG, CTSS, CTSB, and CTSD (Fig. 10A–E). 5 μM ZER-LCNs showed greater

potential to inhibit migration than 50 μM ZER, which is highlighted by greater downregulation of DKK1 and CTSB in the presence of 5 μM ZER-LCNs relative to 50 μM ZER (Fig. 10A–D).

Discussion

Our *in vitro* investigation in A549 cell line has demonstrated the beneficial anti-cancer activity of ZER-LCNs. We have shown that ZER-LCNs remarkably inhibits key processes of cancer progression proliferation and migration, and down-regulate the various protein expression linked with cancer progression. The results of the present study indicate that ZER-LCNs provide superior anti-cancer potency and efficacy through increased inhibition A549 cell proliferation and migration at 10- to 20-fold lower concentrations of free ZER used. Mechanistically, ZER-LCNs inhibited cancer cell proliferation and migration by upregulating the mRNA levels of *P53* and *PTEN*, downregulating the mRNA levels of *KRT18*, as well as by downregulating the levels of several proteins involved in the promotion of cancer cell proliferation, migration, and invasion.

Fig. 9 Regulation of expression of proteins-related to cancer cell proliferation by ZER and ZER-LCNs. After treatment of A549 cells with 50 μM ZER, 2.5 μM ZER-LCNs, or 5 μM ZER-LCNs for 24 h, the proteins were extracted and the expression of proteins-associated with cell proliferation was evaluated with proteome profiler human oncogenic array kit. The figure shows the protein expression of AXL (A), HER1 (B), PGRN (C), and BIRC5 (D). The data are expressed as mean \pm SEM of 3 independent experiments. * $p < 0.05$, ** $p < 0.01$, *** $p < 0.001$, and **** $p < 0.0001$



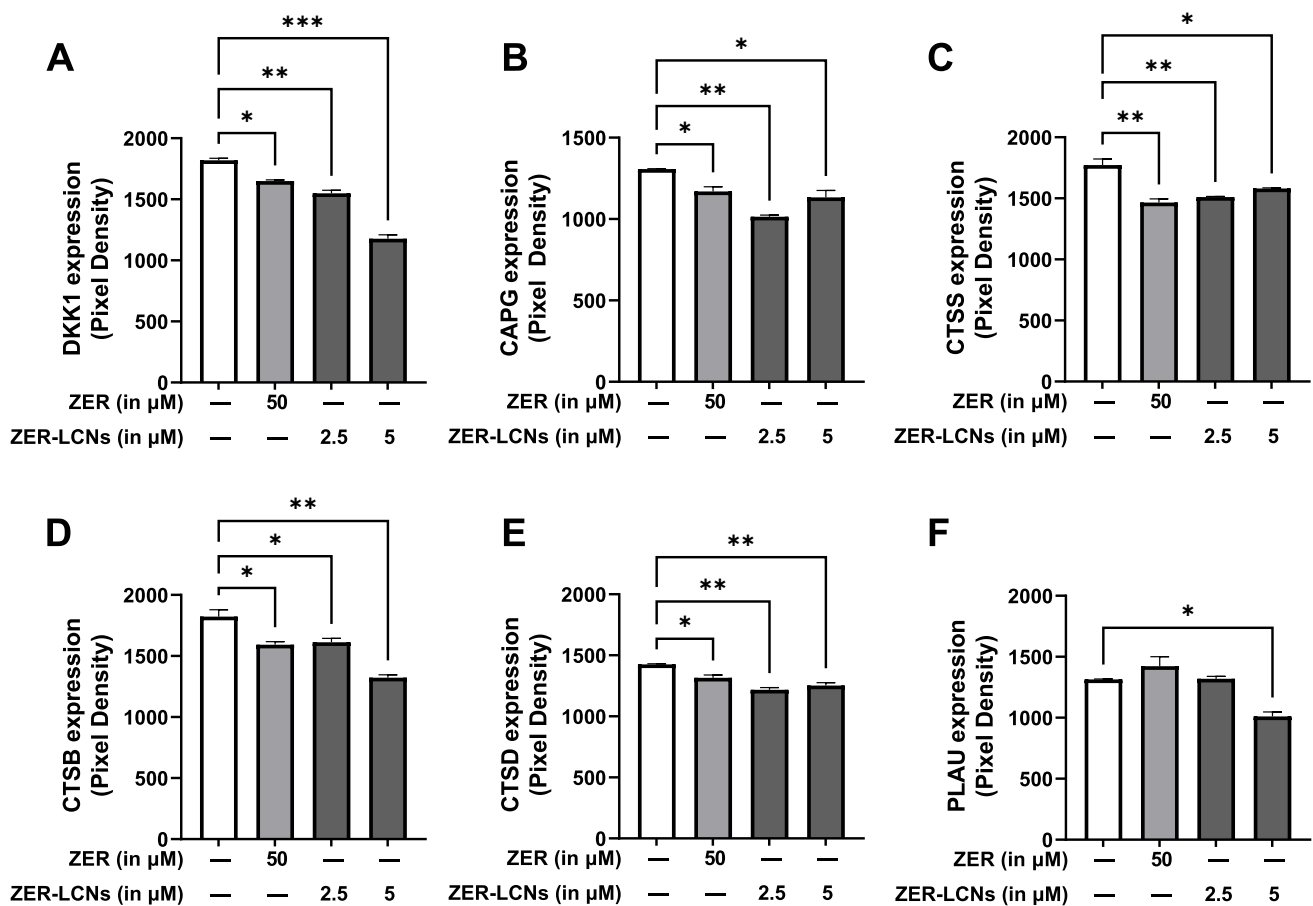


Fig. 10 Regulation of proteins-associated with cancer cell migration by ZER and ZER-LCNs. After treatment of A549 cells with 50 μM ZER, 2.5 μM ZER-LCNs, or 5 μM ZER-LCNs for 24 h, the proteins were extracted and the expression of proteins-associated with cell proliferation was evaluated with proteome profiler human oncogenic

array kit. The figure shows the protein expression of DKK1 (A), CAPG (B), CTSS (C), CTSB (D), CTSD (E), and PIAU (F). The data are expressed as mean \pm SEM of 3 independent experiments. * $p < 0.05$, ** $p < 0.01$, and *** $p < 0.001$

Despite a wide range of promising pharmacological benefits of ZER, it has several limitations, including low dissolution rates, poor gastrointestinal absorption and low oral bioavailability, owing to the fact that it is very slightly soluble in water, thus limiting its clinical applications (Devkota et al. 2021). To overcome these shortcomings, it is essential to develop alternative drug delivery system for ZER utilizing nanotechnology and advanced pharmaceutical approach. The encapsulation of molecules within nanoparticles is advantageous because, besides improving solubility, it improves the stability and cellular uptake of the loaded molecules, simultaneously allowing selective cell targeting (Ng et al. 2020; Paudel et al. 2022). This results in an increased therapeutic efficacy of encapsulated drugs, with substantially lower doses necessary to achieve therapeutic effect compared to free, non-encapsulated drug, and subsequently reduced adverse effects (Paudel et al. 2022). A few studies have shown that formulating ZER with cyclodextrin (Hassan et al. 2020) and nanostructured lipid carriers

(Foong et al. 2018) improves its solubility and bioavailability. Pharmaceutical formulations using nanoparticles have been suggested and developed for a better and more effective drug delivery system for ZER as an anti-cancer agent. LCN drug delivery system is one of such nanotechnology-based systems that offers versatility in designing and delivery of therapeutic moiety to manage chronic respiratory diseases (Chan et al. 2021). We have previously shown that rutin-, naringenin-, and berberine-loaded LCNs offer better anti-cancer activity along with activity against oxidative stress and inflammation than using powder form of these compounds (Alnuqaydan et al. 2022; Alnuqaydan et al. 2022; Mehta et al. 2021; Mehta et al. 2021; Paudel et al. 2022; Paudel et al. 2022; Paudel et al. 2020; Paudel et al. 2021; Wadhwa et al. 2021). Continuing with the similar research hypothesis, we have formulated ZER-LCNs and investigated its anticancer potential.

In this study, the formulation of ZER using the monoolein (MO)-based LCN technology was successfully produced

by dissolving the drug into the MO and then adding it to the chosen solubilizer which was P407. MO or also known as glyceryl monooleate is an amphiphilic molecule that is generally recognized as safe (GRAS) status by the FDA. It can self-assemble itself in environments that are made of aqueous surrounding because of intermolecular forces, thus allowing it to produce a liquid crystalline structure that consist of hydrophobic and hydrophilic sections inside of the lipid core (Loo et al. 2020). MO has rather low cytotoxicity when used in nanoparticles in previous studies (Bode et al. 2013; Leesajakul et al. 2004) in comparison to phytantriol-based LCNs (Hinton et al. 2014). However, MO does have the tendency to cause haemolysis when distributed through the intravenous route. Therefore, in order to reduce the likelihood of this occurring, it was proposed that the addition of P407 stabilizer would be useful as it can play the role of giving steric stabilization and coverage to the outer surfaces of the dispersed colloidal particles. This would in turn also reduce the immediate exposure of MO to the red blood cells (Loo et al. 2020).

The mean diameter of LCN is usually between 70 and 130 nm (Lee et al. 2016), whereas the ZER-LCN had a mean diameter of 180.6 ± 3 nm which also corresponds with the addition of ZER into the formulation thus slightly increasing the overall mean size. Additionally, the PDI obtained for the ZER-LCN were all negative values of less than 0.4 which indicates that the sample had low polydisperse and an overall more uniform sample (Danaei et al. 2020). Additionally, high entrapment efficiency was also observed for the ZER-LCN formulation at $90.63 \pm 0.13\%$. The entrapment efficiency is the difference between the initial drug and the free drug in the supernatant with respect to the total amount added into the nanoformulation. The in vitro drug release study is an important study for the identification of the efficacy, safety as well as the quality of nanoparticle-based drug delivery systems (Weng et al. 2020). Our results suggested that the ZER-LCN was able to release a larger amount of drug in comparison to pure ZER. Additionally, a sustained release of the drug for over 24 h was observed and this prolonged release is an added benefit as it ensures that patients would reap the benefits of the safe drug dosage over a longer period as well as being able to reduce the frequency of the drug consumption.

Once we confirmed that our ZER-LCNs exert favorable characterization data in terms of particle size, polydispersity index, entrapment efficiency, and in vitro release, we proceeded with the investigation of in vitro biological activity against A549 cells. The two key events of tumorigenesis are (a) proliferation and (b) migration/metastasis, which are governed by several pathways, and transcription and expression of cancer-related genes and proteins, respectively. P53 is a nuclear protein whose main physiological role is to regulate the progression of cells through the cell cycle,

arresting the cell cycle in case of DNA damage, and initiating apoptosis if the damage is irreparable (Chasov et al. 2021). Loss-of-function mutations of p53 are very frequent in different types of cancer (Jin et al. 2010). This makes p53 an intriguing option as a therapeutic target, with many approaches emerging recently in an attempt to restore its function (Hassin and Oren 2022). Another important tumor suppressor whose function is often loss in many cancers, including LC, is PTEN (Gkoutakos et al. 2019; Jin et al. 2010). The PTEN protein is a potent oncosuppressor whose physiological function is to maintain the homeostasis of the mitogenic Phosphatidylinositol-3-kinase (PI3K)/AKT pathway by dephosphorylating phosphatidylinositol-3, 4, 5-phosphate (PIP3) (Jin et al. 2010; Molinari and Frattini 2013). The loss of expression and/or function of oncosuppressors such as p53 and PTEN results, through different pathways, in increased cell proliferation and reduced cell death (Jin et al. 2010). This is often accompanied by the aberrant expression of specific proteins that may be used as a cancer biomarker such as KRT18 (Zhang et al. 2019).

Our cell proliferation assay revealed that ZER-LCNs remarkably inhibited the A549 proliferation by ~45% at a dose of 5 μ M (Fig. 4). Interestingly, the pure ZER upto the dose of 50 μ M did not significantly change the cell proliferation indicating ZER-LCN is more potent than its pure form. Furthermore, this was supported by our colony formation assay where ZER-LCNs at a dose of 5 μ M inhibited the colony formation of A549 compared to both control (only media treated) and pure ZER at 50 μ M (Fig. 5). Mechanistically, we have revealed that the decrease in A549 cell proliferation was due to the inhibition of protein expression of Axl, progranulin, Survivin/BIRC5, and ErbB1/HER1 that are involved in cell proliferation/growth (Fig. 9). The expression of oncogene Axl is observed in 60% of NSCLC cell line and it is known to facilitate tumor cell growth and adhesion (Kim et al. 2015; Wimmel et al. 2001). *Progranulin* expression is correlated with A549 growth and induce tumor growth in vivo (He and Bateman 1999). Survivin/BIRC5 inhibits apoptosis of tumor cells, and therefore supports cancer cell survival (Hirano et al. 2015; Schott et al. 1995). HER1 is a member of epidermal growth factor receptor (EGFR) family with crucial function of mediating NSCLC proliferation (Guo et al. 2016). *P53* and *PTEN* are well known tumor suppressor genes in NSCLC (Andjelkovic et al. 2011). It is interesting to note that tumor suppressor gene *P53* and *PTEN* were upregulated by only ZER-LCN but not by pure ZER (Fig. 8).

In relation to A549 migration, we have observed that ZER-LCNs drastically inhibits the A549 would closure in scratch wound healing assay and trans-well chamber assay, the methods to quantify cell migration. This was evident by ~27% inhibition of wound closure by 5 μ M ZER-LCNs while pure ZER could not significantly close the wound

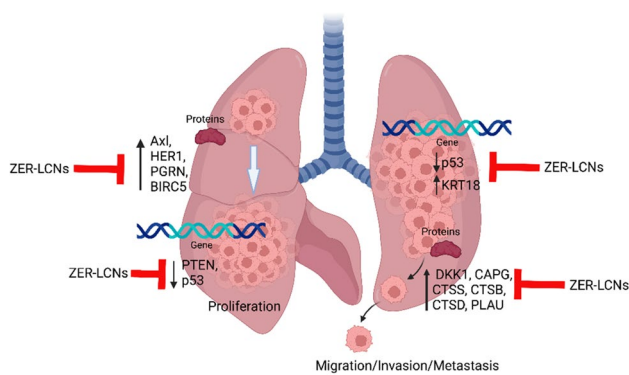


Fig. 11 Anticancer mechanism of action of ZER-LCNs in vitro in A549 cells. (Abbreviations: ZER-LCNs, Zerumbone-liquid crystalline nanoparticles; p53, tumor protein 53; KRT18, keratin 18; PTEN, phosphatase and tensin homolog; Axl, AXL receptor tyrosine kinase; HER1, epidermal growth factor receptor; PGRN, progranulin; BIRC5, Baculoviral IAP repeat containing 5; DKK1, Dickkopf1; CAPG, actin capping protein, gelsolin like; CTSS, Cathepsin S; CTSB, Cathepsin B; CTSD, Cathepsin D; PLAU, urokinase-type plasminogen activator)

compared to the untreated control (Fig. 6). Similarly, in trans-well chamber assay, 5 μ M ZER-LCNs inhibited the migration of A549 by \sim 60% while pure ZER could only inhibit \sim 32% (Fig. 7). Mechanistically, we have revealed that the decrease of A549 cell proliferation was due to the inhibition of protein expression of CTSS, DKK1, CAPG, and PLAU that are involved in cell migration/metastasis (Fig. 10). CTSS protein is associated with NSCLC progression as CTSS can cleave proteoglycan of interstitial matrix such as decorin (Kehlet et al. 2017) and nidogen-1 (Willumsen et al. 2017) to facilitate the invasion of NSCLC cell. DKK1, CTSB, CTSD, and CAPG are also associated with the metastatic potential of cancer (Shao et al. 2011; Tan et al. 2013; Zhang et al. 2017). Our biological study clearly suggests that ZER-LCNs possess more significant anti-cancer potential against A549 cells compared to pure ZER. *KRT18* gene is overexpressed in human cancer and positively correlated with tumor invasion/metastasis (Zhang et al. 2014). In our study, we observed that *KRT18* gene expression was significantly downregulated by ZER-LCNs but not by pure ZER. These findings are diagrammatically summarized in Fig. 11.

We cannot neglect the various limitations in our study that could be a research platform for us and other researcher for further expansion of our current study. Our study lacks the inclusion of the expression of other lung cancer related genes besides *P53*, *PTEN*, and *KRT18*. It would be interesting to explore further to validate whether the genes encoding the proteins in Figs. 9 and 10 are inhibited by ZER-LCNs. As our research outcomes is based on in vitro experimental data, there is a scope for further expansion of our hypothesis utilizing in vivo animal

models of lung cancer. Furthermore, apart for the A549 cell line, there are many other cells line of both NSCLC and SCLC where we can study the therapeutic potential of ZER-LCNs as anticancer agents. Moving forward, it would be useful and compelling to conduct in vivo biological analysis of ZER in the LCN formulation through the inhalation delivery method in experimental mice model with other models that have been established. Using an animal model would also allow us to determine the long-term safety, pharmacokinetics, herb-drug complexities, and many other factors as these plays a pivotal part in determining toxicity and the bioavailability of drugs. Nevertheless, our study suggests that with further strengthening of research with Zerumbone -LCNs, it can be a promising therapeutic option for lung cancer.

Conclusion

In conclusion, ZER-LCNs show significant anti-proliferative and anti-migratory activity in A549 cells by regulating the mRNA expression of *P53*, *PTEN*, and *KRT18* and the expression of several proteins associated with cell proliferation and migration such as AXL, HER1, PGRN, BIRC5, DKK1, CAPG, CTSS, CTSB, CTSD, and PLAU. This study highlights successful application of nanotechnology in formulating LCN-encapsulated ZER to generate superior efficacy and potency compared to free ZER for the treatment of NSCLC. Formulating ZER into LCNs poses much greater pharmacological and biological benefits in comparison to free ZER on its own. The potent biological activities of ZER-LCN prove that it is able to overcome many of the unfavorable characteristics of pure ZER using the nanoformulation method. This study will help to direct future research towards the investigation and development of ZER as a potential anti-cancer drug therapy with the help of nanotechnology.

Acknowledgements KD is supported by a project grant from the Rebecca L Cooper Medical Research Foundation and the Maridulu Budyari Gumal Sydney Partnership for Health, Education, Research and Enterprise (SPHERE) RSEOH CAG Seed grant, fellowship and extension grant, Uttaranchal University grant, and the Faculty of Health MCR/ECR Mentorship Support Grant. PMH is funded by a fellowship and grants from the National Health and Medical Research Council (NHMRC) of Australia (1059238, 1175134, 2010287), and UTS. KRP is supported by a joint fellowship from Prevent Cancer Foundation and International Association for the Study of Lung Cancer (IASLC) USA.

Author contributions KD, KRP, PMH, FCZ, KW, LGP, MEW, BGO, RM, were involved in funding acquisition, development of research hypotheses and visualisation of this project, BM, KRP, GDR were involved in experimental design, data acquisition, statistical analyses, writing original draft, and DDC, TM, JP, and DKC were directly involved in development of ZER-LCN formulations. GG, SKS and

all other authors were involved in review & editing. All authors have contributed to drafting of this manuscript and have read and approved the final manuscript. The authors declare that all data were generated in-house and that no paper mill was used.

Funding Open Access funding enabled and organized by CAUL and its Member Institutions This research was funded by the University of Technology Sydney, Australia, as Global Strategic Partnerships Seed Funding Scheme to KRP, PMH, FCZ, KW, LP, MEW, and KD.

Data availability The data and materials that support the findings of this study will be made available by the corresponding author, upon reasonable request.

Declarations

Ethical approval This study was performed in vitro using human cell line and did not involve human and/or animal studies. Hence, this declaration is “not applicable”.

Competing interests The authors declare no competing interests.

Open Access This article is licensed under a Creative Commons Attribution 4.0 International License, which permits use, sharing, adaptation, distribution and reproduction in any medium or format, as long as you give appropriate credit to the original author(s) and the source, provide a link to the Creative Commons licence, and indicate if changes were made. The images or other third party material in this article are included in the article's Creative Commons licence, unless indicated otherwise in a credit line to the material. If material is not included in the article's Creative Commons licence and your intended use is not permitted by statutory regulation or exceeds the permitted use, you will need to obtain permission directly from the copyright holder. To view a copy of this licence, visit <http://creativecommons.org/licenses/by/4.0/>.

References

- Alamil JMR, Paudel KR, Chan Y, Xenaki D, Panneerselvam J, Singh SK, Gulati M, Jha NK, Kumar D, Prasher P, Gupta G, Malik R, Oliver BG, Hansbro PM, Dua K, Chellappan DK (2022) Rediscovering the therapeutic potential of agarwood in the management of chronic inflammatory diseases. *Molecules* 27(9):3038
- Alnuqaydan AM, Almutary AG, Azam M, Manandhar B, De Rubis G, Madheswaran T, Paudel KR, Hansbro PM, Chellappan DK, Dua K (2022) Phytantriol-based berberine-loaded liquid crystalline nanoparticles attenuate inflammation and oxidative stress in lipopolysaccharide-induced RAW264.7 Macrophages. *Nanomaterials* (Basel) 12(23):4312
- Alnuqaydan AM, Almutary AG, Azam M, Manandhar B, Yin GHS, Yen LL, Madheswaran T, Paudel KR, Hansbro PM, Chellappan DK, Dua K (2022) Evaluation of the cytotoxic activity and anti-migratory effect of berberine-phytantriol liquid crystalline nanoparticle formulation on non-small-cell lung cancer in vitro. *Pharmaceutics* 14(6):1119
- Andjelkovic T, Bankovic J, Stojsic J, Milinkovic V, Podolski-Renic A, Ruzdijic S, Tanic N (2011) Coalterations of p53 and PTEN tumor suppressor genes in non-small cell lung carcinoma patients. *Trans Res* 157(1):19–28
- Baci D, Cekani E, Imperatori A, Ribatti D, Mortara L (2022) Host-related factors as targetable drivers of immunotherapy response in non-small cell lung cancer patients. *Front Immunol* 13:914890
- Bode JC, Kuntsche J, Funari SS, Bunjes H (2013) Interaction of dispersed cubic phases with blood components. *Int J Pharm* 448(1):87–95
- Chan Y, Mehta M, Paudel KR, Madheswaran T, Panneerselvam J, Gupta G, Su QP, Hansbro PM, McLoughlin R, Dua K, Chellappan DK (2021) Versatility of liquid crystalline nanoparticles in inflammatory lung diseases. *Nanomedicine (Lond)* 16(18):1545–1548
- Chasov V, Zaripov M, Mirgayazova R, Khadiullina R, Zmievskaia E, Ganeeva I, Valiullina A, Rizvanov A, Bulatov E (2021) Promising new tools for targeting p53 mutant cancers: humoral and cell-based immunotherapies. *Front Immunol* 12:707734
- Clarence DD, Paudel KR, Manandhar B, Singh SK, Devkota HP, Panneerselvam J, Gupta V, Chitranshi N, Verma N, Saad S, Gupta G, Hansbro PM, Oliver BG, Madheswaran T, Dua K, Chellappan DK (2022) Unravelling the therapeutic potential of nano-delivered functional foods in chronic respiratory diseases. *Nutrients* 14(18):3828
- Danaei M, Dehghankhold M, Ataei S, Davarani FH, Javanmard R, Dokhani A, Khorasani S, Mozafari MR (2020) Impact of particle size and polydispersity index on the clinical applications of lipidic nanocarrier systems. *Pharmaceutics* 10(2):57
- Devkota HP, Paudel KR, Hassan MM, Dirar AI, Das N, Adhikari-Devkota A, Echeverría J, Logesh R, Jha NK, Singh SK (2021) Bioactive compounds from Zingiber montanum and their pharmacological activities with focus on zerumbone. *Appl Sci* 11(21):10205
- Foong JN, Selvarajah GT, Rasedee A, Rahman HS, How CW, Beh CY, Teo GY, Ku CL (2018) Zerumbone-loaded nanostructured lipid carrier induces apoptosis of canine mammary adenocarcinoma cells. *Biomed Res Int* 2018:8691569
- Ghasemzadeh A, Jaafar HZ, Rahmat A, Swamy MK (2017) Optimization of microwave-assisted extraction of zerumbone from Zingiber zerumbet L. rhizome and evaluation of antiproliferative activity of optimized extracts. *Chem Cent J* 11:5
- Girisa S, Shabnam B, Monisha J, Fan L, Halim CE, Arfuso F, Ahn KS, Sethi G, Kunnumakara AB (2019) Potential of zerumbone as an anti-cancer agent. *Molecules* 24(4):734
- Gkoutakos A, Sartori G, Falcone I, Piro G, Ciuffreda L, Carbone C, Tortora G, Scarpa A, Briani E, Milella M, Rosell R, Corbo V, Pilotto S (2019) PTEN in lung cancer: dealing with the problem, Building on New Knowledge and Turning the Game Around. *Cancers (Basel)* 11(8):1141
- Guo R, Zhang Y, Li X, Song X, Li D, Zhao Y (2016) Discovery of ERBB3 inhibitors for non-small cell lung cancer (NSCLC) via virtual screening. *J Mol Model* 22(6):135
- Hassan MM, Mohammed AFA, Elamin KM, Devkota HP, Ohno Y, Motoyama K, Higashi T, Imai T (2020) Improvement of pharmaceutical properties of zerumbone, a multifunctional compound, using cyclodextrin derivatives. *Chem Pharm Bull (Tokyo)* 68(11):1117–1120
- Hassin O, Oren M (2022) Drugging p53 in cancer: one protein, many targets. *Nat Rev Drug Discov* 22:127–144
- He Z, Bateman A (1999) Progranulin gene expression regulates epithelial cell growth and promotes tumor growth in vivo. *Cancer Res* 59(13):3222–9
- Hinton TM, Grusche F, Acharya D, Shukla R, Bansal V, Waddington LJ, Monaghan P, Muir BW (2014) Bicontinuous cubic phase nanoparticle lipid chemistry affects toxicity in cultured cells. *Toxicol Res-Uk* 3(1):11–22
- Hirano H, Maeda H, Yamaguchi T, Yokota S, Mori M, Sakoda S (2015) Survivin expression in lung cancer: association with smoking, histological types and pathological stages. *Oncol Lett* 10(3):1456–1462
- Hu Z, Zeng Q, Zhang B, Liu H, Wang W (2014) Promotion of p53 expression and reactive oxidative stress production is involved in zerumbone-induced cisplatin sensitization of non-small cell lung cancer cells. *Biochimie* 107:257–62. <https://doi.org/10.1016/j.biochi.2014.09.001>
- Jain V, Swarnakar NK, Mishra PR, Verma A, Kaul A, Mishra AK, Jain NK (2012) Paclitaxel loaded PEGylated glyceryl monooleate based nanoparticulate carriers in chemotherapy. *Biomaterials* 33(29):7206–20

- Jun G, Kim MJ, Jeon H-S, Choi JE, Kim DS, Lee EB, Cha SI, Yoon GS, Kim CH, Jung TH, Park JY (2010) PTEN mutations and relationship to EGFR, ERBB2, KRAS, and TP53 mutations in non-small cell lung cancers. *Lung Cancer* 69(3):279–283
- Kehlet SN, Bager CL, Willumsen N, Dasgupta B, Brodmerkel C, Curran M, Brix S, Leeming DJ, Karsdal MA (2017) Cathepsin-S degraded decorin are elevated in fibrotic lung disorders - development and biological validation of a new serum biomarker. *BMC Pulm Med* 17(1):110
- Kim KC, Baek SH, Lee C (2015) Curcumin-induced downregulation of Axl receptor tyrosine kinase inhibits cell proliferation and circumvents chemoresistance in non-small lung cancer cells. *Int J Oncol* 47(6):2296–303
- Kim M, Miyamoto S, Yasui Y, Oyama T, Murakami A, Tanaka T (2009) Zerumbone, a tropical ginger sesquiterpene, inhibits colon and lung carcinogenesis in mice. *Int J Cancer* 124(2):264–71
- Kumbhar P, Manjappa A, Shah R, Jha NK, Singh SK, Dua K, Disouza J, Patravale V (2022) Inhalation delivery of repurposed drugs for lung cancer: approaches, benefits and challenges. *J Control Release* 341:1–15
- Lee DR, Park JS, Bae IH, Lee Y, Kim BM (2016) Liquid crystal nanoparticle formulation as an oral drug delivery system for liver-specific distribution. *Int J Nanomed* 11:853–871
- Leesajakul W, Nakano M, Taniguchi A, Handa T (2004) Interaction of cubosomes with plasma components resulting in the destabilization of cubosomes in plasma. *Colloids Surf B Biointerfaces* 34(4):253–8
- Li C, Qiu Y, Zhang Y (2022) Research progress on therapeutic targeting of cancer-associated fibroblasts to tackle treatment-resistant NSCLC. *Pharmaceuticals (Basel)* 15(11):1411
- Loo YS, Madheswaran T, Rajendran R, Bose RJC (2020) Encapsulation of berberine into liquid crystalline nanoparticles to enhance its solubility and anticancer activity in MCF7 human breast cancer cells. *J Drug Deliv Sci Tec* 57:101756
- Malya V, Paudel KR, Shukla SD, Donovan C, Wadhwa R, Pickles S, Chimankar V, Sahu P, Bielefeldt-Ohmann H, Bebowy M, Hansbro PM, Dua K (2020) Recent advances in experimental animal models of lung cancer. *Future Med Chem* 12(7):567–570
- Manandhar B, Kim HJ, Rhyu DY (2020) Caulerpa okamurae extract attenuates inflammatory interaction, regulates glucose metabolism and increases insulin sensitivity in 3T3-L1 adipocytes and RAW 264.7 macrophages. *J Integr Med* 18(3):253–264
- Mehta M, Malya V, Paudel KR, Chellappan DK, Hansbro PM, Oliver BG, Dua K (2021) Berberine loaded liquid crystalline nanostructure inhibits cancer progression in adenocarcinomic human alveolar basal epithelial cells in vitro. *J Food Biochem* 45(11):e13954
- Mehta M, Paudel KR, Shukla SD, Shastri MD, Satija S, Singh SK, Gulati M, Dureja H, Zaccaroni FC, Hansbro PM, Chellappan DK, Dua K (2021) Rutin-loaded liquid crystalline nanoparticles attenuate oxidative stress in bronchial epithelial cells: a PCR validation. *Future Med Chem* 13(6):543–549
- Molinari F, Frattini M (2013) Functions and regulation of the PTEN gene in colorectal cancer. *Front Oncol* 3:326
- Muller RH, Radtke M, Wissing SA (2002) Solid lipid nanoparticles (SLN) and nanostructured lipid carriers (NLC) in cosmetic and dermatological preparations. *Adv Drug Deliv Rev* 54(Suppl 1):S131–55
- Ng PQ, Ling LSC, Chellian J, Madheswaran T, Panneerselvam J, Kunath AP, Gupta G, Satija S, Mehta M, Hansbro PM, Collet T, Dua K, Chellappan DK (2020) Applications of nanocarriers as drug delivery vehicles for active phytoconstituents. *Curr Pharm Des* 26(36):4580–4590
- Pardeike J, Hommoss A, Muller RH (2009) Lipid nanoparticles (SLN, NLC) in cosmetic and pharmaceutical dermal products. *Int J Pharm* 366(1–2):170–84
- Paudel KR, Chellappan DK, MacLoughlin R, Pinto TJA, Dua K, Hansbro PM (2022) Editorial: Advanced therapeutic delivery for the management of chronic respiratory diseases. *Front Med (Lausanne)* 9:983583
- Paudel KR, Dua K, Panth N, Hansbro PM, Chellappan DK (2022) Advances in research with rutin-loaded nanoformulations in mitigating lung diseases. *Future Med Chem* 14(18):1293–1295
- Paudel KR, Mehta M, Yin GHS, Yen LL, Malya V, Patel VK, Panneerselvam J, Madheswaran T, MacLoughlin R, Jha NK, Gupta PK, Singh SK, Gupta G, Kumar P, Oliver BG, Hansbro PM, Chellappan DK, Dua K (2022) Berberine-loaded liquid crystalline nanoparticles inhibit non-small cell lung cancer proliferation and migration in vitro. *Environ Sci Pollut Res Int* 12(23):4312
- Paudel KR, Mehta M, Yin GHS, Yen LL, Malya V, Patel VK, Panneerselvam J, Madheswaran T, MacLoughlin R, Jha NK, Gupta PK, Singh SK, Gupta G, Kumar P, Oliver BG, Hansbro PM, Chellappan DK, Dua K (2022) Berberine-loaded liquid crystalline nanoparticles inhibit non-small cell lung cancer proliferation and migration in vitro. *Environ Sci Pollut Res Int* 29(31):46830–46847
- Paudel KR, De Rubis G, Panth N, Singh SK, Chellappan DK, Hansbro PM, Dua K (2022) Nanomedicine and medicinal plants: emerging symbiosis in managing lung diseases and associated infections. *EXCLI J* 21:1299–1303
- Paudel KR, Wadhwa R, Mehta M, Chellappan DK, Hansbro PM, Dua K (2020) Rutin loaded liquid crystalline nanoparticles inhibit lipopolysaccharide induced oxidative stress and apoptosis in bronchial epithelial cells in vitro. *Toxicol Vitro : Int J Pub Assoc BIBRA* 68:104961
- Paudel KR, Wadhwa R, Tew XN, Lau NJX, Madheswaran T, Panneerselvam J, Zeeshan F, Kumar P, Gupta G, Anand K, Singh SK, Jha NK, MacLoughlin R, Hansbro NG, Liu G, Shukla SD, Mehta M, Hansbro PM, Chellappan DK, Dua K (2021) Rutin loaded liquid crystalline nanoparticles inhibit non-small cell lung cancer proliferation and migration in vitro. *Life Sci* 276:119436
- Rahman HS, Rasedee A, Yeap SK, Othman HH, Chartrand MS, Namvar F, Abdul AB, How CW (2014) Biomedical properties of a natural dietary plant metabolite, zerumbone, in cancer therapy and chemoprevention trials. *Biomed Res Int* 2014:920742
- Schott AF, Apel IJ, Nuñez G, Clarke MF (1995) Bcl-XL protects cancer cells from p53-mediated apoptosis. *Oncogene* 11(7):1389–94
- Shao F, Zhang R, Don L, Ying K (2011) Overexpression of gelsolin-like actin-capping protein is associated with progression of lung adenocarcinoma. *Tohoku J Exp Med* 225(2):95–101
- Sharma A, Hawthorne S, Jha SK, Jha NK, Kumar D, Girgis S, Goswami VK, Gupta G, Singh S, Dureja H, Chellappan DK, Dua K (2021) Effects of curcumin-loaded poly(lactic-co-glycolic acid) nanoparticles in MDA-MB231 human breast cancer cells. *Nanomedicine (Lond)* 16(20):1763–1773
- Sidahmed HM, Hashim NM, Abdulla MA, Ali HM, Mohan S, Abdelwahab SI, Taha MM, Fai LM, Vadivelu J (2015) Antisecretory, gastroprotective, antioxidant and anti-Helicobacter pylori activity of zerumbone from Zingiber zerumbet (L.) Smith. *PLoS One* 10(3):e0121060
- Solanki N, Mehta M, Chellappan DK, Gupta G, Hansbro NG, Tambuwala MM, Aa Aljabali A, Paudel KR, Liu G, Satija S, Hansbro PM, Dua K, Dureja H (2020) Antiproliferative effects of boswellic acid-loaded chitosan nanoparticles on human lung cancer cell line A549. *Future Med Chem* 12(22):2019–2034
- Su CC, Wang SC, Chen IC, Chiu FY, Liu PL, Huang CH, Huang KH, Fang SH, Cheng WC, Huang SP, Yeh HC, Liu CC, Lee PY, Huang MY, Li CY (2021) Zerumbone suppresses the LPS-induced inflammatory response and represses activation of the NLRP3 inflammasome in macrophages. *Front Pharmacol* 12:652860
- Sung H, Ferlay J, Siegel RL, Laversanne M, Soerjomataram I, Jemal A, Bray F (2021) Global Cancer Statistics 2020: GLOBOCAN

- Estimates of Incidence and Mortality Worldwide for 36 Cancers in 185 Countries. *CA Cancer J Clin* 71(3):209–249
- Tan GJ, Peng ZK, Lu JP, Tang FQ (2013) Cathepsins mediate tumor metastasis. *World J Biol Chem* 4(4):91–101
- Wadhwa R, Paudel KR, Chin LH, Hon CM, Madheswaran T, Gupta G, Panneerselvam J, Lakshmi T, Singh SK, Gulati M, Dureja H, Hsu A, Mehta M, Anand K, Devkota HP, Chellian J, Chellappan DK, Hansbro PM, Dua K (2021) Anti-inflammatory and anticancer activities of Naringenin-loaded liquid crystalline nanoparticles in vitro. *J Food Biochem* 45(1):e13572
- Weng JW, Tong HHY, Chow SF (2020) In vitro release study of the polymeric drug nanoparticles: development and validation of a novel method. *Pharmaceutics* 12(8):732
- Willumsen N, Bager CL, Leeming DJ, Bay-Jensen AC, Karsdal MA (2017) Nidogen-1 degraded by cathepsin S can be quantified in serum and is associated with non-small cell lung cancer. *Neoplasia (New York, N.Y.)* 19(4):271–278
- Wimmel A, Glitz D, Kraus A, Roeder J, Schuermann M (2001) Axl receptor tyrosine kinase expression in human lung cancer cell lines correlates with cellular adhesion. *Eur J Cancer (Oxford England :1990)* 37, (17):2264–74
- Yazbeck V, Alesi E, Myers J, Hackney MH, Cuttino L, Gewirtz DA (2022) An overview of chemotoxicity and radiation toxicity in cancer therapy. *Adv Cancer Res* 155:1–27
- Zhang H, Chen X, Wang J, Guang W, Han W, Zhang H, Tan X, Gu Y (2014) EGR1 decreases the malignancy of human non-small cell lung carcinoma by regulating KRT18 expression. *Sci Rep* 4:5416
- Zhang J, Hu S, Li Y (2019) KRT18 is correlated with the malignant status and acts as an oncogene in colorectal cancer. *Biosci Rep* 39(8):BSR20190884
- Zhang J, Zhang X, Zhao X, Jiang M, Gu M, Wang Z, Yue W (2017) DKK1 promotes migration and invasion of non-small cell lung cancer via beta-catenin signaling pathway. *Tumour Biol* 39(7):1010428317703820
- Publisher's note** Springer Nature remains neutral with regard to jurisdictional claims in published maps and institutional affiliations.

Authors and Affiliations

Bikash Manandhar^{1,2} · Keshav Raj Paudel³ · Dvya Delilaa Clarence⁴ · Gabriele De Rubis^{1,2} · Thiagarajan Madheswaran⁵ · Jithendra Panneerselvam⁵ · Flavia C. Zacconi^{6,7,8} · Kylie A. Williams¹ · Lisa G. Pont¹ · Majid Ebrahimi Warkiani^{9,10} · Ronan MacLoughlin^{11,12,13} · Brian Gregory Oliver^{14,15} · Gaurav Gupta^{16,17} · Sachin Kumar Singh^{2,18} · Dinesh Kumar Chellappan¹⁹ · Philip M. Hansbro³ · Kamal Dua^{1,2}

✉ Philip M. Hansbro
philip.hansbro@uts.edu.au

✉ Kamal Dua
kamal.dua@uts.edu.au

¹ Discipline of Pharmacy, Graduate School of Health, University of Technology Sydney, Sydney, NSW 2007, Australia

² Australian Research Centre in Complementary and Integrative Medicine, Faculty of Health, University of Technology Sydney, Sydney, NSW 2007, Australia

³ Centre for Inflammation, Centenary Institute and University of Technology Sydney, Faculty of Science, School of Life Sciences, Sydney NSW 2050, Australia

⁴ School of Postgraduate Studies, International Medical University (IMU), 57000 Kuala Lumpur, Malaysia

⁵ Department of Pharmaceutical Technology, School of Pharmacy, International Medical University, 57000 Kuala Lumpur, Malaysia

⁶ Departamento de Química Orgánica, Facultad de Química y de Farmacia, Pontificia Universidad Católica de Chile, Av. Vicuña Mackenna 4860, 7820436 Macul, Santiago, Chile

⁷ Centro de Investigación en Nanotecnología y Materiales Avanzados, CIEN-UC, Pontificia Universidad Católica de Chile, Av. Vicuña Mackenna 4860, 7820436 Macul, Santiago, Chile

⁸ Institute for Biological and Medical Engineering, Schools of Engineering, Medicine and Biological Sciences, Pontificia Universidad Católica de Chile, Santiago, Chile

⁹ School of Biomedical Engineering, University of Technology Sydney, Sydney, New South Wales, Australia

¹⁰ Institute for Biomedical Materials and Devices, Faculty of Science, University of Technology Sydney, Sydney, New South Wales, Australia

¹¹ Research and Development, Aerogen Limited, IDA Business Park, Galway, Connacht H91 HE94, Ireland

¹² School of Pharmacy & Biomolecular Sciences, Royal College of Surgeons in Ireland, Dublin, Leinster D02 YN77, Ireland

¹³ School of Pharmacy & Pharmaceutical Sciences, Trinity College, Dublin, Leinster D02 PN40, Ireland

¹⁴ Woolcock Institute of Medical Research, Macquarie University, Sydney, NSW 2137, Australia

¹⁵ School of Life Sciences, Faculty of Science, University of Technology Sydney, Sydney, NSW 2007, Australia

¹⁶ School of Pharmacy, Suresh Gyan Vihar University, Jaipur, Rajasthan, India

¹⁷ Center for Transdisciplinary Research, Saveetha Institute of Medical and Technical Science, Saveetha University, Chennai, India

¹⁸ School of Pharmaceutical Sciences, Lovely Professional University, Jalandhar-Delhi G.T Road, Phagwara 144411, India

¹⁹ Department of Life Sciences, School of Pharmacy, International Medical University, 57000 Kuala Lumpur, Malaysia